Heinrich Heine Universität Düsseldorf

JÜLICH Forschungszentrum

Lipase-catalyzed kinetic resolution: Synthesis and application of axially chiral biphenols

Ruth Christine Ganardi

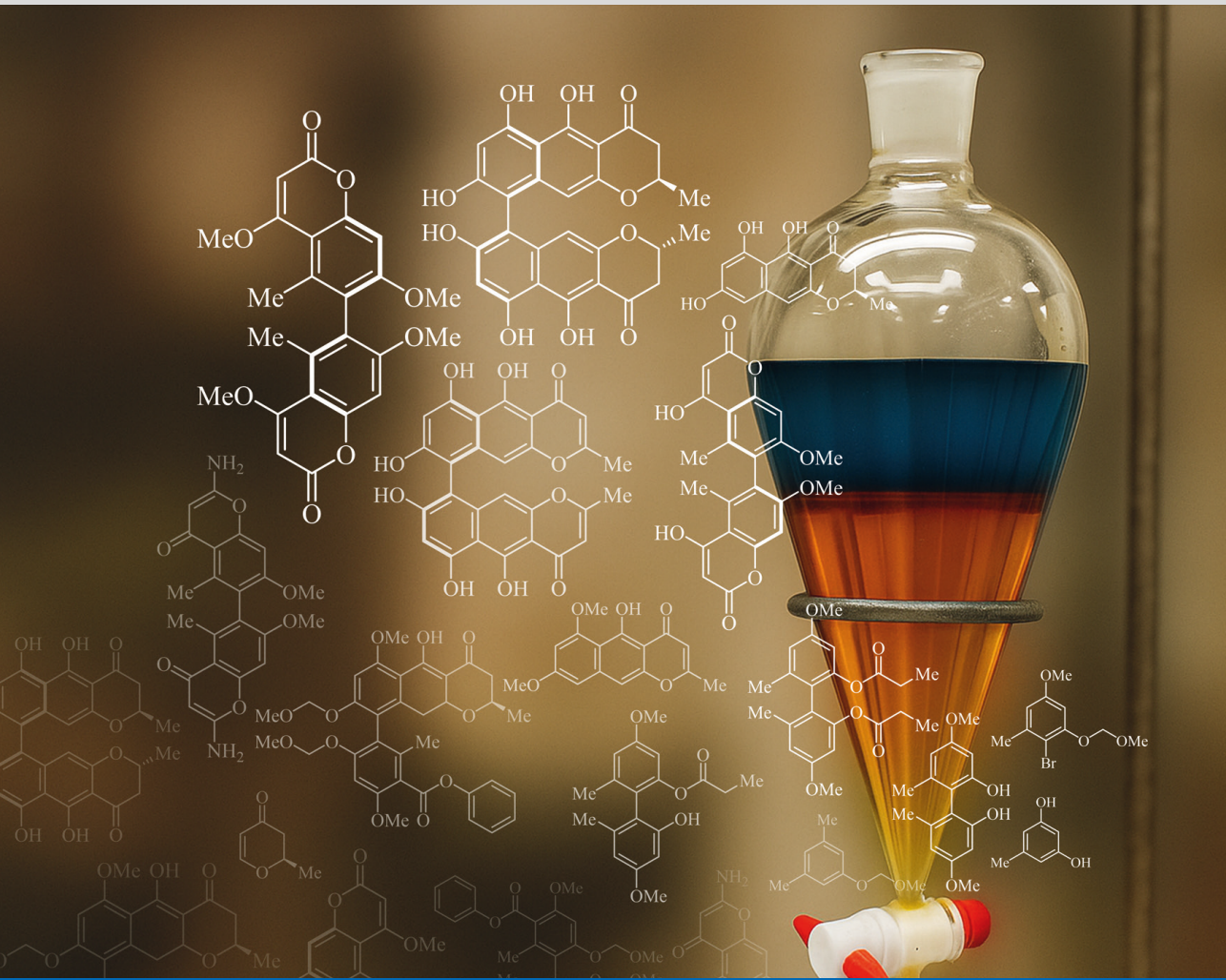

Bioorganische Chemie an der Heinrich-Heine-Universität im Forschungszentrum Jülich

Forschungszentrum Jülich GmbH
Institut für Bio- und Geowissenschaften
IBOC – Bioorganische Chemie

Lipase-catalyzed kinetic resolution: Synthesis and application of axially chiral biphenols

Ruth Christine Ganardi

Bioorganische Chemie an der Heinrich-Heine-Universität
im Forschungszentrum Jülich

Band 51

ISBN 978-3-95806-854-4

Bioorganische Chemie an der Heinrich-Heine-Universität im Forschungszentrum Jülich

Band 51

Herausgegeben von Jörg Pietruszka

Heinrich Heine
Universität
Düsseldorf

Lipase-catalyzed kinetic resolution: Synthesis and application of axially chiral biphenols

Inaugural-Dissertation

zur Erlangung des Doktorgrades
der Mathematisch-Naturwissenschaftlichen Fakultät
der Heinrich-Heine-Universität Düsseldorf

vorgelegt von

Ruth Christine Ganardi
aus Köln

Düsseldorf, September 2025

Bibliografische Information der Deutschen Nationalbibliothek.
Die Deutsche Nationalbibliothek verzeichnet diese Publikation in der
Deutschen Nationalbibliografie; detaillierte Bibliografische Daten
sind im Internet über http://dnb.d-nb.de abrufbar.

Gedruckt mit der Genehmigung der
Mathematisch-Naturwissenschaftlichen Fakultät
der Heinrich-Heine-Universität Düsseldorf

Referent:	Prof. Dr. Jörg Pietruszka
Korreferent:	Prof. Dr. Thomas J.J. Müller
Tag der mdl. Prüfung:	25.02.2025
Herausgeber:	Prof. Jörg Pietruszka
Umschlaggestaltung:	Grafische Medien, Forschungszentrum Jülich GmbH
Druck:	Grafische Medien, Forschungszentrum Jülich GmbH
Copyright:	Forschungszentrum Jülich 2025

Bioorganische Chemie an der Heinrich-Heine-Universität Düsseldorf
im Forschungszentrum Jülich, Band 51

D 61 (Diss. Düsseldorf, Univ., 2025)

ISBN 978-3-95806-854-4

Publications

Parts of this thesis have been published in scientific journals or presented at scientific conferences.

Published in Journals

R. C. Ganardi, J. Greb, B. Henßen, J. Pietruszka, *Adv. Synth. Catal.,* **2023***, 365,* 3512–3520; "Atroposelective Total Synthesis of (+)-Isokotanin A via Combined Metal and Enzyme Catalysis".

This publication contains the following work of my own: The experimental work has been done independently. This includes the lipase screening and EKR optimization towards the lipase-catalyzed enantioselective hydrolysis of biphenyl diesters. The scale up of the enzymatic reaction allowed isolation of the enantiomeric pure biphenol building block, which was used in the total synthesis of (*M*)-isokotanin A. Development of HPLC separation methods have been developed by *B. Henßen*. Writing of the manuscript has been done in cooperation with *J. Greb*.

Conference participation

Poster, 22nd Tetrahedron Symposium, in Lisbon, Portugal (28th June–01st July 2022); R. C. Ganardi, J. Greb, M. Klischan, J. Pietruszka, "Investigations on Atroposelective Synthesis of Biphenols"

Poster, 22nd ORCHEM, in Münster, Germany (05th–07th September 2022); R. C. Ganardi, J. Greb, M. Klischan, J. Pietruszka, "Investigations on Atroposelective Synthesis of Axial Chiral Biphenols"

Table of Contents

1 Abstract **1**

2 Kurzzusammenfassung **3**

3 Introduction **5**

4 Objectives **8**

5 State of knowledge **10**

5.1 Hydrolases in organic synthesis **10**

5.1.1 General 10

5.1.2 Enzyme kinetics 12

5.2 Axially chiral biaryls **18**

5.2.1 General 18

5.2.2 Atroposelective synthesis 20

5.3 *γ*-Naphthopyrone **34**

5.4 Isokotanin **39**

6 Results and Discussion **45**

6.1 Synthesis of axially chiral biphenol building block *rac*-1 **45**

Summary Chapter 6.1 49

6.2 Enzymatic kinetic resolution **50**

6.2.1 Synthesis of biphenyl diesters **181a–e** and monoesters **182a–e** 50

6.2.2 Enzyme screening of commercially available hydrolases 52

6.2.3 Assignment of absolute configuration 56

6.2.4 Studies of *Candida cylindracea* lipase 57

6.2.5 Optimization of the enzymatic kinetic resolution 60

6.2.6 Screening of whole cell extracts 63

6.2.7 Scaled up enzymatic kinetic resolution 64

6.2.8 Kinetics of the enzymatic kinetic resolution 66

Summary Chapter 6.2 68

6.3 Investigations on dynamic enzymatic kinetic resolution 69

6.3.1 Enzymatic esterification of biphenol *rac*-**1** and monoester *rac*-**182a** 70

6.3.2 Racemization of biphenol **1** 73

Summary Chapter 6.3 74

6.4 Substrate scope of axially chiral biphenols 75

6.4.1 Homocoupling of bromophenols 76

6.4.2 Aryl homocoupling *via* directed *ortho*-metalation 80

6.4.3 Derivatization of axially chiral biphenols 86

6.4.4 Synthesis of substrate scope of biphenyl mono- and dipropionates 89

Summary Chapter 6.4 92

6.5 Application of EKR on scope of axially chiral biphenols 93

Summary Chapter 6.5 97

6.6 Investigations on the total syntheses of *γ*-naphthopyrones 98

6.6.1 Synthesis of monomeric *ortho*-toluates **231** and **232** 99

6.6.2 Synthesis of rubrofusarin B (**123**) 100

6.6.3. Synthesis of hemiustilaginoidin F (**125**) 102

6.6.4 Investigations on the synthesis of ustilaginoidin F (**3**) 106

6.6.5. *Myers*' annulation *via* benzylic halogenation 110

Summary Chapter 6.6 116

6.7 Total synthesis of (*M*)-isokotanin A (*M*)-(4) 117

6.7.1 Racemic synthesis of isokotanin A (**4**) 117

6.7.2 Synthesis of atropoenantiopure (*M*)-isokotanin A (*M*)-(**4**) 125

Summary Chapter 6.7 128

6.8 Investigation on total synthesis of (*P*)-isokotanin C (*P*)-(5) 129

Summary Chapter 6.8 132

7 Summary and Outlook 133

8 Experimental **141**

8.1 General Information (Chemical Syntheses) **141**

8.2 General Information (Enzymes) **144**

8.2.1 Determination of specific activity of hydrolases 145

8.3 Synthesis Procedures and Analytics **147**

8.3.1 Synthesis of biphenol building block *rac*-**1** 151

8.3.2 Synthesis of biphenyl diester *rac*-**181a–e** and monoester *rac*-**182a–e** 162

8.3.3 Enzymatic kinetic resolution: Atroposelective hydrolysis 171

8.3.4 Scaled up enzymatic kinetic resolution 174

8.3.5 Investigations on dynamic enzymatic kinetic resolution 176

8.3.6 Synthesis of tetra-*ortho*-substituted biphenol scope 177

8.3.7 Approach towards total synthesis of ustilaginoidin A (**2**) and F (**3**) 229

8.3.8 Total synthesis towards isokotanin A (**4**) and isokotanin C (**5**) 244

9 References **257**

10 Acknowledgements **277**

11 Declaration **279**

12 List of Abbreviations **280**

13 List of synthesized molecules **282**

14 Appendix **290**

1 Abstract

In this work, the atroposelective synthesis of tetra-*ortho*-substituted biphenols was studied. The focus was on the construction and application of the important 2,2′-biphenol building block **1**, which represents a common motif of various aromatic polyketide dimers (Figure 1). Central aspects of this study were the enzymatic kinetic resolution for the isolation of enantiopure biphenol **1** and the application of the biphenol building block **1** in the total synthesis of dimeric polyketides.

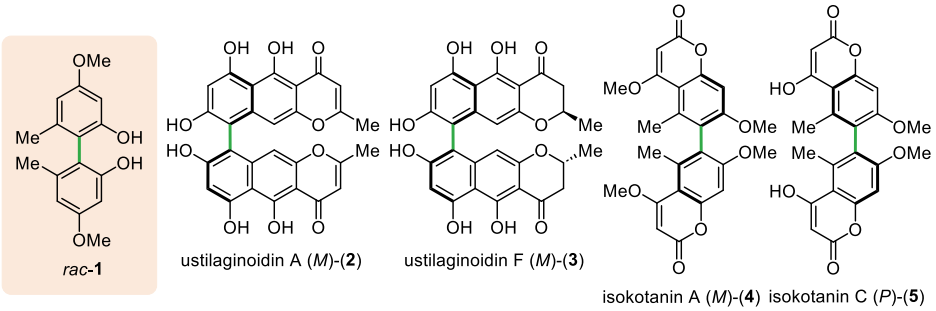

Figure 1 Structure of 2,2′-biphenol building block *rac*-**1** and target natural products: γ-binaphthopyrones **2**–**3** and bicoumarins **4**–**5**.

The challenging construction of the sterically hindered 2,2′-biphenol building block *rac*-**1** was performed and discussed, based on the reaction procedures of *Greb et al.*[1, 2] Therefore, racemic homocouplings *via Lipshutz* coupling and *Miyaura* borylation *Suzuki* coupling (MBSC) were compared, leading to the isolation of the axially chiral biphenol *rac*-**1** in overall 50% yield over eight steps starting from commercially available starting material.

The atroposelective transformation of the racemic biphenol substrate *rac*-**1** was investigated by an enzyme screening of hydrolases. A scalable enzymatic kinetic resolution method was established by applying commercially available *Candida rugosa* lipase (CRL) for the atroposelective hydrolysis of biphenyl dipropionate. Optimization of this reaction system revealed the major influence of the diester's fatty acid chain length and the choice of the solvent system on the enzyme's selectivity and activity.

In addition to the established resolution method, investigations were carried out to evaluate the applicability of the enzymatic kinetic resolution on a biphenol substrate scope. The aim was to study the influence of the substitution pattern on the enzyme's activity and selectivity. In order to address a broader substrate scope, the homocoupling *via* directed

ortho-metalation was investigated. This eliminated the need for regioselective bromination. A homocoupling *via* directed *ortho*-cupration (DOC) using an organoamidocuprate was used for the isolation of biphenyl products in yields up to 64%. Yet, this method proved to exhibit different regioselectivities depending on the substitution pattern. In summary, a dedicated library of eight axially chiral biphenols were obtained, which were used in the CRL-catalyzed resolution under the optimized conditions. The results of the enzymatic kinetic resolution showed that the choice of the *para*-substituents had a minor effect on the enzyme's activity (47–58%) and selectivity (79–>99% *ee*). In contrast, the *ortho*-substituents had a major effect on the enzyme's activity and selectivity and resulted in a drop of conversion and selectivity.

Finally, the isolated enantiopure biphenol **1** was applied in the total synthesis of dimeric polyketides. Here, the total syntheses towards γ-binaphthopyrones ustilaginoidin A (**2**) and F (**3**) were investigated (Figure 1). The key step in this approach is the annulation reaction with the electrophilic pyrone. The first total synthesis of the γ-naphthopyrone monomer of ustilaginoidin F (**3**) was achieved with a total yield of 49% in two steps. The optimized conditions for the synthesis of the γ-naphthopyrone monomer were transferred on the total synthesis of dimeric ustilaginoidin F (**3**). However, bidirectional *Myers*' annulation proved to be rather challenging and led only to mono-annulation.

At last, the axially chiral bicoumarins (*M*)-isokotanin A (**4**) and (*P*)-isokotanin C (**5**) were chosen as alternative targets (Figure 1). Upon utilization of the enantiopure biphenol **1** in the developed synthesis route, enantiopure (*M*)-isokotanin A (**4**) was successfully obtained in 11% overall yield over eight steps. Compared to known asymmetric routes, the combination of the metal-catalyzed homocoupling and the enzymatic resolution enables a scalable and more efficient method towards a common intermediate in the synthetic pathway with a reduction of hazardous chemicals.

2 Kurzzusammenfassung

In dieser Arbeit wurde die atropselektive Synthese von tetra-*ortho*-substituierten Biphenolen untersucht. Der Schwerpunkt lag auf dem Aufbau und der Anwendung des wichtigen 2,2′-Biphenol Bausteins **1**, der ein gemeinsames Motiv verschiedener aromatischer Polyketid-Dimere darstellt (Abbildung 1). Zentrale Aspekte dieser Arbeit war die enzymatische kinetische Racematspaltung zur Isolierung von enantiomerenreinem Biphenol **1** und die Anwendung des Biphenol-Bausteins **1** in der Totalsynthese von dimeren Polyketiden.

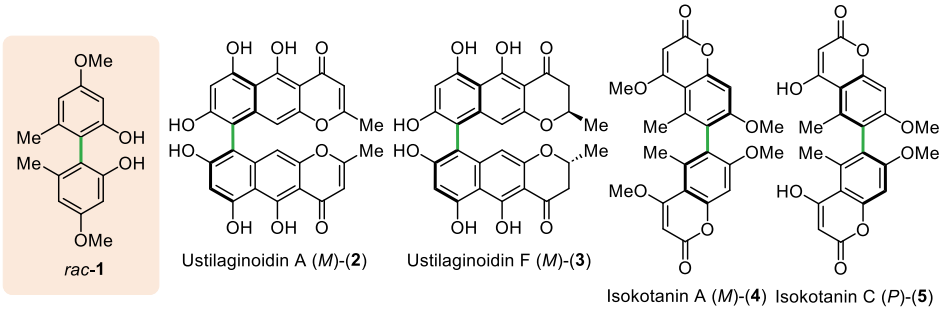

Abbildung 1 Struktur des 2,2′-Biphenol Bausteins *rac*-**1** und der Zielnaturstoffe: γ-Binaphthopyrone **2**–**3** und Bicoumarine **4**–**5**.

Der anspruchsvolle Aufbau des sterisch gehinderten 2,2′-Biphenol Bausteins *rac*-**1** wurde basierend auf den Reaktionsverfahren von *Greb et al*. durchgeführt und diskutiert.[1, 2] Dazu wurden racemische Homokupplungen, *Lipshutz*-Kupplung und *Miyaura* Borylierung *Suzuki* Kupplung (MBSC), verglichen. Diese führten zur Herstellung des axial chiralen Biphenols *rac*-**1** in insgesamt 50 % Ausbeute über acht Schritte ausgehend von kommerziell erhältlichem Ausgangsmaterial.

Die atropselektive Umwandlung des racemischen Biphenols *rac*-**1** wurde durch ein Enzymscreening von Hydrolasen untersucht. Eine skalierbare enzymatische kinetische Racematspaltung wurde etabliert, indem die kommerziell erhältliche *Candida rugosa* Lipase (CRL) für die atropselektive Hydrolyse von Biphenyldipropionate eingesetzt wurde. Die Optimierung dieses Reaktionssystems zeigte den großen Einfluss der Alkylkettenlänge des Diesters und der Wahl des Lösungsmittelsystems auf die Selektivität und Aktivität des Enzyms.

Weiterhin wurde die Anwendbarkeit der enzymatischen kinetischen Racematspaltung an verschiedenen Biphenol-Substraten evaluiert. Ziel war es, den Einfluss des

Substitutionsmusters auf die Aktivität und Selektivität des Enzyms zu analysieren. Um ein breiteres Substratspektrum abzudecken, wurde die Homokupplung über eine *ortho*-Metallierung untersucht. Dadurch war die regioselektive Bromierung der Phenol Monomere nicht mehr notwendig. Eine Homokupplung über eine o*rtho*-Cuprierung unter Verwendung eines Organoamidocuprats wurde für die Isolierung der Biphenyle in Ausbeuten von bis zu 64 % verwendet. Diese Methode wies jedoch je nach Substitutionsmuster unterschiedliche Regioselektivitäten auf. Zusammenfassend lässt sich sagen, dass eine Bibliothek von acht axial chiralen Biphenolen erhalten wurde, die in der CRL-katalysierten Racematspaltung unter den optimierten Bedingungen verwendet wurden. Die Ergebnisse der enzymatischen kinetischen Racematspaltung zeigten, dass die Wahl der *para*-Substituenten einen geringen Einfluss auf die Enzymaktivität (47–58 %) und die Selektivität (79–>99 % *ee*) hatte. Im Gegensatz dazu hatten die *ortho*-Substituenten eine größere Auswirkung auf die Aktivität und Selektivität des Enzyms und führten zu einem Abfall des Umsatzes und der Selektivität.

Schließlich wurde das isolierte enantiomerenreine Biphenol **1** in der Totalsynthese von dimeren Polyketiden eingesetzt. Hier wurden die Totalsynthesen zu den γ-Binaphthopyronen (*M*)-Ustilaginoidin A (**2**) und F (**3**) untersucht (Abbildung 1). Der Schlüsselschritt in diesem Ansatz ist die Anellierung mit dem elektrophilen Pyron. Die erste Totalsynthese des γ-Naphthopyron-Monomers von Ustilaginoidin F (**3**) wurde mit einer Gesamtausbeute von 49 % in zwei Schritten erreicht. Die optimierten Bedingungen für die Synthese des γ-Naphthopyron-Monomers wurden auf die Totalsynthese von dimerem Ustilaginoidin F (**3**) übertragen. Die doppelte *Myers*-Anellierung erwies sich jedoch als schwierig und führte nur zu einer Monoanellierung.

Zuletzt wurden die axial chiralen Bicoumarine (*M*)-Isokotanin A (**4**) und (*P*)-Isokotanin C (**5**) als alternative Zielnaturstoffe ausgewählt (Abbildung 1). Unter Verwendung des enantiomerenreinen Biphenols **1** wurde erfolgreich enantiomerenreines (*M*)-Isokotanin A (**4**) in einer Gesamtausbeute von 11 % über acht Schritte erhalten. Im Vergleich zu bekannten asymmetrischen Synthesewegen ermöglicht die Kombination aus metallkatalysierter Homokupplung und enzymatischer Racematspaltung eine skalierbare und effizientere Methode zur Herstellung eines gemeinsames Intermediats mit einer Reduzierung gefährlicher Chemikalien.

3 Introduction

Since ancient times humans have used natural products, such as those isolated from plants, animals, or microorganisms, to treat all kinds of ailments. The World Health Organization (WHO) reported that around 80% of the global population relies on natural bioactive compounds as the primary care for treating various disorders.[3] Therefore, since the 19th century natural compounds have always been an inspiration for lead structures for medicinal chemistry.[4, 5] The application of either the natural products itself, or modified derivatives in drug discovery has gained increased attention for the development of structural motifs with promising physicochemical and pharmacological properties.[6, 7] One example is the natural product artemisinin (**6**) from *Artemisia annua*, which is used as an antimalarial pharmaceutical (Figure 2).[8] The discovery of the natural product penicillin (**7**) by *Alexander Fleming* in 1928 led to a big breakthrough in medicine. The *β*-lactam antibiotic, produced by mold fungus *Penicillium notatum*, was utilized as a treatment against gram-positive bacteria and thereby revealed to be a lifesaving drug in the second world war.[9] Since then many other natural antibiotics have been discovered, like tetracycline (**8**) (Figure 2).[10] Another example is shown by the structure of HMG-CoA-reductase inhibitor atorvastatin (**9**), which is known as Lipitor® from *Pfizer*. It was developed on the basis of the lead structure of the natural product lovastatin (**10**) from *Aspergillus terreus* (Figure 2).[8, 11, 12] Therefore, investigations towards the isolation and synthesis of natural products are highly attractive. One important example is the antitumor agent paclitaxel (**11**), known as Taxol® (Figure 2). Paclitaxel (**11**) is applied as a chemotherapeutic agent against cancer, for instance ovarian cancer or metastatic breast cancer. In the year 1971, Taxol® (**11**) was first isolated by *Wall* and *Wani* from the bark of the Pacific yew tree, *Taxus brevifolia*.[13, 14] Ongoing investigations for an alternative production of paclitaxel (**11**) have been performed, like semisynthesis, chemical synthesis or cultivation in plant cell culture. Known total syntheses were rather complicated and involved a high number of steps, resulting in very low yields.[15] Nowadays, the company *Phyton Biotech* in Canada became the biggest supplier for paclitaxel (**11**), whereby a plant cell fermentation technology is utilized for a large scale production.[16, 17] Since paclitaxel (**11**) became a successful drug, further taxane analoga were developed and approved, for instance the anti-cancer drug docetaxel (**12**), known as Taxotere® (Figure 2). Docetaxel (**12**) could be produced *via* semisynthesis of isolated taxoid of the European yew tree, *Taxus baccata*.[18] New

approaches towards the total syntheses of Taxol® (**11**) continued to be developed. However, none of them were able to substitute the fermentation process.

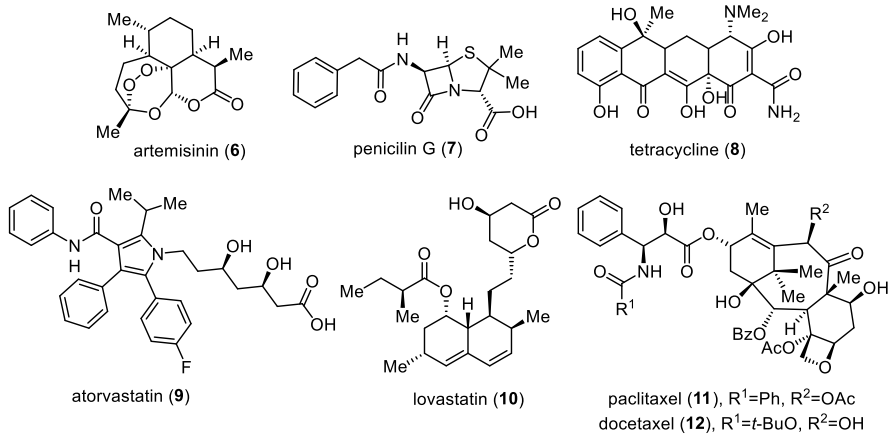

Figure 2 Examples of natural products or lead structures applied as pharmaceuticals.[8, 11, 19-21]

In most cases, isolation of natural compounds from their natural habitat is possible. However, these processes are often neither efficient, nor scalable for industrial application. Therefore, chemical synthetic methods are required to be used for the generation of natural compounds and their derivatives. Structural modification of natural products enables access towards compounds with possibly higher pharmacological potential. Moreover, a greater understanding of the structure-activity relationship can thus be obtained.[6] The aim within the chemical syntheses is to obtain the desired compound in as few steps and in as high of a total yield and purity as possible. Furthermore, essential is the consideration of enantioselectivity of the reactions. There are examples of pharmaceuticals produced as a racemate, for instance the anti-inflammatory drug ibuprofen. The nonactive (*R*)-enantiomer undergoes an *in vivo* racemization of the stereogenic center resulting in an enrichment of the therapeutically active (*S*)-ibuprofen. However, the rate of isomerization is relatively low, resulting in a higher therapeutical effect when consuming the enantiopure (*S*)-ibuprofen.[22, 23] However, it is known that different absolute configurations of API's can exhibit different pharmacological activities.[24] The most prominent example is the commercialization of the hypnotic and sedative drug thalidomide, known under its marketed name contergan. After the company Grünenthal sold the drug as a racemic mixture, evaluations revealed that only the (*R*)-enantiomer functions as the active sedative drug, while the (*S*)-enantiomer exhibits effects in teratogenicity and leads to fetal malformations.[25-27] Moreover, different therapeutic effects were studied for instance in propranolol.

While the (*S*)-enantiomer is 100 times more active in its potential as a beta-blocker, the (*R*)-isomer can be used for the treatment of hyperthyroidism by inhibiting the conversion of thyroxin to triiodothyronin.[28, 29] In 1992, the Food and Drug Administration in the United States published a guideline for the production of enantiopure pharmaceuticals. Since then, the investigation on asymmetric synthesis of natural products and possible lead structures has become of great importance.[30, 31] The complex structural scaffolds of natural products therefore require the development of modern chemical methods. The application of enzymes as highly regio- and stereoselective biocatalysts is here a promising tool.[32] The high acceptability of a broad substrate scope can reduce the overall number of reaction steps and increase the total yield. The combination of biocatalysis and classic organochemical methods provides great opportunities for the highly selective synthesis of the target molecule.[33]

The fight against yet untreatable or newly discovered diseases and recurring resistance places high demands on the development of active drugs. Nature remains here the greatest inspiration and source for new classes of active substances. The continuous development of modern synthetic methods is therefore an important contribution to the progress in medicine and healthcare.

4 Objectives

This work focuses on the investigations towards the synthesis of axially chiral biphenols. In contrast to already existing methods, a scalable and more efficient approach towards the rotationally hindered stereogenic axis is to be developed. For this study the axially chiral biphenol *rac*-**1** is chosen as the model substrate, which is an important building block for the synthesis of various dimeric polyketides. Based on the work of *Julian Greb*,[1, 2] synthesis methods of *rac*-**1** are to be performed and compared regarding their efficiency and safety. In addition to the already developed coupling methods, further strategies shall be investigated towards the synthesis of a dedicated library of different substituted biphenols *rac*-**15** (Scheme 1).

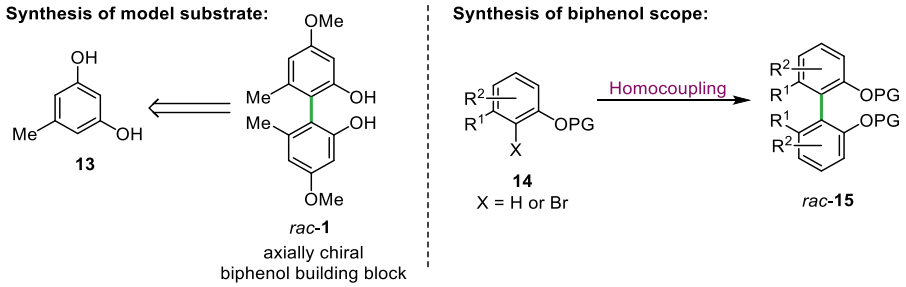

Scheme 1 Synthesis of axially chiral model substrate *rac*-**1** (left) and biphenol scope *rac*-**15** (right).

In order to obtain enantiopure biphenol from *rac*-**1**, a hydrolase is to be utilized for the enzymatic kinetic resolution (EKR), which is to be determined in an enzyme screening (Scheme 2).[34, 35] The reaction conditions of the enzymatic hydrolysis of *rac*-**16** are to be optimized, regarding the choice of solvent, acyl moiety, pH-media, or the use of additives.

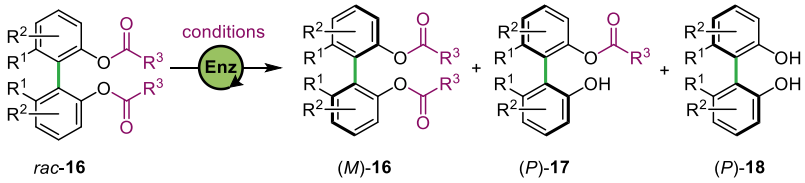

Scheme 2 Enzymatic kinetic resolution of biphenyl diesters *rac*-**16**.

Afterwards, the optimized conditions are to be applied in a preparative gram scale. Development and optimization of chiral HPLC methods should be performed for the analysis of the optical purities and kinetics of the sequential enzymatic process towards monoester **17** and biphenol **18**. After establishing a robust and viable process, the optimized EKR should

be applied to the synthesized scope of racemic biphenols with various substitution patterns. The influence of the electronic properties and the steric hindrance of the substituents on the EKR is to be analyzed.

The isolated enantiopure biphenol building block (*M*)- and (*P*)-**1** should be applied afterwards in the total synthesis of dimeric polyketides. Here, the dimeric *γ*-binaphthopyrones (*M*)-ustilaginoidin A (*M*)-(**2**) and (*M*)-ustilaginoidin F (*M*)-(**3**) and bicoumarins (*M*)-isokotanin A (*M*)-(**4**) and (*P*)-isokotanin C (*P*)-(**5**) were chosen as possible target products (Scheme 3).[36-39]

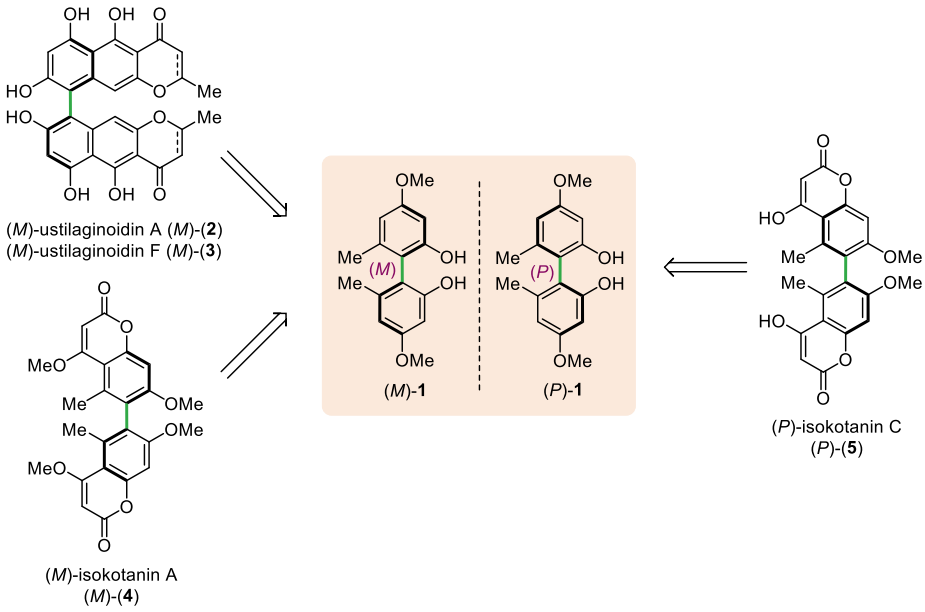

Scheme 3 Target natural products for the total synthesis starting from enantiopure biphenol (*M*)-/(*P*)-**1**.

5 State of knowledge

5.1 Hydrolases in organic synthesis

5.1.1 General

Hydrolases (E.C.3.x.x.x.) are enzymes, which catalyze hydrolytic bond cleavage and the corresponding reverse synthetic reaction.[40] Important subclasses are glycoside- (E.C.3.2.x.x.), peptide- (E.C.3.4.x.x.), or ester hydrolases (E.C.3.1.x.x.).[41, 42] One important class of the ester hydrolases is the triacylglycerol hydrolase (EC.3.1.1.3), so called lipase, which can be found in various microorganisms, plants and animals. Their biological task is to hydrolyze triglycerides in the digestive tract.[40, 43, 44] However, lipases are also highly attractive for industrial application due to their broad acceptance of a wide range of unnatural substrates.[45] The high commercial availability of hydrolases with high catalytic efficiency facilitates the acceleration of environmentally friendly organic processes under mild reaction conditions.[40, 46] Catalysis by hydrolases can result in highly enantioselective reactions of racemic substrates.[40] In the presence of more than one functional group, the reactions can proceed with high regio- and chemoselectivity.[43, 44] Another attractive property of hydrolases is their high stability. Hydrolases function at the lipid-water interface and are therefore suitable for the application in different mixtures of water-miscible solvents, as well as in neat organic solvents.[40] In comparison to many other enzymes such as oxidoreductases, hydrolases do not require a cofactor for regeneration.[42] One example of an industrial application of lipases is the enantioselective hydrolysis of racemic acetamide *rac*-**19** developed by BASF in the 1990s (Scheme 4A).

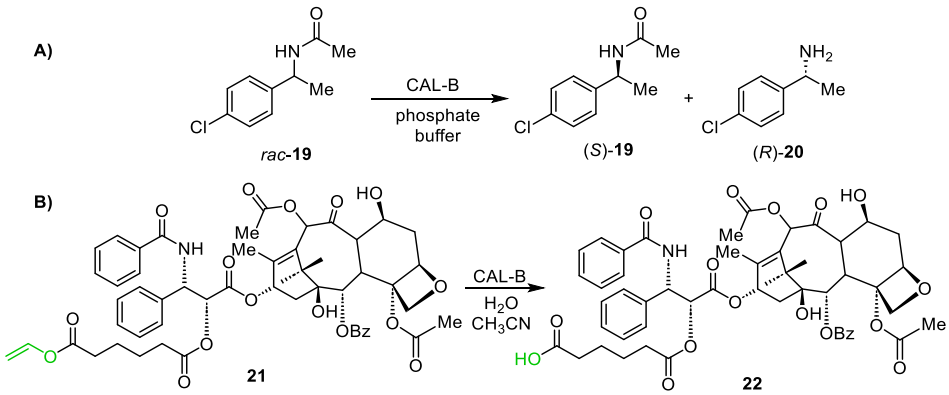

Scheme 4 Industrial application of lipases: A) Enantioselective hydrolysis of racemic acetamide *rac*-**19** by BASF; B) Enzymatic synthesis of paclitaxel derivative **22**.[45]

Treatment with *Candida antarctica* lipase B (CAL-B) generated the free amine (*R*)-**20** in 48% conversion and in excellent enantiomeric excess (>99% *ee*).[47] CAL-B has also found application using much bulkier substrate for the synthesis of a library of paclitaxel derivatives **22** (Scheme 4B).[45] The mechanism of hydrolases was first discovered by *Carter et al*.[48] Scheme 5 shows the so-called catalytic triad exemplarily for the lipase from *Rhizopus oryzae*.[43, 44] Here, three catalytically active amino acids serine, histidine, aspartic acid or glutamic acid interact with the substrate.[42] In the first step the deprotonation of serine leads to a proton transfer to the histidine (A). This facilitates the nucleophilic attack by the oxygen atom of the serine side chain at the carboxylate of the substrate, resulting in a tetrahedral intermediate (B). Liberating the alcohol generates the acyl-enzyme complex (C), which acts as the potential acylation reagent. The attack of the nucleophile towards the acyl-enzyme complex results again in a formation of a tetrahedral intermediate (D), which subsequently releases the product and regenerates the enzyme active site (A).

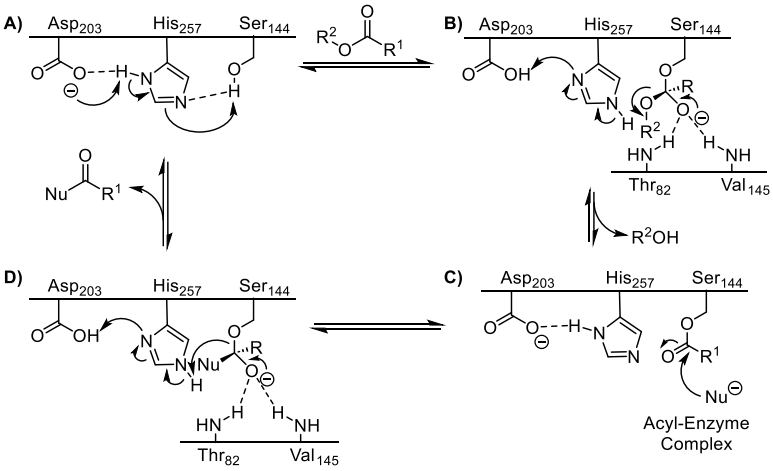

Scheme 5 Reaction mechanism of catalytic triad exemplarily for lipase from *Rhizopus oryzae*.[43, 44]

Depending on the chosen nucleophile a wide range of different products can be generated (Scheme 6).[42-44] In the presence of an aqueous media, water acts as a nucleophile, which results in the formation of a carboxylic acid. However, at low water concentrations the attack of other nucleophiles comprises a great variety of useful biotransformations. Treatment with alcohols or amines results in the so-called enzymatic acyl transfer or aminolysis, while for example the addition of hydrogen peroxide or hydroxylamine generates peracids or hydroxamic acids.[42]

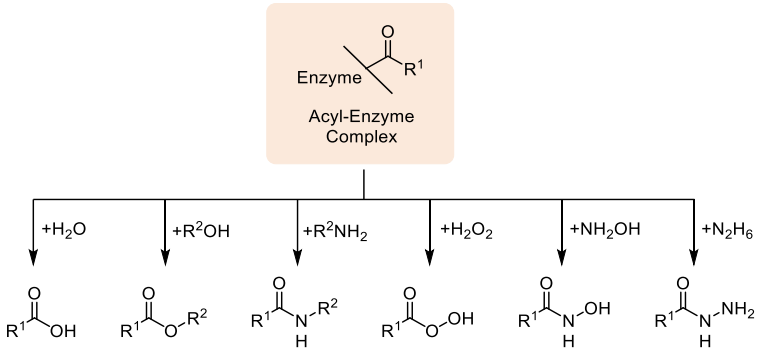

Scheme 6 Possible biotransformations catalyzed by hydrolases.

5.1.2 Enzyme kinetics

Lipases can be used as catalysts for the enantioselective synthesis of chiral products from a racemic mixture. There are three processes for the transformation to chiral products: A) Kinetic Resolution (KR), B) Dynamic Kinetic Resolution (DKR) and C) Desymmetrization (Scheme 7).[49, 50] While in a KR only 50% theoretical yield of the enantiopure product can be reached, in a DKR and a desymmetrization theoretically 100% yield of one product can be obtained.

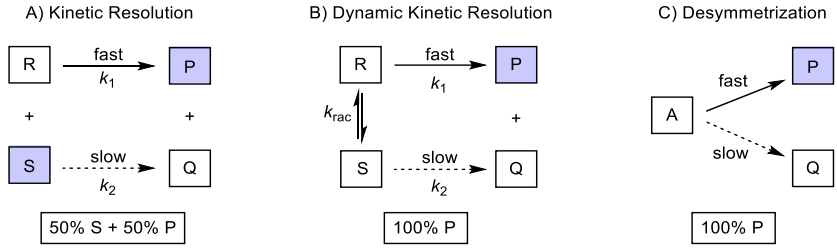

Scheme 7 Strategies for the preparation of enantiopure compounds through enzymatic processes.

The KR is based on the different rate constants of the irreversible transformation of both enantiomers in the racemic mixture ($k_1 >> k_2$) (Scheme 7A). This results in a conversion of selectively one enantiomer (P) at a faster rate, while the other corresponding enantiomer (S) is transformed relatively more slowly. This would lead to a highly enantioselective reaction towards one optically pure product (P) in 50% yield and the non-converted enantiomer (S) in 50% yield.[49] One of the first EKR processes in the food industry was the

synthesis of L-methionin (*S*)-**24** by *Degussa* (Scheme 8).[51, 52] They applied an acylase for the resolution of *N*-acetyl-methionin *rac*-**23**, which was developed by *Seiyaku* in 1969.[53]

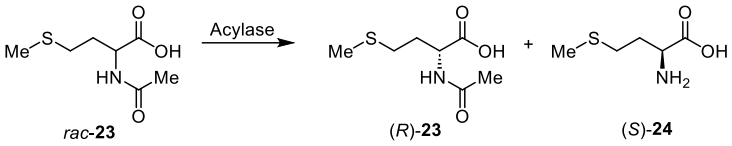

Scheme 8 Acylase-catalyzed resolution of *N*-acetyl-methionine *rac*-**23**.[51, 52]

To reach 100% yield of the desired enantiopure product, a dynamization of the KR is favored (Scheme 7B). Therefore, an *in-situ* racemization of the substrate is required. This racemization must be at least as fast as the enzymatic resolution ($k_{rac} \geq k_1$). Thus, when the more favored enantiomer (R) is transformed by the enzyme, the racemization equilibrium results in continuous supply of the required enantiomer (R) until the enzymatic reaction reaches full conversion towards the enantiopure product (P). Once the product is formed, it must not racemize under the given conditions.[40] The first enzymatic DKR was developed by *Sih et al.* (Scheme 9).[54] Here, they succeeded to synthesize ketorolac (*S*)-**26** by the hydrolysis of racemic ketorolac-ethylester *rac*-**25** catalyzed by a protease of *Streptomyces griseus*. The racemization was performed under basic conditions.

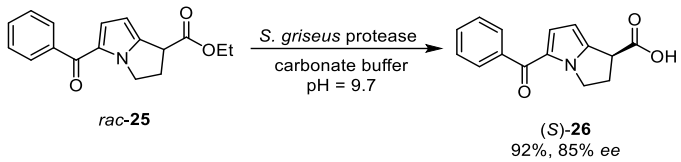

Scheme 9 Enzymatic dynamic kinetic resolution of ketorolac ester *rac*-**25**.[54]

During a desymmetrization a prochiral or *meso* substrate (A) is transformed into a single enantiomer (P) with a possible theoretical yield of 100% (Scheme 7C). Both sides of the substrates can be differentiated by the enzyme and are converted with different rate constants.[55] For instance, *Williams et al.* applied an enzymatic desymmetrization using porcine pancreas lipase (PPL) for the synthesis of enantiomerically enriched *Evans* auxiliaries (Scheme 10).[56] The acylation of *N*-Boc-protected serinol **27** using vinyl acetate resulted in the formation of enantiopure product (*R*)-**28**, which was used in further steps in the enantioselective synthesis of different oxazolidine-2-one derivatives (*S*)-**29**.

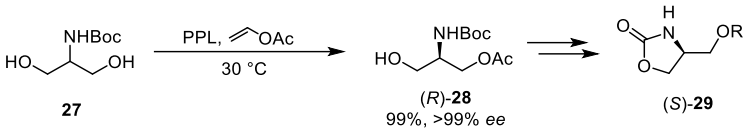

Scheme 10 Enzymatic desymmetrization towards the enantioselective synthesis of *Evans* auxiliaries.[56]

In order to quantify the KR, mathematical parameters have been established. In 1982 *Sih et al*. have developed the mathematical basis to describe kinetics of a resolution.[57] For the description of the optical purity of a product, an enantiomeric excess (*ee*) is defined (Equation 1). Here, n_P and n_Q represent the molar concentration of each enantiomeric product.

$$\%\, \boldsymbol{ee(P)} = \frac{\boldsymbol{n_P - n_Q}}{\boldsymbol{n_P + n_Q}} \cdot \mathbf{100} \qquad \textbf{Equation 1}$$

The enantioselectivity (E-value) is introduced to quantify the enantioselectivity of the reaction, which measures the ability of the enzyme to differentiate between the enantiomers of the substrate (Equation 2 and Equation 3).[57, 58] The enantioselectivity of the resolution is only controlled by the ratio of the rate constants (k_1/k_2) and remains constant regardless of the extent of conversion. The selectivity is inherently dependent on the reaction conditions and can thus be influenced by the choice of substrate or enzyme, variation in cosolvents, pH or temperature. Based on Michaelis-Menten kinetics the E-value corresponds to the k_{cat} and the Michaelis constant K_M values of both enantiomers (R) and (S) (Equation 2). The Michaelis equation describes the reaction rate v_0 as a function of the substrate concentration [S] (Equation 4). K_M is the substrate concentration at a reaction rate that is half of maximum rate v_{max}. k_{cat} represents the turnover number of catalytic reactions per active enzymatic center and time unit.[59] Without determining the rate constants, the E-value can be calculated by the enantiomeric excesses of substrate (ee_S) or product (ee_P) and the respective conversion (c) of the starting material.[42, 60]

$$\boldsymbol{E} = \frac{\boldsymbol{k_1}}{\boldsymbol{k_2}} = \frac{\left[\frac{\boldsymbol{k_{cat}}}{\boldsymbol{K_M}}\right]_2}{\left[\frac{\boldsymbol{k_{cat}}}{\boldsymbol{K_M}}\right]_1} = \frac{\ln\left[(\mathbf{1}-\boldsymbol{c})\cdot(\mathbf{1}-\boldsymbol{ee_S})\right]}{\ln\left[(\mathbf{1}-\boldsymbol{c})\cdot(\mathbf{1}+\boldsymbol{ee_S})\right]} \qquad \textbf{Equation 2}$$

$$\boldsymbol{E} = \frac{\ln\left[\mathbf{1}-\boldsymbol{c}\cdot(\mathbf{1}+\boldsymbol{ee_P})\right]}{\ln\left[\mathbf{1}-\boldsymbol{c}\cdot(\mathbf{1}-\boldsymbol{ee_P})\right]} \qquad \textbf{Equation 3}$$

$$\boldsymbol{v_0} = \boldsymbol{v_{max}}\frac{[\boldsymbol{S}]}{[\boldsymbol{S}]+\boldsymbol{K_M}} = \frac{\boldsymbol{k_{cat}}}{\boldsymbol{k_M}}[\boldsymbol{E}][\boldsymbol{S}] \qquad \textbf{Equation 4}$$

The higher the E-value, the greater is the difference between both rate constants of the enzymatic reaction. If the enzymatic reaction exhibits low selectivities, a low E-value is

determined (Figure 3A). At a conversion of 50% product and substrate can be obtained in low optical purity. Higher conversion of >80% is needed for an isolation of enantiopure substrate (>90% *ee*) with low yield. In contrast, reactions with higher E-values (according to *Bornscheuer et al.* E>20) are desired and useful for preparative synthesis of enantiopure products (Figure 3B).[40]

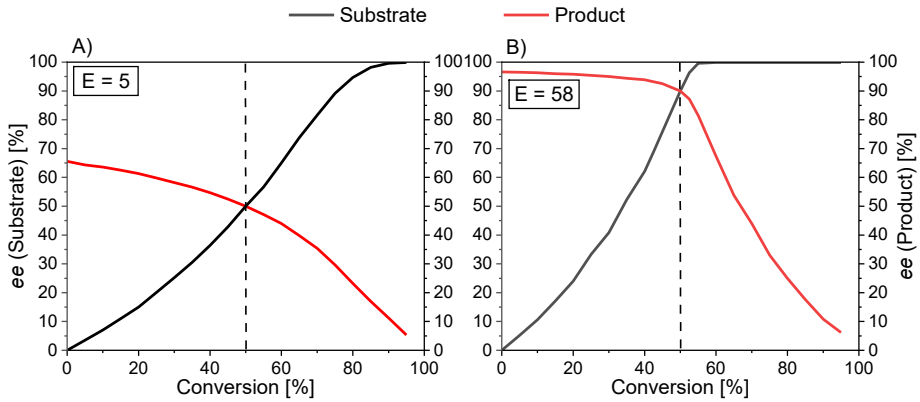

Figure 3 Dependence of *ee* on conversion for reaction with low and high enantioselectivities.

As the E-value is a logarithmic function, higher E-values above 100 are usually not reported, as the determination of the correct E-value becomes less accurate. This mathematical parameter is a useful method to compare different biocatalytic transformations, especially for screening studies. Therefore, certain assumptions were made to apply this equation. This equation describes an irreversible reaction from one single substrate towards one single product, where no product inhibition takes place.[40] Under these conditions the enantioselectivity should remain constant, regardless of the conversion rate. If a mixture of enzymes, for example different isoenzymes, is used as the catalyst, the calculated E-value represents a weighted average of the mixture. However, if the enzymes in the mixture exhibit different affinities towards the substrate, the E-value could vary over the course of the reaction and between batches of the enzyme. As the substrate depletes, different isoenzymes control the activity at different substrate concentrations. Furthermore, if the enzymes in the mixture differ in their stability, the E-value could also vary here between shorter or longer reaction times. Therefore, the determination of the enantioselectivity of a specific reaction using purified enzyme is recommended.[40] When a substrate with two chemically identical reactive groups is applied in an EKR, a sequential KR takes place, where the substrate enters the catalytical center twice (Figure 4). In the first step the KR of the starting material (R and S) towards the intermediates (N and O) is controlled by the rate

constant k_1 and k_2. In the second step the intermediates (N and O) are converted *via* the second resolution step towards the product (P and Q). The selectivity of the second consecutive resolution step is governed by k_3 and k_4. If both reaction steps exhibit the same enantiopreference (k_1>>k_2 and k_3>>k_4), the enantiomeric purity can be enhanced by the sequential resolution, resulting in the formation of ideally 50% yield of enantiopure substrate (S) and product (P).[42]

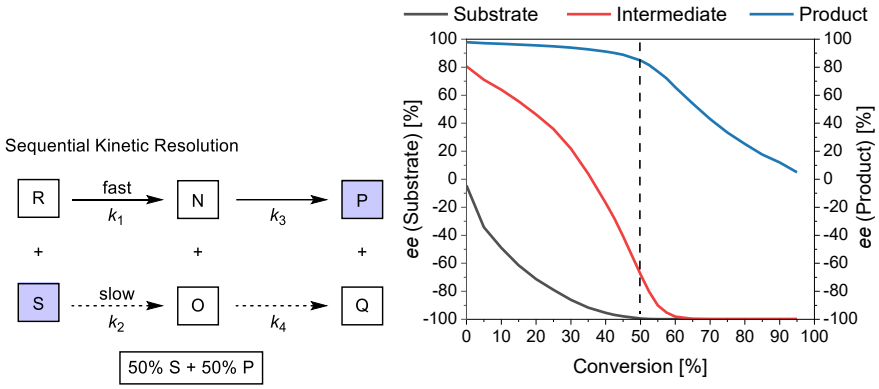

Figure 4 Dependence of optical purity on conversion for a sequential enzymatic kinetic resolution.

The overall kinetics of a sequential KR can become very complex, as the products from the first resolution step become the substrate for the second step. To describe and compare a sequential KR, two E-values have to be determined for each step (E_1 and E_2).[42] The single enantioselectivities (E_1 and E_2) can be determined either experimentally or *via* computational simulations. *Kazlauskas* described the determination of the E-values of his sequential resolution of binaphthyl dipentanoate *rac*-**30** using cholesterol esterase as the biocatalyst (Scheme 11).[35] Here, he treated each hydrolysis step separately. In the first step, E_1 was calculated by the conversion of diester *rac*-**30** and the enantiomeric excess of the recovered diester **30** (ee_S) (Equation 2). For *Kazlauskas*' enzymatic hydrolysis of binaphthyl dipentanoate *rac*-**30** a high enantioselectivity was determined for the first step (E_1>400).

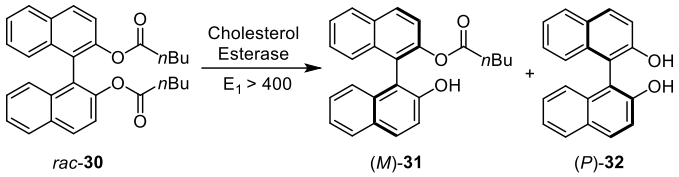

Scheme 11 First step of sequential EKR of binaphthyl dipentanoate *rac*-**30** by *Kazlauskas*.[35]

For the second E-value (E_2) the KR starting from the racemic intermediate *rac*-**31** was performed (Scheme 12). E_2 could afterwards be determined *via* Equation 2 using the enantiomeric excess of the recovered monopentanoate **31** (ee_S) or *via* Equation 3 based on the enantiomeric excess of the binaphthol **32** as the product (ee_P). In the case of *Kazlauskas'* second hydrolysis step, the conversion monopentanoate **31** towards binaphthol **32** was less selective (E=4.9).

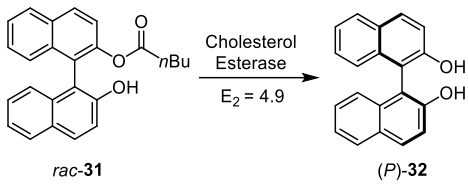

Scheme 12 Second step of sequential EKR of binaphthyl dipentanoate *rac*-**30** by *Kazlauskas*.[35]

Kroutil and his group have developed a program to simulate and analyze sequential KRs.[61, 62] The resolution can be analyzed based on experimental data. The four rate constants ($k_{1\text{-}4}$) can be calculated by concentrations of both enantiomers of substrate and intermediate or product measured at a specific time. Both E-values can be determined with the obtained rate constants *via* Equation 2. With this program, sequential KRs can also be simulated by given assumed rate constants. At every point of conversion, it is possible to determine the conversion and optical purity of each substrate, intermediate and product. Thereby the point of conversion can be defined, where each species can be obtained with a maximum yield or enantiomeric excess.

The overall E-value E_{total} can be calculated from both single enantioselectivities (E_1 and E_2) (Equation 5). E_{total} describes the enantioselectivity of the sequential KR as a single step resolution.

$$\boldsymbol{E_{total} = \frac{E_1 \cdot E_2}{2}} \qquad \textbf{Equation 5}$$

5.2 Axially chiral biaryls

5.2.1 General

Axial chirality was initially described by *Christie* and *Kenner* in 1922, and the term "atropisomerism" was first established by *Kuhn* in 1933.[63] The origin of the word represents the essential characteristic of an axially chiral molecule: Greek, *a* = not and *tropos* = turn.[64, 65] Axially chiral biaryls contain a rotational stability in their aryl-aryl single bond and different substituents on both sides of the chiral axis ($R^1 \neq R^2$, $R^3 \neq R^4$) (Figure 5). The configurational stability is determined by the height of the rotational barrier between ground and transition state and the required thermal energy to overcome this barrier.[66] The height of the rotational barrier is influenced by the choice of substituents in the proximity to the axis (Figure 5). It increases with the steric demand of the substituents in *ortho*-position to the axis. Biaryls with mono-*ortho*-substitution **33** do not exhibit rotational stability along their axis and undergo isomerization at room temperature. Rotational stability could only be observed starting with di-*ortho*-substituted biaryls **34** with bulkier substituents, like trifluoromethyl or naphthyl. For di- and tri-*ortho*-substituted biaryls **34** and **35** with smaller substituents, racemization can occur at room temperature on the timescale of hours. In contrast, atropisomerism can always be observed for tetra-*ortho*-substituted biaryls **36** regardless of the size of substituent. Even at higher temperatures no isomerization takes place.[64, 65]

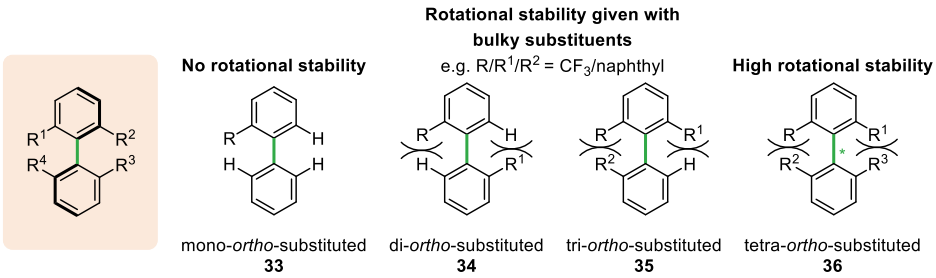

Figure 5 Representation of configurational stability of mono- to tetra-*ortho*-substituted biaryls.[64, 65]

Biaryls with a rotationally hindered and stereogenic axis are an essential part for a great number of natural products (Figure 6). A wide range of axially chiral metabolites has been isolated, which show remarkable bioactivities.[64, 65, 67, 68] Dimeric compounds revealed to be efficient drug candidates, as they contain two available binding sites on a single receptor. This would rise their selectivity and potency.[69, 70] Furthermore, atropisomerism is often a

significant factor in the modification of the pharmacological properties.[71] Although many axially chiral natural products were isolated as a single atrop(diastereo)isomer, there are also natural products, which were only obtained as racemic mixtures of diastereomers.[66] Michellamines for instance only occur as mixtures of atropodiastereomers. The atropodiastereomer michellamine B (*P,M*)-(**37**) exhibits significant activity against human immunodeficiency virus (HIV) type 1 and 2.[72, 73] Various other "mixed" unsymmetric biaryls containing two different coupled aromatic monomers occur in nature. Examples are the most prominent axially chiral antibiotics vancomycin (**38**) or the antimalarial and antitumoral anthraquinone knipholone (*P*)-(**39**).[64, 65, 74-76] Moreover, symmetric axially chiral natural products are for instance the nerve growth stimulating biphenyl mastigophorene A (*P*)-(**40**) or (*P*)-gossypol (*P*)-(**41**), a binaphthalene which exhibits antitumor and antimalarial activities. While the antitumor properties were first reported in racemic mixture of gossypol (**41**), the antiproliferative activity in cancer cell lines of the (*M*)-enantiomer revealed to be 10-fold greater than of (*P*)-gossypol (*P*)-(**41**).[77-79]

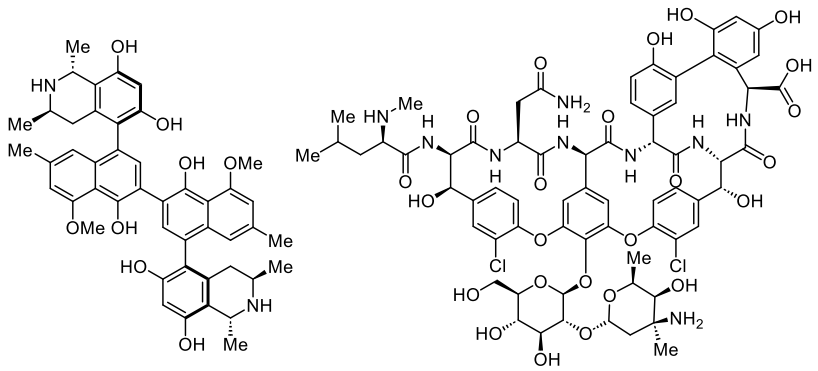

Figure 6 Axially chiral bioactive natural products.

Furthermore, biaryls are not only found in natural products but are important scaffolds for chiral auxiliaries and catalysts in asymmetric synthesis.[64, 65, 80] BINOL (**42**) or the diphosphine ligand BINAP (**43**) are prominent examples of such ligands (Figure 7). In 1980, *Noyori et al*. described the potential of axially chiral compounds to exhibit stereocontrol on a reaction. It was applied in the Rh-catalyzed asymmetric hydrogenation of C–C and C–O double bonds.[81] Since then, the development of asymmetric catalysis using axially chiral biaryl catalysts, ligands or auxiliaries has grown tremendously. Besides further binaphthyl ligands, like NOBIN (**44**) and BINAM (**45**), other biaryl structures have also found application such as biphenanthrol VAPOL (**46**), which was used for an asymmetric *Diels-Alder* reaction.[82-84] Another example is the biphenyl **47** or the non-C_2-symmetrical tertiary aminophenol **48**, which is used as a catalysts in the enantioselective addition of diethylzinc to aldehydes.[85, 86]

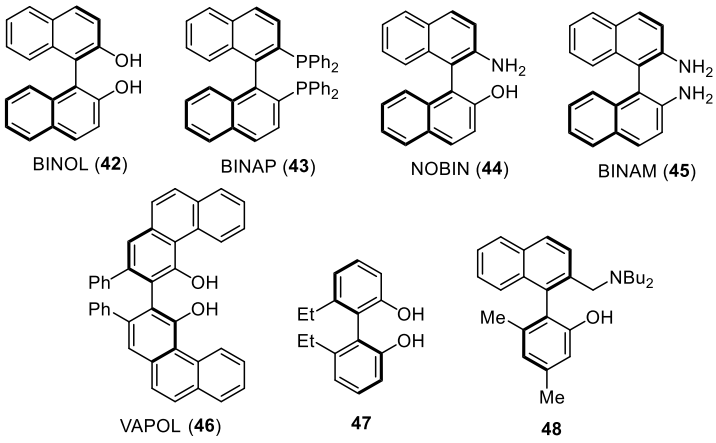

Figure 7 Axially chiral ligands.

The wide applicability as biologically active products or in asymmetric catalysis makes axially chiral biaryls rewarding target compounds. However, the unique structure poses a great challenge in stereoselective synthesis and results in ongoing investigations towards efficient and highly selective methods.[87]

5.2.2 Atroposelective synthesis

The great interest in axially chiral biaryls has led to the development of a wide variety of approaches for the atroposelective construction of biaryls. Two important strategies to access optically pure axially chiral biaryls atroposelectively are shown in Scheme 13.[64, 65,

[70, 80, 88] The most straightforward route is an asymmetric C–C coupling of two aromatic building blocks **49** and **50** (section 5.2.2.1). Another strategy is the atroposelective transformation of prochiral precursors **51** towards biaryls with a defined stereoselective axis (section 5.2.2.2 and 5.2.2.3).[64, 65, 68]

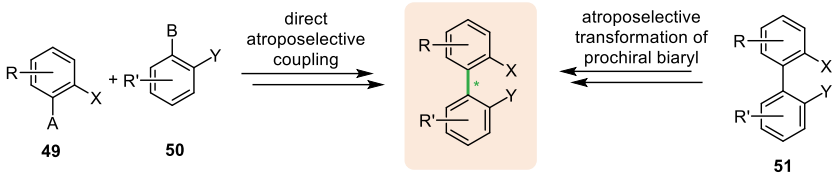

Scheme 13 Overview of strategies for atroposelective synthesis of axially chiral biaryls.

5.2.2.1 Atroposelective C–C coupling

The asymmetric information of an atroposelective C–C coupling is given directly in one step while generating the new C–C axis. There are different strategies to prepare the biaryl compounds atroposelectively. Several approaches are shown in Scheme 14.[64, 65]

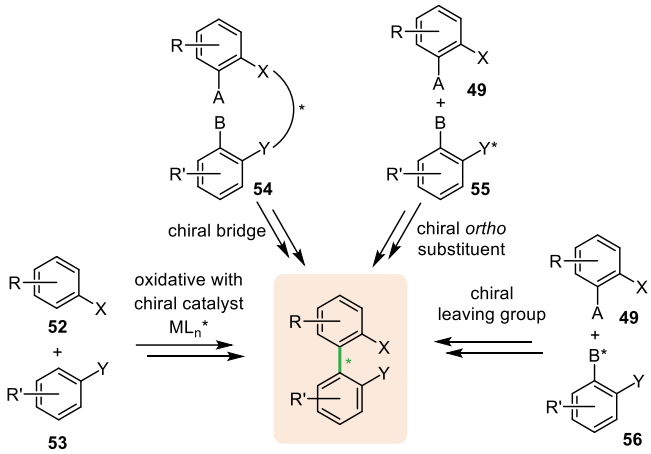

Scheme 14 Strategies for the direct atroposelective synthesis of biaryl axes.

The most widespread synthetic strategy is the biomimetic asymmetric oxidative homocoupling of monomer **52** and **53** for the synthesis of biaryl natural products. This requires catalysts with a high stereoselectivity and catalytic activity for the construction of axially chiral compounds.[80] This method has been widely investigated for the synthesis of binaphthyl derivatives. In 2001 *Kozlowski et al.* published the Cu(I)-catalyzed oxidative

coupling of 2-naphthol derivatives **57**.[89, 90] Binaphthol derivatives **58** was synthesized in good yields with up to 94% *ee* by using CuI, (*S*,*S*)-1,5-diazadecalin as the chiral ligand (10 mol%) and O_2 as the oxidant (Scheme 15A). This method was successfully applied in the total synthesis of various natural products such as nigerone, hypocrellin A and (+)-phleichrome.[91-94] However, the presence of a coordinating substituent in C3-position was essential for high atroposelectivities, which limited the scope of this method. Over the years further strategies have been developed for the asymmetric oxidative coupling towards binaphthols, which have proven to be rather easily accessible.[95, 96] Yet the asymmetric oxidative coupling of phenols revealed to be more challenging due to a higher oxidation potential and a greater number of reactive sites, resulting in low regioselectivity.[97] Therefore, there are fewer strategies of a direct atroposelective coupling towards biphenyls compared to binaphthyls. The group of *Kozlowski* was able to create a chiral vanadium catalyst **[V]-1** for the asymmetric coupling of phenol **59** (Scheme 15B).[97] The regioselectivity of the coupling was determined by the substitution pattern of the monomer. Following this method, the first total synthesis of chaetoglobin A was published (Scheme 15C).[98]

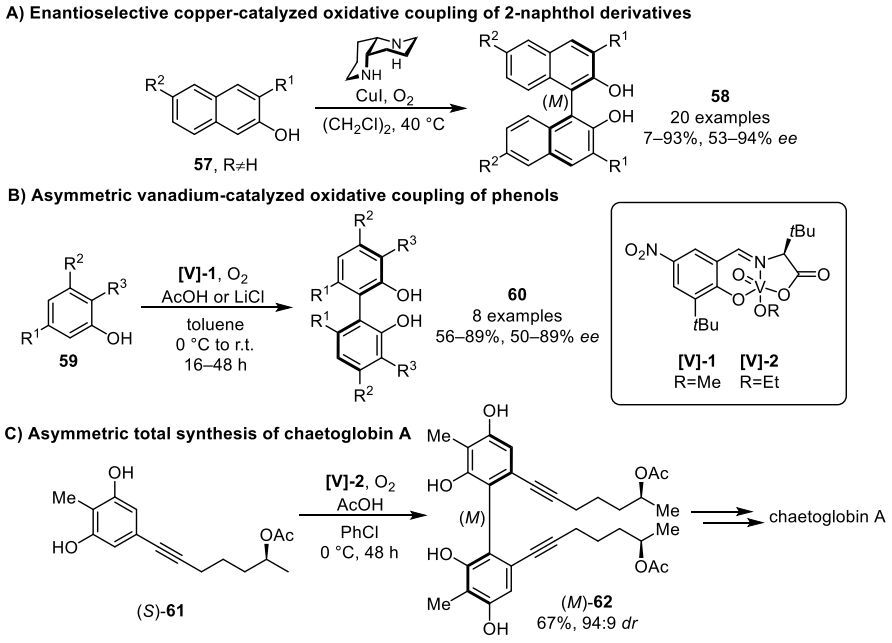

Scheme 15 Oxidative homocoupling of aryls in the presence of chiral additives or catalyst by *Kozlowski's* group.[89, 97, 98]

Suzuki cross couplings are also of great importance in the challenging construction of sterically hindered biaryl axis. In 2002 the group of *Buchwald* first reported biaryl monophosphine ligands for the palladium-catalyzed *Suzuki-Miyaura* cross coupling reaction of unsymmetrical and symmetrical biaryls. Since then, various reports for sterically hindered *Suzuki-Miyaura* couplings have been published.[99-102] In year 2013 the group of *Tang* developed efficient biaryl monophosphorus ligands **L1** and **L2** for the palladium-catalyzed *Suzuki-Miyaura* cross-coupling towards a broad scope of tetra-*ortho*-substituted biaryls (Scheme 16).[103, 104] In contrast to the previously published approaches, this method required lower catalyst and ligand loadings and facilitated the preparation of biaryls with larger *ortho*-substituents.

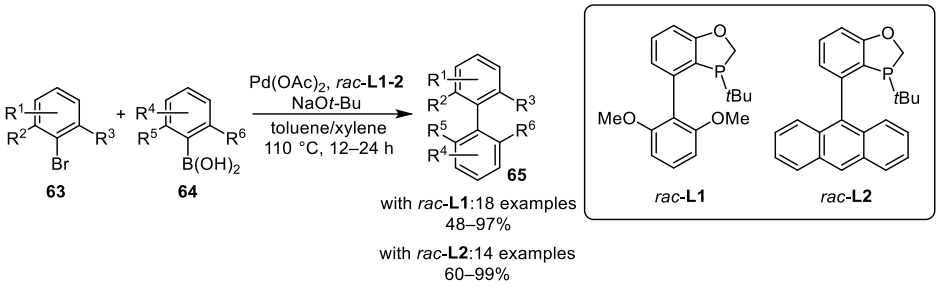

Scheme 16 Racemic *Suzuki-Miyaura* cross coupling towards sterically hindered biaryls.[103]

After the *Suzuki-Miyaura* cross coupling revealed to be an efficient strategy towards the synthesis of sterically hindered biaryls, investigations were made on asymmetric *Suzuki* cross couplings.[105-107] In 2014 and 2020 *Tang et al*. described the application of chiral monophosphorus biaryl ligands **L5–8** on an asymmetric *Suzuki-Miyaura* coupling to generate chiral biaryls **68** and **69** in high yields and excellent enantiomeric excesses of up to 99% *ee* (Scheme 17A). By using **L5–7**, they were able to access chiral tri-*ortho*-substituted biaryls **69** leveraging a polar-π interaction. This method was successfully applied on the first asymmetric total syntheses of korupensamine A and B and michellamine B (Scheme 17B).[108, 109] For the challenging synthesis of tetra-*ortho*-substituted biaryls the group of *Tang* developed a new chiral monophosphorus ligand **L8** to successfully obtain a broad scope of enantiomerically enriched products (Scheme 17A). This ligand was used to achieve an asymmetric total synthesis towards the antitumor agent (*M*)-gossypol (Scheme 17C).[110]

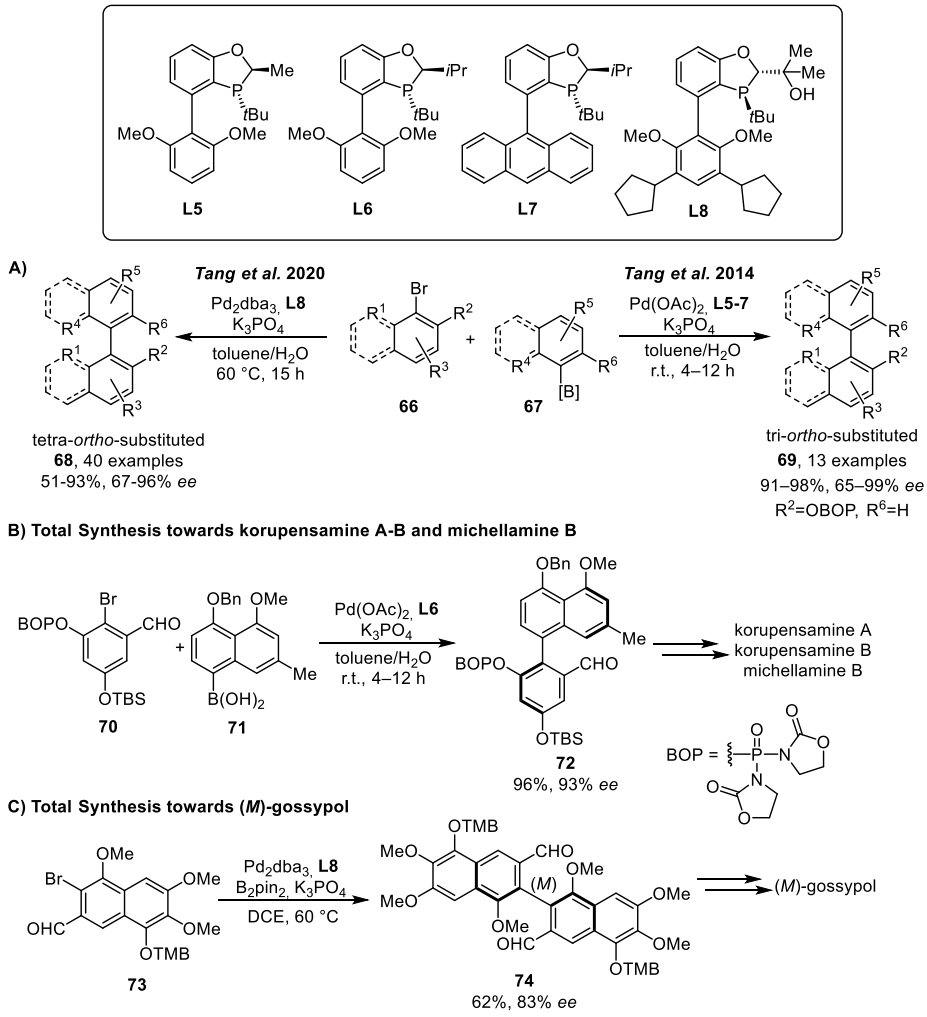

Scheme 17 Asymmetric *Suzuki-Miyaura* cross coupling towards biaryl products by *Tang*'s group.[109, 110]

Moreover, the coupling of chiral bridged aryls is an efficient way for the asymmetric synthesis of biaryls. This strategy facilitates the generation of homo- and cross-coupled biaryl products. The chiral bridge can either remain as a part of the formed product or can function as a chiral auxiliary and is eliminated afterwards.[64, 65] Scheme 18A shows an atroposelective intramolecular oxidative coupling established by *Lipshutz et al*. Two consecutive *Mitsunobu* reactions of *ortho*-bromophenols **75** and **76** with chiral L-threitol (*R*,*R*)-**77** resulted in the formation of the tethered diether (*S*,*S*)-**78**. Homocoupling *via* cuprate formation led to the atroposelective construction of the biaryl axis in (*P*)-**79**.[111, 112] This method has been applied by *Lin et al*. to various total syntheses of natural products, like the

natural bicoumarin (*P*)-kotanin (Scheme 18B).[66, 113, 114] Analogously to *Lipshutz'* method, the tethered diether (*S*,*S*)-**82** was prepared under *Mitsunobu* conditions and afterwards coupled *via* the formation of an intramolecular cyanocuprate. The removal of the chiral auxiliary was performed in four steps yielding the free biphenol (*P*)-**223f** in 71%, which was used to synthesize the natural product (*P*)-kotanin in five further steps.[115]

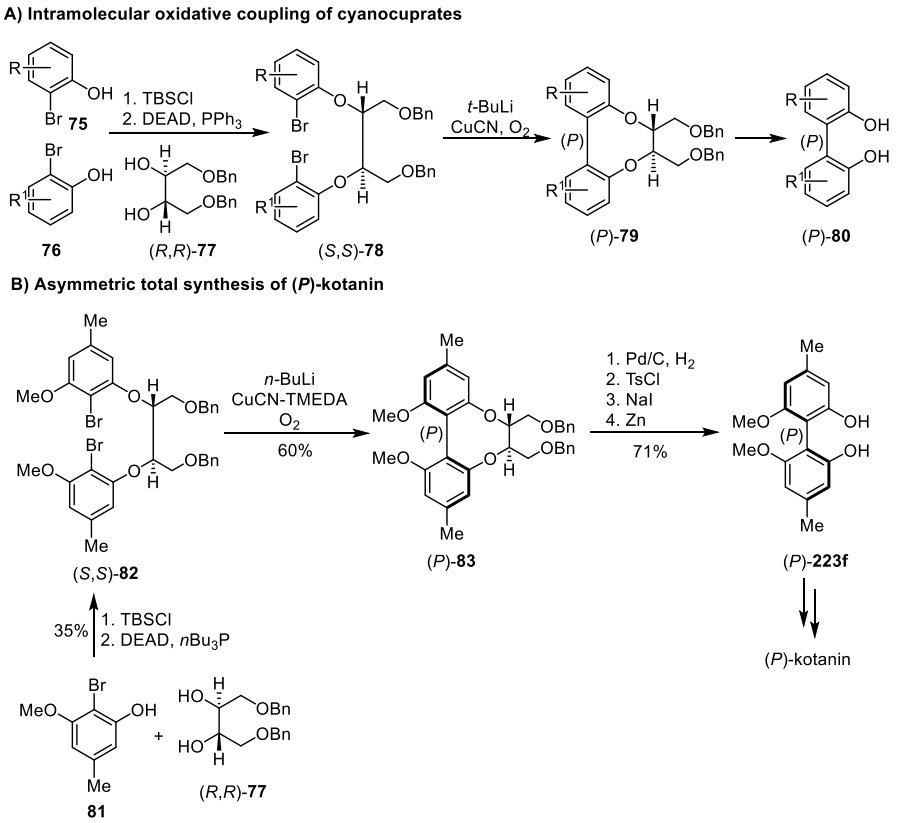

Scheme 18 Atroposelective biaryl coupling using chiral bridges.[111, 112, 115]

The intermolecular coupling of two aryl compounds can also take place atroposelectively by the introduction of a substituent bearing chiral information in the *ortho*-position to the coupling site. In comparison to the use of chiral bridges, only one monomer needs to be modified, providing more freedom for the substitution pattern of the second aryl ring. *Meyers* and his group published an efficient method to synthesize axially chiral compounds stereoselectively by introducing chiral oxazoline substituents (Scheme 19A).[116, 117] An *Ullmann* homocoupling of naphthalene (*S*)-**84** generated binaphthyl (*P*)-**85** with excellent diastereomeric excess (94% *de*). *Meyers* used this method to establish an atroposelective

total synthesis of (*P*)-gossypol (Scheme 19B).[118, 119] The axially chiral biaryl (*P*)**-87** was obtained in 80% yield and good diastereomeric excess (89% *de*), which was used to prepare the natural product in five steps (98% *de*).

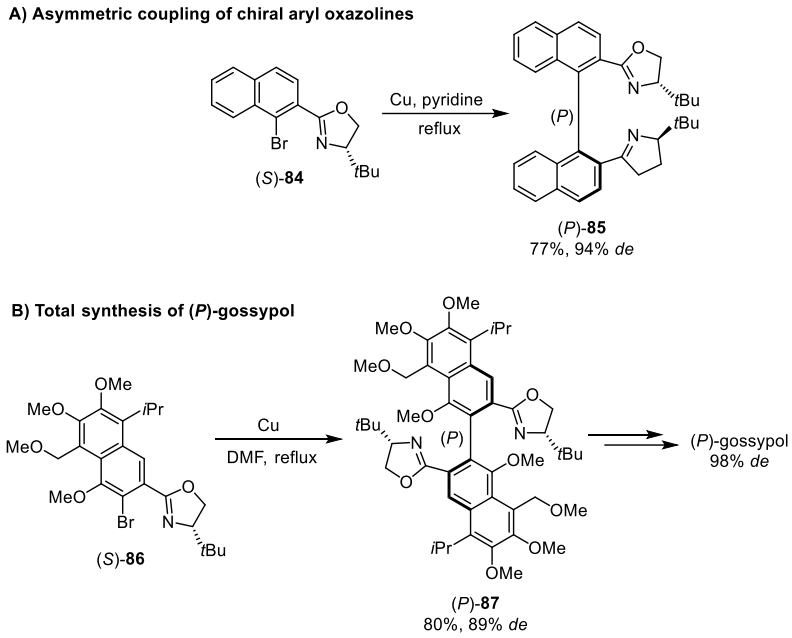

Scheme 19 Atroposelective synthesis of biaryls *via* chiral aryl oxazolines.[116, 119]

A further method is the nucleophilic aromatic substitution by applying chiral leaving groups. In contrast to the application of a chiral substituents, employing a chiral leaving group provides an easy way to introduce asymmetric information without the need for an additional step to remove an auxiliary. This strategy was first reported by *Wilson* and *Cram* to produce binaphthyl compounds (*P*)**-90** by the coupling of *Grignard* reagent **88** with 1-(*R*)-menthoxynaphtalenes (*R*)-(**89**) (Scheme 20A).[120-122] The application of (*R*)-menthol as the chiral leaving group resulted in the most selective chirality transfer. The group of *Hattori* later used this method for the synthesis of tetra-*ortho*-substituted biphenyl compounds (*M*)**-93** (Scheme 20B).[123] However, the coupling of phenols exhibited lower reactivities and only moderate selectivities.

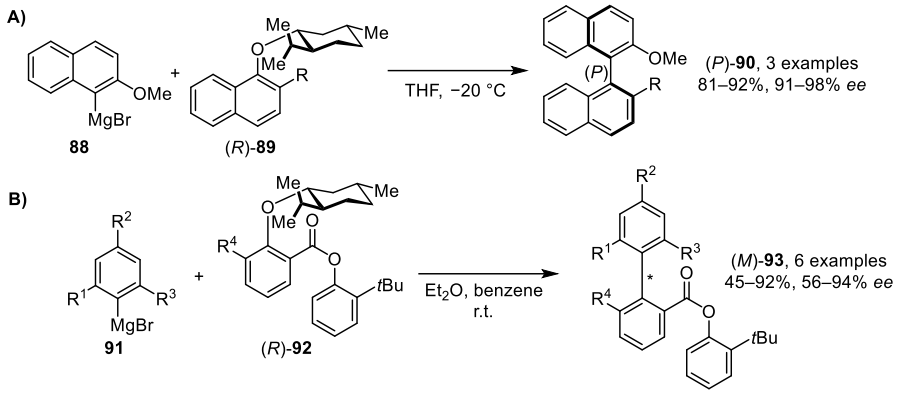

Scheme 20 Atroposelective coupling with (*R*)-menthol as chiral leaving group.[121, 123]

5.2.2.2 Non-enzymatic atroposelective transformation of racemic biaryls

In comparison to the direct atroposelective coupling, transformation of prochiral or racemic biaryls towards axially chiral biaryls is a widely known and efficient alternative. There have been strategies established, including desymmetrization or (dynamic) KR.[68, 80] In this section non-enzymatic strategies are discussed, while the enzymatic methods are described in section 5.2.2.3. KR is a useful tool for the enantioenrichment of axially chiral biaryls and were investigated extensively.[64, 65, 71, 80] An example is the efficient chemical resolution of BINOL and NOBIN by *N*-heterocyclic carbene (NHC) catalysis (Scheme 21). The group of *Zhao* performed an enantioselective acylation with the application of functionalized aldehydes **95** and the NHC-catalyst **98** to yield 12 examples of enantiopure BINOL and biphenyl derivatives **96** and **97** with good chemical yields and good enantioselectivities (E = 22–116, up to 99% *ee*).[124, 125]

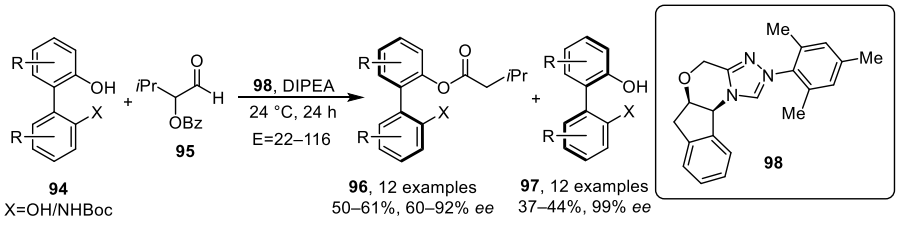

Scheme 21 NHC catalyzed kinetic resolution of BINOL and NOBIN by *Zhao et al.*[124, 125]

Furthermore, various desymmetrizations have been developed, where a functionalization of an enantiotopic *ortho*-substituent is performed to break the symmetry of the compound and to obtain a chiral axis. *Hayashi et al.* published the chiral palladium catalyzed cross

coupling of achiral 2,6-ditriflates **99** with *Grignard* reagents leading to a desymmetrization of biphenyls **100** in excellent yields and optical purity (Scheme 22A).[126-128] In 2020 *Smith* and *Cheong* developed an atroposelective acylative desymmetrization catalyzed by chiral isothiourea-catalysts (Scheme 22B).[129, 130] The choice of catalyst, BTM **102** or HyperBTM **103**, controls the stereoselectivity towards the formed biaryl **104** and **105**.

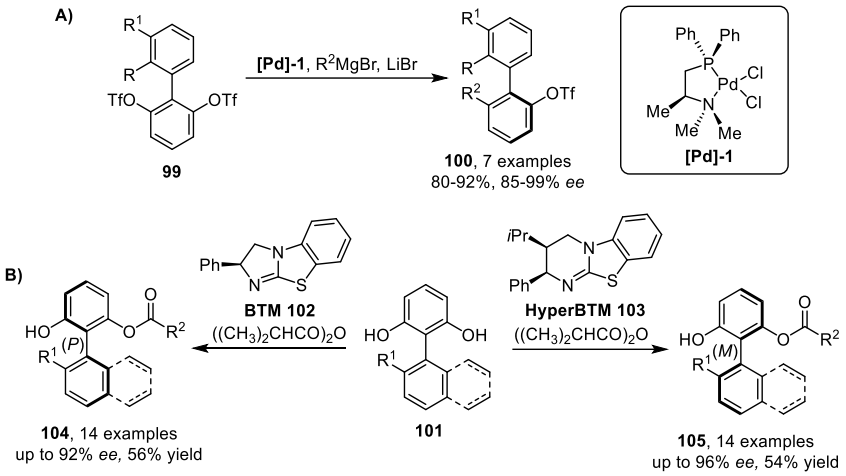

Scheme 22 Biaryl desymmetrization catalyzed by A) palladium catalyst or B) isothiourea catalysts.[126-130]

Copper-mediated deracemization has also proven to be an efficient method for obtaining axially chiral biphenols, for instance the chiral ligand VANOL (*P*)-**107** (Scheme 23A).[131, 132] The formation of the sparteine copper complex leads to lowering of the rotational barrier and an epimerization towards the thermodynamically more stable complex.[132] Recently, this method was applied by *Greb et al.* for the atroposelective synthesis of biphenol (*P*)-**1**, which was used afterwards for the synthesis of di-epi-gonytolide A (Scheme 23B).[1]

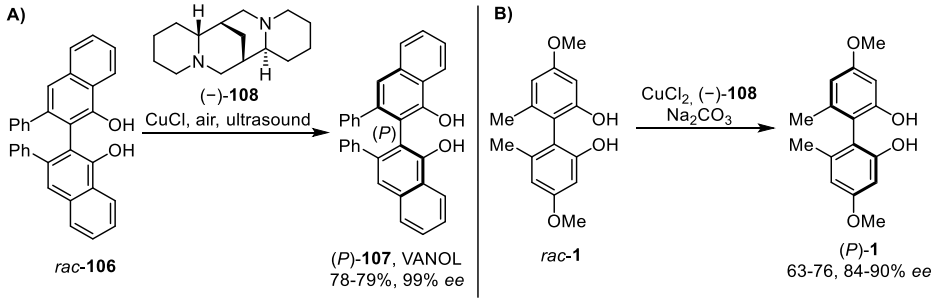

Scheme 23 Copper-mediated deracemization of biphenols.[1, 131]

In 1992 *Bringmann* developed the so called "lactone methodology" for a DKR to obtain configurationally stable biaryls (Scheme 24).[64, 65, 133, 134] An intramolecular cross-coupling of ester-bridged aryls leads to the formation of the configurationally unstable biaryl lactone **108**. An atroposelective ring opening results in the formation of the desired axially chiral atropisomer **109** (Scheme 24A). This method has been extended to different atroposelective lactone ring openings.[133] Most commonly, chiral anionic nucleophiles, such as chiral alcoholates or amines, have been employed for the ring opening (Scheme 24B). Additionally, asymmetric reduction of the lactone in the presence of chiral hydride transfer reagents, like the *Corey-Bakshi-Shibata* (CBS) reagent or *Noyori*'s chiral lithium aluminium hydride has proven to be highly selective.[135] Another strategy is the lactone activation through the application of a chiral Lewis acids or through a η^6-coordination of a chiral transition metal complex (Scheme 24C and D). Following activation, the application of an achiral nucleophile results in the ring opening and the formation of one enantioenriched atropisomer. Depending on the choice of the chiral nucleophile or auxiliary, both atropisomers can be accessed *via* the same precursor in high yield and optical purity. This method has already served as the asymmetric key step for the atroposelective total synthesis of axially chiral natural products, like (*M*)-bismurrayaquinone A or (*M*)-mastigophorene A.[37, 136-140]

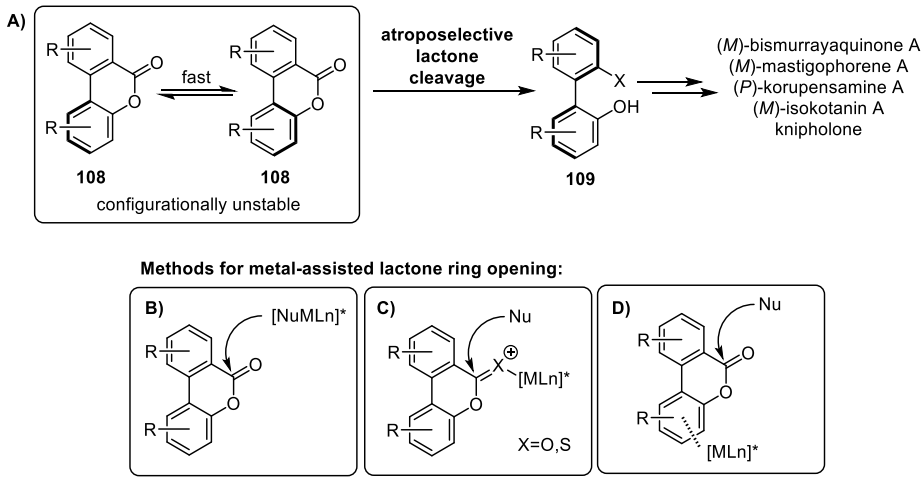

Scheme 24 Dynamic kinetic resolution of axially chiral biaryls *via* the "lactone methodology".

5.2.2.3 Enzymatic atroposelective transformation of prochiral biaryls

The application of biocatalysts for the asymmetric synthesis of axially chiral biaryls has increasingly gained attention. The great opportunities in enzyme discovery and engineering reveal an important part of the synthetic toolbox, including the stereoselective synthesis of atropisomers.[87] In contrast to conventional non-enzymatic methods, enzymatic processes bring several advantages to the challenging synthetic question.[141, 142] Enzymes are sustainable catalyst, which enable highly enantio-, regio- and chemoselective reactions under mild reaction conditions with a reduced application of hazardous substances.[40] They are commonly used in two different approaches for the atroposelective synthesis of axially chiral biaryls. Following the biosynthetic pathway, the most direct approach towards the synthesis of biaryls is the oxidative coupling. Therefore, laccases, monooxygenases or peroxidases were applied for the direct asymmetric construction of axially chiral biaryl bonds.[143-145] This chapter will focus on the second biocatalytic methodology, where hydrolases are used for the asymmetric transformation of prochiral or racemic axially chiral precursors.[87] Hydrolases have often been applied in the KR of atropisomers, where acylation, hydrolysis or acyl transfer reactions take place. An early approach of an enzymatic resolution of BINOL was developed in the year 1989 by *Kazlauskas* (Scheme 25).[35] He was able to establish the enantioselective hydrolysis of binaphthol ester *rac*-**30**, catalyzed by a cholesterol esterase (bovine pancreatic acetone powder) yielding the enantiomers with high enantiomeric purity of 99% *ee* (E_1>400).

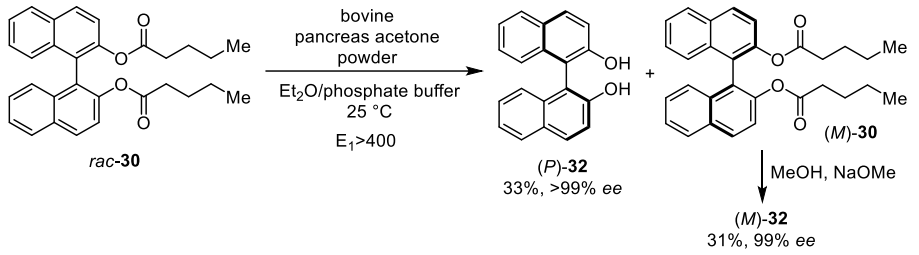

Scheme 25 Enzymatic kinetic resolution of binaphthyl dipentanoate *rac*-**30** by *Kazlauskas*.[35]

Since then, continuous studies at improving this system can be found in literature addressing lipase catalyzed KR of binaphthyl substrates.[146-151] Only few examples have been reported for biphenyl derivatives.[87, 152-154] In the year 2003 *Sanfilippo et al.* described the first lipase catalyzed KR of biphenyls (Scheme 26).[67] Here, they performed an enantioselective esterification of biphenol *rac*-**223b** with vinyl acetate as acyl donor,

catalyzed by *Pseudomonas cepacia* lipase (PSL). The lipase was immobilized on various supports, giving different results. The best conditions employed the lipase immobilized on ceramic resulting in the formation of (*M*)-**110** and (*P*)-**223b** in 49–51% and 90–96% *ee* after 1–3 days (E = 74).

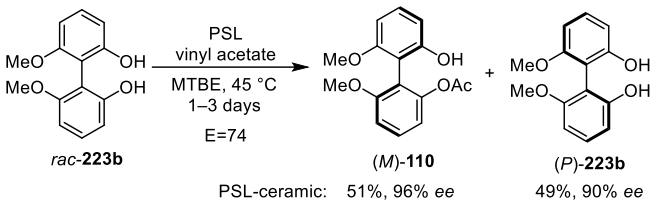

Scheme 26 First enzymatic acetylation of axially chiral biphenol using PSL by *Sanfilippo et al.*[67]

A highly efficient EKR of binaphthols and biphenols was reported by *Akai's* group., who used a commercially available immobilized lipoprotein lipase from *Pseudomonas* sp. (LIP301) and vinyl acetate as the acyl donor (Scheme 27).[155] The addition of sodium carbonate resulted in the acceleration of the enzymatic acetylation, due to the increased nucleophilicity of the biaryl hydroxy groups. This method was a great improvement for the enzymatic enantioselective transformation of racemic biaryls. Former EKRs of axially chiral biaryls were limited in their substrate scope and required longer reaction times 1–3 days.[67] In contrast, this approach is applicable to a broader binaphthyl substrate scope. However, the scope contained only two biphenol compounds. This approach leads to both enantioenriched isomers (*P*)-**111** and (*M*)-**112** in good yields of around 50% and good to excellent enantiomeric excesses within a shorter reaction time.

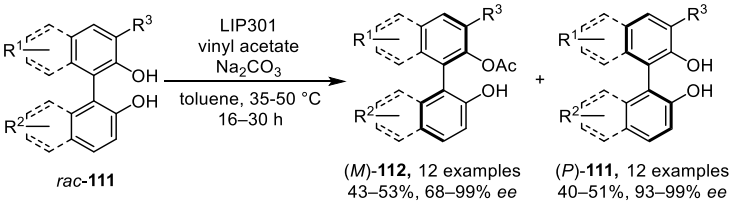

Scheme 27 Enzymatic kinetic resolution of axially chiral biaryl diols by *Akai et al.*[155]

To date, only a few DKR of biaryls have been reported. Based on *Bringmann*'s lactone concept, investigations towards a lipase-catalyzed lactone ring opening was reported by *Deska et al.* (Scheme 28).[134, 156] However, the screened lipases exhibited low selectivities and reactivities. The best result was observed with pig liver esterase (PLE) resulting in only 6% conversion and poor optical purity.

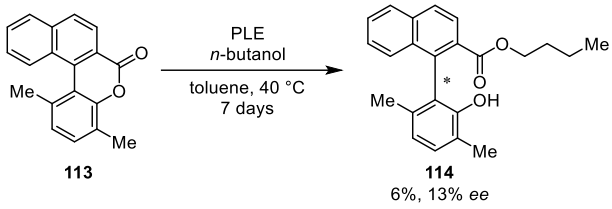

Scheme 28 Lipase-catalyzed lactone opening by *Deska et al.*[156]

The combination of lipases and metal catalysis for a DKR have been an attractive and promising method to afford enantiopure alcohols and amines.[157] In 2018 *Akai* and coworkers published the first DKR of racemic biaryls *rac*-**111** (Scheme 29).[158, 159] They made use of the combination of a Ru-catalyzed racemization and a highly enantioselective lipase-catalyzed acylation, using immobilized lipoprotein lipase from *Pseudomonas* sp. (LIP301). By the application of the Ru-catalyst **[Ru]-1**, an SET process takes place, which results in the formation of a radical intermediate with an sp^3 carbon at the biaryl axis. This lowers the energetic barrier of the rotation along the former biaryl bond resulting in racemization. A subsequent ester hydrolysis with potassium carbonate in methanol led to the formation of the desired enantiopure biaryl products (*M*)-**111**. This method was successfully applied to a scope of 16 examples with high enantiomeric excess and chemical yield, including only one example of a biphenyl compound.

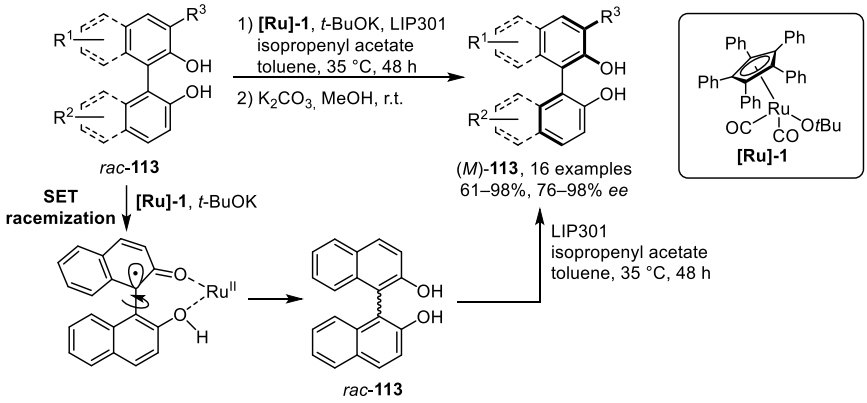

Scheme 29 Enzymatic dynamic kinetic resolution of axially chiral biaryls by *Akai*'s group.[155]

Besides KRs, various desymmetrization reactions of prochiral biphenyls have been reported, which access the formation of enantioenriched atropisomers in ideally 100% yield. The group of *Matsumoto* utilized different lipases, including porcine pancreatic lipase (PPL), *Rhizopus oryzae* lipase (ROL) or *Pseudomonas cepacia* lipase (PCL), for the

enantioselective desymmetrization of diacetates **116** (Scheme 30A).[160-162] Depending on the choice of the lipase a specific stereogenic control towards one of both atropisomers with high selectivity was observed. The enantioenriched monoacetate (*M*)-**115** was for instance obtained by the enzymatic desymmetrization catalyzed by PPL, while ROL catalyzed the reaction towards monoacetate (*P*)-**115** in excellent optical purity. *Matsumoto's* group applied this method in the following years in the first asymmetric total synthesis of the natural product (*M*)-euxanmodin B (*M*)-**119** (Scheme 30B).[161, 163]

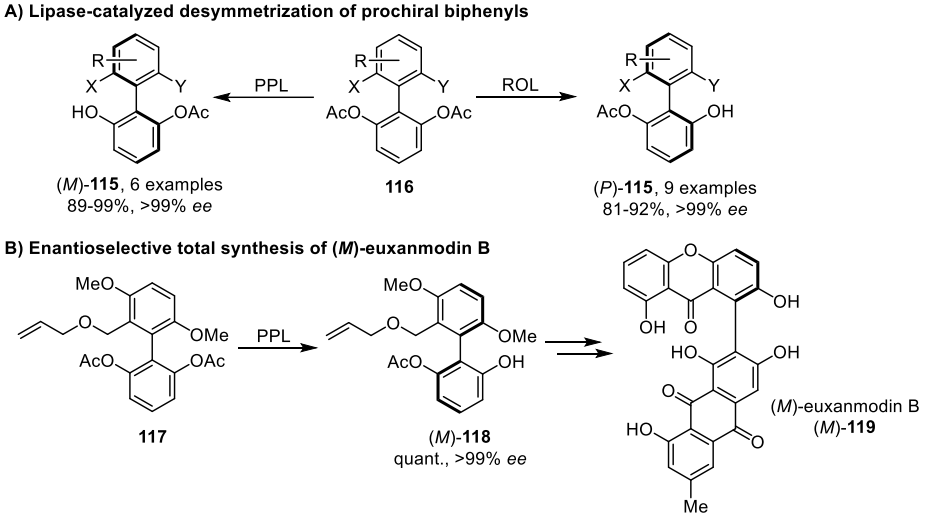

Scheme 30 Enzymatic desymmetrization of symmetric biaryl diacetates.[160-162]

In 2020, *Akai et al*. presented an enantiodivergent synthesis of both enantiomers of tri-*ortho*-substituted biphenols using a single immobilized *Burkholderia cepacia* lipase (PS-IM). The enzymatic acylative desymmetrization with vinyl acetate resulted in the formation of the monoester (*M*)-**115** in good to excellent yield and optical purity. Under aqueous conditions a hydrolytic desymmetrization led to the generation of (*P*)-**115** (Scheme 31).[164]

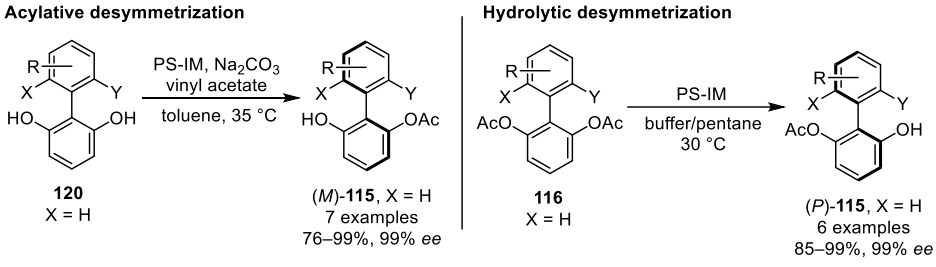

Scheme 31 Enzymatic enantiodivergent synthesis of tri-*ortho*-substituted biphenols.[164]

5.3 γ-Naphthopyrone

γ-Naphthopyrones **121** are an important group of aromatic polyketides, which are built up as tricycles. They are in essence naphthalenes with linearly annulated γ-pyrones (Figure 8). The monomeric form, as well as their dimeric form: γ-binaphthopyrones **122** , can be found in various fungal species, like *Villosiclava virens* or *Ustilaginoidea virens*, the pathogen of the disease affecting rice called "false smut".[165, 166] The monomeric units are connected by an axis in C9-position, leading to the formation of an axially chiral dimer. Additionally, the pyrone can occur in an unsaturated or dihydro form, which introduces a further stereogenic center in C2-position.

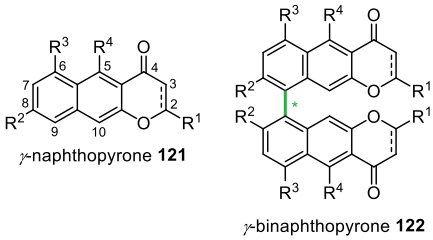

Figure 8 Chemical structure of γ-naphthopyrone **121** and axially chiral γ-binaphthopyrone **122**.

As of date, a large number of monomeric and dimeric γ-naphthopyrones with a diverse range of biological activities, like antiviral, antimicrobial or insecticidal activity, have been reported.[165, 167] Antimicrobial activity has already been discovered in 1895 from the red pigment from a rice fungus *Ustilaginoidea virens*.[167, 168] Other isolated dimeric γ-binaphthopyrones were evaluated to exhibit cytotoxicity against human epidermoid carcinoma cells and ovarian cancer cells.[169] The first γ-naphthopyrone rubrofusarin (**123**) was isolated in the year of 1937 and its structure was elucidated in 1961 by *Stout* and *Jensen*.[170, 171] Their biological importance in combination with their interesting structural scaffold makes these compounds an attractive field of research. In the context of this work the γ-binaphthopyrones: ustilaginoidin A (*M*)-(**2**) and ustilaginoidin F (*M*)-(**3**) and their monomeric units norrubrofusarin (**124**) and hemiustilaginoidin F (**125**) will be discussed in greater detail (Figure 9).

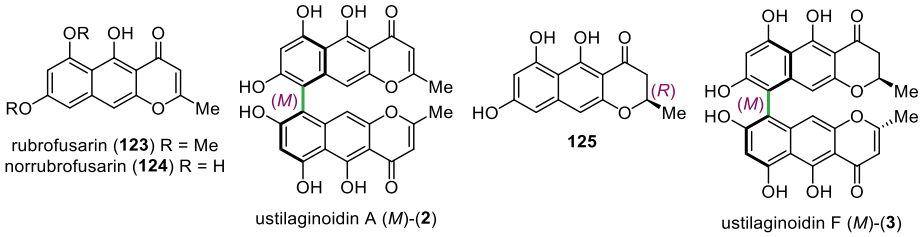

Figure 9 Chemical structure of ustilaginoidin A (*M*)-(**2**) and ustilaginoidin F (*M*)-(**3**) and their monomeric units norrubrofusarin (**124**) and hemiustilaginoidin F (**125**).

The biosynthesis of γ-naphthopyrones proceeds *via* the polyketide pathway in different fungal species, like *Fusarium graminearum, Aspergillus niger*, or *Ustilaginoidea virens*.[172-174] Scheme 32 shows the biosynthetic pathway towards γ-naphthopyrones and γ-binaphthopyrones in *U. virens*. In the first step a non-reducing polyketide synthase PKS catalyzes the condensation of one acetyl-CoA and six malonyl-CoA forming the intermediate YWA1 (**126**). Dehydration of YWA1 (**126**) by UsgD results in the formation of the orange pigment norrubrofusarin (**124**).

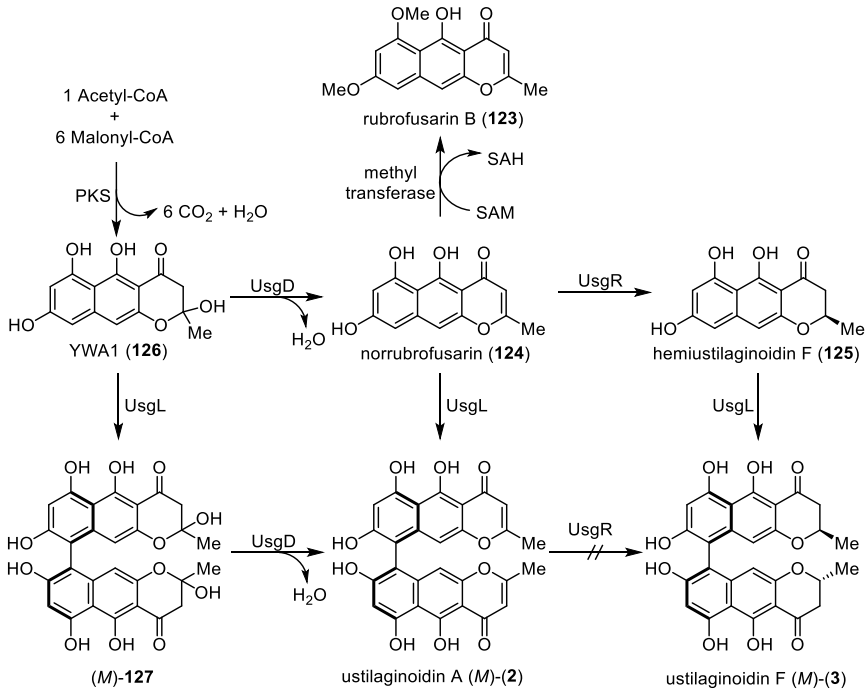

Scheme 32 Biosynthetic pathway towards γ-naphthopyrones and γ-binaphthopyrones in *U. virens*.[175]

In the next step a double *O*-methylation forms the γ-naphthopyrone rubrofusarin B (**123**). The reductase UsgR is responsible for the reduction of the pyrone ring towards the dihydro form in hemiustilaginoidin F (**125**). In the last step, the laccase UsgL catalyzes the phenol coupling towards the γ-naphthopyrone dimers. It was shown that all three different naphthopyrone monomers **124**, **125** and **126** can be dimerized atroposelectively by UsgL towards the (*M*)-configurated dimers (*M*)-**127**, ustilaginoidin A (*M*)-(**2**) and ustilaginoidin F (*M*)-(**3**). Afterwards dimer **127** is directly dehydrated by UsgD towards the natural ustilaginoidin A (*M*)-(**2**). However, reduction of dimer **2** towards ustilaginoidin F (*M*)-(**3**) is not observed.[175]

The first synthesis of rubrofusarin B (**123**) was established by *Shibata et al.* in 1963 (Scheme 33).[176] In the first step, an *Arndt-Eistert* reaction was performed starting from benzoic acid **128** to gain diazoketone **129**. In the presence of silver oxide, **129** was converted to an aryl acetic acid, followed by the formation towards the acid chloride **130**. Treatment with ethyl acetoacetate (EAA) and magnesium resulted in **131**, which underwent cyclization during vacuum distillation at elevated temperature. The obtained **132** was subjected to a *Claisen* condensation with ethyl acetate. Lastly, the condensation product **133** was cyclized in the presence of acetic acid and hydrochloric acid towards the desired γ-naphthopyrone rubrofusarin B (**123**).

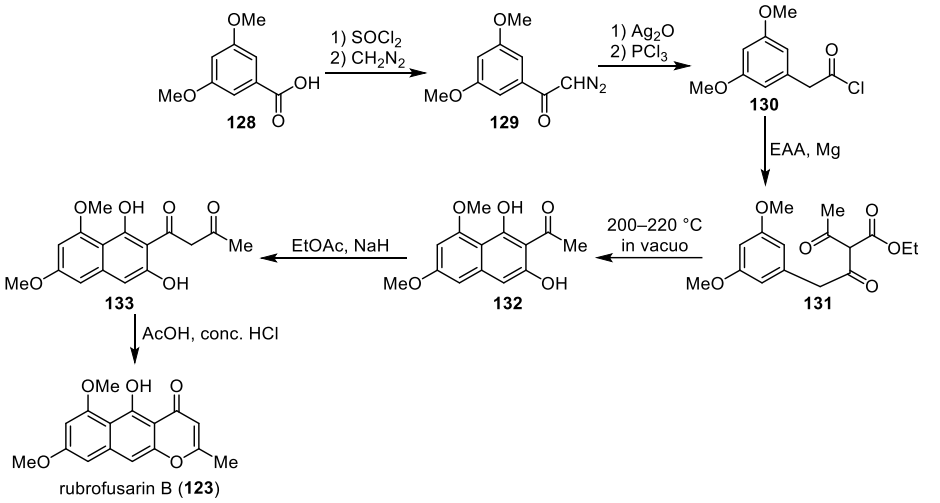

Scheme 33 Synthesis of rubrofusarin B (**123**) by *Shibata et al.*[176]

Shibata's group continued to investigate the synthesis of racemic ustilaginoidin A (**2**) by an oxidative phenol coupling with $FeCl_3$ (Scheme 34).[177] The direct oxidative coupling of

norrubrofusarin (**124**) towards ustilaginoidin A (**2**) was not possible. Therefore, dimethyl ether protected norrubrofusarin **134** was required. In the presence of $FeCl_3$, *γ*-binaphthopyrone **135** was obtained in 27% isolated yield. Treatment with dimethyl sulfate and potassium carbonate as a base resulted in the permethylated *γ*-binaphthopyrone **136**, which was afterwards demethylated using hydroiodic acid to yield racemic ustilaginoidin A (**2**) in 29% yield.

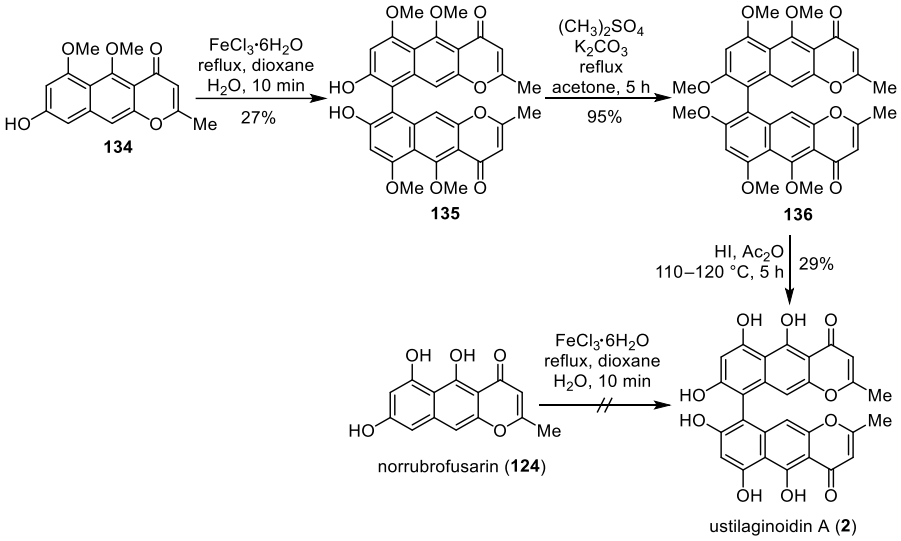

Scheme 34 Synthesis of racemic ustilaginoidin A (**2**) by *Shibata et al.*[176]

Staunton et al. described an alternative total synthesis towards rubrofusarin B (**123**) (Scheme 35).[178] Following this procedure, orsellinate **228** reacts with pyrylium salt **137** in the presence of LDA to form pyrone **234** in 25–35% yield. Repeated treatment with LDA induces the cyclization towards the *γ*-naphthopyrone **123** in 17% yield.

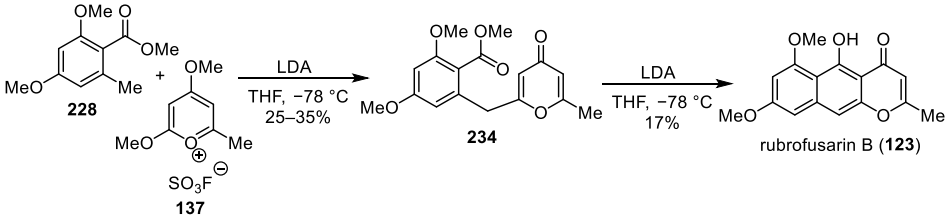

Scheme 35 Synthesis of rubrofusarin B (**123**) by *Staunton et al.*[178]

In the year of 2019, the group of *Müller* investigated a group of laccases to catalyze the phenol coupling reactions in the biosynthetic pathway of ustilaginoidins.[173, 174] They

started with the synthesis of norrubrofusarin (**124**), which functioned as the monomer for the desired coupling reaction (Scheme 36). Analogous to *Staunton*'s group an annulation was performed using methyl benzoate **228** and pyrylium tetrafluoroborate **233**. In two steps, the γ-naphthopyrone **123** was formed using LDA as the base and a subsequent acidic hydrolysis. Treatment with BBr_3 resulted in a double methyl ether cleavage towards norrubrofusarin (**124**). In the next step *A. niger* UstL expression culture were used for the investigation of the enzymatic coupling. Full conversions of norrubrofusarin (**124**) towards the coupling product **2** were observed in the presence of laccase-containing lysate. High regioselectivity was observed, as the 9,9′-dimer was exclusively formed. In the next step the atroposelectivity of four different laccases AshL, CheL, MytL and UstL were analyzed. The first three laccases AshL, CheL and MytL all exhibited atroposelectivity towards the (*P*)-configuration (84–99% *ee*). However, the selectivity of UstL varied depending on the lysate concentration. At low concentration (*P*)-ustilaginoidin A (*P*)-**2** was formed (up to 32% *ee*). At higher concentrations of UstL the atroposelectivity changed towards the (*M*)-configuration (up to 55% *ee*).

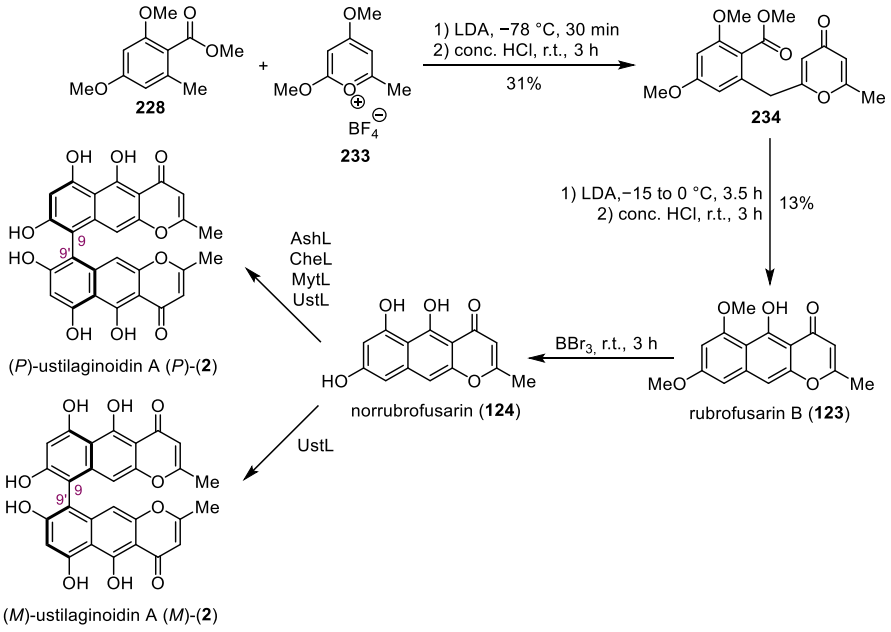

Scheme 36 Laccase-catalyzed phenol coupling towards ustilaginoidin A (**2**) by the group of *Müller*.[173, 174]

5.4 Isokotanin

One further important class of axially chiral dimeric polyketides is bicoumarins. Fungal species, like *Aspergillus*, *Emericella* or *Petromyces* produce a broad spectrum of natural bicoumarins by regio- and stereoselective dimerization of siderin (**138**) or its demethylated derivative **139** (Scheme 37).[179] This work focused on the axially chiral bicoumarins isokotanin A (**4**) and C (**5**), which has been isolated first from the sclerotia of *Aspergillus alliaceus* by *Gloer et al.* in 1994.[180] Shortly afterwards, *Udagawa*'s group has extracted isokotanin B (**146**) from its teleomorph *Petromyces alliaceus*.[181] The difference in the structure of isokotanin A–C (**4**), (**146**) and (**5**) and their regioisomers is the connectivity of the two monomeric coumarin units. While kotanin (**140**), demethylkotanin (**141**), orlandin (**142**) are C8-C8′ bridged, and desertorin A–C (**143**)–(**145**) are C6-C8′ bridged, the chiral axis of isokotanin A–C (**4**), (**146**) and (**5**) is connecting in C6 and C6′ position.

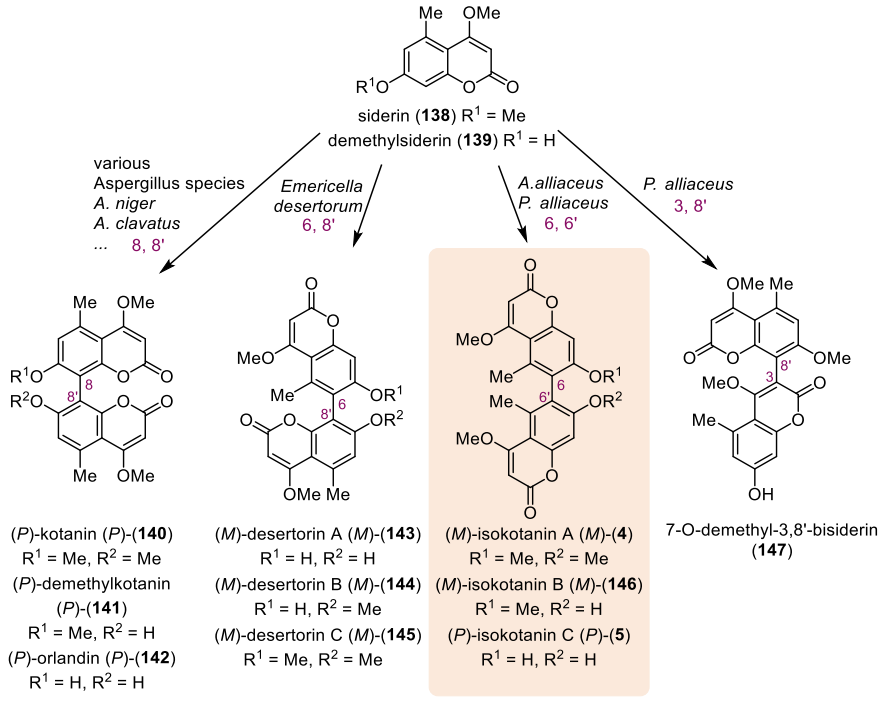

Scheme 37 Bicoumarins isolated from *Aspergillus*, *Emericella* or *Petromyces* species.

The biosynthesis of bicoumarin kotanin (**140**) has been investigated by studies of the regio- and stereoselective coumarin coupling in *A. niger* and compared to the results gained by the isolation of isokotanin A–C (**4**), (**146**) and (**5**) in *A. allicaeus*.[179-181] It was shown that

a dimerization of demethylsiderin (**139**) takes place in *A. niger* regioselectively towards (*P*)-orlandin (*P*)-(**142**). The coupling using siderin (**138**) proved to be stereoselective, as all three isolated bicoumarins kotanin (**140**), demethylkotanin (**141**) and orlandin (**142**) have a (*P*)-configuration. In contrast, a less regioselective phenol coupling was observed in *A. alliaceus*. A mixture of isokotanin A–C and its C8-C8′ and C3-C8′ bridged regioisomers have been isolated.[180, 181] While the dimerization in *A. niger* exhibited high stereoselectivity, the phenol coupling of demethylsiderin (**139**) in *A. alliaceus* took place non-stereoselectively towards *rac*-isokotanin C *rac*-(**5**). A subsequent stereospecific *O*-methylation resulted in the formation of enantioenriched isokotanin A (*M*)-(**4**) and isokotanin B (*M*)-(**146**).[179] *Gloer* described the activity of isokotanin B (**146**) and isokotanin C (**5**) against corn earworm *Helicoverpa zea* and *Carpophilus hemipterus*, which is a fungivorous dried fruit beetle.[180] The bioactivities and their interesting structures made the investigations towards the atroposelective total synthesis of the axially chiral bicoumarins attractive.

Three different methods were established for the asymmetric synthesis of the same building block (*M*)-**152**, which was used for the total synthesis towards (*M*)-isokotanin A (*M*)-**4**. The first asymmetric total synthesis of (*M*)- and (*P*)-isokotanin A (**4**) and the assignment of the absolute configuration of the naturally occurring bicoumarins was published by *Lin et al.* in the year 1996 (Scheme 38).[36] This route followed the protocol of *Meyers et al.* by the construction of the axially chiral biaryl axis utilizing chiral bromo-oxazoline (*R*)-**148**, which was discussed in section 5.2.2.1 (Scheme 19) before.[116] An asymmetric *Ullmann* coupling of (*R*)-**148** resulted in the formation of axially chiral (*M*)-**149**, which was directly converted to (*M*)-**150** under acidic conditions in 51% yield over two steps. The following reduction with $LiAlH_4$ led to the diol (*M*)-**151** in a yield of 80%, which was reduced in the presence of Pd/C and catalytic amount of TFA to the building block (*M*)-**152** in 54% yield. Thus, (*M*)-**152** could be obtained in four steps with an overall yield of 22%. The absolute configuration of isokotanin A (**4**) was assigned to be (*M*) by the comparison of the optical rotation of tetraol (*M*)-**153** with literature data.[182]

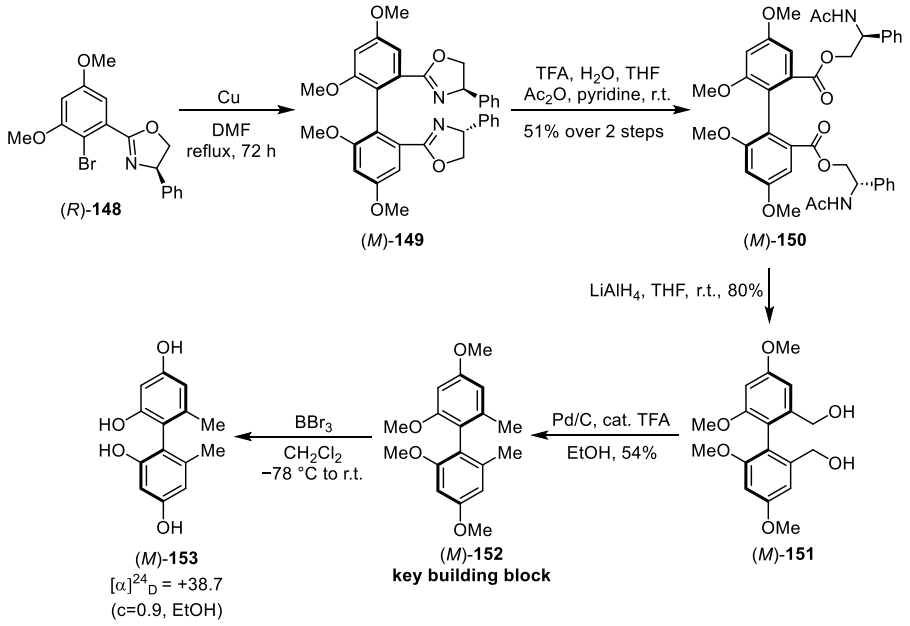

Scheme 38 Asymmetric synthesis of building block (*M*)-**152** by *Lin et al.*[36]

In the year 2002, the group of *Bringmann* applied their resolution method *via* a biaryl lactone to the asymmetric formation of (*M*)-**152** (Scheme 39) (see section 5.2.2.2, Scheme 24).[37] Analogously to *Lin*, the construction of the sterically hindered biaryl axis was performed *via* an *Ullmann* coupling of **154** in a yield of 89%, which was followed by a reduction with $LiAlH_4$ towards diol *rac*-**151** in 97% yield. *Rac*-**151** was afterwards oxidized in the presence of MnO_2 towards the dialdehyde *rac*-**155** in a yield of 92%. A *Cannizzaro* disproportionation converted *rac*-**155** towards hydroxy acid *rac*-**156** in 94%. In the next step hydroxy acid *rac*-**156** was subjected in a *Steglich* esterification using DCC and DMAP to obtain the key lactone *rac*-**157** in 72% yield. *Bringmann* established the atroposelective CBS reduction of the stable seven membered biaryl lactone *rac*-**157**. Therefore, oxazaborolidine-activated borane was used for a KR by an atroposelective ring cleavage towards a 1:1 mixture of diol (*M*)-**151** (46%) and lactone (*P*)-**157** (43%) in good to excellent enantiomeric excesses of 75–96% *ee*. Crystallization was used to increase the optical purity of (*M*)-**151**. The building block (*M*)-**152** was afforded afterwards by a hydroxy-bromo exchange and a subsequent reduction with $LiAlH_4$ in 83% over two steps. Overall, the preparation of the building block (*M*)-**152** took place in nine steps and 12% overall yield. The assignment of the absolute configuration by *Lin et al.* was confirmed by CD spectrum measurements.

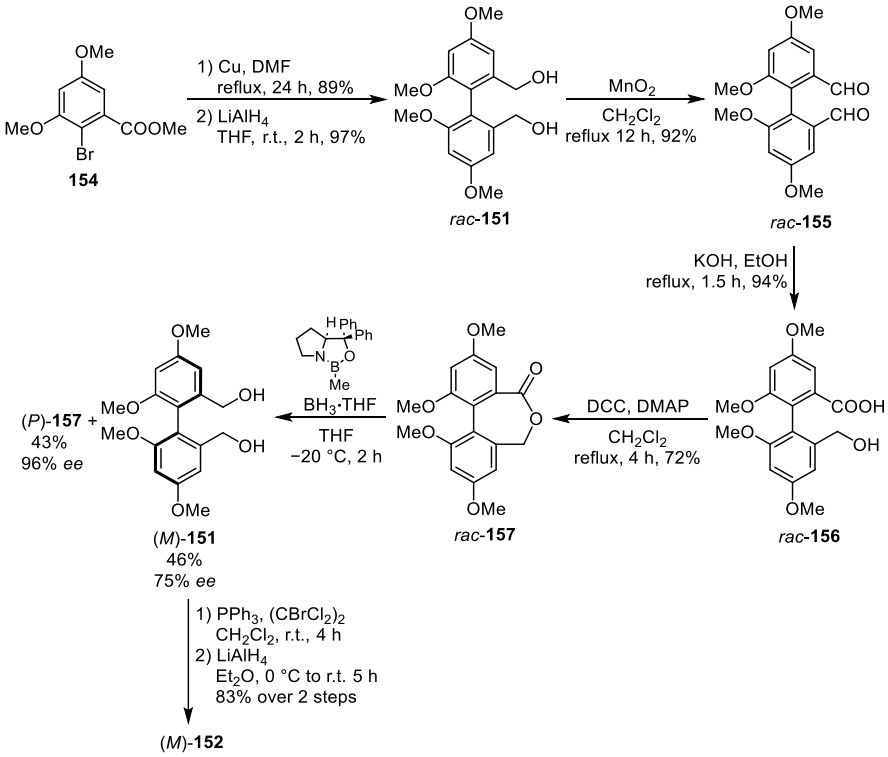

Scheme 39 Asymmetric synthesis of building block (*M*)-**152** by *Bringmann et al.*[37]

Finally, the group of *Graff* developed a desymmetrization *via* a direct asymmetric bromine-lithium exchange for the synthesis of building block (*M*)**-152**, which can be used in the formal synthesis of (*M*)-isokotanin A (*M*)-(**4**) (Scheme 40).[39] Their synthesis started with the oxidative coupling of 1,3,5-tribromobenzene (**158**) to form *rac*-**159**, which was followed by a nucleophilic substitution with sodium methoxide. The product *rac*-**160** was obtained in a yield of 70%. Afterwards, by applying stoichiometric amounts of chiral ligand, an asymmetric bromine lithium exchange was performed with the subsequent addition of methyl iodide. The enantioenriched biaryl (*M*)**-161** was obtained in 84% yield and moderate enantiomeric excess of 68% *ee*. In the last step, a copper-mediated dimethoxylation resulted in the formation of the desired building block (*M*)**-152** in 42% yield with >72% *ee*. Thus, (*M*)**-152** was synthesized in four steps with an overall yield of 15%.

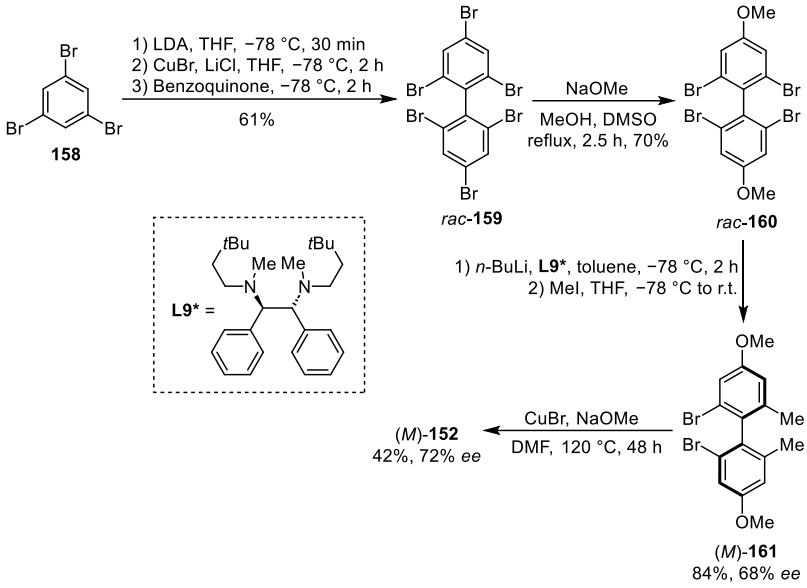

Scheme 40 Asymmetric synthesis of building block (*M*)-**152** by *Graff et al.*[39]

Lin and *Bringmann* used the same procedure towards the total synthesis of (*M*)-isokotanin A (*M*)-(**4**) starting from building block (*M*)-**152** (Scheme 41). In the first step a double acylation was performed in the presence of $TiCl_4$. Treatment with $TiCl_4$ resulted in the regioselective cleavage of both *para*-methyl ethers towards (*M*)-**162**. Afterwards, decarbonate (*M*)-**163** was obtained by the reaction with methyl chloroformate. In the last step, a base-catalyzed cyclization of (*M*)-**163**, and a subsequent methylation led to the formation of the natural product (*M*)-isokotanin A (*M*)-(**4**). The dimeric natural product was obtained in five steps with 9–46% overall yield starting from the building block (*M*)-**152**.

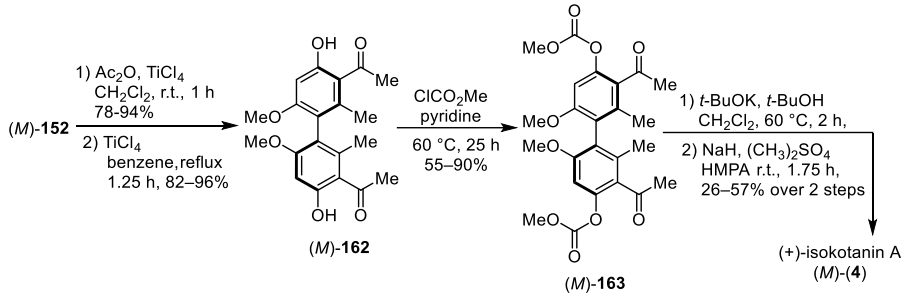

Scheme 41 Synthesis towards (*M*)-isokotanin A (*M*)-(**4**) by *Lin* and *Bringmann*.[36, 37]

In contrast, *Müller*'s group published an alternative racemic route towards isokotanin A *rac*-(**4**), kotanin *rac*-(**140**) and desertorin C *rac*-(**145**) (Scheme 42).[38] Here, the route started with an unselective oxidative coupling of methyl benzoate **164** in the presence of $FeCl_3$ on SiO_2 as the oxidant. This coupling gave a mixture of the three regioisomeric biaryl esters *rac*-**268**, *rac*-**165** and *rac*-**166**. The 5,5′-dimer *rac*-**268** was converted to the diamino-bichromenone *rac*-**270** by treatment with lithiated acetonitrile in 77%. In the last step, acidic hydrolysis and double *O*-methylation led to the racemic natural product *rac*-**4**. Overall, *rac*-isokotanin A *rac*-(**4**) was obtained in four steps with 13% overall yield.

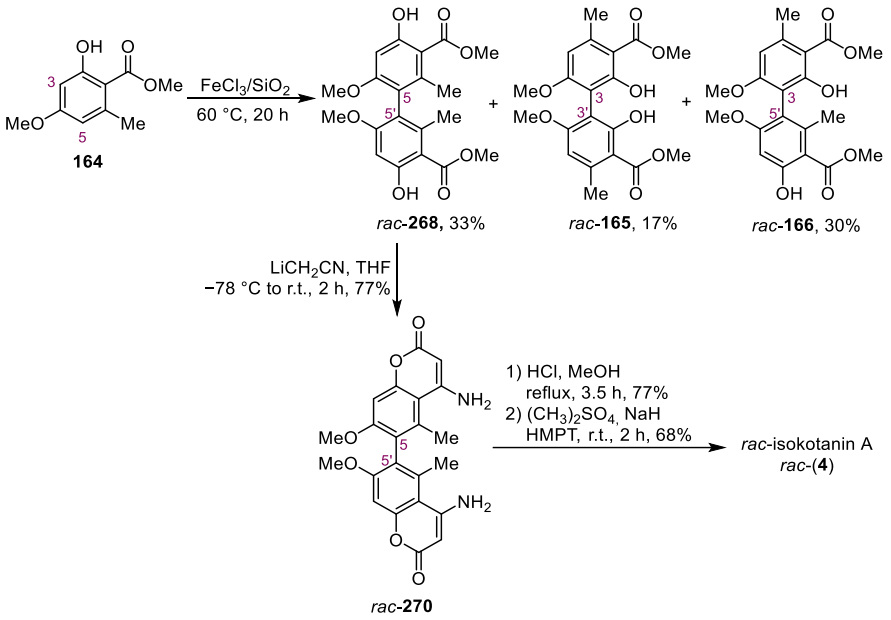

Scheme 42 Racemic total synthesis towards *rac*-isokotanin A *rac*-(**4**) by *Müller et al.*[38]

6 Results and Discussion

6.1 Synthesis of axially chiral biphenol building block *rac*-1

For the investigation of atroposelective synthesis of tetra-*ortho*-substituted biphenols, one important axially chiral building block has been chosen. Biphenol *rac*-**1** represents a common biphenyl motif, which can be found in various bioactive aromatic dimeric natural products, like isokotanin A–C[180], gonytolide A[183] or viriditoxin[184]. The broad applicability and synthetic challenge make the investigation towards the atroposelective construction of *rac*-**1** very attractive. In the following chapter, the racemic synthesis of *rac*-**1** is described, which is based on the work of *Julian Greb* and *Till Drennhaus*.[1, 185] This represents a more robust, scalable and efficient way towards *rac*-**1**, in comparison to former reported procedures (Scheme 43).[182, 186-189]

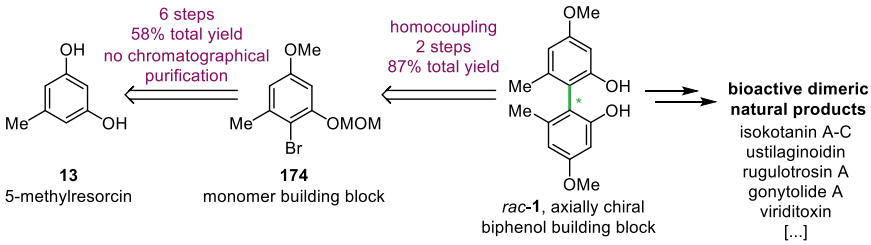

Scheme 43 Overview of the synthesis of axially chiral 2,2′-biphenol building block *rac*-**1**.

The challenging construction of the tetra-*ortho*-substituted biphenyl axis was to be performed by a homocoupling of MOM-protected bromophenol **174**. The monomer building block **174** was to be obtained by a six-step synthesis from commercially available and cheap 5-methylresorcin (**13**). The preparation was known to be scalable and efficient, as no chromatographical purification would be needed. By the robust synthesis route towards bromophenol **174**, challenges of late-stage introductions of the desired 1,3,5-substitution pattern could be overcome. The synthesis of the monomeric unit bromophenol **174** was carried out according to the scalable method of *Greb et al.* (Scheme 44).[1] In the first step a permethylation of the commercially available orcinol **13** was performed in the presence of dimethyl sulfate (DMS) and potassium carbonate in 98% yield on a 15 g scale. Afterwards the synthesized dimethyl orcinol **167** was mono-demethylated towards **168**. Herein, a highly selective mono methylether cleavage took place using sodium *n*-propyl thiolate in DMF. After the first demethylation, the generated negatively charged phenolate restricts a subsequent nucleophilic attack by sodium *n*-propyl thiolate.[190, 191] Purification *via*

distillation facilitated an efficient and scalable way to isolate desired phenol **168** in high purity and in 86% yield. In the next step, a regioselective bromination of phenol **168** in 2-position was required for later homocoupling. Here, the established method of *O*-acetylation followed by bromination of phenol **168** led to a mixture of mono-brominated regioisomers **170** and **171**.[1] The introduction of an acetyl group facilitated better regio-control towards the bromination products **170** and **171** (~1:6). The crude mixture was deprotected in the presence of sodium carbonate in methanol affording a mixture of the free bromophenols **172** and **173**. The regioisomers were separated *via* distillation, affording 73% isolated yield of the desired 2-bromophenol **172** and 13% of its regioisomer **173**. Finally, **172** was protected with the MOM and EOM protecting groups, giving final products **174** and **175** respectively in six steps with an excellent overall yield (58%) with no chromatographic purification required. In the next step, two different synthetic methods were used for the racemic homocoupling towards tetra-*ortho*-substituted biphenol *rac*-**1**, which were developed by *Greb et al*.[1, 2]

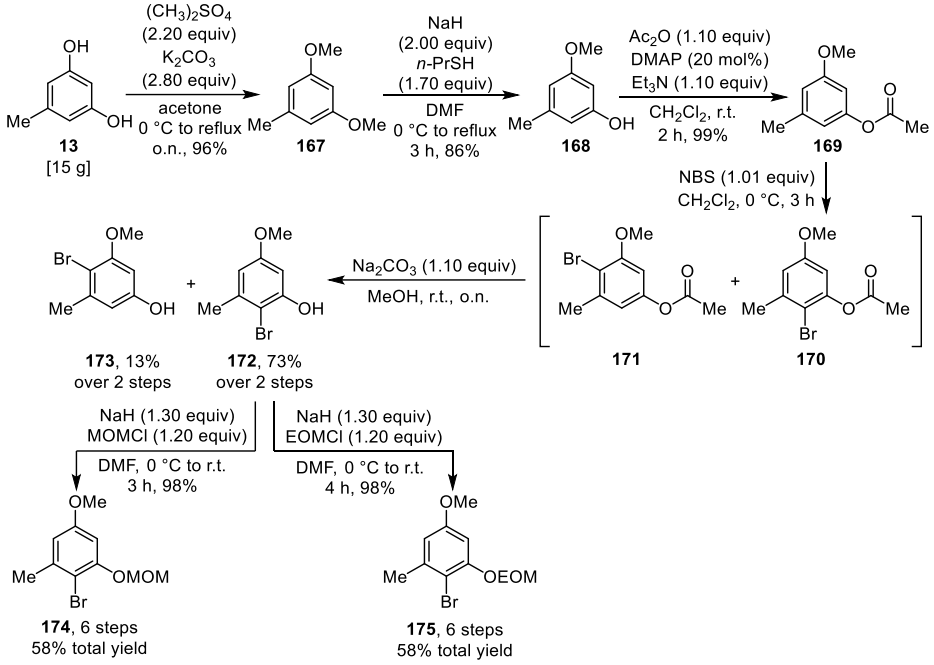

Scheme 44 Synthesis of MOM- and EOM-protected bromophenol **174** and **175**.

In both methods, the application of the MOM- and EOM-protected bromophenol **174** and **175** were compared. The chosen MOM group was advantageous as it coordinates alkyl-

lithium species in the *Lipshutz* homocouplings, and can be easily removed under acidic conditions.[192] However, for the introduction of the MOM group (chloromethyl)-methylether is used, which is reported to be highly carcinogenic. Traces of highly carcinogenic bis(chloromethyl)ether, which is a byproduct of its production may be present in the reagent.[193, 194] To reduce the risks, the use of the less hazardous EOM group was compared.

In the first step, the homocoupling *via* an oxidation of a *Lipshutz* cuprate was performed (Scheme 45).[1] A halogen-metal exchange with *tert*-butyllithium and the subsequent addition of copper(I)cyanide di-lithium chloride solution led to the formation of the cyano cuprate $Ar_2Cu(CN)Li_2$. Oxidation of the cuprate with tetra-*tert*-butyldiphenoquinone (DPQ) (**179**) generated the sterically demanding biaryl bond in *rac*-**176a–b**. Here, the reduced byproduct $DPQH_2$ **180** could be recycled by reoxidation under alkaline conditions towards DPQ **179**. Main side reactions were protodehalogenation towards **177a–b** and oxidation towards **178a–b**. When using MOM-protected bromophenol **174**, biaryl *rac*-**176a** was obtained in 87%. However, when changing to EOM-protected bromophenol **175** the conversion towards homocoupling decreased (52%), leading to a 1:1 mixture of product and side products. This might be caused by the increased steric hindrance of the ethyl group during metal coordination, which might result in lower reactivity towards the cuprate.

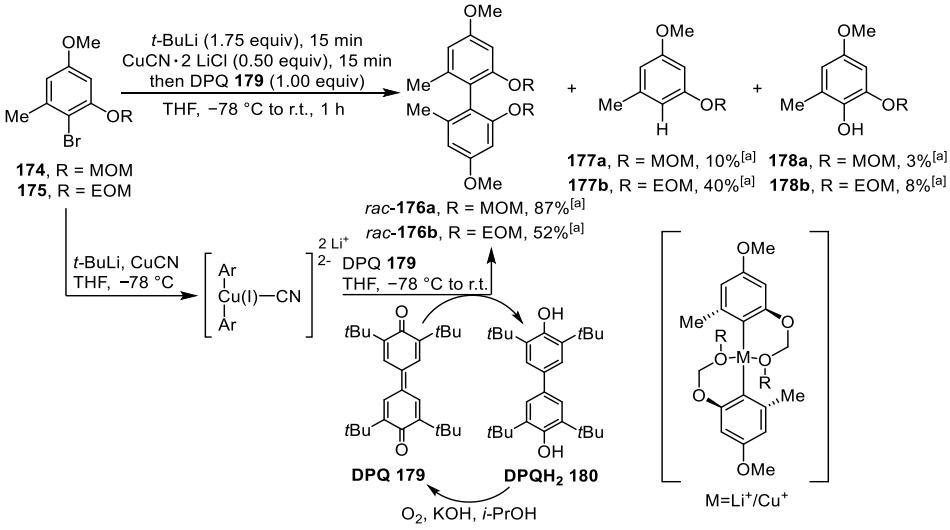

Scheme 45 Homocoupling *via Lipshutz* cuprate towards tetra-*ortho*-substituted 2,2′-biphenyl *rac*-**176a–b**; [a] Conversions were determined *via* ^{1}H-NMR.

The second method for the formation of the tetra-*ortho*-substituted biaryl *rac*-**176a–b** was a one pot MBSC (Scheme 46).[2] For the MBSC, *Buchwald*'s G4 SPhos precatalyst (SPhos

PdG4) (2.50 mol%),[195-197] combined with SPhos as ligand, was applied as the palladium source in a THF/water mixture (4:1). In comparison to other common palladium sources, the use of the precatalyst SPhosPdG4 was reported not to lead to any formation of palladium black,[2] resulting in higher activities towards the desired product. K_3PO_4 was used for catalyst activation. The reaction mixture was heated up to 70 °C and a solution of bis(pinacolato)diboron (B_2pin_2) in THF was added dropwise *via* syringe pump. Slow addition prevented the hydrolysis of B_2pin_2.[198] After 16 hours the conversion was observed *via* ^{1}H-NMR. When residues of bromophenol **174** or **175** were still visible, further 0.55 equiv B_2pin_2 with respect to the remaining starting material was added. When using MOM-protected bromophenol **174**, homocoupling product *rac*-**176a** was formed in 73%, while protodehalogenated phenol **177a** was obtained in 21%. Analogously to the *Lipshutz* homocoupling, the EOM-protected bromophenol **175** led to a decreased conversion of 49% towards the biaryl *rac*-**176b** and a higher conversion of protodehalogenated product **177b**.

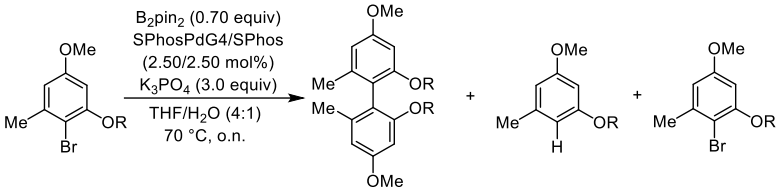

Scheme 46 One-pot MBSC sequence for the synthesis of tetra-*ortho*-substituted 2,2′-biphenyl *rac*-**176a–b**; [a] Conversions were determined *via* ^{1}H-NMR.

Despite the lower risk of using an EOM protecting group rather than a MOM protecting group, MOM-protected bromophenol **174** showed in both coupling procedures higher reactivities towards the desired homocoupling. Therefore, both coupling reactions were scaled up, starting from MOM-protected bromophenol **174**. The desired biaryl *rac*-**176a** could be isolated in 83% yield from the *Lipshutz* coupling on a 19.15 mmol-scale and in 68% yield from the MBSC on a 5 mmol-scale. In general, both homocoupling reactions proved to be robust and scalable methods for the construction of tetra-*ortho*-substituted biaryl *rac*-**176a**. However, the one pot MBSC showed several advantages. In contrast to the *Lipshutz* coupling, the MBSC reaction is less hazardous, as only catalytic amount of palladium is used instead of the stoichiometric application of organolithium reagents and copper cyanide. The handling and removal of high amount of *tert*-butyllithium, copper cyanide and DPQ **179** required caution.

In the last step, the isolated biphenyl *rac*-**176a** was deprotected under acidic conditions in quantitative yield (Scheme 47). Overall, the 2,2′-biphenol building block *rac*-**1** was obtained in up to 50% total yield over eight steps starting from commercially available orcinol **13**.

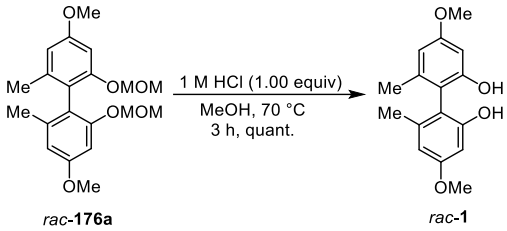

rac-**176a** *rac*-**1**

Scheme 47 Deprotection towards free tetra-*ortho*-substituted 2,2′-biphenol *rac*-**1**.

Summary Chapter 6.1

1. Synthesis of monomer building block **174** and **175**:
   - 58% total yield in six steps without chromatographical purification

2. For both homocoupling methods MOM proved to be a better protecting group than EOM:
   - Homocoupling *via Lipshutz* cuprate: 87% yield (MOM) vs. 52% yield (EOM)
   - MBSC sequence: 73% yield (MOM) vs. 49% yield (EOM)

3. Free biphenol *rac*-**1** could be obtained in up to 50% yield in eight steps.

6.2 Enzymatic kinetic resolution

To achieve the atroposelective synthesis of the important 2,2′-biphenol building block **1**, an EKR method was developed. In this chapter, the investigations towards the enzymatic hydrolysis of axially chiral biphenyl diesters are discussed. A screening of different hydrolases was conducted to convert diesters of the building block **1**. The sequential reaction towards the monoester and free biphenol was analyzed with the help of ^{1}H-NMR and chiral HPLC. In this study the influence of different variables, such as the ester alkyl chain length, cosolvent and pH value, was investigated. Kinetic studies of the sequential KR were performed to give better understanding of the enzyme's activity and selectivity towards substrate, intermediate, and product.

6.2.1 Synthesis of biphenyl diesters 181a–e and monoesters 182a–e

In the first step, a set of linear fatty acid diesters *rac*-**181a–e** and their corresponding monoesters *rac*-**182a–e**, both ranging from acetate to hexanoate, were synthesized starting from biphenol *rac*-**1** (Table 1). Both diesters and monoesters were obtained as a mixture in a single reaction, in the presence of 1.50 equiv anhydride, and isolated through column chromatography.

Table 1 Synthesis of linear fatty acid diesters *rac*-**181a–e** and monoesters *rac*-**182a–e**.

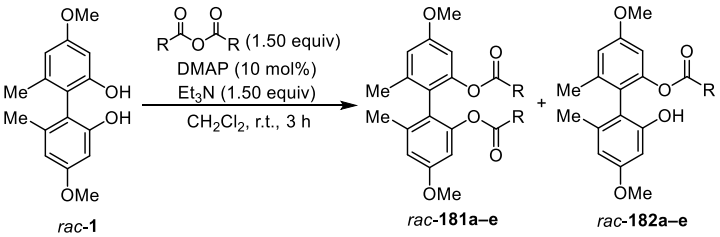

Entry	R	*rac*-181a–e [%][a]	*rac*-182a–e [%][a]
1	Me	67	33
2	Et	52	10
3	*n*-Pr	33	12
4	*n*-Bu	39	17
5	*n*-Pe	32	44

[a] Isolated yields.

All ten substrates were prepared in low to moderate yields. The isolated yield of the monoesters *rac*-**182a–e** was for the most part lower than the yields of the corresponding diesters *rac*-**181a–e**. Subsequently, the isolated substrates were used for the enzyme screening and served as reference compounds for the analysis of the enantioselectivities *via* chiral HPLC. HPLC separation methods for the respective diesters, monoesters and biphenol were developed by *Birgit Henßen* and are reported in the experimental part.

6.2.2 Enzyme screening of commercially available hydrolases

A screening of 14 commercially available hydrolases was carried out for the hydrolysis of biphenyl diesters *rac*-**181a–e** towards monoesters **182a–e** and biphenol **1** (Table 2). The specific enzyme activities of all hydrolases were first determined based on the hydrolysis of *p*-nitrophenyl hexanoate.[199] All information about the specific enzyme activities and suppliers is given in Table 19. The initial screening was performed on a scale of 1 mg of substrates *rac*-**181a–e** in a two-phase system (MTBE/0.1 M KP_i-buffer, pH=7.4; 1:1) at 40 °C. Conversions were determined *via* ^{1}H-NMR after 48 hours (Table 2).

Table 2 Enzyme screening of biphenyl diesters *rac*-**181a–e** in a two-phase system.

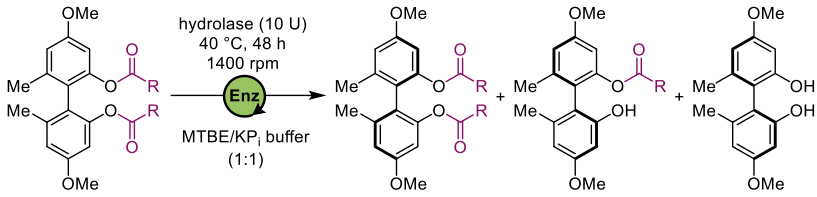

Entry	Hydrolase	Conversion of *rac*-181a–e[a]				
		Me	Et	*n*-Pr	*n*-Bu	*n*-Pe
1	*Aspergillus niger* lipase[b]	36	14	0	0	0
2	*Candida cylindracea* lipase	33	20	32	7	0
3[c]	Cholesterol esterase from porcine pancreas	61	22	46	7	8
4	Lipase from porcine pancreas	0	0	0	0	0
5	Esterase from porcine liver	0	0	0	0	0
6	*Pseudomonas* lipase (LPL 311)	0	0	0	0	0
7	*Pseudomonas cepacia* lipase	0	0	0	0	0
8	*Mucor javanicus* lipase	0	0	0	0	0
19	*Rhizopus niveus* lipase	0	0	0	0	0
10	*Rhizopus oryzae* lipase	0	0	0	0	0
11	*Rhizopus oryzae* esterase	0	0	0	0	0
12	*Burkholderia cepacia* lipase	0	0	0	0	0
13[c]	*Candida antarctica* lipase	0	0	0	0	0
14	Pancreatin from porcine pancreas	0	0	0	0	0

Conversion legend:

0	1-10	11-20	21-30	31-40	41-50	51-60	61-70	71-80	81-90	91-100

Hydrolase (10 U), 40 °C, 48 h, 1400 rpm, in MTBE/KP_i-buffer (pH=7.4) (1:1); [a] Conversion of *rac*-**181a–e** towards **182a–e** and **1** was determined *via* ^{1}H-NMR; [b] Only 3 U of ANL was used; [c] While other hydrolases were provided as lysates, CEPP was used as a purified enzyme and CAL-B was used as an immobilized lipase.

The results of the screening show that only three hydrolases exhibited activity towards the hydrolysis of the different biphenyl diester *rac*-**181a–e**, namely *Aspergillus niger* lipase (ANL) (entry 1), *Candida cylindracea* lipase (CCL) (entry 2), and Cholesterol esterase from porcine pancreas (CEPP) (entry 3). All other hydrolases showed no hydrolytic activity towards the substrate, hinting at the challenging enzymatic conversion of tetra-*ortho*-substituted biphenyls. While ANL only accepted diacetate *rac*-**181a** and dipropionate *rac*-**181b**, CCL and CEPP converted a broader range of substrate. However, lower conversions of substrates with longer ester chain lengths C ≥ 5 were observed for both. CEPP exhibited the highest conversions, resulting in the hydrolysis of diacetate *rac*-**181a** in 61% and of dibutyrate *rac*-**181c** in 46%.

In the next step, the enantioselectivities of the hydrolysis using the three active hydrolases were thoroughly investigated. Therefore, the crude product was analyzed to determine the product ratios and enantiomeric excesses of all three substrates. These results and the calculated E_1-values of the respective conversions of diesters **181a–e** are shown in Figure 10. As this enzymatic process consists of two sequential steps towards biphenol **1**, two E-values were needed for the complete description of the whole reaction. In the first step, enantioselectivity E_1 of the first hydrolysis step was used as a measure for the KR efficiency. In later steps the enantioselectivity E_2 of the second hydrolysis step was analyzed afterwards. The E_1-value was calculated by the conversion and enantiomeric excess of recovered starting material *rac*-**181a–e**.[35, 199] Indeed, Figure 10 shows that the choice of chain length had not only a profound influence on the enzyme's activity, but also on the respective enantioselectivity. ANL exhibited moderate to good conversions of diacetate *rac*-**181a** and dipropionate *rac*-**181b** but displayed low enantioselectivities ($E_1 = 3$ or $E_1 = 2$). A cutout of the ^{1}H-NMR spectrum and HPLC chromatogram of the crude product of diacetate *rac*-**181a** is shown exemplarily in Figure 11 and Figure 12. Similar behavior could be observed in the hydrolysis of diacetate *rac*-**181a** with CCL ($E_1 = 5$). Interestingly, the application of dipropionate *rac*-**181b** resulted in a significant increase in enantioselectivity ($E_1 = 66$). However, the presence of one additional methylene group on the ester side chain (*rac*-**181c**) resulted in decreased enantioselectivities again ($E_1 = 34$). Besides the activities, the enantioselectivities of CCL towards longer chained substrates (*rac*-**181d–e**) were rather low ($E_1 < 4$). Although CEPP exhibited high activities towards the hydrolysis of diacetate *rac*-**181a** and dibutyrate *rac*-**181c**, low enantioselectivities were observed for all substrates ($E_1 < 17$). Hence, after the enzyme screening CCL in

combination with dipropionate *rac*-**181b** was chosen to proceed with, as here the highest enantioselectivity was determined (E_1 = 66).

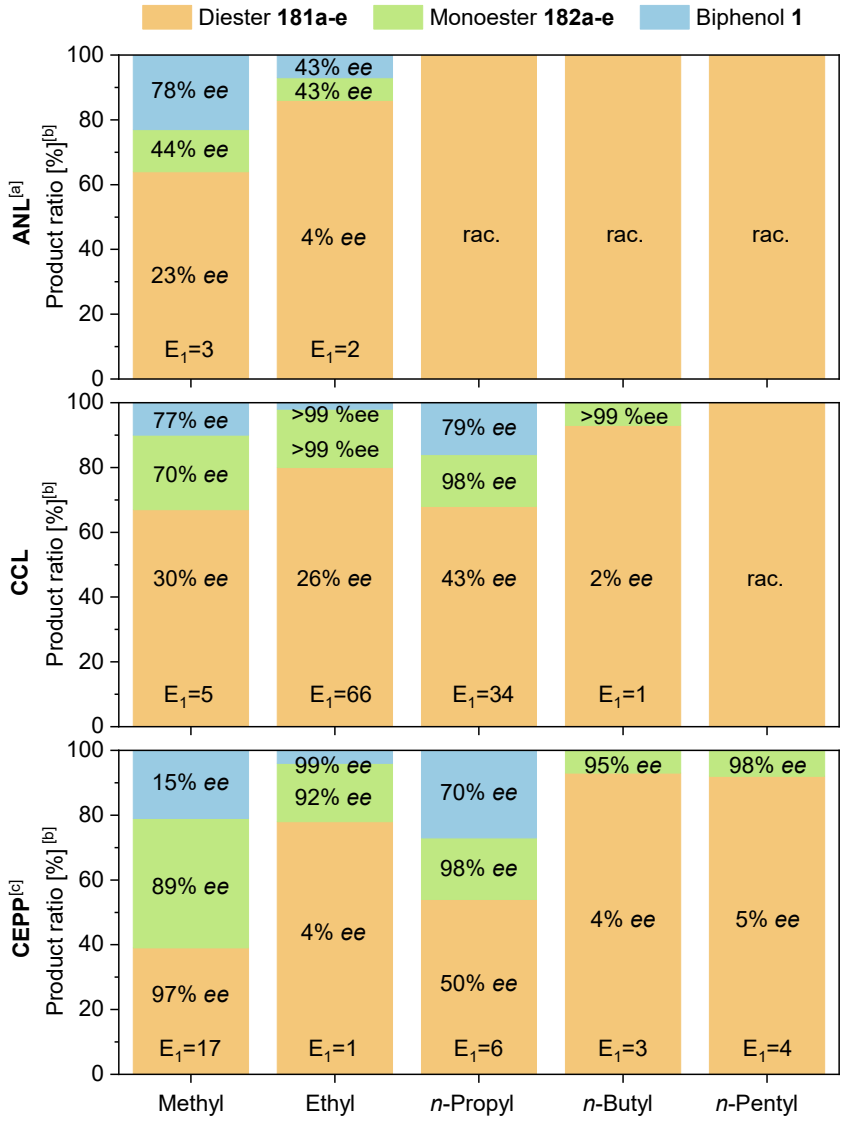

Figure 10 Enantioselectivities of enzymatic hydrolysis with *Aspergillus niger* lipase (ANL), *Candida cylindracea* lipase (CCL) and Cholesterol esterase from porcine pancreas (CEPP); Hydrolase (10 U), 40 °C, 48 h, 1400 rpm, in MTBE/KP_i-buffer (pH=7.4) (1:1); E_1-value was determined by the conversion and *ee* of the recovered diester; [a] Only 3 U of ANL was used; [b] Product ratio was determined *via* ^{1}H-NMR; *ee* was determined *via* chiral HPLC; [c] While other hydrolases were provided as lysates, CEPP was used as a purified enzyme.

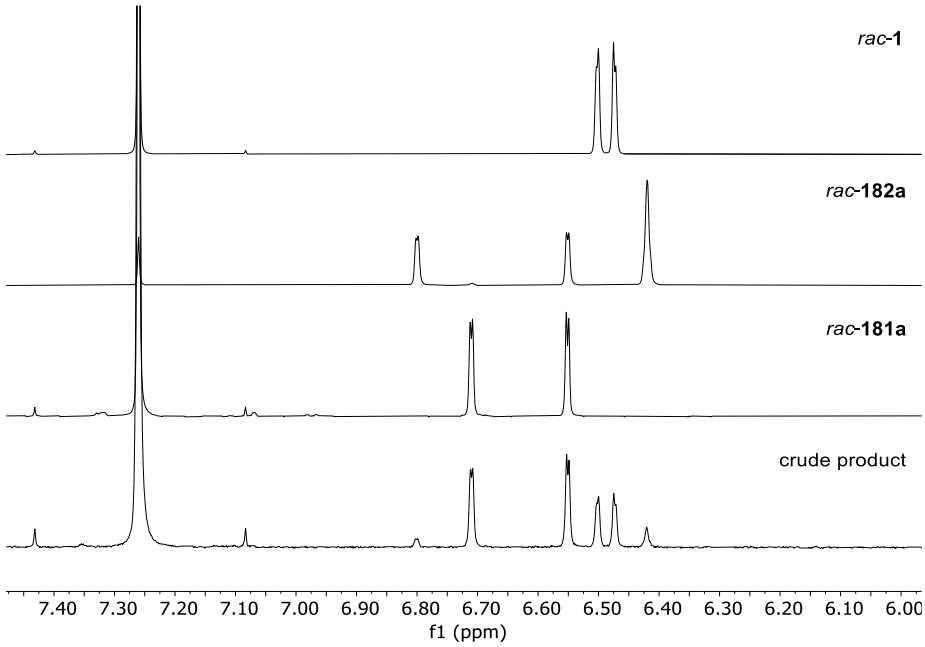

Figure 11 Cutout of stacked ^{1}H-NMR spectra in $CDCl_3$ of crude product of ANL-catalyzed hydrolysis of *rac*-**181a** and the reference products *rac*-**181a**, *rac*-**181b** and *rac*-**1**.

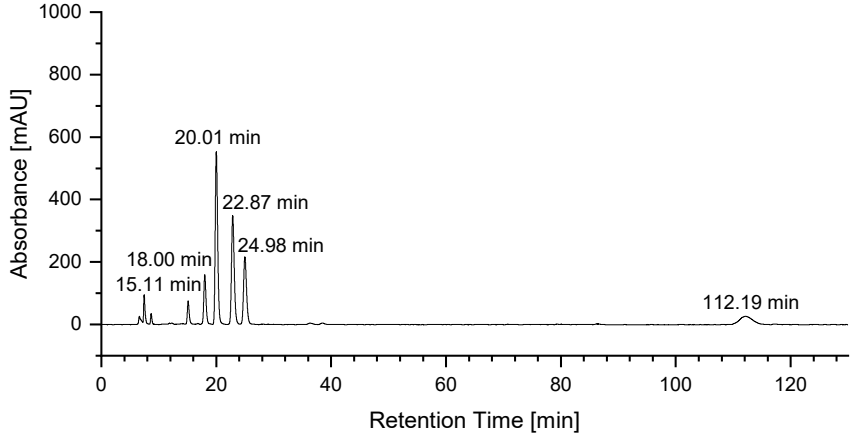

	t_{R1} [min]	Area [mAu*min]	t_{R2} [min]	Area [mAu*min]	*ee* [%]
181a	20.01	272.95	22.87	190.56	23
182a	15.11	27.35	18.00	70.07	44
1	24.98	127.89	112.19	73.08	78

Figure 12 HPLC chromatogram of crude product of ANL-catalyzed hydrolysis of *rac*-**181a**; Column: Chiralpak-IC, *Fa. Daicel* (250x4.6 mm); 5 µL, 25 °C, 0.5 mL/min, 205 nm; solvent: *n*-heptane:2-propanol (90:10).

6.2.3 Assignment of absolute configuration

Before further optimization of the EKR of dipropionate *rac*-**181b** was executed, theabsolute configuration of the different enantiomers was assigned. The enantiomers of biphenol *rac*-**1** were separated *via* preparative HPLC. The method was established by *Birgit Henßen* (Figure 13). Starting from *rac*-**1** (520 mg, 1.9 mmol), both enantiomers (*M*)-**1** (39%, >99% *ee*) and (*P*)-**1** (40%, >99% *ee*) could be isolated in high yields. Comparison of the optical rotation with literature facilitated the assignment of the absolute configuration.[1]

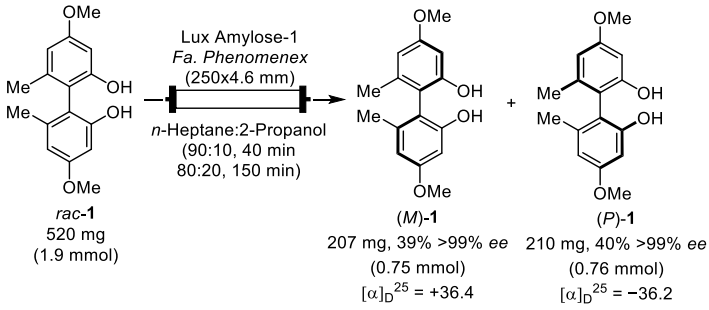

Figure 13 Separation of (*M*)- and (*P*)-**1** on preparative HPLC.

Esterification of the enantiopure biphenol (*P*)**-1** (t_R = 57.18 min) and (*M*)**-1** (t_R = 167.2 min) allowed the assignment of the enantiomers of diester (*M*)**-181b** (t_R = 9.79 min) and (*P*)-**181b** (t_R = 10.62 min) and monoester (*M*)**-182b** (t_R = 21.91 min) and (*P*)**-182b** (t_R = 35.45 min) (Figure 14).

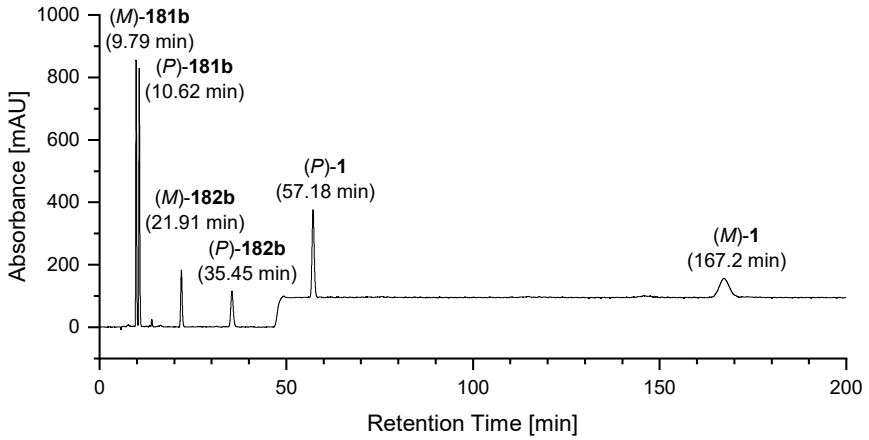

Figure 14 HPLC chromatogram of racemic mixture of *rac*-**1**, *rac*-**181b** and *rac*-**182b**; Column: Lux Amylose-1, *Fa. Phenomenex* (250x4.6 mm); 5 µL, 25 °C, 0.5 mL/min, 274 nm; solvent: *n*-heptane:2-propanol (90:10) for 40 min then (80:20) for 150 min.

6.2.4 Studies of *Candida cylindracea* lipase

In the previous enzyme screening (section 6.2.2), CCL proved to be a suitable lipase for the resolution of axially chiral biphenyl esters. The yeast *Candida cylindracea* is also known as *Candida rugosa* and was reclassified as *Diutina rugosa*.[200, 201] It was applied frequently in several biotransformations and can be found in industrial processes. However, studies in literature revealed problems in reproducibility in the use of this lipase. [200, 202, 203] Based on the current state of knowledge, *Candida rugosa* lipase secretes eight isoenzymes, each of which exhibits different biocatalytic properties such as different selectivities and affinities. Depending on the supplier and their conditions of fermentation, a different lipase loading and isoenzymatic profile is given.[200] Therefore, a comparison was made between the application of CRL obtained from different suppliers for the resolution of dipropionate *rac*-**181b**.

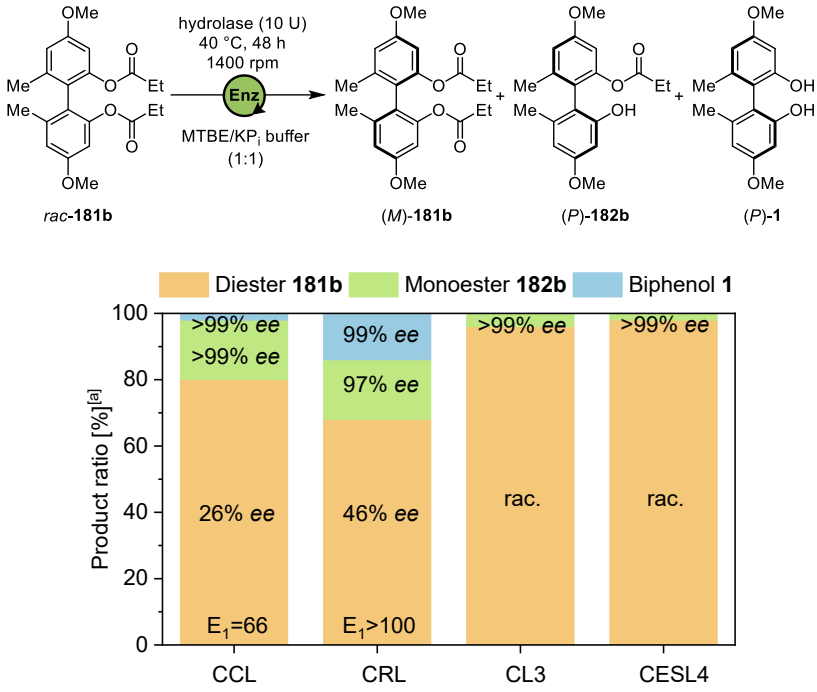

Figure 15 Enzyme screening of *Candida rugosa* lipases from different suppliers; Hydrolase (10 U), 40 °C, 48 h, 1400 rpm, in MTBE/KP_i-buffer (pH=7.4) (1:1); *Candida cylindracea* lipase from *Fluka* (CCL), *Candida rugosa* lipase from *Sigma Aldrich* (CRL), Chirazym L3 from *Roche Diagnostics* (CL3), lipase from *Candida sp.* (CESL4); [a] Product ratio was determined *via* ^{1}H-NMR; *ee* was determined *via* chiral HPLC.

Since the previously used active CCL was no longer manufactured by *Fluka* anymore and is now available under the name *Candida rugosa* lipase (CRL) from *Sigma Aldrich*,[204] a

test reaction was conducted for the enzymatic hydrolysis using the new CRL from *Sigma Aldrich*. Both lipases, CCL and CRL were compared to commercially available CRL from *Roche Diagnostics* (Chirazym L-3, CL3) and a lipase from a *Candida sp.* from *Amano enzymes* (Figure 15). All hydrolases were applied with the same specific enzyme activity (10 U), which was determined before based on the hydrolysis of *p*-nitrophenyl hexanoate (Table 19).[199] Reproducing the results of CCL using CRL from *Sigma Aldrich* was successful. CRL led even to higher conversions at high enantioselectivities ($E_1 > 100$). However, the application of the lipases from *Roche Diagnostics* and *Amano enzymes* (CL3 and CESL4) confirmed the issue of reproducibility. Both lipases CL3 and CESL4 showed poor activity towards the hydrolysis of biphenyl dipropionate *rac*-**181b** compared to the batches of CCL and CRL. This result confirms the hypothesis that different lipase loadings and compositions depend on the supplier and conditions of fermentation. This leads to varying catalytic performance.

This raised the question of the isoenzymatic profile of the applied CRL. This will give a better understanding of the responsible isoenzyme for the enantioselective hydrolysis, as the supplier did not provide any information in this regard. One of the eight isoenzymes of CRL (LIP-3) is characterized as a cholesterol esterase.[200, 205] Therefore, different cholesterol esterases were additionally screened (Figure 16). *Kazlauskas* made use of taurocholate, which is a bile salt activating cholesterol esterases in bovine pancreas by formation of more active dimers and hexamers.[35] Thus, the effect of taurocholate salt as an additive was investigated in combination with lipase from porcine pancreas (PPL) and CCL (Figure 16). Previous enzyme screenings had already shown that CEPP exhibited a good activity, but low enantioselectivity towards substrate *rac*-**181b** ($E_1 = 1$). The application of cholesterol esterase from bovine pancreas (CEBP) resulted in a similar activity and selectivity ($E_1 = 4$). In contrast, a cholesterol esterase from *Pseudomonas fluorescens* (CEPF) did not exhibit any activity towards the hydrolysis of *rac*-**181b**. While PPL without any additive did not result in any conversion of *rac*-**181b**, the addition of taurocholate increased the conversion with good enantioselectivity ($E_1 = 125$). Overall, the results from the cholesterol esterase screening indicated such an enzyme being active in the PPL batch to hydrolyze the biphenyl substrate *rac*-**181b**. However, the addition of taurocholate to CCL did not lead to a significant increase in activity, but to a decrease in selectivity ($E_1 = 7$). This indicates that no cholesterol esterase is probably responsible in the CRL for the enantioselective hydrolysis of *rac*-**181b**.

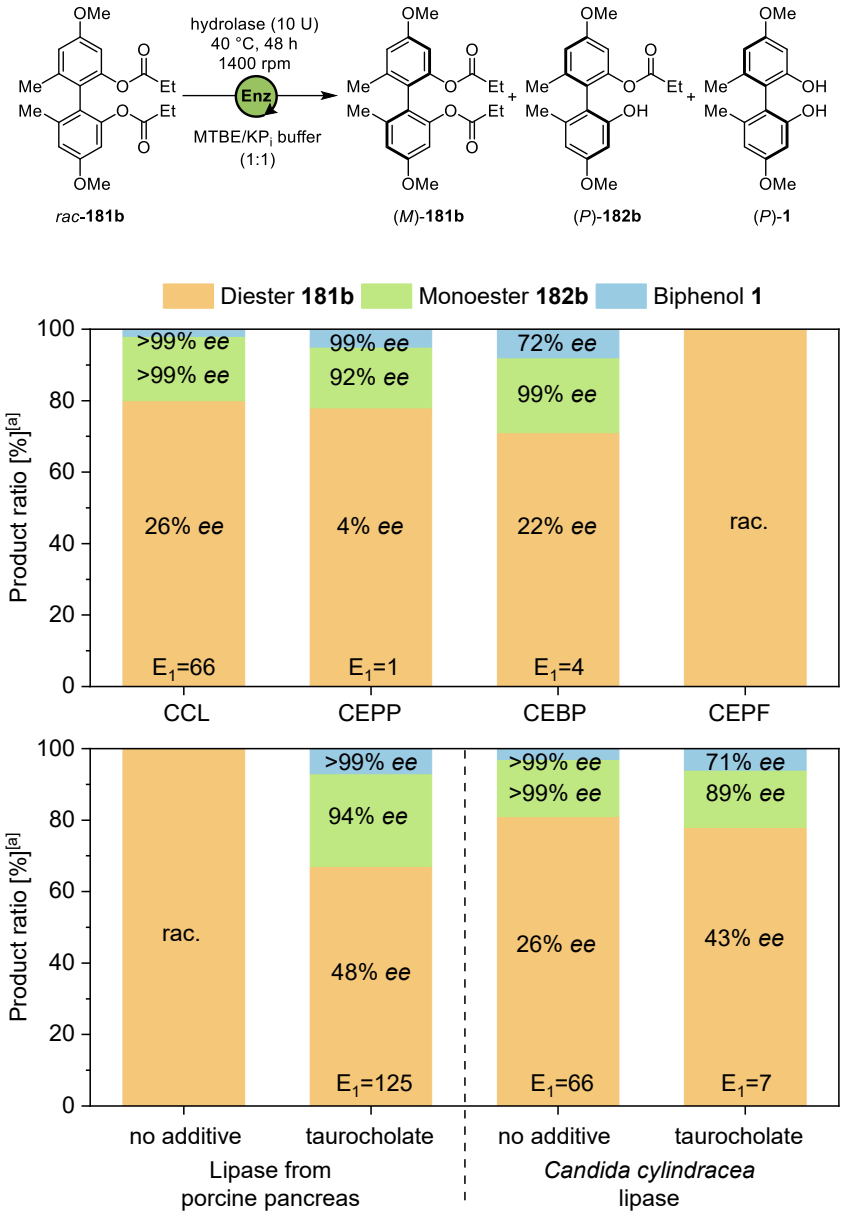

Figure 16 Enzyme screening of different cholesterol esterases and investigation on the effect of addition of taurocholate (0.70 equiv); Hydrolase (10 U), 40 °C, 48 h, 1400 rpm, in MTBE/KP_i-buffer (pH=7.4) (1:1); *Candida cylindracea* lipase from *Fluka* (CCL), Cholesterol esterase from porcine liver (CEPP), Cholesterol esterase from bovine pancreas (CEBP), Cholesterol esterase from *Pseudomonas fluorescens* (CEPF); [a] Product ratio was determined *via* ^{1}H-NMR; *ee* was determined *via* chiral HPLC.

In summary, these investigations revealed the importance of the choice of the specific CRL batch, taking the supplier and their production protocols into consideration. In order to gain

more information about the specific active isoenzyme for this atroposelective biocatalytic process, production and screening of the individual isoenzymes needs to be performed. The combination of PPL and the addition of taurocholate salt would be a possible system for the enzymatic resolution of biphenyl diester *rac*-**181b** as well. However, further optimization was continued using CRL, as here high activity and selectivity was reached without any need for an additive.

6.2.5 Optimization of the enzymatic kinetic resolution

In this section, optimization of the reaction conditions regarding the solvent system was performed. Different two-phase systems of organic solvent and KP_i-buffer (1:1) were tested for the enzymatic hydrolysis of *rac*-**181b**. The results were compared to the one-phase reaction with DMSO (10 vol%) (Figure 17).

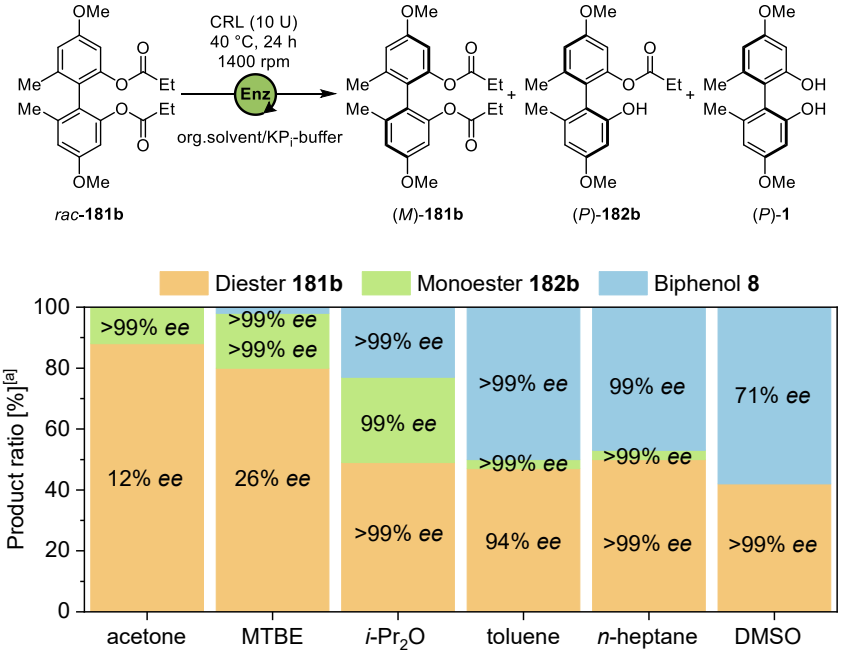

Figure 17 Screening of solvents for EKR: CRL (10 U), 40°C, 24 h, 1400 rpm; Ratio of organic solvent and KP_i-buffer (pH=7.4): 1:1; One-phase reaction was performed with 10 vol% DMSO KP_i-buffer (pH=7.4); [a] Product ratio was determined *via* ^{1}H-NMR; *ee* was determined *via* chiral HPLC.

In general, high enantioselectivities were observed regardless of solvent. However, the choice of cosolvent had a profound influence on the respective enzyme's activity. Solvents

with a higher polarity, like acetone and MTBE led to lower conversions of *rac*-**181b**. This showed the direct correlation between the enzyme activity and the log P of the solvent, which represents the solvent's hydrophobicity. High solvent concentrations with a log P < 4 are more likely to remove the essential water layer around the lipase, affecting the enzymatic activity and leading possibly to protein denaturation.[141, 206-208] In contrast, using more unpolar solvents, such as toluene or *n*-heptane, resulted in higher conversions of around 50%. Here, water-immiscible solvents could lead to no distortion of the water layer, which would keep the enzyme in its active state.[208] The lipase' activity is enhanced in a more hydrophobic surrounding, as unpolar solvents have the characteristics of shifting the equilibrium from a closed to an open conformation of the lipase.[209] In comparison to the two-phase systems, the enzymatic hydrolysis in a one-phase reaction systems with 10 vol% DMSO led to even higher conversion >50%. The enzyme water layer was unlikely to be removed by the low concentration of water-miscible DMSO, which may have affected the enzymes activity.[206, 207]

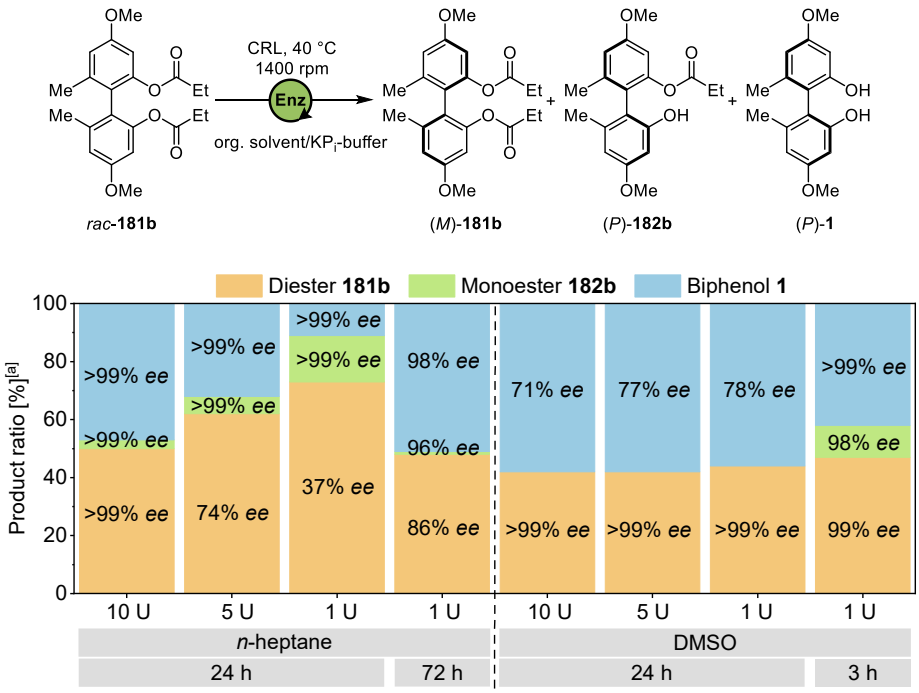

Figure 18 Optimization of enzyme loading for EKR: CRL, 40 °C, 1400 rpm; Two-phase reaction was performed in *n*-heptane and KP_i-buffer (pH=7.4): 1:1; One-phase reaction was performed with 10 vol% DMSO/KP_i-buffer (pH=7.4); [a] Product ratio was determined *via* ^{1}H-NMR; *ee* was determined *via* chiral HPLC.

In the next step, the enzyme loading was optimized in the two solvent systems, which had the highest activities (*n*-heptane and DMSO). Figure 18 shows that in a two-phase system (*n*-heptane:KP_i-buffer) a higher enzyme loading (10 U) was needed for high conversions of 50% within 24 hours. Lowering the enzyme loading to 1 U resulted in a decrease of activity towards the hydrolysis of *rac*-**181b**. When the reaction time was extended to 72 hours, a conversion of around 50% could be reached at a low enzyme loading (1 U). However, in a one-phase system with 10 vol% DMSO, the hydrolytic activity and enantioselectivity remained constant at low enzyme loading (1 U), leading to conversion >50%. The reaction time could be reduced to 3 hours to gain 50% conversion of *rac*-**181b**. Therefore, the application of a low enzyme loading (1 U) in a one-phase system with DMSO as cosolvent (10 vol%) was chosen as the conditions for the EKR of dipropionate *rac*-**181b**.

Finally, the influence of the pH value of the KP_i-buffer was examined. A pH range of 6.5 to 8 was screened in combination with DMSO as a cosolvent (10 vol%). Table 3 demonstrates that the conversion of biphenyl dipropionate *rac*-**181b** was higher at higher pH-values. A conversion rate of 50% could be achieved at a pH of 7 to 8. To ensure consistency of previous optimizations described with these findings, the previously used pH value of 7.4 was maintained for all subsequent reactions.

Table 3 Screening of pH value of KP_i-buffer for EKR.

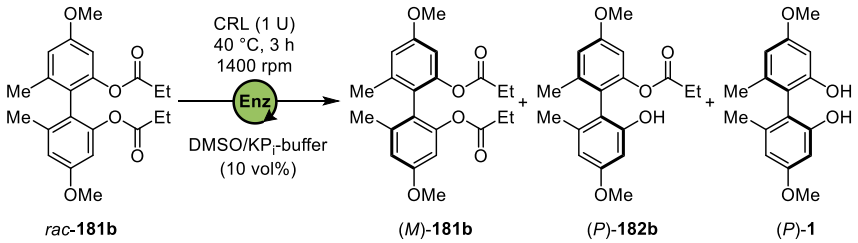

Entry	pH value of KP_i-buffer	Product ratio [%][a]		
		(*M*)-181b	(*P*)-182b	(*P*)-1
1	6.5	68	3	29
2	7	54	2	44
3	8	48	6	46

CRL (1 U), 40 °C, 3 h, 1400 rpm; 10 vol% DMSO/KP_i-buffer; [a] Product ratio was determined *via* ^{1}H-NMR.

6.2.6 Screening of whole cell extracts

Besides commercially available hydrolases, hydrolases as whole cell extracts were provided by *Stephan Thies* and *Alexander Bollinger* from the institute of molecular enzyme technology (IMET, HHU Düsseldorf).[210-212] Eight organic solvent tolerant hydrolases were screened for the hydrolysis of biphenyl dipropionate *rac*-**181b**. A list of all screened hydrolases can be found in Table 20. Among all eight hydrolases only one lipase, specifically (pelB)TB035 from the organism *Pseudomonas aestusnigri*, exhibited hydrolytic activity. Therefore, this lipase was used for further screening of all five biphenyl ester substrates *rac*-**181a–e** (Figure 19). Following the reaction conditions of the reported screening systems for the used hydrolases, the reaction was performed in a one-phase system of DMSO and KP_i-buffer (1:1) and at a lower temperature of 30 °C.[210]

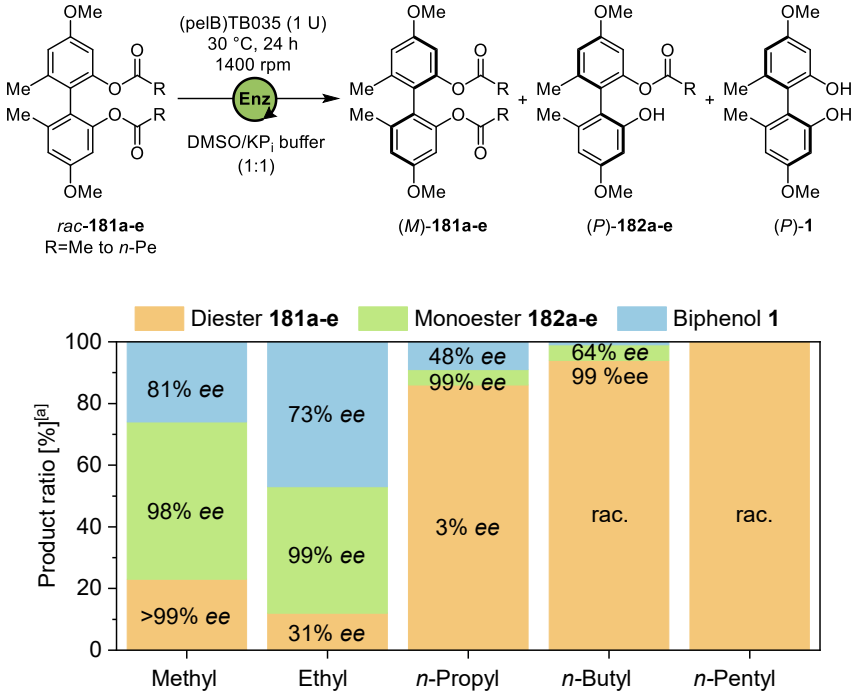

Figure 19 Screening of substrates *rac*-**181a–e** on EKR with (pelB)TB035 (1 U), 30 °C, 24 h, 1400 rpm; Ratio of DMSO and KP_i-buffer (pH=7.4): 1:1; [a] Product ratio was determined *via* ^{1}H-NMR; *ee* was determined *via* chiral HPLC.

The results demonstrate that the hydrolase exhibited greater acceptance of substrates with shorter fatty acid esters. High enantioselectivities of the hydrolysis of diacetate *rac*-**181a** and dipropionate *rac*-**181b** could be observed, leading to a ~1:1 mixture of both products

with high enantiomeric excesses of 73–99% *ee*. Substrates with longer ester chains, however, were converted in low amounts and with poor selectivities. These results show that the hydrolase (pelB)TB035 could be a good candidate for enantioselective conversion of biphenyl substrates. In contrast to the commercially available lipases, the protein sequence of the given hydrolase is known. Thus, further studies focused on this enzyme need to be performed, regarding enzyme engineering towards the optimal conditions.

6.2.7 Scaled up enzymatic kinetic resolution

Based on the optimizations described in the previous chapters, the EKR was performed in a preparative scale (Table 4). The scale was increased in several steps to gain knowledge about practical handling of the enzymatic reaction regarding stirring, work up and isolation.

Table 4 Enzymatic kinetic resolution of *rac*-**181b** in different scales.

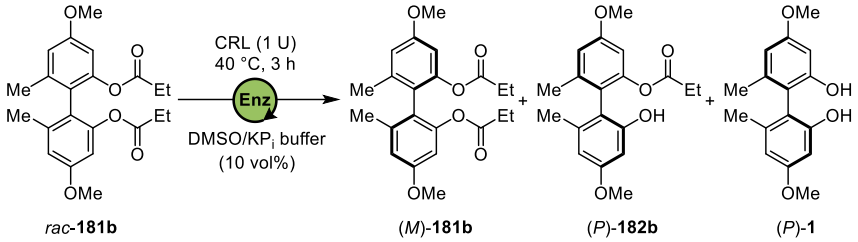

Entry	Scale[a]	181b [%][b]	181b % *ee*[c]	182b [%][b]	182b % *ee*[c]	1 [%][b]	1 % *ee*[c]
1[d]	1 mg	47	99	11	98	42	>99
2[e][f]	50 mg	42 (25)	94	7 (6)	96	51 (34)	99
3[e][g]	200 mg	50 (26)	99	4 (4)	>99	48 (43)	>99
4[e][g]	1 g	44 (43)	99	6 (5)	92	51 (40)	>99

CRL (1 U), 40 °C, 3 h, 10vol% DMSO/KP$_i$-buffer (pH=7.4); [a] Mass of *rac*-**181b**, [b] Conversion was determined *via* ^{1}H-NMR, yields of isolated products are given in parentheses, [c] *ee* was determined *via* chiral HPLC; [d] Reaction was performed in a LockSure Eppendorf vial and shaked in a Thermo-Shaker at 1400 rpm; [e] Reaction was performed in a round bottom flask and stirred with a Teflon coated stirring bar; [f] Direct extraction with EtOAc from crude product; [g] Removal of enzyme by precipitation with ammonium sulfate.

Entry 1 shows the conversions and enantiomeric excesses of the optimized enzymatic hydrolysis of *rac*-**181b** in a 1 mg scale from the screening results. Mixing of the reaction mixture was done by shaking in a Thermo-Shaker. In the next step, the scale was increased by a factor of 50, 200 and 1000. In contrast to the screening reactions, the scaled-up reactions were executed in a round bottom flask with a Teflon coated stirring bar. Racemic

diester *rac*-**181b** and CRL were stirred at 40 °C in a one-phase system of 10 vol% DMSO/KP_i-buffer. Conversions and enantioselectivities remained constant, regardless of the scale of the reaction. However, isolation of the enantiopure products proved to be challenging. In the first step, the enzymatic resolution was performed starting from 50 mg racemic biphenyl dipropionate *rac*-**181b** (entry 2). After 3 hours, the crude product was directly extracted with EtOAc three times, leading to a low combined isolated yield of 65%. Addition of organic solvent to the aqueous enzyme mixture resulted in the formation of an interphase. Products had the tendency to get trapped in the interphase and could not be easily extracted. Therefore, the work up was modified by removing the enzyme before performing the extraction of the products (entry 3–4). After the reaction time, enzyme precipitation was done by the addition of solid ammonium sulfate. The suspension was filtered through a celite pad over a wide Büchner funnel, followed by extensive washing of the precipitate with EtOAc. In this way, the formation of the interphase could be significantly reduced. Afterwards, extraction of the aqueous phase was performed five times, leading to an improved combined isolated yield of 73% or 88% (entry 3–4). Scheme 48 outlines the EKR in preparative scale starting from 1 g *rac*-**181b**, leading to the synthesis of (*M*)- and (*P*)-**1**. After 3 hours, diester (*M*)-**181b** and biphenol (*P*)-**1** could be obtained in 43% and 40% yield with excellent enantiomeric excesses of ≥99% each. The isolated dipropionate (*M*)-**181b** was subjected to alkaline methanolysis, yielding enantiopure biphenol (*M*)-**1** in excellent yield (98%, 99% *ee*). Thus, all in all starting from 1 g (2.6 mmol) biphenyl dipropionate *rac*-**181b** around 280–300 mg (1.0 mmol) of each pure enantiomer of the important building block **1** could be obtained. The assignment of the absolute configuration was confirmed based on the comparison of the optical rotation of isolated biphenol **1** (see section 6.2.3).

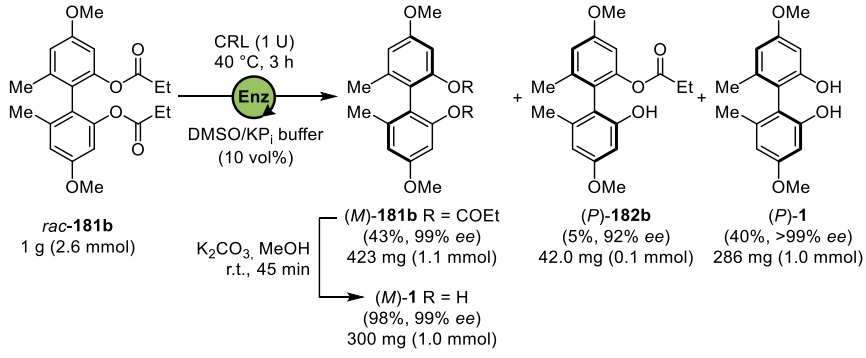

Scheme 48 Scaled up synthesis of (*M*)- and (*P*)-**1**.

6.2.8 Kinetics of the enzymatic kinetic resolution

With the successfully optimized EKR in hand, investigations of the kinetics were to be done. Here, the procedure of *Kazlauskas* was followed.[35, 57] In order to gain a greater understanding about the enantioselectivities of the sequential KR kinetics of both single steps were analyzed separately. Therefore, both enantioselectivities E_1 and E_2 for each step were determined *via* Equation 6 and 7. In the first step, the time-course of the lipase-catalyzed hydrolysis of diester *rac*-**181b** was recorded (Figure 20). As observed before, high conversions of 50% of the starting material *rac*-**181b** were measured after only 3 hours. A gradual increase of the enantiomeric excess to >99% *ee* was determined, while the enantiomeric excess of monoester (*P*)-**182b** and biphenol (*P*)-**1** remained constant at 99% *ee*. The enantioselectivity E_1 was calculated by the enantiomeric excess of diester **181b**, representing the conversion of *rac*-**181b**. For the first step of the EKR, a high enantioselectivity of $E_1 = 80$ was determined, which correlates with the high enantiomeric excess of the recovered starting material (*M*)-**181b**.

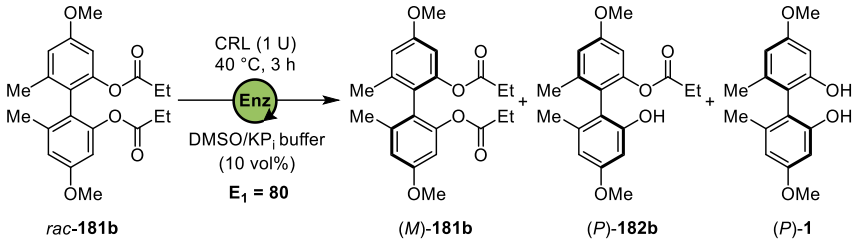

$$E_1 = \frac{\ln[(1-c)\cdot(1-ee_{Diester})]}{\ln[(1-c)\cdot(1+ee_{Diester})]} = 80 \qquad \textbf{Equation 6}$$

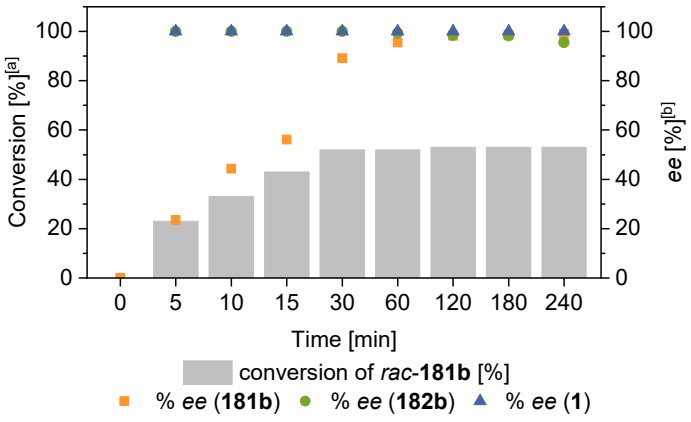

Figure 20 Time-course of EKR of *rac*-**181b**: CRL (1 U), 40 °C, 1400 rpm; 10 vol% DMSO/KP_i-buffer (pH=7.4); [a] Conversion was determined *via* ^{1}H-NMR, [b] *ee* was determined *via* chiral HPLC.

In the second step, the kinetics and enantioselectivities of the second hydrolysis step were analyzed. Thus, racemic monoester *rac*-**182b** was applied as starting material in the enzymatic hydrolysis reaction under the same optimized conditions (Figure 21). The time-course of *rac*-**182b** demonstrates a faster hydrolysis rate in comparison to the diester *rac*-**181b**. After only 1 hour, high conversions of 60% were recorded. However, in contrast to the highly enantioselective first hydrolysis step, a low enantioselectivity of $E_2 = 2$ was determined for the second step, as low enantiomeric excess of both monoester **182b** and biphenol **1** were measured.

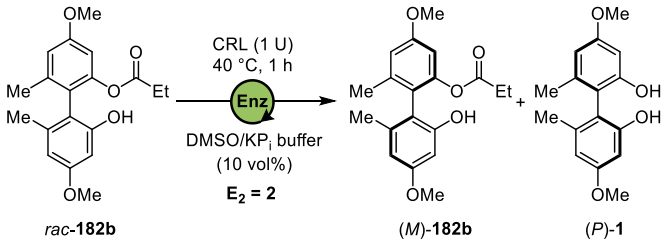

$$E_2 = \frac{\ln\left[(1-c)\cdot(1+ee_{Biphenol})\right]}{\ln\left[(1-c)\cdot(1-ee_{Biphenol})\right]} = 2 \qquad \textbf{Equation 7}$$

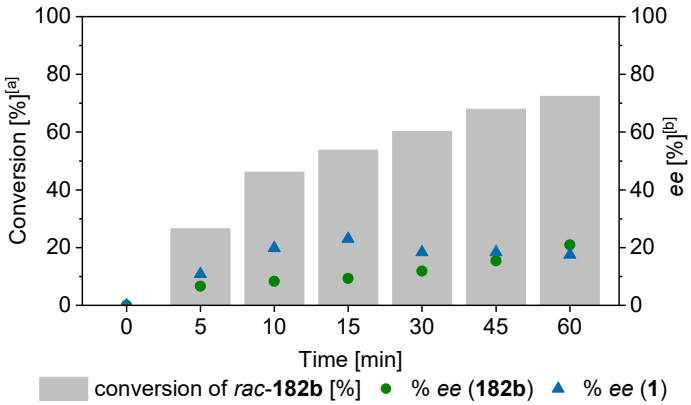

Figure 21 Time-course of EKR of *rac*-**182b**: CRL (1 U), 40 °C, 1400 rpm; 10vol% DMSO/KP_i-buffer (pH=7.4); [a] Conversion was determined *via* ^{1}H-NMR, [b] *ee* was determined *via* chiral HPLC.

Thus, the overall high atroposelectivity is mainly controlled by the first enzymatic hydrolysis step of dipropionate *rac*-**181b**. This result corresponds to the observations of the cholesterol esterase catalyzed resolution of binaphthyl esters published by *Kazlauskas*.[35]

Summary Chapter 6.2

1. Synthesis of five biphenyl diester and monoester substrates for enzyme screening and as reference compounds for chiral HPLC

2. Enzyme screening and optimization of enzymatic kinetic resolution:
   - 3 of 14 commercially available hydrolases exhibited hydrolytic activity towards biphenyl diester.
   - 1 of 8 whole cell extracts (provided by IMET) exhibited hydrolytic activity towards biphenyl diester.
   - CRL-catalyzed hydrolysis of biphenyl dipropionate *rac*-**181b** took place highly enantioselectively.
   - Because of unknown isoenzymatic profile of the lysate, specific CRL needed to be applied, considering supplier and production.
   - EKR showed the highest activity in a one-phase system (1 U CRL in 10 vol% DMSO/KP_i-buffer, pH=7.4)

3. EKR could be successfully scaled up to 1 g-scale:
   - Isolation of (*P*)-biphenol (*P*)-**1**: 40% yield, >99% *ee*
   - Isolation of (*M*)-biphenol (*M*)-**1**: 42% yield, 99% *ee*

4. High atroposelectivity is mainly controlled by the first enzymatic hydrolysis step (E_1 = 80)

6.3 Investigations on dynamic enzymatic kinetic resolution

The successfully optimized EKR facilitates the preparation of both enantiomers of biphenol **1** in excellent optical purity. However, both enantiomers can only be obtained in at most 50% yield. A dynamic enzymatic kinetic resolution (DEKR) brings the advantage of the formation of a single enantiomeric product in 100% theoretical yield. In this chapter the investigations on a DEKR towards enantiopure biphenol **1** are described. Figure 22 shows exemplarily the DEKR, where the enzymatic esterification of the (*P*)-configurated biphenol (*P*)-**1** or monoacetate (*P*)-**182a** takes place faster. The main requirement for a DEKR is the fast racemization of the enantiomeric starting material. Here, possible racemization of 2,2′-biphenol **1** or biphenyl monoester **182a** by redox processes was anticipated.[158, 159, 213] While in the previously established EKR the enzymatic hydrolysis of biphenyl diesters was performed, here the inverse enzymatic esterification of the to be racemized 2,2′-biphenol **1** or biphenyl monoester **182a** was to be developed. The high enantioselectivity of the lipase would lead to the enzymatic conversion of the more favored enantiomer to its monoester or diester at a high reaction rate in ideally 100%.

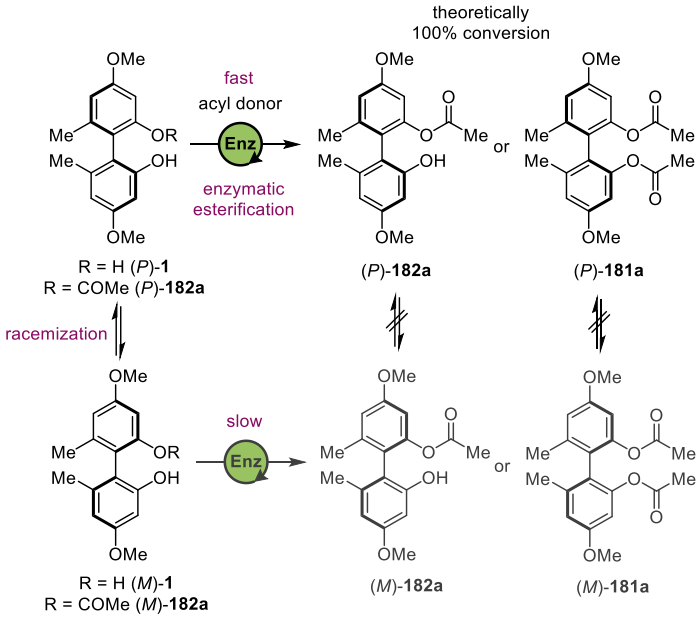

Figure 22 Dynamic enzymatic kinetic resolution of biphenol **1** or **182a**.

In the following, studies towards the atroposelective enzymatic esterification and racemization of 2,2′-biphenol *rac*-**1** or biphenyl monoester **182a** are discussed.

6.3.1 Enzymatic esterification of biphenol *rac*-1 and monoester *rac*-182a

In order to find an enzyme for the enantioselective esterification of biphenyl *rac*-**1** or monoacetate *rac*-**182a**, 13 commercially available hydrolases were screened (Table 5). Here, vinyl acetate was used as an acyl donor for the named acetylation. The reaction was performed in anhydrous toluene and in presence of molecular sieves (4 Å).[155]

Table 5 Enzyme screening for acetylation of biphenol *rac*-**1** and biphenyl monoacetate *rac*-**182a**.

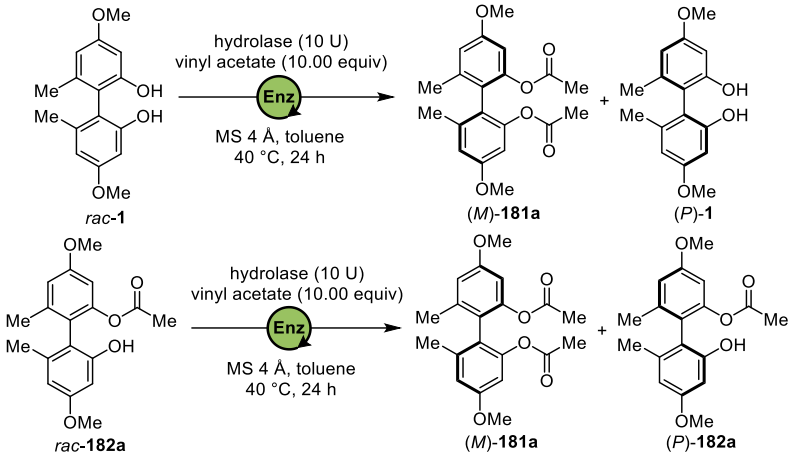

Entry	Hydrolase	Conv. of *rac*-1 [%][a]	Conv. of *rac*-182a [%][a]
1	*Aspergillus niger* lipase[b]	0	n.d.
2	*Candida rugosa* lipase	0	0
4	Lipase from porcine pancreas	0	0
5	Esterase from porcine liver	0	n.d.
6	*Pseudomonas* lipase (LPL 311)	0	0
7	*Pseudomonas cepacia* lipase	0	0
8	*Mucor javanicus* lipase	0	n.d.
9	*Rhizopus niveus* lipase	0	n.d.
10	*Rhizopus oryzae* lipase	0	n.d.
12	*Burkholderia cepacia* lipase	0	0
13[c]	*Candida antarctica* lipase	0	0

Conversion legend:

0	1-10	11-20	21-30	31-40	41-50	51-60	61-70	71-80	81-90	91-100

Hydrolase (10 U), 40 °C, 24 h, 1400 rpm, vinyl acetate (10.00 equiv) in toluene; [a] Conversion was determined *via* ^{1}H-NMR; [b] Only 3 U of ANL was used; [c] While other hydrolases were provided as lysates, CAL-B was used as an immobilized lipase.

After a reaction time of 24 hours none of the tested hydrolases resulted in any conversion towards the esterification products. Since *Candida rugosa* lipase exhibited high hydrolytic activity on the biphenyl diester, more comprehensive screening for the theoretically possible reverse reaction using CRL was conducted. Here, CRL was combined with different acyl donors and bases under the same previous conditions (Table 6).

Table 6 Screening of CRL-catalyzed esterification of biphenol *rac*-**1**.

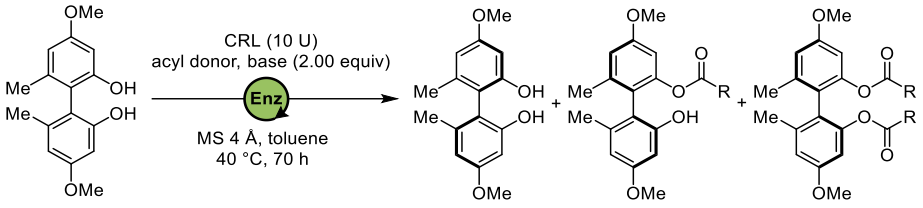

Entry	Acyl donor	Equiv	Base	1 [%][a]	182a–b [%][a]	181a–b [%][a]
1	Vinyl acetate	10	-	100	0	0
2	Vinyl propionate	10	-	100	0	0
3	Isopropyl acetate	10	-	100	0	0
4	Isopropenyl acetate	10	-	97	3	0
5	Isopropenyl acetate	10	Na_2CO_3	91 (7% *ee*)	9 (11% *ee*)	0
6	Isopropenyl acetate	10	K_3PO_4	67 (3% *ee*)	27 (3% *ee*)	7 (rac.)
7[b]	Isopropenyl acetate	10	K_3PO_4	1	54	46
8	4-nitrophenyl acetate	10	-	100	0	0
9	3-chlorophenyl acetate	10	-	96	4	0
10	3-chlorophenyl acetate	20	-	95	5	0
11	3-chlorophenyl acetate	40	-	75 (2% *ee*)	25 (rac.)	0

CRL (10 U), 40 °C, 70 h, 1400 rpm, MS 4 Å, toluene; [a] Conversion was determined *via* ^{1}H-NMR; *ee* was determined *via* chiral HPLC and are given in parenthesis; [b] Reaction was performed without any lipase.

The reaction was monitored *via* ^{1}H-NMR after 70 hours. The application of vinyl acyl donors or isopropenyl acetate is useful, as the tautomerized by-product acetaldehyde or acetone can be released and would lead to an irreversible transformation.[214] However, CRL in combination with the application of acyl donors, like vinyl acetate,[158, 159, 164, 215] vinyl propionate[152] or isopropyl acetate[216] did not result in any conversion towards esterification (entry 1–3). In the presence of isopropenyl acetate[155, 158, 159] low conversion towards biphenyl monoacetate **182a** was observed (entry 4). In order to obtain higher conversions, bases were added to increase the nucleophilicity of the biphenolic hydroxyl

groups and thus facilitate the enzymatic esterification (entry 5–6). The addition of Na_2CO_3 and K_3PO_4 led to higher conversions towards monoacetate **182a**, however with poor enantioselectivities. A negative control reaction, omitting the lipase in the presence of K_3PO_4, proved the competitive non-enzymatic base catalyzed acylation to cause the poor enantioselectivities. In contrast to the enzymatic reaction, the K_3PO_4 catalyzed esterification resulted in high conversions towards a mixture of **181a** and **182a** (entry 7). In the next step, aromatic acyl donors were tested. While the application of 4-nitrophenyl acetate did not lead to any conversions, low amounts of monoacetate **182a** were observed in the presence of 3-chlorophenyl acetate[158, 159, 217] (entry 9). Raising the equivalents of the acyl donor resulted in the formation of monoacetate **182a** in 25%, however in a racemic way (entry 11). As the CRL-catalyzed acylation of biphenol *rac*-**1** proved not to be enantioselective, the second esterification step from the monoester *rac*-**182a** towards diester **181a** was analyzed, envisioning similar high enantioselectivities as in the enzymatic hydrolysis of diester *rac*-**181b**. The enzyme catalyzed esterification of biphenyl monoacetate *rac*-**182a** was performed under the same conditions using those two acyl donors, which showed highest activity towards the desired product before (isopropenyl acetate and 3-chlorophenyl acetate). However, Table 7 shows that CRL did not promote the enzymatic esterification of biphenyl monoacetate *rac*-**182a**.

Table 7 Screening of CRL-catalyzed esterification of biphenyl monoacetate *rac*-**182a**.

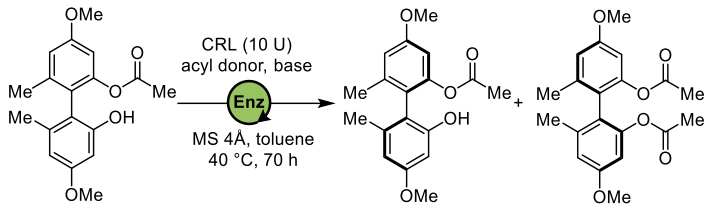

rac-**182a** (*M*)-**182a** (*P*)-**181a**

Entry	Acyldonor	Equiv	Base[a]	182a [%][b]	181a [%][b]
1	Isopropenyl acetate	10	-	100	0
2	3-chlorophenyl acetate	10	-	100	0

CRL (10 U), 40 °C, 70 h, 1400 rpm, MS 4 Å, toluene; [a] Base (2.00 equiv); [b] Conversion was determined *via* ^{1}H-NMR.

Overall, no suitable hydrolase could be found for the enantioselective enzymatic esterification of biphenol *rac*-**1** or biphenyl monoacetate *rac*-**182a**. The use of CRL, which exhibited the highly enantioselective hydrolysis of biphenyl dipropionate *rac*-**181b**,

resulted in the presence of 3-chlorophenyl acetate in the formation of monoacetate **182a** in poor selectivity.

6.3.2 Racemization of biphenol 1

Besides the enzymatic esterification, the racemization of the starting material is essential for the establishment of a DEKR. Therefore, different metal-based catalysts were screened for the racemization of biphenol (*M*)-**1** (Table 8). The enantiopure biphenol (*M*)-**1** was stirred for 24 hours in the presence of the catalyst in toluene at 40 °C. Chiral HPLC was employed to identify a drop in enantiomeric excesses.

Table 8 Screening of catalysts for the racemization of biphenol (*M*)-**1**.

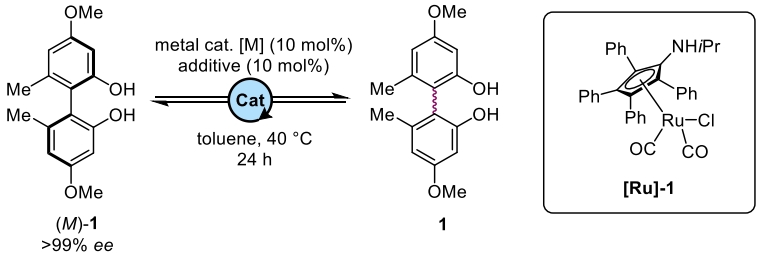

Entry	Metal catalyst [M]	Additive	1 % *ee*[a]
1	$Rh_2(OAc)_4$	-	>99
2	$FeCl_3$	-	Substrate decomposition
3	Pd/C	-	75
4	**[Ru]-1**	-	99
5	**[Ru]-1**	*t*-BuOK	43

[a] *ee* was determined *via* chiral HPLC.

Readily available redox metal catalysts were chosen, which had been used before to racemize chiral alcohols or for the oxidative coupling of naphthols or phenols.[158, 159, 218-220] $Rh_2(OAc)_4$ is a commonly used metal catalyst for the racemization of chiral secondary alcohols *via* hydrogenation transfer.[218] However, $Rh_2(OAc)_4$ was ineffective for the racemization of biphenol (*M*)-**1** (entry 1). Therefore, the goal was to aim a metal-catalyzed single electron transfer towards a radical intermediate, which contains a sp^3 carbon at the chiral axis. This would lead to an elongation of the C-C bond and would facilitate the free rotation around the axis, leading to the desired racemization.[155] In the presence of $FeCl_3$, the starting material (*M*)-**1** decomposed and led to a formation of black solids. This could

be caused by oxidative phenol polymerization. A significant decrease in the enantiomeric excesses of (*M*)-**1** was determined when Pd/C or **[Ru]-1**/*t*-BuOK was used (entry 3 and 5). **[Ru]-1** was developed by *Park et al.* for the racemization of secondary alcohols without the need of hydrogen mediators.[217, 221, 222] In later years, the group of *Akai* utilized the same Ruthenium catalyst for highly efficient racemization of axially chiral binaphthols.[158, 159] Here they described that the addition of *t*-BuOK as a strong base was crucial for the activation of **[Ru]-1**. This corresponds with the results in entry 4–5. The application of **[Ru]-1** in absence of any base led to no decrease in optical purity of (*M*)**-1**. All in all, this screening reveals the possibilities of racemization processes of axially chiral biphenols, which were to be further studied and optimized. For its application in an EKR, a high compatibility with the lipase and high racemization rate needs to be ensured.

Summary Chapter 6.3

1. Enzymatic esterification of biphenol *rac*-**1** and biphenyl monoacetate *rac*-**182a**:
   - 13 commercially available hydrolases were screened for the acetylation with vinyl acetate: No enzymatic activity was observed.
   - CRL-catalyzed esterification with isopropenyl acetate and 3-chloro-phenylacetate exhibited low conversions, with no selectivities.

2. Racemization of biphenol-**1**:
   - Drop in enantiomeric excess of (*M*)**-1** could be observed in the presence of Pd/C or **[Ru]-1** activated by *t*-BuOK.

6.4 Substrate scope of axially chiral biphenols

The EKR using CRL proved to be an efficient and robust method for the atroposelective synthesis of the important biphenol building block **1**. There is, however a great variety of other axially chiral biphenol building blocks that can be used for the synthesis of dimeric natural products or chiral auxiliaries.[66, 223] Therefore, the developed enzymatic resolution method was investigated for its applicability on a broader substrate scope (Scheme 49). The effect of different substituents regarding steric and electronic effects on the resolution was studied.

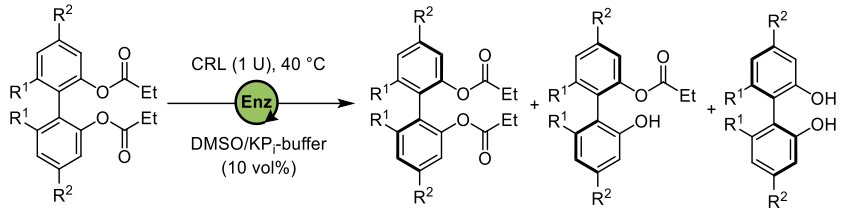

Scheme 49 Enzymatic kinetic resolution on biphenol scope with different *ortho* and *para* substituents.

In the following chapters the synthesis of a substrate scope of tetra-*ortho*-substituted biphenols was performed. Parts of the experiments were carried out in collaboration with *Jacqueline Kühnel* and *Alesia Hysenaj*. A specific library was chosen with different *para*- and *ortho*-substituents, based on the model substrate **1**. Here, substituents were selected with increasing steric hindrance and different electronic effects (Figure 23).

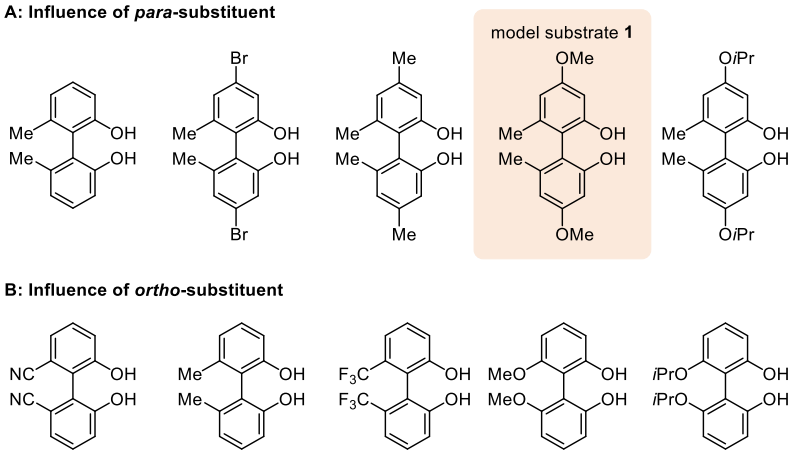

Figure 23 Choice of biphenol scope based on different *ortho*- and *para*-substituents.

Additionally, further tetra-*ortho*-substituted biphenol building blocks were selected, which can be used for further synthesis of dimeric natural products, like kotanin[224] and cupressuflavone[225] or axial chiral phosphine ligands, like SYNPhos[226] and SEGPhos[227] (Figure 24).

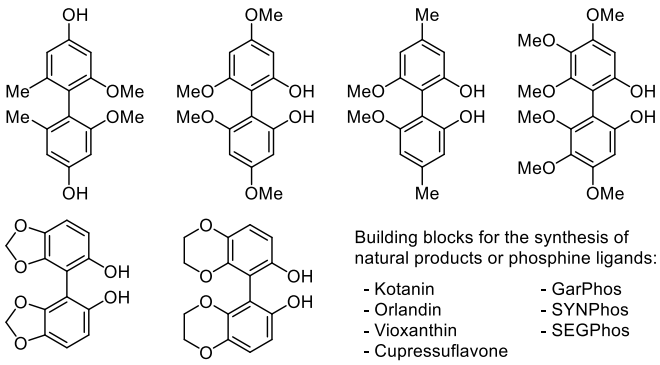

Figure 24 Choice of further biphenol building blocks.

6.4.1 Homocoupling of bromophenols

For the synthesis of the scope of 2,2′-biphenols, the established methods for the homocouplings of MOM-protected bromophenols were intended to be used. While some bromophenols were commercially available, others needed to be synthesized first. Therefore, bromination with NBS were executed starting from the free phenols (Scheme 50). The bromination of unprotected 3,5-dimethylphenol (**183**) led to a mixture of isomers, whereas the desired bromination in 2-position was obtained in 43% yield. The bromination in 4-position and double bromination could be observed as side reactions.[107] Analogously the bromination of 3,5-dimethoxyphenol (**188**) was performed in the presence of NBS and *para*-toluenesulfonic acid, following the procedures of *Jiang et al.* (Scheme 50).[228] The desired bromination in 2-position was obtained 62% conversion. However, the formed regioisomer **190** could not be separated *via* column chromatography. Therefore, as described before in chapter 4.1, a highly regioselective bromination with NBS was executed *via* an *O*-acetylation. This route towards the brominated dimethoxyphenol **189** was described by the group of *Haufe* before.[229] After *O*-acetylation the product **191** could be obtained in 99% yield. Then, bromination and subsequent methanolysis led to formation of the desired brominated product **189** in 98% total yield over two steps.

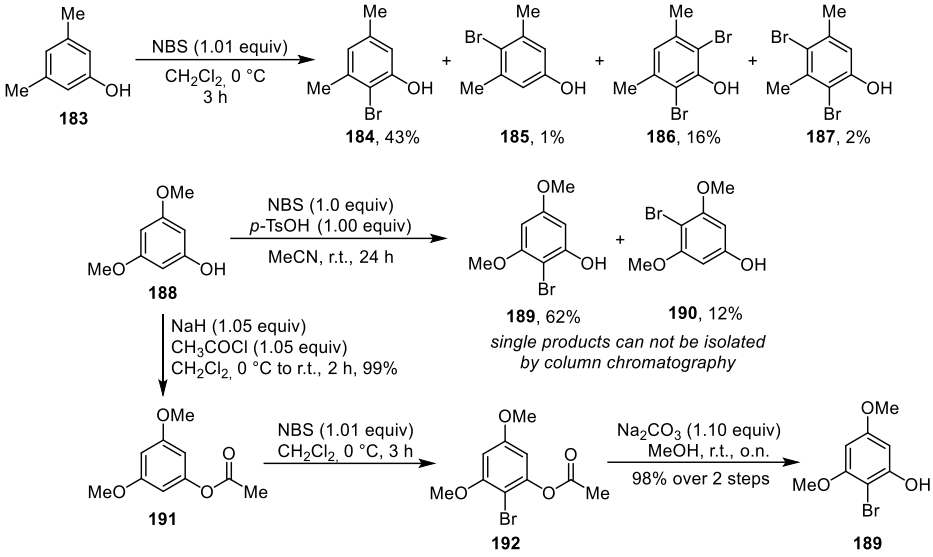

Scheme 50 Bromination with NBS of phenols **183** and **188**.

In the next step, MOM protection of the commercially available and synthesized bromophenols was performed using MOMCl and NaH as a base (Scheme 51). All protected bromophenols **193a–e** were obtained in very good isolated yields of 84–99%. They were used without any purification for the homocoupling towards the respective biaryls.

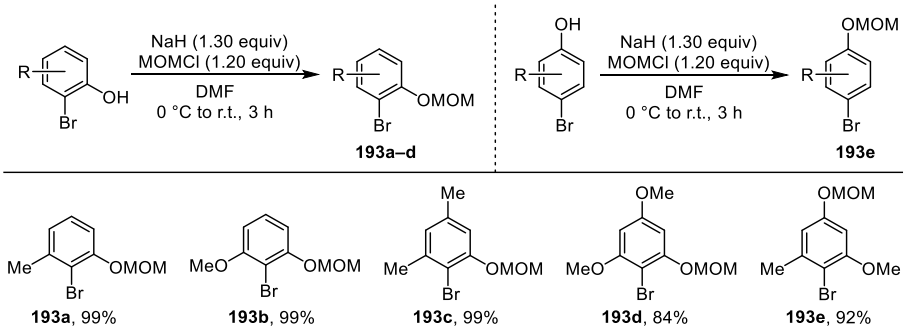

Scheme 51 MOM protection of bromophenols **193a–e**.

In contrast to the previous brominated phenols, the synthesis of brominated 3,4,5-trimethoxyphenol **193f** was performed in a different order (Scheme 52). In the first step, a MOM protection was performed, as this monomer **201d** was needed for the directed *ortho*-metalation described in section 6.4.2. Afterwards treatment with NBS caused a mono-bromination towards **193f** in 92% isolated yield.

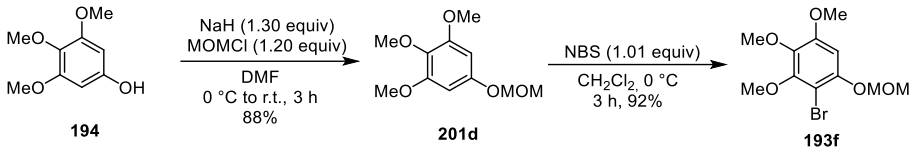

Scheme 52 Bromination of 3,4,5-trimethoxyphenol (**194**).

Furthermore, 2-bromoresorcinol (**195**) was used to synthesize *O*-monoalkylated bromophenols **193g–h**. In the first step, the mono-acetalization with MOMCl or mono alkylation with dimethyl sulfate was tested in the presence of a base (Scheme 53). Here, in both cases a mixture of starting material, mono- and difunctionalized product was obtained. Isolation *via* column chromatography enabled access to monomethylated resorcinol **196** in 32% yield and mono-MOM-protected resorcinol **198** in 34% yield. The selectivity towards the mono-functionalization was for both cases similar. In the second step, a more bulky ether substituent was aimed to be introduced. Therefore, the MOM-protected bromoresorcinol **198** was alkylated with 2-bromopropane and benzylbromide in the presence of potassium carbonate as a base in DMF. Isopropylated bromoresorcinol **193g** was afforded in 64% yield and benzylated bromoresorcinol **193h** in 96% yield.

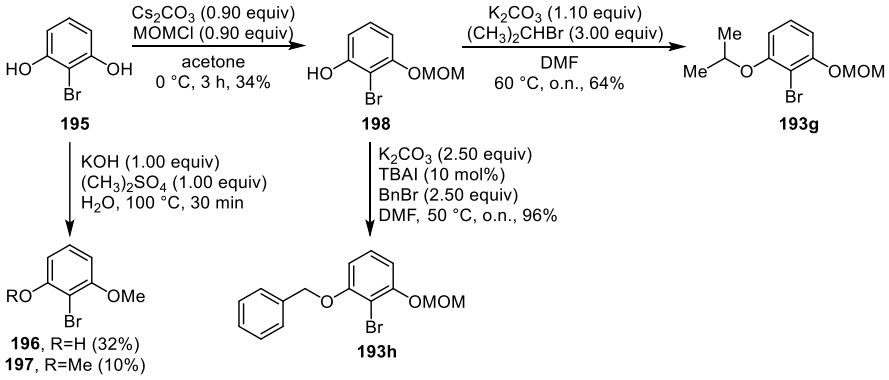

Scheme 53 Synthesis of MOM-protected bromophenol **193g** and **193h**.

With the monomeric bromophenols in hand, the synthesis of the tetra-*ortho*-substituted biphenyls *rac*-**199a–h** was performed. Here, both established methods: *Lipshutz* coupling and MBSC were compared (Scheme 54). The application of methyl- **193a** and **193c** and methoxy-substituted bromophenol **193b** and **193d** resulted in the formation of the desired homocoupling products in 38–66% yield (entry 1–4). While for all previous cases the conversions of both *Lipshutz* coupling and MBSC were similar, a difference could be observed in the formation of *rac*-**199e**, where the MOM-protected hydroxy group was in *para*-

position to the axis (entry 5). Here, the coupling *via* a *Lipshutz* cuprate led to a lower yield, half as high as the MBSC. This might be caused by the absence of the MOM group, as a strong coordinating group in *ortho*-position towards the bromide. Therefore, the coordination of the formed lithiated aryl or cuprate might not be as good, which could lead to a lower conversion towards the oxidation of the *Lipshutz* cuprate. The homocoupling of the electron rich trimethoxy bromophenol **193f** did not result in any conversion (entry 6).

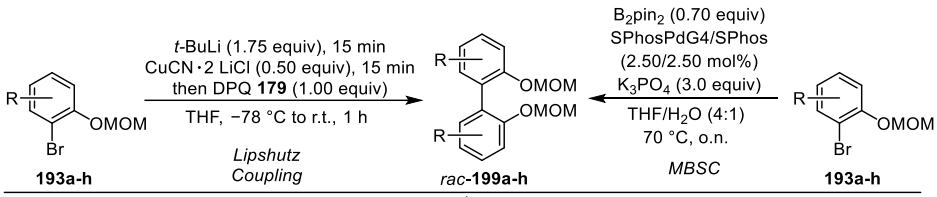

Entry	Substrate	Product	Yield [%][a] *Lipshutz*	Yield [%][a] *MBSC*	Entry	Substrate	Product	Yield [%][a] *Lipshutz*	Yield [%][a] *MBSC*
1	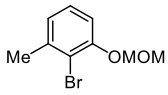 **193a**	*rac*-**199a**	55%	66%	5	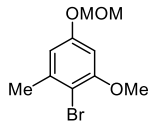 **193e**	*rac*-**199e**	33%	63%
2	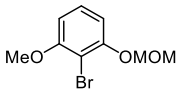 **193b**	*rac*-**199b**	40%	38%	6	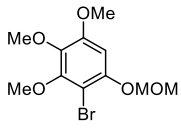 **193f**	*rac*-**199f**	0%	0%
3	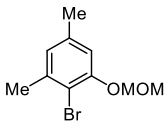 **193c**	*rac*-**199c**	52%	n.d.	7	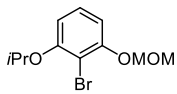 **193g**	*rac*-**199g**	0%	0%
4	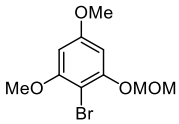 **193d**	*rac*-**199d**	45%	49%	8	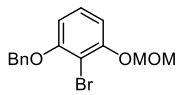 **193h**	*rac*-**199h**	0%	5%

Scheme 54 Substrate scope of tetra-*ortho*-substituted biaryl couplings; [a] Isolated yield.

The coupling of 2-bromophenols with more bulky substituents in *ortho*-position showed very poor or no conversion towards the desired axially chiral dimer (entry 7–8). The high steric hindrance of the *ortho*-substituents probably restricted the construction of the crowded biaryl bond. All in all, five different tetra-*ortho*-substituted biphenols

rac-**199a–e** were obtained by the established homocoupling methods in a range of yields of 40–66%.

6.4.2 Aryl homocoupling *via* directed *ortho*-metalation

For the synthesis of 2,2′-biphenols *via* the developed *Lipshutz* coupling or MBSC, MOM-protected 2-bromophenols are required.[1, 2] This restricts the range of scope, as a regioselective bromination could often be challenging. As a MOM protecting group is a direct metalation group (DMG), MOM-protected phenols could be utilized to perform directed *ortho*-metalation and subsequently lead to an oxidative biaryl coupling in the same position (Scheme 55). Therefore, the challenge of regioselective bromination can be avoided and a broader substrate scope of 2,2′-biphenols could be addressed.

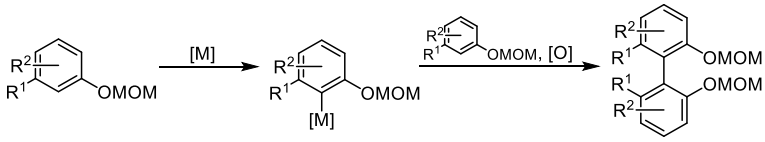

Scheme 55 Preparation of tetra-*ortho*-substituted biphenols *via* directed *ortho*-metalation.

To test this approach, phenols with different substitution patterns were chosen as substrates. First, protections with a MOM protecting group were performed under common procedure (Scheme 56). All protections took place in very good conversion and the desired products could be gained in 60–99% isolated yields.

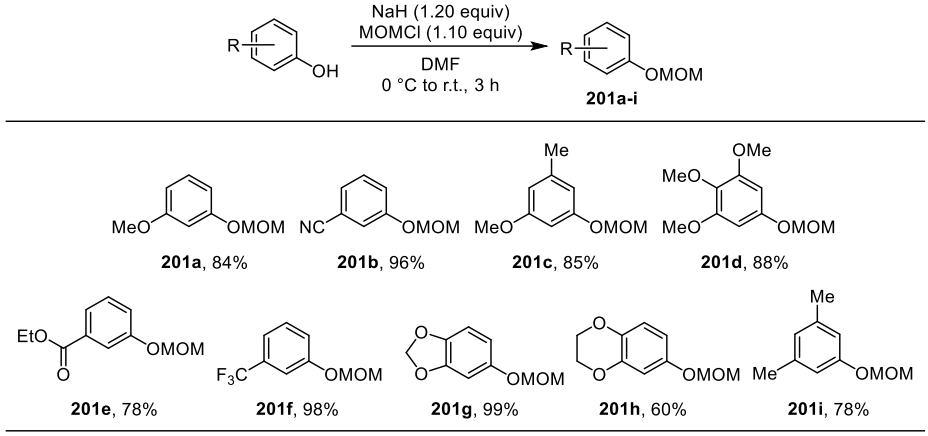

Scheme 56 Synthesis of MOM-protected phenols **203a–k**.

With the MOM-protected phenols **201a–i** in hand, the aryl homocoupling *via* directed *ortho*-metalation was investigated. **201a** was used as the monomer for first screenings and optimizations, as it contained a strong and a moderate DMG in 1,3-position. The metalation was expected to take place in 2-position through a cooperative coordination of the alkyllithium. The first approach was the formation of the *Lipshutz* cuprate *via* a directed *ortho*-lithiation with the help of TMEDA. TMEDA was used as a bidentate amine to break up aggregates of butyllithium.[230, 231] To ensure full conversion of the *ortho*-metalation, deuteration experiments were performed first (Scheme 57).

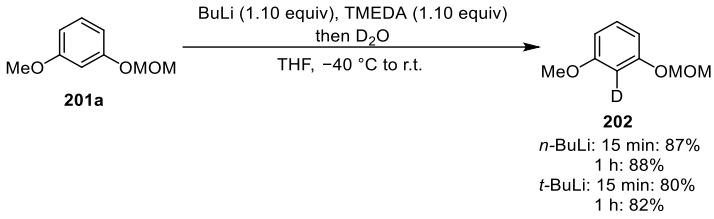

Scheme 57 Deuteration *via ortho*-metalation of **201a**; [a] Conversions were determined *via* ^{1}H-NMR.

Two different alkyl lithium bases were added in combination with TMEDA to a solution of the monomer **201a** in THF at −40 °C. After 15 minutes and 1 hour an aliquot was taken out of the reaction mixture and quenched with D_2O. ^{1}H-NMR showed a slightly higher conversion using *n*-butyllithium. The results suggest that a reaction time of 15 minutes would be sufficient, and longer times do not significantly increase the conversion. Therefore, further *ortho*-metalation steps were performed with *n*-butyllithium and a reaction time of 15 minutes.

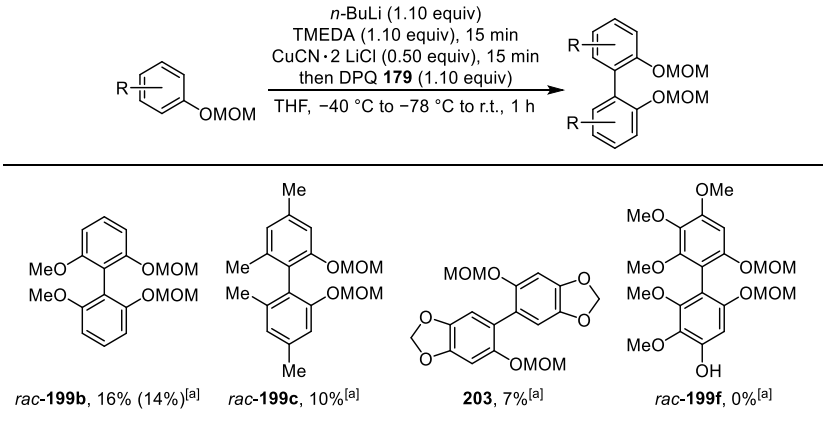

Scheme 58 Oxidative homocoupling of *Lipshutz* cuprates *via* directed *ortho*-metalation; [a] Conversions were determined *via* ^{1}H-NMR; isolated yields are given in parenthesis.

The optimized conditions for the directed *ortho*-metalation were applied on the oxidative homocoupling of MOM-protected phenols (Scheme 58). Analogously to the previously described *Lipshutz* coupling, the metalation was followed by the formation of the *Lipshutz* cuprate with copper(I)cyanide di-lithium chloride solution and a subsequent oxidation with DPQ **179** to the axially chiral biphenyl. This reaction was tested on five different examples. However, the coupling product of *rac*-**199b** and *rac*-**199c** could only be obtained in 16% and 10%. The application of MOM-protected sesamol **201g** resulted in the formation of the wrong regioisomer **203** in 7% conversion. The electron rich trimethoxy phenol **201d** led to no conversion towards the coupling product, which could be caused by the high electron density of the substrate. In all cases the starting material could be reisolated again *via* column chromatography and no formation of any side product was observed. As high conversions of directed *ortho*-lithiation were likely under the given conditions, the formation of the needed cuprate might have been the restricting step, leading to low conversions.

Due to the so far observed low conversions, a directed *ortho*-cupration was tested using an organoamidocuprate, developed by *Uchiyama et al*.[232-234] Here, 2,2,6,6-tetramethylpiperidine was used as a bulky amido ligand. Lithiated TMP and copper(I)cyanide generates *in situ* the homoleptic amidocuprate $(TMP)_2Cu(CN)Li_2$, which functions as a non-transferable dummy group for a highly regioselective directed *ortho*-cupration (DOC). It was shown that functionalization with various electrophiles is possible, as well as cross coupling towards biphenyl product in the presence of an oxidizing agent. This method was first applied on the homocoupling of 1-methoxy-3-(methoxymethoxy)benzene (**201a**) (Scheme 59). In the first step, the starting material **201a** was added to the *in situ* generated cuprate base $(TMP)_2Cu(CN)Li_2$, deprotonating two aromatic C-H bonds and forming a homoleptic biaryl cuprate. The subsequent addition of DPQ **179** led to the oxidative coupling and furnished the biphenyl *rac*-**199b**. The desired coupling product *rac*-**199b** was formed in 57%. Besides the starting material, the side product was the regioisomer **204**, which was generated in 11%. Surprisingly, here the DOC took place at the 6-position adjacent to the methoxy group, instead of next to the MOM group, which was supposed to be the stronger DMG. In comparison to the *Lipshutz* coupling of MOM-protected bromophenols, this method showed a more efficient way towards the challenging synthesis of tetra-*ortho*-substituted biphenyl *rac*-**199b**. The coupling using the respective bromophenol **193b** required a tedious and less efficient preparation of the bromophenol **193b**, which led to the biphenyl *rac*-**199b** in an overall yield of 13% over three steps. However, applying

the homocoupling method *via* DOC, the same desired biphenyl *rac*-**199b** could be synthesized in 47% total yield over only two steps.

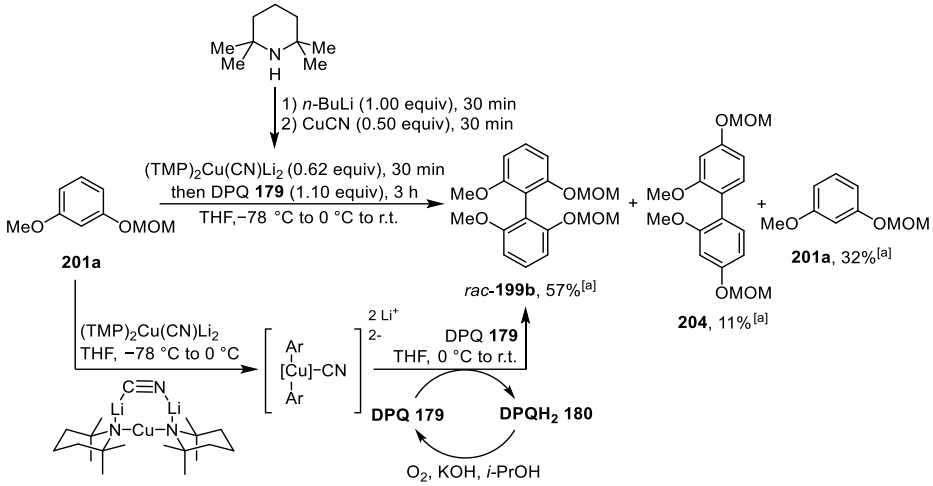

Scheme 59 Homocoupling of phenol **201a** *via* DOC; [a] Conversions were determined *via* ^{1}H-NMR.

As the synthesized biphenyls were going to be used for the enzymatic hydrolysis of biphenyl propionates, the homocoupling *via* DOC was tested on 3-methoxyphenyl propionate **205** (Scheme 60). In this way, steps of MOM-protection and deprotection could be eliminated. However, the reaction only resulted in the hydrolysis of the propionate. No conversion towards the desired biphenyl was observed.

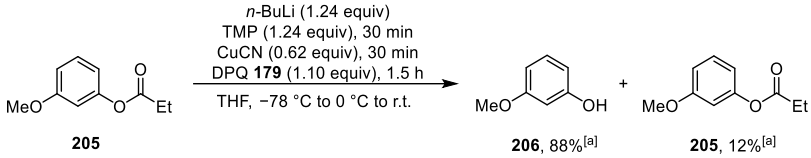

Scheme 60 Homocoupling of 3-methoxyphenyl propionate **205** *via* directed *ortho*-cupration; [a] Conversions were determined *via* ^{1}H-NMR.

The developed homocoupling *via* DOC was afterwards applied on a broad scope of ten different MOM-protected phenols **201a–h** (Scheme 61). The *ortho*-position to the MOM group, which was aimed for the construction of the chiral biaryl axis, is highlighted. Scheme 61 shows that the homocoupling succeeded for methoxy- and nitrile-substituted phenols (entry 1–3). The desired biphenyls *rac*-**199b**, *rac*-**207**–**208** were formed regioselectively in 37–64% yield. Analogously to previous reactions *via* a MBSC or

Lipshutz coupling, the trimethoxy substituted biphenyl *rac*-**199f** could not be obtained (entry 4). In comparison to the previous *Lipshutz* coupling *via* directed *ortho*-lithiation, conversion of the MOM-protected ethyl benzoate **209** *via* a DOC coupling was observed (entry 5). However, the coupling did not show the desired regioselectivity and the biphenyl axis was generated at the 4-position in 20%. Besides electron poor 3-cyanophenol **201b**, protected 3-trifluoromethylphenol **201f** was applied to generate tetra-*ortho*-substituted biphenyls with electron withdrawing substituents. However, the DOC coupling resulted also in the formation of the wrong regioisomer **210** in 55% (entry 6). The same wrong regioselectivity was observed in the reaction using benzannulated phenols **201g** and **201h** (entry 7-8). In general, this method is efficient, significantly reducing the number of reaction steps required for the synthesis of biphenyls. Therefore, it is attractive regarding waste reduction and lowering synthetic costs. The coupling also exhibited a broad functional group tolerance with fair to good conversions, without the necessity of introducing a bromide. However, the results highlight a regioselectivity issue. Depending on the substrate, the biphenyl axis can be constructed at either of the two positions *ortho* to the DMG. In this case, homocoupling methods *via* brominated substrates are still required to ensure high regioselectivity.

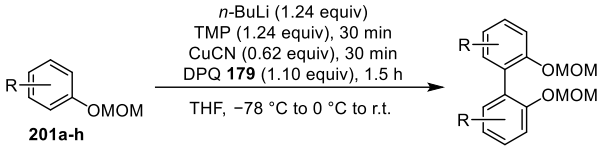

Entry	Substrate	Product, Yield[a]	Entry	Substrate	Product, Yield[a]
1	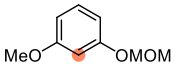 **201a**	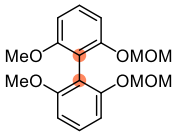 *rac*-**199b**, 57%	5	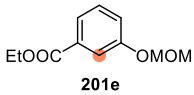 **201e**	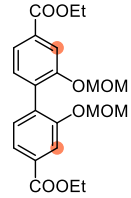 **209**, 20%
2	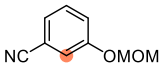 **201b**	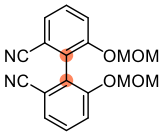 *rac*-**207**, 64%	6	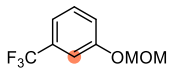 **201f**	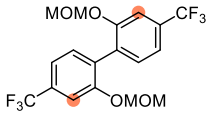 **210**, 55%
3	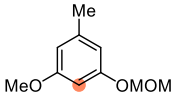 **201c**	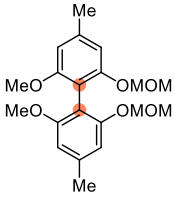 *rac*-**208**, 37%	7	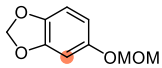 **201g**	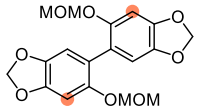 **203**, 30%
4	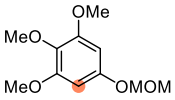 **201d**	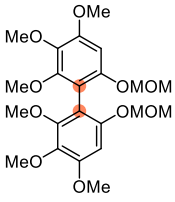 *rac*-**199f**, 0%	8	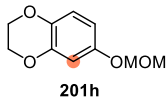 **201h**	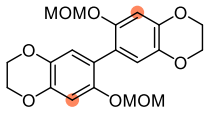 **211**, 17%

Scheme 61 Substrate scope of tetra-*ortho*-substituted biaryl couplings *via* directed *ortho*-cupration; aimed position for the construction of the biaryl axis is highlighted in orange; [a] Isolated yield.

6.4.3 Derivatization of axially chiral biphenols

In order to expand the scope of axial chiral biphenols, derivatizations of synthesized biphenols were performed. Here, the goal was to introduce different functional groups in the *para*-position to the biphenyl axis. In the first step, the introduction of a bulky alkyoxy group was targeted. The idea was to cleave both methyl ether in *para*-position of *rac*-**1** and afterwards alkylate the hydroxy groups in *para*-position. The hypothesis was that due to the higher steric hindrance of both *ortho*-hydroxy groups, alkylation would be more likely occur in *para*-position than in *ortho*-position. Therefore, the methyl ether cleavage was performed by treatment with BBr_3 in CH_2Cl_2 (Scheme 62). After stirring overnight, free tetraol *rac*-**153** was obtained in 82% isolated yield and the mono-deprotected side product *rac*-**213** was isolated in 18%.

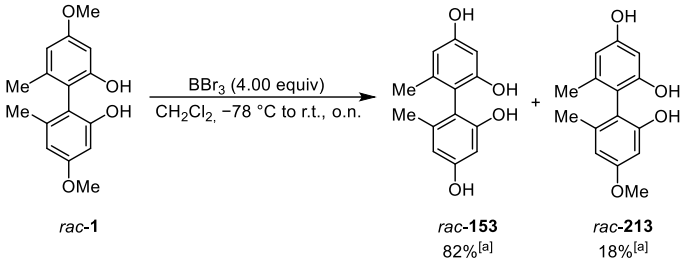

Scheme 62 Methyl ether cleavage of *rac*-**1**; [a] Isolated yield.

Potassium carbonate was used to deprotonate the hydroxy group before isopropylbromide was applied as the alkylating reagent (Table 9). Regardless of the solvent, no conversion could be observed at room temperature (entry 1–2). At elevated temperature a mixture of three alkylation products was detected (entry 3). In contrast to the hypothesis, the first *O*-alkylation took place in *ortho*-position, forming *rac*-**214**. In the second step, one of both *para*-hydroxy groups got alkylated, leading to *rac*-**215** and *rac*-**216**.

Table 9 Alkylation of biphenyl tetraol *rac*-**153**.

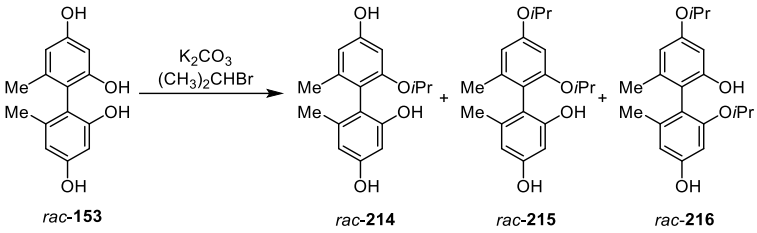

Entry	K_2CO_3 (equiv)	$(CH_3)_2CHBr$ (equiv)	Solvent	Temp.	Time	214[a]	215[a]	216[a]
1	2.00	2.00	Acetone	r.t.	24 h	−	−	−
2	2.00	2.00	DMF	r.t.	24 h	−	−	−
3	2.00	6.00	DMF	60 °C	48 h	+	+	+

[a] Product formation was determined *via* mass spectrometry (ESI): + = mass of product visible, − = no conversion; structural elucidation was performed *via* 2D-NMR.

As the alkylation of tetraol *rac*-**153** showed low chemoselectivity, a protection of both hydroxy groups in *ortho*-position was performed (Scheme 63). First, the formation of the silylether of both *ortho* hydroxy groups was planned, following the procedure of *Sawada*, who applied this protection on dibenzofurans.[235, 236] However, the addition of *t*-$Bu_2Si(OTf)_2$ and lutidine to tetraol *rac*-**153** in DMF did not lead to any conversion towards the protected product.

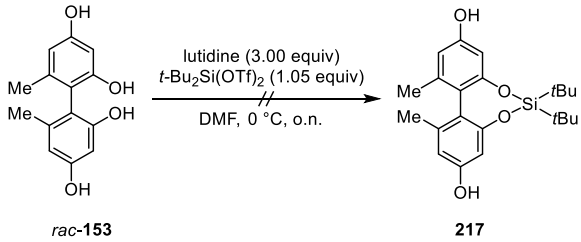

Scheme 63 Protection *ortho*-hydroxy groups of *rac*-**153** with silylether.

Alternatively, *rac*-**1** should be protected with benzyl groups as an orthogonal protecting group (Scheme 64). Subsequently the deprotection of the methyl ether should take place selectively. Benzylated biphenyl *rac*-**218** was obtained in 66% yield by alkylation with BnBr, potassium carbonate and catalytic *tert*-butylammoniumiodide. However, the following methyl ether cleavage with BBr_3 or BCl_3 did not proceed selectively. In the presence of BBr_3 both benzyl ether and methyl ether were not stable and were removed,

affording tetraol *rac*-**153**. Treatment with BCl_3 led first to the cleavage of the benzyl ether, while the methyl ether remained.

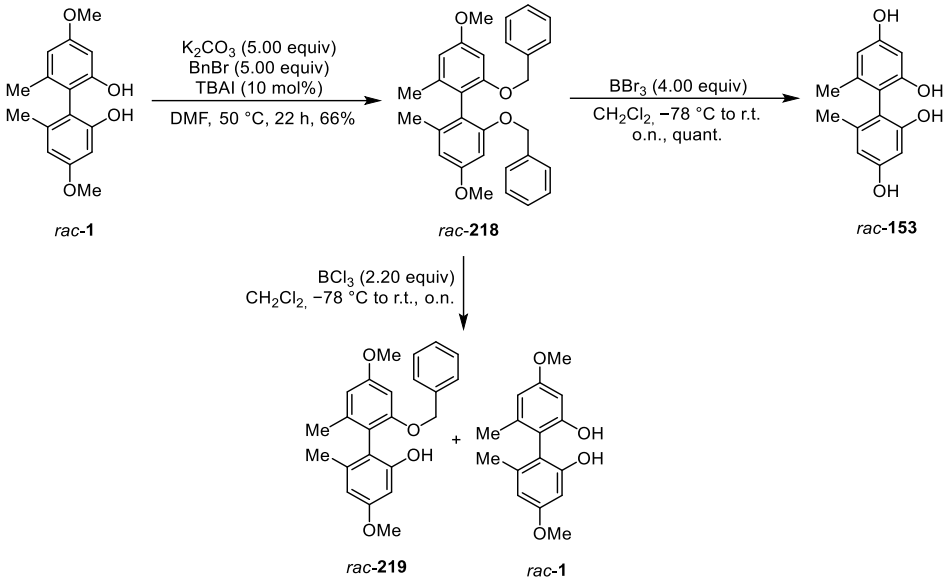

Scheme 64 Selective protection of *ortho*-hydroxy groups of *rac*-**1**.

After derivatization of the *para*-hydroxy groups of *rac*-**153** did not succeed, an alternative functionalization *via* iridium catalysis was performed. Here, regioselective borylation was achieved by applying $[Ir(COD)OMe]_2$ as a catalyst in combination with the dtbpy ligand and B_2pin_2 (Scheme 65).[237-240] This reaction was established and performed by *Moritz Klischan* starting from *rac*-**199a**.[241, 242] The iridium-catalyzed borylation led to a ~1:1 mixture of diborylated *rac*-**220** and monoborylated biphenyl *rac*-**221**, which was separated *via* column chromatography.

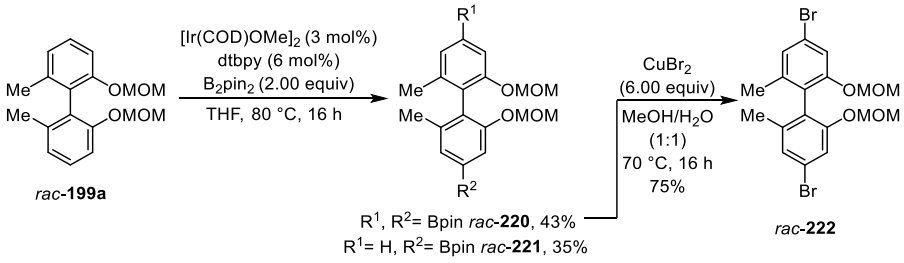

Scheme 65 Regioselective borylation and bromination using iridium catalysis.

Biphenyl boronate ester *rac*-**220** is a versatile building block for diverse functionalization or cross coupling. Here, a conversion of the boronate ester to the bromide using copper(II) bromide was performed, following the procedure of *Huffman*.[243] Biphenyl bromide *rac*-**222** was isolated in 75% yield. Analogously to the biphenyl boronate ester, cross coupling of brominated biphenyl *rac*-**222** would expand the biphenyl substrate scope.

6.4.4 Synthesis of substrate scope of biphenyl mono- and dipropionates

In total eight different tetra-*ortho*-substituted axially chiral biphenyls could be synthesized, which in the next step should be deprotected to the free biphenols *rac*-**223a–h**. Here, the MOM protecting group was removed under acidic conditions (Scheme 66). All eight biphenols *rac*-**223a–h** were isolated in good to excellent yields from 66–99%.

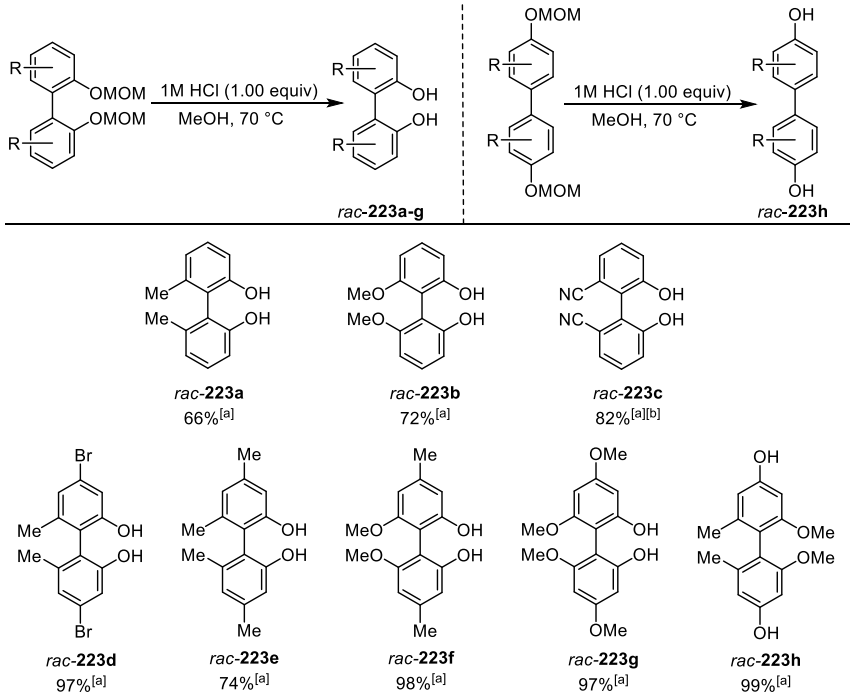

Scheme 66 Substrate scope of deprotected tetra-*ortho*-substituted biphenols *rac*-**223a–h**; [a] Isolated yield; [b] in dioxane at 60 °C.

For the application in the EKR, biphenyl mono- and dipropionates needed to be synthesized. For the first two examples of *rac*-**223a** and *rac*-**223g**, the synthesis of mono- and dipropionates proceeded separately with either 1.00 or 2.00 equiv of propionic anhydride

and triethyl amine (Scheme 67). Both diesters *rac*-**224a** and **224g** and monoesters **225a** and **225g** were obtained in good yields of 74–83%.

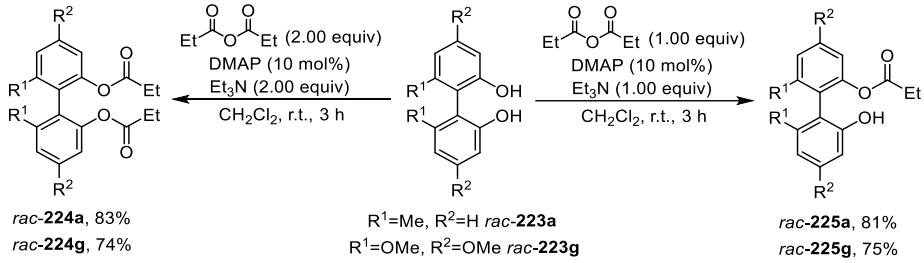

Scheme 67 Synthesis of biphenyl mono- and dipropionate *rac*-**228a,g** and *rac*-**229a,g**.

The remaining six biphenyls monoesters *rac*-**225b–h** and diesters *rac*-**225b–h** were prepared in one step using 1.50 equiv of propionic anhydride and triethyl amine (Scheme 68). The mixture of monoester and diester products were separated *via* column chromatography. Here, dipropionates *rac*-**224b–h** were obtained in 47–83% yield and the monopropionates *rac*-**225b–h** in 9–48% yield.

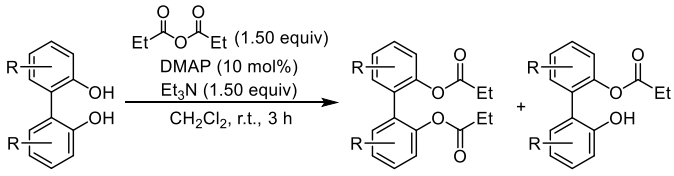

rac-**223b-h** *rac*-**224b-h** *rac*-**225b-h**

Entry	Substrate	Yield [%][a] *rac*-**224b-h**	Yield [%][a] *rac*-**225b-h**	Entry	Substrate	Yield [%][a] *rac*-**224b-h**	Yield [%][a] *rac*-**225b-h**
1	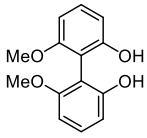 *rac*-**223b**	47%	48%	4	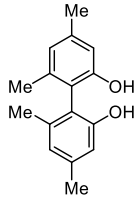 *rac*-**223e**	67%	9%
2	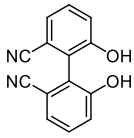 *rac*-**223c**	57%	26%	5	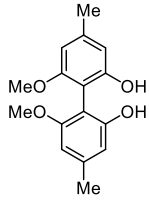 *rac*-**223f**	52%	28%
3	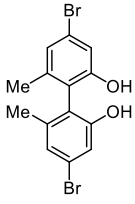 *rac*-**223d**	66%	24%	6	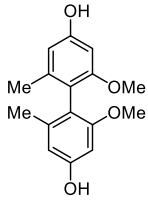 *rac*-**223h**	83%	0%

Scheme 68 Substrate scope of biphenyl mono- *rac*-**225b–h** and dipropionates *rac*-**224b–h**; [a] Isolated yield.

Summary Chapter 6.4

1. Eight MOM-protected bromophenols **193a–h** were synthesized.

2. Homocoupling of MOM-protected bromophenols
   - Reactivities between *Lipshutz* coupling and MBSC were similar for MOM-protected 2-bromophenols.
   - The use of bromophenols with bulky *ortho*-substituents or high electron density could not be realized in the coupling reaction.
   - 5 of 8 biphenols could be obtained (40–60% isolated yield)

3. 8 MOM-protected phenols **201a–h** were synthesized for the homocoupling *via* directed *ortho*-metalation.

4. Homocoupling *via* directed *ortho*-lithiation:
   - Directed o*rtho*-lithiation was quantified *via* deuteration experiment.
   - 3 of 5 coupling products were obtained in low conversions.

5. Homocoupling *via* directed *ortho*-cupration (DOC):
   - 3 of 8 axially chiral biphenyls were obtained (37–64% yield)
   - 4 of 8 biphenyl regioisomers were obtained (17–55% yield)

6. Ir-catalyzed regioselective borylation facilitated further derivatization of axially chiral biphenols.

7. MOM deprotection results in a scope of eight tetra-*ortho*-substituted biphenols *rac*-**223a–h** (66–99% isolated yield).

8. Eight biphenyl dipropionates *rac*-**224a–h** and monopropionates *rac*-**225a–h** were prepared for EKR.

6.5 Application of EKR on scope of axially chiral biphenols

After a scope of eight biphenyl dipropionates *rac*-**224a–h** was prepared, the investigations towards the EKR regarding the different axially chiral substrates were performed. *Rac*-**224a–h** were treated with CRL under the optimized conditions in a one-phase system (DMSO 10 vol%) at 40 °C. The enzyme activity and enantioselectivity towards the different substituted biphenols were analyzed after 3 hours reaction time.

First, the enzymatic hydrolysis of *rac*-**224h** was tested, to prove the importance of the position of the targeted and hydrolyzed ester functionality (Scheme 69). Within less than 15 minutes full conversion of *rac*-**224h** was reached towards its racemic free biphenol *rac*-**223h**. This showed that the addressed ester functionality must be in *ortho*-position relative to the chiral axis to control the atroposelectivity of the enzymatic resolution.

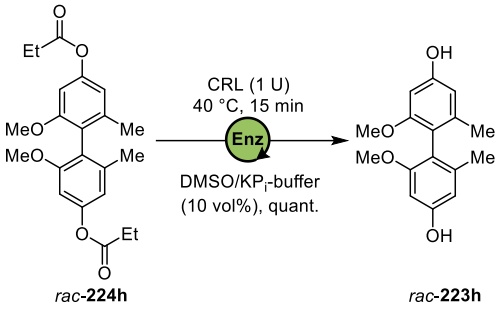

Scheme 69 Enzymatic hydrolysis of *rac*-**224h** with CRL (1 U), 40 °C, 15 min; 1400 rpm; 10 vol% DMSO/KP_i-buffer (pH=7.4); [a] Conversion was determined *via* ^{1}H-NMR.

In the next step, the influence of the *para*-substituent was studied, where biphenyl dipropionate *rac*-**181b** was used as a benchmark. Here, four substrates with different *para*-substituents with increasing steric hindrance were compared (Figure 25). CRL exhibited a constant high hydrolytic activity for the biphenyl diesters *rac*-**224a**, **224d**, **224e**, **181b** regardless of their substitution pattern in *para*-position. After 3 hours, conversions of 47–58% could be reached. The choice of *para*-substituent had only a minor effect on the enantioselectivity, which led to the formation of enantiopure biphenol **223a**, **223d**, **223e**, **1** with good to excellent enantiomeric excesses of 79–>99% *ee*. This indicates that the active center of the lipase accepts substrates with different *para*-substituent without significantly affecting the enantioselectivity.

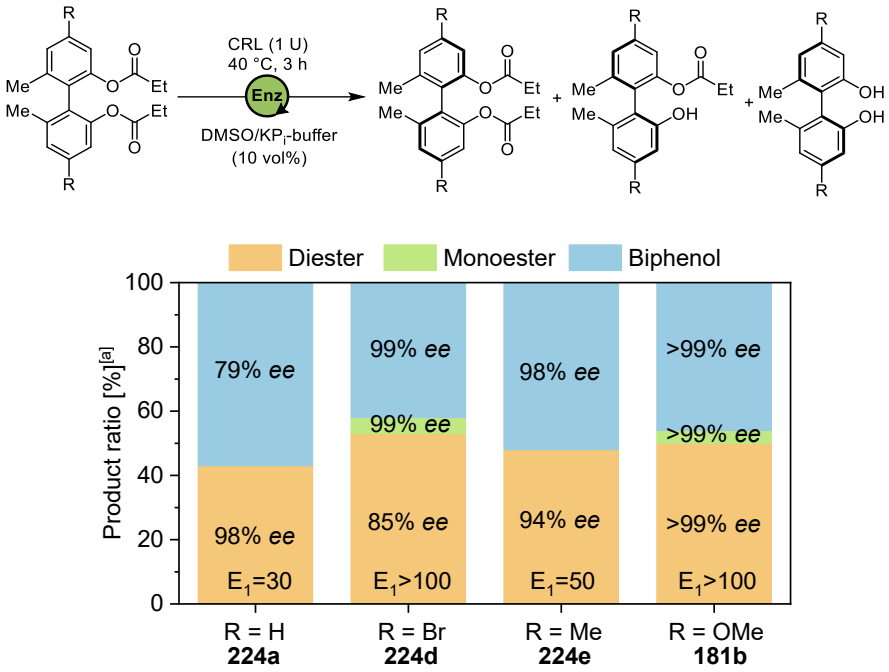

Figure 25 Effect of *para*-substituent of biphenyl diester *rac*-**224a**, **224d**, **224e**, **181b** on EKR; CRL (1 U), 40 °C, 3 h, 1400 rpm; 10 vol% DMSO/KP_i-buffer (pH=7.4); [a] Conversion was determined *via* ^{1}H-NMR; *ee* was determined *via* chiral HPLC.

In the last step, the effect of the substitution pattern in *ortho*-position to the chiral axis was investigated (Figure 26). In contrast to the *para*-position, the substituent in *ortho*-position had a major influence on the hydrolytic activity and selectivity of the lipase. In comparison to the 6,6′-dimethylbiphenyl dipropionate *rac*-**224a**, which was hydrolyzed selectively with good conversions ($E_1 = 30$), similar conversions of 6,6′-dimethoxybiphenyl diester *rac*-**224b** of 49% were observed, but with lower selectivities ($E_1 = 6$). The second hydrolysis step towards biphenol **223b** was more slowly and led to a formation of a mixture of monoester **225b** and biphenol **223b** with moderate enantiomeric excesses of 54% *ee* and 73% *ee*. 6,6′-dinitrilebiphenyl diester *rac*-**224c** was not well accepted as a substrate for the enzymatic resolution either. Low conversion of 23% and poor enantioselectivities were determined ($E_1 = 2$).

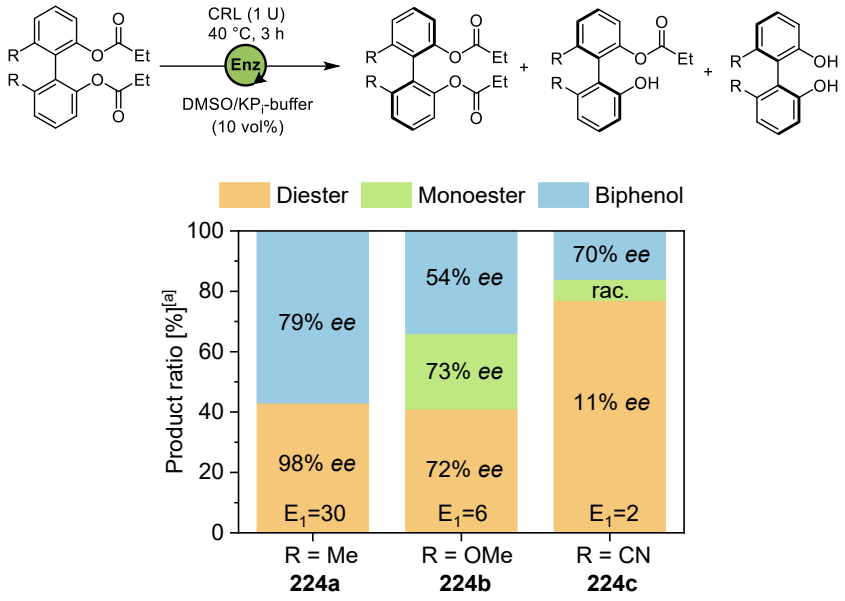

Figure 26 Effect of *ortho*-substituent of biphenyl diester *rac*-**224a–c** on EKR; CRL (1 U), 40 °C, 3 h, 1400 rpm; 10 vol% DMSO/KP_i-buffer (pH=7.4); [a] Conversion was determined *via* ^{1}H-NMR; *ee* was determined *via* chiral HPLC.

In the last step EKR was performed using substrates with additional *para*-substituents introduced to the 6,6′-dimethoxybiphenyl *rac*-**224f** and *rac*-**224g** (Figure 27). In contrast to *rac*-**224b**, *rac*-**224f** was enzymatically hydrolyzed in 53% conversions, resulting in a mixture of monoester and biphenol products with good enantiomeric excess of 78–81% *ee* (E_1 = 25). The introduction of a methoxy group led to lower conversions and moderate enantioselectivities (34% conversion, 71–80% *ee*, E_1 = 9).

From these results a better understanding of the applicability of CRL on the EKR of 2,2′-biphenols was gained. The EKR facilitates the asymmetric synthesis of various 2,2′-biphenols. However, limitations regarding the substitution pattern have been revealed. The choice of the substitution pattern is essential for the EKR with high atroposelectivity. Axially chiral biphenyl dipropionates only with methyl-substitution in *ortho*-position were converted atroposelectively. The application of other *ortho*-substituents resulted in a drop of activity and selectivity. In contrast, the *para*-substitution pattern showed a lesser impact on conversions and atroposelectivity. Substituents with different steric hindrance and electronic characteristics were accepted well with good conversions and high atroposelectivities. The highly selective synthesis of bromide-substituted biphenol **223d** should be highlighted, which can function as a good building block for the asymmetric preparation of

biphenols with various *para*-substituents *via* cross-coupling reactions or other functionalization.

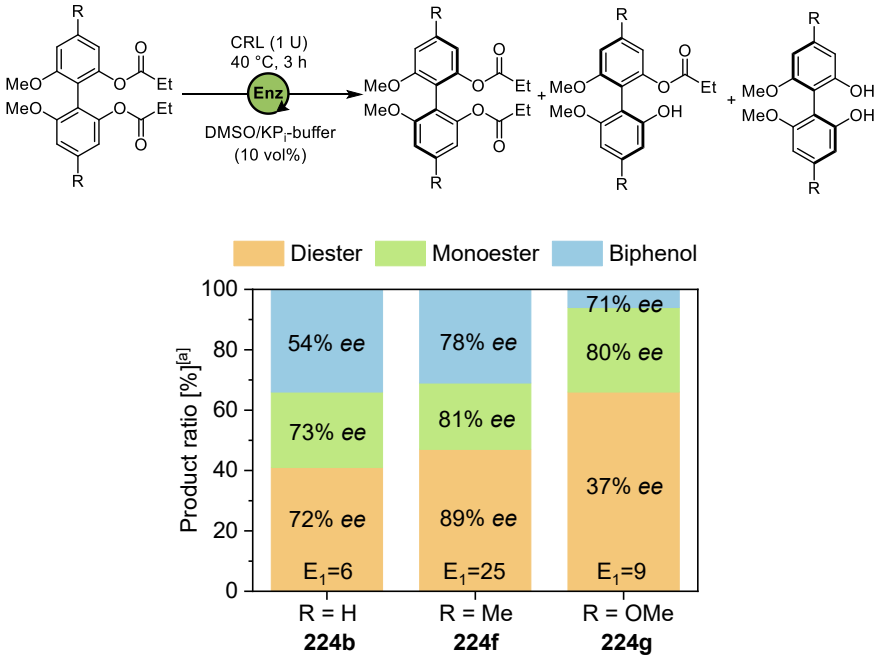

Figure 27 Effect of *ortho*- and *para*-substituent of biphenyl diester *rac*-**224f–g** on EKR; CRL (1 U), 40 °C, 3 h, 1400 rpm; 10 vol% DMSO/KP_i-buffer (pH=7.4); [a] Conversion was determined *via* ^{1}H-NMR; *ee* was determined *via* chiral HPLC.

Summary Chapter 6.5

1. Ester functionality has to be in *ortho*-position to the chiral axis to control the atroposelectivity of the enzymatic resolution.

2. Four biphenols with different *para*-substituents were tested for the EKR:
   - Choice of *para*-substituents has a minor effect on the enzyme's activity and selectivity.
   - Formation of four biphenols with good to excellent enantiomeric excesses (79–>99% *ee*, 47–58% conversion)

3. Five biphenols with different *ortho*-substituents were tested for the EKR:
   - Choice of *ortho*-substituents has a major effect on the enzyme's activity and selectivity.
   - Only 6,6′-dimethylbiphenyl *rac*-**224a** could be converted in high conversions and with high selectivities.
   - Other *ortho*-substituents (methoxy, nitrile) resulted in a drop of conversion and selectivity.

6.6 Investigations on the total syntheses of γ-naphthopyrones

The atropoenantiopure 2,2′-biphenol building block (*M*)- and (*P*)-**1** were to be utilized in a total synthesis of dimeric axial chiral polyketides. There are various known polyketides, which contain the chosen 2,2′-biphenol building block **1**, including dimeric γ-binaphthopyrones (Scheme 70).[173, 174, 244]

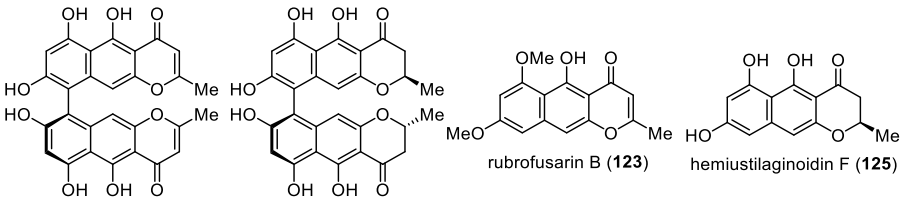

Scheme 70 Examples of monomeric and dimeric γ-naphthopyrones.

In the next chapters, the investigations on the total synthesis of (*M*)-ustilaginoidin A (*M*)-(**2**) and F (*M*)-(**3**) are described. Here, studies were performed first on the synthesis of the monomeric unit rubrofusarin (**123**) and hemiustilaginoidin F (**125**). The optimizations were afterwards implemented on the synthesis of the dimeric natural products. Scheme 71 shows the retrosynthetic analysis of (*M*)-ustilaginoidin A (*M*)-(**2**) and F (*M*)-(**3**). The key step of the total synthesis is the double construction of the polycycle.

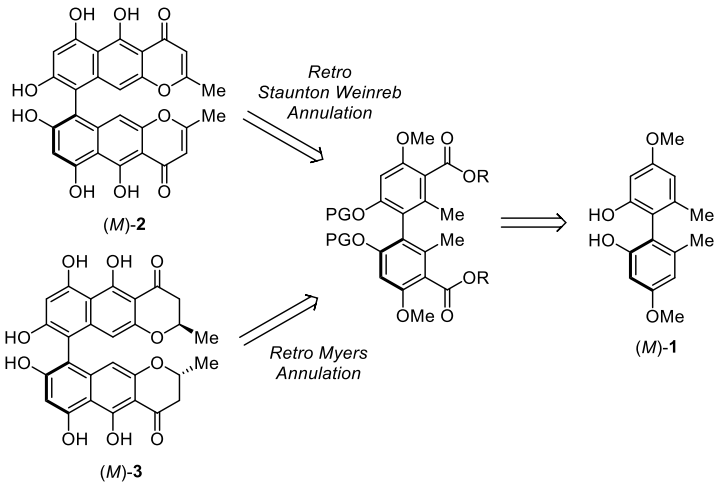

Scheme 71 Retrosynthetic analysis of γ-binaphthopyrones.

Here, *ortho*-toluates should be converted either in a *Staunton-Weinreb* or in a *Myers'* annulation, depending on the choice of the electrophile.[173, 174, 178, 245] The required dimeric

ortho-toluate, acting as the nucleophile, can be prepared starting from the 2,2′-biphenol building block (*M*)-**1**. In the upcoming chapters the detailed results of the racemic synthesis strategies are presented.

6.6.1 Synthesis of monomeric *ortho*-toluates 231 and 232

To investigate the annulation towards the monomeric *γ*-naphthopyrones, *ortho*-toluates needed to be synthesized. In addition to the more commonly used methyl benzoate **228**, phenyl benzoate **229** was prepared as well to compare the suitability of both for the annulation due to their differences in steric hindrance and reactivity. Scheme 72 and Scheme 73 show the syntheses of both *ortho*-toluates **228** and **229**, which were carried out according to known procedures.[246, 247]

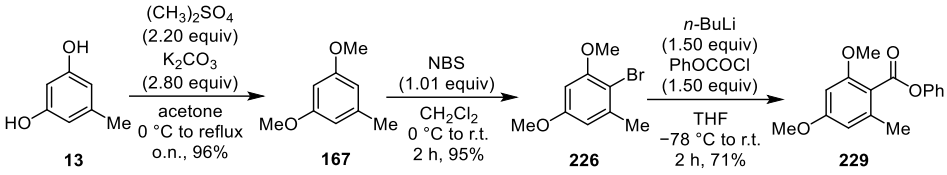

Scheme 72 Synthesis of monomeric phenyl benzoate **229**.

Dimethylation of 5-methylresorcinol (**13**) was performed as described in section 6.1. In the presence of NBS 3,5-dimethoxytoluene (**167**) was brominated in 2-position. Due to the slight excess of NBS double bromination occurred in small quantities, which was easily removed through column chromatography. Starting from bromophenol **226**, both methyl **228** and phenyl benzoate **229** were prepared. The phenyl benzoate **229** was directly synthesized *via* halogen-metal exchange with *n*-butyllithium and nucleophilic addition to phenyl chloroformate in 71% yield. However, the methyl ester **228** was obtained *via* carboxylation towards benzoic acid **230** and subsequent methylation, to avoid the use of methyl chloroformate. Here, different methods for the methylation of benzoic acid **230** were tested (Scheme 73). The desired methyl benzoate **228** could be obtained by methylation using trimethylsilyl diazomethane in methanol in 90% yield. The reaction took place at room temperature and very short reaction time. However, a high amount of methylating reagent (10.00 equiv) was required. When using potassium carbonate as a base with methyl iodide, the yield dropped to 51%. The high reflux temperature of DMF might have caused evaporation of methyl iodide and led to low conversions. Substitution of

methyl iodide with dimethyl sulfate led to excellent conversion (91% yield). Overall, phenyl benzoate **229** was afforded in 65% yield over three steps and methyl benzoate **228** in 70% yield over five steps.

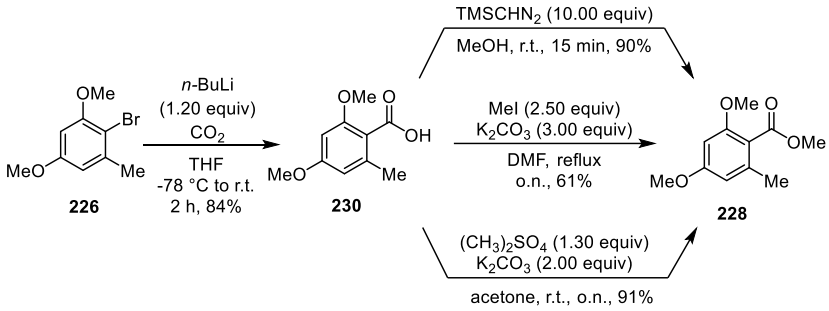

Scheme 73 Synthesis of monomeric methyl benzoate **228**.

6.6.2 Synthesis of rubrofusarin B (123)

In the first step the synthesis of the monomeric *γ*-naphthopyrone rubrofusarin B (**123**) was reproduced following *Müller's* procedure.[173, 174] A *Staunton-Weinreb* annulation was performed with methyl benzoate **228** and pyrylium tetrafluoroborate **233** as the electrophile. The required electrophile **233** was prepared starting from methylation of commercially available 4-hydroxy-6-methyl-2H-pyran-2-one (**231**) in quantitative yield (Scheme 74).[248] The pyrylium salt was synthesized by addition of silver tetrafluoroborate and methyl iodide. The desired salt **233** was purified by recrystallization and was obtained in higher yields of 33% than those published.[173, 174]

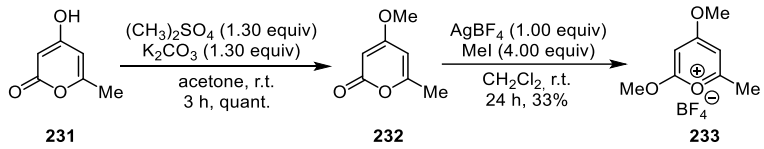

Scheme 74 Synthesis of 2,4-dimethoxy-6-methylpyrylium tetrafluoroborate (**233**).

After the electrophile was prepared, the annulation was performed with methyl ester **228** in two steps according to *Müller*'s procedure (Scheme 75).[173, 174] Lithium diisopropylamide (LDA) was used as a base to deprotonate the benzylic position of the *ortho*-toluate. The formed anion was observed by the characteristic red coloration. When adding the electrophile, the toluate anion was supposed to attack to the pyrylium **233** in

β-position and remove the methoxy group as a leaving group under acidic conditions. However, contrary to *Müller*'s result only traces of the addition product **234** were observed by mass spectrometry. Changing the *ortho*-toluate to phenyl benzoate **229**, the addition took place in 32% conversion. Subsequent treatment with LDA was supposed to deprotonate the acidic proton and lead to cyclization towards the desired *γ*-naphthopyrone rubrofusarin B (**123**). However, no conversion of the phenyl ester intermediate **235** was visible. Contrary to the observed results, the phenyl benzoate was supposed to be more reactive towards the cyclization, as the phenolate functions as a good leaving group. This was also observed by *Myers*' in the preparation of tetracycline antibiotics.[249]

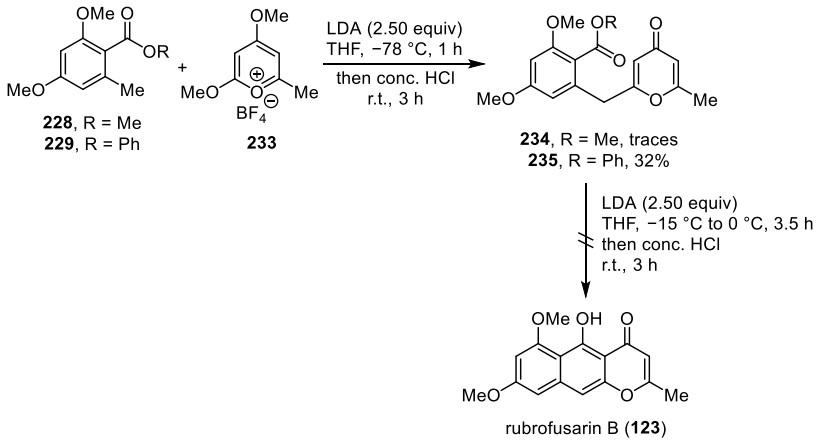

Scheme 75 Approach towards the synthesis of rubrofusarin B (**123**).

In summary, synthesis of the nucleophilic (section 6.6.1) and electrophilic building blocks for the *Staunton-Weinreb* annulation was successfully performed. However, there was a challenge to reproduce published synthesis of the monomeric rubrofusarin B (**123**). By changing the orsellinate it was possible only to isolate the addition product **235**, which did not undergo further cyclization.

6.6.3. Synthesis of hemiustilaginoidin F (125)

As the synthesis of rubrofusarin (**123**) did not succeed, in the following chapter investigations on the *Myers*' annulation towards the monomer building block hemiustilaginoidin F (**125**) are described. Therefore, electrophile hydropyran-4-one **241** was needed. The synthesis of the enantiopure pyrone **241** was performed according to the procedure of *Merifield et al.* (Scheme 76).[250]

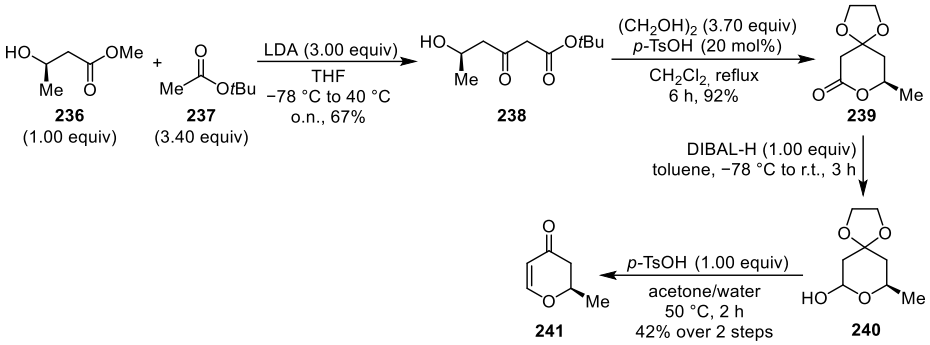

Scheme 76 Synthesis of hydropyran-4-one **241**.

Keto ester **238** was obtained by a *Claisen* condensation of *in situ* generated lithium ester enolate of *tert*-butylacetate (**237**) and commercially available methyl (*S*)-3-hydroxybutyrate (**236**) in 67% yield.[251] Treatment with *p*-TsOH and ethylene glycol led to the cyclization and protection of the ketone in one step in excellent yield. The formed lactone **239** was then reduced with DiBAl-H under mild conditions to afford lactol **240**. The gained mixture of both epimers of lactol **240** was used without further purification. It was afterwards applied in an elimination reaction followed by the deprotection of the acetal under acidic conditions in a single step. Thus, overall (*S*)-hydropyran-4-one **241** could be afforded in 22% total yield over four steps. As previous results pointed out that phenyl benzoate **229** showed higher reactivity towards the annulation reaction, it was also used for further screening of the *Myers*' annulation towards **242** (Table 10). In this reaction, LDA was again used as the base to deprotonate the *ortho*-toluate **229**. Hydropyranone **241** was added afterwards as the electrophile. In the first step, the number of equivalents of the base LDA was screened. Entries 1–3 show that with more equivalents of LDA higher conversions towards the desired product **242** could be reached. Using 3.0 equivalents of LDA a quantitative conversion of **229** was observed and the annulation product could be isolated in 61% yield. Besides the desired cyclization product, another side product was

observed. When the amount of base was increased, the conversion to this side product decreased.

Table 10 Optimization of *Myers'* annulation towards **242**.

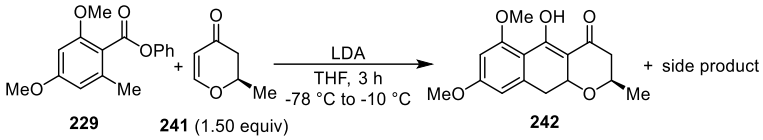

Entry	LDA equiv	Additive	229 [%][a]	242 [%][a]	Side prod. [%][a]
1	1.0	-	16	57	26
2	2.0	-	16	71	13
3	3.0	-	0	Quant. (61)	0
4	1.1	DMPU[b]	25	50	25
5	1.1	TMEDA[b]	17	62	21
6	1.1	LiHMDS[c]	39	61	0
7	1.1	LiHMDS[c] + $NEt_3 \cdot HCl$[d]	28	72	0

[a] Conversions were determined *via* ^{1}H-NMR; isolated yields are given in parenthesis; [b] 2.0 equiv; [c] 1.0 equiv; [d] 5 mol%

The side product could be isolated in mixed fractions with the annulation product *via* column chromatography. ^{1}H-NMR was used for structure elucidation of the side product. However, the structure could not be clearly elucidated and only assumptions could be made. Figure 28 shows the stacked ^{1}H-NMR spectra of annulation product **242**, a mixed fraction of product **242** and side product and phenyl benzoate **229** as the starting material. The ^{1}H-NMR spectrum of the side product still shows the presence of the phenyl ester (green box). However, the singlet of the initial methyl group of the toluate is not visible anymore (red box), which indicates that an addition to the electrophile took place, but no subsequent cyclization.

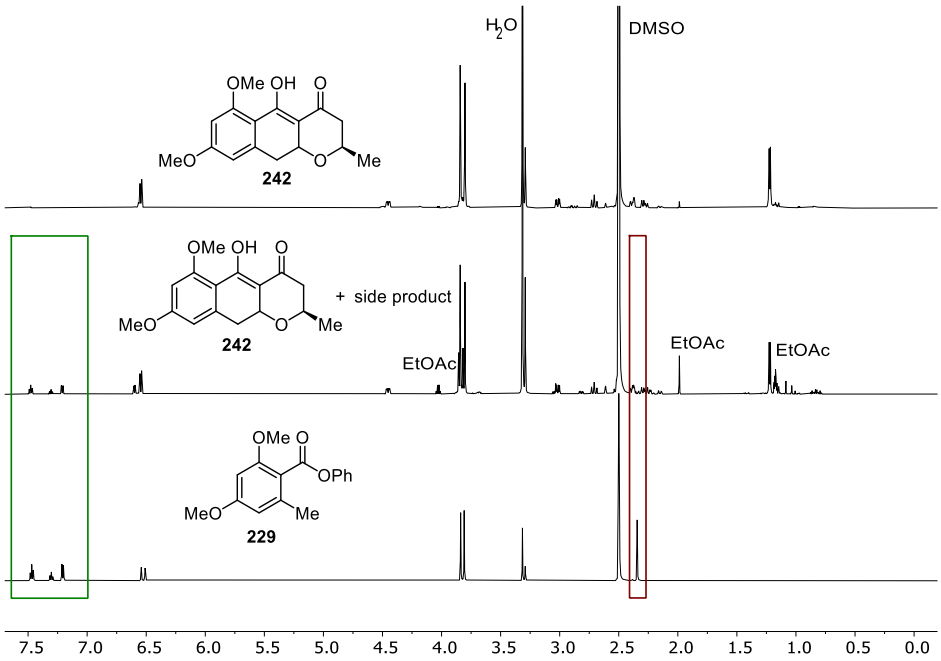

Figure 28 Overview of ^{1}H-NMR spectra (DMSO-d_6, 600 MHz) of annulation product **242**, mixed fraction of **242** and side product, and phenyl benzoate **229**.

Scheme 77 shows a possible mechanism for the formation of the desired product **242** and a possible side product **iii**. In the first step, the deprotonated *ortho*-toluate **229** attacks the *β*-position of the *Michael* system, forming lithium enolate **i**. Afterwards the enolate attacks the ester carbonyl group, whereas the phenoxy group leaves as a leaving group. One hypothesis could be that at higher amount of LDA, the formation of lithium enolate **i** is ensured, which, in turn, would promote the cyclization leading to the desired product **242** (blue path). At lower amounts of LDA, **i** might not be stable enough. Before the enolate attacks the ester, ring opening of the pyrone ring may have already occurred, potentially resulting in the formation of side product **iii** (green path). As depicted in Scheme 77, the annulated product **242** could exist in two tautomers: enol-**242** and keto-**242**, which could both be observed in the ^{1}H-NMR spectra and on TLC depending on the solvent. On the TLC of a solution in $CDCl_3$ two compounds were visible. The ^{1}H-NMR spectrum of the same solution a mixture of enol-**242** and keto-**242** was determined. However, the TLC of a solution in DMSO-d_6 showed only one spot, which could be determined as the enol-**242** in the ^{1}H-NMR spectrum. In comparison to the nonpolar solvent $CDCl_3$, the polar solvent DMSO is a strong polar hydrogen bond acceptor, which is able to stabilize the enol tautomer.[252]

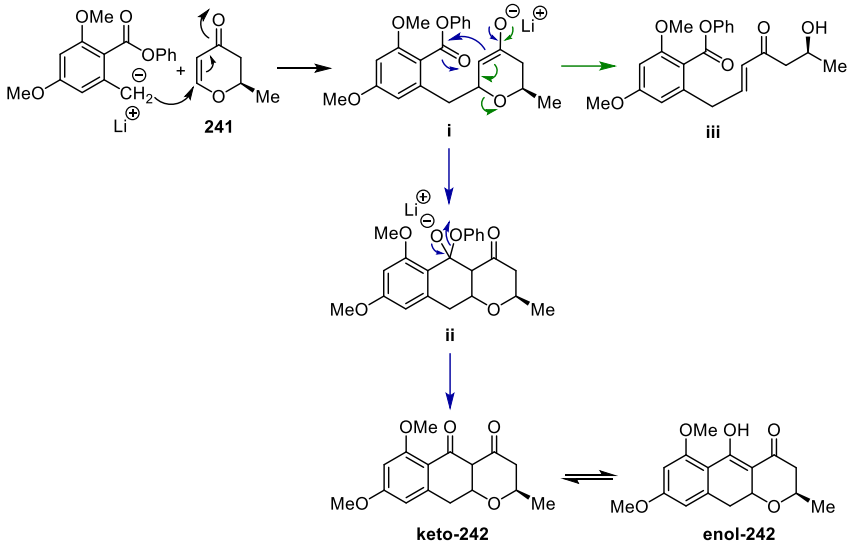

Scheme 77 Possible mechanism of annulation towards product **244** and side product **iii**.

In the next step, different additives were screened to increase conversion towards the desired annulated product **242** at lower quantities of LDA (Table 10) (entry 4–7). It is known that LDA is present as disolvated dimers in ethereal solvents.[253] Additives, like DMPU or TMEDA, are commonly used as ligands to coordinate the metal cation and displace THF. This would lead to the breaking up of aggregates and to higher reactivities.[253, 254] However, entries 4–5 show that addition of DMPU or TMEDA did not result in an increase in conversion. Previous results highlighted the importance of the lithium enolate of the addition product, required for the following cyclization. Observations from the group of *Ronn* showed that subsequent addition of a weaker base, like LiHMDS, would lead to the deprotonation of the acidic proton towards the enolate, thus inducing the cyclization.[255, 256] Entry 6 confirms these observations. Although the overall conversion towards product **242** remained the same, no formation of side product was detected. This would also support the suggested mechanism towards the side product (Scheme 77). The presence of LiHMDS ensured the formation of the lithium enolate **i** leading to cyclization towards the desired product, rather than ring opening. Furthermore, *Ronn et al.* stated to add NEt_3·HCl as a rate-enhancing additive. The combination of NEt_3·HCl with LDA generates *in situ* anhydrous LiCl and Et_3N as a byproduct, which does not influence the lithiation.[257] They showed that LiCl catalyzes the deaggregation of the LDA dimer to the highly reactive LDA monomer.[258, 259] In entry 7 a combination of LiHMDS and NEt_3·HCl was used for the annulation

reaction. After 3 hours an increase of the overall conversion and no side product was observed, which indicated the higher reactivity of the deaggregated LDA monomer.

After the annulated product **242** was isolated, the oxidative aromatization towards **243** needed to be performed. Here, different oxidation conditions were tested (Table 11). After a short reaction time of 2 hours, oxidation with DDQ led to complete degradation of the starting material (entry 1). In entries 2–4 chloranil was applied as an alternative benzoquinone oxidizing agent. Here, the results show that a long reaction time under reflux was required to reach full conversion. After refluxing for 6 days, the desired product **243** was obtained successfully in very good yield of 80%. The long reaction time might be caused by inhibition due to complexation of the hydroquinone side product of chloranil and the starting material **242**, which was previously observed by *White et al.*[260] Overall the *γ*-naphthopyrone dimethylether **243** for the synthesis of ustilaginoidin F (**3**) was successfully synthesized in overall 49% yield over two steps.

Table 11 Screening of oxidation conditions towards *γ*-naphthopyrone **243**.

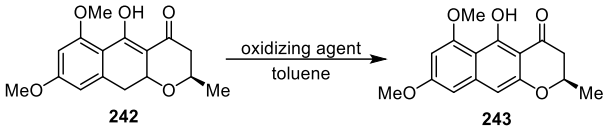

242 **243**

Entry	Oxidizing agent	Equiv	Temp.	Time	242 [%][a]	243 [%][a]	Side prod. [%][a]
1	DDQ	1.1	r.t.	2 h	0	0	0
2	chloranil	1.1	reflux	33 h	63	29	8
3	chloranil	4.0	reflux	2 d	60	32	8
4	chloranil	4.0	reflux	6 d	0	82 (80)	18

[a] Conversions were determined *via* ^{1}H-NMR; isolated yields are given in parenthesis.

6.6.4 Investigations on the synthesis of ustilaginoidin F (3)

The gained knowledge from the synthesis of *γ*-naphthopyrone monomer **243** was next applied to the synthesis of the dimeric ustilaginoidin F (**3**). Therefore, dimeric *ortho*-toluate *rac*-**245** was prepared, starting from MOM-protected biphenol *rac*-**176a**. In contrast to the monomer synthesis, here the MOM protecting groups were kept in 2,2′-position, as isolated from the homocoupling. Thereby, two steps of acidic deprotection and double *O*,*O*′-methylation were avoided. In order to obtain the final natural product, all four

hydroxy groups would need to be deprotected. Therefore, a more labile MOM-protecting group was preferred over a methyl ether. In Scheme 78, the synthetic route towards the dimeric phenyl benzoate *rac*-**245** is shown, which was performed following the monomer synthesis. A highly regioselective double bromination of MOM-protected biphenol *rac*-**176a** with NBS took place in excellent yield (99%). Afterwards, dimeric phenyl benzoate *rac*-**245** was prepared *via* a double halogen-metal exchange and a nucleophilic addition to phenyl chloroformate in 60% yield. Mono-deprotohalogenation was observed as the main side product.

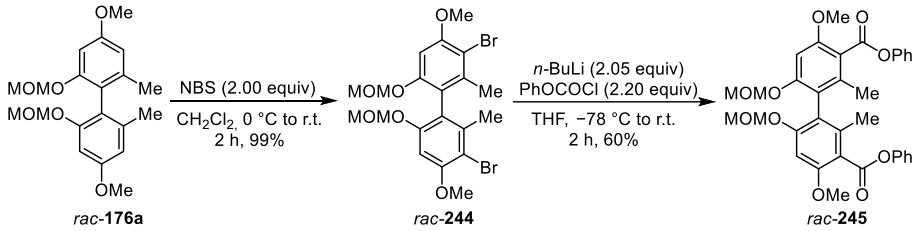

Scheme 78 Synthesis of dimeric phenyl benzoate *rac*-**245**.

First, the bidirectional *Myers*' annulation was performed with the optimized conditions of the monomer synthesis with a doubled amount of base and pyranone **241** (Scheme 79). After 3 hours reaction time, the mass of the mono-annulation product *rac*-**246** could be detected. However, no conversion towards the desired double annulation was observed.[261]

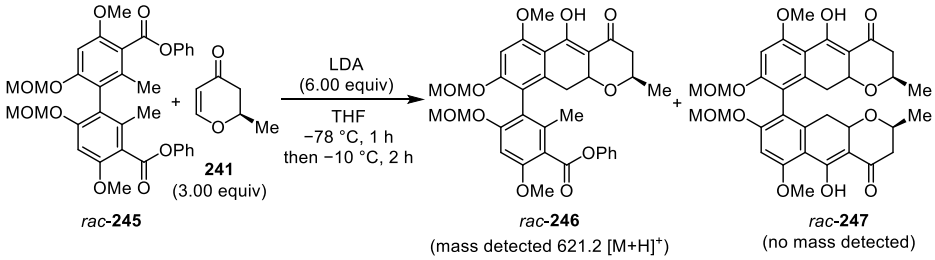

Scheme 79 Initial test reaction for double *Myers*' annulation towards *rac*-**247**.

Based on this observation, three hypotheses were formulated for this reaction under the given conditions:

1) Double benzylic deprotonation did not proceed completely.
2) Equivalents of electrophilic hydropyranone **241** were too low.
3) After the first annulation the second benzylic anion was reprotonated.

In the next step, further investigations were performed to address the named hypotheses. To ensure a complete double benzylic deprotonation of the dimeric toluate, deuteration experiments were performed under different conditions (Scheme 80). Here, the starting material *rac*-**245** was added to 6.00 equiv of LDA in THF at given temperature. Samples were taken from the reaction mixture hourly and quenched with D_2O. The crude samples were analyzed by ^{1}H-NMR to determine the conversion towards the desired double deuteration. Scheme 80 shows that at a lower temperature of −78 °C complete deprotonation required a longer reaction time of 3 hours. However, when adding NEt_3·HCl the reaction time could be shortened to 2 hours, which could be traced back to the catalyzed deaggregation of LDA and the following higher reactivity. When raising the temperature to −40 °C quantitative deprotonation could be observed after 1 hour.

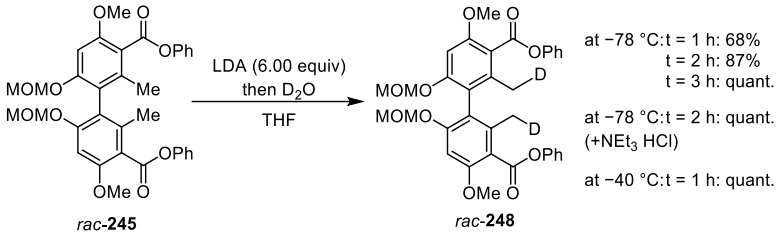

Scheme 80 Deuteration experiments for optimization of double benzylic deprotonation of *rac*-**245**; Conversions were determined *via* ^{1}H-NMR.

Therefore, in the following, for further optimizations benzylic deprotonation with LDA was performed at −40 °C. In the next step, the influence of the amount of the electrophile **241** was analyzed (Table 12). First, the reaction was performed at the optimized temperature (−40 °C) with 3.0 equivalents of pyranone **241**. Deuteration experiments have shown that double deprotonation proceeds completely under these conditions. However, after the addition of the pyranone **241**, only mono-annulated product *rac*-**246** was observed *via* mass spectrometry. Increasing the reaction time after the addition of pyranone **241** did not have any influence on the formation of *rac*-**247** (entry 2). In a third experiment, the amount of pyranone **241** was raised to 6.0 equivalents. After 2 hours the reaction was quenched with D_2O, in order to determine the amount of remaining deprotonated mono-functionalized product *rac*-**246**. Besides the mass of *rac*-**246**, no formation of double annulation *rac*-**247** was visible. Thus, the increased amount of pyranone **241** did not have a positive effect on the desired double annulation. Moreover, the ^{1}H-NMR of the crude product indicated that deuteration of the second methyl group of *rac*-**246** did not take place. Thus, the second

benzylic anion was likely to get reprotonated before the second addition towards the electrophile could take place. However, the origin of the protonation source is still unclear.

Table 12 Optimization of double *Myers*' annulation towards *rac*-**247**.

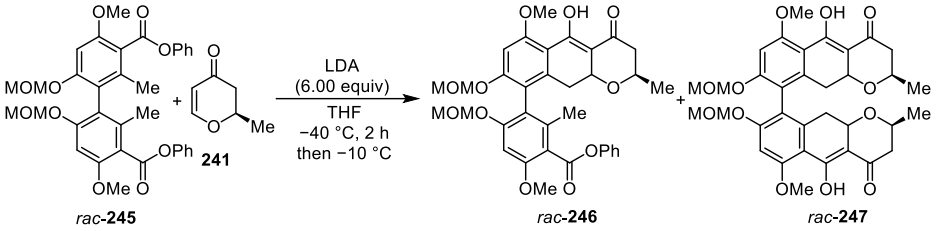

Entry	Equiv (241)	Time after addition of 241	*rac*-246[a]	*rac*-247[a]
1	3.0	2 h	+	−
2	3.0	o.n.	+	−
3[b]	6.0	2 h	+	−

[a] Product formation was determined *via* mass spectrometry (ESI); + = mass of product visible; − = no conversion; [b] Reaction was quenched with D_2O instead of H_2O.

As a direct double *Myers*' annulation reaction could not be executed, a stepwise annulation was envisioned (Scheme 81). The mono-functionalized product *rac*-**246** should be applied as a starting material for a second annulation reaction. However, LDA is likely to deprotonate the two acidic protons in 10-position or *α*-position to the ketone first. Therefore, an oxidative aromatization of the polycycle was tested to eliminate the acidic protons in 10-position first. For the oxidation the same optimized conditions as for the synthesis of monomeric *γ*-naphthopyrone **243** were used. However, stirring *rac*-**246** in the presence of chloranil in toluene at 110 °C resulted only in the degradation of the starting material and no conversion towards the oxidation product *rac*-**249**.

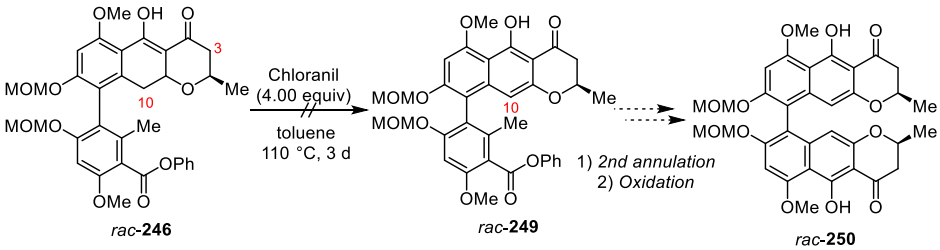

Scheme 81 Stepwise double *Myers*' annulation towards *rac*-**250**.

The challenge of the double *Myers*' annulation might be influenced by the choice of dimeric *ortho*-toluate. It might be possible that the steric hindrance of the mono-annulated product

rac-**246** might be too high. Thus, the addition of the second pyranone **241** might be sterically hindered and protonation of the benzylic anion would take place faster. In order to reduce the steric hindrance, the double annulation reaction was tested with dimeric methyl benzoate *rac*-**266** under the same optimized conditions (Scheme 82). The synthesis of *rac*-**266** is described in section 6.7.1. Besides the mass of the mono-annulated product *rac*-**252**, the mass of the mono-addition product *rac*-**251** was detected *via* mass spectrometry as well. This observation is consistent with the lower reactivity of the methyl benzoate *rac*-**266** towards the desired cyclization. Thus, the application of a less sterically hindered benzoate had no positive influence on the double addition or annulation reaction under the given conditions. Longer reaction times might prove whether the formation of the double annulation product would take place in the presence of the methyl ester.

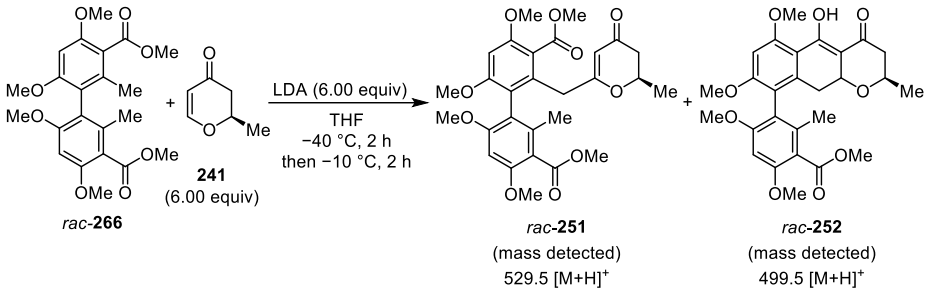

Scheme 82 Double *Myers*' annulation of dimeric methyl benzoate *rac*-**266** towards *rac*-**247**.

Despite the successful synthesis of the monomeric *γ*-naphthopyrone **243**, the double *Myers*' annulation to the desired dimeric natural product **3** pointed out to be rather challenging.

6.6.5. *Myers*' annulation *via* benzylic halogenation

After the attempts towards the synthesis of ustilaginoidin F (**3**) did not succeed, another alternative for the challenging double annulation reaction was tested. Here, benzylic halogenations were utilized. Scheme 83 shows two possible routes: When benzyl bromide *rac*-**253** is applied, the annulation undergoes a lithium-halogen exchange and generates *in situ* the required benzylic anion. After a fast lithium-halogen exchange, the formed anion could directly attack pyranone **241** in high concentration. This method proved to be effective for annulation reactions towards tetracycline analogues. [249, 256] Another possibility is the introduction of benzyl fluorides, which have several advantages. The generated benzylic anion would be more stabilized by the high electronegativity of fluorine.

This would lead to the formation of *rac*-**255** upon addition of the electrophile **241**. Without isolation of fluorinated tricycle *rac*-**255**, a formal elimination of HF with 2,2,2-trifluoroethanol (TFE) would result directly in an aromatization towards *rac*-**250**.[262] Thereby, the use of oxidizing agents like DDQ or chloranil could also be avoided.

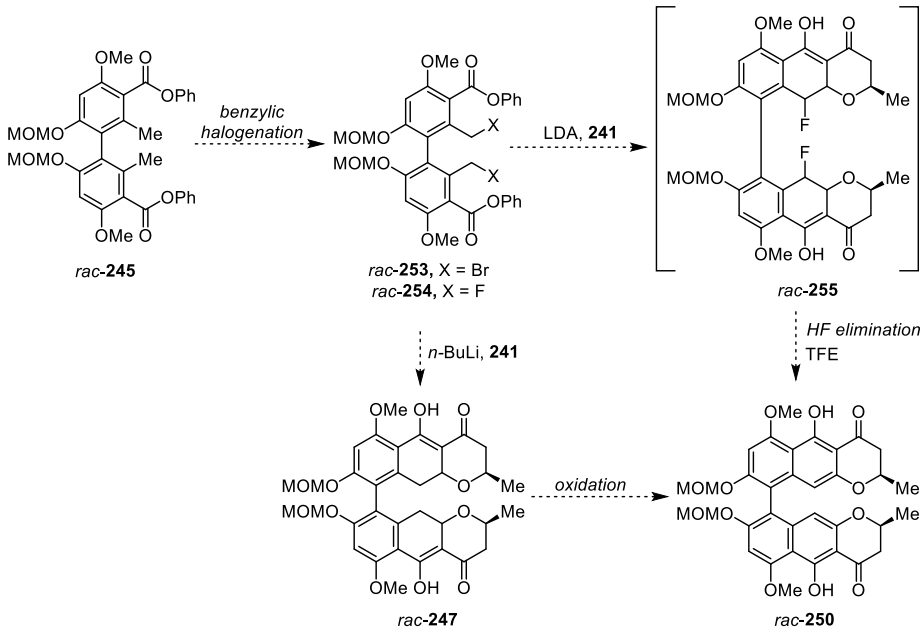

Scheme 83 Proposed synthesis path towards γ-naphthopyrone *rac*-**250** *via* benzylic halogenation.

In the first step, annulation reactions were tested on monomeric benzyl halides. Therefore, investigations towards the synthesis of monomeric benzyl halides were performed. Here, different electrophilic halogenation reactions were tested (Table 13). LDA was used as a base to perform selective benzylic deprotonation. After 1 hour at −78 °C different electrophilic halogenating reagents were added. For the synthesis of benzyl bromide **256**, NBS and $(BrCF_2)_2$ were used, inspired by the procedure of *Shair et al*.[262] However, while the application of NBS led to no conversion and $(BrCF_2)_2$ to only 21% isolated yield, aromatic bromination occurred as the main side product. Similarly, using NFSI or Selectfluor for an electrophilic fluorination only poor conversions could be observed (entry 3–4).[263, 264] A reason for the low conversions might be the low amount of base (1.00–1.50 equiv), as previous optimization showed that higher base equivalents are required for an increased conversion towards the functionalization of the *ortho*-toluate **229** (Table 10).

Table 13 Benzylic halogenation of phenyl benzoate **229** *via* electrophilic halogenation.

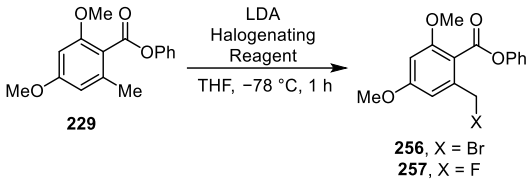

Entry	Equiv (LDA)	Halogenating Reagent	Conv. (256) [%][a]	Conv. (257) [%][a]
1	1.00	NBS[b]	0	/
2	1.50	$(BrCF_2)_2$[c]	(21)	/
3	1.00	NFSI[b]	/	10
4	1.00	Selectfluor[b]	/	0

[a] Conversions were determined *via* ^{1}H-NMR; isolated yields are given in parenthesis; [b] 1.30 equiv were used; [c] 2.05 equiv were used.

As the electrophilic halogenation was not successful, other halogenation methods were performed. Scheme 84 shows a persulfate-promoted selective fluorination using Selectfluor as the fluorine source, which was established by *Yi et al.*[265] They proposed a radical mechanism, where the persulfate was used to activate the benzylic hydrogen atoms. After 24 hours, no conversion towards the benzyl fluoride **257** was observed. However, only aromatic mono- and difluorination took place, which indicates that the used persulfate did not initiate a radical pathway, and Selectfluor acted itself in an electrophilic aromatic substitution. Similar results could be observed in radical halogenation using AIBN and NBS (Scheme 84). The radical initiator AIBN did not induce radical formation, with the result that only an electrophilic aromatic substitution with NBS took place.

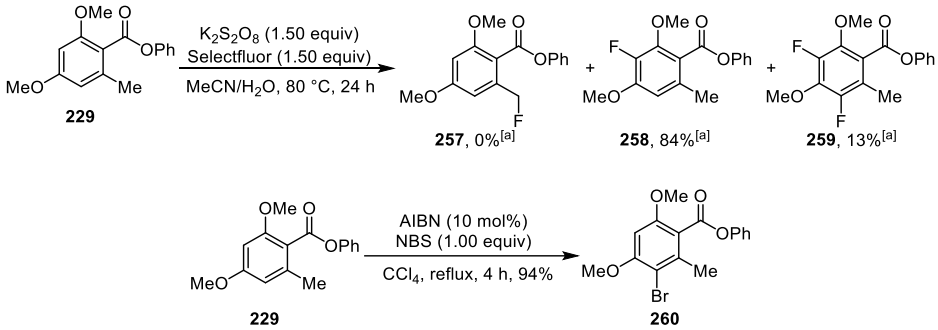

Scheme 84 Radical halogenation of phenyl benzoate **229**; [a] Conversions were determined *via* ^{1}H-NMR.

In *Shair*'s *Michael-Claisen* annulation, a nucleophilic displacement to convert a benzyl bromide with *tert*-butylammonium difluorotriphenylsilicate (TBAT) towards the desired benzyl fluoride was performed.[262, 266] Following *Shair*'s conditions isolated benzyl bromide **256** was stirred with TBAT over night at 80 °C (Scheme 85). The desired fluorinated product **257** was obtained in 57% conversion in the crude product. However, there was a challenge to isolate the product *via* column chromatography without impurities. Therefore, benzyl fluoride **257** could not be applied in the annulation reactions. In contrast to *Shair*'s procedure (47% yield over two steps), benzyl fluoride **257** could be synthesized only in 12% total yield over two steps starting from phenyl benzoate **229**.

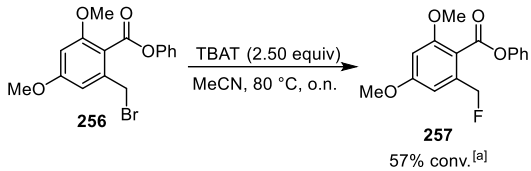

Scheme 85 Fluorination *via* nucleophilic displacement of bromide **256**; [a] Conversions were determined *via* ^{1}H-NMR.

In the next step, a *Myers*' annulation was performed with benzyl bromide **256** *via* a lithium-halogen exchange with *n*-butyllithium (Scheme 86). In contrast to the previous annulation with LDA, *n*-butyllithium was added dropwise to a solution of both benzyl bromide **256** and pyranone **241** in THF. After 4 hours reaction time, the annulated product **242** was formed in 86% conversion. The main side reaction was protodehalogenation of the starting material **256**. In comparison to the annulation *via* selective deprotonation with LDA, this reaction was more robust, leading to very good conversion. However, an additional step is required to prepare the required benzyl bromide **256**.

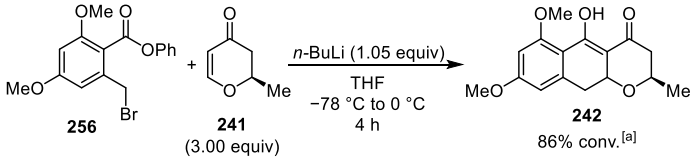

Scheme 86 *Myers*' annulation *via* lithium-halogen exchange towards **242**; [a] Conversions were determined *via* ^{1}H-NMR.

Afterwards, the *Myers*' annulation *via* a lithium-halogen exchange was applied on the dimeric benzyl bromide *rac*-**253**. Therefore, benzylic halogenation should be executed on the dimeric phenyl benzoate *rac*-**245** *via* selective deprotonation with LDA and $(BrCF_2)_2$ as electrophilic halogenating reagent (Scheme 87). The same conditions as the monomer

synthesis were applied on the dimer synthesis, whereas the equivalents of LDA and $(BrCF_2)_2$ were doubled. After 1 hour reaction time, only the mono-brominated dimeric orsellinate *rac*-**261** was obtained in excellent conversion of 92%. However, there was no indication of dibromination. The bromination reaction was repeated with isolated mono-brominated product *rac*-**261** under the same conditions. Nevertheless, no conversion was observed, and the starting material was reisolated.

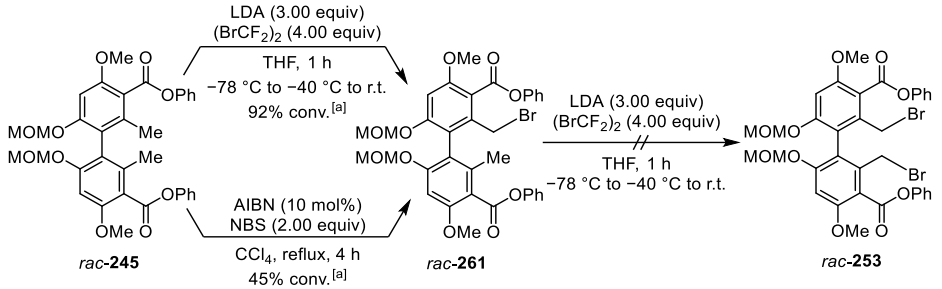

Scheme 87 Attempted synthesis of dimeric benzyl bromide *rac*-**253** *via* electrophilic halogenation and radical halogenation; [a] Conversions were determined *via* ^{1}H-NMR.

When performing a radical bromination with AIBN and NBS, mono-brominated dimer *rac*-**261** was formed only in 45% conversion (Scheme 87). In contrast to the monomeric radical bromination, no aromatic bromination product was visible as a side product, as the favored position was blocked by the biphenyl axis. As double bromination of the *ortho*-toluate was challenging, bromination of mono-annulation product *rac*-**246** was tested (Scheme 88). However, again no conversion towards the desired bromination was observed.

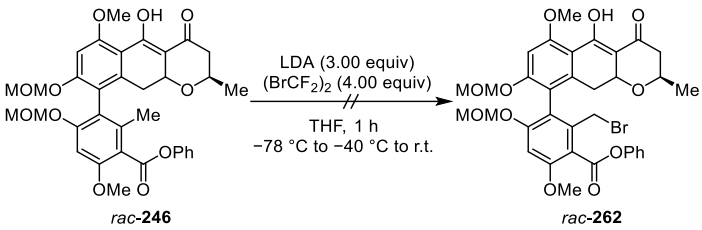

Scheme 88 Attempted bromination of mono-annulated dimer *rac*-**246**.

The results point out that specific two-directional annulation reactions of biphenyls can be challenging (Scheme 89). Bidirectional *Staunton-Weinreb* annulations with the *para*-substituent to the axis have been already applied in the synthesis of dimeric axially chiral polyketides, like vioxanthin or hibarimicinone (blue).[262, 267-270]

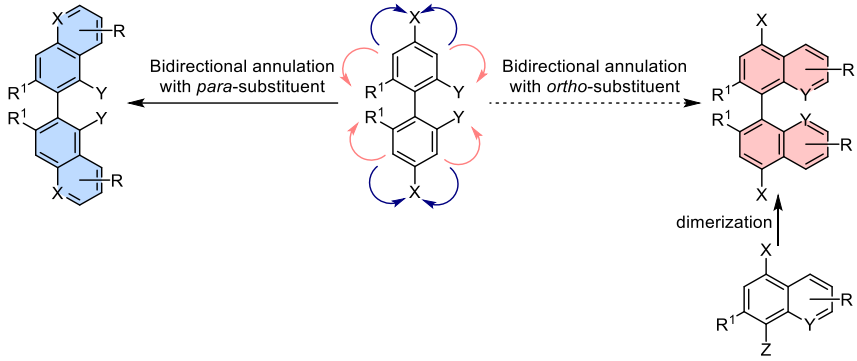

Scheme 89 Challenges of bidirectional annulation towards the synthesis of dimeric axially chiral polyketides.

However, bidirectional *Staunton Weinreb* or *Myers*' annulations with the *ortho*-substituents, extending orthogonal to the axis, appear to be restricted (red). Therefore, literature more often describes to access these dimers by dimerization of the final monomeric building blocks.[173, 174, 271-273] Further investigations on bidirectional annulation reactions thus need to be done.

Summary Chapter 6.6

1. Synthesis of monomeric and dimeric *ortho*-toluates:
   - Monomeric methyl benzoate **228** was isolated in 70% yield over five steps.
   - Monomeric phenyl benzoate **229** was isolated in 65% yield over three steps.
   - Dimeric phenyl benzoate *rac*-**245** was isolated in 59% yield over two steps.

2. Reproduction of total synthesis of rubrofusarin B (**123**) did not succeed:
   - Addition product **235** was only formed using phenyl benzoate **229** (32% yield)

3. Synthesis of monomeric *γ*-naphthopyrone dimethylether **243** (49% yield over two steps)
   - Annulation of phenyl benzoate *rac*-**229** and **241** was possible (61% yield)
     - Higher equivalent of LDA was required for higher conversion.
     - LiHMDS and NEt_3·HCl could be used as additive to increase the reactivity and to facilitate cyclization.
   - Oxidative aromatization using chloranil was successful (80% yield)

4. Approach towards total synthesis of ustilaginoidin F (**3**):
   - Deuteration experiments were used to determine conditions for complete double benzylic deprotonation.
   - Annulation of dimeric benzoate *rac*-**245** led only to mono-annulation.
   - Bidirectional *Myers*' annulation of dimeric methyl benzoate: Lower reactivity of toluate led to mixture of mono-addition and mono-annulation.
   - Oxidative aromatization of mono-annulated product led to degradation.

5. *Myers*' annulation *via* benzylic halogenation was used as possible alternative:
   - Monomeric benzylic halogenation was possible *via* selective deprotonation and electrophillic halogenation in low conversions.
   - Annulation with monomeric benzyl bromide **256** was successful (86% conv.)
   - Dimeric benzylic halogenation led only to mono-bromination.
   - Subsequent bromination of mono-brominated product was not possible.

6.7 Total synthesis of (*M*)-isokotanin A (*M*)-(4)

After the approach towards the total synthesis of chosen *γ*-naphthopyrones did not succeed, another natural product was chosen, which features the same biphenol building block **1**: (*M*)-isokotanin A (*M*)-(**4**). The antifeedant bicoumarin was first isolated in 1994 by *Gloer* and since then different atroposelective total syntheses have been published.[36, 37, 39, 180] By the application of the metal-catalyzed homocoupling reaction and the scalable EKR strategy, a more efficient and robust total synthesis was aimed to be established. The retrosynthetic analysis of (*M*)-isokotanin A (*M*)-(**4**) is shown in Scheme 90. The strategy was inspired by the racemic total synthesis of the group of *Müller*.[38] The dimeric bicoumarins were to be prepared by double cyclizations of dimeric orsellinate (*M*)-**268**, which could be gained from the biphenol building block (*M*)-**1**.

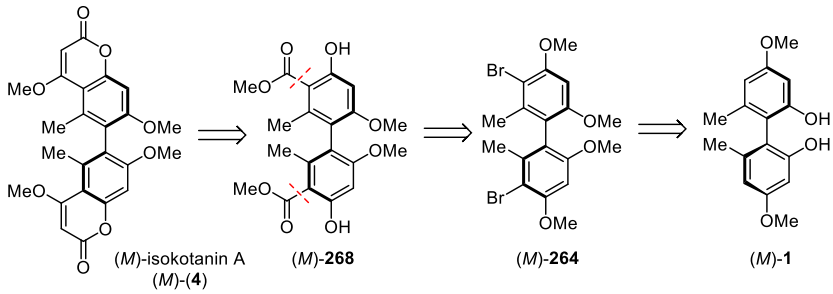

Scheme 90 Retrosynthetic analysis of the total synthesis of (*M*)-isokotanin A (*M*)-(**4**).

6.7.1 Racemic synthesis of isokotanin A (4)

The synthesis steps towards (*M*)-isokotanin A (*M*)-(**4**) were initially developed and optimized using racemic biphenol *rac*-**1**. In the first step, a double methylation of biphenol *rac*-**1** was performed (Table 14). Common conditions using potassium carbonate as base and dimethyl sulfate (DMS) as methylating agent in acetone were applied.[271, 272, 274, 275] However, after stirring for 24 hours at room temperature as well as at elevated temperatures, insufficient amounts of the desired double-methylated biphenol *rac*-**152** were isolated (entry 1–2). The crude ^{1}H-NMR showed the formation of monomethylated product *rac*-**263** and side products, which could not be identified. The steric hindrance of both *ortho*-substituents next to the axis might lead to the low reactivity. Addition of higher equivalents of dimethyl sulfate did also not increase the conversion (entry 3). During the reaction dimethyl sulfate might decompose in aqueous basic conditions, which would

explain the low conversions.[276] When the methylating agent was added slowly over a period of 10 hours, fresh dimethyl sulfate was continuously available in the reaction mixture and the desired *O*,*O*′-dimethyl biphenol *rac*-**152** was isolated in 99% (entry 4).

Table 14 *O*,*O*′-Double methylation of biphenol *rac*-**1**.

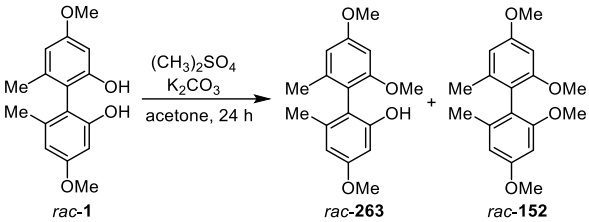

Entry	K_2CO_3 (equiv)	DMS (equiv)	Temp.	Addition[a]	263 [%][a]	152 [%][a]
1	2.5	2.1	Reflux	Fast	33 (27)	67 (56)
2	3.0	2.5	r.t.	Fast	n.d.	89 (58)
3	3.0	5.0	r.t.	Fast	42 (32)	58 (47)
4	3.0	10.0	r.t.	Slow over 10 h	n.d.	(99)

[a] Way of adding $(CH_3)_2SO_4$; [b] Conversions were determined *via* ^{1}H-NMR; isolated yields are given in parenthesis.

Afterwards a highly regioselective dibromination was performed in excellent yield (97%), providing exclusively the 4,4′-substituted product *rac*-**264** (Scheme 91). Brominated biphenyl *rac*-**264** was carboxylated *via* halogen-metal exchange and nucleophilic addition to carbon dioxide in 94% yield. Here, it was important to purge the reaction mixture with gaseous carbon dioxide, instead of adding solid carbon dioxide directly. The presence of condensed water would otherwise lead to a high amount of protodehalogenation product *rac*-**152**.

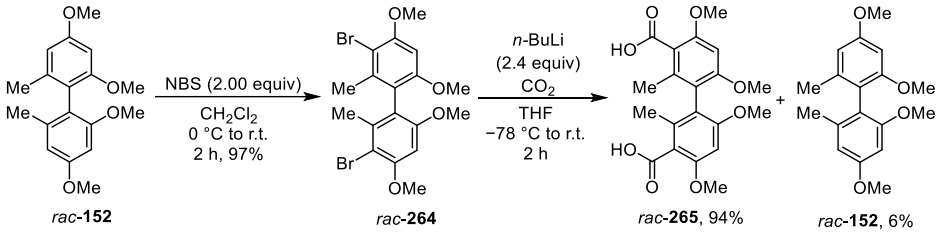

Scheme 91 Synthesis of dicarboxylate *rac*-**265** *via* double bromination of *rac*-**152**.

The crude dicarboxylate *rac*-**265** was subsequently methylated to the corresponding methyl benzoate dimer *rac*-**266** (Table 15). Therefore, dimethyl sulfate was used as the

methylating agent. Different bases and solvents were screened for optimal conditions. As in previous methylation reactions, acetone and potassium carbonate were initially tested (entry 1). However, very low conversions were observed possibly due to the poor solubility of the starting material in acetone. Therefore, the solvent was changed to ethanol which ensured good solubility and consequently resulted in higher conversions (entry 2–4). Nevertheless, the use of sodium hydroxide also led to the formation of mono-decarboxylated side product *rac*-**267** after longer reaction times. When using potassium carbonate as a weaker base in ethanol, the desired double esterified product *rac*-**266** was obtained in very good yields (73%) (entry 4).

Table 15 Esterification of dicarboxylate *rac*-**265**.

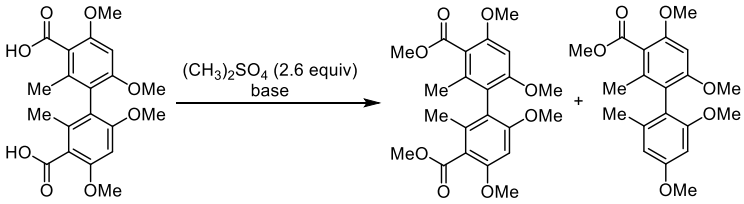

Entry	Base	Equiv	Solvent	Temp.	Time	266 [%][a]	267 [%][a]
1	K_2CO_3	4.0	Acetone	r.t.	o.n.	5 (2)	n.d.
2	NaOH	2.5	EtOH	Reflux	o.n.	31 (14)	34 (15)
3	NaOH	2.5	EtOH	r.t.	o.n.	30	40
4	K_2CO_3	4.0	EtOH	r.t.	5 h	90 (73)	10

[a] Conversions were determined *via* ^{1}H-NMR; isolated yields are given in parenthesis.

In the next step, a regioselective double methyl ether cleavage in 5,5′-position was performed by treatment with BCl_3 giving dimeric orsellinate *rac*-**268** in good yields (76%) (Scheme 92).[277] At this point, the synthesis route is intersecting the published racemic total synthesis by the group of *Müller*.[38] Here the aim was to reproduce the synthesis of diaminobichromenone *rac*-**270** in the reaction with lithiated acetonitrile. According to the given procedure, orsellinate *rac*-**268** was added to *in situ* lithiated acetonitrile. After a reaction time of 1.5 hours, the desired product was supposed to be isolated in 77% yield.[38] However, only traces of a mixture of mono-functionalized *rac*-**269** and dimeric aminochromenone *rac*-**270** was observed (Scheme 92).

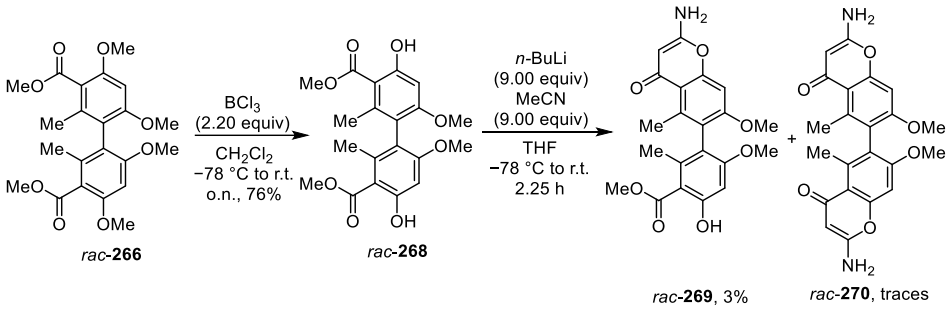

Scheme 92 Synthesis of diaminobichromenone *rac*-**270**.

When considering the mechanism of the aminochromenone synthesis, different reactions might be possible. Scheme 93 illustrates the different possible mechanisms based on the monomer orsellinate **271**. When orsellinate **271** is added to lithiated acetonitrile, $LiCH_2CN$ is expected to attack the carbonyl group and form the *β*-keto nitrile i**v**, as described by *Müller* (Route A).[38, 278] In the next step, the hydroxy group needs to be deprotonated either by the excess of *n*-butyllithium, the lithiated acetonitrile or the methoxide. The phenolate **vi** would attack the nitrile group, which would result in an intramolecular cyclization. Acidic work up would lead to the desired product aminochromenone **viii**.

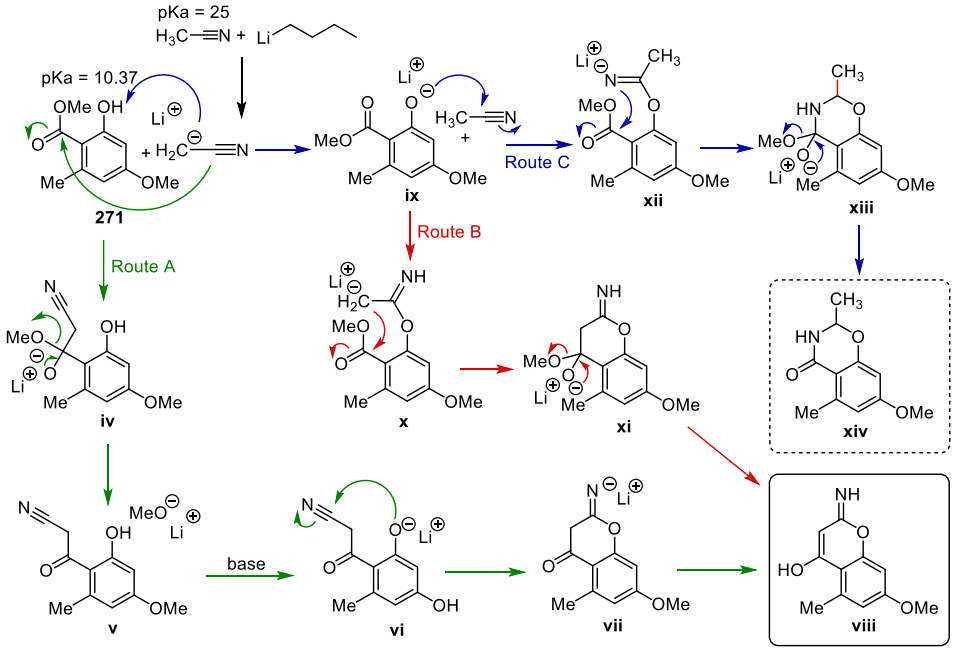

Scheme 93 Possible mechanism for the synthesis of aminochromenone.

Moreover, lithiated acetonitrile could also act as a base, deprotonating the phenol (pKa = 10)[279], which is more acidic than acetonitrile (pKa = 25)[280]. The phenolate **ix** would attack the acetonitrile, which would lead to two possible routes. An intramolecular cyclization of **x** would lead to the formation of the desired aminochromenone **viii** (Route B). Although the higher acidity of the used orsellinate in contrast to acetonitrile would theoretically propose the deprotonation of orsellinate **271** as a first step, Müller described the formation of the *β*-keto nitrile.[38] On the other hand, the phenolate i**x** could also attack the acetonitrile and induce a subsequent intramolecular cyclization of **xii** towards lactam **xiv**. However, no lactam formation was observed. In case of the formation of the *β*-keto nitrile three hypotheses could be made, to increase the conversion to the desired diamino-bichromenone:

1) Longer reaction time and higher temperatures are needed to enhance the nucleophilic attack of $LiCH_2CN$.
2) Longer reaction time and higher temperatures are needed to enhance the intramolecular cyclization.
3) Additional base is needed to deprotonate phenol **v** and to facilitate cyclization towards **viii**.

Based on the hypotheses, different conditions were screened to improve the conversions (Table 16). The procedure was adjusted, by adding additional *n*-butyllithium (4.0 equiv) after orsellinate *rac*-**268** was mixed with lithiated acetonitrile. First, the effect of additional base was analyzed (entry 1). The reaction time and temperature were kept the same as in the published procedure. The addition of extra base increased the conversions, allowing for the isolation of both the mono- *rac*-**269** and difunctionalized product *rac*-**270**. This result confirms the third hypothesis. Although there is already an excess of base in the reaction mixture, additional base is required to ensure the deprotonation of the hydroxy group of the *β*-keto nitrile, which promotes the intramolecular cyclization. In the next step, reaction time and temperature were screened. Entry 2 shows that longer reaction times led to further increase of the conversion. However, when rising the temperature for a longer duration, conversions dropped again (entry 3). The intermediates might not be stable at elevated temperatures. Therefore, the temperature was maintained at −78 °C and the reaction time was further extended, resulting in more optimal conditions (entry 4–5). After 6.5 hours a ~1:1 mixture of mono- and dimeric aminochromenone was observed. The mono-

aminochromenone *rac*-**269** was obtained in 38% and the diaminobichromenone *rac*-**270** in 43% isolated yield (entry 5).

Table 16 Optimization of conditions for the synthesis of diaminobichromenone *rac*-**271**.

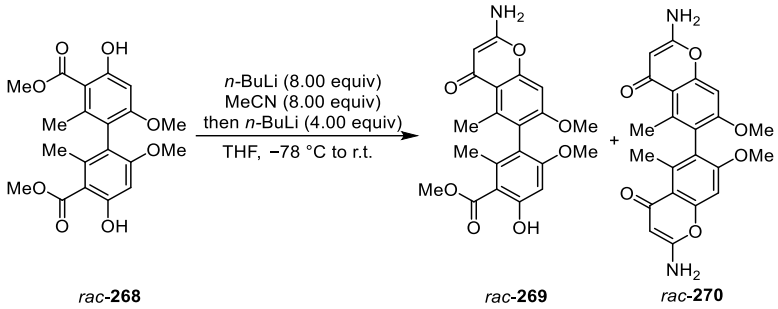

rac-**268** *rac*-**269** *rac*-**270**

Entry	Time and Temp after addition of 268	Time and Temp after 2nd addition of *n*-BuLi	268 [%][a]	269 [%][a]	270 [%][a]
1	30 min at −78 °C, 45 min at r.t.	1 h at r.t.	80	15	5
2	1.5 h at −78 °C	30 min at −78 °C, 1 h at r.t.	40	28	33
3	1.5 h at −78 °C, 1 h at r.t.	30 min at −78 °C, 1 h at r.t.	84	12	4
4	3 h at −78 °C	30 min at −78 °C, 1 h at r.t.	34	25	41
5	5 h at −78 °C	30 min at −78 °C, 1 h at r.t.	19	(38)	(43)

[a] Conversions were determined *via* ^{1}H-NMR; isolated yields are given in parenthesis.

When applying isolated monoproduct *rac*-**269** under the same optimized conditions, the desired dimeric product *rac*-**270** was afforded in 59% isolated yield (Scheme 94). Thus, diaminobichromenone *rac*-**270** was obtained in 65% total yield over two steps.

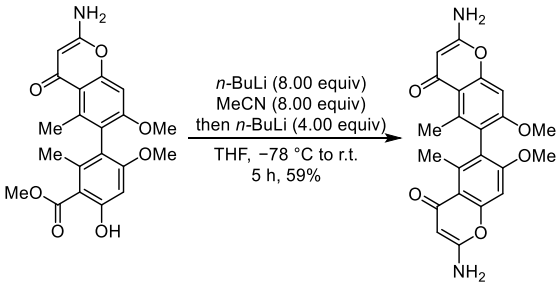

rac-**269** *rac*-**270**

Scheme 94 Conversion of mono-aminochromenone *rac*-**269** towards dimeric aminochromenone *rac*-**270**.

The synthesized dimeric cyclization product could possibly exist in two tautomers: 2-aminochromen-4-one *rac*-**270** and 2-iminochromen-4-ol *rac*-**270** (Scheme 95). In the HMBC-spectrum the relevant correlation is marked (Figure 29). In the ^{1}H-NMR spectrum (DMSO-d_6) the singlet for both amino groups are visible at δ = 7.15 ppm. These protons 1-H/1′-H show a correlation with C-3/C-3′, which are the α-carbon atoms of the *Michael* systems. Hence, only the presence of the 2-aminochromen-4-one tautomer was confirmed, which correspond with the results of *Müller*.[38]

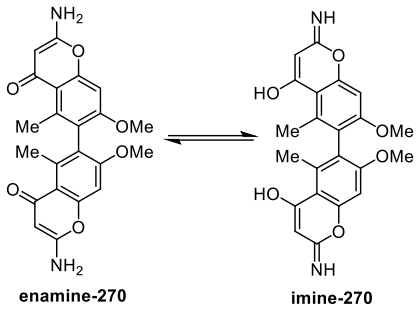

Scheme 95 Possible tautomers of diaminobichromenone *rac*-**270**.

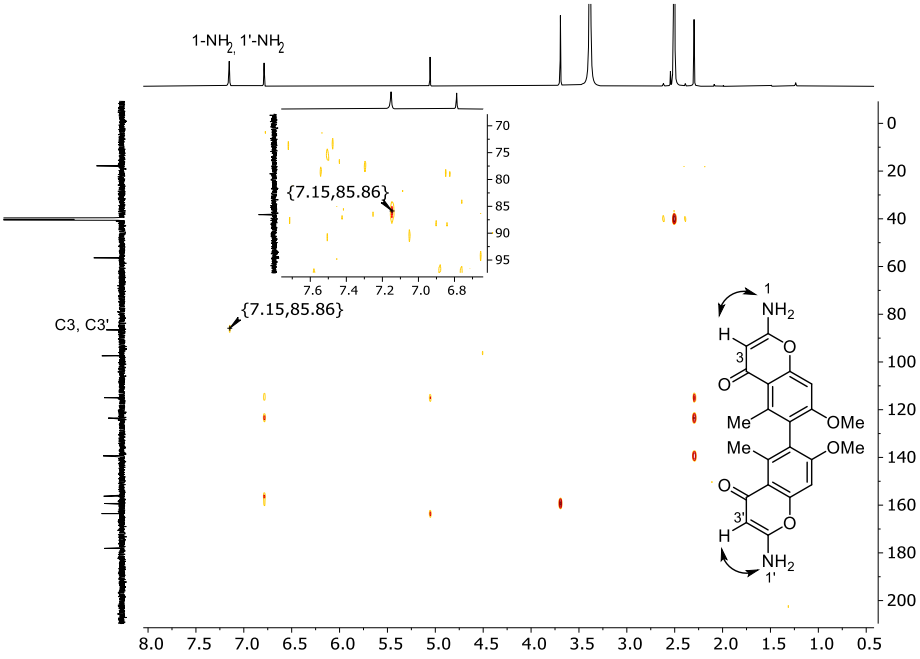

Figure 29 HMBC-Spectrum of dimeric cyclization product *rac*-**270**.

In the last step, diaminobichromenone *rac*-**270** was hydrolyzed towards the hydroxychromenone *rac*-**272** (Scheme 96). Following *Müller*'s procedure, the hydrolysis was performed in the presence of concentrated hydrochloric acid and methanol. After the stated 3.5 hours, the hydroxychromenone *rac*-**272** could not be isolated in high purity, as stated in the publication. Unknown side products were formed, which could not be removed by column chromatography or recrystallization. Therefore, the crude product was used without further purification. The hydroxychromenone *rac*-**272** was methylated towards the desired *rac*-isokotanin A *rac*-(**4**) in overall 30% yield over two steps. Overall, the racemic dimeric natural product *rac*-**4** could be synthesized in 10% total yield in eight steps, starting from the biphenol building block *rac*-**1**.

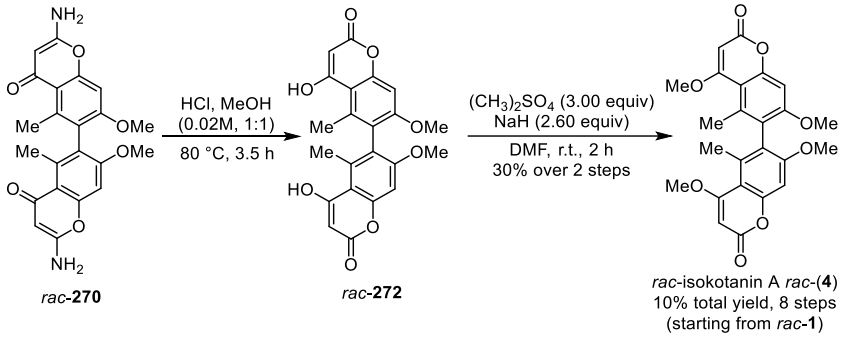

Scheme 96 Synthesis towards *rac*-isokotanin A *rac*-(**4**).

6.7.2 Synthesis of atropoenantiopure (*M*)-isokotanin A (*M*)-(4)

In this chapter the atropoenantiopure biphenol (*M*)**-1** was applied in the total synthesis towards the natural product (*M*)-isokotanin A (*M*)-(**4**) (Scheme 97). The biphenol building block (*M*)**-1** was synthesized *via* the EKR, described in section 6.2.7. The conditions of the optimized racemic total synthesis towards the natural bicoumarin *rac*-isokotanin A *rac*-(**4**) (section 6.7.1) were implemented.

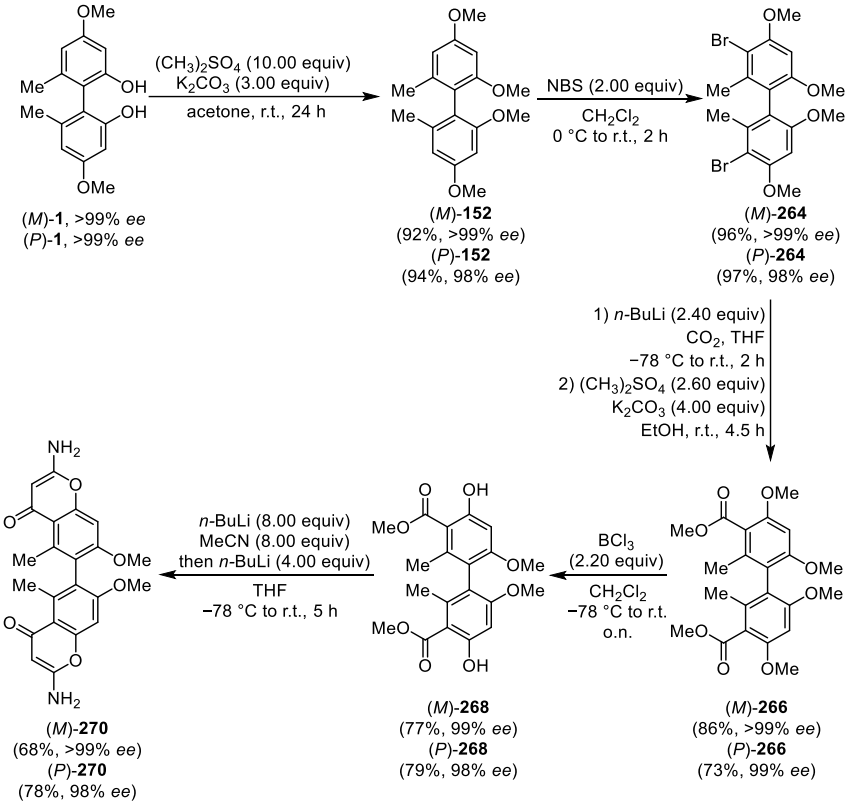

Scheme 97 Atropoenantiopure synthesis of diaminobichromenone (*M*)-**270** and (*P*)-**270**.

Analogously to the preparation of racemic material, the total synthesis of enantiopure product **270** started with the double *O*-methylation and regioselective bromination from enantiopure biphenol (*P*)-/(*M*)-**1** in excellent yields. Afterwards, the formation of the double methyl ester (*P*)-/(*M*)-**266** was performed in 73% and 86% yield over two steps. In the presence of BCl_3, the desired regioselective double methyl ether cleavage in 5,5′-position took place in good yields of 77% and 79% respectively. The synthesized dimeric orsellinate (*P*)-/(*M*)-**268** was used in the optimized reaction towards

diaminobichromenone (*P*)-/(*M*)-**270**. In comparison to the racemic synthesis, the enantiopure synthesis occurred with higher conversions and without the formation of mono-functionalized product (*P*)-/(*M*)-**269**. The desired product (*M*)-**270** could be isolated directly in one step in 68% yield and (*P*)-**270** in 78% yield.

In the last steps, only the diaminobichromenone (*M*)-**270** was used to complete the total synthesis, as the natural product was assigned the (*M*)-configuration. In two steps the dimeric diaminobichromenone (*M*)-**270** was hydrolyzed and methylated in 26% total yield (Scheme 98).

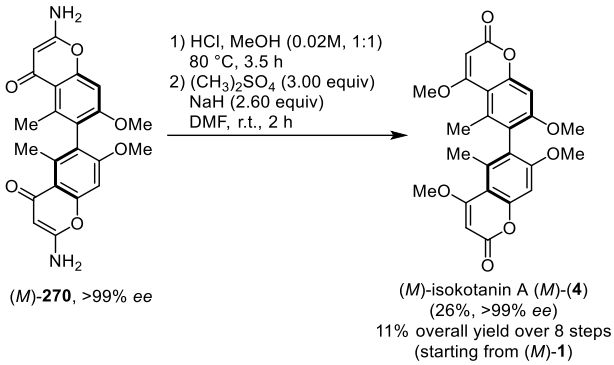

Scheme 98 Atropoenantiopure synthesis of (*M*)-isokotanin A (*M*)-(**4**).

In summary, the atroposelective total synthesis of (*M*)-isokotanin A (*M*)-(**4**) starting from the enantiopure axially chiral 2,2′-biphenol building block (*M*)-**1** was established in 11% overall yield over eight steps. The enantiopurity of all compounds remained constant. Minimal fluctuations of the enantiomeric excesses were likely caused by measuring inaccuracy of the chiral HPLC. The absolute configuration of the natural product was confirmed by the comparison of its optical rotation ($[\alpha]_D^{25} = +48.0$ (c = 1.0, $CHCl_3$)) with literature data ($[\alpha]_D^{25} = +21.4$ (c = 0.22, $CHCl_3$)).[180]

In comparison to previously published asymmetric total syntheses of (*M*)-isokotanin A (*M*)-(**4**), [36, 37, 39] all routes, including the one presented here, intersect the same common enantiopure intermediate (*M*)-**152**. However, the application of the Pd-catalyzed MBSC in combination with the EKR for the synthesis of building block (*M*)-**1** had several advantages, which makes this route more efficient (Figure 30). In contrast to *Lin*'s chiral bromo-oxazoline monomers (*R*)-**148**, which had to be synthesized with stoichiometric amounts of chiral phenylglycinol, the monomer building block bromophenol **174** could be prepared in

a robust and scalable way. Furthermore, in contrast to the former total syntheses, the established homocoupling *via* Pd-catalyzed MBSC eliminates the need of stoichiometric amounts of copper, high temperatures and hazardous reagents. Using catalytic amounts of palladium, a scalable one-pot MBSC could be performed for the construction of the challenging tetra-*ortho*-substituted biaryl bond.

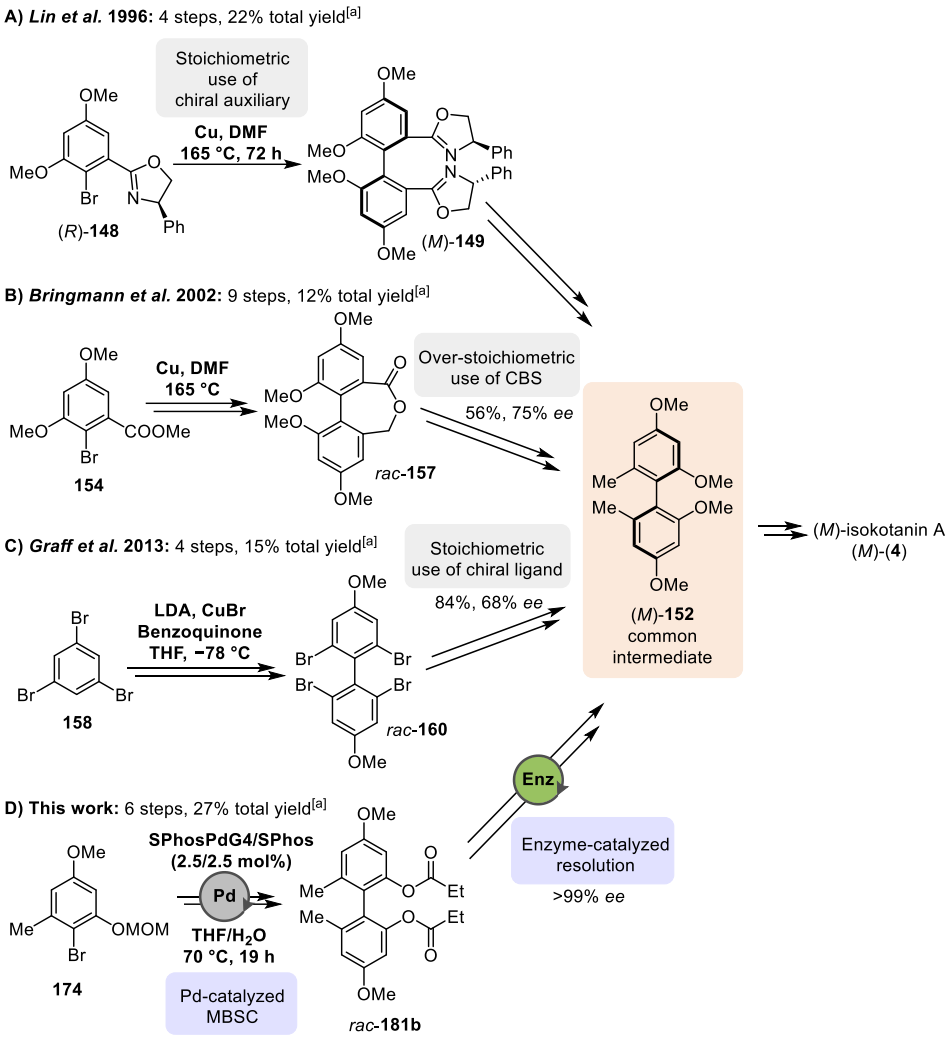

Figure 30 Strategies of asymmetric total syntheses of (*M*)-isokotanin A (*M*)-(**4**); [a] overall total yield and step count from monomer building block towards common intermediate (*M*)-**152**.

The atroposelective preparation of enantiopure (*M*)-**152** formerly required the stoichiometric application of chiral reagents or auxiliaries, which only led to an enantiomeric excess of 68–75% *ee* before recrystallization. The group of *Lin* did not report any

enantiomeric excess of the axially chiral dimer (*M*)-**149**. In contrast, the catalytic EKR facilitates a highly atroposelective transformation of *rac*-**1** towards enantiopure product (*M*)- and (*P*)-**1** (≥99% *ee*) on a gram-scale using cheap and commercially available CRL. Thus, compared to former asymmetric routes, a more efficient and scalable way was developed, resulting in the common intermediate (*M*)-**152** in a higher total yield and in excellent enantiomeric excess.

Summary Chapter 6.7

1. Racemic total synthesis of *rac*-isokotanin A *rac*-(**4**) (10% overall yield in eight steps)
   - Synthesis of dimeric orsellinate *rac*-**268** was developed (50% over five steps)
   - Subsequent synthesis of isokotanin A *rac*-(**4**) was inspired by *Müller*'s route.[38]
   - In addition to the publication of *Müller et al.*[38], studies towards the synthesis of diaminobichromenone *rac*-**270** was performed: additional base was essential for the bidirectional functionalization in high conversions
   - Hydrolysis and dimethylation took place in low yields.

2. Racemic synthesis route could be applied on the synthesis of enantiopure (*M*)-isokotanin A (*M*)-(**4**) (11% overall yield in eight steps)
   - Enantiopure biphenol building block (*M*)-**1** was successfully applied in the total synthesis.
   - In contrast to racemic route, synthesis of enantiopure diaminobichromenone (*M*)-**270** took place exclusively *via* difunctionalization

3. In contrast to previous publications, a more scalable way was developed to obtain the common intermediate (*M*)-**152** in a higher total yield and excellent enantiomeric excess.

6.8 Investigation on total synthesis of (*P*)-isokotanin C (*P*)-(5)

A great advantage of the EKR of biphenol **1** is that both enantiomers (*M*)- and (*P*)-**1** are accessible. In this way it would be also possible to access the natural product (*P*)-isokotanin C (*P*)-(**5**), of which no total synthesis has been published before. The small but defining difference between both is, beside the opposite configuration, that the 2,2′-dimethyl ether is replaced with a 2,2′-bihydroxy moiety. Therefore, the goal is to cleave the double methyl ether late stage of the diaminobichromenone (*P*)-**270** or the hydroxychromenone (*P*)-**272** (Scheme 99). An acid-catalyzed etherification of the unprotected hydroxychromenone (*P*)-**273** would lead to the desired natural product (*P*)-**5**. This reaction has been performed on the monomer building block towards demethylsiderin **139**.[179]

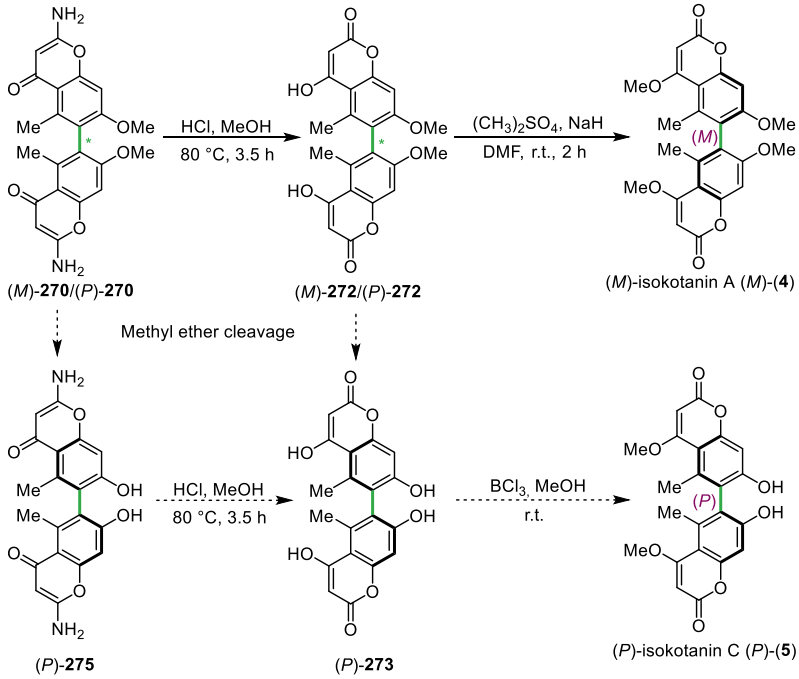

Scheme 99 Proposed total synthesis of (*P*)-isokotanin C (*P*)-(**5**).

First, different conditions were tested for the demethylation of hydroxychromenone *rac*-**272** (Table 17). Treatment with BBr_3 in CH_2Cl_2 did not show any conversion, as the starting material was not soluble in CH_2Cl_2 (entry 1).[281, 282] A heterogeneous reaction after 24 hours was not possible. Hydroxychromenone *rac*-**272** showed low solubility in most organic solvents. Therefore, combinations of strong nucleophiles in DMF were chosen

(entry 2–3). While sodium *n*-propyl thiolate did not show any conversions, the treatment with potassium diphenyl phosphide led to the detection of the mass of the product (404.8 $[M+Na]^+$; 420.8 $[M+K]^+$).[283] ^{31}P-NMR was measured in $CDCl_3$ to identify possible phosphine side products. The corresponding methylated phosphine was visible in its oxidized form in the ^{31}P-NMR (methyldiphenylphosphine oxide: δ=29.07 ppm). Additionally, oxidation side products like diphenyl phosphine oxide (δ =21.46 ppm; 202.9 $[M+H]^+$) and diphenyl phosphinic acid (218.9 $[M+H]^+$) were observed in the mass spectrum and ^{31}P-NMR. However, the desired demethylated product was not able to be isolated.

Table 17 Conditions for demethylation of hydroxychromenone *rac*-**272**.

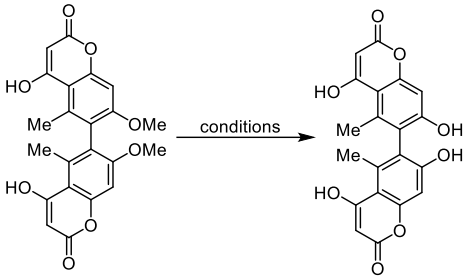

rac-**272** *rac*-**273**

Entry	Reagent	Equiv	Solvent	Temp.	Time	Product formation[a]
1	BBr_3	2.2	CH_2Cl_2	r.t.	24 h	−
2	*n*-PrSNa[b]	4.0	DMF	80 °C	5 h	−
3	PPh_2K[c]	8.0	DMF	80 °C	o.n.	+

[a] Product formation was determined *via* mass spectrometry (ESI): + = mass of product visible, − = no conversion; [b] prepared from *n*-PrSH (4.0 equiv) and NaH (60% in mineral oil, 4.4 equiv); [c] prepared from $HPPh_2$ (8.0 equiv) and *t*-BuOK (1 M in THF, 8.0 equiv).

As the deprotected hydroxychromenone *rac*-**273** could not be isolated, different conditions towards the deprotection of diaminobichromenone *rac*-**270** were tested (Table 18). In the reaction with BBr_3 in CH_2Cl_2, mono-deprotected aminochromenone *rac*-**274** could be detected in the mass spectrum (377.2 $[M+H]^+$) and was isolated in 5% yield (entry 1). Treatment with trimethylsilyl iodide in the microwave (300 W) did not show any conversion. After longer reaction time only decomposition of the starting material was visible.[284, 285] Diphenyl phosphide was previously the most promising demethylating agent, hence different diphenyl phosphides were tested (entry 3–5). However, no conversion towards mono- **274** or double deprotected product **275** was identified.

Table 18 Conditions for demethylation of diaminobichromenone *rac*-**270**.

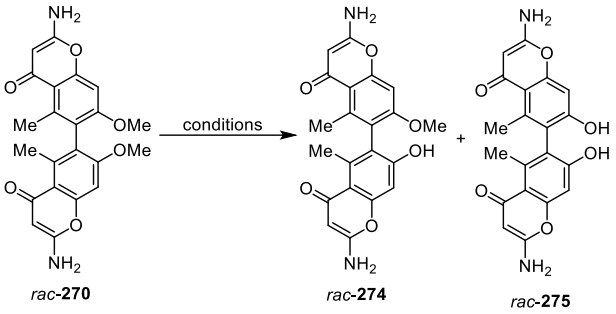

Entry	Reagent	Equiv	Solvent	Temp.	Time	Product formation[a]
1	BBr_3	2.2	CH_2Cl_2	40 °C	24 h	+ (*rac*-**274**)
2	TMSI	3.5	MeCN	MW: 300 W	15 min	−
3	PPh_2K[b]	8.0	DMF	80 °C	o.n.	−
4	PPh_2Li[c]	8.0	THF	80 °C	o.n.	−
5	PPh_2Na[d]	8.0	DMF	80 °C	o.n.	−

[a] Product formation was determined *via* mass spectrometry (ESI): + = mass of product visible, − = no conversion; [b] prepared from $HPPh_2$ (8.0 equiv) and *t*-BuOK (1 M in THF, 8.0 equiv); [c] prepared from $HPPh_2$ (8.0 equiv) and *n*-butyllithium (2.5 M in pentane, 8.0 equiv); [d] prepared from $HPPh_2$ (8.0 equiv) and NaH (60% in mineral oil, 8.0 equiv).

The deprotection of a dimeric biphenyl with high steric hindrance and low solubility in organic solvents proved to be challenging. Therefore, deprotection was tested on dimeric orsellinate *rac*-**268**, which is less bulky and has a good solubility in most organic solvents. *rac*-**268** was treated with potassium diphenyl phosphide overnight (Scheme 100). After work up only the mono-deprotected orsellinate *rac*-**276** was visible and was isolated in 8% yield. Applying the isolated mono-product *rac*-**276** under the same conditions did not lead to any further conversion towards the desired product *rac*-**277**.

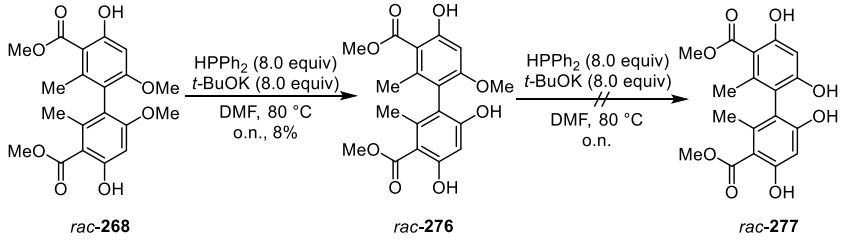

Scheme 100 Dimethyl ether cleavage of dimeric orsellinate *rac*-**268**.

The results show the great challenge of the double methyl ether cleavage. The choice of a suitable substrate could improve the conversion due to better solubility. However, in general the access towards both free hydroxy groups in the 2,2′-biphenol proved to be difficult, due to the high steric hindrance.

Summary Chapter 6.8

1. Double methyl ether cleavage of hydroxychromenone *rac*-**272** could be observed in the mass spectrum:
   - Deprotection was possible in the presence of PPh_2K in DMF.
   - Desired deprotected product *rac*-**273** could not be isolated.

2. Methyl ether cleavage of diaminobichromenone *rac*-**270** or dimeric orsellinate *rac*-**268** led only to mono-deprotection in low yields.

7 Summary and Outlook

In this work, investigations on the atroposelective synthesis of axially chiral biphenols were carried out. Therefore, methods for the racemic synthesis of a dedicated library of tetra-*ortho*-substituted biphenols were studied. An enzymatic kinetic resolution was established for the atroposelective transformation of the important biphenol building block **1**. The applicability of the used lipase was tested on a scope of different biphenols to evaluate the influence of the substitution pattern on the enzyme's activity and selectivity. The isolated enantiopure biphenol **1** was afterwards applied in the total synthesis towards dimeric polyketides.

In the first part of this work, different homocoupling methods for the construction of tetra-*ortho*-substituted biphenols were applied. The MBSC or *Lipshutz* coupling facilitated the homocoupling of various MOM-protected 2-bromophenols (six examples, 33–87% yield) (Scheme 101). However, the coupling methods were not applicable to bromophenols with bulky *ortho*-substituents or high electron density, resulting in no conversion.

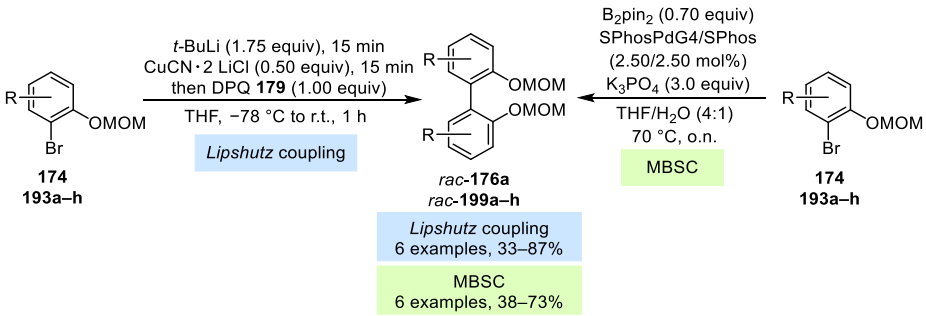

Scheme 101 *Lipshutz* coupling and MBSC towards axially chiral biphenol scope.

In the next step, homocoupling methods *via* directed *ortho*-metalation were investigated, which would broaden the accessible substrate scope. The phenol monomer can be more easily prepared, as no regioselective bromination was required anymore. The developed homocoupling *via* directed *ortho*-cupration with the cuprate base $(TMP)_2Cu(CN)Li_2$ provided the access towards biphenyls in yields up to 64%. Overall, this method was found to be efficient in reducing the number of steps required for the synthesis of tetra-*ortho*-substituted biphenyls. It exhibits a wide functional group tolerance, waste reduction and cost savings. Yet, this method proved to show different regioselectivities depending on the substitution pattern. In 3 of 8 examples the desired tetra-*ortho*-substituted biphenyl was

obtained (37–64% yield), while 4 of 8 examples led to the formation of the di-*ortho*-substituted regioisomer (17–55% yield). In order to improve regioselectivity a screening of different organoamidocuprates can be performed (Scheme 102).

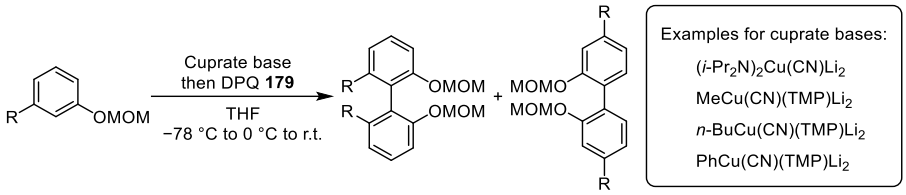

Scheme 102 Possible screening of different cuprate bases for the homocoupling of MOM-protected phenols.

The reported results of the group of *Uchiyama* shows the potential of further cuprate bases for the directed *ortho*-functionalization.[232, 233] A less bulky base could potentially form the homoleptic biaryl cuprate more selectively towards the more sterically hindered tetra-*ortho*-substituted biphenyl. In future investigations, the synthesis of unsymmetric axially chiral biphenols can be performed using the developed methods. Besides the MBSC or *Lipshutz* coupling methods of two different 2-bromophenols, a sequential directed *ortho*-cupration can be done following the developed method of *Uchiyama et al.* (Scheme 103).[234] Here, the question of the right regioselectivity needs to be answered.

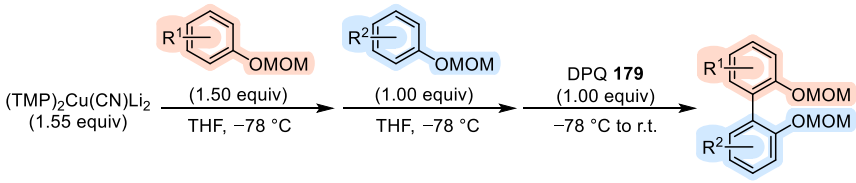

Scheme 103 Sequential directed *ortho*-cupration towards the synthesis of asymmetric axially chiral biphenols.

For the atroposelective transformation of racemic biphenols, a scalable and efficient EKR was developed. The application of the commercially available CRL (1 U) resulted in the atroposelective hydrolysis of biphenyl dipropionate *rac*-**181b** under mild conditions (10 vol% DMSO/KP_i-buffer, 40 °C) and a short reaction time of 3 hours. The resolution was performed on a gram-scale, leading to the isolation of enantiopure biphenols (*P*)-**1** and (*M*)-**1** in 40 and 42% yield and excellent optical purities of ≥99% *ee*. However, comparison of CRL from different suppliers revealed problems in reproducibility. Due to an unknown isoenzymatic profile of the lysates, different batches of the CRL revealed different activities and selectivities in the enzymatic hydrolysis. This was most likely caused by different isoenzymatic profiles, given by different production conditions. Therefore, more

information needs to be gained about the specific responsible isoenzyme for this atroposelective biocatalytic hydrolysis. Future experiments would involve the production of individual isoenzymes. Previous publications described the heterologous expression of isoenzymes LIP1–4 in the yeast *P. pastoris*. Additionally, LIP1 had been expressed in *S. cerevisiae* and LIP4 in *E. coli* before.[202, 286-288] Screening of the individual isoenzymes on the activity and selectivity towards the transformation of axially chiral compounds would reveal the responsible isoenzyme. In this way, the lipase loading could also be reduced by using a specific purified lipase, instead of the crude lyophilizate.

The developed EKR method was furthermore applied on the library of different biphenol substrates (Scheme 104). The results of the EKR revealed that the ester functionality in *ortho*-position to the chiral axis is essential to control the atroposelectivity of the EKR. The choice of the *para*-substituents had a minor effect on the enzyme's activity and selectivity. The biphenols **223a**, **d** and **e** were obtained in excellent conversions (47–58%) and with good to excellent enantiomeric excesses (79–>99% *ee*). However, the enzyme's activity and selectivity were influenced by the *ortho*-substituents, resulting in a drop of conversion and selectivity.

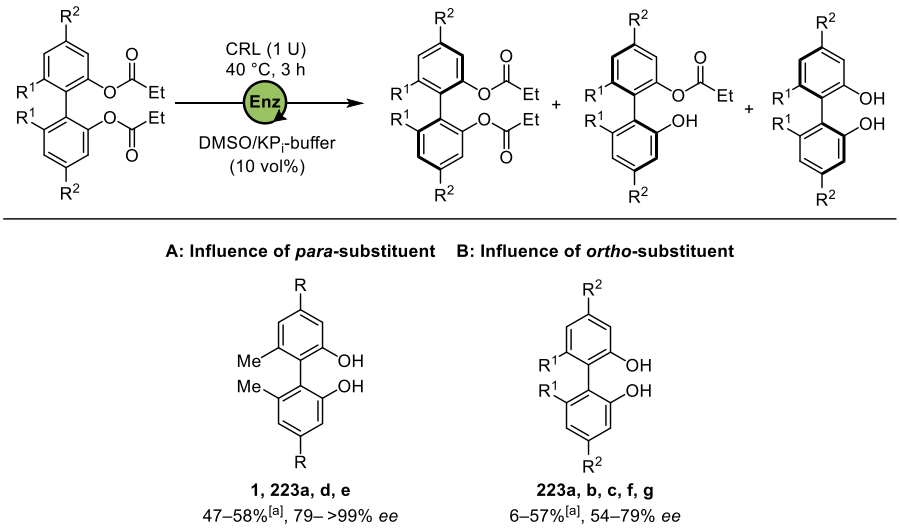

Scheme 104 Enzymatic kinetic resolution of axially chiral biphenol scope; [a] Conversion towards biphenol was determined *via* ^{1}H-NMR.

As the structure of the different isoenzymes is known, docking studies of biphenol substrates with different substitution pattern can be performed. If the responsible active isoenzyme can be determined, designing of the active side might expand the applicability

towards a highly atroposelective transformation of a broader scope regardless the substitution pattern. Analogously, docking studies and enzyme engineering of the hydrolase (pelB)TB035 from the IMET can be performed to improve lipase's activity and selectivity. The enzymatic hydrolysis of biphenyl diacetate *rac*-**181a** and dipropionate *rac*-**181b** exhibited high enantioselectivities (73–99% *ee*), revealing the potential for further investigations.

For the dynamization of the EKR, a second enzyme screening was performed for the acetylation of biphenol *rac*-**1** and biphenyl monoacetate *rac*-**182b**, as an oxidative racemization of the starting material was envisaged. However, it was not possible to find a suitable hydrolase for the enantioselective esterification of *rac*-**1** or *rac*-**182b**. The combination of CRL with isopropenyl acetate or 3-chlorophenylacetate exhibited low conversions and no enantioselectivity. The determination of the active CRL isoenzyme for the atroposelective hydrolysis may help to understand why the same crude lysate does not catalyze the atroposelective acetylation. First screenings of metal catalysts revealed the potential for the racemization of enantiopure biphenol **1** using Pd/C or **[Ru]-1** activated by *t*-BuOK. To find a suitable racemization catalyst, the redox potential of the substrate **1** can be determined *via* cyclic voltammetry.

The combination of the racemic coupling methods with the CRL-catalyzed KR has proven to be a suitable tool for a robust and scalable synthesis of enantiopure biphenols. This can provide access towards further various natural products, such as the dimeric xanthone rugulotrosin A (*P*)-(**278**), preanthraquinone atrovirin B_2 (*P*)-(**279**) or binaphthopyran-2-one pigmentosin A (*M*)-(**280**), which are based on the common motif **1** (Figure 31).[275, 289, 290]

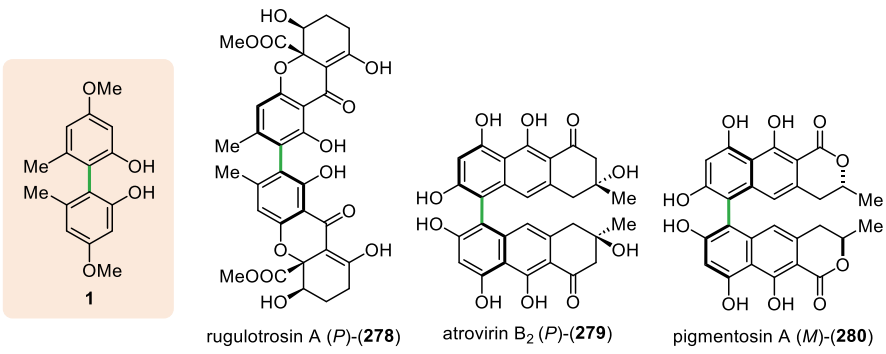

Figure 31 Examples of further possible axially chiral target products based on model substrate **1**.

Furthermore, optimization of the lipase' selectivity would facilitate the synthesis of a broad variety of further symmetric or asymmetric axially chiral target products. This would include natural products, like vioxanthin (*P*)-(**281**), orlandin (*P*)-(**142**) or desertorin A (*M*)-(**143**), and also chiral ligands, such as Garphos (**282**) or SYNPHOS (**283**) (Figure 32).[226, 267, 291, 292]

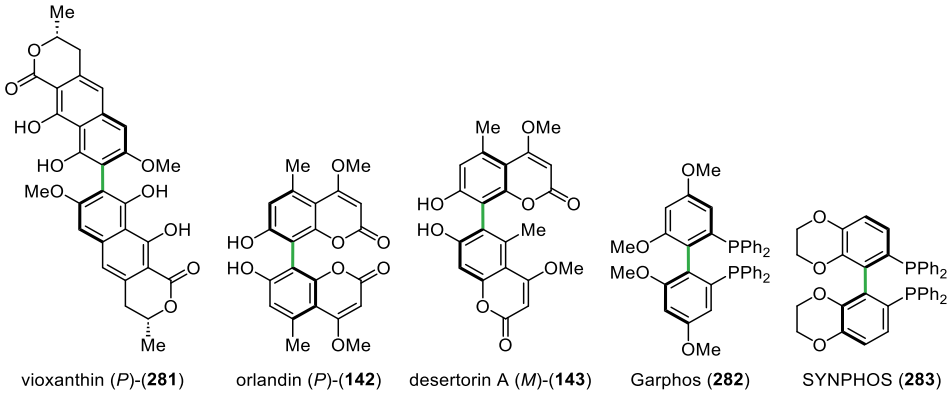

Figure 32 Examples of further possible axially chiral target products.

In the further course of this work the isolated enantiopure biphenol (*M*)-/(*P*)-**1** were applied the total syntheses of axially chiral dimeric polyketides, such as the γ-binaphthopyrones (*M*)-ustilaginoidin A (*M*)-(**2**) and F (*M*)-(**3**). The monomeric γ-naphthopyrone **242** was successfully synthesized by the annulation of phenyl benzoate **229** and pyranone **241**. Oxidative aromatization using chloranil was successful, giving γ-naphthopyrone **243** in 49% total yield over two steps. However, limitations occurred when performing the bidirectional *Myers*' annulation on dimeric toluate *rac*-**245**. The bidirectional *Myers*' annulation of *rac*-**245** with pyranone **241** led only to mono-annulation. Scheme 105 shows an alternative approach towards (*M*)-ustilaginoidin F (*M*)-(**3**). Here, a double benzylic bromination should be tested in early stage using less sterically hindered substrate (*M*)-**176a**. The benzylic bromide (*M*)-**284** should be then converted to fluoride (*M*)-**285**. Following the previous procedures, the dimeric phenyl benzoate (*M*)-**254** should be prepared, which then should be applied in the bidirectional *Myers*' annulation. The formed benzylic anion was envisaged to be more stabilized by the fluorine and therefore the annulation would be more favored. In the last step, aromatization in the presence of TFE and acidic deprotection should result in the formation of the natural product (*M*)-**3**.

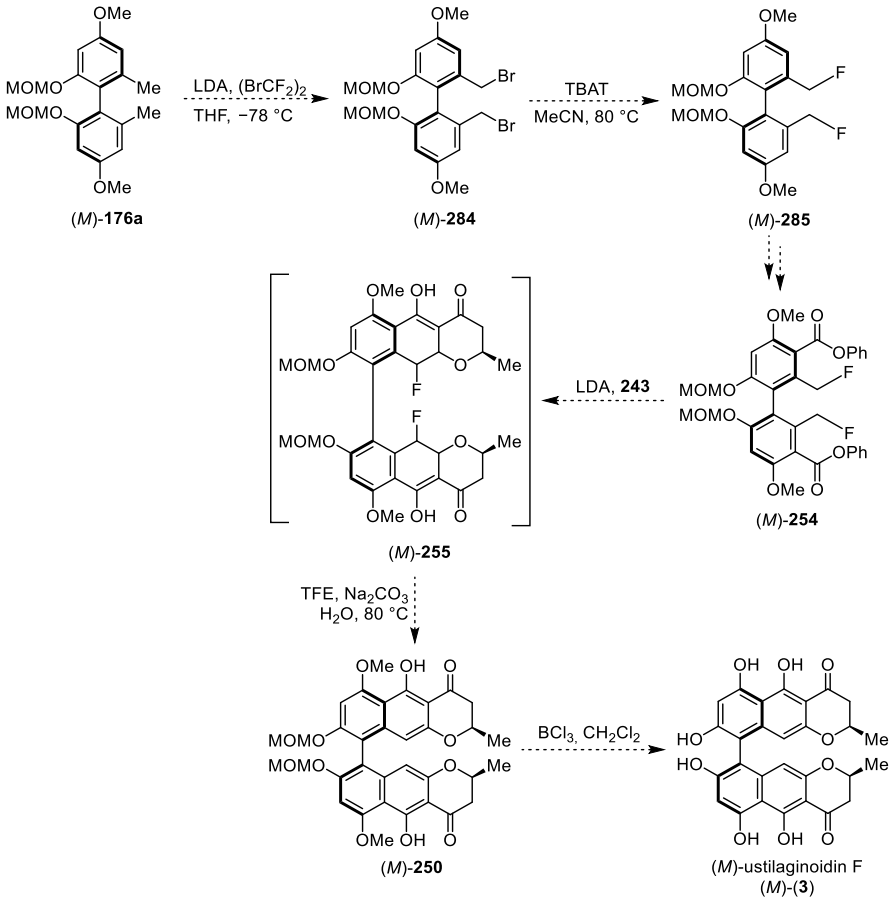

Scheme 105 Alternative approach towards (*M*)-ustilaginoidin F (*M*)-(**3**).

However, if the double benzylic functionalization of (*M*)**-176a** would not be possible due to the molecule's internal high steric hindrance, another alternative would be to approach the double fluorinated biaryl **285** by homocoupling of fluorinated monomer **286** (Scheme 106). Here, an open question would be whether the fluorinated biphenol is a suitable substrate for the EKR, leading to the required enantiopure dimer (*M*)**-288**. Analogously to previous procedure, this dimer would then be used for the synthesis of phenyl benzoate (*M*)-**254**.

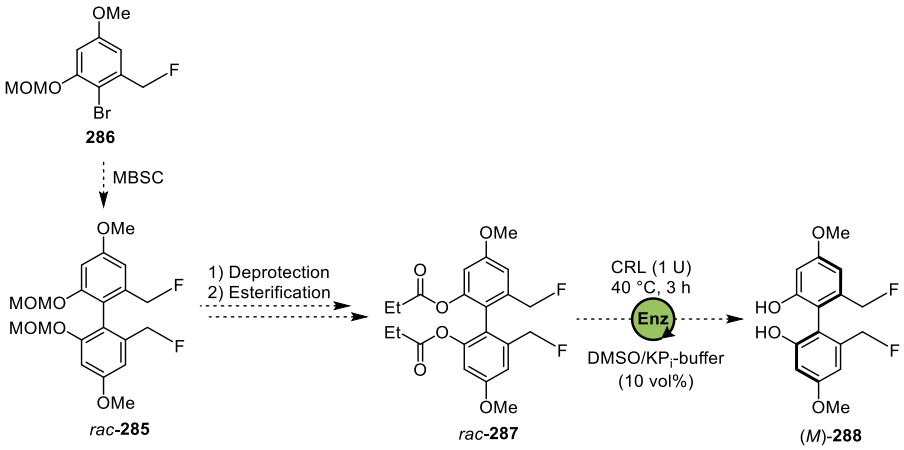

Scheme 106 Alternative approach towards (*M*)-**288.**

Finally, the asymmetric total synthesis of the axially chiral bicoumarin (*M*)-isokotanin A (*M*)-(**4**) and (*P*)-isokotanin C (*P*)-(**5**) was investigated. The enantiopure (*M*)-**1** applied in the established total synthesis, resulting in the isolation of enantiopure (*M*)-isokotanin A (*M*)-(**4**) in 11% overall yield in 8 steps. Additionally, in this work the approach towards the bicoumarin (*P*)-isokotanin C (*P*)-(**5**) was described. However, the total synthesis could not be completed due to the challenging double methyl ether cleavage. Therefore, future experiments using a more labile protecting group for both *ortho*-hydroxy substituents should be performed. Scheme 107 shows the planned synthesis route using a MOM protecting group as the substitute. Analogously to the previous pathway, the dimeric methyl ester (*P*)-**289** should be generated, which should be afterwards deprotected in the presence of BCl_3. Under the given acidic condition, the MOM protecting group would most likely also get removed. The double cyclization towards the diaminobichromenone (*P*)-**275** using tetraol (*P*)-**277** as a starting material needs to be tested. The synthesis of the respective monomeric aminochromenone was described before by *Müller et al.*[179] In the last step, acidic hydrolysis and regioselective etherification should then result in generating the desired bicoumarin (*P*)-**5**.

In addition to the development of the atroposelective methodology, the access towards dimeric polyketides in both absolute configurations allows the investigation of their biological activities depending on their structural configuration. Testing of the natural and unnatural enantiomer can give greater understanding about the structure activity relationship.

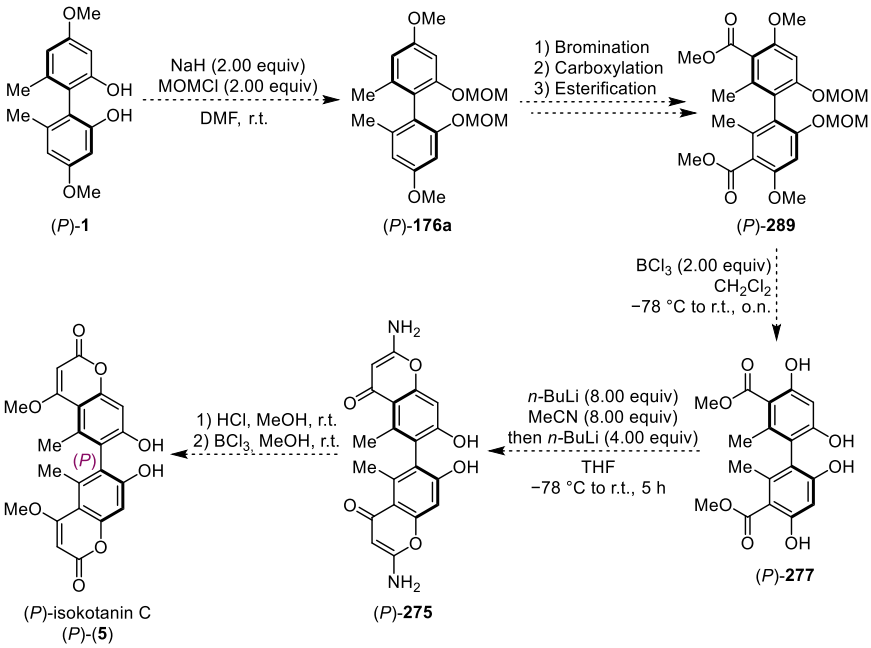

Scheme 107 Alternative approach towards (*P*)-isokotanin C (*P*)-(**5**).

8 Experimental

8.1 General Information (Chemical Syntheses)

Materials and Methods

All air- and moisture-sensitive reactions were performed under a nitrogen atmosphere using oven dried glassware and dried solvents. The chemicals were either purchased from the companies *Alfa Aesar* GmbH & Co KG, *Merck* KGaA, *Sigma Adrich* Co, *Carl Roth* GmbH + Co KG, Fluka, *AppliChem* GmbH, *Roche*, *Codexis* and *TCI* Europe or have been already available in the laboratory. The dried solvents THF, toluene, Et_2O and CH_2Cl_2 were taken from the solvent purification system. The evaporation of the solvents was performed at the rotary evaporator within a water bath with a temperature of 40 °C. Acetone was distilled over 4 Å molecular sieve and stored over it.

Flash Column Chromatography

Flash column chromatography was executed using silica gel 60 (40–63 µm, 230–240 mesh, *Macherey*-Nagel). Depending on the substrate different solvent mixtures were used, such as petroleum ether (PE)/EtOAc, CH_2Cl_2/MeOH, PE/toluene or PE/CH_2Cl_2.

Thin Layer Chromatography

Analytical thin layer chromatography (TLC) was carried out using precoated plastic sheets (*Macherey-Nagel* POLYGRAM® SIL G/UV254). Visualization on TLC was achieved by UV light or by treatment with *p*-anisaldehyde stain (5 mL concentrated sulfuric acid, 1.5 mL glacial acetic acid and 3.7 mL *p*-anisaldehyde in 135 mL absolute ethanol) or cerium molybdate stain (12 g ammonium molybdate, 0.5 g ceric ammonium molybdate and 15 mL conc. sulfuric acid in 235 mL distilled water).

NMR-Spectroscopy

^{1}H- and ^{13}C-NMR spectra were recorded on an Advance/DRX 600 nuclear magnetic resonance spectrometer (*Bruker*, Billerica, USA) at 600 MHz and 151 MHz. Chemical shifts δ

are given in ppm and were referenced to residual chloroform at $\delta = 7.26$ ppm (^{1}H) or $\delta = 77.16$ ppm (^{13}C). Spectra which were taken in CD_3OD, were referenced to methanol at $\delta = 3.31$ ppm (^{1}H) or $\delta = 49.00$ ppm (^{13}C). Spectra which were taken in DMSO-d_6, were referenced at $\delta = 2.50$ ppm (^{1}H) or $\delta = 39.52$ ppm (^{13}C). Multiplicities are labelled by s (singlet), d (doublet), t (triplet), doublet of doublet (dd), m (multiplet) and broad singlet (brs). Coupling constants (J) are given in Hz.

Infrared Spectroscopy

IR data were recorded on a SpectrumOne spectrometer (*PerkinElmer*, Waltham, USA) as a thin film. The absorption bands $\tilde{\nu}$ are reported in cm^{-1}.

Mass Spectrometry

Low resolution mass spectra were recorded on the ADVION EXPRESSion CMS. The mass spectrometry was recorded on the hybrid mass spectrometer LTQ FT Ultra from *Thermo Fisher*. Ionization was performed by electrospray ionization (ESI).

High Resolution Mass Spectrometry (HRMS)

High resolution mass spectra were recorded on the UHR-QTOF maXis 4G (*Bruker Daltonics*) at the Heinrich-Heine-University Düsseldorf. Ionization was performed by electrospray ionization (ESI).

High Performance Liquid Chromatography (HPLC)

Enantiomeric excess of chiral compounds was determined with the help of the HPLC-chromatograms (*Dionex* UltiMate 3000 Column Compartment, *Thermo Scientific*). The solvents used for this purpose were degassed before use. The parameters such as flow rate, column, wavelength, and solvent are given in the experimental section for each compound.

Melting Point

Melting point was measured at the melting point system *Büchi* melting-point B-540.

Polarimetry

Optical rotations were measured using *A. Krüss* Optronic P8000 polarimeter in a 0.1 dm cuvette tempered to 20 °C. The specific optical rotation is calculated according to Equation 8, where the parameter *c* stands for the concentration [g/100 mL], *α* for the measured optical rotation and *l* for the length of the measuring cuvette [dm].

$$[\alpha]_D^{Temp} = \frac{\alpha}{c \cdot l} in\ [mL \cdot dm^1 \cdot g^{-1}] \qquad \textbf{Equation 8}$$

8.2 General Information (Enzymes)

All used enzymes were either purchased from the companies *Fluka*, *Amano*, *Sigma* and *Toboyo*, or were donated by commercial (*Roche Diagnostics* and *Amano*) or academic providers (IMET: Institute for molecular enzyme technology, Heinrich-Heine-University Düsseldorf at Forschungszentrum Jülich). A complete list of the hydrolases used can be found in Table 19 and Table 20.

Table 19 Listing of the commercially available enzymes used, their organism, their suppliers, and their specific activity.

Abbr.	Enzyme	Organism	Supplier	Activity [U/mg][a]
ANL	Lipase	*Aspergillus niger*	*Fluka*	0.017
CCL	Lipase	*Candida cylindracea*	*Fluka*	0.170
CRL	Lipase	*Candida rugosa*	*Fluka*	0.120
CEPP[b]	Cholesterol esterase	*Porcine pancreas*	*Alfaaesar*	0.380
PPL	Lipase	*Porcine pancreas*	*Fluka*	0.120
PLE	Esterase	*Porcine liver*	*Sigma*	7.510
LPL	Lipase	*Pseudomonas*	*Toyobo*	20.72
PCL	Lipase	*Pseudomonas cepacia*	*Sigma*	4.120
MJL	Lipase	*Mucor javanicus*	*Sigma*	0.060
RNL	Lipase	*Rhizopus niveus*	*Sigma*	0.009
ROL	Lipase	*Rhizopus oryzae*	*Fluka*	0.050
ROE	Esterase	*Rhizopus oryzae*	*Sigma*	0.007
BCL	Lipase	*Burkholderia cepacia*	*Amano*	0.480
CAL-B[c]	Lipase	*Candida antarctica*	*Fluka*	9.020
PPP	Pancreatin	*Porcine pancreas*	*Sigma*	0.004
CL3	Hydrolase	*Candida rugosa*	*Roche*	1.070
CESL4	Lipase	*Candida sp.*	*Amano*	0.570
CEBP	Cholesterol esterase	*Bovine pancreas*	*Sigma*	0.060
CEPF	Cholesterol esterase	*Pseudomonas fluorescens*	*Sigma*	3.750

[a] Specific enzyme activity was determined according to the hydrolysis of *p*-nitrophenyl hexanoate; [b] While other hydrolases were provided as lysates, CEPP was used as a purified enzyme; [c] CAL-B was used as an immobilized lipase.

Table 20 Listing of hydrolases provided by IMET, their organism, and the specific activity.

Abbr.	Enzyme	Organism	Activity [U/mL][a]
Dim008	Carboxylic ester hydrolase	*Aneurinibacillus thermoaerophilus Hz*	800
(pelB)TB035	Carboxylic ester hydrolase	*Pseudomonas aestusnigri* VGXO14	20
CycTB025	Carboxylic ester hydrolase	*Pseudonocardia thermophila*	40
Abo_Est3	Carboxylic ester hydrolase	*Alcanivorax borkumensis* SK2	1.5
Abo_LipD	Carboxylic ester hydrolase	*Alcanivorax borkumensis* SK2	15
Aku_Est3	Carboxylic ester hydrolase	*Pseudomonas aestusnigri* VGXO14	20
PE-H Y250S	Polyester Hydrolase	*Pseudomonas aestusnigri* VGXO14	80
PE-H	Polyester Hydrolase	*Pseudomonas aestusnigri* VGXO14	80

Hydrolases were used as whole cell extracts; [a] Specific enzyme activity was determined according to the hydrolysis of *p*-nitrophenyl butyrate. The data was provided by IMET.

8.2.1 Determination of specific activity of hydrolases

Specific enzyme activity was determined according to the hydrolysis of *p*-nitrophenyl hexanoate under slightly basic conditions (Scheme 108).[199] The formed hydrolysis product *p*-nitrophenolate was measured photometrically at 410 nm. All measurements were performed in triplica.

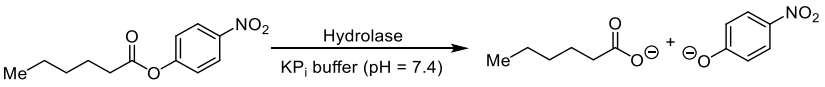

Scheme 108 Enzymatic hydrolysis of *p*-nitrophenyl hexanoate.

First a calibration was performed to determine the extinction coefficient of *p*-nitrophenyl hexanoate. A dilution serie of substrate solutions in acetonitrile in the range of 0.001–0.5 mM was prepared. In a 96-microwell plate 15 µL of the calibration sample was added to 135 µL KP_i-buffer solution (pH = 7.4). The absorption was measured at λ = 410 nm. The measured absorption [mAu] was plotted against the concentration of the corresponding

substrate solution [mM] (Figure 33). The extinction coefficient was given by the slope of the calibration curve: ε_{calib} = 5.53 mAu/mM.

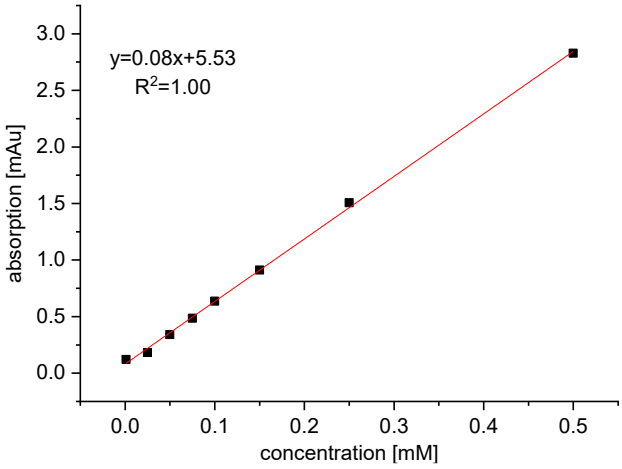

Figure 33 Calibration curve of *p*-nitrophenyl hexanoate.

A master mix solution was prepared, containing 0.25 mM *p*-nitrophenyl hexanoate solution in KP_i buffer (100 mM, pH = 7.4) and 10% acetonitrile. Afterwards a solution of enzyme in KP_i-buffer with a specific concentration (0.01–1 mg/mL) was prepared. 30 µL enzyme solution was pipetted to 120 µL master mix solution in the microwell plate. The autohydrolysis rate was determining by measuring the absorbance of 30 µL buffer solution with 120 µL master mix solution. The absorbance was measured at λ = 410 nm over a reaction time up to 5 minutes. It is important to ensure linear change in the absorbance, otherwise the enzyme solution must be further diluted. In the next step, the blank values of the autohydrolysis were subtracted from the measured absorption values of each reaction. The specific activity was calculated afterwards by using Equation 9.

$$\boldsymbol{U_{spec} = \frac{\Delta E \cdot 5}{\varepsilon_{calib} \cdot c}} \qquad \textbf{Equation 9}$$

U_{spec} = specific enzyme activity [U/mg]

ΔE = change in absorbance at 410 nm per minute [1/min]

ε_{calib} = slope of calibration curve [mAu/mM]

c = concentration of enzyme solution [mg/mL]

8.3 Synthesis Procedures and Analytics

General Procedure A: NBS Bromination

Phenol (1.00 equiv) was dissolved in dry CH_2Cl_2 (0.3 M) and cooled down to 0 °C. NBS (1.01 equiv) was added, and the reaction mixture was stirred at 0 °C. After full conversion, the reaction was quenched by adding 10% aqueous sodium sulfite solution. The reaction mixture was extracted with CH_2Cl_2 three times and washed with brine. The combined organic layer was dried over $MgSO_4$. After concentration at reduced pressure the product could be used without further purification.

General Procedure B: MOM-Protection

Phenol (1.00 equiv) was given in anhydrous DMF (0.3 M). The reaction mixture was cooled down to 0 °C and NaH (60% dispersion in mineral oil, 1.30 equiv) was added in one portion. The mixture was stirred at 0 °C for 1 hour. After adding (chloromethyl)methylether (1.20 equiv) dropwise at 0 °C, the reaction mixture was stirred at r.t. until full conversion was observed. The mixture was quenched by the addition of water. The reaction mixture was extracted three times with EtOAc. The combined organic phase was washed with saturated $NaHCO_3$ solution, dried over $MgSO_4$. After drying at reduced pressure, the residual oil was washed three times with ice to remove any residual DMF.

General Procedure C: Esterification of benzoic acid

Benzoic acid (1.00 equiv) was given in dry ethanol (1 M). Conc. H_2SO_4 (20 mol%) was added dropwise and the mixture was stirred at reflux overnight. The reaction was quenched by addition of saturated aqueous $NaHCO_3$ solution. Afterwards the mixture was diluted with EtOAc and water. The organic phase was extracted with EtOAc three times, and the combined organic phases were dried over $MgSO_4$. After concentration at reduced pressure the product could be used without further purification.

General Procedure D: Lipshutz Coupling

The copper-mediated homocoupling was performed following the given procedure.[1]

Protected bromophenol (1.00 equiv) was dissolved in anhydrous THF (0.2 M) and cooled down to −78 °C. After *tert*-butyllithium solution (2.5 M in pentane, 1.75 equiv) was added dropwise, the cooled mixture was continuously stirred for 30 minutes. A solution of CuCN·2LiCl (1.0 M in anhydrous THF, 0.50 equiv) was added dropwise and stirring was continued for 30 minutes. Simultaneously a solution of tetra-*tert*-butyldiphenoquinone (**179**) (1.10 equiv) in anhydrous THF (2.5 M) was prepared and afterwards added in one shot to the reaction mixture. After the mixture was stirred at −78 °C for 30 minutes, the cooling bath was removed, and the mixture warmed up to r.t. The reaction mixture was continuously stirred at r.t. for 30 minutes and quenched by adding water. The CuCN precipitated and went back into solution by adding aqueous 30% ammonia solution. The organic phase was extracted with CH_2Cl_2 three times. The combined organic phase was dried over $MgSO_4$ and concentrated under reduced pressure. The oxidizing agent biquinone **179** could be recycled by filtering off with methanol. Afterwards purification by column chromatography was performed to isolate the desired product. If an oxidation side product was observed, the residue was dissolved in EtOAc and washed with aqueous 1 M NaOH solution.

General Procedure E: Miyaura Borylation Suzuki Coupling (MBSC)

The MSBC was performed following the given procedure.[2]

Protected bromophenol (1.00 equiv), SPhos (2.5 mol%) and SPhosPdG4 (2.5 mol%) were given in a schlenk flask and dissolved in degassed THF (0.25 M) under inert conditions. A solution of K_3PO_4 (3.00 equiv) in degassed water (3 M) was added. The mixture was stirred and heated to 70 °C. A solution of B_2pin_2 (0.70 equiv) in THF (1 M) was added *via* syringe pump over 3.5 hours. The reaction mixture was continuously stirred at 70 °C. The conversion was observed *via* ^{1}H-NMR. After full conversion, the mixture was cooled down to r.t., filtered through a celite pad and washed thoroughly with EtOAc. The aqueous phase was extracted with EtOAc three times, and the combined organic phases were dried over $MgSO_4$. After the combined organic phases were concentrated under reduced pressure, purification by column chromatography was performed to isolate the desired product.

General Procedure F: Coupling *via ortho*-directed cupration

Lithiumtetramethylpiperidide (LiTMP) was prepared *in situ*, by adding *tert*-butyllithium (2.5 M in pentane, 1.24 equiv) to a solution of tetramethylpiperidine (1.24 equiv) in anhydrous THF (0.75 M) at −78 °C. The solution was stirred at 0 °C for 30 minutes. Simultaneously CuCN (0.62 equiv) was given in anhydrous THF (0.4 M) and cooled down to −78 °C. LiTMP was transferred dropwise to the CuCN dispersion at 0 °C and continuously stirred for 30 minutes. Afterwards a solution of protected phenol (1.00 equiv) in anhydrous THF (0.6 M) was added dropwise and stirred for 30 minutes at 0 °C. Meanwhile a solution of tetra-*tert*-butyldiphenoquinone (**179**) (1.10 equiv) in anhydrous THF (2.5 M) was prepared and afterwards added in one shot to the reaction mixture. Afterwards the mixture was stirred for 30 minutes at 0 °C, and for 2.5 hours at r.t. The reaction mixture was quenched by adding water. The CuCN precipitated and went back into solution by adding aqueous 30% ammonia solution. When no CuCN precipitate was observed anymore, the organic phase was extracted with CH_2Cl_2 three times. The combined organic phase was dried over $MgSO_4$ and concentrated under reduced pressure. The oxidizing agent diphenoquinone **179** could be recycled by filtering off with methanol. Afterwards purification by column chromatography was performed to isolate the desired product.

General Procedure G: MOM-Deprotection

The protected biphenyl (1.00 equiv) was dissolved in degassed methanol (0.25 M). 1 M aqueous HCl solution (1.00 equiv) was added. The mixture was stirred at 70 °C. After full conversion the mixture was cooled down and quenched by the addition of 0.1 M KP_i-buffer solution (pH = 7.4). The organic phase was extracted three times with EtOAc. The combined organic phases were dried over $MgSO_4$ and concentrated at reduced pressure. If necessary, purification by column chromatography was performed to isolate the desired product.

General Procedure H: Esterification of biphenol to a mixture of biphenyl diester and monoester

Biphenol (1.00 equiv) and DMAP (10 mol%) were dissolved in anhydrous CH_2Cl_2 (0.05 M). Afterwards the anhydride (1.50 equiv) and triethylamine (1.50 equiv) were added dropwise.

After the mixture was stirred for 3 hours at 0 °C, water was added. 1 M HCl was applied to acidify the reaction mixture. The aqueous phase was extracted with CH_2Cl_2 three times. The combined organic phases were washed with saturated aq. $NaHCO_3$ and brine, dried over $MgSO_4$, and concentrated under reduced pressure. The residue was purified by column chromatography.

General Procedure I: Esterification of biphenol to biphenyl diester

The exclusive synthesis of biphenyl monoester was performed according to general procedure H with adjusted equivalents of the reagents: Biphenol (1.00 equiv) and DMAP (10 mol%) were dissolved in anhydrous CH_2Cl_2 (0.05 M). Afterwards the anhydride (2.00 equiv) and triethylamine (2.00 equiv) were added dropwise. After the mixture was stirred for 3 hours at 0 °C, water was added. 1 M HCl was applied to acidify the reaction mixture. The aqueous phase was extracted with CH_2Cl_2 three times. The combined organic phases were washed with saturated aq. $NaHCO_3$ and brine, dried over $MgSO_4$, and concentrated under reduced pressure. The residue was purified by column chromatography.

General Procedure J: Esterification of biphenol to biphenyl monoester

The exclusive synthesis of biphenyl monoester was performed according to general procedure H with adjusted equivalents of the reagents: Biphenol (1.00 equiv) and DMAP (10 mol%) were dissolved in anhydrous CH_2Cl_2 (0.05 M). Afterwards the anhydride (1.00 equiv) and triethylamine (1.00 equiv) were added dropwise. After the mixture was stirred for 3 hours at 0 °C, water was added. 1 M HCl was applied to acidify the reaction mixture. The aqueous phase was extracted with CH_2Cl_2 three times. The combined organic phases were washed with saturated aq. $NaHCO_3$ and brine, dried over $MgSO_4$, and concentrated under reduced pressure. The residue was purified by column chromatography.

8.3.1 Synthesis of biphenol building block *rac*-1

1,3-Dimethoxy-5-methylbenzene (167)

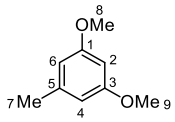

167

5-Methylresorcinol (15.00 g, 120.8 mmol) and anhydrous potassium carbonate (47.76 g, 345.6 mmol) was given in a flask. Acetone (140 mL) was added to dissolve the starting material. While stirring the reaction mixture dimethyl sulfate (25.21 mL, 265.8 mmol) was added. The mixture was stirred at reflux. After 22 hours the reaction mixture was quenched by adding 10% aqueous sodium sulfite solution. The mixture continued to stir for 30 minutes at r.t and afterwards acidified with 1 M HCl. The organic phase was extracted three times with EtOAc and washed with brine. The combined organic phase was dried over $MgSO_4$ and concentrated by solvent evaporation at reduced pressure to give 1,3-dimethoxy-5-methylbenzene (**167**) (17.64 g, 117.9 mmol) in 96% yield as brown oil. The product could be used without further purification.

R_f (PE:EE, 80:20) = 0.75

^{1}H-NMR ($CDCl_3$, 600 MHz) δ 6.34 (d, $^4J_{4/6,2}$ = 2.2 Hz, 2H, 4-H, 6-H), 6.29 (t, $^4J_{4,6,2}$ = 2.3 Hz, 1H, 2-H), 3.78 (s, 6H, 8-OC$\underline{H}_3$, 10-OC$\underline{H}_3$), 2.31 (s, 3H, 7-C$\underline{H}_3$).

^{13}C-NMR ($CDCl_3$, 151 MHz) δ 160.84 (C-1, C-3), 140.35 (C-5), 107.40 (C-4, C-6), 97.65 (C-2), 55.37 (C-8, C-10), 21.96 (C-7).

IR: ν[cm^{-1}]: 3000, 2939, 2837, 1594, 1458, 1425, 1320, 1203, 1146, 1067, 1057, 826, 684.

MS (ESI): m/z = 53.0 $[M+H]^+$

The analytical data correspond to the data given in literature.[1, 224, 293]

3-Methoxy-5-methylphenol (168)

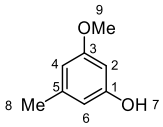

168

NaH (60% dispersion in mineral oil, 12.80 g, 320.0 mmol) was given in anhydrous DMF (120 mL) and cooled down to 0 °C. 1-Propanethiol (24.37 mL, 268.8 mmol) in DMF (30 mL) was added dropwise. The reaction mixture was warmed to r.t. and stirred for 10 minutes. Dimethyl orcinol (**167**) (24.35 g, 160.0 mmol) in DMF (80 mL) was added dropwise. The formed foam was stirred at reflux. The condenser was connected to an aqueous sodium hypochlorite solution to quench released thioether. After 7 hours the reaction mixture was quenched by adding cold water. The mixture was washed three times with PE. The organic phase was discarded. Afterwards the aqueous phase was acidified with 4 M hydrochloric acid solution and extracted three times with MTBE. The combined organic phase was dried over $MgSO_4$ and concentrated by solvent evaporation at reduced pressure. Purification *via* Kugelrohr-Destillation at 150 °C gave 3-methoxy-5-methylphenol (**168**) (19.11 g, 138.3 mmol) in 86% yield as orange oil.

R_f (PE:EE, 80:20) = 0.38

^{1}H-NMR ($CDCl_3$, 600 MHz) δ 6.32 (d, $^4J_{4,2,6}$ = 2.1 Hz, 1H, 4-H), 6.26 (t, $^4J_{6,2,4}$ = 1.7 Hz, 1H, 6-H), 6.23 (d, $^4J_{2,4,6}$ = 2.3 Hz, 1H, 2-H), 3.76 (s, 3H, 9-OC$\underline{H}_3$), 2.27 (s, 3H, 8-C$\underline{H}_3$).

^{13}C-NMR ($CDCl_3$, 151 MHz) δ 160.99 (C-3), 156.62 (C-1), 140.74 (C-5), 108.72 (C-6), 107.50 (C-4), 98.71 (C-2), 55.38 (C-9), 21.73 (C-8).

IR: ν[cm^{-1}]: 3309, 2921, 2841, 1592, 1459, 1336, 1194, 1142, 1014, 973, 828, 682.

MS (ESI): m/z = 139.0 $[M+H]^+$

The analytical data correspond to the data given in literature.[1, 191]

3-Methoxy-5-methylphenyl acetate (169)

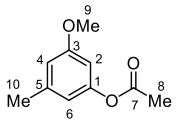

169

3-Methoxy-5-methylphenol (**168**) (19.11 g, 138.3 mmol), DMAP (0.34 g, 2.8 mmol) and trimethylamine (21.21 mL, 152.2 mmol) were given in anhydrous CH_2Cl_2 (140 mL). The reaction mixture was cooled down to 0 °C. Acetic anhydride (14.36 mL, 152.2 mmol) was added dropwise. The mixture was stirred at room temperature for 2 hours and quenched by addition of water. After acidifying with 1 M hydrochloric acid solution the mixture was extracted three times with CH_2Cl_2. The combined organic phase was dried over MgSO4 and dried at reduced pressure to give 3-methoxy-5-methylphenyl acetate (**169**) (24.92 g, 138.3 mmol) in 99% yield as light yellow oil.

R_f (PE:EE, 80:20) = 0.48

^{1}H-NMR ($CDCl_3$, 600 MHz) δ 6.60 (t, $^4J_{4,2,6}$ = 1.7 Hz, 1H, 4-H), 6.51 (d, $^4J_{6,2,4}$ = 2.1 Hz, 1H, 6-H), 6.45 (t, $^4J_{2,4,6}$ = 2.2 Hz, 1H, 2-H), 3.77 (s, 3H, 9-OC$\underline{H}_3$), 2.32 (s, 3H, 10-C$\underline{H}_3$), 2.28 (s, 3H, 8-C$\underline{H}_3$).

^{13}C-NMR ($CDCl_3$, 151 MHz) δ 169.67 (C-7), 160.44 (C-3), 151.57 (C-1), 140.46 (C-5), 114.74 (C-6), 112.70 (C-4), 104.76 (C-2), 55.50 (C-9), 21.71 (C-10), 21.29 (C-8).

IR: ν[cm^{-1}]: 2940, 1765, 1609, 1294, 1191, 1162, 1151, 1128, 1062, 1023.

MS (ESI): m/z = 139.0 $[M\text{-}CH_3CO+H]^+$

The analytical data correspond to the data given in literature.[3]

2-Bromo-5-methoxy-3-methylphenol (172)

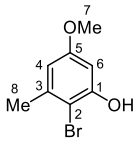

172

3-Methoxy-5-methylphenyl acetate (**169**) (24.92 g, 138.3 mmol), was dissolved in anhydrous CH_2Cl_2 (460 mL) at 0 °C. NBS (24.86 g, 139.7 mmol) was added in one portion. The mixture was stirred at 0 °C for 3 hours and quenched by addition of 10% aqueous sodium sulfite solution. The reaction mixture was extracted three times with CH_2Cl_2. The combined organic phase was washed with saturated $NaHCO_3$ solution, dried over $MgSO_4$, and dried at reduced pressure. The crude brominated product was used without further purification and dissolved in methanol (280 mL). After sodium bicarbonate (12.78 g, 152.1 mmol) was added, the mixture was stirred over night at room temperature. The reaction mixture was quenched by acidifying with 1 M hydrochloric acid solution. The organic phase was extracted three times with CH_2Cl_2 and dried over $MgSO_4$. The crude ^{1}H-NMR shows a ratio of 85:15 between the desired product and its regioisomer. Therefore, purification *via* Kugelrohr-Destillation was performed (3×10^{-2} mbar, 100 °C; collecting flask cooled to 0 °C). The desired brominated product (**172**) (21.92 g, 101.0 mmol) could be obtained in 73% yield as white solid. The regioisomer (**173**) (3.90 g, 18.0 mmol) was isolated in 13% yield as light orange crystals.

R_f (PE:EE, 80:20) = 0.49

^{1}H-NMR ($CDCl_3$, 600 MHz) δ 6.66 (d, $^4J_{6,4}$ = 2.5 Hz, 1H, 6-H), 6.42 (d, $^4J_{4,6}$ = 2.3 Hz, 1H, 4-H), 5.57 (s, 1H, OH), 3.76 (s, 3H, 7-OC$\underline{H}_3$), 2.36 (s, 3H, 8-C$\underline{H}_3$).

^{13}C-NMR ($CDCl_3$, 151 MHz) δ 159.77 (C-5), 153.14 (C-1), 139.02 (C-2), 109.33 (C-4), 104.12 (C-3), 98.93 (C-6), 55.59 (C-7), 23.36 (C-8).

IR: ν[cm^{-1}]: 3338, 1578, 1343, 1305, 1252, 1193, 1159, 1041, 1020, 977, 837, 809, 625, 582, 554

MS (ESI): m/z = 217.9 $[M+H]^+$.

Mp: 70–73 °C **Lit. Mp:** 73–75 °C[1]

The analytical data correspond to the data given in literature.[1]

4-Bromo-3-methoxy-5-methylphenol (173)

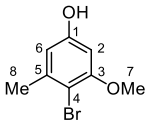

173

R_f (PE:EE, 80:20) = 0.33

^{1}H-NMR ($CDCl_3$, 600 MHz) δ 6.36 (s, 1H, 6-H), 6.31 (s, 1H, 2-H), 4.69 (s, 1H, OH), 3.85 (s, 3H, 7-OC$\underline{H}_3$), 2.35 (s, 3H, 8-C$\underline{H}_3$).

^{13}C-NMR ($CDCl_3$, 151 MHz) δ 156.85 (C-5), 155.15 (C-1), 140.09 (C-3), 109.54 (C-2), 104.98 (C-4), 97.75 (C-6), 56.25 (C-7), 23.20 (C-8).

IR: ν[cm^{-1}]: 3328, 1605, 1584, 1330, 1184, 1152, 1087, 1014, 831, 626, 597

MS (ESI): m/z = 216.9 $[M+H]^+$.

Mp: 112–115 °C **Lit. Mp:** 122–124 °C[1]

The analytical data correspond to the data given in literature.[1]

2-Bromo-5-methoxy-1-(methoxymethoxy)-3-methylbenzene (174)

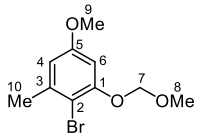

174

The product was synthesized according to general procedure B. The MOM-protected product **174** (14.15 g, 54.17 mmol) was obtained from 2-bromo-5-methoxy-1-(methoxymethoxy)-3-methylbenzene (**172**) (12.00 g, 55.28 mmol) in 98% yield as colorless oil.

R_f (PE:EE, 80:20) = 0.65

^{1}H-NMR ($CDCl_3$, 600 MHz) δ 6.60 (d, $^4J_{6,4}$ = 2.8 Hz, 1H, 6-H), 6.50 (d, $^4J_{4,6}$ = 2.8 Hz, 1H, 4-H), 5.2 (s, 2H, 7-C$\underline{H}_2$), 3.77 (s, 3H, 9-OC$\underline{H}_3$), 3.52 (s, 3H, 8-OC$\underline{H}_3$), 2.39 (s, 3H, 10-C$\underline{H}_3$).

^{13}C-NMR ($CDCl_3$, 151 MHz) δ 159.29 (C-5), 154.62 (C-1), 140.00 (C-3), 109.48 (C-4), 106.44 (C-2), 100.67 (C-6), 95.37 (C-7), 56.50 (C-8), 55.63 (C-9), 23.78 (C-10).

IR: ν[cm^{-1}]: 2923, 1582, 1465, 1322, 1149, 1069, 1047, 1021, 996, 923, 834.

HRMS (ESI): m/z = Found: 261.0122 ($C_{10}H_{14}BrO_3$) $[(M+H)]^+$, calculated: 261.0121.

The analytical data correspond to the data given in literature.[1]

2-Bromo-5-methoxy-1-(ethoxymethoxy)-3-methylbenzene (175)

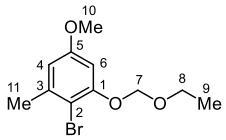

175

Bromophenol **172** (10.50 g, 48.37 mmol) was given in anhydrous DMF (150 mL). The reaction mixture was cooled down to 0 °C and NaH (60% dispersion in mineral oil, 2.52 g, 62.9 mmol) was added in one portion. The mixture was stirred at 0 °C for 1 hour. After adding (chloromethyl)ethylether (5.38 mL, 58.1 mmol) dropwise at 0 °C, the reaction mixture was stirred at r.t. for 3 hours. The mixture was quenched by addition of water. The reaction mixture was extracted three times with EtOAc. The combined organic phase was washed with saturated $NaHCO_3$ solution, dried over $MgSO_4$. Drying at reduced pressure gave EOM-protected product **175** (13.04 g, 47.40 mmol) in 98% yield as colorless oil.

R_f (PE:EE, 80:20) = 0.58

^{1}H-NMR ($CDCl_3$, 600 MHz) δ 6.63 (d, $^4J_{4,6}$ = 2.9 Hz, 1H, 4-H), 6.49 (d, $^4J_{6,4}$ = 2.9 Hz, 1H, 6-H), 5.27 (s, 2H, 10-C$\underline{H}_2$), 3.79 (m, 2H, 8-C$\underline{H}_2$) 3.77 (s, 3H, 10-OC$\underline{H}_3$), 2.39 (s, 3H, 11-C$\underline{H}_3$), 1.23 (t, $^3J_{9,8}$ = 7.1 Hz, 3H, 9-C$\underline{H}_3$).

^{13}C-NMR ($CDCl_3$, 151 MHz) δ 159.27 (C-1), 154.78 (C-5), 139.91 (C-2), 109.36 (C-4), 106.42 (C-3), 100.71 (C-6), 94.08 (C-10), 64.75 (C-8), 55.62 (C-7), 23.77 (C-11), 15.26 (C-9).

IR: ν[cm^{-1}]: 2975, 1583, 1466, 1322, 1197, 1159, 1113, 1069, 1045, 1020, 995, 918, 836.

HRMS (ESI): m/z = Found: 275.0280 ($C_{11}H_{16}BrO_3$) $[(M+H)]^+$, calculated: 275.0277.

4,4'-Dimethoxy-2,2'-bis(methoxymethoxy)-6,6'-dimethyl-1,1'-biphenyl *rac*-(176a)

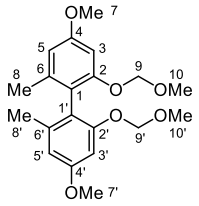

rac-**176a**

The homocoupling was performed according to general procedure D. After column chromatography (PE:EtOAc = 90:10 to 80:20) the coupling product *rac*-**176a** (1.21 g, 3.34 mmol) was obtained from 2-bromo-5-methoxy-1-(methoxymethoxy)-3-methylbenzene **174** (2.00 g, 7.66 mmol) in 87% yield as yellow oil. The protodehalogenation side product **177a** (0.14 g, 0.77 mmol) was isolated in 10% yield as colorless oil. Washing with aqueous 1 M NaOH solution led to removal of the oxidation side product **178a** (45 mg, 0.23 mmol), which was isolated in 3% yield as orange oil.

R_f (PE:EE, 80:20) = 0.43

^{1}H-NMR ($CDCl_3$, 600 MHz) δ 6.64 (s, 2H, 3-H, 3'-H), 6.52 (s, 2H, 5-H, 5'-H), 4.99 (d, $^2J_{9a/9'a,9b/9'b}$ = 18.5 Hz, 4H, 9-H, 9'-H), 3.82 (s, 6H, 7-OC$\underline{H}_3$, 7'-OC$\underline{H}_3$), 3.30 (s, 6H, 10-OC$\underline{H}_3$, 10'-OC$\underline{H}_3$), 1.95 (s, 6H, 8-C$\underline{H}_3$, 8'- C$\underline{H}_3$).

^{13}C-NMR ($CDCl_3$, 151 MHz) δ 159.47 (C-4, C-4'), 155.97 (C-2, C-2'), 139.50 (C-6, C-6'), 119.85 (C-1, C-1'), 108.52 (C-5, C-5'), 99.64 (C-3, C-3'), 94.93 (C-9, C-9'), 55.85 (C-10, C-10'), 55.31 (C-7, C-7'), 20.26 (C-8, C-8').

IR: ν[cm^{-1}]: 2952, 2835, 1602, 1582, 1466, 1309, 1145, 1041, 994, 922, 833.

HRMS (ESI): m/z = Found: 363.1805 ($C_{20}H_{27}O_6$) $[(M+H)]^+$, calculated: 383.1802.

1-Methoxy-3-(methoxymethoxy)-5-methylbenzene (177a)

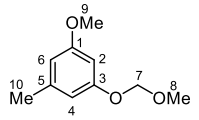

177a

R_f (PE:EE, 80:20) = 0.65

^{1}H-NMR ($CDCl_3$, 600 MHz) δ 6.48 (dd, J = 2.2, 1.2 Hz, 1H, 4-H), 6.42 (d, J = 2.3 Hz, 1H, 2-H), 6.41 – 6.38 (m, 1H, 6-H), 5.15 (s, 2H, 7-C$\underline{H}_2$-), 3.77 (s, 3H, 9-C$\underline{H}_3$), 3.48 (s, 3H, 8-C$\underline{H}_3$), 2.30 (s, 3H, 10-C$\underline{H}_3$).

^{13}C-NMR ($CDCl_3$, 151 MHz) δ 160.75 (C-1), 158.42 (C-3), 140.43 (C-5), 109.33 (C-4), 108.57 (C-6), 99.82 (C-2), 94.56 (C-7), 56.13 (C-8), 55.38 (C-9), 21.91 (C-10).

IR: ν[cm^{-1}]: 2954, 1593, 1466, 1141, 1063, 1027, 991, 923, 832, 686.

MS (ESI): m/z = 150.0 $[M\text{-}CH_3OH+H]^+$

4-Methoxy-2-(methoxymethoxy)-6-methylphenol (178a)

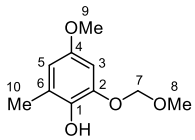

178a

R_f (PE:EE, 80:20) = 0,37

^{1}H-NMR ($CDCl_3$, 600 MHz) δ 6.57 (d, $^{4}J_{3,5}$ = 2.8 Hz, 1H, 3-H), 6.40 – 6.36 (m, 1H, 5-H), 5.53 (s, 1H, OH), 5.18 (s, 2H, 7-C$\underline{H}_2$-), 3.73 (s, 3H, 9-OC$\underline{H}_3$), 3.51 (s, 3H, 8-OC$\underline{H}_3$), 2.25 (s, 3H, 10-C$\underline{H}_3$).

^{13}C-NMR ($CDCl_3$, 151 MHz) δ 152.71 (C-4), 144.53 (C-2), 138.68 (C-1), 124.83 (C-6), 109.27 (C-5), 100.41 (C-3), 96.15 (C-7), 56.52 (C-8), 55.90 (C-9), 16.07 (C-10).

IR: ν[cm^{-1}]: 3444, 2951, 2834, 1614, 1497, 1226, 1291, 1143, 1036, 990, 922, 834, 785.

HRMS (ESI): m/z = Found: 199.0967 ($C_{10}H_{15}O_4$) $[(M+H)]^+$, calculated: 199.0965.

4,4'-Dimethoxy-2,2'-bis(ethoxymethoxy)-6,6'-dimethyl-1,1'-biphenyl *rac*-(176b)

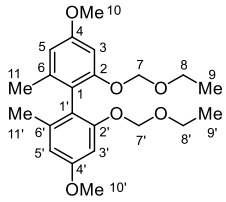

rac-**176b**

The homocoupling was performed according to general procedure D. After column chromatography (PE:EtOAc = 80:20 to 60:40) the coupling product *rac*-**176b** (77 mg, 0.20 mmol) was obtained from 2-bromo-5-methoxy-1-(methoxymethoxy)-3-methylbenzene (**175**) (0.10 g, 0.38 mmol) in 52% yield as orange oil and the protodehalogenation side product **177b** (29 mg, 0.15 mmol) in 40% yield as colorless oil.

R_f (PE:EE, 80:20) = 0.4

^{1}H-NMR ($CDCl_3$, 600 MHz) δ 6.67 (d, $^4J_{3/3',5/5'}$ = 2.6 Hz, 2H, 3-H, 3'-H), 6.51 (d, $^4J_{5/5',3/3'}$ = 2.7 Hz, 2H, 5-H, 5'-H), 5.03 (d, $^2J_{7a/7'a,7b/7'b}$ = 16.6 Hz, 4H, 7-C$\underline{H}_2$-, 7'-C$\underline{H}_2$-), 3.82 (s, 6H, 10-OC$\underline{H}_3$, 10'-OC$\underline{H}_3$), 3.57 – 3.51 (m, 4H, 8-C$\underline{H}_2$-, 8'-C$\underline{H}_2$-), 1.93 (s, 6H, 11-C$\underline{H}_3$, 11'-C$\underline{H}_3$), 1.14 (d, $^3J_{9/9',8/8'}$ = 7.1 Hz, 6H, 9-C$\underline{H}_3$, 9'-C$\underline{H}_3$).

^{13}C-NMR ($CDCl_3$, 151 MHz) δ 159.43 (C-4, C-4'), 156.16 (C-2, C-2'), 139.39 (C-1, C-1'), 119.83 (C-6, C-6'), 108.40 (C-5, C-5'), 99.68 (C-3, C-3'), 93.66 (C-7, C-7'), 63.96 (C-8, C-8'), 55.31 (C-10, C-10'), 20.26 (C-11, C-11'), 15.25 (C-9, C-9').

IR: ν[cm^{-1}]: 2975, 1602, 1583, 1466, 1442, 1311, 1194, 1150, 1108, 1040, 994, 920, 836.

HRMS (ESI): m/z = Found: 391.2117 ($C_{22}H_{31}O_6$) $[(M+H)]^+$, calculated: 391.2115.

1-(Ethoxymethoxy)-3-methoxy-5-methylbenzene (177b)

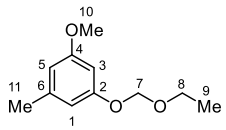

177b

R_f (PE:EE, 80:20) = 0.6

^{1}H-NMR ($CDCl_3$, 600 MHz) δ 6.48 (s, 1H, 1-H), 6.43 (t, $^4J_{3,1,5}$ = 2.3 Hz, 1H, 3-H), 6.39 (s, 1H, 5-H), 5.20 (s, 2H, 7-C$\underline{H}_2$-), 3.77 (s, 3H, 10-C$\underline{H}_3$), 3.73 (q, $^3J_{8,9}$ = 7.1 Hz, 2H, 8-C$\underline{H}_2$-), 2.30 (s, 3H, 11-C$\underline{H}_3$), 1.23 (t, $^3J_{9,8}$ = 7.1 Hz, 3H, 9-C$\underline{H}_3$).

^{13}C-NMR ($CDCl_3$, 151 MHz) δ 160.73 (C-4), 158.60 (C-2), 140.39 (C-6), 109.36 (C-1), 108.45 (C-5), 99.80 (C-3), 93.30 (C-7), 64.37 (C-8), 55.39 (C-10), 21.92 (C-11), 15.26 (C-9).

IR: ν[cm^{-1}]: 2976, 1597, 1470, 1197, 1148, 1105, 1065, 1030, 834.

HRMS (ESI): m/z = Found: 197.1172 ($C_{11}H_{17}O_3$) $[(M+H)]^+$, calculated: 197.1172.

3,3',5,5'-Tetra-*tert*-butyl-[1,1'-bi(cyclohexylidene)]-2,2',5,5'-tetraene-4,4'-dione (179)

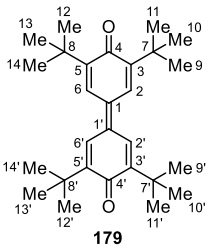

179

In a round-bottom flask 2,6-di-*tert*-butylphenol (20.0 g, 96.9 mmol) was dissolved in 2-propanol (200 mL). Potassium hydroxide (20.1 g, 356 mmol) in 30 mL water was added. The reaction mixture was purged with oxygen, while stirring for 3 hours at r.t. Afterwards 200 mL water was added, and the precipitated product was filtered off. After washing the precipitate with water, the crude product was recrystallized in 2-propanol, resulting in the biquinone **179** (32.5 g, 79.5 mmol) in 82% yield as purple/brown crystals.

R_f (PE:EE, 95:5) = 0.81

^{1}H-NMR ($CDCl_3$, 600 MHz) δ 7.70 (s, 4H, 2-H, 2′-H, 6-H, 6′-H), 1.36 (s, 36H, 9-C$\underline{H}_3$, 9′-C$\underline{H}_3$, 10-C$\underline{H}_3$, 10′-C$\underline{H}_3$, 11-C$\underline{H}_3$, 11′-C$\underline{H}_3$, 12-C$\underline{H}_3$, 12′-C$\underline{H}_3$, 13-C$\underline{H}_3$, 13′-C$\underline{H}_3$, 14-C$\underline{H}_3$, 14′-C$\underline{H}_3$).

^{13}C-NMR ($CDCl_3$, 151 MHz) δ 186.64 (C-4, C-4′), 150.62 (C-3, C-3′, C-5, C-5′), 136.29 (C-1, C-1′), 126.16 (C-2, C-2′, C-6, C-6′), 36.18 (C-7, C-7′, C-8, C-8′), 29.62 (C-9, C-9′, C-10, C-10′, C-11, C-11′, C-12, C-12′, C-13, C-13′, C-14, C-14′).

IR: ν[cm^{-1}]: 2956, 1601, 1361, 1090, 898.

MS (ESI): m/z = 409.2 $[M+H]^+$.

Mp: 240–243 °C **Lit. Mp:** 245–246 °C[1]

The analytical data correspond to the data given in literature.[1]

4,4'-Dimethoxy-6,6'-dimethyl-[1,1'-biphenyl]-2,2'-diol *rac*-(1)

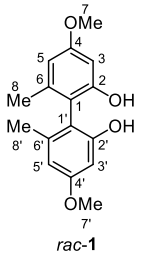

rac-**1**

The deprotection was performed according to general procedure G. After column chromatography (PE:EtOAc = 80:20) the biphenol *rac*-**1** (0.90 g, 3.3 mmol) was obtained from 4,4'-dimethoxy-2,2'-bis(methoxymethoxy)-6,6'-dimethyl-1,1'-biphenyl *rac*-(**176a**) (1.21 g, 3.31 mmol) in 99% yield as yellow solid.

R_f (PE:EE, 80:20) = 0.18

^{1}H-NMR ($CDCl_3$, 600 MHz) δ 6.50 (d, $^4J_{5/5',3/3'}$ = 2.5 Hz, 2H, 5-H, 5'-H), 6.47 (d, $^4J_{3/3',5/5'}$ = 2.5 Hz, 2H, 3-H, 3'-H), 4.77 (s, 2H, 7-OH, 7'-OH), 3.82 (s, 6H, 8-O$\underline{C}H_3$, 8'-O$\underline{C}H_3$), 1.97 (s, 6H, 9-$C\underline{H}_3$, 9'- $C\underline{H}_3$).

^{13}C-NMR ($CDCl_3$, 151 MHz) δ 161.29 (C-4, C-4'), 155.57 (C-2, C-2'), 140.60 (C-6, C-6'), 111.34 (C-1, C-1'), 109.10 (C-5, C-5'), 98.56 (C-3, C-3'), 55.42 (C-8, C-8'), 19.92 (C-9, C-9').

IR: ν[cm^{-1}]: 3436, 2943, 2836, 1610, 1573, 1328, 1194, 1141, 1068, 1035, 832.

HRMS (ESI): m/z = Found: 275.1280 ($C_{16}H_{19}O_4$) $[(M+H)]^+$, calculated: 275.1278.

HPLC: Column: Chiracel OD-H (250x4.6 mm); 5 µL, 25 °C, 0.5 mL/min, 274 nm; solvent: *n*-heptane:2-propanol (90:10), t_R = 26.7, 35.2 min.

8.3.2 Synthesis of biphenyl diester *rac*-181a–e and monoester *rac*-182a–e

4,4′-Dimethoxy-6,6′-dimethyl-[1,1′-biphenyl]-2,2′-diyl diacetate *rac*-(181a)

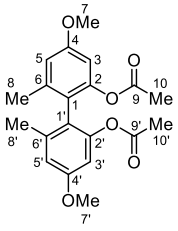

rac-**181a**

Diacetate *rac*-**181a** and monoacetate *rac*-**182a** were synthesized according to the general procedure H, starting from biphenol *rac*-**1** (0.10 g, 0.36 mmol). After purification by column chromatography (PE/EtOAc = 80:20) diacetate *rac*-**181a** (86 mg, 0.24 mmol) was obtained in 67% yield as white crystals and monoacetate *rac*-**182a** (38 mg, 0.12 mmol) in 33% yield as colorless oil.

R_f (PE:EE, 70:30) = 0.48

^{1}H-NMR ($CDCl_3$, 600 MHz) δ 6.71 (d, $^4J_{5/5',3/3'}$ = 2.6 Hz, 2H, 5-H, 5′-H), 6.55 (d, $^4J_{3/3',5/5'}$ = 2.5 Hz, 2H, 3-H, 3′-H), 3.81 (s, 3H, 7-OC$\underline{H}_3$, 7′-OC$\underline{H}_3$), 2.00 (s, 3H, 8-C$\underline{H}_3$, 8′-C$\underline{H}_3$), 1.91 (s, 3H, 10-C$\underline{H}_3$, 10′-C$\underline{H}_3$).

^{13}C-NMR ($CDCl_3$, 151 MHz) δ 169.31 (C-9, C-9′)., 159.35 (C-4, C-4′), 149.84 (C-2, C-2′), 140.25 (C-6, C-6′), 121.17 (C-1, C-1′), 113.34 (C-5, C-5′), 105.71 (C-3, C-3′), 55.32 (C-7, C-7′), 20.73 (C-10, C-10′), 19.86 (C-8, C-8′).

IR: ν[cm^{-1}]: 2922, 1752, 1609, 1466, 1367, 1312, 1203, 1188, 1140, 1067, 890, 849, 840, 588, 590.

HRMS (ESI): m/z = Found: 359.1494 ($C_{20}H_{23}O_6$) $[(M+H)]^+$, calculated: 359.1489.

Mp: 120–122 °C

HPLC: Column: Chiralpak IC, *Fa. Daicel* (250x4.6 mm); 5 µL, 25 °C, 0.5 mL/min, 205 nm; solvent: *n*-heptane:2-propanol (90:10), t_R = 20.1, 23.0 min.

2′-Hydroxy-4,4′-dimethoxy-6,6′-dimethyl-[1,1′-biphenyl]-2-yl acetate *rac*-(182a)

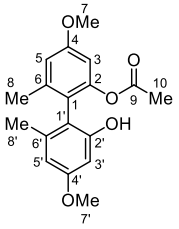

rac-**182a**

R_f (PE:EE, 70:30) = 0.42

^{1}H-NMR ($CDCl_3$, 600 MHz) δ 6.80 (s, 1H, 5-H), 6.55 (s, 1H, 3-H), 6.42 (s, 2H, 3′-H, 5′-H), 4.90 (s, 1H, 9′-OH), 3.83 (s, 3H, 7-OC$\underline{H}_3$), 3.79 (s, 3H, 7′-OC$\underline{H}_3$), 2.00 (s, 3H, 8-C$\underline{H}_3$), 1.93 (s, 3H, 10-C$\underline{H}_3$), 1.91 (s, 3H, 8′-C$\underline{H}_3$).

^{13}C-NMR ($CDCl_3$, 151 MHz) δ 170.48 (C-9), 160.40 (C-4), 160.31 (C-4′), 154.59 (C-2′), 151.59 (C-2), 141.55 (C-1′), 139.14 (C-1), 120.18 (C-6′), 114.96 (C-6), 114.22 (C-5), 108.57 (C-5′), 105.86 (C-3), 98.91 (C-3′), 55.56 (C-7), 55.28 (C-7′), 20.49 (C-10), 20.03 (C-8), 19.96 (C-8′).

IR: ν[cm^{-1}]: 3484, 2939, 2840, 1612, 1576, 1467, 1313, 1191, 1139, 1067, 1037, 837.

HRMS (ESI): m/z = Found: 317.1387 ($C_{18}H_{21}O_5$) $[(M+H)]^+$, calculated: 317.1384.

HPLC: Column: Chiralpak IC, *Fa. Daicel* (250x4.6 mm); 5 µL, 25 °C, 0.5 mL/min, 205 nm; solvent: *n*-heptane:2-propanol (90:10), t_R = 15.0, 17.8 min.

4,4′-Dimethoxy-6,6′-dimethyl-[1,1′-biphenyl]-2,2′-diyl dipropionate *rac*-(181b)

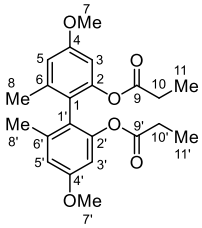

rac-**181b**

Dipropionate *rac*-**181b** and monopropionate *rac*-**182b** were synthesized according to the general procedure H, starting from biphenol *rac*-**1** (500 mg, 1.82 mmol). After purification by column chromatography (PE/EtOAc = 95:5 to 90:10 to 80:20) dipropionate *rac*-**181b** (366 mg, 946 µmol) was obtained in 52% yield as white crystals and monopropionate *rac*-**182b** (60 mg, 0.18 mmol) in 10% yield as colorless oil.

R_f (PE:EE, 80:20) = 0.51

^{1}H-NMR ($CDCl_3$, 600 MHz) δ 6.70 (d, $^4J_{5/5',3/3'}$ = 2.5 Hz, 2H, 5-H, 5′-H), 6.55 (d, $^4J_{3/3',5/5'}$ = 2.5 Hz, 2H, 3-H, 3′-H), 3.81 (s, 6H, 7-OC$\underline{H}_3$, 7′-OC$\underline{H}_3$), 2.19 (p, $^2J_{10a/10'a,10b/10'b}$ = 8.1 Hz, $^3J_{10,11,10',11'}$ = 7.7 Hz, 4H, 10-C$\underline{H}_2$-, 10′-C$\underline{H}_2$-), 2.00 (s, 6H, 8-C$\underline{H}_3$, 8′-C$\underline{H}_3$), 0.90 (t, $^3J_{11/11',10/10'}$ = 7.6 Hz, 6H, 11-C$\underline{H}_3$, 11′-C$\underline{H}_3$).

^{13}C-NMR ($CDCl_3$, 151 MHz) δ 172.68 (C-9, C-9′), 159.34 (C-4, C-4′), 149.86 (C-2, C-2′), 140.23 (C-6, C-6′), 121.20 (C-1, C-1′), 113.26 (C-5, C-5′), 105.62 (C-3, C-3′), 55.50 (C-7, C-7′), 27.66 (C-10, C-10′), 19.85 (C-8, C-8′), 9.03 (C-11, C-11′).

IR: ν[cm^{-1}]: 2920, 1750, 1616, 1575, 1470, 1415, 1325, 1309, 1196, 1148, 1067, 875, 857, 562, 494.

HRMS (ESI): m/z = Found: 387.1808 ($C_{22}H_{27}O_6$) $[(M+H)]^+$, calculated: 387.1802.

Mp: 89–90 °C

HPLC: Column: Lux Amylose-1, *Fa. Phenomenex* (250x4.6 mm); 5 µL, 25 °C, 0.5 mL/min, 274 nm; solvent: *n*-heptane:2-propanol (90:10), t_R = 9.7, 10.6 min.

2′-Hydroxy-4,4′-dimethoxy-6,6′-dimethyl-[1,1′-biphenyl]-2-yl propionate *rac*-(182b)

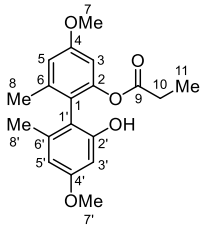

rac-**182b**

R_f (PE:EE, 80:20) = 0.38

^{1}H-NMR ($CDCl_3$, 600 MHz) δ 6.80 (d, $^4J_{5,3}$ = 2.5 Hz, 1H, 5-H), 6.55 (d, $^4J_{3,5}$ = 2.5 Hz, 1H, 3-H), 6.41 (s, 2H, 3′-H, 5′-H), 4.91 (s, 1H, 9′-OH), 3.83 (s, 3H, 7-OC$\underline{H}_3$), 3.78 (s, 3H, 7′-OC$\underline{H}_3$), 2.21 (m, $^2J_{10a,10b}$ = 15.6 Hz, $^3J_{10,11}$ = 7.6 Hz, 2H, 10-C$\underline{H}_2$-), 2.01 (s, 3H, 8′-C$\underline{H}_3$), 1.90 (s, 3H, 8-C$\underline{H}_3$), 0.89 (t, $^3J_{11,10}$ = 7.6 Hz, 3H, 11-C$\underline{H}_3$).

^{13}C-NMR ($CDCl_3$, 151 MHz) δ 173.94 (C-9), 160.45 (C-4), 160.41 (C-4′), 154.70 (C-2′), 151.10 (C-2), 141.52 (C-1′), 139.20 (C-1), 120.21 (C-6′), 115.12 (C-6), 114.19 (C-5),

108.57 (C-5′), 105.92 (C-3), 99.03 (C-3′), 55.57 (C-7), 55.34 (C-7′), 27.61 (C-10), 20.02 (C-8), 19.94 (C-8′), 9.07 (C-11).

IR: ν[cm^{-1}]: 3483, 2941, 1753, 1612, 1576, 1465, 1314, 1182, 1188, 1066, 1039, 838, 497.

HRMS (ESI): m/z = Found: 331.1543 ($C_{19}H_{23}O_5$) $[(M+H)]^+$, calculated: 331.1540.

HPLC: Column: Lux Amylose-1, *Fa. Phenomenex* (250x4.6 mm); 5 µL, 25 °C, 0.5 mL/min, 274 nm; solvent: *n*-heptane:2-propanol (90:10), t_R = 21.7, 35.0 min.

4,4′-Dimethoxy-6,6′-dimethyl-[1,1′-biphenyl]-2,2′-diyl dibutyrate *rac*-(181c)

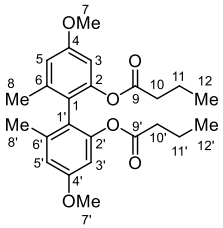

rac-**181c**

Dibutyrate *rac*-**181c** and monobutyrate *rac*-**182c** were synthesized according to the general procedure H, starting from biphenol *rac*-**1** (0.10 g, 0.36 mmol). After purification by column chromatography (PE/EtOAc = 98:2 to 85:15) dibutyrate *rac*-**181c** (25 mg, 0.12 mmol) was obtained in 33% yield as yellow oil.and monobutyrate *rac*-**182c** (15 mg, 40 µmol) in 12% yield as colorless oil.

R_f (PE:EE, 80:20) = 0.48

^{1}H-NMR ($CDCl_3$, 600 MHz) δ 6.69 (d, $^4J_{5/5',3/3'}$ = 2.6 Hz, 2H, 5-H, 5′-H), 6.54 (d, $^4J_{3/3',5/5'}$ = 2.5 Hz, 2H, 3-H, 3′-H), 3.80 (s, 6H, 7-OC$\underline{H}_3$, 7′-OC$\underline{H}_3$), 2.20 – 2.11 (m, 4H, 10-C$\underline{H}_2$-, 10′-C$\underline{H}_2$-), 2.01 (s, 6H, 8-C$\underline{H}_3$, 8′-C$\underline{H}_3$), 1.40 (ddt, $^2J_{11a/11'a,11b/11'b}$ = 14.1 Hz, $^3J_{11/11',10/10',12/12'}$ = 7.0 Hz, 4H, 11-C$\underline{H}_2$-, 11′-C$\underline{H}_2$-), 0.77 (t, $^3J_{12/12',11/11'}$ = 7.4 Hz, 6H, 12-OC$\underline{H}_3$, 12′-OC$\underline{H}_3$).

^{13}C-NMR ($CDCl_3$, 151 MHz) δ 171.83 (C-9, C-9′), 159.28 (C-4, C-4′), 149.88 (C-2, C-2′), 140.25 (C-6, C-6′), 121.29 (C-1, C-1′), 113.30 (C-5, C-5′), 105.65 (C-3, C-3′), 55.52 (C-7, C-7′), 36.04 (C-10, C-10′), 19.86 (C-8, C-8′), 18.25 (C-11, C-11′), 13.55 (C-12, C-12′).

IR: ν[cm^{-1}]: 2963, 1756, 1611, 1573, 1466, 1309, 1241, 1188, 1137, 1068, 842.

HRMS (ESI): m/z = Found: 415.2115 ($C_{24}H_{31}O_6$) $[(M+H)]^+$, calculated: 415.2115.

HPLC: Column: Chiralpak IC, *Fa. Daicel* (250x4.6 mm); 5 µL, 25 °C, 0.5 mL/min, 205 nm; solvent: *n*-heptane:2-propanol (90:10), t_R = 10.8, 13.9 min.

2′-Hydroxy-4,4′-dimethoxy-6,6′-dimethyl-[1,1′-biphenyl]-2-yl butyrate *rac*-(182c)

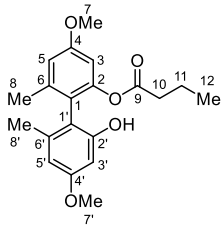

rac-**182c**

R_f (PE:EE, 80:20) = 0.11

^{1}H-NMR ($CDCl_3$, 600 MHz) δ 6.80 (d, $^4J_{5,3}$ = 2.5 Hz, 1H, 5-H), 6.54 (d, $^4J_{3,5}$ = 2.6 Hz, 1H, 3-H), 6.41 (q, $^4J_{3',5'}$ = 2.5 Hz, 2H, 3′-H, 5′-H), 4.92 (s, 1H, 9′-OH), 3.83 (s, 3H, 7-OC$\underline{H}_3$), 3.78 (s, 3H, 7′-OC$\underline{H}_3$), 2.23 – 2.14 (m, 2H, 10-C$\underline{H}_2$-), 2.00 (s, 3H, 8′-C$\underline{H}_3$), 1.90 (s, 3H, 8-C$\underline{H}_3$), 1.40 (ddt, $^2J_{11a,11b}$ = 15.9 Hz, $^3J_{11,10,12}$ = 7.0 Hz, 2H, 11-C$\underline{H}_2$-), 0.75 (t, $^3J_{12,11}$ = 7.4 Hz, 3H, 12-C$\underline{H}_3$).

^{13}C-NMR ($CDCl_3$, 151 MHz) δ 173.15 (C-9), 160.40 (C-4), 160.40 (C-4′), 154.65 (C-2′), 151.02 (C-2), 141.52 (C-1′), 139.15 (C-1), 120.26 (C-6′), 115.15 (C-6), 114.18 (C-5), 108.60 (C-5′), 105.86 (C-3), 99.09 (C-3′), 55.56 (C-7), 55.35 (C-7′), 35.96 (C-10), 20.05 (C-8), 19.99 (C-8′), 18.33 (C-11), 13.48 (C-12).

IR: ν[cm^{-1}]: 2963, 1749, 1612, 1576, 1467, 1314, 1192, 1138, 1068, 1040, 837, 497.

HRMS (ESI): m/z = Found: 345.1702 ($C_{20}H_{25}O_5$) $[(M+H)]^+$, calculated: 345.1697.

HPLC: Column: Chiralpak IC, *Fa. Daicel* (250x4.6 mm); 5 µL, 25 °C, 0.5 mL/min, 205 nm; solvent: *n*-heptane:2-propanol (90:10), t_R = 12.2, 15.6 min.

4,4′-Dimethoxy-6,6′-dimethyl-[1,1′-biphenyl]-2,2′-diyl dipentanoate *rac*-(181d)

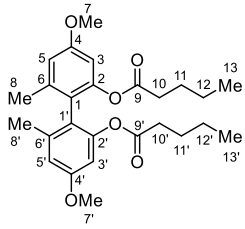

rac-**181d**

Dipentanoate *rac*-**181d** and monopentanoate *rac*-**182d** were synthesized according to the general procedure H, starting from biphenol *rac*-**1** (195 mg, 711 µmol). After purification by column chromatography (PE/EtOAc = 95:5 to 90:10) dipentanoate *rac*-**181d** (123 mg, 277 µmol) was obtained in 39% yield as yellow oil and monopentanoate *rac*-**182d** (44 mg, 0.12 mmol) in 17% yield as yellow oil.

R_f (PE:EE, 80:20) = 0.46

^{1}H-NMR ($CDCl_3$, 600 MHz) δ 6.70 (d, $^4J_{5/5',3/3'}$ = 2.5 Hz, 2H, 5-H, 5′-H), 6.53 (d, $^4J_{3/3',5/5'}$ = 2.5 Hz, 2H, 3-H, 3′-H), 3.80 (s, 6H, 7-OC$\underline{H}_3$, 7′-OC$\underline{H}_3$), 2.18 (td, $^2J_{10a/10'a,10b/10'b}$ = 7.5 Hz, $^3J_{10/10',11/11'}$ = 3.3 Hz, 4H, 10-C$\underline{H}_2$-, 10′-C$\underline{H}_2$-), 2.00 (s, 6H, 8-C$\underline{H}_3$, 8′-C$\underline{H}_3$), 1.31 (tt, $^2J_{11a/11'a,11b/11'b}$ = 15.2 Hz, $^3J_{11/11',10/10',12/12'}$ = 7.3 Hz, 4H, 11-C$\underline{H}_2$-, 11′-C$\underline{H}_2$-), 1.14 (ddt, $^2J_{12a/12'a,12b/12'b}$ = 13.8 Hz, $^3J_{12/12',11/11'}$ = 9.0 Hz, $^3J_{12/12',13/13'}$ = 6.7 Hz, 4H, 12-C$\underline{H}_2$-, 12′-C$\underline{H}_2$-), 0.79 (t, $^3J_{13/13',12/12'}$ = 7.3 Hz, 6H, 13-C$\underline{H}_3$, 13′-C$\underline{H}_3$).

^{13}C-NMR ($CDCl_3$, 151 MHz) δ 171.96 (C-9, C-9′), 159.43 (C-4, C-4′), 149.96 (C-2, C-2′), 140.27 (C-6, C-6′), 121.132 (C-1, C-1′), 113.28 (C-5, C-5′), 105.71 (C-3, C-3′), 55.46 (C-7, C-7′), 34.03 (C-10, C-10′), 26.94 (C-11, C-11′), 22.15 (C-12, C-12′), 19.84 (C-8, C-8′), 13.81 (C-13, C-13′).

IR: ν[cm^{-1}]: 2958, 1755, 1612, 1573, 1466, 1309, 1227, 1190, 1142, 1068, 1001, 946, 856.

HRMS (ESI): m/z = Found: 443.2430 ($C_{26}H_{35}O_6$) $[(M+H)]^+$, calculated: 443.2428.

HPLC: Column: Chiralpak IC, *Fa. Daicel* (250x4.6 mm); 5 µL, 25 °C, 0.5 mL/min, 205 nm; solvent: *n*-heptane:2-propanol (90:10), t_R = 10.1, 13.8 min.

2′-Hydroxy-4,4′-dimethoxy-6,6′-dimethyl-[1,1′-biphenyl]-2-yl pentanoate *rac*-(182d)

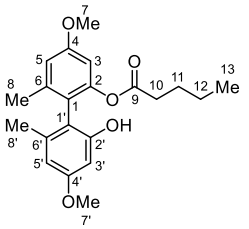

rac-**182d**

R_f (PE:EE, 80:20) = 0.34

^{1}H-NMR ($CDCl_3$, 600 MHz) δ 6.79 (dd, $^4J_{5,3}$ = 2.6, 0.8 Hz, 1H, 5-H), 6.54 (d, $^4J_{3,5}$ = 2.4, 1H, 3-H), 6.41 (m, 2H, 3′-H, 5′-H), 4.92 (s, 1H, 9′-OH), 3.83 (s, 3H, 7-OC$\underline{H}_3$), 3.78 (s, 3H, 7′-OC$\underline{H}_3$), 2.21 (td, J = 7.5, 3.5 Hz, 2H, 10-C$\underline{H}_2$-), 2.00 (s, 3H, 8′-C$\underline{H}_3$), 1.90 (s, 3H, 8-C$\underline{H}_3$), 1.34 – 1.27 (m, 2H, 11-C$\underline{H}_2$-), 1.13 – 1.05 (m, 2H, 12-C$\underline{H}_2$-), 0.78 (t, J = 7.3 Hz, 3H, 13-C$\underline{H}_3$).

^{13}C-NMR ($CDCl_3$, 151 MHz) δ 173.36 (C-9), 160.40 (C-4), 160.39 (C-4′), 154.67 (C-2′), 151.02 (C-2), 141.53 (C-1′), 139.16 (C-1), 120.28 (C-6′), 114.12 (C-6), 114.17 (C-5), 108.58 (C-5′), 105.87 (C-3), 99.08 (C-3′), 55.56 (C-7), 55.28 (C-7′), 33.93 (C-10), 26.97 (C-11), 22.05 (C-12), 20.05 (C-8), 19.98 (C-8′), 13.79 (C-13).

IR: ν[cm^{-1}]: 3490, 2958, 1751, 1612, 1576, 1466, 1313, 1231, 1192, 1139, 1068, 1000, 938, 838, 497.

HRMS (ESI): m/z = Found: 359.1857 ($C_{21}H_{27}O_5$) $[(M+H)]^+$, calculated: 359.1853.

HPLC: Column: Chiralpak IC, *Fa. Daicel* (250x4.6 mm); 5 µL, 25 °C, 0.5 mL/min, 205 nm; solvent: *n*-heptane:2-propanol (90:10), t_R = 12.1, 15.2 min.

4,4′-Dimethoxy-6,6′-dimethyl-[1,1′-biphenyl]-2,2′-diyl dihexanoate *rac*-(181e)

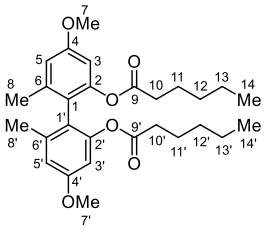

rac-**181e**

Dihexanoate *rac*-**181e** and monohexanoate *rac*-**182e** were synthesized according to the general procedure H, starting from biphenol *rac*-**1** (312 mg, 1.14 mmol). After purification by column chromatography (PE/EtOAc = 95:5 to 90:10) dihexanoate *rac*-**181e** (175 mg, 372 µmol) was obtained in 32% yield as yellow oil and monohexanoate *rac*-**182e** (188 mg, 505 µmol) in 44% yield as yellow oil.

R_f (PE:EE, 80:20) = 0.67

^{1}H-NMR ($CDCl_3$, 600 MHz) δ 6.69 (s, 2H, 5-H, 5′-H), 6.53 (s, 2H, 3-H, 3-H′), 3.80 (s, 6H, 7-OC$\underline{H}_3$, 7′-OC$\underline{H}_3$), 2.16 (q, $^2J_{10a/10'a,10b/10'b}$ = 6.9 Hz, $^3J_{10/10',11/11'}$ = 6.5 Hz, 4H, 10-C$\underline{H}_2$-, 10′-C$\underline{H}_2$-), 2.00 (s, 6H, 8-C$\underline{H}_3$, 8′-C$\underline{H}_3$), 1.37-1.28 (m, $^2J_{11a/11'a,11b/11'b}$ = 8.3 Hz, $^3J_{11/11',10/10',12/12'}$ = 7.5 Hz, 4H, 11-C$\underline{H}_2$-, 11-C$\underline{H}_2$-), 1.22-1.17 (m, $^3J_{12/12',10/10',11/11'}$ = 7.0 Hz, 4H, 12-C$\underline{H}_2$-, 12′-C$\underline{H}_2$-), 1.13-1.08 (q, $^3J_{13/13',12/12',14/14'}$ = 7.0 Hz, 4H, 13-C$\underline{H}_2$-, 13′-C$\underline{H}_2$-), 0.84 (q, $^3J_{14/14',13/13'}$ = 6.9 Hz, 6H, 14-C$\underline{H}_3$, 14′-C$\underline{H}_3$).

^{13}C-NMR ($CDCl_3$, 151 MHz) δ 172.08 (C-9, C-9′), 159.37 (C-4, C-4′), 149.92 (C-2, C-2′), 140.26 (C-6, C-6′), 121.27 (C-1, C-1′), 113.28 (C-5, C-5′), 105.62 (C-3, C-3′), 55.42 (C-7, C-7′), 34.02 (C-10, C-10′), 31.19 (C-13, C-13′), 24.52 (C-11, C-11′), 22.41 (C-12, C-12′), 19.85 (C-8, C-8′), 13.96 (C-14, C-14′).

IR: ν[cm^{-1}]: 2931, 1756, 1611, 1574, 1466, 1309, 1216, 1191, 1142, 1091, 1068, 855.

HRMS (ESI): m/z = Found: 471.2743 ($C_{28}H_{39}O_6$) $[(M+H)]^+$, calculated: 471.2741

HPLC: Column: Chiralpak IC, *Fa. Daicel* (250x4.6 mm); 5 µL, 25 °C, 0.5 mL/min, 205 nm; solvent: *n*-heptane:2-propanol (90:10), t_R = 9.7, 13.0 min.

2′-Hydroxy-4,4′-dimethoxy-6,6′-dimethyl-[1,1′-biphenyl]-2-yl hexanoate *rac*-(182e)

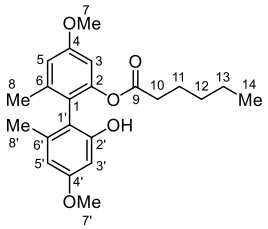

rac-**182e**

R_f (PE:EE, 80:20) = 0.47

^{1}**H-NMR** ($CDCl_3$, 600 MHz) δ 6.80 (d, $^4J_{5,3}$ = 2.5 Hz, 1H, 5-H), 6.54 (d, $^4J_{3,5}$ = 2.5 Hz, 1H, 3-H), 6.41 (s, 2H, 3′-H, 5′-H), 4.93 (s, 1H, 9′-OH), 3.83 (s, 3H, 7-OC$\underline{H}_3$), 3.77 (s, 3H, 7′-OC$\underline{H}_3$), 2.23 – 2.17 (m, 2H, 10-C$\underline{H}_2$-), 2.00 (s, 3H, 8′-C$\underline{H}_3$), 1.90 (s, 3H, 8-C$\underline{H}_3$), 1.32 (m, $^2J_{11a,11b}$ = 14.7 Hz, $^3J_{11,10}$ = 7.2 Hz, $^3J_{11,12}$ = 3.1 Hz, 2H, 11-C$\underline{H}_2$-), 1.19 (m, $^3J_{12,11,13}$ = 7.2 Hz, 2H, 12-C$\underline{H}_2$-), 1.07 (dqd, $^2J_{13a,13b}$ = 15.0 Hz, $^3J_{13,12}$ = 7.9 Hz, $^3J_{13,14}$ = 7.2 Hz, 2H, 13-C$\underline{H}_2$-), 0.83 (t, $^3J_{14,13}$ = 7.3 Hz, 3H, 14-C$\underline{H}_3$).

^{13}C-NMR ($CDCl_3$, 151 MHz) 173.38 (C-9), 160.39 (C-4), 160.37 (C-4′), 154.67 (C-2′), 151.02 (C-2), 141.53 (C-1′), 139.15 (C-1), 120.28 (C-6′), 114.84 (C-6), 114.18 (C-5), 108.56 (C-5′), 105.85 (C-3), 99.08 (C-3′), 55.56 (C-7), 55.24 (C-7′), 34.20 (C-10), 31.07 (C-13), 24.58 (C-11), 22.51 (C-12), 20.06 (C-8), 19.98 (C-8′), 13.87 (C-14).

IR: ν[cm^{-1}]: 3483, 2941, 1752, 1612, 1576, 1465, 1314, 1268, 1192, 1138, 1066, 1039, 838, 497.

HRMS (ESI): m/z = Found: 373.2014 ($C_{22}H_{29}O_5$) $[(M+H)]^+$, calculated: 373.2010.

HPLC: Column: Chiralpak IC, *Fa. Daicel* (250x4.6 mm); 5 µL, 25 °C, 0.5 mL/min, 205 nm; solvent: *n*-heptane:2-propanol (90:10), t_R = 11.7, 14.4 min.

8.3.3 Enzymatic kinetic resolution: Atroposelective hydrolysis

General procedure K: EKR in a two-phase system

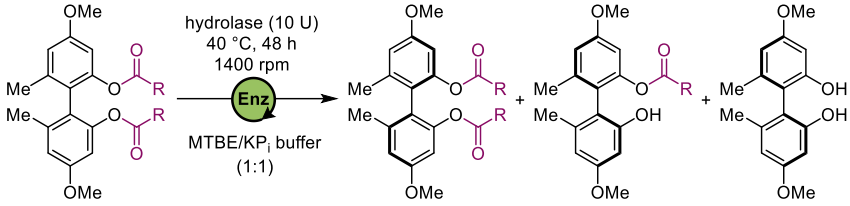

rac-**181a-e** (*M*)-**181a-e** (*P*)-**182a-e** (*P*)-**1**

Scheme 109 Enzyme screening of biphenyl diesters *rac*-**181a–e** in a two-phase system.

In a 2 mL *SureLock Eppendorf* vial the hydrolase (10 U) was weighed in and 0.1 M KP_i-buffer (pH = 7.4) was added (500 µL). A solution of diester *rac*-**181a–e** in MTBE (2 mg/mL, 500 µL) was added. The *Eppendorf* vial was shaken for 48 hours at 40 °C with 1400 rpm. The reaction was quenched by centrifugation of the mixture and extracting the organic phase. The aqueous phase was extracted for three times with EtOAc, by shaking the enzyme suspension with 1 mL EtOAc, centrifugating and extracting the organic phase. The combined organic phase was dried over $MgSO_4$ and concentrated under reduced pressure. The residue was dissolved in $CDCl_3$ to determine relative conversions *via* ^{1}H-NMR and used for separation on chiral HPLC for the determination of the enantiomeric excess.

Enzyme screening with addition of taurocholate salt

The enzymatic reaction in a two-phase system was performed according to general procedure K. Sodium taurocholate salt (0.70 equiv) was added before shaking for 48 hours. Work up and quantification was executed as described before.

Screening of solvents and enzyme amount

Two-phase system:

The enzymatic reaction in a two-phase system was performed as described in general procedure K with different organic solvents (acetone, MTBE, 2-propanol, toluene, *n*-heptane and DMSO) and different enzyme loadings (10, 5 and 1 U)

One-phase system:

For reactions in a one-phase system using DMSO as a cosolvent, the DMSO concentration was lowered to 10 vol%. In a 2 mL *SureLock Eppendorf* vial CRL (10, 5 and 1 U) was weighed in and 0.1 M KP_i-buffer (pH = 7.4) was added (900 µL). A solution of diester *rac*-**181b** in DMSO (10 mg/mL, 100 µL) was added. The vial was shaken for 24 hours at 40 °C with 1400 rpm. The work up and quantification of the products was executed as described in general procedure K.

Screening of pH value of KP_i buffer

In a 2 mL *SureLock Eppendorf* vial CRL (1 U) was weighed in and 0.1 M KP_i-buffer (pH = 6.5, 7, 8) was added (900 µL). A solution of diester *rac*-**181b** in DMSO (10 mg/mL, 100 µL) was added. The vial was shaken for 3 hours at 40 °C with 1400 rpm. The work up and quantification of the products was executed as described in general procedure K.

Screening of whole cell extracts

In a 2 mL *SureLock Eppendorf* vial the whole cell extract (1 U) was added and 0.1 M KP_i-buffer (pH = 7.4) was added (500 µL). A solution of diester *rac*-**181a–e** in DMSO (2 mg/mL, 500 µL) was added. The vial was shaken for 24 hours at 30 °C with 1400 rpm. The work up and quantification of the products was executed as described in general procedure K.

Investigation towards time-course of EKR of *rac*-181b

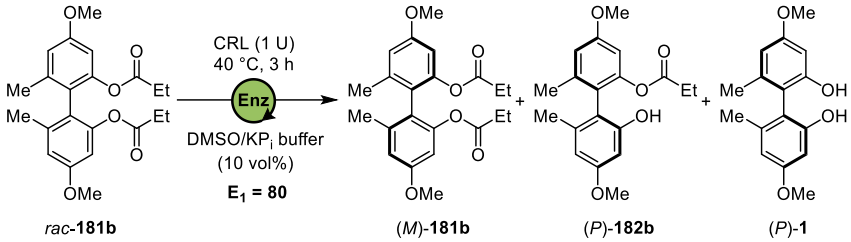

Scheme 110 Investigation of time-course of the first step of sequential EKR.

To record the time-course of EKR of *rac*-**181b** six reactions were set up in a *SureLock Eppendorf* vial to monitor the reaction over 4 hours. In a 2 mL vial CRL was weighed in and 0.1 M KP_i-buffer (pH = 7.4) was added (900 µL). A solution of diester *rac*-**181b** in DMSO (10 mg/mL, 100 µL) was added. The reaction mixtures were shaken for a specific amount of time (5, 10, 15, 30, 60, 120, 180 and 240 minutes) at 40 °C with 1400 rpm. The reaction was quenched by centrifugation of the mixture and extracting the organic phase. The aqueous phase was extracted for three times with EtOAc, by shaking the enzyme suspension with 1 mL EtOAc, centrifugating and extracting the organic phase. The combined organic phase was dried over $MgSO_4$ and concentrated under reduced pressure. The residue was dissolved in $CDCl_3$ to determine relative conversions *via* ^{1}H-NMR and used for separation on chiral HPLC for the determination of the enantiomeric excess.

Investigation towards time-course of EKR of *rac*-182b

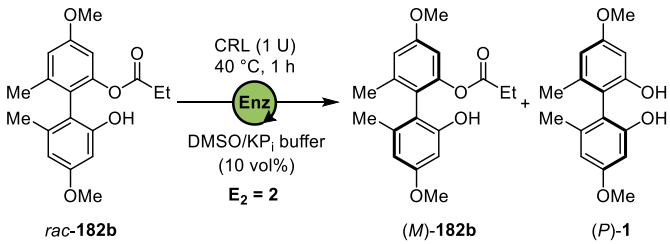

Scheme 111 Investigation of time-course of the second step of sequential EKR.

For the time-course of EKR of *rac*-**182b** eight reactions were set up in a *SureLock Eppendorf* vial to monitor the reaction over 1 hour. In a 2 mL vial the hydrolase was weighed in and 0.1 M KP_i-buffer (pH = 7.4) was added (900 µL). A solution of monoester *rac*-**182b** in DMSO (10 mg/mL, 100 µL) was added. The reaction mixtures were shaken for a specific

amount of time (5, 10, 15, 30, 45, 60 minutes) at 40 °C with 1400 rpm. The reaction was quenched by centrifugation of the mixture and extracting the organic phase. The aqueous phase was extracted for three times with EtOAc, by shaking the enzyme suspension with 1 mL EtOAc, centrifugating and extracting the organic phase. The combined organic phase was dried over $MgSO_4$ and concentrated under reduced pressure. The residue was dissolved in $CDCl_3$ to determine relative conversions *via* ^{1}H-NMR and used for separation on chiral HPLC for the determination of the enantiomeric excess.

8.3.4 Scaled up enzymatic kinetic resolution

CRL (6.00 g, 6 w/w) and 0.1 M KP_i buffer (450 mL, pH = 7.4) was given in a round bottom flask. The substrate solution of diester *rac*-**181b** (1.00 g, 2.60 mmol) dissolved in DMSO (20 mg/mL, 50 mL) was added. The mixture was stirred with a Teflon coated stirring bar with 1000 rpm at 40 °C for 3 hours. The reaction was quenched by adding solid ammonium sulfate in portions until the enzyme completely precipitated. The suspension was filtered over a wide *Büchner* funnel covered with a celite pad. The aqueous phase was extracted five times with EtOAc. The combined organic phase was washed with brine, dried over $MgSO_4$, and concentrated under reduced pressure. The residue was diluted in EtOAc and washed with ice water to remove the residual DMSO. After concentration, the mixture was purified by column chromatography on silica gel (PE/EtOAc = 95:5 to 90:10 to 80:20).

***(M)*-4,4′-Dimethoxy-6,6′-dimethyl-[1,1′-biphenyl]-2,2′-diyl dipropionate *(M)*-(181b)**

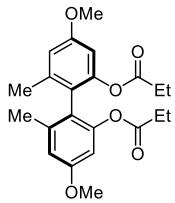

(*M*)-**181b**

The enzymatic kinetic resolution resulted in the isolation of (*M*)-biphenyl diester (*M*)-**181b** (432 mg, 1.10 mmol, 99% *ee*) in 43% yield as colorless oil. The spectroscopic data were in accordance with those previously obtained for racemic material.

$[\alpha]_D^{25} = -45$ (c = 1.0, $CHCl_3$)

***(P)*-2′-Hydroxy-4,4′-dimethoxy-6,6′-dimethyl-[1,1′-biphenyl]-2-yl propionate *(P)*-(182b)**

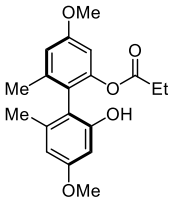

(*P*)-**182b**

The enzymatic kinetic resolution resulted in the isolation of (*P*)-biphenyl monoester (*P*)-**182b** (42 mg, 0.13 mmol, 92% *ee*) in 5% yield as colorless oil. The spectroscopic data were in accordance with those previously obtained for racemic material.

***(P)*-4,4′-Dimethoxy-6,6′-dimethyl-[1,1′-biphenyl]-2,2′-diol (*P*)-(1)**

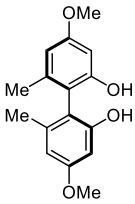

(*P*)-**1**

The enzymatic kinetic resolution resulted in the isolation of (*P*)-biphenol (*P*)-**1** (286 mg, 1.00 mmol, >99% *ee*) in 40% yield as white crystals. The spectroscopic data were in accordance with those previously obtained for racemic material.

Mp: 175 °C **Lit. Mp:** 172–174 °C[1]

$[\alpha]_D^{25} = -36.2$ (c = 1.0, $CHCl_3$) **Lit.** $[\alpha]_D^{25} = -31.9$ (c = 1.0, $CHCl_3$)[1]

Hydrolysis to enantiopure biphenyl (*M*)-1

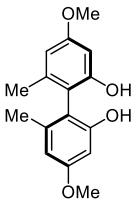

(*M*)-**1**

The enantiopure diester (*M*)-**181b** (432 mg, 1.10 mmol) was dissolved in methanol (10 mL) and potassium carbonate (0.61 g, 4.4 mmol) was added. The mixture was stirred at r.t. for 2 hours. After full conversion the mixture was acidified with 1 M HCl. The aqueous phase was extracted with EtOAc for three times. The combined organic phases were dried over $MgSO_4$ and concentrated under reduced pressure. (*M*)-biphenol (*M*)-**1** was obtained as light orange crystals (0.30 g, 1.1 mmol, >99% *ee*) in 98% yield. The spectroscopic data were in accordance with those previously obtained for racemic material.

Mp: 173 °C **Lit. Mp:** 155–160 °C[189]

$[\alpha]_D^{25} = 36.4$ (c = 1.0, $CHCl_3$) **Lit.** $[\alpha]_D^{25} = 15.0$ (c = 1.0, CH_3OH)[189]

8.3.5 Investigations on dynamic enzymatic kinetic resolution

General procedure L: Enzymatic esterification

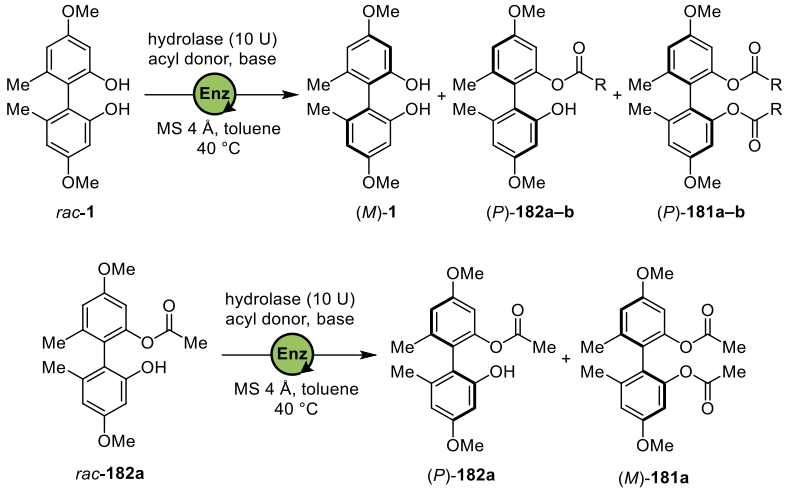

Scheme 112 Enzyme screening of enzymatic esterification of *rac*-**1** and *rac*-**182a**.

In a 2 mL *SureLock Eppendorf* vial the hydrolase (10 U) and molecular sieve (4 Å, 10 mg) was weighed in. A solution of biphenol *rac*-**1** or monoester *rac*-**182a** in anhydrous toluene (1 mg/mL, 1000 µL), the acyl donor (10 equiv), and if needed the base (2.00 equiv) was added. The *Eppendorf* vial was shaken for 24 or 70 hours at 40 °C with 1400 rpm. The reaction was quenched by adding KP_i-buffer (500 µL, pH = 7.4). The solids were washed for three times with EtOAc, by shaking the solids with 1 mL EtOAc, centrifugating and extracting the solvent. The combined organic phase was dried over $MgSO_4$ and concentrated under reduced pressure. The residue was dissolved in $CDCl_3$ to determine relative conversions *via* ^{1}H-NMR and used for separation on chiral HPLC for the determination of the enantiomeric excess.

General procedure M: Racemization of biphenol 1

500 µL of a stock solution of the catalyst (10.00 mol%) and if needed the additive (10.00 mol%) in anhydrous toluene was given in a 2 mL *SureLock Eppendorf* vial. A solution of (*M*)-biphenol (*M*)-**1** in anhydrous toluene (2 mg/mL, 500 µL) was added afterwards. The vial was shaken for 24 hours at 40 °C. The reaction was quenched by filtering through a celite pad and washing with EtOAc for three times. The combined organic phase was

concentrated under reduced pressure. The residues were analyzed on chiral HPLC for the determination of the enantiomeric excess.

8.3.6 Synthesis of tetra-*ortho*-substituted biphenol scope

2-Bromo-3,5-dimethylphenol (184)

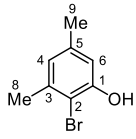

184

The product was synthesized according to general procedure A. After purification by column chromatography (PE/EtOAC = 98:2 to 95:5), the brominated product **184** (0.21 g, 1.1 mmol) was obtained from 3,5-dimethylphenol (**183**) (0.30 g, 2.5 mmol) in 43% yield as light yellow oil.

R_f (PE:EE, 90:10) = 0.48

^{1}H-NMR ($CDCl_3$, 600 MHz) δ 6.69 (d, $^4J_{6,4}$ = 2.2 Hz, 1H, 6-H), 6.64 (d, $^4J_{4,6}$ = 2.1 Hz, 1H, 4-H), 5.50 (s, 1H, OH), 2.35 (s, 3H, 8-C$\underline{H}_3$), 2.25 (s, 3H, 9-C$\underline{H}_3$).

^{13}C-NMR ($CDCl_3$, 151 MHz) δ 152.16 (C-1), 138.46 (C-5), 138.17 (C-3), 123.68 (C-4), 113.94 (C-6), 109.95 (C-2), 23.08 (C-8), 21.09 (C-9).

IR: ν[cm^{-1}]: 3339, 1444, 1315, 1271, 1172, 1029, 955, 839, 582, 574.

MS (ESI): m/z = 202.9 [M+H]+

The analytical data correspond to the data given in literature.[107]

3,5-Dimethoxyphenyl acetate (191)

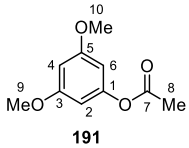

191

3,5-Dimethoxyphenol (**188**) (1.00 g, 6.49 mmol) was dissolved in CH_2Cl_2 (25 mL) and cooled down to 0 °C. NaH (60% dispersion in mineral oil, 0.27 g, 6.8 mmol) was added.

After the mixture was stirred for 1 hour at r.t., acetylchloride (0.49 mL, 6.8 mmol) was added dropwise at 0 °C. The reaction mixture was stirred again at r.t. until full conversion was observed. The reaction was quenched by adding ice cold water and the organic phase was extracted three times with CH_2Cl_2. The combined organic phase was washed with brine and dried over $MgSO_4$. Concentrating at reduced pressure led to the product **191** (1.27 g, 6.47 mmol) in 99% yield as light yellow oil.

R_f (PE:EE, 80:20) = 0.40

^{1}H-NMR ($CDCl_3$, 600 MHz) δ 6.34 (t, $^4J_{4,2,6}$ = 2.2 Hz, 1H, 4-H), 6.26 (d, $^4J_{6,2,4}$ = 2.2 Hz, 2H, 2-H, 6-H), 3.77 (s, 6H, 9-OC$\underline{H}_3$, 10-OC$\underline{H}_3$), 2.29 (s, 3H, 8-C$\underline{H}_3$).

^{13}C-NMR ($CDCl_3$, 151 MHz) δ 169.44 (C-7), 161.29 (C-3, C-5), 152.36 (C-1), 100.38 (C-2, C-6), 98.42 (C-4), 55.62 (C-9, C-10), 21.29 (C-8).

IR: ν[cm^{-1}]: 2841, 1764, 1593, 1200, 1151, 1126, 1050, 1017, 827, 677.

MS (ESI): m/z = 197.0 $[M+H]^+$.

The analytical data correspond to the data given in literature.[294]

2-Bromo-3,5-dimethoxyphenyl acetate (192)

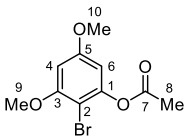

192

The product was synthesized according to general procedure A. Brominated phenol **192** was gained (1.4 g, 5.1 mmol) from 3,5-dimethoxyphenyl acetate (**191**) (1.0 g, 5.1 mmol) in quantitative yield. The crude product was used without further purification.

R_f (PE:EE, 80:20) = 0.33

^{1}H-NMR ($CDCl_3$, 600 MHz) δ 6.39 (d, $^4J_{4,6}$ = 2.6 Hz, 1H, 4-H), 6.33 (d, $^4J_{6,4}$ = 2.6 Hz, 1H, 6-H), 3.87 (s, 3H, 9-OC$\underline{H}_3$), 3.79 (s, 3H, 10-OC$\underline{H}_3$), 2.35 (s, 3H, 8-C$\underline{H}_3$).

^{13}C-NMR ($CDCl_3$, 151 MHz) δ 168.45 (C-7), 160.06 (C-3), 157.51 (C-5), 149.84 (C-1), 100.59 (C-2), 97.62 (C-6), 97.39 (C-4), 56.48 (C-9), 55.69 (C-10), 20.84 (C-8).

IR: ν[cm^{-1}]:1755, 1584. 1196, 1160, 1091, 1070, 1028, 887, 818, 605, 568.

MS (ESI): m/z = 232.9 $[M\text{-}CH_3C{=}O{+}H]^+$.

Mp: 93–95 °C **Lit. Mp:** 92–93 °C[295]

The analytical data correspond to the data given in literature.

2-Bromo-3,5-dimethoxyphenol (189)

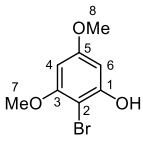

189

Bromophenylacetate **192** (0.60 g, 2.2 mmol) was dissolved in methanol (5 mL). Sodium bicarbonate (0.20 g, 2.4 mmol) was added, and the mixture was stirred at r.t. until full conversion was observed. The reaction mixture was quenched by acidifying with 1 M aqueous HCl solution. The organic phase was extracted three times with CH_2Cl_2 and dried over $MgSO_4$. Concentrating at reduced pressure gave the free bromophenol **189** (0.49 g, 2.1 mmol) in 98% yield as a white solid. The product was used without further purification.

R_f (PE:EE, 80:20) = 0.36

^{1}H-NMR ($CDCl_3$, 600 MHz) δ 6.26 (d, $^4J_{6,4}$ = 2.9 Hz, 1H, 6-H), 6.11 (d, $^4J_{4,6}$ = 2.8 Hz, 1H, 4-H), 5.65 (s, 1H, OH), 3.85 (s, 3H, 8-OC$\underline{H}_3$), 3.78 (s, 3H, 7-OC$\underline{H}_3$).

^{13}C-NMR ($CDCl_3$, 151 MHz) δ 160.87 (C-3), 156.96 (C-5), 154.01 (C-1), 93.34 (C-6), 92.68 (C-4), 91.20 (C-2), 56.44 (C-8), 55.71 (C-7).

IR: ν[cm^{-1}]: 1776, 1584, 1431, 1215, 1198, 1100, 874, 805, 693.

MS (ESI): m/z = 234.8 $[M+H]^+$.

Mp: 81–83 °C **Lit. Mp:** 79–81 °C[295]

The analytical data correspond to the data given in literature.[296]

2-Bromo-1-(methoxymethoxy)-3-methylbenzene (193a)

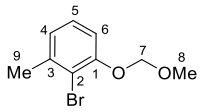

193a

The product was synthesized according to general procedure B. MOM-protected product **193a** (1.23 g, 5.30 mmol) was obtained from 2-bromo-3-methylphenol (1.00 g, 5.35 mmol) in 99% yield as light yellow oil.

R_f (PE:EE, 80:20) = 0.71

^{1}H-NMR ($CDCl_3$, 600 MHz) δ 7.14 (t, $^3J_{6,5}$ = 7.9 Hz, 1H, 6-H), 6.98 – 6.95 (m, 1H, 5-H), 6.94 – 6.89 (m, 1H, 4-H), 5.24 (s, 2H, 7-C$\underline{H}_2$-), 3.52 (s, 3H, 8-OC$\underline{H}_3$), 2.42 (s, 3H, 9-C$\underline{H}_3$).

^{13}C-NMR ($CDCl_3$, 151 MHz) δ 153.98 (C-1), 139.94 (C-2), 127.62 (C-6), 124.28 (C-4), 115.68 (C-3), 113.49 (C-5), 95.30 (C-7), 56.51 (C-8), 23.53 (C-9).

IR: ν[cm^{-1}]: 2924, 1466, 1260 ,1153, 1086, 1044, 1026, 985, 922, 769.

MS (ESI): m/z = 200.8 $[M\text{-}CH_3OH+H]^+$

The analytical data correspond to the data given in literature.[297]

2-Bromo-1-methoxy-3-(methoxymethoxy)benzene (193b)

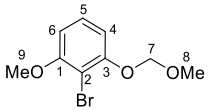

193b

The product was synthesized according to general procedure B. MOM-protected product **193b** (1.72 g, 6.96 mmol) was obtained from 2-bromo-3-methoxyphenol (1.43 g, 7.03 mmol) in 99% yield as colorless oil.

R_f (PE:EE, 80:20) = 0.5

^{1}H-NMR ($CDCl_3$, 600 MHz) δ 7.21 (t, $^3J_{5,6,4}$ = 8.3 Hz, 1H, 5-H), 6.80 (dd, $^3J_{4,5}$ = 8.3 Hz, $^5J_{4,7}$ = 1.2 Hz, 1H, 4-H), 6.61 (dd, $^3J_{6,5}$ = 8.3 Hz, $^5J_{6,9}$ = 1.2 Hz, 1H, 6-H), 5.25 (s, 2H, 7-C$\underline{H}_2$-), 3.90 (s, 3H, 9-OC$\underline{H}_3$), 3.52 (s, 3H, 8-OC$\underline{H}_3$).

^{13}C-NMR ($CDCl_3$, 151 MHz) δ 157.36 (C-1), 155.18 (C-3), 128.36 (C-5), 108.72 (C-4), 105.75 (C-6), 102.63 (C-2), 95.27 (C-7), 56.60 (C-9), 56.55 (C-8).

IR: ν[cm^{-1}]: 2939, 1591, 1470, 1435, 1249, 1153, 1096, 1066, 1036, 996 766.

MS (ESI): m/z = 214.0 $[M\text{-}CH_3OH\text{-}H]^-$

The analytical data correspond to the data given in literature.[298]

2-Bromo-1-(methoxymethoxy)-3,5-dimethylbenzene (193c)

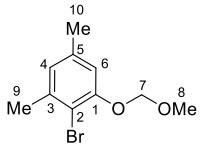

193c

The product was synthesized according to general procedure B. MOM-protected product **193c** (2.42 g, 9.87 mmol) was obtained from 2-bromo-3,5-dimethylphenol (**184**) (2.01 g, 10.0 mmol) in 99% yield as white solid.

R_f (PE:EE, 80:20) = 0.83

^{1}H-NMR ($CDCl_3$, 600 MHz) δ 6.80 (d, $^4J_{6,4}$ = 1.9 Hz, 1H, 6-H), 6.77 – 6.73 (m, 1H, 4-H), 5.23 (s, 2H, 7-C$\underline{H}_2$-), 3.53 (s, 3H, 8-OC$\underline{H}_3$), 2.37 (s, 3H, 9-C$\underline{H}_3$), 2.27 (s, 3H, 10-C$\underline{H}_3$).

^{13}C-NMR ($CDCl_3$, 151 MHz) δ 153.71 (C-1), 139.33 (C-3), 137.75 (C-5), 125.23 (C-2), 114.37 (C-4), 112.28 (C-6), 95.27 (C-7), 56.50 (C-8), 23.37 (C-9), 21.34 (C-10).

IR: ν[cm^{-1}]: 2921, 1579, 1466, 1314, 1151, 1049, 1027, 989, 968, 924, 836.

HRMS (ESI): m/z = Found: 245.0173 ($C_{10}H_{14}BrO_2$) $[(M+H)]^+$, calculated: 245.0172.

2-Bromo-1,5-dimethoxy-3-(methoxymethoxy)benzene (193d)

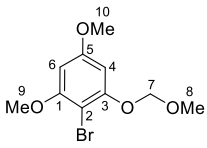

193d

The product was synthesized according to general procedure B. MOM-protected product **193d** (1.39 g, 5.97 mmol) was obtained from 2-bromo-3,5-dimethoxyphenol (**189**) (1.41 g, 6.03 mmol) in 84% yield as colorless oil.

R_f (PE:EE, 80:20) = 0.57

^{1}H-NMR ($CDCl_3$, 600 MHz) δ 6.42 (d, $^4J_{4,6}$ = 2.6 Hz, 1H, 4-H), 6.22 (d, $^4J_{6,4}$ = 2.5 Hz, 1H, 6-H), 5.23 (s, 2H, 7-C$\underline{H}_2$-), 3.87 (s, 3H, 9-OC$\underline{H}_3$), 3.80 (s, 3H, 10-OC$\underline{H}_3$), 3.52 (s, 3H, 8-C$\underline{H}_3$).

^{13}C-NMR ($CDCl_3$, 151 MHz) δ 160.48 (C-5), 157.57 (C-1), 155.56 (C-3), 95.38 (C-7), 94.80 (C-4), 93.68 (C-2), 93.52 (C-6), 56.56 (C-8), 56.51 (C-9), 55.72 (C-10).

IR: ν[cm^{-1}]: 2940, 1587, 1461, 1230, 1211, 1159, 1115, 1085, 1064, 1008.

HRMS (ESI): m/z = Found: 277.0067 ($C_{10}H_{14}BrO_4$) $[(M+H)]^+$, calculated: 277.0070.

2-Bromo-1-methoxy-5-(methoxymethoxy)-3-methylbenzene (193e)

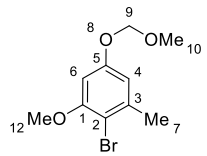

193e

The product was synthesized according to general procedure B. MOM-protected product **193e** (2.24 g, 8.57 mmol) was obtained from 4-bromo-3-methoxy-5-methylphenol (**173**) (2.02 g, 9.31 mmol) in 92% yield as light yellow oil.

R_f (PE:EE, 80:20) = 0.52

^{1}H-NMR ($CDCl_3$, 600 MHz) δ 6.59 (s, 1H, 4-H), 6.48 (s, 1H, 6-H), 5.15 (s, 2H, 9-C$\underline{H}_2$-), 3.86 (s, 3H, 12-OC$\underline{H}_3$), 3.48 (s, 3H, 10-OC$\underline{H}_3$), 2.38 (s, 3H, 7-C$\underline{H}_3$).

^{13}C-NMR ($CDCl_3$, 151 MHz) δ 157.10 (C-5), 156.79 (C-1), 140.11 (C-2), 110.17 (C-4), 106.52 (C-3), 99.03 (C-6), 94.72 (C-9), 56.46 (C-12), 56.22 (C-10), 23.65 (C-7).

IR: ν[cm^{-1}]: 2925, 1589, 1465, 1323, 1150, 1095, 1044, 1022, 928.

MS (ESI): m/z = 263.0 $[M+H]^+$.

The analytical data correspond to the data given in literature.[299]

2-Bromo-3,4,5-trimethoxy-1-(methoxymethoxy)benzene (193f)

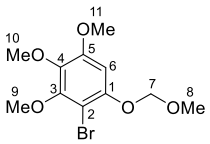

193f

The product was synthesized according to general procedure A. Brominated product **193f** (2.20 g, 7.16 mmol) was obtained from (3,4,5-trimethoxyphenoxy)methanol **201d** (1.78 g, 7.80 mmol) in 92% yield as colorless oil.

R_f (PE:EE, 80:20) = 0.45

^{1}H-NMR ($CDCl_3$, 600 MHz) δ 6.62 (s, 1H, 6-H), 5.20 (s, 2H, 7-C$\underline{H}_2$-), 3.91 (s, 3H, 9-OC$\underline{H}_3$), 3.85 (s, 3H, 11-OC$\underline{H}_3$), 3.83 (s, 3H, 10-OC$\underline{H}_3$), 3.54 (s, 3H, 8-OC$\underline{H}_3$).

^{13}C-NMR ($CDCl_3$, 151 MHz) δ 153.03 (C-5), 151.61 (C-3), 150.62 (C-1), 138.44 (C-4), 99.58 (C-2), 97.38 (C-6), 95.85 (C-7), 61.26 (C-9), 61.06 (C-10), 56.47 (C-8), 56.24 (C-11).

IR: ν[cm^{-1}]: 2937, 1716, 1576, 1481, 1393, 1152, 1108, 1050, 1005, 920, 812.

HRMS (ESI): m/z = Found: 307.0170 ($C_{11}H_{16}BrO_5$) $[(M+H)]^+$, calculated: 307.0176.

2-Bromo-1-isopropoxy-3-(methoxymethoxy)benzene (193g)

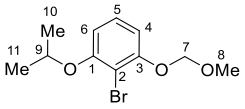

193g

Potassium carbonate (0.19 g, 1.4 mmol) and the MOM-protected phenol **198** (0.30 g, 1.3 mmol) was dissolved in DMF (30 mL). 2-Bromopropane (0.36 mL, 3.9 mmol) was added slowly, and the mixture was stirred at 60 °C. After full conversion was observed, the reaction was quenched by adding 1 M aqueous HCl solution to acidify the mixture. The organic phase was extracted three times with EtOAc and dried over $MgSO_4$. Purification *via* column chromatography (PE:EtOAc = 95:5) gave the desired product **193g** (0.23 g, 0.83 mmol) in 64% yield as light yellow oil.

R_f (PE:EE, 90:10) = 0.47

^{1}H-NMR ($CDCl_3$, 600 MHz) δ 7.16 (t, $^3J_{5,4,6}$ = 8.3 Hz, 1H, 5-H), 6.77 (d, $^3J_{4,5}$ = 8.3 Hz, 1H, 4-H), 6.62 (d, $^3J_{6,5}$ = 8.4 Hz, 1H, 6-H), 5.24 (s, 2H, 7-C$\underline{H}_2$-), 4.56 (hept, $^3J_{9,10,11}$ = 6.1 Hz, 1H, 9-H), 3.52 (s, 3H, 8-C$\underline{H}_3$), 1.38 (d, $^3J_{10,11,9}$ = 6.1 Hz, 6H, 10-C$\underline{H}_3$, 11-C$\underline{H}_3$).

^{13}C-NMR ($CDCl_3$, 151 MHz) δ 156.09 (C-1), 155.34 (C-3), 128.08 (C-5), 109.31 (C-6), 108.59 (C-4), 104.72 (C-2), 95.26 (C-7), 72.35 (C-9), 56.53 (C-8), 22.26 (C-10, C-11).

IR: ν[cm^{-1}]: 2978, 1593, 1463, 1249, 1154, 1117, 1092, 1046, 768.

HRMS (ESI): m/z = Found: 275.0276 ($C_{11}H_{16}BrO_3$) $[(M+H)]^+$, calculated: 275.0277.

1-(Benzyloxy)-2-bromo-3-(methoxymethoxy)benzene (193h)

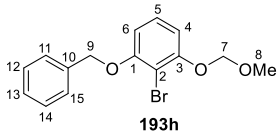

193h

MOM-protected phenol **198** (0.08 g, 0.3 mmol), potassium carbonate (0.12 g, 0.86 mmol) and *tert*-butylammoniumiodide (12 mg, 30 µmol) was given in dry DMF (3 mL). The mixture was heated up to 50 °C. Benzyl bromide (0.10 mL, 0.86 mmol) was added slowly. After full conversion the reaction was quenched by adding water. The mixture was continuously stirred at 60 °C for 1 hour. After cooling down, the organic phase was extracted

three times with EtOAc and dried over $MgSO_4$. After concentrating the combined organic phase at reduced pressure, the residue was washed three times with ice to remove any residual DMF. Purification *via* column chromatography (PE:EtOAc = 90:10) gave the benzylated product **193h** (0.11 g, 0.33 mmol) in 96% yield as colorless oil.

R_f (PE:EE, 80:20) = 0.51

^{1}H-NMR ($CDCl_3$, 600 MHz) δ 7.49 (d, $^3J_{11/15,12,14}$ = 7.3 Hz, 2H, 11-H, 15-H), 7.39 (t, $^3J_{12/14,11,13,15}$ = 7.6 Hz, 2H, 12-H, 14-H), 7.35 – 7.29 (m, 1H, 13-H), 7.17 (t, $^3J_{5,4,6}$ = 8.3 Hz, 1H, 5-H), 6.81 (dd, $^3J_{4,5}$ = 8.4 Hz, 1H, 4-H), 6.65 (dd, $^3J_{6,5}$ = 8.32 Hz, 1H, 6-H), 5.26 (s, 2H, 7-C$\underline{H}_2$-), 5.17 (s, 2H, 9-C$\underline{H}_2$-), 3.53 (s, 3H, 8-C$\underline{H}_3$).

^{13}C-NMR ($CDCl_3$, 151 MHz) δ 156.49 (C-1), 155.29 (C-3), 136.76 (C-10), 128.70 (C-12, C-14), 128.28 (C-5), 128.03 (C-13), 127.11 (C-11, C-15), 108.96 (C-4), 107.55 (C-6), 103.47 (C-2), 95.28 (C-7), 71.09 (C-9), 56.56 (C-8).

IR: ν[cm^{-1}]: 2902, 1592, 1461, 1251, 1153, 1094, 1056, 1036, 1029, 1000, 921, 765, 734, 695.

HRMS (ESI): m/z = Found: 323.0280 ($C_{15}H_{16}BrO_3$) $[(M+H)]^+$, calculated: 323.0277.

2-Bromo-3-methoxyphenol (196)

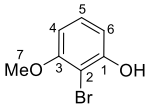

196

2-Bromoresorcinol (**195**) (1.86 g, 9.81 mmol) and potassium hydroxide pellets (0.55 g, 9.8 mmol) were given in a flask filled with distilled water (25 mL). Dimethyl sulfate (0.93 mL, 9.8 mmol) was added slowly. After full addition the mixture was stirred at 100 °C for 30 minutes. The reaction was quenched by adding 10% aq. sodium sulfite solution and 1 M aqueous HCl solution until the mixture turned acidic. The organic phase was extracted three times with EtOAc and afterwards dried over $MgSO_4$. After concentration at reduced pressure the crude product was purified *via* column chromatography (PE: EtOAc = 90:10), leading to the desired monomethylated product (**196**) (0.63 g, 3.1 mmol) in 32% yield as a white solid and the double methylated side product (**197**) (0.22 g, 1.0 mmol) in 10% yield as a white solid.

R_f (PE:EE, 80:20) = 0.15

^{1}H-NMR ($CDCl_3$, 600 MHz) δ 7.17 (t, $^3J_{5,4,6}$ = 8.2 Hz, 1H, 5-H), 6.68 (dd, $^3J_{6,5}$ = 8.3 Hz, $^4J_{6,4}$ = 1.3 Hz, 1H, 6-H), 6.48 (dd, $^3J_{4,5}$ = 8.3 Hz, $^4J_{4,6}$ = 1.3 Hz, 1H, 4-H), 5.62 (s, 1H, OH), 3.89 (s, 3H, 7-OC$\underline{H}_3$).

^{13}C-NMR ($CDCl_3$, 151 MHz) δ 156.64 (C-3), 153.66 (C-1), 128.82 (C-5), 108.69 (C-6), 103.81 (C-4), 100.15 (C-2), 56.54 (C-7).

IR: ν[cm^{-1}]: 3483, 1592, 1467, 1437, 1263, 1292, 1164, 1073, 1031, 765.

MS (ESI): m/z = 204.7 $[M+H]^+$.

Mp: 74–77 °C **Lit. Mp:** 79–80 °C[300]

The analytical data correspond to the data given in literature.[107]

2-Bromo-1,3-dimethoxybenzene (197)

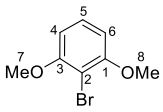

197

R_f (PE:EE, 80:20) = 0.28

^{1}H-NMR ($CDCl_3$, 600 MHz) δ 7.23 (td, $^3J_{5,4,6}$ = 8.3 Hz, $^4J_{5,8}$ = 1.1 Hz, 1H, 5-H), 6.58 (dd, $^3J_{4/6,5}$ = 8.4 Hz, $^4J_{4,6}$ = 1.2 Hz, 2H, 4-H, 6-H), 3.90 (d, $^5J_{7/8,4/6}$ = 1.2 Hz, 6H, 7-OC$\underline{H}_3$, 8-OC$\underline{H}_3$).

^{13}C-NMR ($CDCl_3$, 151 MHz) δ 157.36 (C-1, C-3), 128.38 (C-5), 104.84 (C-4, C-6), 101.11 (C-2), 56.60 (C-7, C-8).

IR: ν[cm^{-1}]: 3009, 2920, 1590, 1472, 1455, 1433, 1254, 1097, 1034, 763, 628.

MS (ESI): m/z = 204.7 $[M+H]^+$.

Mp: 91–95 °C **Lit. Mp:** 91–92 °C[301]

The analytical data correspond to the data given in literature.[302, 303]

2-Bromo-3-(methoxymethoxy)phenol (198)

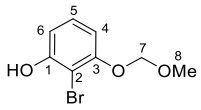

198

2-Bromoresorcinol (**195**) (1.00 g, 5.29 mmol) was given in anhydrous acetone (10 mL). The reaction mixture was cooled down to 0 °C and caesium carbonate (1.57 g, 4.81 mmol) was added in one portion. The mixture was stirred at 0 °C for 1 hour. After adding (chloromethyl)methylether (0.37 mL, 4.8 mmol) dropwise at 0 °C, the reaction mixture was stirred at 0 °C for 3 hours. The mixture was quenched by addition of water. The reaction mixture was extracted three times with EtOAc. The combined organic phase was washed with saturated $NaHCO_3$ solution, dried over $MgSO_4$. After drying at reduced pressure, the residual oil was purified by column chromatography (PE/EtOAc = 95:5), leading to the MOM-protected phenol **198** (0.42 g, 1.8 mmol) in 34% yield as yellow crystals.

R_f (PE:EE, 90:10) = 0.33

^{1}H-NMR ($CDCl_3$, 600 MHz) δ 7.15 (t, $^3J_{5,4,6}$ = 8.3 Hz, 1H, 5-H), 6.72 (q, $^3J_{6,5}$ = 1.3 Hz, 1H, 6-H), 6.71 (q, $^3J_{4,5}$ = 1.3 Hz, 1H, 4-H), 5.63 (s, 1H, OH), 5.24 (s, 2H, 7-C$\underline{H}_2$-), 3.52 (s, 3H, 8-OC$\underline{H}_3$).

^{13}C-NMR ($CDCl_3$, 151 MHz) δ 154.44 (C-3), 153.66 (C-1), 128.85 (C-5), 109.58 (C-6), 107.54 (C-4), 101.47 (C-2), 95.23 (C-7), 56.57 (C-8).

IR: ν[cm^{-1}]: 3492, 2926, 1592, 1465, 1190, 1154, 1087, 1031, 929, 772.

MS (ESI): m/z = 202.7 $[M\text{-}CH_3OH+H]^+$.

Mp: 57–58 °C **Lit. Mp:** 55–56 °C[304]

The analytical data correspond to the data given in literature.[23]

***rac*-2,2'-Bis(methoxymethoxy)-6,6'-dimethyl-1,1'-biphenyl *rac*-(199a)**

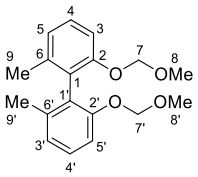

rac-**199a**

The homocoupling was performed according to general procedure E. After column chromatography (PE:EtOAc = 95:5) the coupling product *rac*-**199a** (43 mg, 0.14 mmol) was obtained from 2-bromo-1-(methoxymethoxy)-3-methylbenzene (**193a**) (0.10 g, 0.43 mmol) in 66% yield as yellow crystals.

R_f (PE:EE, 80:20) = 0.46

^{1}H-NMR ($CDCl_3$, 600 MHz) δ 7.21 (t, $^3J_{3/3',4/4'}$ = 7.9 Hz, 2H, 3-H, 3′-H), 7.03 (d, $^3J_{4/4',3/3',5/5'}$ = 8.2 Hz, 2H, 4-H, 4′-H), 6.96 (d, $^3J_{5/5',4/4'}$ = 7.5 Hz, 2H, 5-H, 5′-H), 5.03 – 4.99 (m, 4H, 7-C$\underline{H}_2$-, 7′-C$\underline{H}_2$-), 3.29 (s, 6H, 8-OC$\underline{H}_3$, 8′-OC$\underline{H}_3$), 1.97 (s, 6H, 9-C$\underline{H}_3$, 9′-C$\underline{H}_3$).

^{13}C-NMR ($CDCl_3$, 151 MHz) δ 154.74 (C-2, C-2′), 138.45 (C-1, C-1′), 128.12 (C-3, C-3′), 127.64 (C-6, C-6′), 123.63 (C-5, C-5′), 112.62 (C-4, C-4′), 94.85 (C-7, C-7′), 55.83 (C-8, C-8′), 19.8 (C-9, C-9′).

IR: ν[cm^{-1}]: 2923, 1463, 1244, 1150, 1085, 1041, 983, 921, 777, 741.

MS (ESI): m/z = 271.0 $[M\text{-}CH_3OH+H]^+$

The analytical data correspond to the data given in literature.[305]

***rac*-2,2'-Dimethoxy-6,6'-bis(methoxymethoxy)-1,1'-biphenyl *rac*-(199b)**

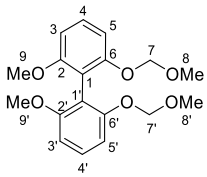

rac-**199b**

The homocoupling was performed according to general procedure D. After column chromatography (PE:EtOAc = 90:10) the coupling product *rac*-**199b** (28 mg, 80 µmol) was obtained from 2-bromo-1-methoxy-3-(methoxymethoxy)benzene (**193b**) (0.10 g, 0.42 mmol) in 40% yield as yellow crystals.

R_f (PE:EE, 70:30) = 0.33

^{1}H-NMR ($CDCl_3$, 600 MHz) δ 7.28 (t, $^3J_{4/4',3/3',5/5'}$ = 8.3 Hz, 2H, 4-H, 4′-H), 6.86 (dd, $^3J_{5/5',4/4'}$ = 8.3 Hz, $^5J_{5/5',7/7'}$ = 0.9 Hz, 2H, 5-H, 5′-H), 6.69 (dd, $^3J_{3/3',4/4'}$ = 8.3 Hz, $^5J_{3/3',9/9'}$ = 0.9 Hz, 2H, 3-H, 3′-H), 5.07 – 4.98 (m, 4H, 7-C$\underline{H}_2$-, 7′-C$\underline{H}_2$-), 3.72 (s, 6H, 9-OC$\underline{H}_3$, 9′-OC$\underline{H}_3$), 3.32 (s, 6H, 8-OC$\underline{H}_3$, 8′-OC$\underline{H}_3$).

^{13}C-NMR ($CDCl_3$, 151 MHz) δ 158.51 (C-2, C-2′), 156.19 (C-6, C-6′), 128.93 (C-4, C-4′), 114.16 (C-1, C-1′), 108.57 (C-5, C-5′), 105.35 (C-3, C-3′), 95.15 (C-7, C-7′), 56.10 (C-9, C-9′), 55.77 (C-8, C-8′).

IR: ν[cm^{-1}]: 2936, 1589, 1466, 1244, 1151, 1100, 1066, 1016, 996, 727.

MS (ESI): m/z = 302.9 $[M\text{-}CH_3OH+H]^+$

Mp: 79–86 °C

The analytical data correspond to the data given in literature.[306]

***rac*-2,2'-Bis(methoxymethoxy)-4,4',6,6'-tetramethyl-1,1'-biphenyl *rac*-(199c)**

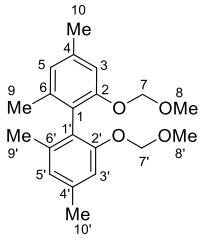

rac-**199c**

The homocoupling was performed according to general procedure D. After column chromatography (PE:EtOAc = 95:5) the coupling product *rac*-**199c** (35 mg, 0.11 mmol) was obtained from 2-bromo-1-(methoxymethoxy)-3,5-dimethylbenzene (**193c**) (0.10 g, 0.41 mmol) in 52% yield as light yellow oil.

R_f (PE:EE, 80:20) = 0.61

^{1}H-NMR ($CDCl_3$, 600 MHz) δ 6.86 (s, 2H, 3-H, 3′-H), 6.79 (s, 2H, 5-H, 5′-H), 5.06 – 4.93 (m, 4H, 7-C$\underline{H}_2$-, 7′-C$\underline{H}_2$-), 3.31 (s, 6H, 8-OC$\underline{H}_3$, 8′-OC$\underline{H}_3$), 2.35 (s, 6H, 10-C$\underline{H}_3$, 10′-C$\underline{H}_3$), 1.93 (s, 6H, 9-C$\underline{H}_3$, 9′-C$\underline{H}_3$).

^{13}C-NMR ($CDCl_3$, 151 MHz) δ 154.81 (C-2, C-2′), 138.20 (C-6, C-6′), 137.79 (C-4, C-4′), 124.59 (C-1, C-1′), 124.49 (C-5, C-5′), 113.46 (C-3, C-3′), 94.79 (C-7, C-7′), 55.81 (C-8, C-8′), 21.71 (C-10, C-10′), 19.85 (C-9, C-9′).

IR: ν[cm^{-1}]: 2918, 1444, 1315, 1149, 1100, 1045, 989, 927, 832.

HRMS (ESI): m/z = Found: 331.1896 ($C_{20}H_{27}O_4$) $[(M+H)]^+$, calculated: 331.1904.

***rac*-2,2',4,4'-Tetramethoxy-6,6'-bis(methoxymethoxy)-1,1'-biphenyl *rac*-(199d)**

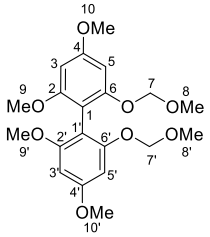

rac-**199d**

The homocoupling was performed according to general procedure E. After column chromatography (PE:EtOAc = 90:10 to 80:20) the coupling product *rac*-**199d** (35 mg, 90 µmol) was obtained from 2-bromo-1,5-dimethoxy-3-(methoxymethoxy)benzene (**193d**) (0.10 g, 0.36 mmol) in 50% yield as light orange oil.

R_f (PE:EE, 80:20) = 0.15

^{1}H-NMR ($CDCl_3$, 600 MHz) δ 6.46 (d, $^4J_{5/5',3/3'}$ = 2.3 Hz, 2H, 5-H, 5′-H), 6.27 (d, $^4J_{3/3',5/5'}$ = 2.3 Hz, 2H, 3-H, 3′-H), 5.05 – 4.96 (m, 4H, 7-C$\underline{H}_2$-, 7′-C$\underline{H}_2$-), 3.83 (s, 6H, 10-OC$\underline{H}_3$, 10′-OC$\underline{H}_3$), 3.70 (s, 6H, 9-OC$\underline{H}_3$, 9′-OC$\underline{H}_3$), 3.34 (s, 6H, 8-OC$\underline{H}_3$, 8′-OC$\underline{H}_3$).

^{13}C-NMR ($CDCl_3$, 151 MHz) δ 160.60 (C-4, C-4′), 159.21 (C-2, C-2′), 157.03 (C-6, C-6′), 106.51 (C-1, C-1′), 95.32 (C-7, C-7′), 94.51 (C-5, C-5′), 93.05 (C-3, C-3′), 56.04 (C-9, C-9′), 55.82 (C-8, C-8′), 55.41 (C-10, C-10′).

IR: ν[cm^{-1}]: 2934, 1598, 1473, 1206, 1150, 1113 1064, 1021, 925, 825.

HRMS (ESI): m/z = Found: 395.1712 ($C_{20}H_{27}O_8$) $[(M+H)]^+$, calculated: 395.1700.

***rac*-2,2'-Dimethoxy-4,4'-bis(methoxymethoxy)-6,6'-dimethyl-1,1'-biphenyl *rac*-(199e)**

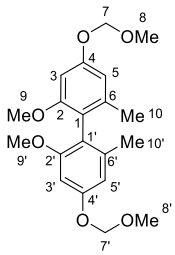

rac-**199e**

The homocoupling was performed according to general procedure E. After column chromatography (PE:EtOAc = 80:20) the coupling product *rac*-**199e** (0.87 g, 2.4 mmol) was obtained from 2-bromo-1-methoxy-5-(methoxymethoxy)-3-methylbenzene (**193e**) (2.00 g, 7.66 mmol) in 63% yield as yellow oil.

R_f (PE:EE, 80:20) = 0.41

^{1}H-NMR ($CDCl_3$, 600 MHz) δ 6.59 (d, $^4J_{5/5',3/3'}$ = 2.4 Hz, 2H, 5-H, 5′-H), 6.51 (d, $^4J_{3/3',5/5'}$ = 2.3 Hz, 2H, 3-H, 3′-H), 5.23 – 5.17 (m, 2H, 7-C$\underline{H}_2$-, 7′-C$\underline{H}_2$-), 3.68 (s, 6H, 9-OC$\underline{H}_3$, 9′-OC$\underline{H}_3$), 3.53 (s, 6H, 8-C$\underline{H}_3$, 8′-C$\underline{H}_3$), 1.92 (s, 6H, 10-C$\underline{H}_3$, 10′-C$\underline{H}_3$).

^{13}C-NMR ($CDCl_3$, 151 MHz) δ 158.21 (C-2, C-2′), 157.39 (C-4, C-4′), 139.44 (C-1, C-1′), 119.66 (C-6, C-6′), 109.08 (C-5, C-5′), 98.00 (C-3, C-3′), 94.78 (C-7, C-7′), 56.29 (C-9, C-9′), 55.94 (C-8, C-8′), 20.12 (C-10, C-10′).

IR: ν[cm^{-1}]: 2952, 1600, 1581, 1143, 1082, 1027, 998, 923, 831.

HRMS (ESI): m/z = Found: 363.1808 ($C_{20}H_{27}O_6$) $[(M+H)]^+$, calculated: 363.1802.

Ethyl 3-hydroxybenzoate (200)

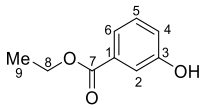

200

The product was synthesized according to general procedure C. Ethylbenzoate **200** (1.12 g, 6.74 mmol) was obtained from 3-hydroxybenzoate (1.00 g, 7.24 mmol) in 93% yield as white powder.

R_f (PE:EE, 80:20) = 0.54

^{1}H-NMR ($CDCl_3$, 600 MHz) δ 7.62 (dt, $^3J_{5,3,4}$ = 7.8, $^5J_{5,2}$ = 1.2 Hz, 1H, 5-H), 7.54 (dd, $^3J_{4,5}$ = 2.7 Hz, $^4J_{4,2}$ = 1.5 Hz, 1H, 4-H), 7.31 (t, $^4J_{2,4,6}$ = 2.9 Hz, 1H, 2-H), 7.04 (dd, $^3J_{6,5}$ = 8.1 Hz, $^4J_{6,2}$ = 2.7 Hz, 1H, 6-H), 5.19 (s, 1H, OH), 4.37 (q, $^3J_{8,9}$ = 7.1 Hz, 2H, 8-C$\underline{H}_2$-), 1.39 (t, $^3J_{9,8}$ = 7.1 Hz, 3H, 9-C$\underline{H}_3$).

^{13}C-NMR ($CDCl_3$, 151 MHz) δ 166.58 (C-7), 155.75 (C-1), 132.09 (C-3), 129.82 (C-2), 122.17 (C-5), 120.15 (C-6), 116.37 (C-4), 61.31 (C-8), 14.44 (C-9).

IR: ν[cm^{-1}]: 3296, 1675, 1597, 1448, 1304, 1237, 755, 676, 655.

MS (ESI): m/z = 166.9 $[M+H]^+$

Mp: 73–75 °C **Lit. Mp:** 70–72 °C[307]

The analytical data correspond to the data given in literature.[308]

1-Methoxy-3-(methoxymethoxy)benzene (201a)

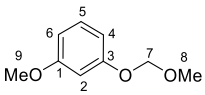

201a

The product was synthesized according to general procedure B. MOM-protected product **201a** (1.14 g, 6.75 mmol) was obtained from 3-methoxyphenol (1.00 g, 8.06 mmol) in 84% yield as light yellow oil.

R_f (PE:EE, 90:10) = 0.58

^{1}H-NMR ($CDCl_3$, 600 MHz) δ 7.19 (t, $^{4}J_{2,4,6}$ = 8.2 Hz, 1H, 2-H), 6.65 (ddd, $^{3}J_{4,5}$ = 8.2 Hz, $^{4}J_{4,6}$ = 2.3, $^{6}J_{4,2}$ = 0.9 Hz, 1H, 4-H), 6.61 (t, $^{3}J_{5,4,6}$ = 2.4 Hz, 1H, 5-H), 6.57 (ddd, $^{3}J_{6,5}$ = 8.2 Hz, $^{4}J_{6,4}$ = 2.3, $^{6}J_{6,2}$ = 0.9 Hz, 1H, 6-H), 5.17 (s, 2H, 7-C$\underline{H}_2$-), 3.79 (s, 3H, 9-C$\underline{H}_3$), 3.48 (s, 3H, 8-C$\underline{H}_3$).

^{13}C-NMR ($CDCl_3$, 151 MHz) δ 160.91 (C-1), 158.59 (C-3), 130.05 (C-2), 108.52 (C-4), 107.64 (C-6), 102.77 (C-5), 94.60 (C-7), 56.16 (C-8), 55.43 (C-9).

IR: ν[cm^{-1}]: 2955, 2835, 1591, 1490, 1142, 1007, 989, 922, 764, 687.

MS (ESI): m/z = 168.9 $[M+H]^+$

The analytical data correspond to the data given in literature.[298]

3-(Methoxymethoxy)benzonitrile (201b)

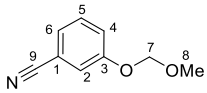

201b

The product was synthesized according to general procedure B. MOM-protected product **201b** (1.31 g, 8.03 mmol) was obtained from 3-hydroxybenzonitrile (1.00 g, 8.39 mmol) in 96% yield as light yellow oil.

R_f (PE:EE, 80:20) = 0.43

^{1}H-NMR ($CDCl_3$, 600 MHz) δ 7.38 (m, 1H, 2-H), 7.33 (dd, $^{3}J_{4,5}$ = 2.6 Hz, $^{4}J_{4,2}$ = 1.5 Hz, 1H, 4-H), 7.31 – 7.26 (m, 2H, 5-H, 6-H), 5.19 (s, 2H, 7-C$\underline{H}_2$-), 3.48 (s, 3H, 8-OC$\underline{H}_3$).

^{13}C-NMR ($CDCl_3$, 151 MHz) δ 157.52 (C-3), 130.50 (C-2), 125.72 (C-4), 121.33 (C-5, C-6), 119.71 (C-5, C-6), 118.74 (C-1), 113.44 (C-9), 94.62 (C-7), 56.38 (C-8).

IR: ν[cm^{-1}]: 2959, 2231, 1579, 1484, 1252, 1152, 1081, 1009, 987.

MS (ESI): m/z = 163.9 $[M+H]^+$.

The analytical data correspond to the data given in literature.[312]

1-Methoxy-3-(methoxymethoxy)-5-methylbenzene (201c)

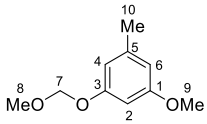

201c

The product was synthesized according to general procedure B. MOM-protected product **201c** (3.37 g, 18.5 mmol) was obtained from 3-methoxy-5-methylphenol (**168**) (3.00 g, 21.7 mmol) in 85% yield as colorless oil.

R_f (PE:EE, 80:20) = 0.65

^{1}H-NMR ($CDCl_3$, 600 MHz) δ 6.48 (m, 1H, 4-H), 6.42 (d, $^4J_{2,4,6}$ = 2.3 Hz, 1H, 2-H), 6.41 – 6.38 (m, 1H, 6-H), 5.15 (s, 2H, 7-C$\underline{H}_2$-), 3.77 (s, 3H, 9-C$\underline{H}_3$), 3.48 (s, 3H, 8-C$\underline{H}_3$), 2.30 (s, 3H, 10-C$\underline{H}_3$).

^{13}C-NMR ($CDCl_3$, 151 MHz) δ 160.75 (C-1), 158.42 (C-3), 140.43 (C-5), 109.33 (C-4), 108.57 (C-6), 99.82 (C-2), 94.56 (C-7), 56.13 (C-8), 55.38 (C-9), 21.91 (C-10).

IR: ν[cm^{-1}]: 2954, 1593, 1466, 1141, 1063, 1027, 991, 923, 832, 686.

MS (ESI): m/z = 150.0 $[M\text{-}CH_3OH+H]^+$.

The analytical data correspond to the data given in literature.[313]

(3,4,5-Trimethoxyphenoxy)methanol (201d)

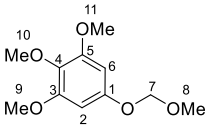

201d

The product was synthesized according to general procedure B. MOM-protected product **201d** (2.01 g, 8.81 mmol) was obtained from 3,4,5-trimethoxyphenol (**194**) (1.84 g, 9.97 mmol) in 88% yield as colorless oil.

R_f (PE:EE, 80:20) = 0.44

^{1}H-NMR ($CDCl_3$, 600 MHz) δ 6.31 (s, 2H, 2-H, 6-H), 5.14 (s, 2H, 7-C$\underline{H}_2$-), 3.84 (s, 6H, 9-OC$\underline{H}_3$, 11-OC$\underline{H}_3$), 3.79 (s, 3H, 10-OC$\underline{H}_3$), 3.50 (s, 3H, 8-OC$\underline{H}_3$).

^{13}C-NMR ($CDCl_3$, 151 MHz) δ 154.12 (C-1), 153.82 (C-3, C-5), 133.02 (C-4), 95.17 (C-7), 94.18 (C-2, C-6), 61.14 (C-10), 56.23 (C-9, C-11), 56.18 (C-8).

IR: ν[cm^{-1}]: 2939, 2827, 1592, 1504, 1462, 1418, 1226, 1144, 1125, 1009, 920.

HRMS (ESI): m/z = Found: 229.1076 ($C_{11}H_{17}O_5$) $[(M+H)]^+$, calculated: 229.1071.

Ethyl 3-(methoxymethoxy)benzoate (201e)

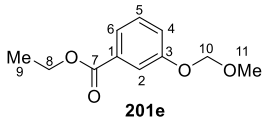

201e

The product was synthesized according to general procedure B. MOM-protected product **201e** (0.99 g, 4.7 mmol) was obtained from ethyl-3-hydroxybenzoate (**200**) (1.00 g, 6.02 mmol) in 78% yield as colorless oil.

R_f (PE:EE, 80:20) = 0.55

^{1}H-NMR ($CDCl_3$, 600 MHz) δ 7.69 (m, 2H, 5-H, 6-H), 7.35 (t, $^{4}J_{2,4,6}$ = 8.1 Hz, 1H, 2-H), 7.22 (m, 1H, 4-H), 5.22 (s, 2H, 10-C$\underline{H}_2$-), 4.37 (q, $^{3}J_{8,9}$ = 7.1 Hz, 2H, 8-C$\underline{H}_2$-), 3.49 (s, 3H, 11-C$\underline{H}_3$), 1.39 (t, $^{3}J_{9,8}$ = 7.1 Hz, 3H, 9-C$\underline{H}_3$).

^{13}C-NMR ($CDCl_3$, 151 MHz) δ 166.46 (C-7), 157.28 (C-3), 132.08 (C-1), 129.54 (C-2), 123.22 (C-5 or C-6), 121.05 (C-4), 117.23 (C-5 or C-6), 94.58 (C-10), 61.19 (C-8), 56.25 (C-11), 14.46 (C-9).

IR: ν[cm^{-1}]: 2930, 1717, 1271, 1152, 1102, 1076, 1007, 990, 755.

MS (ESI): m/z = 210.9 $[M+H]^+$.

The analytical data correspond to the data given in literature.[314]

1-(Methoxymethoxy)-3-(trifluoromethyl)benzene (201f)

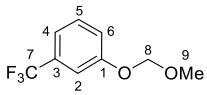

201f

The product was synthesized according to general procedure B. MOM-protected product **201f** (1.24 g, 6.03 mmol) was obtained from 3-(trifluoromethyl)phenol (1.00 g, 6.17 mmol) in 98% yield as light yellow oil.

R_f (PE:EE, 80:20) = 0.68

^{1}H-NMR ($CDCl_3$, 600 MHz) δ 7.39 (m, 1H, 2-H), 7.29 (t, $^4J_{4,2}$ = 2.0 Hz, 1H, 4-H), 7.27 – 7.24 (m, 1H, 5-H), 7.21 (dd, $^3J_{6,5}$ = 8.3 Hz, $^4J_{6,2}$ = 2.5 Hz, 1H, 6-H), 5.21 (s, 2H, 8-C$\underline{H}_2$-), 3.49 (s, 3H, 9-OC$\underline{H}_3$).

^{13}C-NMR ($CDCl_3$, 151 MHz) δ 157.54 (C-1), 131.94 (C-7), 130.12 (C-2), 123.13 (C-3), 119.68 (C-6), 118.66 (C-5), 113.44 (C-4), 94.64 (C-8), 56.30 (C-9).

^{19}F NMR ($CDCl_3$, 300 MHz) δ -63.68

IR: ν[cm^{-1}]: 2929, 1456, 1324, 1153, 1121, 1082, 1066, 1005, 991, 871, 790, 697.

MS (ESI): m/z = 174.9 $[M\text{-}CH_3OH+H]^+$.

The analytical data correspond to the data given in literature.[266]

5-(Methoxymethoxy)benzo[d][1,3]dioxole (201g)

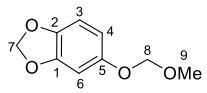

201g

The product was synthesized according to general procedure B. MOM-protected product **201g** (3.90 g, 21.4 mmol) was obtained from sesamol (3.00 g, 21.7 mmol) in 99% yield as colorless oil.

R_f (PE:EE, 80:20) = 0.74

^{1}H-NMR ($CDCl_3$, 600 MHz) δ 6.70 (d, $^{3}J_{3,4}$ = 8.4 Hz, 1H, 3-H), 6.62 (d, $^{4}J_{6,4}$ = 2.5 Hz, 1H, 6-H), 6.49 (dd, $^{3}J_{4,3}$ = 8.5 Hz, $^{4}J_{4,6}$ = 2.4 Hz, 1H, 4-H), 5.92 (s, 2H, 7-C$\underline{H}_2$-), 5.08 (s, 2H, 8-C$\underline{H}_2$-), 3.48 (s, 3H, 9-OC$\underline{H}_3$).

^{13}C-NMR ($CDCl_3$, 151 MHz) δ 152.68 (C-5), 148.27 (C-1), 142.70 (C-2), 108.62 (C-4), 108.19 (C-3), 101.35 (C-7), 99.91 (C-6), 95.67 (C-8), 56.06 (C-9).

IR: ν[cm^{-1}]: 2897, 1501, 1483, 1212, 1175, 1150, 1129, 1066, 1037, 998, 937, 920, 814.

MS (ESI): m/z = 151.0 $[M\text{-}CH_3OH+H]^+$.

The analytical data correspond to the data given in literature.[315]

6-(Methoxymethoxy)-2,3-dihydrobenzo[b][1,4]dioxine (201h)

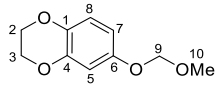

201h

The product was synthesized according to general procedure B. MOM-protected product **201h** (0.77 g, 3.9 mmol) was obtained from 2,3-dihydrobenzo[b][1,4]dioxin-6-ol (1.00 g, 6.57 mmol) in 60% yield as colorless oil.

R_f (PE:EE, 90:10) = 0.29

^{1}H-NMR ($CDCl_3$, 600 MHz) δ 6.77 (d, $^{3}J_{8,7}$ = 8.8 Hz, 1H, 8-H), 6.61 (d, $^{4}J_{5,7}$ = 2.8 Hz, 1H, 5-H), 6.54 (dd, $^{3}J_{7,8}$ = 8.8 Hz, $^{4}J_{7,5}$ = 2.8 Hz, 1H, 7-H), 5.08 (s, 2H, 9-C$\underline{H}_2$-), 4.26 – 4.22 (m, 2H, 3-C$\underline{H}_2$-), 4.22 – 4.19 (m, 2H, 2-C$\underline{H}_2$-), 3.47 (s, 3H, 10-OC$\underline{H}_3$).

^{13}C-NMR ($CDCl_3$, 151 MHz) δ 151.81 (C-6), 143.88 (C-4), 138.83 (C-1), 117.51 (C-8), 109.90 (C-7), 105.96 (C-5), 95.33 (C-9), 64.68 (C-3), 64.30 (C-2), 56.02 (C-10).

IR: ν[cm^{-1}]: 2933, 1596, 1500, 1301, 1240, 1196, 1148, 1065, 1000, 913, 885.

HRMS (ESI): m/z = Found: 197.0811 ($C_{10}H_{13}O_4$) $[(M+H)]^+$, calculated: 197.0808.

1-(Methoxymethoxy)-3,5-dimethylbenzene (201i)

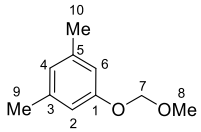

203k

The product was synthesized according to general procedure B. MOM-protected product **201i** (1.06 g, 6.38 mmol) was obtained from 3,5-dimethylphenol (1.00 g, 8.19 mmol) in 78% yield as light yellow oil.

R_f (PE:EE, 80:20) = 0.79

^{1}H-NMR ($CDCl_3$, 600 MHz) δ 6.67 (s, 2H, 2-H, 2-H, 6-H), 6.66 (s, 1H, 4-H), 5.15 (s, 2H, 7-C$\underline{H}_2$-), 3.48 (s, 3H, 8-OC$\underline{H}_3$), 2.29 (s, 6H, 9-C$\underline{H}_3$, 10-C$\underline{H}_3$).

^{13}C-NMR ($CDCl_3$, 151 MHz) δ 157.39 (C-1), 139.40 (C-3, C-5), 123.81 (C-4), 114.05 (C-2, C-6), 94.50 (C-7), 56.08 (C-8), 21.55 (C-9, C-10).

IR: ν[cm^{-1}]: 2921, 1596, 1292, 1146, 1084, 1036, 988, 924, 835, 689.

MS (ESI): m/z = 167.0 [M+H]+.

The analytical data correspond to the data given in literature.[316]

6,6'-Bis(methoxymethoxy)-5,5'-bibenzo[d][1,3]dioxole (203)

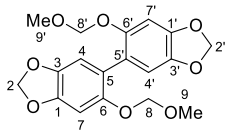

203

The homocoupling was performed according to general procedure F. After column chromatography (PE:EtOAc = 80:20) the coupling product **203** (30 mg, 80 µmol) was obtained from 5-(methoxymethoxy)benzo[d][1,3]dioxole (**201g**) (0.10 g, 0.55 mmol) in 30% yield as light yellow oil.

R_f (PE:EE, 70:30) = 0.36

^{1}H-NMR ($CDCl_3$, 600 MHz) δ 6.76 – 6.69 (m, 4H, 4-H, 4'-H, 7-H, 7'-H), 5.93 (dd, $^2J_{2a/2'a,2b/2'b}$ = 9.0, $^5J_{2/2',4/4',7/7'}$ =1.5 Hz, 4H, 2-CH_2-, 2'-CH_2-), 5.04 – 4.97 (m, 4H, 8-CH_2-, 8'-CH_2-), 3.35 (s, 6H, 9-CH_3, 9'-CH_3).

^{13}C-NMR ($CDCl_3$, 151 MHz) δ 150.73 (C-6, C-6′), 146.66 (C-1, C-1′), 142.66 (C-3, C-3′), 108.52 (C-4, C-4′), 107.78 (C-7, C-7′), 106.82 (C-5, C-5′), 101.54 (C-2, C-2′), 96.55 (C-8, C-8′), 55.97 (C-9, C-9′).

IR: ν[cm^{-1}]: 2897, 1438, 1399, 1235, 1152, 1085, 1041, 939, 918, 795.

HRMS (ESI): m/z = Found: 363.1076 ($C_{18}H_{19}O_8$) $[(M+H)]^+$, calculated: 363.1074.

***rac*-6,6'-Bis(methoxymethoxy)-[1,1'-biphenyl]-2,2'-dicarbonitrile *rac*-(207)**

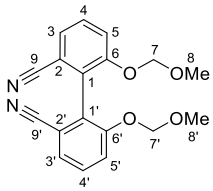

rac-**207**

The homocoupling was performed according to general procedure F. After column chromatography (PE:EtOAc = 80:20 to 70:30) the coupling product *rac*-**207** (63 mg, 0.19 mmol) was obtained from 3-(methoxymethoxy)benzonitrile (**201b**) (0.10 g, 0.61 mmol) in 64% yield as yellow solid.

R_f (PE:EE, 70:30) = 0.31

^{1}H-NMR ($CDCl_3$, 600 MHz) δ 7.56 (d, $^3J_{4/4',3/3',5/5'}$ = 8.4, 2H, 4-H, 4′-H), 7.48 (d, $^3J_{5/5',4/4'}$ = 8.4 Hz, 2H, 5-H, 5′-H), 7.44 (d, $^3J_{3/3',4/4'}$ = 7.7 Hz, 2H, 3-H, 3′-H), 5.23 – 5.08 (m, 4H, 7-C$\underline{H}_2$-, 7′-C$\underline{H}_2$-), 3.41 (s, 6H, 8-OC$\underline{H}_3$, 8′-OC$\underline{H}_3$).

^{13}C-NMR ($CDCl_3$, 151 MHz) δ 155.53 (C-6, C-6′), 130.78 (C-5, C-5′), 127.98 (C-2, C-2′), 126.12 (C-3, C-3′), 119.79 (C-4, C-4′), 117.53 (C-9, C-9′), 115.02 (C-1, C-1′), 95.32 (C-7, C-7′), 56.51 (C-8, C-8′).

IR: ν[cm^{-1}]: 2908, 2229, 1574, 1459, 1256, 1153, 1016, 997, 921, 795.

HRMS (ESI): m/z = Found: 299.1281 ($C_{17}H_{17}NO_4$) $[(M-CN+H)]^+$, calculated:299.1158.

Mp: 113–118 °C

***rac*-2,2'-Dimethoxy-6,6'-bis(methoxymethoxy)-4,4'-dimethyl-1,1'-biphenyl *rac*-(208)**

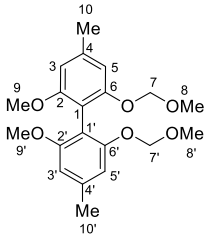

rac-**208**

The homocoupling was performed according to general procedure F. After column chromatography (PE:EtOAc = 90:10) the coupling product *rac*-**208** (37 mg, 0.10 mmol) was obtained from 1-methoxy-3-(methoxymethoxy)-5-methylbenzene (**201c**) (0.10 g, 0.55 mmol) in 37% yield as colorless oil.

R_f (PE:EE, 70:30) = 0.46

^{1}H-NMR ($CDCl_3$, 600 MHz) δ 6.69 (d, $^4J_{5/5',3/3'}$ = 1.4 Hz, 2H, 5-H, 5′-H), 6.51 (s, 2H, 3-H, 3′-H), 5.06 – 4.95 (m, 4H, 7-C$\underline{H}_2$-, 7′-C$\underline{H}_2$-), 3.70 (s, 6H, 9-OC$\underline{H}_3$, 9′-OC$\underline{H}_3$), 3.33 (s, 6H, 8-OC$\underline{H}_3$, 8′-OC$\underline{H}_3$), 2.38 (s, 6H, 10-C$\underline{H}_3$, 10′-C$\underline{H}_3$).

^{13}C-NMR ($CDCl_3$, 151 MHz) δ 158.26 (C-2, C-2′), 156.08 (C-6, C-6′), 138.94 (C-4, C-4′), 111.09 (C-1, C-1′), 109.42 (C-5, C-5′), 106.46 (C-3, C-3′), 95.10 (C-7, C-7′), 56.03 (C-9, C-9′), 55.75 (C-8, C-8′), 22.35 (C-10, C-10′).

IR: ν[cm^{-1}]: 2934, 1604, 1576, 1460, 1396, 1233, 1150, 1111, 1069, 1021, 998, 922, 814.

HRMS (ESI): m/z = Found: 363.1806 ($C_{20}H_{27}O_6$) $[(M+H)]^+$, calculated: 363.1802.

2,2'-Bis(methoxymethoxy)-4,4'-bis(trifluoromethyl)-1,1'-biphenyl (210)

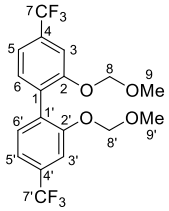

210

The homocoupling was performed according to general procedure F. After column chromatography (PE:EtOAc = 95:5 to 85:15) the coupling product **210** (55 mg, 0.13 mmol) was obtained from 1-(methoxymethoxy)-3-(trifluoromethyl)benzene (**201f**) (0.10 g, 0.49 mmol) in 55% yield as yellow oil.

R_f (PE:EE, 80:20) = 0.57

^{1}H-NMR ($CDCl_3$, 600 MHz) δ 7.50 – 7.47 (m, 2H, 3-H, 3′-H), 7.37 – 7.30 (m, 4H, 5-H, 5′-H, 6-H, 6′-H), 5.12 (s, 4H, 8-C$\underline{H}_2$-, 8′-C$\underline{H}_2$-), 3.37 (s, 6H, 9-OC$\underline{H}_3$, 9′-OC$\underline{H}_3$).

^{13}C-NMR ($CDCl_3$, 151 MHz) δ 155.15 (C-2, C-2′), 131.71 (C-4, C-4′), 131.69 (C-1, C-1′), 131.50 (C-6, C-6′), 124.94 (C-7, C-7′), 118.64 (C-5, C-5′), 112.21 (C-3, C-3′), 95.29 (C-8, C-8′), 56.28 (C-9, C-9′).

^{19}F NMR ($CDCl_3$, 300 MHz) δ -63.47

IR: ν[cm^{-1}]: 2960, 1427, 1391, 1324, 1157, 1118, 1081, 986, 874.

HRMS (ESI): m/z = Found: 428.1285 ($C_{18}H_{20}F_6NO_4$) $[(M+NH_4)]^+$, calculated: 428.1291.

***rac*-6,6'-Dimethyl-[1,1'-biphenyl]-2,2',4,4'-tetraol *rac*-(153)**

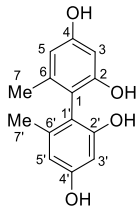

***rac*-153**

Biphenol *rac*-**1** (0.20 g, 0.73 mmol) was dissolved in anhydrous CH_2Cl_2 (30 mL). The mixture was then cooled down to −78 °C. A solution of boron tribromide (2.92 mL, 2.92 mmol,

1.0 M in CH_2Cl_2) was added dropwise. The mixture was stirred overnight in a warming cooling bath. The reaction was afterwards quenched by adding KP_i-buffer (pH = 7.4). The mixture was extracted three times with EtOAc and dried over $MgSO_4$. After concentrating the combined organic phase at reduced pressure, the crude product was purified *via* column chromatography (PE:EtOAc = 50:50) gave tetraol *rac*-**153** (0.15 g, 0.60 mmol) in 82% yield as light yellow oil.

R_f (PE:EE, 50:50) = 0.16

^{1}H-NMR ($CDCl_3$, 600 MHz) δ 6.28 (d, $^4J_{5/5',3/3'}$ = 2.4 Hz, 2H, 5-H, 5′-H), 6.23 (d, $^4J_{3/3',5/5'}$ = 2.3 Hz, 2H, 3-H, 3′-H), 1.87 (s, 6H 7-C$\underline{H}_3$, 7′-C$\underline{H}_3$).

^{13}C-NMR ($CDCl_3$, 151 MHz) δ 158.33 (C-4, C-4′), 157.00 (C-2, C-2′), 141.00 (C-6, C-6′), 115.93 (C-1, C-1′), 109.54 (C-5, C-5′), 101.07 (C-3, C-3′), 20.09 (C-7, C-7′).

IR: ν[cm^{-1}]: 3233, 2922, 1595, 1450, 1247, 1143, 1042, 989, 837, 593.

MS (ESI): m/z = 247.0 $[M+H]^+$.

Mp: 234–238 °C **Lit. Mp:** 238–239 °C[317]

The analytical data correspond to the data given in literature.[317]

***rac*-2,2'-Bis(benzyloxy)-4,4'-dimethoxy-6,6'-dimethyl-1,1'-biphenyl *rac*-(218)**

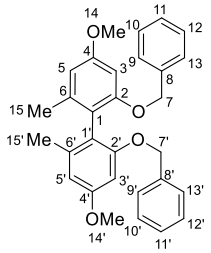

rac-**218**

Biphenol *rac*-**1** (0.20 g, 0.73 mmol), potassium carbonate (0.50 g, 3.7 mmol) and *tert*-butylammoniumiodide (27 mg, 70 µmol) was given in dry DMF (8 mL). The mixture was heated up to 50 °C. Benzylbromide (0.43 mL, 3.7 mmol) was added slowly over 2.5 hours with a syringe pump. After full conversion the reaction was quenched by adding water. The mixture was continuously stirred at 60 °C for 1 hour. After cooling down, the organic phase was extracted three times with EtOAc and dried over $MgSO_4$. After concentrating the

combined organic phase at reduced pressure, the residue was washed three times with ice to remove any residual DMF. Purification *via* column chromatography (PE:EtOAc = 90:10) gave the benzylated product *rac*-**218** (0.22 g, 0.48 mmol) in 66% yield as light yellow oil.

R_f (PE:EE, 80:20) = 0.46

^{1}H-NMR ($CDCl_3$, 600 MHz) δ 7.19 (qd, $^3J_{10/10',11/11',12/12'}$ = 5.0, $^4J_{11/11',9/9',13/13'}$ = 1.5 Hz, 6H, 10-H, 10'-H, 11-H, 11'-H, 12-H, 12'-H), 7.15 – 7.10 (m, 4H, 9-H, 9'-H, 13-H, 13'-H), 6.49 (d, $^4J_{5/5',3/3'}$ = 2.4 Hz, 2H, 5-H, 5'-H), 6.41 (d, $^4J_{3/3',5/5'}$ = 2.3 Hz, 2H, 3-H, 3'-H), 4.97 (d, $^4J_{7/7',9/9',13/13'}$ = 2.0 Hz, 4H, 7-CH_2-, 7'-CH_2-), 3.80 (s, 6H, 14-CH_3, 14'-CH_3), 2.00 (s, 6H, 15-CH_3, 15'-CH_3).

^{13}C-NMR ($CDCl_3$, 151 MHz) δ 159.46 (C-4, C-4'), 157.37 (C-2, C-2'), 139.57 (C-6, C-6'), 137.91 (C-8, C-8'), 128.37 (C-11, C-11'), 127.31 (C-10, C-10', C-12, C-12'), 126.53 (C-9, C-9', C-13, C-13'), 119.70 (C-1, C-1'), 107.03 (C-5, C-5'), 98.29 (C-3, C-3'), 70.23 (C-7, C-7'), 55.34 (C-14, C-14'), 20.32 (C-15, C-15').

IR: ν[cm^{-1}]: 2937. 1600, 1580, 1463, 1315, 1192, 1152, 1066, 1000, 733, 695.

HRMS (ESI): m/z = Found: 455.2220 ($C_{30}H_{31}O_4$) $[(M+H)]^+$, calculated: 455.2217.

***rac*-2,2'-(2,2'-Bis(methoxymethoxy)-6,6'-dimethyl-[1,1'-biphenyl]-4,4'-diyl)bis(4,4,5,5-tetramethyl-1,3,2-dioxaborolane) *rac*-(220)**

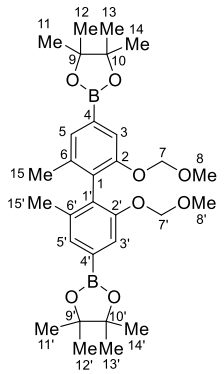

rac-**220**

R_f (PE:EE, 80:20) = 0.34

^{1}H-NMR ($CDCl_3$, 600 MHz) δ 7.41 (d, $^{4}J_{3/,3',5/5'}$ = 6.2 Hz, 4H, 3-H, 3′-H, 5-H, 5′-H), 5.11 – 4.99 (m, 4H, 7-C$\underline{H}_2$-, 7′-C$\underline{H}_2$-), 3.26 (s, 6H, 8-OC$\underline{H}_3$, 8′-OC$\underline{H}_3$), 1.94 (s, 6H, 15-C$\underline{H}_3$, 15′-C$\underline{H}_3$), 1.35 (s, 24H, 11-C$\underline{H}_3$, 11′-C$\underline{H}_3$, 12-C$\underline{H}_3$, 12′-C$\underline{H}_3$, 13-C$\underline{H}_3$, 13′-C$\underline{H}_3$, 14-C$\underline{H}_3$, 14′-C$\underline{H}_3$).

^{13}C-NMR ($CDCl_3$, 151 MHz) δ 154.13 (C-2, C-2′), 137.72 (C-1, C-1′), 131.06 (C-6, C-6′), 130.09 (C-5, C-5′), 117.85 (C-3, C-3′), 94.64 (C-7, C-7′), 83.92 (C-9, C-9′, C-10, C-10′), 56.01 (C-8, C-8′), 25.08 (C-11, C-11′, C-12, C-12′, C-13, C-13′, C-14, C-14′), 19.58 (C-15, C-15′).

IR: ν[cm^{-1}]: 2977, 1391, 1356, 1241, 1144, 1047, 967, 851.

HRMS (ESI): m/z = Found: 572.3574 ($C_{30}H_{48}B_2NO_8$) $[(M+NH_4)]^+$, calculated: 572.3561.

Mp: 168–170 °C

***rac*-2-(2,2'-Bis(methoxymethoxy)-6,6'-dimethyl-[1,1'-biphenyl]-4-yl)-4,4,5,5-tetramethyl-1,3,2-dioxaborolane *rac*-(221)**

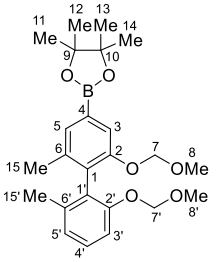

rac-**221**

R_f (PE:EE, 90:10) = 0.43

^{1}H-NMR ($CDCl_3$, 600 MHz) δ 7.42 (d, $^{4}J_{3,5}$ = 2.7 Hz, 2H, 3-H, 5-H), 7.21 (t, $^{3}J_{3',4'}$ = 7.9 Hz, 1H, 3′-H), 7.03 (d, $^{3}J_{4',3',5'}$ = 8.3 Hz, 1H, 4′-H), 6.95 (d, $^{3}J_{5',4'}$ = 7.6 Hz, 1H, 5′-H), 5.08 (d, $^{2}J_{7'a,7'b}$ = 6.5 Hz, 1H, 7′-C$\underline{H}_2$-), 5.05 – 5.01 (m, 2H, 7-C$\underline{H}_2$-), 4.97 (d, $^{2}J_{7'a,7'b}$ = 6.8 Hz, 1H, 7′-C$\underline{H}_2$-), 3.29 (s, 3H, 8-C$\underline{H}_3$), 3.26 (s, 3H, 8′-C$\underline{H}_3$), 1.97 (s, 3H, 15-C$\underline{H}_3$), 1.94 (s, 3H, 15′-C$\underline{H}_3$), 1.36 (s, 12H, 11-C$\underline{H}_3$, 12-C$\underline{H}_3$, 13-C$\underline{H}_3$, 14-C$\underline{H}_3$).

^{13}C-NMR ($CDCl_3$, 151 MHz) δ 154.59 (C-2), 154.29 (C-2′), 138.23 (C-1′), 137.96 (C-1), 131.18 (C-6), 130.17 (C-5), 128.14 (C-3′), 127.54 (C-6′), 123.56 (C-5′), 118.14 (C-3),

112.39 (C-4′), 94.84 (C-7′), 94.70 (C-7), 83.93 (C-9, C-10), 55.97 (C-8′), 55.86 (C-8), 25.08 (C-11, C-12, C-13, C-14), 19.82 (C-15′), 19.62 (C-15).

IR: ν[cm^{-1}]: 2926, 1361, 1244, 1151, 1047, 989, 968, 853.

HRMS (ESI): m/z = Found: 446.2719 ($C_{24}H_{37}BNO_6$) $[(M+NH_4)]^+$, calculated: 446.2708.

***rac*-4,4'-Dibromo-2,2'-bis(methoxymethoxy)-6,6'-dimethyl-1,1'-biphenyl *rac*-(222)**

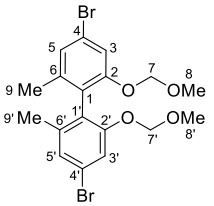

rac-**222**

To a solution of borylated biaryl *rac*-**220** (80 mg, 0.14 mmol) dissolved in methanol (10 mL) an aqueous solution of copper bromide (0.19 g, 0.87 mmol) in water (10 mL) was added. The mixture was stirred for 16 hours at 70 °C. After cooling the mixture to r.t, EtOAc was added for dilution. The reaction was quenched with aqueous 0.1 mM EDTA solution. The organic phase was extracted with EtOAc three times and washed with aqueous 0.1 mM EDTA solution and brine. The combined organic phases were dried over $MgSO_4$ and concentrated under reduced pressure. After purification *via* column chromatography (PE:EtOAc = 95:5 to 90:10), the brominated product *rac*-**222** (55 mg, 0.12 mmol) could be obtained in 86% yield as white solid.

R_f (PE:EE, 90:10) = 0.44

^{1}H-NMR ($CDCl_3$, 600 MHz) δ 7.22 – 7.19 (m, 2H, 3-H, 3′-H), 7.12 (d, $^4J_{5/5',3/3'}$ = 2.1 Hz, 2H, 5-H, 5′-H), 5.02 – 4.97 (m, 4H, 7-C$\underline{H}_2$-, 7′-C$\underline{H}_2$-), 3.31 (s, 6H, 8-C$\underline{H}_3$, 8′-C$\underline{H}_3$), 1.92 (s, 6H, 9-C$\underline{H}_3$, 9′-C$\underline{H}_3$).

^{13}C-NMR ($CDCl_3$, 151 MHz) δ 155.28 (C-2, C-2′), 139.98 (C-1, C-1′), 126.56 (C-5, C-5′), 125.48 (C-6, C-6′), 121.55 (C-4, C-4′), 115.87 (C-3, C-3′), 94.76 (C-7, C-7′), 56.03 (C-8, C-8′), 19.59 (C-9, C-9′).

IR: ν[cm^{-1}]: 2954, 1570, 1390, 1252, 1154, 1046, 990, 927, 818

HRMS (ESI): m/z = Found: 476.0064 ($C_{18}H_{24}BrNO_4$) $[(M+NH_4)]^+$, calculated: 476.0067.

***rac*-6,6'-Dimethyl-[1,1'-biphenyl]-2,2'-diol *rac*-(223a)**

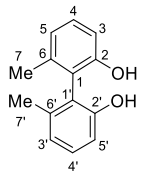

rac-**223a**

The deprotection was performed according to general procedure G. After column chromatography (PE:EtOAc = 80:20) the biphenol *rac*-**223a** (0.33 g, 1.5 mmol) was obtained from 2,2'-bis(methoxymethoxy)-6,6'-dimethyl-1,1'-biphenyl *rac*-(**199a**) (0.70 g, 2.3 mmol) in 66% yield as light yellow crystals.

R_f (PE:EE, 70:30) = 0.37

^{1}H7-NMR ($CDCl_3$, 600 MHz) δ 7.07 (t, $^3J_{3/3',4/4'}$ = 7.8 Hz, 2H, 3-H, 3′-H), 6.79 (d, $^3J_{5/5',4/4'}$ = 7.5 Hz, 2H, 5-H, 5′-H), 6.72 (d, $^3J_{4/4',3/3',5/5'}$ = 8.1 Hz, 2H, 4-H, 4′-H), 1.93 (s, 6H, 7-C$\underline{H}_3$, 7'-C$\underline{H}_3$).

^{13}C-NMR ($CDCl_3$, 151 MHz) δ 155.70 (C-2, C-2′), 139.59 (C-1, C-1′), 129.14(C-6, C-6′), 125.14 (C-3, C-3′), 122.25 (C-5, C-5′), 113.83 (C-4, C-4′), 19.87 (C-7, C-7′).

IR: ν[cm^{-1}]: 3462, 3409, 1574, 1463, 1281,1259, 1175, 1162, 792, 782.

MS (ESI): m/z = 215.1 $[M+H]^+$.

HPLC: Column: Lux Amylose-1, *Fa. Phenomenex* (250x4.6 mm); 3 µL, 25 °C, 1.0 mL/min, 210 nm; solvent: *n*-heptane:2-propanol (90:10), t_R = 14.9, 28.1 min.

The analytical data correspond to the data given in literature.[318]

***rac*-6,6'-Dimethoxy-[1,1'-biphenyl]-2,2'-diol *rac*-(223b)**

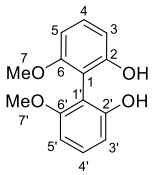

rac-**223b**

The deprotection was performed according to general procedure G. After column chromatography (PE:EtOAc = 90:10 to 80:20) the biphenol *rac*-**223b** (0.22 g, 0.91 mmol) was obtained from 2,2'-dimethoxy-6,6'-bis(methoxymethoxy)-1,1'-biphenyl *rac*-(**199b**) (0.42 g, 1.2 mmol) in 73% yield as white solid.

R_f (PE:EE, 80:20) = 0.22

^{1}H-NMR ($CDCl_3$, 600 MHz) δ 7.31 (t, $^3J_{4/4',3/3',5/5'}$ = 8.3 Hz, 2H, 4-H, 4′-H), 6.72 (dd, $^3J_{3/3',4/4'}$ = 8.2 Hz, $^4J_{3,8}$ = 1.0 Hz, 2H, 3-H, 3′-H), 6.62 (dd, $^3J_{5/5',4/4'}$ = 8.3 Hz, $^5J_{5/5',7/7'}$ = 1.0 Hz, 2H, 5-H, 5′-H), 5.04 (s, 2H, OH), 3.77 (s, 6H, 7-OC$\underline{H}_3$, 7′-OC$\underline{H}_3$).

^{13}C-NMR ($CDCl_3$, 151 MHz) δ 158.09 (C-6, C-6′), 155.49 (C-2, C-2′), 130.78 (C-4, C-4′), 109.40 (C-1, C-1′), 107.08 (C-3, C-3′), 103.69 (C-5, C-5′), 56.22 (C-7, C-7′).

IR: ν[cm^{-1}]: 3412, 1578, 1462, 1436, 1251, 1198, 1171, 1073, 780, 727.

MS (ESI): m/z = 247.0 $[M+H]^+$.

Mp: 146–150 °C **Lit. Mp:** 144–146 °C[306]

HPLC: Column: Lux Amylose-1, *Fa. Phenomenex* (250x4.6 mm); 5µL, 25 °C, 1.0 mL/min, 205 nm; solvent: *n*-heptane:2-propanol (80:20), t_R = 16.1, 26.6 min.

The analytical data correspond to the data given in literature.[306]

***rac*-6,6'-Dihydroxy-[1,1'-biphenyl]-2,2'-dicarbonitrile *rac*-(223c)**

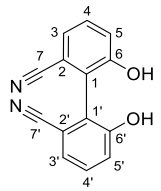

rac-**223c**

MOM-protected biphenol *rac*-**207** (0.16 g, 0.49 mmol) was dissolved in dioxane (8 mL) and 4 M aq. HCl solution (0.49 mL, 2.0 mmol) was added. The reaction mixture was stirred at 60 °C for 4 hours. After full conversion, the mixture was cooled down and quenched by adding 0.1 M KP_i-buffer solution. The organic phase was extracted with CH_2Cl_2 three times. The combined organic phases were dried over $MgSO_4$ and concentrated at reduced pressure. The residue was purified *via* column chromatography (PE:EtOAc = 45:55), giving the free biphenol *rac*-**223c** (95 mg, 0.40 mmol) in 82% yield as white powder.

R_f (PE:EE, 50:50) = 0.36

^{1}H-NMR (CH_3OD, 600 MHz) δ 7.41 (t, $^3J_{5/5',4/4'}$ = 8.0 Hz, 2H, 5-H, 5′-H), 7.30 (d, $^3J_{3/3',4/4'}$ = 7.7 Hz, 2H, 3-H, 3′-H), 7.22 (d, $^3J_{4/4',3/3',5/5'}$ = 8.3 Hz, 2H, 4-H, 4′-H).

^{13}C-NMR (CH_3OD, 151 MHz) δ 157.33 (C-6, C-6′), 131.45 (C-5, C-5′), 126.94 (C-3, C-3′), 124.78 (C-4, C-4′), 121.63 (C-7, C-7′), 118.76 (C-2, C-2′), 115.72 (C-1, C-1′).

IR: ν[cm^{-1}]: 3257, 2246, 1577, 1455, 1291, 1261, 960, 796, 727, 685.

HRMS (ESI): m/z = Found: 237.0661 ($C_{14}H_9N_2O_2$) $[(M+H)]^+$, calculated: 237.0659.

Mp: 138–142 °C

HPLC: Column: Lux Amylose-1, *Fa. Phenomenex* (250x4.6 mm); 5 µL, 25 °C, 0.3 mL/min, 205 nm; solvent: *n*-heptane:2-propanol (80:20), t_R = 5.6, 5.9 min.

***rac*-4,4'-Dibromo-6,6'-dimethyl-[1,1'-biphenyl]-2,2'-diol *rac*-(223d)**

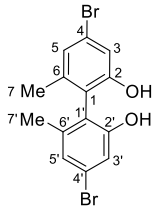

rac-**223d**

The deprotection was performed according to general procedure G without any further purifications. The biphenol *rac*-**223d** (38 mg, 0.10 mmol) was obtained from 4,4'-dibromo-2,2'-bis(methoxymethoxy)-6,6'-dimethyl-1,1'-biphenyl *rac*-(**222**) (49 mg, 0.11 mmol) in 91% yield as white solid.

R_f (PE:EE, 90:10) = 0.13

^{1}H-NMR ($CDCl_3$, 600 MHz) δ 7.10 (d, $^4J_{5/5',3/3'}$ = 1.9 Hz, 2H, 5-H, 5′-H), 7.08 (d, $^4J_{3/3',5/5'}$ = 1.9 Hz, 2H, 3-H, 3′-H), 1.98 (s, 6H, 7-C$\underline{H}_3$, 7′-C$\underline{H}_3$).

^{13}C-NMR ($CDCl_3$, 151 MHz) δ 154.56 (C-2, C-2′), 140.80 (C-1, C-1′), 126.05 (C-5, C-5′), 123.89 (C-4, C-4′), 118.10 (C-6, C-6′), 117.06 (C-3, C-3′), 19.44 (C-7, C-7′).

IR: ν[cm^{-1}]: 3503, 1592, 1570, 1406, 1280, 1162, 1037, 1004, 829.

HRMS (ESI): m/z = Found: 370.3546 ($C_{14}H_{13}Br_2O_2$) $[(M+H)]^+$, calculated: 370.9277.

Mp: 102–106 °C

HPLC: Column: Chiralpak IB, *Fa. Daicel* (250x4.6 mm); 5 µL, 25 °C, 0.5 mL/min, 205 nm; solvent: *n*-heptane:2-propanol (95:5), t_R = 25.4, 35.3 min.

***rac*-4,4',6,6'-Tetramethyl-[1,1'-biphenyl]-2,2'-diol *rac*-(223e)**

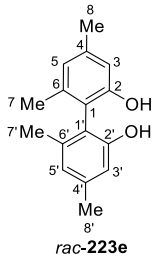

rac-**223e**

The deprotection was performed according to general procedure G. After purification by column chromatography (PE/EtOAc = 90:10), biphenol *rac*-**223e** (74 mg, 0.30 mmol) was obtained from 4,4',6,6'-tetramethyl-[1,1'-biphenyl]-2,2'-diol *rac*-(**199c**) (98 mg, 0.30 mmol) in 99% yield as yellow solid.

R_f (PE:EE, 80:20) = 0.38

^{1}H-NMR ($CDCl_3$, 600 MHz) δ 6.75 (d, $^4J_{5/5',3/3'}$ = 1.8 Hz, 2H, 5-H, 5′-H), 6.72 (d, $^4J_{3/3',5/5'}$ = 1.6 Hz, 2H, 3-H, 3′-H), 4.64 (s, 2H, OH), 2.33 (s, 6H, 8-C$\underline{H}_3$, 8′-C$\underline{H}_3$), 1.97 (s, 6H, 7-C$\underline{H}_3$, 7′-C$\underline{H}_3$).

^{13}C-NMR ($CDCl_3$, 151 MHz) δ 153.99 (C-2, C-2′), 140.36 (C-4, C-4′), 138.90 (C-6, C-6′), 123.69 (C-5, C-5′), 116.55 (C-1, C-1′), 113.78 (C-3, C-3′), 21.50 (C-8, C-8′), 19.60 (C-7, C-7′).

IR: ν[cm^{-1}]: 3477, 1618, 1565, 1305, 1305, 1183, 1043, 839.

MS (ESI): m/z = 243.0 [M+H]+.

Mp: 170–172 °C **Lit. Mp:** 170 °C[319]

HPLC: Column: Lux Amylose-1, *Fa. Phenomenex* (250x4.6 mm); 5 µL, 25 °C, 0.2 mL/min for 20 min then 1.0 mL/min, 205 nm; solvent: *n*-heptane:2-propanol (85:15), t_R = 36.3, 62.7 min.

The analytical data correspond to the data given in literature.[320]

***rac*-6,6'-Dimethoxy-4,4'-dimethyl-[1,1'-biphenyl]-2,2'-diol *rac*-(223f)**

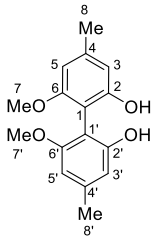

rac-**223f**

The deprotection was performed according to general procedure G without any further purifications. The biphenol *rac*-**223f** (20 mg, 70 µmol) was obtained from 2,2'-dimethoxy-6,6'-bis(methoxymethoxy)-4,4'-dimethyl-1,1'-biphenyl *rac*-(**208**) (27 mg, 80 µmol) in 88% yield as yellow crystals.

R_f (PE:EE, 80:20) = 0.23

^{1}H-NMR ($CDCl_3$, 600 MHz) δ 6.57 – 6.53 (m, 2H, 5-H, 5′-H), 6.43 (d, $^4J_{3/3',5/5'}$ = 1.4 Hz, 2H, 3-H, 3′-H), 5.01 (s, 2H, OH), 3.75 (s, 6H, 7-OC$\underline{H}_3$, 7′-OC$\underline{H}_3$), 2.36 (s, 6H, 8-C$\underline{H}_3$, 8′-C$\underline{H}_3$).

^{13}C-NMR ($CDCl_3$, 151 MHz) δ 157.87 (C-6, C-6′), 155.27 (C-2, C-2′), 141.13 (C-4, C-4′), 109.97 (C-3, C-3′), 104.81 (C-5, C-5′), 104.08 (C-1, C-1′), 56.14 (C-7, C-7′), 22.10 (C-8, C-8′).

IR: ν[cm^{-1}]: 3477, 2923, 2855, 1616, 1576, 1464, 1199, 1098, 816.

MS (ESI): m/z = 275.1 $[M+H]^+$.

Mp: 181–187 °C **Lit. Mp:** 182–189 °C[115]

HPLC: Column: Lux Amylose-1, *Fa. Phenomenex* (250x4.6 mm); 2 µL, 25 °C, 0.5 mL/min, 210 nm; solvent: *n*-heptane:2-propanol (55:45), t_R = 19.1, 38.3 min.

***rac*-4,4',6,6'-Tetramethoxy-[1,1'-biphenyl]-2,2'-diol *rac*-(223g)**

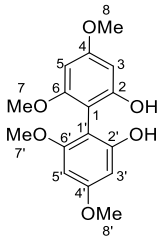

rac-**223g**

The deprotection was performed according to general procedure G without any further purification. Biphenol *rac*-**223g** (0.23 g, 0.74 mmol) was obtained from 4,4',6,6'-tetramethoxy-[1,1'-biphenyl]-2,2'-diol *rac*-(**199d**) (0.30 g, 0.77 mmol) in 97% yield as yellow solid.

R_f (PE:EE, 50:50) = 0.44

^{1}H-NMR ($CDCl_3$, 600 MHz) δ 6.28 (d, $^4J_{5/5',3/3'}$ = 2.3 Hz, 2H, 5-H, 5′-H), 6.20 (d, $^4J_{3/3',5/5'}$ = 2.4 Hz, 2H, 3-H, 3′-H), 5.09 (s, 2H, OH), 3.82 (s, 6H, 7-OC$\underline{H}_3$, 7′-OC$\underline{H}_3$), 3.73 (s, 6H, 8-OC$\underline{H}_3$, 8′-OC$\underline{H}_3$).

^{13}C-NMR ($CDCl_3$, 151 MHz) δ 162.21 (C-6, C-6′), 159.14 (C-4, C-4′), 156.57 (C-2, C-2′), 98.78 (C-1, C-1′), 93.64 (C-5, C-5′), 92.22 (C-3, C-3′), 56.13 (C-8, C-8′), 55.54 (C-7, C-7′).

IR: ν[cm^{-1}]: 3455, 1613, 1583, 1456, 1207, 1150, 1096.

MS (ESI): m/z = 307.2 $[M+H]^+$.

Mp: 152–154 °C **Lit. Mp:** 165–166 °C[113]

HPLC: Column: Lux Amylose-1, *Fa. Phenomenex* (250x4.6 mm); 5 µL, 25 °C, 1.0 mL/min, 205 nm; solvent: *n*-heptane:2-propanol (80:20), t_R = 31.6. 77.8 min.

The analytical data correspond to the data given in literature.[113]

***rac*-2,2'-Dimethoxy-6,6'-dimethyl-[1,1'-biphenyl]-4,4'-diol *rac*-(223h)**

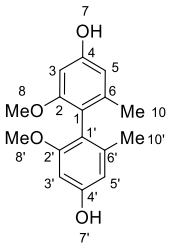

rac-**223h**

The deprotection was performed according to general procedure G. After column chromatography (PE:EtOAc = 60:40) the biphenol *rac*-**223h** (0.53 g, 1.9 mmol) was obtained from 2,2'-dimethoxy-4,4'-bis(methoxymethoxy)-6,6'-dimethyl-1,1'-biphenyl *rac*-(**199e**) (0.71 g, 2.0 mmol) in 99% yield as orange needles.

R_f (PE:EE, 60:40) = 0.38

^{1}H-NMR (CH_3OD, 600 MHz) δ 6.32 (d, $^4J_{5/5',3/3'}$ = 2.2 Hz, 2H, 5-H, 5′-H), 6.30 (d, $^4J_{3/3',5/5'}$ = 2.3 Hz, 2H, 3-H, 3′-H), 3.60 (s, 6H, 8-OC$\underline{H}_3$, 8′-OC$\underline{H}_3$), 1.81 (s, 6H, 10-C$\underline{H}_3$, 10′-C$\underline{H}_3$).

^{13}C-NMR (CH_3OD, 151 MHz) δ 159.56 (C-2, C-2′), 158.12 (C-4, C-4′), 140.26 (C-1, C-1′), 118.81 (C-6, C-6′), 109.63 (C-5, C-5′), 97.70 (C-3, C-3′), 55.89 (C-8, C-8′), 19.98 (C-10, C-10′).

IR: ν[cm^{-1}]: 3368, 2924, 1589, 1462, 1323, 1154, 1090, 1015, 833.

MS (ESI): m/z = 275.1 $[M+H]^+$.

Mp: 202 °C **Lit. Mp:** 200–202 °C[186]

The analytical data correspond to the data given in literature.[186]

***rac*-6,6'-Dimethyl-[1,1'-biphenyl]-2,2'-diyl dipropionate *rac*-(224a)**

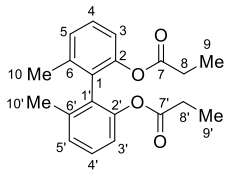

rac-**224a**

The product was synthesized according to general procedure I. After purification *via* column chromatography (PE:EtOAc = 90:10), the dipropionate *rac*-**224a** (0.23 g, 0.70 mmol) was obtained from 6,6'-dimethyl-[1,1'-biphenyl]-2,2'-diol *rac*-(**223a**) (0.18 g, 0.84 mmol) in 83% yield as colorless oil.

R_f (PE:EE, 90:10) = 0.44

^{1}H-NMR (CH_3OD, 600 MHz) δ 7.31 (t, $^3J_{5/5',4/4'}$ = 7.9 Hz, 2H, 5-H, 5′-H), 7.18 (d, $^3J_{4/4',3/3',5/5'}$ = 7.6 Hz, 2H, 4-H, 4′-H), 7.00 (d, $^3J_{3/3',4/4'}$ = 8.0 Hz, 2H, 3-H, 3′-H), 2.21 – 2.08 (m, $^3J_{8/8',9/9'}$ = 8.0 Hz, 4H, 8-C$\underline{H}_2$-, 8′-C$\underline{H}_2$-), 2.01 (s, 6H, 10-C$\underline{H}_3$, 10′-C$\underline{H}_3$), 0.84 (t, $^3J_{9/9',8/8'}$ = 7.6 Hz, 6H, 9-C$\underline{H}_3$, 9′-C$\underline{H}_3$).

^{13}C-NMR (CH_3OD, 151 MHz) δ 174.08 (C-7, C-7′), 149.98 (C-1, C-1′), 140.06 (C-6, C-6′), 130.25 (C-2, C-2′), 129.41 (C-5, C-5′), 128.33 (C-4, C-4′), 121.09 (C-3, C-3′), 28.22 (C-8, C-8′), 19.52 (C-10, C-10′), 9.10 (C-9, C-9′).

IR: ν[cm^{-1}]: 2982, 1757, 1458, 1227, 1188, 1135, 1061, 749.

HRMS (ESI): m/z = Found: 327.1596 ($C_{20}H_{23}O_4$) $[(M+H)]^+$, calculated: 327.1591.

HPLC: Column: Lux Amylose-1, *Fa. Phenomenex* (250x4.6 mm); 5 µL, 25 °C, 1 mL/min, 210 nm; solvent: *n*-heptane:2-propanol (90:10), t_R = 3.8, 3.9 min.

***rac*-2'-Hydroxy-6,6'-dimethyl-[1,1'-biphenyl]-2-yl propionate *rac*-(225a)**

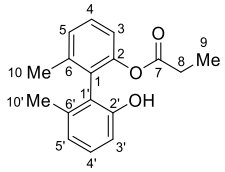

rac-**225a**

The product was synthesized according to general procedure J. After purification *via* column chromatography (PE:EtOAc = 95:5), the monoester *rac*-**225a** (0.10 g, 0.37 mmol) was obtained from 6,6'-dimethyl-[1,1'-biphenyl]-2,2'-diol *rac*-(**223a**) (0.10 g, 0.47 mmol) in 81% yield as colorless oil.

R_f (PE:EE, 90:10) = 0.25

^{1}H-NMR (CH_3OD, 600 MHz) δ 7.31 (t, $^3J_{3,4}$ = 7.8 Hz, 1H, 3-H), 7.22 (d, $^3J_{5,4}$ = 7.6 Hz, 1H, 5-H), 7.10 (t, $^3J_{3',4'}$ = 7.8 Hz, 1H, 3′-H), 7.00 (d, $^3J_{4,3,5}$ = 8.1 Hz, 1H, 4-H), 6.78 (d, $^3J_{5',4'}$ = 7.5 Hz, 1H, 5′-H), 6.72 (d, $^3J_{4',3',5'}$ = 8.1 Hz, 1H, 4′-H), 2.16 (qd, $^3J_{8,9}$ = 7.7, 2.0 Hz, 2H, 8-C$\underline{H}_2$-), 2.06 (s, 3H, 10-C$\underline{H}_3$), 1.92 (s, 3H, 10′-C$\underline{H}_3$), 0.84 (t, $^3J_{9,8}$ = 7.6 Hz, 3H, 9-C$\underline{H}_3$).

^{13}C-NMR (CH_3OD, 151 MHz) δ 173.09 (C-7), 154.28 (C-2′), 149.05 (C-2), 138.93 (C-1), 137.85 (C-1′), 130.38 (C-6), 128.16 (C-3′), 127.64 (C-3), 126.98 (C-5), 122.81 (C-6′), 120.73 (C-5′), 119.50 (C-4), 112.44 (C-4′), 26.90 (C-8), 18.36 (C-10′), 18.28 (C-10), 7.79 (C-9).

IR: ν[cm^{-1}]: 3484, 2980, 1749, 1578, 1459, 1225, 1148, 1062, 778, 744.

HRMS (ESI): m/z = Found: 271.1330 ($C_{17}H_{19}O_3$) $[(M+H)]^+$, calculated: 271.1329.

HPLC: Column: Lux Amylose-1, *Fa. Phenomenex* (250x4.6 mm); 5 µL, 25 °C, 1 mL/min, 210 nm; solvent: *n*-heptane:2-propanol (90:10), t_R = 5.4, 6.0 min.

***rac*-6,6'-Dimethoxy-[1,1'-biphenyl]-2,2'-diyl dipropionate *rac*-(224b)**

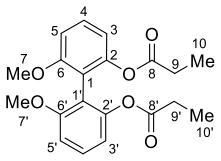

rac-**224b**

Dipropionate *rac*-**224b** and monopropionate *rac*-**225b** were synthesized according to general procedure H, starting from 6,6'-dimethoxy-[1,1'-biphenyl]-2,2'-diol *rac*-(**223b**) (50 mg, 0.20 mmol). After purification *via* column chromatography (PE:EtOAc = 80:20 to 70:30), dipropionate *rac*-**224b** (34 mg, 90 µmol) was obtained in 47% yield as white solid and monopropionate *rac*-**225b** (30 mg, 0.10 mmol) in 50% yield as colorless oil.

R_f (PE:EE, 80:20) = 0.4

^{1}H-NMR ($CDCl_3$, 600 MHz) δ 7.34 (t, $^3J_{4/4',3/3',5/5'}$ = 8.3 Hz, 2H, 4-H, 4′-H), 6.83 (dq, $^3J_{3/3',4/4'}$ = 8.2 Hz, $^4J_{3/3',5/5'}$ = 1.0 Hz, 4H, 3-H, 3′-H, 5-H, 5′-H), 3.74 (s, 6H, 7-OC$\underline{H}_3$, 7′-OC$\underline{H}_3$), 2.24 (qd, $^2J_{9a/9'a,9b/9'b}$ = 7.6 Hz, $^3J_{9/9',10/10'}$ = 2.4 Hz, 4H, 9-C$\underline{H}_2$-, 9′-C$\underline{H}_2$-), 0.96 (t, $^3J_{10/10',9/9'}$ = 7.6 Hz, 6H, 10-C$\underline{H}_3$, 10′-C$\underline{H}_3$).

^{13}C-NMR ($CDCl_3$, 151 MHz) δ 172.35 (C-8, C-8′), 158.56 (C-6, C-6′), 149.68 (C-2, C-2′), 129.05 (C-4, C-4′), 115.82 (C-3, C-3′ or C-5, C-5′), 115.09 (C-1, C-1′), 108.28 (C-3, C-3′ or C-5, C-5′), 56.25 (C-7, C-7′), 27.70 (C-9, C-9′), 8.99 (C-10, C-10′).

IR: ν[cm^{-1}]: 2924, 1751, 1469, 1436, 1264, 1139, 1087, 1070, 783, 744, 726.

HRMS (ESI): m/z = Found: 359.1493 ($C_{20}H_{23}O_6$) $[(M+H)]^+$, calculated: 359.1489.

Mp: 85–88 °C

HPLC: Column: Lux Amylose-1, *Fa. Phenomenex* (250x4.6 mm); 5µL, 25 °C, 1.0 mL/min, 205 nm; solvent: *n*-heptane:2-propanol (80:20), t_R = 5.1, 9.1 min.

***rac*-2'-Hydroxy-6,6'-dimethoxy-[1,1'-biphenyl]-2-yl propionate *rac*-(225b)**

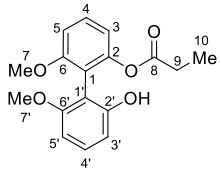

rac-**225b**

R_f (PE:EE, 80:20) = 0.25

^{1}H-NMR ($CDCl_3$, 600 MHz) δ 7.42 (t, $^3J_{5',4'}$ = 8.3 Hz, 1H, 5′-H), 7.23 (t, $^3J_{5,4}$ = 8.2 Hz, 1H, 5-H), 6.95 – 6.91 (m, 1H, 3′-H), 6.83 (t, $^3J_{4',3',5'}$ = 8.2 Hz, 1H, 4′-H), 6.65 (t, $^3J_{4,3,5}$ = 8.3, 1H, 4-H), 6.56 – 6.52 (m, 1H, 3-H), 4.97 (s, 1H, OH), 3.78 (s, 3H, 7′-OC$\underline{H}_3$), 3.70 (s, 3H, 7-OC$\underline{H}_3$), 2.30 – 2.16 (m, 2H, 9-C$\underline{H}_2$-), 0.91 (t, $^3J_{10,9}$ = 7.6 Hz, 3H, 10-C$\underline{H}_3$).

^{13}C-NMR ($CDCl_3$, 151 MHz) δ 173.37 (C-8), 158.79 (C-6′), 158.12 (C-6), 154.77 (C-2′), 150.93 (C-2), 130.34 (C-1′) 130.21 (C-5′), 129.88 (C-5), 115.30 (C-4′), 115.12 (C-1′) 109.29 (C-4), 109.17 (C-3′), 103.26 (C-3), 56.42 (C-7′), 56.11 (C-7), 27.65 (C-9), 9.04 (C-10).

IR: ν[cm^{-1}]: 3456, 2941, 1748, 1600, 1463, 1435, 1252, 1069, 725.

HRMS (ESI): m/z = Found: 303.1230 ($C_{17}H_{19}O_5$) $[(M+H)]^+$, calculated: 303.1227.

HPLC: Column: Lux Amylose-1, *Fa. Phenomenex* (250x4.6 mm); 5µL, 25 °C, 1.0 mL/min, 205 nm; solvent: *n*-heptane:2-propanol (80:20), t_R = 10.2, 12.9 min.

***rac*-6,6'-Dicyano-[1,1'-biphenyl]-2,2'-diyl dipropionate *rac*-(224c)**

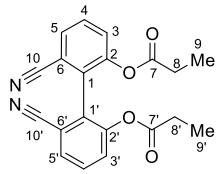

rac-**224c**

Dipropionate *rac*-**224c** and monopropionate *rac*-**225c** were synthesized according to general procedure H, starting from 6,6'-dihydroxy-[1,1'-biphenyl]-2,2'-dicarbonitrile *rac*-(**223c**) (60 mg, 0.25 mmol). After purification *via* column chromatography

(PE:EtOAc = 60:40 to 0:100), dipropionate *rac*-**224c** (50 mg, 0.14 mmol) was obtained from in 56% yield as white solid and monopropionate *rac*-**225c** (19 mg, 70 µmol) in 26% yield as white solid.

R_f (PE:EE, 50:50) = 0.58

^{1}H-NMR ($CDCl_3$, 600 MHz) δ 7.71 (d, $^3J_{5/5',4/4'}$ = 7.7 Hz, 2H, 5-H, 5′-H), 7.61 (d, $^3J_{4/4',3/3',5/5'}$ = 7.7 Hz, 2H, 4-H, 4′-H), 7.55 (d, $^3J_{3/3',4/4'}$ = 8.4 Hz, 2H, 3-H, 3′-H), 2.37 – 2.23 (m, 4H, 8-C$\underline{H}_2$-, 8′-C$\underline{H}_2$-), 0.98 (t, $^3J_{9/9',8/8'}$ = 7.5 Hz, 6H, 9-C$\underline{H}_3$, 9′-C$\underline{H}_3$).

^{13}C-NMR ($CDCl_3$, 151 MHz) δ 171.67 (C-7, C-7′), 149.07 (C-2, C-2′), 130.90 (C-5, C-5′), 130.42 (C-4, C-4′), 130.23 (C-1, C-1′), 128.11 (C-3, C-3′), 116.33 (C-6, C-6′), 115.27 (C-10, C-10′), 27.47 (C-8, C-8′), 8.74 (C-9, C-9′).

IR: ν[cm^{-1}]: 2235, 1766, 1453, 1235, 1122, 1078, 869, 804, 736.

HRMS (ESI): m/z = Found: 349.1186 ($C_{20}H_{17}N_2O_4$) $[(M+NH_4)]^+$, calculated: 348.1183.

Mp: 117–120 °C

HPLC: Column: Lux Amylose-1, *Fa. Phenomenex* (250x4.6 mm); 5 µL, 25 °C, 0.3 mL/min, 205 nm; solvent: *n*-heptane:2-propanol (80:20), t_R = 9.8, 11.0 min.

***rac*-2',6-Dicyano-6'-hydroxy-[1,1'-biphenyl]-2-yl propionate *rac*-(225c)**

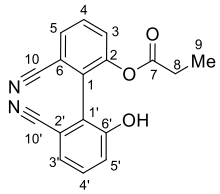

rac-**225c**

R_f (PE:EE, 50:50) = 0.37

^{1}H-NMR ($CDCl_3$, 600 MHz) δ 7.78 (d, $^3J_{4,5,3}$ = 7.6 Hz, 1H, 4-H), 7.67 (t, $^3J_{5',4'}$ = 8.0 Hz, 1H, 5′-H), 7.62 (d, $^3J_{3,4}$ = 8.3 Hz, 1H, 3-H), 7.47 (t, $^3J_{5,4}$ = 8.0 Hz, 1H, 5-H), 7.34 (d, $^3J_{3',4'}$ = 7.6 Hz, 1H, 3'-H), 7.23 (d, $^3J_{4',3',5'}$ = 8.4 Hz, 1H, 4′-H), 2.30 (qd, $^2J_{8a,8b}$ = 7.7 Hz, $^3J_{8,9}$ = 6.0 Hz, 2H, 8-C$\underline{H}_2$-), 0.94 (t, $^3J_{9,8}$ = 7.6 Hz, 3H, 9-C$\underline{H}_3$).

^{13}C-NMR ($CDCl_3$, 151 MHz) δ 172.97 (C-7), 157.35 (C-2), 150.92 (C-6′), 133.33 (C-2), 132.31 (C-5), 131.56 (C-5′), 131.43 (C-4), 129.14 (C-3), 124.92 (C-3′), 121.66 (C-4′), 118.18 (C-10′), 117.84 (C-1′), 116.24 (C-1), 115.47 (C-10), 28.21 (C-8), 9.12 (C-9).

IR: ν[cm^{-1}]: 3231, 2255, 1755, 1465, 1448, 1304, 1186, 1165, 989,795, 739.

HRMS (ESI): m/z = Found: 293.0921. ($C_{17}H_{13}N_2O_3$) $[(M+NH_4)]^+$, calculated: 293.0921.

Mp: 241–248 °C

HPLC: Column: Lux Amylose-1, *Fa. Phenomenex* (250x4.6 mm); 5 µL, 25 °C, 0.3 mL/min, 205 nm; solvent: *n*-heptane:2-propanol (80:20), t_R = 7.2, 8.9 min.

***rac*-4,4'-Dibromo-6,6'-dimethyl-[1,1'-biphenyl]-2,2'-diyl dipropionate *rac*-(224d)**

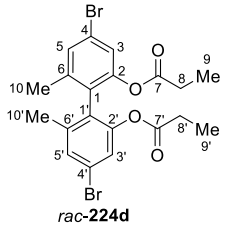

rac-**224d**

Dipropionate *rac*-**224d** and monopropionate *rac*-**225d** were synthesized according to general procedure H, starting from 4,4'-dibromo-6,6'-dimethyl-[1,1'-biphenyl]-2,2'-diol *rac*-(**223d**) (28 mg, 70 µmol). After purification *via* column chromatography (PE:EtOAc = 95:5) the dipropionate *rac*-**224d** (27 mg, 51 µmol) was obtained in 66% yield as colorless oil and monopropionate *rac*-**225d** (7 mg, 17 µmol) in 24% yield as colorless oil.

R_f (PE:EE, 90:10) = 0.57

^{1}H-NMR ($CDCl_3$, 600 MHz) δ 7.32 (d, $^4J_{5/5',3/3'}$ = 2.0 Hz, 2H, 5-H, 5′-H), 7.19 (d, $^4J_{3/3',5/5'}$ = 2.0 Hz, 2H, 3-H, 3′-H), 2.20 (qd, $^2J_{8a/8'a,8b/8'b}$ = 7.5 Hz, $^3J_{8/8',9/9'}$ = 4.0 Hz, 4H, 8-C$\underline{H}_2$-, 8′-C$\underline{H}_2$-), 2.00 (s, 6H, 10-C$\underline{H}_3$, 10′-C$\underline{H}_3$), 0.92 (t, $^3J_{9/9',8/8'}$ = 7.6 Hz, 6H, 9-C$\underline{H}_3$, 9′-C$\underline{H}_3$).

^{13}C-NMR ($CDCl_3$, 151 MHz) δ 172.23 (C-7, C-7′), 149.01 (C-2, C-2′), 140.61 (C-6, C-6′), 130.37 (C-5, C-5′), 127.35 (C-4, C-4′), 123.61 (C-3, C-3′), 121.53 (C-1, C-1′), 27.50 (C-8, C-8′), 19.35 (C-10, C-10′), 8.88 (C-9, C-9′).

IR: ν[cm^{-1}]: 2925, 1764, 1589, 1460, 1183, 1130, 1080, 827.

HRMS (ESI): m/z = Found: 482.9805 ($C_{20}H_{21}Br_2O_4$) $[(M+H)]^+$, calculated: 482.9801.

HPLC: Column: Lux Amylose-1, *Fa. Phenomenex* (250x4.6 mm); 5 µL, 25 °C, 1.0 mL/min, 205 nm; solvent: *n*-heptane:2-propanol (98:2), t_R = 4.1, 4.6 min.

***rac*-4,4'-Dibromo-2'-hydroxy-6,6'-dimethyl-[1,1'-biphenyl]-2-yl propionate *rac*-(225d)**

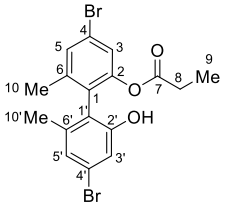

rac-**225d**

R_f (PE:EE, 90:10) = 0.30

^{1}H-NMR ($CDCl_3$, 600 MHz) δ 7.44 – 7.40 (m, 1H, 5-H), 7.19 (d, $^4J_{3,5}$ = 2.0 Hz, 1H, 3-H), 7.02 (s, 2H, 3′-H, 5′-H), 2.23 (dt, $^2J_{8a,8b}$ = 27.2 Hz, $^3J_{8,9}$ = 8.0 Hz, 2H, 8-C$\underline{H}_2$-), 2.01 (s, 3H, 10-C$\underline{H}_3$), 1.90 (s, 3H, 10′-C$\underline{H}_3$), 0.91 (t, $^3J_{9,8}$ = 7.6 Hz, 3H, 9-C$\underline{H}_3$).

^{13}C-NMR ($CDCl_3$, 151 MHz) δ 173.85 (C-7), 154.03 (C-2′), 150.03 (C-2), 141.75 (C-1), 139.51 (C-1′), 131.54 (C-5), 127.07 (C-6), 125.47 (C-3′), 123.80 (C-3), 122.84 (C-4′), 122.64 (C-4), 121.35 (C-6′), 117.85 (C-5′), 27.47 (C-8), 19.54 (C-10′), 19.43 (C-10), 8.99 (C-9).

IR: ν[cm^{-1}]: 3444, 1756, 1590, 1460, 1410, 1251, 1142, 1081, 1004, 825.

HRMS (ESI): m/z = Found: 426.9542 ($C_{17}H_{17}Br_2O_3$) $[(M+H)]^+$, calculated: 426.9539.

HPLC: Column: Lux Amylose-1, *Fa. Phenomenex* (250x4.6 mm); 5 µL, 25 °C, 1.0 mL/min, 205 nm; solvent: *n*-heptane:2-propanol (98:2), t_R = 19.6, 44.1 min.

rac-4,4',6,6'-Tetramethyl-[1,1'-biphenyl]-2,2'-diyl dipropionate _rac_-(224e)

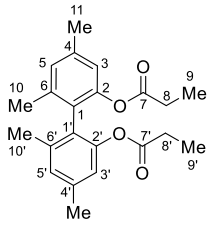

rac-**224e**

The product was synthesized according to general procedure I without any further purifications. The dipropionate _rac_-**248e** (28 mg, 80 µmol) was obtained from 4,4',6,6'-tetramethyl-[1,1'-biphenyl]-2,2'-diol _rac_-(**223e**) (30 mg, 0.12 mmol) in 67% yield as light yellow oil.

R_f (PE:EE, 80:20) = 0.65

^{1}H-NMR ($CDCl_3$, 600 MHz) δ 6.95 (d, $^4J_{5/5',3/3'}$ = 1.7 Hz, 2H, 5-H, 5′-H), 6.81 – 6.78 (m, 2H, 3-H, 3′-H), 2.34 (s, 6H, 11-C$\underline{H}_3$, 11′-C$\underline{H}_3$), 2.17 (qd, $^2J_{8a/8'a,8b/8'b}$ = 7.6 Hz, $^3J_{8/8',9/9'}$ = 6.7 Hz, 4H, 8-C$\underline{H}_2$-, 8′-C$\underline{H}_2$-), 1.98 (s, 6H, 10-C$\underline{H}_3$, 10′-C$\underline{H}_3$), 0.88 (t, $^3J_{9/9',8/8'}$ = 7.6 Hz, 6H, 9-C$\underline{H}_3$, 9′-C$\underline{H}_3$).

^{13}C-NMR ($CDCl_3$, 151 MHz) δ 172.88 (C-7, C-7′), 148.72 (C-2, C-2′), 138.79 (C-6, C-6′), 138.19 (C-4, C-4′), 128.20 (C-5, C-5′), 126.00 (C-1, C-1′), 120.42 (C-3, C-3′), 27.67 (C-8, C-8′), 21.29 (C-11, C-11′), 19.46 (C-10, C-10′), 8.99 (C-9, C-9′).

IR: ν[cm^{-1}]: 2924, 1758, 1714, 1355, 1139, 1082, 529.

HRMS (ESI): m/z = Found: 355.1911 ($C_{22}H_{27}O_4$) $[(M+H)]^+$, calculated: 355.1904.

HPLC: Column: Lux Amylose-1, *Fa. Phenomenex* (250x4.6 mm); 5 µL, 25 °C, 0.2 mL/min for 20 min then 1.0 mL/min, 205 nm; solvent: *n*-heptane:2-propanol (85:15), t_R = 17.0, 18.1 min.

rac-2'-Hydroxy-4,4',6,6'-tetramethyl-[1,1'-biphenyl]-2-yl propionate _rac_-(225e)

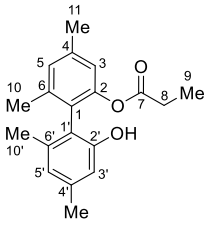

rac-**225e**

The product was synthesized according to general procedure J. After purification *via* column chromatography (PE:EtOAc = 95:5), the monoester _rac_-**225e** (4 mg, 0,01 mmol) was obtained from 4,4',6,6'-tetramethyl-[1,1'-biphenyl]-2,2'-diol _rac_-(**223e**) (40 mg, 0.16 mmol) in 9% yield as light yellow oil.

R_f (PE:EE, 90:10) = 0.28

^{1}H-NMR ($CDCl_3$, 600 MHz) δ 7.05 (d, $^4J_{5,3}$ = 1.8 Hz, 1H, 5-H), 6.82 – 6.79 (m, 1H, 3-H), 6.65 (s, 2H, 3′-H, 5′-H), 2.37 (s, 3H, 11-C$\underline{H}_3$), 2.29 (s, 3H, 11′-C$\underline{H}_3$), 2.25 – 2.13 (m, 2H, 8-C$\underline{H}_2$-), 2.00 (s, 3H, 10-C$\underline{H}_3$), 1.89 (s, 3H, 10′-C$\underline{H}_3$), 0.86 (t, $^3J_{9,8}$ = 7.6 Hz, 3H, 9-C$\underline{H}_3$).

^{13}C-NMR ($CDCl_3$, 151 MHz) δ 174.17 (C-7), 153.21 (C-2′), 149.79 (C-2), 139.97 (C-1), 139.67 (C-4), 138.98 (C-4′), 137.59 (C-1′), 129.17 (C-5), 125.37 (C-6), 123.04 (C-3′), 120.69 (C-3), 119.90 (C-6′), 114.40 (C-5′), 27.61 (C-8), 21.39 (C-11′), 21.29 (C-11), 19.70 (C-10), 19.56 (C-10′), 9.03 (C-9).

IR: ν[cm^{-1}]: 3499, 2921, 1749, 1618, 1459, 1301, 1266, 1154, 1082, 839.

HRMS (ESI): m/z = Found: 299.1645 ($C_{19}H_{23}O_3$) $[(M+H)]^+$, calculated: 299.1642.

HPLC: Column: Lux Amylose-1, *Fa. Phenomenex* (250x4.6 mm); 5 µL, 25 °C, 0.2 mL/min for 20 min then 1.0 mL/min, 205 nm; solvent: *n*-heptane:2-propanol (85:15), t_R = 21.4, 23.7 min.

Mp: 92–95 °C

***rac*-6,6'-Dimethoxy-4,4'-dimethyl-[1,1'-biphenyl]-2,2'-diyl dipropionate *rac*-(224f)**

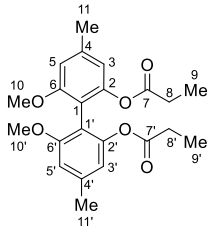

rac-**224f**

Dipropionate *rac*-**224f** and monopropionate *rac*-**225f** were synthesized according to general procedure H, starting from 6,6'-dimethoxy-4,4'-dimethyl-[1,1'-biphenyl]-2,2'-diol *rac*-(**223f**) (15 mg, 50 µmol). After purification *via* column chromatography (PE:EtOAc = 95:5) dipropionate *rac*-**224f** (11 mg, 29 µmol) was obtained in 57% yield as yellow oil and monopropionate *rac*-**225f** (5 mg, 14 µmol) in 28% yield as white solid.

R_f (PE:EE, 80:20) = 0.33

^{1}H-NMR ($CDCl_3$, 600 MHz) δ 6.63 (d, $^4J_{3/3',5/5'}$ = 4.3 Hz, 4H, 3-H, 5-H, 3′-H, 5′-H), 3.71 (s, 6H, 10-C$\underline{H}_3$, 10′-C$\underline{H}_3$), 2.38 (s, 6H, 11-C$\underline{H}_3$, 11′-C$\underline{H}_3$), 2.25 (qd, $^2J_{8a/8'a,8b/8'b}$ = 7.6 Hz, $^3J_{8/8',9/9'}$ = 3.6 Hz, 4H, 8-C$\underline{H}_2$-, 8′-C$\underline{H}_2$-), 0.99 (t, $^3J_{9/9',8/8'}$ = 7.6 Hz, 6H, 9-C$\underline{H}_3$, 9′-C$\underline{H}_3$).

^{13}C-NMR ($CDCl_3$, 151 MHz) δ 172.50 (C-7, C-7′), 158.28 (C-6, C-6′), 149.49 (C-2, C-2′), 139.20 (C-4, C-4′), 115.70 (C-3, C-3′), 112.78 (C-1, C-1′), 109.35 (C-5, C-5′), 56.12 (C-10, C-10′), 27.71 (C-8, C-8′), 21.99 (C-11, C-11′), 9.05 (C-9, C-9′).

IR: ν[cm^{-1}]: 2924, 1758, 1612, 1460, 1222, 1138, 1082, 823.

HRMS (ESI): m/z = Found: 378.1789 ($C_{22}H_{27}O_6$) $[(M+H)]^+$, calculated: 378.1802.

HPLC: Column: Lux Amylose-1, *Fa. Phenomenex* (250x4.6 mm); 2 µL, 25 °C, 0.5 mL/min, 210 nm; solvent: *n*-heptane:2-propanol (55:45), t_R = 7.4, 8.8 min.

***rac*-2'-Hydroxy-6,6'-dimethoxy-4,4'-dimethyl-[1,1'-biphenyl]-2-yl propionate *rac*-(225f)**

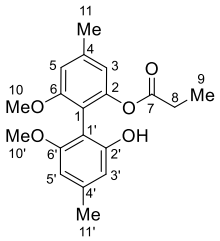

rac-**229f**

R_f (PE:EE, 80:20) = 0.27

^{1}H-NMR ($CDCl_3$, 600 MHz) δ 6.74 – 6.71 (m, 1H, 5′-H), 6.65 (dd, $^4J_{3',5'}$ = 1.5 Hz, $^4J_{3',11'}$ = 0.8 Hz, 1H, 3′-H), 6.47 (dd, $^4J_{3,5}$ = 1.5 Hz, $^4J_{3,11}$ = 0.8 Hz, 1H, 3-H), 6.35 (d, $^4J_{5,3}$ = 1.5 Hz, 1H. 5-H), 3.76 (s, 3H, 10′-OC$\underline{H}_3$), 3.68 (s, 3H, 10-OC$\underline{H}_3$), 2.41 (s, 3H, 11′-C$\underline{H}_3$), 2.33 (s, 3H, 11-C$\underline{H}_3$), 2.23 (qd, $^2J_{8a,8b}$ = 7.6 Hz, $^3J_{8,9}$ = 5.2 Hz, 2H, 8-C$\underline{H}_2$-), 0.94 (t, $^3J_{9,8}$ = 7.6 Hz, 3H, 9-C$\underline{H}_3$).

^{13}C-NMR ($CDCl_3$, 151 MHz) δ 173.41 (C-7), 158.51 (C-6′), 157.93 (C-6), 154.50 (C-2), 150.72 (C-2′), 140.57 (C-4′), 140.01 (C-4), 116.00 (C-5′), 111.95 (C-1′), 110.19 (C-3′), 109.75 (C-3), 106.30 (C-1), 104.35 (C-5), 56.34 (C-10′), 56.02 (C-10), 27.67 (C-8), 22.05 (C-11), 21.99 (C-11′), 9.06 (C-9).

IR: ν[cm^{-1}]: 3542, 2939, 1755, 1613, 1462, 1199, 1149, 1094.

HRMS (ESI): m/z = Found: 331.1543 ($C_{19}H_{23}O_5$) $[(M+H)]^+$, calculated: 331.1540.

HPLC: Column: Lux Amylose-1, *Fa. Phenomenex* (250x4.6 mm); 2 µL, 25 °C, 0.5 mL/min, 210 nm; solvent: *n*-heptane:2-propanol (55:45), t_R = 12.9, 15.8 min.

***rac*-4,4',6,6'-Tetramethoxy-[1,1'-biphenyl]-2,2'-diyl dipropionate *rac*-(224g)**

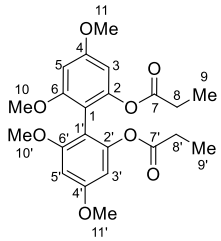

rac-**224g**

The product was synthesized according to general procedure I without any further purifications. The dipropionate *rac*-**224g** (29 mg, 70 µmol) was obtained from 4,4',6,6'-tetramethoxy-[1,1'-biphenyl]-2,2'-diol *rac*-(**223g**) (27 mg, 90 µmol) in 77% yield as white solid.

R_f (PE:EE, 60:40) = 0.37

^{1}H-NMR ($CDCl_3$, 600 MHz) δ 6.40 (d, $^4J_{5/5',3/3'}$ = 2.3 Hz, 2H, 5-H, 5′-H), 6.36 (d, $^4J_{3/3',5/5'}$ = 2.4 Hz, 2H, 3-H, 3′-H), 3.81 (s, 6H, 11-OC$\underline{H}_3$, 11′-OC$\underline{H}_3$), 3.70 (s, 6H, 10-OC$\underline{H}_3$, 10′-OC$\underline{H}_3$), 2.27 (qd, $^2J_{8a/8'a,8b/8'b}$ = 7.8 Hz, $^3J_{8/8',9/9'}$ = 3.7 Hz, 4H, 8-C$\underline{H}_2$-, 8′-C$\underline{H}_2$-), 1.00 (t, $^3J_{9/9',8/8'}$ = 7.6 Hz, 6H, 9-C$\underline{H}_3$, 9′-C$\underline{H}_3$).

^{13}C-NMR ($CDCl_3$, 151 MHz) δ 172.22 (C-7, C-7′), 160.21 (C-4, C-4′), 159.08 (C-6, C-6′), 150.32 (C-2, C-2′), 108.07 (C-1, C-1′), 99.55 (C-3, C-3′), 96.43 (C-5, C-5′), 55.95 (C-10, C-10′), 55.45 (C-11, C-11′), 27.58 (C-8, C-8′), 8.92 (C-9, C-9′).

IR: ν[cm^{-1}]: 2999, 1753, 1583, 1455, 1217, 1145, 1089, 1071, 1061, 932, 819.

HRMS (ESI): m/z = Found: 419.1698 ($C_{22}H_{27}O_8$) $[(M+H)]^+$, calculated: 419.1700.

Mp: 94–96 °C

HPLC: Column: Lux Amylose-1, *Fa. Phenomenex* (250x4.6 mm); 5 µL, 25 °C, 1.0 mL/min, 205 nm; solvent: *n*-heptane:2-propanol (80:20), t_R = 6.2, 7.1 min.

rac-2'-Hydroxy-4,4',6,6'-tetramethoxy-[1,1'-biphenyl]-2-yl propionate _rac_-(225g)

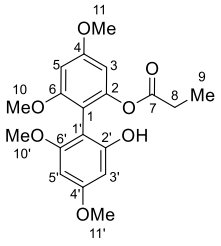

rac-**225g**

The product was synthesized according to general procedure J. After purification *via* column chromatography (PE:EtOAc = 80:20), the monoester _rac_-**225g** (88 mg, 0.24 mmol) was obtained from 4,4',6,6'-tetramethoxy-[1,1'-biphenyl]-2,2'-diol _rac_-(**223g**) (0.10 g, 0.33 mmol) in 73% yield as white solid.

R_f (PE:EE, 50:50) = 0.40

^{1}H-NMR ($CDCl_3$, 600 MHz) δ 6.48 (d, $^4J_{5,3}$ = 2.4 Hz, 1H, 5-H), 6.37 (d, $^4J_{3,5}$ = 2.3 Hz, 1H, 3-H), 6.21 (d, $^4J_{3',5'}$ = 2.3 Hz, 1H, 3′-H), 6.12 (d, $^4J_{5',3'}$ = 2.3 Hz, 1H, 5′-H), 5.05 (s, 1H, OH), 3.83 (s, 3H, 11-OC$\underline{H}_3$), 3.80 (s, 3H, 11′-OC$\underline{H}_3$), 3.75 (s, 3H, 10-OC$\underline{H}_3$), 3.68 (s, 3H, 10′-OC$\underline{H}_3$), 2.25 (qd, $^2J_{8a,8b}$ = 7.6 Hz, $^3J_{8,9}$ = 6.2 Hz, 2H, 8-C$\underline{H}_2$-), 0.96 (t, $^3J_{9,8}$ = 7.6 Hz, 3H, 9-C$\underline{H}_3$).

^{13}C-NMR ($CDCl_3$, 151 MHz) δ 173.32 (C-7), 161.42 (C-4′), 161.41 (C-4) 159.62 (C-6), 159.00 (C-6′), 155.67 (C-2′), 151.93 (C-2), 107.00 (C-1), 101.53 (C-1′), 100.10 (C-3), 97.21 (C-5), 93.38 (C-3′), 91.84 (C-5′), 56.33 (C-10), 56.01 (C-10′), 55.66 (C-11), 55.44 (C-11′), 27.66 (C-8), 9.10 (C-9).

IR: ν[cm^{-1}]: 1608, 1578, 1207, 1191, 1148, 1089, 1063, 820, 532.

HRMS (ESI): m/z = Found: 363.1440 ($C_{19}H_{23}O_7$) $[(M+H)]^+$, calculated: 363.1438.

Mp: 112–114 °C

HPLC: Column: Lux Amylose-1, *Fa. Phenomenex* (250x4.6 mm); 5 µL, 25 °C, 1.0 mL/min, 205 nm; solvent: *n*-heptane:2-propanol (80:20), t_R = 18.6, 28.1 min.

***rac*-2,2'-Dimethoxy-6,6'-dimethyl-[1,1'-biphenyl]-4,4'-diyl dipropionate *rac*-(224h)**

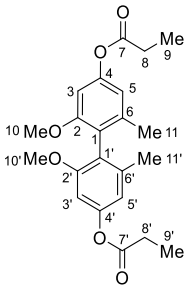

rac-**224h**

The product was synthesized according to general procedure I. After purification *via* column chromatography (PE:EtOAc = 85:15), the dipropionate *rac*-**224h** (59 mg, 0.15 mmol) was obtained from 2,2'-dimethoxy-6,6'-dimethyl-[1,1'-biphenyl]-4,4'-diol *rac*-(**223h**) (50 mg, 0.18 mmol) in 80% yield as white solid.

R_f (PE:EE, 80:20) = 0.38

^{1}H-NMR ($CDCl_3$, 600 MHz) δ 6.65 (d, $^4J_{5/5',3/3'}$ = 2.2 Hz, 2H, 5-H, 5′-H), 6.56 (d, $^4J_{3/3',5/5'}$ = 2.2 Hz, 2H, 3-H, 3′-H), 3.66 (s, 6H, 10-OC$\underline{H}_3$, 10′-OC$\underline{H}_3$), 2.60 (q, $^3J_{8/8',9/9'}$ = 7.6 Hz, 4H, 8-C$\underline{H}_2$-, 8′-C$\underline{H}_2$-), 1.93 (s, 7H, 11-C$\underline{H}_3$, 11′-C$\underline{H}_3$), 1.28 (t, $^3J_{9/9',8/8'}$ = 7.5 Hz, 7H, 9-C$\underline{H}_3$, 9′-C$\underline{H}_3$).

^{13}C-NMR ($CDCl_3$, 151 MHz) δ 172.98 (C-7, C-7′), 157.51 (C-2, C-2′), 150.63 (C-4, C-4′), 139.17 (C-6, C-6′), 122.83 (C-1, C-1′), 114.81 (C-5, C-5′), 102.32 (C-3, C-3′), 55.77 (C-10, C-10′), 27.88 (C-8, C-8′), 19.72 (C-11, C-11′), 9.15 (C-9, C-9′).

IR: ν[cm^{-1}]: 2921, 1759, 1586, 1461, 1307, 1131, 1091, 1001, 889, 822.

HRMS (ESI): m/z = Found: 387.1799 ($C_{22}H_{27}O_6$) $[(M+H)]^+$, calculated: 387.1802.

Mp: 96–98 °C

8.3.7 Approach towards total synthesis of ustilaginoidin A (2) and F (3)

2-Bromo-1,5-dimethoxy-3-methylbenzene (226)

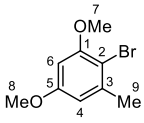

226

The product was synthesized according to general procedure A. After purification *via* column chromatography (PE:EtOAc = 98:2), the brominated product **226** (13.02 g, 56.36 mmol) was obtained from 3,5-dimethoxytoluene (**167**) (9.00 g, 59.1 mmol) in 95% yield as white crystals. Double brominated side product **227** (0.55 g, 1.8 mmol) was isolated in 3% yield as white crystals.

R_f (PE:EE, 90:10) = 0.52

^{1}H-NMR ($CDCl_3$, 600 MHz) δ 6.45 – 6.41 (m, 1H, 4-H), 6.35 (d, $^4J_{6,4}$ = 2.7 Hz, 1H, 6-H), 3.86 (s, 3H, 7-OC$\underline{H}_3$), 3.79 (s, 3H, 8-OC$\underline{H}_3$), 2.39 (s, 3H, 9-C$\underline{H}_3$).

^{13}C-NMR ($CDCl_3$, 151 MHz) δ 159.45 (C-5), 156.78 (C-1), 139.97 (C-2), 107.36 (C-4), 105.26 (C-3), 97.39 (C-6), 56.42 (C-7), 55.61 (C-8), 23.72 (C-9).

IR: ν[cm^{-1}]: 2945, 2841, 1713, 1584, 1460, 1410, 1337, 1202, 1161, 1981, 1022, 817, 607.

MS (ESI): m/z = 153.0 $[M+H]^+$.

Mp: 56–59 °C **Lit. Mp:** 53–54 °C[321]

The analytical data correspond to the data given in literature.[247]

2,4-Dibromo-1,5-dimethoxy-3-methylbenzene (227)

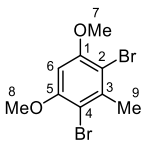

227

R_f (PE:EE, 90:10) = 0.15

^{1}H-NMR ($CDCl_3$, 600 MHz) δ 6.42 (s, 1H, 6-H), 3.90 (s, 6H, 7-OC$\underline{H}_3$, 8-OC$\underline{H}_3$), 2.62 (s, 3H, 9-C$\underline{H}_3$).

^{13}C-NMR ($CDCl_3$, 151 MHz) δ 155.89 (C-1, C-5), 139.40 (C-2, C-4), 105.91 (C-3), 95.00 (C-6), 56.60 (C-7, C-8), 24.33 (C-9).

IR: ν[cm^{-1}]: 2840, 1574, 1449, 1325, 1208, 1080, 1046, 934, 799, 681, 616.

MS (ESI): m/z = 310.8 $[M+H]^+$.

Mp: 161–167 °C **Lit. Mp:** 168–169 °C[322]

The analytical data correspond to the data given in literature.[322]

Phenyl 2,4-dimethoxy-6-methylbenzoate (229)

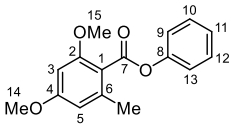

229

Bromophenol **226** (0.50 g, 2.2 mmol) was dissolved in anhydrous THF (50 mL) and cooled down to −78 °C. *n*-Butyllithium (2.5 M in pentane, 1.30 mL, 3.25 mmol) was added dropwise at –78 °C. After stirring for 1 hour, phenyl chloroformiate (0.41 mL, 3.3 mmol) was added. The reaction mixture was stirred for 30 minutes at r.t. After full conversion the reaction was quenched by adding water and extracted with EtOAc three times. The combined organic phases were dried over $MgSO_4$ and concentrated under reduced pressure. Purification *via* column chromatography (PE:EtOAc = 85:15) led to the phenyl benzoate **229** (0.42 g, 1.5 mmol) in 71% yield as light yellow crystals.

R_f (PE:EE, 80:20) = 0.36

^{1}H-NMR ($CDCl_3$, 600 MHz) δ 7.45 – 7.39 (m, 2H, 9-H, 13-H), 7.25 – 7.24 (m, 1H, 11-H), 7.24 – 7.21 (m, 3H, 10-H, 12-H), 6.38 (d, $^{4}J_{5,3}$ = 2.3 Hz, 1H, 5-H), 6.37 (d, $^{4}J_{3,5}$ = 2.4 Hz, 1H, 3-H), 3.87 (s, 3H, 15-OC$\underline{H}_3$), 3.83 (s, 3H, 14-OC$\underline{H}_3$), 2.44 (s, 3H, 16-C$\underline{H}_3$).

^{13}C-NMR ($CDCl_3$, 151 MHz) δ 166.77 (C-7), 161.98 (C-4), 158.94 (C-2), 151.21 (C-8), 139.00 (C-1), 129.58 (C-9, C-13), 125.93 (C-11), 121.91 (C-12, C-10), 115.62 (C-6), 107.02 (C-5), 96.49 (C-3), 56.18 (C-15), 55.56 (C-14), 20.29 (C-16).

IR: ν[cm^{-1}]: 3001, 2851, 1736, 1584, 1458, 1327, 1254, 1188, 1157, 1095, 1070, 1042, 825, 742, 688.

HRMS (ESI): m/z = Found: 273.1102 ($C_{16}H_{17}O_4$) $[(M+H)]^+$, calculated: 273.1121.

Mp: 72–74 °C

2,4-Dimethoxy-6-methylbenzoic acid (230)

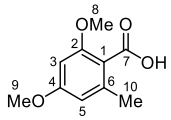

230

Brominated phenol **226** (7.00 g, 30.3 mmol) was given in a schlenk flask and dissolved in anhydrous THF (300 mL). The reaction mixture was cooled down to −78 °C. *n*-Butyllithium (2.5 M in pentane, 14.54 mL, 36.35 mmol) was added dropwise at −78 °C. After stirring for 30 minutes, gaseous CO_2 is purged into the reaction mixture which evolved by solid CO_2 in a syringe. The reaction mixture was first stirred for further 5 minutes at −78 °C and then warmed to r.t. over 1 hour. The reaction was quenched by addition of saturated NH_4Cl solution and acidified with 1 M HCl. After three extractions with EtOAc, the combined organic phase was dried over $MgSO_4$ and concentrated under reduced pressure. The benzoic acid **230** (5.91 g, 30.1 mmol) was obtained in quantitative yield as light yellow crystals without any further purification.

R_f (PE:EE, 80:20) = 0.08

^{1}H-NMR ($CDCl_3$, 600 MHz) δ 6.44 (d, $^4J_{5,3}$ = 2.4 Hz, 1H, 5-H), 6.39 (d, $^4J_{3,5}$ = 2.4 Hz, 1H, 3-H), 3.95 (s, 3H, 8-OC$\underline{H}_3$), 3.84 (s, 3H, 9-OC$\underline{H}_3$), 2.57 (s, 3H, 10-C$\underline{H}_3$).

^{13}C-NMR ($CDCl_3$, 151 MHz) δ 167.78 (C-1), 162.50 (C-4), 159.79 (C-2), 144.75 (C-1), 112.06 (C-6), 109.45 (C-5), 96.75 (C-3), 56.71 (C-8), 55.37 (C-9), 22.96 (C-10).

IR: ν[cm^{-1}]: 2967, 2850, 2645, 2528, 1623, 1598, 1584, 1285, 1204, 1162, 1088, 824, 611.

MS (ESI): m/z = 179.0 $[M-H_2O+H]^+$.

Mp: 143–145 °C **Lit. Mp:** 142–144 °C[323]

The analytical data correspond to the data given in literature.[323, 324]

Methyl 2,4-dimethoxy-6-methylbenzoate (228)

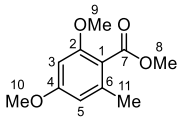

228

Benzoic acid **230** (2.70 g, 3.76 mmol) and potassium carbonate (3.80 g, 27.5 mmol) was given in acetone (70 mL). Dimethyl sulfate (1.70 mL, 17.9 mmol) was added dropwise. The reaction mixture was stirred overnight at r.t. After full conversion the reaction was quenched by adding 10% aqueous sodium sulfite solution. The mixture was stirred for 30 minutes at r.t. and afterwards acidified with aqueous 1 M HCl solution and extracted with EtOAc three times. The combined organic phase was dried over $MgSO_4$ and concentrated under reduced pressure. After purification *via* column chromatography (PE:EtOAc = 85:15), the methyl benzoate **228** (1.81 g, 8.61 mmol) could be isolated in 62% yield as yellow crystals.

R_f (PE:EE, 80:20) = 0.40

^{1}H-NMR ($CDCl_3$, 600 MHz) δ 6.31 (q, $^4J_{5,3}$ = 2.3 Hz, 2H, 3-H, 5-H), 3.88 (s, 3H, 8-OC$\underline{H}_3$), 3.80 (s, 3H, 9-OC$\underline{H}_3$), 3.80 (s, 3H, 10-OC$\underline{H}_3$), 2.28 (s, 3H, 11-C$\underline{H}_3$).

^{13}C-NMR ($CDCl_3$, 151 MHz) δ 168.88 (C-7), 161.51, (C-1) 158.36 (C-4), 138.43 (C-1), 116.53 (C-6), 106.80 (C-3/5), 96.32 (C-3/5), 56.05 (C-10), 55.49 (C-9), 52.18 (C-8), 20.10 (C-10).

IR: ν[cm^{-1}]: 3002, 2952, 2836, 1724, 1604, 1584, 1324, 1260, 1197, 1153, 1092, 1051, 935, 843, 810, 640.

MS (ESI): m/z = 179.0 $[M\text{-}CH_3OH+H]^+$.

Mp: 43–45 °C **Lit. Mp:** 42–44 °C[325]

The analytical data correspond to the data given in literature.[247]

4-Methoxy-6-methyl-2H-pyran-2-one (232)

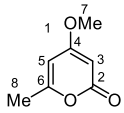

232

Pyrone **231** (1.00 g, 7.93 mmol) and potassium carbonate (1.43 g, 10.3 mmol) was given in acetone (30 mL). Dimethyl sulfate (0.98 mL, 10 mmol) was added dropwise. The reaction mixture was stirred at reflux for 3 hours. After full conversion the reaction was quenched by adding 10% aqueous sodium sulfite solution. The mixture was stirred at r.t. for 30 minutes and afterwards acidified with aqueous 1 M HCl solution and extracted with EtOAc three times. The combined organic phase was dried over $MgSO_4$ and concentrated under reduced pressure. The desired product **232** (1.10 g, 7.83 mmol) was isolated in 99% yield as white powder.

R_f (PE:EE, 80:20) = 0.12

^{1}H-NMR ($CDCl_3$, 600 MHz) δ 5.77 (dq, $^4J_{5,3}$ = 1.9 Hz, $^4J_{5,8}$ = 0.9 Hz, 1H, 5-H), 5.40 (d, $^4J_{3,5}$ = 2.2 Hz, 1H, 3-H), 3.79 (s, 3H, 7-OC$\underline{H}_3$), 2.23 – 2.19 (m, 3H, 8-C$\underline{H}_3$).

^{13}C-NMR ($CDCl_3$, 151 MHz) δ 171.47 (C-4), 165.13 (C-2), 162.21 (C-6), 100.50 (C-5), 87.53 (C-3), 55.93 (C-7), 19.96 (C-8).

IR: ν[cm^{-1}]: 3094, 3021, 1736, 1716, 1650, 1567, 1462, 1406, 1325, 1250, 1148, 1027, 939, 867, 817, 545.

MS (ESI): m/z = 141.0 $[M+H]^+$.

Mp: 87–89 °C **Lit. Mp:** 86–90 °C[326]

The analytical data correspond to the data given in literature.[327, 328]

2,4-Dimethoxy-6-methylpyrylium tetrafluoroborate (233)

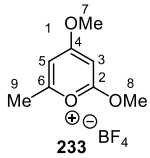

233

$AgBF_4$ (0.69 g, 3.6 mmol) was added to pyranone **232** (0.50 g, 3.6 mmol) dissolved in anhydrous CH_2Cl_2 (4 mL). Methyliodide (0.89 mL, 14 mmol) was added, and the reaction mixture was stirred over night at r.t. Afterwards the precipitated AgI was filtered off and washed with CH_2Cl_2. The combined filtrate was concentrated under reduced pressure and purified by recrystallization in THF. The tetrafluoroborate **233** (0.28 g, 1.2 mmol) could be obtained in 33% yield as white solid.

^{1}H-NMR ($CDCl_3$, 600 MHz) δ 6.82 – 6.75 (m, 2H, 3-H, 5-H), 4.45 (s, 3H, 7-OC$\underline{H}_3$), 4.30 (s, 3H, 8-OC$\underline{H}_3$), 2.66 (s, 3H, 9-C$\underline{H}_3$).

^{13}C-NMR ($CDCl_3$, 151 MHz) δ 184.18 (C-2), 170.21 (C-4), 157.87 (C-6), 107.57 (C-3/C-5), 88.42 (C-3/C-5), 60.53 (C-7), 60.20 (C-8), 20.05 (C-9).

IR: ν[cm^{-1}]: 1667, 1542, 1486, 1249, 1163, 1098, 1051, 1034, 944, 911, 521.

Mp: 154–155 °C

The analytical data correspond to the data given in literature.[173, 174]

Phenyl 2,4-dimethoxy-6-((6-methyl-4-oxo-4H-pyran-2-yl)methyl)benzoate (235)

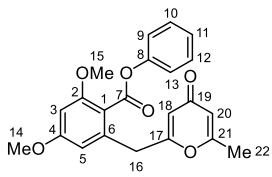

235

Diisopropylamine (0.13 mL, 0.92 mmol) was given in anhydrous THF (1 mL) and cooled down to –78 °C. *n*-Butyllithium (2.5 M in pentane, 0.37 mL, 0.92 mmol) was added dropwise at –78 °C. After stirring for 15 minutes at −78 °C, a solution of toluate **229** (0.10 g, 0.37 mmol) dissolved in anhydrous THF (1 mL) was added dropwise. The reaction mixture

was stirred at −78 °C for 30 minutes. Pyrylium tetrafluoroborate (**233**) (88 mg, 0.37 mmol) was added in one shot. After 30 minutes mixing at −78 °C 1.5 mL conc. HCl solution was added, and the mixture was stirred at r.t. for 3 hours. The mixture was diluted with water and neutralized with Na_2CO_3. The organic phase was extracted with EtOAc and dried over $MgSO_4$. Purification *via* column chromatography (PE:EtOAc = 60:40) led to isolation of the desired product **235** (44 mg, 0.12 mmol) in 32% yield as yellow oil.

R_f (PE:EE, 60:40) = 0.21

^{1}H-NMR ($CDCl_3$, 600 MHz) δ 7.44 (t, $^3J_{9/13,10/12}$ = 7.7 Hz, 2H, 9-H, 13-H), 7.31 – 7.26 (m, 1H, 11-H), 7.17 (s, 2H, 10-H, 12-H), 6.49 (d, $^4J_{3,5}$ = 2.7 Hz, 1H, 3-H), 6.35 (d, $^4J_{5,3}$ = 2.7 Hz, 1H, 5-H), 5.98 (s, 1H, 18-H), 5.95 (s, 1H, 20-H), 3.93 (s, 3H, 15-OC$\underline{H}_3$), 3.86 (s, 3H, 14-OC$\underline{H}_3$), 3.82 (s, 3H, 16-C$\underline{H}_2$-), 2.19 (s, 3H, 22-C$\underline{H}_3$).

^{13}C-NMR ($CDCl_3$, 151 MHz) δ 207.80 (C-19), 166.42 (C-6), 163.28 162.53 (C-4), 161.85 (C-21), 159.59 (C-2), 157.85 (C-7), 150.97 (C-8), 137.72 (C-17), 129.68 (C-9, C-13), 126.14 (C-11), 121.66 (C-10, C-12), 115.83 (C-1), 110.79 (C-18), 107.28 (C-5), 105.41 (C-20), 97.81 (C-3), 56.32 (C-15), 55.92 (C-16), 55.69 (C-14), 38.95 (C-16), 20.03 (C-22).

IR: ν[cm^{-1}]: 1728, 1605, 1561, 1458, 1329, 1261, 1189, 1160, 1074, 1039, 852, 749, 691.

HRMS (ESI): m/z = Found: 381.1328 ($C_{22}H_{21}O_6$) $[(M+H)]^+$, calculated: 381.1333.

***tert*-Butyl (*R*)-5-hydroxy-3-oxohexanoate (238)**

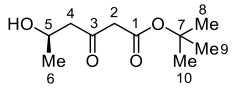

238

Diisopropylamine (17.03 mL, 121.1 mmol) was given in anhydrous THF (24 mL) and cooled down to −78 °C. *n*-Butyllithium (2.25 M in pentane, 42.88 mL, 96.91 mmol) was added dropwise. The mixture was stirred for 15 minutes at −78 °C. *tert*-Butylacetate (**237**) (14.46 mL, 109.5 mmol) was added dropwise and stirring was continued for 20 minutes. A solution of (*R*)-3-hydroxybutyrate (**236**) (3.60 mL, 32.3 mmol) in anhydrous THF (20 mL) was added dropwise. The reaction mixture was stirred afterwards at −40 °C for 2 hours. After full conversion, the reaction was quenched by adding ice cold water. The organic phase was extracted with EtOAc three times. The combined organic phases were dried over

$MgSO_4$ and concentrated under reduced pressure. The residue was purified *via* column chromatography (PE:EtOAc = 80:20), leading to the desired ketoester **238** (4.38 g, 21.6 mmol) in 67% yield as yellow oil.

R_f (PE:EE, 50:50) = 0.42

^{1}H-NMR ($CDCl_3$, 600 MHz) δ 4.25 (dqd, $^3J_{5,4}$ = 9.1 Hz, $^3J_{5,6}$ = 6.3 Hz, $^4J_{5,3}$ = 2.9 Hz, 1H. 5-H), 3.37 (d, $^4J_{2,4}$ = 2.2 Hz, 2H, 2-C$\underline{H}_2$-), 2.73 (dd, $^3J_{4,5}$ = 17.7 Hz, $^4J_{4,2}$ = 2.9 Hz, 1H, 4-C$\underline{H}_2$-), 2.63 (dd, $^3J_{4,5}$ = 17.7 Hz, $^4J_{4,2}$ = 2.9 Hz, 1H, 4-C$\underline{H}_2$-), 1.47 (s, 9H, 9-C$\underline{H}_3$, 10-C$\underline{H}_3$, 11-C$\underline{H}_3$), 1.21 (d, $^3J_{6,5}$ = 6.3 Hz, 3H, 6-C$\underline{H}_3$).

^{13}C-NMR ($CDCl_3$, 151 MHz) δ 204.40 (C-3), 166.28 (C-1), 82.46 (C-8), 63.91 (C-5), 51.27 (C-2), 51.08 (C-4), 28.10 (C-9, C-10, C-11), 22.48 (C-6).

IR: ν[cm^{-1}]: 3423. 2977, 1707, 1369, 1321, 1253, 1144, 1054, 958, 840, 746.

MS (ESI): m/z = 203.3 $[M+H]^+$.

$[\alpha]_D^{25} = -42.2$ (c = 1.0, $CHCl_3$) **Lit.** $[\alpha]_D^{25} = -40.1$ (c = 1.0, $CHCl_3$)[329]

The analytical data correspond to the data given in literature.[330]

(*R*)-9-Methyl-1,4,8-trioxaspiro[4.5]decan-7-one (239)

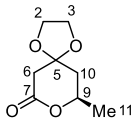

239

Ketoester **238** (2.36 g, 11.7 mmol) was given in dry CH_2Cl_2 (30 mL). Ethylene glycol (2.44 mL, 43.2 mmol), and toluenesulfonic acid (0.44 g, 2.3 mmol) was added. The reaction mixture was stirred at reflux for 6 hours. After cooling down, aqueous saturated $NaHCO_3$ solution was added, and the organic phase was extracted with CH_2Cl_2 three times. The combined organic phases were dried over $MgSO_4$ and concentrated under reduced pressure. The lactone **239** (1.85 g, 10.7 mmol) was obtained in 92% yield as colorless oil. The crude product was used without further purification.

R_f (PE:EE, 60:40) = 0.44

^{1}H-NMR ($CDCl_3$, 600 MHz) δ 4.57 (dqd, $^{3}J_{9,11}$ = 12.6 Hz, $^{3}J_{9,10}$ = 6.4, $^{5}J_{9,6}$ = 2.8 Hz, 1H, 9-H), 4.04 – 3.93 (m, 4H, 2-C$\underline{H}_2$-, 3-C$\underline{H}_2$-), 2.78 (dd, $^{2}J_{6a,6b}$ = 17.3 Hz, $^{4}J_{6,10}$ = 1.9 Hz, 1H, 6-C$\underline{H}_2$-), 2.70 (d, $^{2}J_{6a,6b}$ = 17.3 Hz, 1H, 6-C$\underline{H}_2$-), 2.03 (dt, $^{3}J_{10,9}$ = 14.0 Hz, $^{4}J_{10,11}$ = 2.5 Hz, 1H, 10-C$\underline{H}_2$-), 1.83 (dd, $^{3}J_{10,9}$ = 13.9 Hz, $^{2}J_{10a,10b}$ = 11.7 Hz, 1H, 10-C$\underline{H}_2$-), 1.41 (d, $^{3}J_{11,9}$ = 6.4 Hz, 3H, 11-C$\underline{H}_3$).

^{13}C-NMR ($CDCl_3$, 151 MHz) δ 169.67 (C-7), 105.81 (C-5), 73.54 (C-9), 64.89 (C-2, C-3), 41.11 (C-6), 40.89 (C-10), 21.35 (C-11).

IR: ν[cm^{-1}]: 2981, 2898, 1738, 1386, 1341, 1258, 1117, 1054, 1003, 979, 949, 801.

MS (ESI): m/z = 173.0 $[M+H]^+$.

$[\alpha]_D^{25} = +23.0$ (c = 1.0, $CHCl_3$)

Lit. (*S*)-Enantiomer $[\alpha]_D^{25} = -19.5$ (c = 1.2, $CHCl_3$)[250]

The analytical data correspond to the data given in literature.[250]

(*R*)-2-Methyl-2,3-dihydro-4H-pyran-4-one (241)

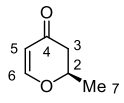

241

Lactone **239** (1.85 g, 10.7 mmol) was given in anhydrous toluene (30 mL) and cooled down to −78 °C. DiBAl-H (1 M in toluene, 11.67 mL, 11.67 mmol) was added dropwise over 30 minutes. After the mixture was continuously stirred at −78 °C for 30 minutes, saturated aqueous NH_4Cl (10 mL) solution was added dropwise, and the mixture was warmed up to r.t. and stirred for 30 minutes. Afterwards sodium sulfate (4 g) and diethyl ether (150 mL) were added and stirred for 30 minutes. The solids were removed by filtration through a celite pad and washed with diethyl ether. The combined filtrate was concentrated under reduced pressure. The crude residue was used without further purification. The crude lactol **240** was given in a mixture of acetone and water (1:1 – 80 mL). Toluenesulfonic acid (2.22 g, 11.7 mmol) was added, and the solution was stirred at 50 °C for 2 hours. Afterwards the reaction mixture was cooled down and quenched by adding saturated aqueous $NaHCO_3$ solution. The mixture was concentrated partially under reduced pressure. The organic phases were then extracted with diethyl ether three times. The combined organic

phases were dried over $MgSO_4$ and concentrated under reduced pressure. The residue was purified *via* column chromatography (PE:EtOAc = 80:20), leading to the desired pyranone **241** (0.51 g, 4.5 mmol) in 42% yield as orange oil.

R_f (PE:EE, 50:50) = 0.40

^{1}H-NMR ($CDCl_3$, 600 MHz) δ 7.36 – 7.32 (m, 1H, 5-H), 5.40 (dd, $^3J_{6,5}$ = 6.0, 1.1 Hz, 1H, 6-H), 4.60 – 4.51 (m, 1H, 2-H), 2.55 – 2.40 (m, 2H, 3-C$\underline{H}_2$-), 1.46 (d, $^3J_{7,2}$ = 6.3 Hz, 3H, 7-C$\underline{H}_3$).

^{13}C-NMR ($CDCl_3$, 151 MHz) δ 192.80 (C-4), 163.44 (C-5), 107.04 (C-6), 76.15 (C-2), 43.63 (C-3), 20.49 (C-7).

IR: ν[cm^{-1}]: 3455, 1924, 1726, 1462, 1380, 1273, 1125, 1076.

MS (ESI): m/z = 157.1 $[M+2Na-H]^+$.

$[\alpha]_D^{25} = +86.5$ (c = 1.0, $CHCl_3$) **Lit.** $[\alpha]_D^{25} = +187.2$ (c = 1.5, $CHCl_3$)[331, 332]

The analytical data correspond to the data given in literature.[250]

(2*R*)-5-Hydroxy-6,8-dimethoxy-2-methyl-2,3,10,10a-tetrahydro-4H-benzo[g]chromen-4-one (242)

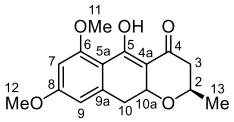

242

Diisopropylamine (1.61 mL, 11.0 mmol) was given in anhydrous THF (50 mL) and cooled down to −78 °C. *n*-Butyllithium (2.5 M in pentane, 4.61 mL, 11.0 mmol) was added dropwise at −78 °C. After stirring for 15 minutes at −78 °C, a solution of toluate **229** (1.00 g, 3.67 mmol) dissolved in anhydrous THF (20 mL) was added dropwise. The reaction mixture was stirred at −78 °C for 1 hour. Pyranone **241** (0.62 g, 5.5 mmol) dissolved in anhydrous THF (20 mL) was added dropwise. The mixture was let warmed up to r.t. over 2 hours and afterwards quenched with saturated aqueous NH_4Cl solution. The organic phase was extracted with EtOAc and dried over $MgSO_4$. Purification *via* column

chromatography (PE:EtOAc = 60:40) led to isolation of the desired product **242** (0.65 g, 2.2 mmol) in 61% yield as yellow oil.

R_f (PE:EE, 60:40) = 0.33

^{1}H-NMR ($CDCl_3$, 600 MHz) δ 15.67 (s, 1H, OH), 6.40 (d, $^4J_{7,9}$ = 2.3 Hz, 1H, 7-H), 6.36 (dd, $^4J_{9,7}$ = 1.1 Hz, $^4J_{9,10}$ = 2.4 Hz, 1H, 9-H), 4.57 – 4.48 (m, 1H, 10a-H), 3.91 (s, 3H, 11-OC$\underline{H}_3$), 3.86 (s, 3H, 12-OC$\underline{H}_3$), 3.86 – 3.79 (m, 1H, 2-H), 3.00 (dd, $^4J_{10,9}$ = 5.1 Hz, $^3J_{10,10a}$ = 14.3 Hz, 1H, 10-C$\underline{H}_2$-), 2.89 (dd, $^3J_{10,10a}$ = 14.0 Hz, $^4J_{10,9}$ = 1.0 Hz, 1H, 10-C$\underline{H}_2$-), 2.43 – 2.33 (m, 2H, 3-C$\underline{H}_2$-), 1.33 (d, $^3J_{13,2}$ = 6.2 Hz, 3H, 13-C$\underline{H}_3$).

^{13}C-NMR ($CDCl_3$, 151 MHz) δ 185.53 (C-5), 176.99 (C-4), 164.38 (C-8), 162.33 (C-6), 143.38 (C-4a), 114.50 (C-9a), 108.06 (C-5a), 106.02 (C-9), 98.03 (C-7), 71.08 (C-10a), 69.79 (C-2), 56.23 (C-11), 55.68 (C-12), 38.00 (C-3), 37.82 (C-10), 21.67 (C-13).

IR: ν[cm^{-1}]: 2939, 1594, 1455, 1314, 1278, 1240, 1200, 1161, 1083, 1040, 980, 939, 707, 517.

HRMS (ESI): m/z = Found: 291.1226 ($C_{16}H_{19}O_5$) $[(M+H)]^+$, calculated: 219.1227.

(2*R*)-5-Hydroxy-6,8-dimethoxy-2-methyl-2,3-dihydro-4H-benzo[g]chromen-4-one (243)

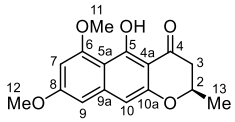

243

Chloranil (98 mg, 0.40 mmol) was given in anhydrous toluene (5 mL). The reduced naphthopyrone **242** (30 mg, 0.10 mmol) dissolved in anhydrous toluene (5 mL) was added. The reaction mixture was stirred at reflux for 24 hours. The reaction was quenched by adding 2 M $NaHSO_3$ solution. The organic phase was extracted with EtOAc and dried over $MgSO_4$. After purification *via* column chromatography (PE:EtOAc = 70:30), the naphthopyrone **243** (23 mg, 80 µmol) was isolated in 82% yield as brown solid.

R_f (PE:EE, 60:40) = 0.52

^{1}H-NMR (DMSO-d_6, 600 MHz) δ 14.29 (s, 1H, OH), 6.68 (d, $^4J_{9,7}$ = 2.3 Hz, 1H, 9-H), 6.59 (s, 1H, 10-H), 6.36 (d, $^4J_{7,9}$ = 2.4 Hz, 1H, 7-H), 4.63 – 4.55 (m, 1H, 2-H), 3.85 (s, 6H, 11-

OC$\underline{H}_3$, 12-OC$\underline{H}_3$), 2.89 (dd, $^2J_{3a,3b}$ = 17.2 Hz, $^3J_{3,2}$ = 11.9 Hz, 1H, 3-C$\underline{H}_2$-), 2.74 (dd, $^2J_{3a,3b}$ = 17.3 Hz, $^4J_{3,13}$ = 3.0 Hz, 1H, 3-C$\underline{H}_2$-), 1.41 (d, $^3J_{13,2}$ = 6.2 Hz, 3H, 13-C$\underline{H}_3$).

^{13}C-NMR (DMSO-d_6, 151 MHz) δ 198.47 (C-4), 164.49 (C-5), 162.18 (C-6/C-8), 160.88 (C-6/C-8), 155.93 (C-10a), 142.83 (C-4a), 106.11 (C-9a), 103.10 (C-5a), 100.95 (C-10), 98.58 (C-9), 96.28 (C-7), 72.87 (C-2), 55.83 (C-11/C-12), 55.40 (C-11/C-12), 43.14 (C-3), 20.48 (C-2).

IR: ν[cm^{-1}]: 2954, 2927, 1708, 1689, 1629, 1603, 1456, 1382, 1342, 1317, 1210, 1168.

MS (ESI): m/z = 289.2 $[M+H]^+$.

Mp: 173–175 °C **Lit. Mp:** 175–177 °C[333]

The analytical data correspond to the data given in literature.[334]

3,3'-Dibromo-4,4'-dimethoxy-6,6'-bis(methoxymethoxy)-2,2'-dimethyl-1,1'-biphenyl *rac*-(244)

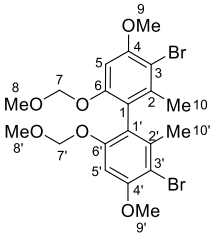

rac-**244**

MOM-protected biphenyl *rac*-**176a** (0.20 g, 0.55 mmol) was dissolved in anhydrous CH_2Cl_2 (2 mL) at 0 °C. NBS (0.19 g, 1.1 mmol) was added in one portion. The mixture was stirred at 0 °C for 3 hours and quenched by addition of 10% aqueous sodium sulfite solution. The reaction mixture was extracted three times with CH_2Cl_2. The combined organic phase was washed with saturated $NaHCO_3$ solution, dried over $MgSO_4$, and dried at reduced pressure. The product was used without further purification. The brominated product *rac*-**244** (0.26 mg, 0.50 mmol) was obtained in 91% yield as orange solid.

R_f (PE:EE, 80:20) = 0.28

^{1}H-NMR ($CDCl_3$, 600 MHz) δ 6.73 (s, 2H, 5-H, 5′-H), 5.07 – 4.93 (m, 4H, 7-C$\underline{H}_2$-, 7′-C$\underline{H}_2$-), 3.92 (s, 6H, 9-OC$\underline{H}_3$, 9′-OC$\underline{H}_3$), 3.31 (s, 6H, 8-OC$\underline{H}_3$, 8′-OC$\underline{H}_3$), 2.06 (s, 6H, 10-C$\underline{H}_3$, 10′-C$\underline{H}_3$).

^{13}C-NMR ($CDCl_3$, 151 MHz) δ 155.91 (C-4, C-4′), 154.91 (C-6, C-6′), 139.23 (C-2, C-2′), 120.87 (C-1, C-1′), 107.34 (C-3, C-3′), 97.93 (C-5, C-5′), 95.08 (C-7, C-7′), 56.43 (C-9, C-9′), 55.96 (C-8, C-8′), 20.70 (C-10, C-10′).

IR: ν[cm^{-1}]: 2912, 1445, 1326, 1312, 1217, 1149, 1090, 1045, 1031, 932, 918, 819, 810.

HRMS (ESI): m/z = Found: 519.0011 ($C_{20}H_{25}Br_2O_6$) $[(M+H)]^+$, calculated: 519.0012.

Mp: 156–157 °C

Diphenyl 4,4'-dimethoxy-6,6'-bis(methoxymethoxy)-2,2'-dimethyl-[1,1'-biphenyl]-3,3'-dicarboxylate *rac*-(245)

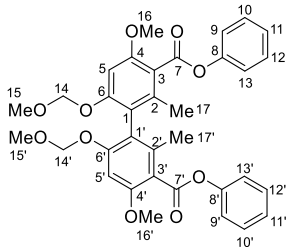

rac-**245**

Dimeric bromophenol *rac*-**244** (1.25 g, 2.40 mmol) was dissolved in anhydrous THF (50 mL) and cooled down to −78 °C. *n*-Butyllithium (2.5 M in pentane, 2.18 mL, 4.93 mmol) was added dropwise at −78 °C. After stirring for 1 hour, phenyl chloroformiate (0.67 mL, 5.3 mmol) was added. The reaction mixture was stirred for 2 hours at r.t. After full conversion the reaction was quenched by adding water and extracted with EtOAc three times. The combined organic phases were dried over $MgSO_4$ and concentrated under reduced pressure. Purification *via* column chromatography (PE:EtOAc = 70:30) led to the phenyl benzoate *rac*-**245** (0.87 g, 1.4 mmol) in 60% yield as white solid.

R_f (PE:EE, 60:40) = 0.21

^{1}H-NMR (DMSO-d_6, 600 MHz) δ 7.48 (t, $^3J_{13/13',9/9',10/10',12/12'}$ = 7.9 Hz, 4H, 9-H, 9′-H, 13-H, 13′-H), 7.32 (t, $^3J_{11/11',10/10',12/12'}$ = 7.4 Hz, 2H, 11-H, 11′-H), 7.23 (d,

$^{3}J_{10/10',9/9',11/11',12/12',11/11',13/13'}$ = 7.9 Hz, 4H, 10-H, 10′-H, 12-H, 12′-H), 6.85 (s, 2H, 5-H, 5′-H), 5.19 (s, 4H, 14-C$\underline{H}_2$-, 14′-C$\underline{H}_2$-), 3.91 (s, 6H, 16-C$\underline{H}_3$, 16′-C$\underline{H}_3$), 3.25 (s, 6H, 15-C$\underline{H}_3$, 15′-C$\underline{H}_3$), 1.96 (s, 6H, 17-C$\underline{H}_3$, 17′-C$\underline{H}_3$).

^{13}C-NMR (DMSO-d_6, 151 MHz) δ 166.31 (C-7, C-7′), 156.71 (C-6, C-6′), 156.50 (C-4, C-4′), 150.55 (C-8, C-8′), 135.84 (C-3, C-3′), 129.71 (C-9, C-9′, C-13, C-13′), 126.08 (C-11, C-11′), 121.74 (C-10, C-10′, C-12, C-12′), 118.18 (C-1, C-1′), 116.34 (C-2, C-2′), 96.74 (C-5, C-5′), 93.95 (C-14, C-14′), 56.05 (C-16, C-16′), 55.54 (C-15, C-15′), 16.60 (C-17, C-17′).

IR: ν[cm^{-1}]: 2927, 1734, 1588, 1489, 1457, 1307, 1243, 1215, 1184, 1160, 1087, 1061, 1040, 932, 690.

HRMS (ESI): m/z = Found: 603.2218 ($C_{34}H_{35}O_{10}$) $[(M+H)]^+$, calculated: 603.2225.

Mp: 154–156 °C

Phenyl 2-(bromomethyl)-4,6-dimethoxybenzoate (256)

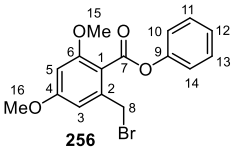

256

Diisopropylamine (0.17 mL, 1.2 mmol) was given in anhydrous THF (2 mL) and cooled down to –78 °C. *n*-Butyllithium (2.5 M in pentane, 0.49 mL, 1.1 mmol) was added dropwise at –78 °C. After stirring for 15 minutes at –78 °C, a solution of toluate **229** (0.20 g, 0.73 mmol) dissolved in anhydrous THF (5 mL) was added dropwise. The reaction mixture was stirred at –78 °C for 1 hour. 1,2-dibromotetrafluoroethane (0.14 mL, 1.2 mmol) was added rapidly. After 5 minutes 5 mL aqueous saturated NH_4Cl solution was added rapidly, and the mixture was warmed to r.t. The organic phase was extracted with EtOAc three times and washed with aqueous saturated NH_4Cl solution. The combined organic phases were dried over $MgSO_4$ and concentrated under reduced pressure. After purification *via* column chromatography (PE:EtOAc = 95:5 to 90:10 to 80:20), the brominated product **256** (50 mg, 0.15 mmol) could be isolated in 21% yield as yellow oil.

R_f (PE:EE, 80:20) = 0.38

^{1}H-NMR ($CDCl_3$, 600 MHz) δ 7.43 (tt, $^{4}J_{10,14}$ = 2.2 Hz, $^{3}J_{1012/,11,13}$ = 7.8 Hz, 2H, 11-H, 13-H), 7.32 – 7.27 (m, 3H, 10-H, 12-H, 14-H), 6.57 (d, $^{4}J_{3,5}$ = 2.3 Hz, 1H, 5-H), 6.49 (d, $^{4}J_{5,3}$ = 2.2 Hz, 1H, 3-H), 4.64 (s, 2H, 8-C$\underline{H}_2$-), 3.89 (s, 3H, 16-OC$\underline{H}_3$), 3.87 (s, 3H, 15-OC$\underline{H}_3$).

^{13}C-NMR ($CDCl_3$, 151 MHz) δ 165.71 (C-7), 162.31 (C-2), 159.54 (C-4), 151.07 (C-8), 138.99 (C-1), 129.62 (C-9, C-10), 126.12 (C-11, C-13), 121.96 (C-12, C-14), 115.30 (C-6), 107.11 (C-5), 99.26 (C-3), 56.42 (C-16), 55.75 (C-15), 30.55 (C-8).

IR: ν[cm^{-1}]: 2936, 1748, 1605, 1456, 1344, 1202, 1160, 1029, 836.

HRMS (ESI): m/z = Found: 351.0223 ($C_{16}H_{16}BrO_4$) $[(M+H)]^+$, calculated: 351.0226.

Phenyl 3-bromo-4,6-dimethoxy-2-methylbenzoate (260)

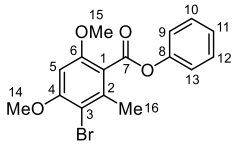

260

Toluate **229** (0.10 g, 0.37 mmol), AIBN (6 mg, 40 µmol), NBS (70 mg, 0.37 mmol) was given in anhydrous chloroform (1 mL). After the mixture was stirred for 4 hours at reflux, it was cooled down to 0 °C. The formed suspension was filtered off and washed with cold EtOAc. Afterwards the combined organic phase was washed with aqueous saturated Na-HCO_3 solution. The organic phase was dried over $MgSO_4$ and concentrated under reduced pressure. The brominated product **260** (0.12 g, 0.35 mmol) was obtained in 94% yield as white powder.

R_f (PE:EE, 80:20) = 0.16

^{1}H-NMR ($CDCl_3$, 600 MHz) δ 7.45–7.42 (m, 2H, 9-H, 13-H), 7.29–7.23 (m, 3H, 10-H, 11-H, 12-H), 6.43 (s, 1H, 5-H), 3.95 (s, 3H, 14-OC$\underline{H}_3$), 3.92 (s, 3H, 15-OC$\underline{H}_3$), 2.51 (s, 3H, 16-C$\underline{H}_3$).

^{13}C-NMR ($CDCl_3$, 151 MHz) δ 166.30 (C-1), 158.00 (C-4), 157.17 (C-6), 151.05 (C-8), 137.57 (C-2), 129.66 (C-9, C-13), 126.16 (C-10, C-12), 121.75 (C-11), 117.30 (C-3), 106.08 (C-1), 94.23 (C-5), 56.62 (C-14), 56.46 (C-15), 20.73 (C-16).

IR: ν[cm^{-1}]: 2940, 1745, 1589, 1457, 1333, 1243, 1210, 1186, 1160, 1087, 1063, 750.

MS (ESI): m/z = 352.9 $[M+H]^+$.

Mp: 154–156 °C

8.3.8 Total synthesis towards isokotanin A (4) and isokotanin C (5)

rac-2,2′,4,4′-Tetramethoxy-6,6′-dimethyl-1,1′-biphenyl *rac*-(152)

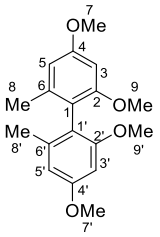

rac-**152**

Biphenyl *rac*-**1** (1.00 g, 3.65 mmol) and anhydrous potassium carbonate (1.51 g, 10.9 mmol) was given in a flask. Acetone (14 mL) was added to dissolve the starting material. While stirring the reaction mixture dimethyl sulfate (3.46 mL, 36.5 mmol) was added dropwise over 10 hours at r.t. After 16 hours the reaction mixture was quenched by adding 10% aq. sodium sulfite solution. The mixture was continued to stir for 30 minutes at r.t and afterwards acidified with 1 M HCl. The organic phase was extracted three times with EtOAc and washed with brine. The combined organic phase was dried over $MgSO_4$ and concentrated by solvent evaporation at reduced pressure to give 2,2′,4,4′-tetramethoxy-6,6′-dimethyl-1,1′-biphenyl *rac*-(**152**) (1.10 g, 3.34 mmol) in 99% yield as white solid. The product could be used without further purifications.

R_f (PE:EE, 80:20) = 0.72

^{1}H-NMR ($CDCl_3$, 600 MHz) δ 6.45 (d, $^4J_{5/5',3/3'}$ = 2.4 Hz, 2H, 5-H, 5′-H), 6.40 (d, $^4J_{3/3',5/5'}$ = 2.6 Hz, 2H, 3-H, 3′-H), 3.83 (s, 6H, 7-OC$\underline{H}_3$, 7′-OC$\underline{H}_3$), 3.68 (s, 6H, 9-OC$\underline{H}_3$, 9′-OC$\underline{H}_3$), 1.93 (s, 6H, 8-C$\underline{H}_3$, 8′-C$\underline{H}_3$).

^{13}C-NMR ($CDCl_3$, 151 MHz) δ 159.58 (C-4, C-4′), 158.38 (C-2, C-2′), 139.39 (C-6, C-6′), 118.64 (C-1, C-1′), 106.32 (C-5, C-5′), 96.36 (C-3, C-3′), 55.94 (C-9, C-9′), 55.28 (C-7, C-7′), 20.17 (C-8, C-′8).

IR: ν[cm^{-1}]: 2995, 2836, 1598, 1455, 1326, 1198, 1151, 1065, 999, 826, 538.

MS (ESI): m/z = 303.0 $[M+H]^+$.

Mp: 101 °C **Lit. Mp:** 107–109 °C[317]

HPLC: Chiralpak IC, *Fa. Daicel* (250x4.6 mm); 5 µL, 25 °C, 0.5 mL/min, 210 nm; solvent: *n*-heptane:2-propanol (99:1), t_R = 19.4, 36.4 min.

The analytical data correspond to the data given in literature.[224, 335, 336]

(*M*)-2,2′,4,4′-Tetramethoxy-6,6′-dimethyl-1,1′-biphenyl (*M*)-(152)

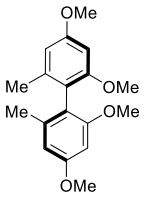

The product was synthesized according to the racemic synthesis of *rac*-**152**. The *(M)*-biaryl (*M*)-**152** (254 mg, 840 µmol, >99% *ee*) was obtained in 92% yield from *(M)*-biphenyl (*M*)-**1** (250 mg, 913 µmol) as white solid. The spectroscopic data were in accordance with those previously obtained for racemic material.

Mp: 128 °C **Lit. Mp:** 127 °C[37]

$[\alpha]_D^{25} = 34.2$ (c = 1.0, $CHCl_3$) **Lit.** $[\alpha]_D^{25} = 35.3$ (c = 0.75, $CHCl_3$)[37]

The analytical data correspond to the data given in literature.

(*P*)-2,2′,4,4′-Tetramethoxy-6,6′-dimethyl-1,1′-biphenyl (*P*)-(152)

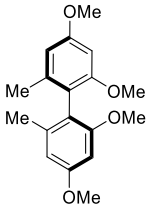

The product was synthesized according to the racemic synthesis of *rac*-**152**. The *(P)*-biaryl (*P*)-**152** (259 mg, 857 µmol, 98% *ee*) was obtained in 94% yield from *(P)*-biphenyl (*M*)-**1** (250 mg, 913 µmol) as white solid. The spectroscopic data were in accordance with those previously obtained for racemic material.

Mp: 126 °C **Lit. Mp:** 125–126 °C[37]

$[\alpha]_D^{25} = -36.8$ (c = 1.0, $CHCl_3$) **Lit.** $[\alpha]_D^{25} = -35.1$ (c = 0.75, $CHCl_3$)[37]

The analytical data correspond to the data given in literature.[37, 38]

rac-3,3′-Dibromo-4,4′,6,6′-tetramethoxy-2,2′-dimethyl-1,1′-biphenyl _rac_-(264)

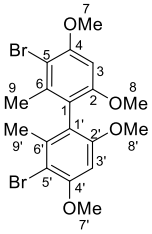

rac-**264**

rac-**152** (1.01 g, 3.34 mmol) was dissolved in dry CH_2Cl_2 (12 mL) and cooled down to 0 °C. NBS (1.19 g, 6.68 mmol) was added, and the reaction mixture was stirred for 1 hour. After full conversion, the reaction was quenched by adding 10% aq. sodium sulfite solution. The reaction mixture was extracted with CH_2Cl_2 for three times and washed with brine. The combined organic layer was dried over $MgSO_4$. After concentration at reduced pressure 3,3′-dibromo-4,4′,6,6′-tetramethoxy-2,2′-dimethyl-1,1′-biphenyl _rac_-(**264**) (1.49 g, 3.24 mmol) was obtained in 97% yield as a white solid. The product could be used without further purification.

R_f (PE:EE, 60:40) = 0.64

^{1}H-NMR ($CDCl_3$, 600 MHz) δ 6.46 (s, 2H, 5-H, 5′-H), 3.95 (s, 6H, 7-OC$\underline{H}_3$, 7′- OC$\underline{H}_3$), 3.71 (s, 6H, 8-OC$\underline{H}_3$, 8′-OC$\underline{H}_3$), 2.03 (s, 6H, 9-C$\underline{H}_3$, 9′-C$\underline{H}_3$).

^{13}C-NMR ($CDCl_3$, 151 MHz) δ 157.13 (C-6, C-6′), 155.95 (C-4, C-4′), 139.26 (C-2, C-2′), 119.75 (C-1, C-1′), 105.89 (C-3, C-3′), 94.44 (C-5, C-5′), 56.43 (C-7, C-7′), 56.18 (C-8, C-8′), 20.55 (C-9, C-9′).

IR: ν[cm^{-1}]: 1588, 1465, 1322, 1203, 1105, 1079, 1032, 810, 651.

MS (ESI): m/z = 460.9 $[M+H]^+$.

Mp: 230 °C **Lit. Mp:** 230–232 °C[224]

HPLC: Column: Lux Amylose-1, *Fa. Phenomenex* (250x4.6 mm); 5 µL, 25 °C, 0.5 mL/min, 274 nm; solvent: *n*-heptane:2-propanol (98:2), t_R = 14.2, 17.0 min.

The analytical data correspond to the data given in literature.[224]

(*M*)-3,3′-Dibromo-4,4′,6,6′-tetramethoxy-2,2′-dimethyl-1,1′-biphenyl (*M*)-(264)

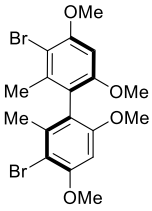

The product was synthesized according to the racemic synthesis of *rac*-**264**. The (*M*)-biaryl (*M*)-**264** (292 mg, 635 µmol, >99% *ee*) was obtained in 96% yield from *(M)*-biaryl (*M*)-**152** (200 mg, 661 µmol) as white solid. The spectroscopic data were in accordance with those previously obtained for racemic material.

Mp: 193 °C; $[\alpha]_D^{25} = 31.4$ (c = 1.0, $CHCl_3$)

(*P*)-3,3′-Dibromo-4,4′,6,6′-tetramethoxy-2,2′-dimethyl-1,1′-biphenyl (*P*)-(264)

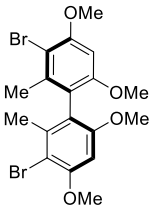

The product was synthesized according to the racemic synthesis of *rac*-**264**. The (*P*)-biaryl (*P*)-**264** (319 mg, 693 µmol, 98% *ee*) was obtained in 97% yield from *(P)*-biaryl (*P*)-**152** (215 mg, 711 µmol) as white solid. The spectroscopic data were in accordance with those previously obtained for racemic material.

Mp: 190 °C; $[\alpha]_D^{25} = -40$ (c = 1.0, $CHCl_3$)

***rac*-Dimethyl-4,4′,6,6′-tetramethoxy-2,2′-dimethyl-[1,1′-biphenyl]-3,3′-dicarboxylate *rac*-(266)**

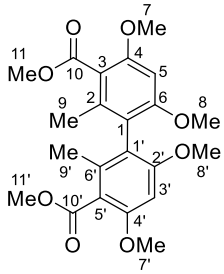

rac-**266**

Brominated biaryl *rac*-**264** (332 mg, 721 µmol) was given in a schlenk flask and dissolved in anhydrous THF (16 mL). The reaction mixture was cooled down to −78 °C. *n*-Butyllithium (2.5 M in pentane, 0.61 mL, 1.7 mmol) was added dropwise at −78 °C. After stirring for 30 minutes, gaseous CO_2 is purged into the reaction mixture which evolved by solid CO_2 in a syringe. The reaction mixture was first stirred for further 5 minutes at −78 °C and

then warmed to r.t. over 1 hour. The reaction was quenched by addition of saturated NH_4Cl solution and acidified with 1 M HCl. After three extractions with EtOAc, the combined organic phase was dried over $MgSO_4$ and concentrated under reduced pressure. The crude product was used without further purification. The formed carboxylic acid and anhydrous potassium carbonate (249 mg, 1.80 mmol) was given in a round bottom flask. Ethanol (8 mL) was added to dissolve the starting material. After 10 minutes stirring at r.t. dimethyl sulfate (0.27 mL, 2.9 mmol) was added dropwise. The reaction mixture was stirred over night at r.t. After full conversion, the mixture was quenched by adding 10% aq. sodium sulfite solution and stirring for 30 minutes at r.t. The organic phase was extracted three times with EtOAc and dried over $MgSO_4$. After the solvent was evaporated under reduced pressure, the crude product was purified by column chromatography (PE/EtOAC = 60:40 to 50:50) affording the methyl ester *rac*-**266** (208 mg, 0.497 mmol) in 69% yield over two steps as a white solid.

R_f (PE:EE, 60:40) = 0.29

^{1}H-NMR ($CDCl_3$, 600 MHz) δ 6.40 (s, 2H, 5-H, 5′-H), 3.89 (s, 6H, 11-OC$\underline{H}_3$, 11′-OC$\underline{H}_3$), 3.87 (s, 6H, 7-OC$\underline{H}_3$, 7′-OC$\underline{H}_3$), 3.70 (s, 6H, 8-OC$\underline{H}_3$, 8′-OC$\underline{H}_3$), 1.84 (s, 6H, 9-C$\underline{H}_3$, 9′-C$\underline{H}_3$).

^{13}C-NMR ($CDCl_3$, 151 MHz) δ 169.40 (C-10, C-10′), 159.05 (C-6, C-6′), 157.17 (C-4, C-4′), 137.16 (C-2, C-2′), 118.11 (C-1, C-1′), 116.82 (C-3, C-3′), 93.18 (C-5, C-5′), 56.03 (C-7, C-7′), 55.93 (C-8, C-8′), 52.24 (C-11, C-11′), 16.94 (C-9, C-9′).

IR: ν[cm^{-1}]: 2952, 1721, 1586, 1317, 1288, 1203, 1075, 938.

MS (ESI): m/z = 419.3 $[M+H]^+$.

Mp: 201 °C **Lit. Mp:** 209 °C[337]

HPLC: Column: Chiracel OD-H (250x4.6 mm); 5 µL, 25 °C, 0.5 mL/min, 331 nm; solvent: *n*-heptane:2-propanol (95:5), t_R = 44.9, 53.4 min.

The analytical data correspond to the data given in literature.[337]

(*M*)-Dimethyl-4,4′,6,6′-tetramethoxy-2,2′-dimethyl-[1,1′-biphenyl]-3,3′-dicarboxylate (*M*)-(266)

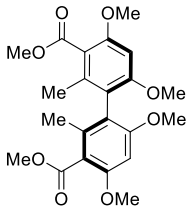

The product was synthesized according to the racemic synthesis of *rac*-**266**. The (*M*)-methyl ester (*M*)-**266** (238 mg, 0.568 mmol, >99% *ee*) was obtained in 86% yield over two steps from (*M*)-biaryl (*M*)-**264** (200 mg, 0.66 mmol) as white solid. The spectroscopic data were in accordance with those previously obtained for racemic material.

Mp: 177 °C; $[\boldsymbol{\alpha}]_{\boldsymbol{D}}^{25} = 11.0$ (c = 1.0, $CHCl_3$)

(*P*)-Dimethyl-4,4′,6,6′-tetramethoxy-2,2′-dimethyl-[1,1′-biphenyl]-3,3′-dicarboxylate (*P*)-(266)

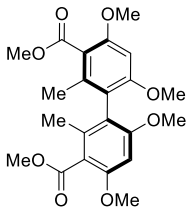

The product was synthesized according to the racemic synthesis of *rac*-**266**. The (*P*)-methyl ester (*P*)-**266** (181 mg, 0.433 mmol, 99% *ee*) was obtained in 73% yield over two steps from (*P*)-biaryl (*P*)-**264** (271 mg, 0.59 mmol) as white solid. The spectroscopic data were in accordance with those previously obtained for racemic material.

Mp: 178 °C; $[\boldsymbol{\alpha}]_{\boldsymbol{D}}^{25} = -22.2$ (c = 1.0, $CHCl_3$)

rac-Dimethyl-4,4′-dihydroxy-6,6′-dimethoxy-2,2′-dimethyl-[1,1′-biphenyl]-3,3′-dicarboxylate _rac_-(268)

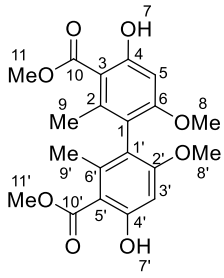

rac-**268**

Methyl ester _rac_-**266** (470 mg, 1.12 mmol) was dissolved in dried CH_2Cl_2 (50 mL) and cooled down to −78 °C. BCl_3 solution (1 M in CH_2Cl_2, 2.46 mL, 2.46 mmol) was added dropwise. The reaction mixture was stirred overnight in the slowly warming acetone-dry ice bath. After full conversion KP_i-buffer was added to quench the reaction. The mixture was extracted three times with CH_2Cl_2 and dried over $MgSO_4$. The combined organic phase was concentrated under reduced pressure. After purification by column chromatography (PE:EtOAc = 80:20 to 60:40), product _rac_-**268** (334 mg, 856 µmol) in 76% yield as a white solid.

R_f (PE:EE, 60:40) = 0.80

^{1}H-NMR ($CDCl_3$, 600 MHz) δ 11.78 (s, 2H, 7-H, 7′-H), 6.43 (s, 2H, 5-H, 5′-H), 3.92 (s, 6H, 11-OC$\underline{H}_3$, 11′-OC$\underline{H}_3$), 3.69 (s, 6H, 8-OC$\underline{H}_3$, 8′-OC$\underline{H}_3$), 2.11 (s, 6H, 9-C$\underline{H}_3$, 9′-C$\underline{H}_3$).

^{13}C-NMR ($CDCl_3$, 151 MHz) δ 172.68 (C-10, C-10′), 164.69 (C-4, C-4′), 162.51 (C-6, C-6′), 141.62 (C-2, C-2′), 119.45 (C-1, C-1′), 105.85 (C-3, C-3′), 97.56 (C-5, C-5′), 55.89 (C-8, C-8′), 51.98 (C-11, C-11′), 19.52 (C-9, C-9′).

IR: ν[cm^{-1}]: 2939, 1575, 1315, 1254, 1225, 1198, 1167, 1086, 1043, 950, 827, 621.

MS (ESI): m/z = 391.0 $[M+H]^+$.

Mp: 183 °C **Lit. Mp:** 183 °C[337, 338]

HPLC: Column: Lux Amylose-1, *Fa. Phenomenex* (250x4.6 mm); 5 µL, 25 °C, 0.5 mL/min, 232 nm; solvent: *n*-heptane:2-propanol (50:50), t_R = 11.3, 17.5 min.

The analytical data correspond to the data given in literature.[337]

(*M*)-Dimethyl-4,4′-dihydroxy-6,6′-dimethoxy-2,2′-dimethyl-[1,1′-biphenyl]-3,3′-dicarboxylate (*M*)-(268)

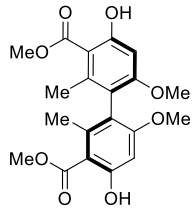

The product was synthesized according to the racemic synthesis of *rac*-**268**. The (*M*)-biaryl (*M*)-**268** (116 mg, 0.297 mmol, 99% *ee*) was obtained in 77% yield from (*M*)-biaryl (*M*)-**266** (162 mg, 0.387 mmol) as white solid. The spectroscopic data were in accordance with those previously obtained for racemic material.

Mp: 169 °C; $[\boldsymbol{\alpha}]_{\boldsymbol{D}}^{25} = 4.2$ (c = 1.0, $CHCl_3$)

(*P*)-Dimethyl-4,4′-dihydroxy-6,6′-dimethoxy-2,2′-dimethyl-[1,1′-biphenyl]-3,3′-dicarboxylate (*P*)-(268)

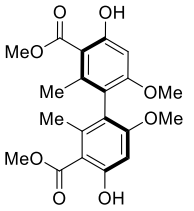

The product was synthesized according to the racemic synthesis of *rac*-**268**. The (*P*)-biaryl (*P*)-**268** (118 mg, 0.302 mmol, 98% *ee*) was obtained in 79% yield from (*P*)-biaryl (*P*)-**266** (160 mg, 0.382 mmol) as white solid. The spectroscopic data were in accordance with those previously obtained for racemic material.

Mp: 135 °C; $[\boldsymbol{\alpha}]_{\boldsymbol{D}}^{25} = -32.2$ (c = 1.0, $CHCl_3$)

***rac*-2,2′-Diamino-7,7′-dimethoxy-5,5′-dimethyl-4H,4′H-[6,6′-bichromene]-4,4′-dione *rac*-(270)**

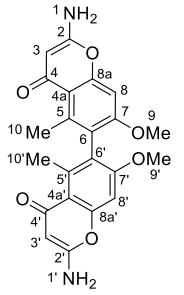

rac-**270**

Anhydrous acetonitrile (0.086 mL, 1.6 mmol) was given in dry THF (10 mL) and cooled down to −78 °C. *n*-Butyllithium (2 M in hexane, 0.82 mL, 1.6 mmol) was added dropwise. The mixture was stirred for 45 minutes at −78 °C. After addition of the orsellinate *rac*-**268** (80 mg, 0.21 mmol) dissolved in dry THF (4 mL) dropwise over 10 minutes, the mixture was continued to stir for 3 hours at −78 °C. Afterwards additional *n*-butyllithium (2 M in hexane, 0.41 mL, 0.82 mmol) was added. The mixture was warmed up to r.t. and stirred for 1 hour. The reaction was quenched by addition of aqueous NH_4Cl solution. The organic phase was extracted three times with EtOAc and dried over $MgSO_4$. After the solvent was evaporated under reduced pressure, the crude product was purified by column chromatography (EtOAc/2-Propanol = 1:0 to 5:1 to 3:1) affording the aminochromenone *rac*-**270** (57 mg, 0.14 mmol) in 68% yield as a light brown solid. The mono-functionalized product *rac*-**269** (30 mg, 75 µmol) in 38% yield could be isolated and was converted in the same procedure towards the desired difunctionalized product.

R_f (EE:*i*PrOH, 3:1) = 0.28

^{1}H-NMR (DMSO, 600 MHz) δ 7.15 (s, 4H,1-N$\underline{H}_2$, 1-N$\underline{H}_2$), 6.79 (s, 2H, 8-H, 8′-H), 5.05 (s, 2H, 3-H, 3′-H), 3.69 (s, 6H, 9-OC$\underline{H}_3$, 9′-OC$\underline{H}_3$), 2.30 (s, 6H, 10-C$\underline{H}_3$, 10′-C$\underline{H}_3$).

^{13}C-NMR (DMSO, 151 MHz) δ 177.61 (C-4, C-4′), 163.02 (C-2, C-2′), 158.77 (C-8a, C-8a′), 155.74 (C-7, C-7′), 138.82 (C-5, C-5′), 122.98 (C-6, C-6′), 114.42 (C-4a, C-4a′), 96.88 (C-8, C-8′), 86.01 (C-3, C-3′), 56.81 (C-9, C-9′), 17.29 (C-10, C-10′).

IR: ν[cm^{-1}]: 3330, 3142, 1647, 1596, 1638, 1439, 1403, 1260, 1200, 1123, 1043, 825, 524.

MS (ESI): m/z = 409.1 $[M+H]^+$.

Mp: 264 °C **Lit. Mp:** 262 °C[38]

HPLC: Column: Lux Amylose-1, *Fa. Phenomenex* (250x4.6 mm); 5 µL, 25 °C, 0.5 mL/min, 238 nm; solvent: *n*-heptane:2-propanol (75:25), t_R = 13.9, 17.3 min.

The analytical data correspond to the data given in literature.[38]

***rac*-Methyl-3-(2-amino-7-methoxy-5-methyl-4-oxo-4H-chromen-6-yl)-6-hydroxy-4-methoxy-2-methylbenzoate *rac*-(269)**

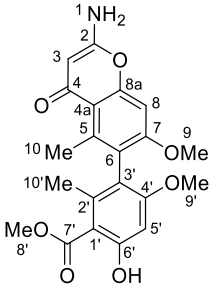

rac-**269**

R_f (EE:*i*PrOH, 3:1) = 0.63

^{1}H-NMR (DMSO-d_6, 600 MHz) δ 10.20 (s, 1H, OH), 7.09 (s, 2H, N$\underline{H}_2$), 6.75 (s, 1H, 8-H), 6.44 (s, 1H, 5′-H), 5.04 (s, 1H, 3-H), 3.78 (s, 3H, 8′-OC$\underline{H}_3$), 3.70 (s, 3H, 9-OC$\underline{H}_3$), 3.58 (s, 3H, 9′-OC$\underline{H}_3$), 2.31 (s, 3H, 10-C$\underline{H}_3$), 1.75 (s, 3H, 10′-C$\underline{H}_3$).

^{13}C-NMR (DMSO-d_6, 151 MHz) δ 178.20 (C-2), 169.23 (C-7′), 163.01 (C-4), 159.03 (C-7), 158.84 (C-4′), 156.79 (C-6′), 155.64 (C-8a), 139.13 (C-4a), 135.40 (C-1′), 123.16 (C-6), 119.22 (C-3′), 116.18 (C-5), 112.61 (C-2′), 97.03 (C-5′), 96.76 (C-8), 85.99 (C-3), 55.78 (C-9), 55.38 (C-9′), 51.48 (C-8′), 17.44 (C-10), 17.22 (C-10′).

IR: ν[cm^{-1}]: 2933, 1651, 1583, 1439, 1407, 1322, 1244, 1200, 1171, 825, 630, 528.

HRMS (ESI): m/z = Found: 400.1389 ($C_{21}H_{22}NO_7$) $[(M+H)]^+$, calculated: 400.1391.

Mp: 97 °C

(*M*)-2,2′-Diamino-7,7′-dimethoxy-5,5′-dimethyl-4H,4′H-[6,6′-bichromene]-4,4′-dione (*M*)-(270)

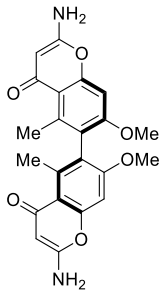

The product was synthesized according to the racemic synthesis *rac*-**270**. The *(M)*-biaryl (*M*)-**270** (65 mg, 0.16 mmol, >99% *ee*) was obtained in 68% yield from (*M*)-biaryl (*M*)-**268** (91 mg, 0.23 mmol) as light yellow crystals. The spectroscopic data were in accordance with those previously obtained for racemic material.

Mp: 263 °C; $[\boldsymbol{\alpha}]_{\boldsymbol{D}}^{25} = 17.2$(c = 1.0, CH_3OH)

(*P*)-2,2′-Diamino-7,7′-dimethoxy-5,5′-dimethyl-4H,4′H-[6,6′-bichromene]-4,4′-dione (*P*)-(270)

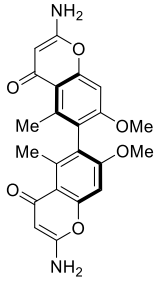

The product was synthesized according to the racemic synthesis *rac*-**270**. The *(P)*-biaryl (*P*)-**270** (69 mg, 0.17 mmol, 98% *ee*) was obtained in 78% yield from (*P*)-biaryl (*P*)-**268** (85 mg, 0.22 mmol) as light yellow crystals. The spectroscopic data were in accordance with those previously obtained for racemic material.

Mp: 264 °C; $[\boldsymbol{\alpha}]_{\boldsymbol{D}}^{25} = -24.2$(c = 1.0, CH_3OH)

***rac*-Isokotanin A *rac*-(4)**

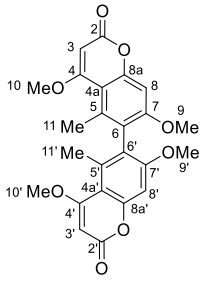

rac-**4**

The aminochromenone *rac*-**270** (130 mg, 0.318 mmol) was dissolved in methanol (20 mL). 36% HCl (20 mL) was added carefully. The mixture was stirred at reflux for 3.5 hours. After cooling down, water was added, where a white solid precipitated. Potassium

carbonate was added carefully to adjust the pH to 1. Methanol was evaporated at the rotary evaporator. The residue was cooled down in an ice bath for 15 minutes, whereas the product precipitated. The precipitate was filtered off, washed with water, and lyophilized overnight.

The precipitated hydroxychromenone *rac*-**272** was used without further purification. NaH (32 mg, 0.80 mmol) was given in a schlenk flask. The chromenone, dissolved in anhydrous DMF (7 mL), was added. After gas evolution has faded, dimethyl sulfate (0.091 mL, 0.96 mmol) was added, and the mixture was stirred for 2 hours at r.t. After full conversion, the mixture was quenched by adding 10% aq. sodium sulfite solution and stirring for 30 minutes at r.t. The mixture was acidified by addition of 1 M HCl. The organic phase was extracted three times with EtOAc and dried over $MgSO_4$. After the solvent was evaporated under reduced pressure, the crude product was purified by column chromatography (CH_2Cl_2/EtOAc = 3:1) affording *rac*-isokotanin A *rac*-(**4**) (44 mg, 0.10 mmol) in 30% yield over two steps as a white solid.

R_f (CH_2Cl_2:EE, 3:1) = 0.32

^{1}H-NMR ($CDCl_3$, 600 MHz) δ 6.78 (s, 2H, 8-H, 8′-H), 5.59 (s, 2H, 3-H, 3′-H), 3.94 (s, 6H, 10-OC<u>H</u>$_3$, 10′-OC<u>H</u>$_3$), 3.72 (s, 6H, 9-OC<u>H</u>$_3$, 9′-OC<u>H</u>$_3$), 2.23 (s, 6H, 11-C<u>H</u>$_3$, 11′-C<u>H</u>$_3$).

^{13}C-NMR ($CDCl_3$, 151 MHz) δ 170.19 (C-2, C-2′), 163.13 (C-4, C-4′), 160.28 (C-7, C-7′), 156.44 (C-8a, C-8a′), 137.33 (C-5, C-5′), 123.57 (C-6, C-6′), 108.24 (C-4a, C-4a′), 97.58 (C-8, C-8′), 88.09 (C-3, C-3′), 56.15 (C-10, C-10′), 56.11 (C-9, C-9′), 18.87 (C-11, C-11′).

IR: ν[cm^{-1}]: 2942, 2848, 1715, 1591, 1365, 1252, 1197, 1170, 1055, 973, 806.

MS (ESI): m/z = 439.2 $[M+H]^+$.

Mp: 337 °C **Lit. Mp:** 321 °C[38]

HPLC: Chiracel OD-H (250x4.6 mm); 5 µL, 25 °C, 0.5 mL/min, 331 nm; solvent: *n*-heptane:2-propanol (30:70), t_R = 21.7, 32.2 min.

The analytical data correspond to the data given in literature.[38]

***(M)*-Isokotanin A (*M*)-(4)**

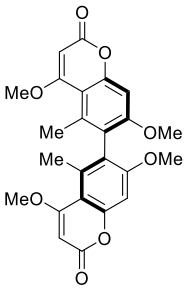

The product was synthesized according to the racemic synthesis of *rac*-**4**. The *(M)*-isokotanin A (*M*)-(**4**) (18 mg, 41 µmol, >99% *ee*) was obtained in 26% yield over two steps from (*M*)-aminochromenone (*M*)-**270** (70 mg, 0.17 mmol) as light yellow crystals. The spectroscopic data were in accordance with those previously obtained for racemic material.

Mp: 288 °C **Lit. Mp:** 286–289 °C[37]

$[\boldsymbol{\alpha}]_{\boldsymbol{D}}^{\mathbf{25}} = 48.0$ (c = 1.0, $CHCl_3$) **Lit.** $[\boldsymbol{\alpha}]_{\boldsymbol{D}}^{\mathbf{25}} = 21.6$ (c = 0.26, $CHCl_3$)[37]

The analytical data correspond to the data given in literature.[37]

9 References

[1] J. Greb, T. Drennhaus, M. K. Klischan, Z. W. Schroeder, W. Frey, J. Pietruszka, *Chem. Eur. J.* **2023**, *29*, e202300941; 'A Common C2-Symmetric 2,2'-Biphenol Building Block and its Application in the Synthesis of (+)-di-*epi*-Gonytolide A'.

[2] R. C. Ganardi, J. Greb, B. Henssen, J. Pietruszka, *Adv. Synth. Catal.* **2023***, 365,* 3512-3520 ; 'Atroposelective Total Synthesis of (+)-Isokotanin A via Combined Metal and Enzyme Catalysis'.

[3] N. R. Farnsworth, O. Akerele, A. S. Bingel, D. D. Soejarto, Z. Guo, *Bull. World Health Organ.* **1985**, *63*, 965; 'Medicinal plants in therapy'.

[4] J. A. Beutler, *Curr. Protoc. Pharmacol.* **2009**, *46*, 9.11.11-19.11.21; 'Natural products as a foundation for drug discovery'.

[5] J. Drews, *Science* **2000**, *287*, 1960-1964; 'Drug discovery: a historical perspective'.

[6] B. Chopra, A. K. Dhingra, *Phytother. Res.* **2021**, *35*, 4660-4702; 'Natural products: A lead for drug discovery and development'.

[7] D. J. Newman, G. M. Cragg, *J. Nat. Prod.* **2020**, *83*, 770-803; 'Natural products as sources of new drugs over the nearly four decades from 01/1981 to 09/2019'.

[8] T. Classen, J. Pietruszka, *Bioorg. Med. Chem.* **2018**, *26*, 1285-1303; 'Complex molecules, clever solutions–Enzymatic approaches towards natural product and active agent syntheses'.

[9] C. Friedrich, *Pharm. Unserer Zeit* **2006**, *35*, 392-398; 'Die Geschichte der *β*-Lactam-Antibiotika: Zwischen Zufall und gezielter Entwicklung'.

[10] A. L. Demain, *Med. Res. Rev.* **2009**, *29*, 821-842; 'Antibiotics: natural products essential to human health'.

[11] Y. Tu, *Nat. Med.* **2011**, *17*, 1217-1220; 'The discovery of artemisinin (qinghaosu) and gifts from Chinese medicine'.

[12] J. Barrios-González, R. U. Miranda, *Appl. Microbiol. Biotechnol.* **2010**, *85*, 869-883; 'Biotechnological production and applications of statins'.

[13] K. Priyadarshini, A. U. Keerthi, *Med. Chem.* **2012**, *2*, 139-141; 'Paclitaxel against cancer: a short review'.

[14] C. Khanna, M. Rosenberg, D. Vail, *J. Vet. Intern. Med.* **2015**, *29*, 1006-1012; 'A review of paclitaxel and novel formulations including those suitable for use in dogs'.

[15] V. Nikolic, I. Savic, I. Savic, L. Nikolic, M. Stankovic, V. Marinkovic, *Open Med.* **2011**, *6*, 527-536; 'Paclitaxel as an anticancer agent: Isolation, Activity, Synthesis and Stability'.

[16] L. Satish, Y. Seher, K. Rakkammal, P. Muthuramalingam, C. R. Lakshmi, A. Hemasundar, K. Prasanth, S. Shamili, M. K. Swamy, M. S. Dhanarajan, in *Paclitaxel*, Elsevier, **2022**, pp. 229-250.

[17] M. Salehi, S. Farhadi, in *Paclitaxel*, Elsevier, **2022**, pp. 129-153.

[18] D. Frense, *Appl. Microbiol. Biotechnol.* **2007**, *73*, 1233-1240; 'Taxanes: perspectives for biotechnological production'.

[19] R. Daghrir, P. Drogui, *Environ. Chem. Lett.* **2013**, *11*, 209-227; 'Tetracycline antibiotics in the environment: a review'.

[20] N. Kardos, A. L. Demain, *Appl. Microbiol. Biotechnol.* **2011**, *92*, 677-687; 'Penicillin: the medicine with the greatest impact on therapeutic outcomes'.

[21] R. Panchagnula, *Int. J. Pharm.* **1998**, *172*, 1-15; 'Pharmaceutical aspects of paclitaxel'.

[22] J. Millership, P. Collier, *Chirality* **1997**, *9*, 313-316; 'Topical administration of racemic ibuprofen'.

[23] H. Cheng, J. D. Rogers, J. L. Demetriades, S. D. Holland, J. R. Seibold, E. Depuy, *Pharm. Res.* **1994**, *11*, 824-830; 'Pharmacokinetics and bioinversion of ibuprofen enantiomers in humans'.
[24] E. Sanganyado, Z. Lu, Q. Fu, D. Schlenk, J. Gan, *Water Res.* **2017**, *124*, 527-542; 'Chiral pharmaceuticals: A review on their environmental occurrence and fate processes'.
[25] C. Meierhofer, S. Dunzendorfer, C. J. Wiedermann, *BioDrugs* **2001**, *15*, 681-703; 'Theoretical basis for the activity of thalidomide'.
[26] Y. Hashimoto, *Bioorg. Med. Chem.* **2002**, *10*, 461-479; 'Structural development of biological response modifiers based on thalidomide'.
[27] K. Roth, *Chem. Unserer Zeit* **2005**, *39*, 212-217; 'Eine unendliche chemische Geschichte'.
[28] K. Stoschitzky, W. Lindner, G. Zernig, *J. Clin. Bas. Cardiol.* **1998**, *1*, 15-19; 'Racemic beta-blockers-fixed combinations of different drugs'.
[29] L. A. Nguyen, H. He, C. Pham-Huy, *Int. J. Biomed. Sci.* **2006**, *2*, 85; 'Chiral drugs: an overview'.
[30] R. Noyori, *Angew. Chem. Int. Ed.* **2002**, *41*, 2008-2022; 'Asymmetric catalysis: science and opportunities (Nobel lecture)'.
[31] R. Noyori, *Angew. Chem.* **2002**, *114*, 2108-2123; 'Asymmetrische Katalyse: Kenntnisstand und Perspektiven (Nobel-Vortrag)'.
[32] E. L. Bell, W. Finnigan, S. P. France, A. P. Green, M. A. Hayes, L. J. Hepworth, S. L. Lovelock, H. Niikura, S. Osuna, E. Romero, *Nat. Rev. Methods Primers* **2021**, *1*, 46; 'Biocatalysis'.
[33] R. Wohlgemuth, *New Biotech.* **2021**, *60*, 113-123; 'Biocatalysis–Key enabling tools from biocatalytic one-step and multi-step reactions to biocatalytic total synthesis'.
[34] B. Skrobo, J. D. Rolfes, J. Deska, *Tetrahedron* **2016**, *72*, 1257-1275; 'Enzymatic approaches for the preparation of optically active non-centrochiral compounds'.
[35] R. J. Kazlauskas, *J. Am. Chem. Soc.* **1989**, *111*, 4953-4959; 'Resolution of binaphthols and spirobiindanols using cholesterol esterase'.
[36] G.-Q. Lin, M. Zhong, *Tetrahedron Lett.* **1996**, *37*, 3015-3018; 'The first synthesis of optically pure (+)-and (−)-isokotanin A and the assignment of their absolute configuration'.
[37] G. Bringmann, J. Hinrichs, P. Henschel, J. Kraus, K. Peters, E. M. Peters, *Eur. J. Org. Chem.* **2002**, *2002*, 1096-1106; 'Atropo-Enantioselective Synthesis of the Natural Bicoumarin (+)-Isokotanin A via a Configurationally Stable Biaryl Lactone'.
[38] W. Hüttel, M. Nieger, M. Müller, *Synthesis* **2003**, 1803-1808; 'A Short and Efficient Total Synthesis of the Naturally Occurring Coumarins Siderin, Kotanin, Isokotanin A and Desertorin C'.
[39] J. Graff, T. Debande, J. Praz, L. Guénée, A. Alexakis, *Org. Lett.* **2013**, *15*, 4270-4273; 'Asymmetric Bromine–Lithium Exchange: Application toward the Synthesis of Natural Product'.
[40] U. T. Bornscheuer, R. J. Kazlauskas, *Hydrolases in organic synthesis: regio-and stereoselective biotransformations*, John Wiley & Sons, **2006**.
[41] E. Shukla, A. D. Bendre, S. M. Gaikwad, *Hydrolases: The Most Diverse Class of Enzymes*, IntechOpen London, **2022**.
[42] K. Faber, *Biotransformations in Organic Chemistry*, Springer, **2004**.
[43] R. D. Schmid, R. Verger, *Angew. Chem. Int. Ed.* **1998**, *37*, 1608-1633; 'Lipases: interfacial enzymes with attractive applications'.
[44] R. D. Schmid, R. Verger, *Angew. Chem.* **1998**, *110*, 1694-1720; 'Lipasen: Grenzflächen-Enzyme mit attraktiven Anwendungen'.

[45] A. Ghanem, H. Y. Aboul-Enein, *Chirality* **2005**, *17*, 1-15; 'Application of lipases in kinetic resolution of racemates'.
[46] D. Méndez-Sánchez, M. López-Iglesias, V. Gotor-Fernández, *Curr. Org. Chem.* **2016**, *20*, 1186-1203; 'Hydrolases in organic chemistry. Recent achievements in the synthesis of pharmaceuticals'.
[47] H. Smidt, A. Fischer, P. Fischer, R. D. Schmid, *Biotechnol. Tech.* **1996**, *10*, 335-338; 'Preparation of optically pure chiral amines by lipase-catalyzed enantioselective hydrolysis of *N*-acyl-amines'.
[48] P. Carter, J. A. Wells, *Nature* **1988**, *332*, 564; 'Dissecting the catalytic triad of a serine protease'.
[49] C. C. Gruber, I. Lavandera, K. Faber, W. Kroutil, *Adv. Synth. Catal.* **2006**, *348*, 1789-1805; 'From a racemate to a single enantiomer: deracemization by stereoinversion'.
[50] K. Faber, *Chem. Eur. J.* **2001**, *7*, 5004-5010; 'Non-sequential processes for the transformation of a racemate into a single stereoisomeric product: proposal for stereochemical classification'.
[51] M. Breuer, K. Ditrich, T. Habicher, B. Hauer, M. Keßeler, R. Stürmer, T. Zelinski, *Angew. Chem. Int. Ed.* **2004**, *43*, 788-824; 'Industrial methods for the production of optically active intermediates'.
[52] M. Breuer, K. Ditrich, T. Habicher, B. Hauer, M. Keßeler, R. Stürmer, T. Zelinski, *Angew. Chem.* **2004**, *116*, 806-843; 'Industrielle Verfahren zur Herstellung von optisch aktiven Zwischenprodukten'.
[53] A. S. Bommarius, M. Schwarm, K. Drauz, *Chimia* **2001**, *55*, 50-50; 'Comparison of different chemoenzymatic process routes to enantiomerically pure amino acids'.
[54] G. Fuelling, C. J. Sih, *J. Am. Chem. Soc.* **1987**, *109*, 2845-2846; 'Enzymatic Second-Order Asymmetric Hydrolysis of Ketorolac Esters: In Situ Racemization'.
[55] T. Suzuki, *Tetrahedron Lett.* **2017**, *58*, 4731-4739; 'Recent topics in the desymmetrization of *meso*-diols'.
[56] C. Neri, J. M. Williams, *Adv. Synth. Catal.* **2003**, *345*, 835-848; 'New routes to chiral Evans auxiliaries by enzymatic desymmetrisation and resolution strategies'.
[57] C. S. Chen, Y. Fujimoto, G. Girdaukas, C. J. Sih, *J. Am. Chem. Soc.* **1982**, *104*, 7294-7299; 'Quantitative analyses of biochemical kinetic resolutions of enantiomers'.
[58] M. D. Greenhalgh, J. E. Taylor, A. D. Smith, *Tetrahedron* **2018**, *74*, 5554-5560; 'Best practice considerations for using the selectivity factor, s, as a metric for the efficiency of kinetic resolutions'.
[59] J. M. Berg, J. L. Tymoczko, L. Stryer, *Biochemie*, Springer, **2018**.
[60] A. J. J. Straathof, J. A. Jongejan, *Enzyme Microb. Tech.* **1997**, *21*, 559-571; 'The enantiomeric ratio: origin, determination and prediction'.
[61] W. Kroutil, A. Kleewein, K. Faber, *Tetrahedron: Asymmetry* **1997**, *8*, 3263-3274; 'A computer program for analysis, simulation and optimization of asymmetric catalytic processes proceeding through two consecutive steps. Type 2: sequential kinetic resolutions'.
[62] W. Kroutil, A. Kleewein, K. Faber, 22.07.2024, http://biocatalysis.uni-graz.at/biocatalysis-tools/sekire2, **2019**.
[63] G. H. Christie, J. Kenner, *J. Chem. Soc., Trans.* **1922**, *121*, 614-620; 'LXXI.—The molecular configurations of polynuclear aromatic compounds. Part I. The resolution of γ-6: 6'-dinitro-and 4:6:4':6'-tetranitro-diphenic acids into optically active components'.

[64] G. Bringmann, A. J. Price Mortimer, P. A. Keller, M. J. Gresser, J. Garner, M. Breuning, *Angew. Chem. Int. Ed.* **2005**, *44*, 5384-5427; 'Atroposelective synthesis of axially chiral biaryl compounds'.
[65] G. Bringmann, A. J. Price Mortimer, P. A. Keller, M. J. Gresser, J. Garner, M. Breuning, *Angew. Chem.* **2005**, *117*, 5518-5563; 'Atropselektive Synthese axial-chiraler Biaryle'.
[66] G. Bringmann, T. Gulder, T. A. M. Gulder, M. Breuning, *Chem. Rev.* **2011**, *111*, 563-639; 'Atroposelective total synthesis of axially chiral biaryl natural products'.
[67] C. Sanfilippo, G. Nicolosi, G. Delogu, D. Fabbri, M. A. Dettori, *Tetrahedron: Asymmetry* **2003**, *14*, 3267-3270; 'Access to optically active 2,2'-dihydroxy-6,6'-dimethoxy-1,1'-biphenyl by a simple biocatalytic procedure'.
[68] G. Ma, M. P. Sibi, *Chem. Eur. J.* **2015**, *21*, 11644-11657; 'Catalytic kinetic resolution of biaryl compounds'.
[69] M. K. Hadden, B. S. J. Blagg, *Anti-Cancer Agents Med. Chem.* **2008**, *8*, 807-816; 'Dimeric approaches to anti-cancer chemotherapeutics'.
[70] J. K. Cheng, S.-H. Xiang, S. Li, L. Ye, B. Tan, *Chem. Rev.* **2021**, *121*, 4805-4902; 'Recent advances in catalytic asymmetric construction of atropisomers'.
[71] G. Ma, C. Deng, J. Deng, M. P. Sibi, *Org. Biomol. Chem.* **2018**, *16*, 3121-3126; 'Dynamic kinetic resolution of biaryl atropisomers by chiral dialkylaminopyridine catalysts'.
[72] M. R. Boyd, Y. F. Hallock, J. H. Cardellina, K. P. Manfredi, J. W. Blunt, J. B. McMahon, R. W. Buckheit Jr, G. Bringmann, M. Schäffer, G. M. Cragg, *J. Med. Chem.* **1994**, *37*, 1740-1745; 'Anti-HIV michellamines from Ancistrocladus korupensis'.
[73] J. Supko, L. Malspeis, *Antimicrob. Agents Chemother.* **1995**, *39*, 9-14; 'Pharmacokinetics of michellamine B, a naphthylisoquinoline alkaloid with in vitro activity against human immunodeficiency virus types 1 and 2, in the mouse and dog'.
[74] E. Dagne, W. Steglich, *Phytochem.* **1984**, *23*, 1729-1731; 'Knipholone: a unique anthraquinone derivative from *Kniphofia foliosa*'.
[75] D. H. Williams, B. Bardsley, *Angew. Chem. Int. Ed.* **1999**, *38*, 1172-1193; 'The vancomycin group of antibiotics and the fight against resistant bacteria'.
[76] D. H. Williams, B. Bardsley, *Angew. Chem.* **1999**, *111*, 1264-1286; 'Die Vancomycin-Antibiotica und der Kampf gegen resistente Bakterien'.
[77] Y. Fukuyama, Y. Asakawa, *J. Chem. Soc., Perkin Trans.* **1991**, 2737-2741; 'Novel neurotrophic isocuparane-type sesquiterpene dimers, mastigophorenes A, B, C and D, isolated from the liverwort *Mastigophora diclados*'.
[78] V. Band, A. P. Hoffer, H. Band, A. E. Rhinehardt, R. C. Knapp, S. A. Matlin, D. J. Anderson, *Gynecol. Oncol.* **1989**, *32*, 273-277; 'Antiproliferative effect of gossypol and its optical isomers on human reproductive cancer cell lines'.
[79] C. C. Benz, M. Keniry, J. M. Ford, A. J. Townsend, F. W. Cox, S. Palayoor, S. A. Matlin, W. N. Hait, K. H. Cowan, *Mol. Pharmacol.* **1990**, *37*, 840-847; 'Biochemical correlates of the antitumor and antimitochondrial properties of gossypol enantiomers'.
[80] J. A. Carmona, C. Rodríguez-Franco, R. Fernández, V. Hornillos, J. M. Lassaletta, *Chem. Soc. Rev.* **2021**, *50*, 2968-2983; 'Atroposelective transformation of axially chiral (hetero)biaryls. From desymmetrization to modern resolution strategies'.
[81] A. Miyashita, A. Yasuda, H. Takaya, K. Toriumi, T. Ito, T. Souchi, R. Noyori, *J. Am. Chem. Soc.* **1980**, *102*, 7932-7934; 'Synthesis of 2,2'-bis (diphenylphosphino)-1,1'-binaphthyl (BINAP), an atropisomeric chiral bis(triaryl)phosphine, and its use

in the rhodium(I)-catalyzed asymmetric hydrogenation of α-(acylamino)acrylic acids'.

[82] J. Bao, W. D. Wulff, A. L. Rheingold, *J. Am. Chem. Soc.* **1993**, *115*, 3814-3815; 'Vaulted biaryls as chiral ligands for asymmetric catalytic Diels-Alder reactions'.

[83] J. Bao, W. D. Wulff, J. B. Dominy, M. J. Fumo, E. B. Grant, A. C. Rob, M. C. Whitcomb, S.-M. Yeung, R. L. Ostrander, A. L. Rheingold, *J. Am. Chem. Soc.* **1996**, *118*, 3392-3405; 'Synthesis, Resolution, and Determination of Absolute Configuration of a Vaulted 2,2'-Binaphthol and a Vaulted 3,3'-Biphenanthrol (VAPOL)'.

[84] S. Yu, C. Rabalakos, W. D. Mitchell, W. D. Wulff, *Org. Lett.* **2005**, *7*, 367-369; 'New synthesis of vaulted biaryl ligands via the snieckus phenol synthesis'.

[85] J. Jie, H. Yang, Y. Zhao, H. Fu, *iScience* **2023**, *26*; 'Development of diverse adjustable axially chiral biphenyl ligands and catalysts'.

[86] G. Bringmann, M. Breuning, *Tetrahedron: Asymmetry* **1998**, *9*, 667-679; 'Enantioselective addition of diethylzinc to aldehydes using novel axially chiral 2-aminomethyl-1-(2'-hydroxyphenyl)naphthalene catalysts'.

[87] O. F. Watts, J. Berreur, B. S. Collins, J. Clayden, *Acc. Chem. Res.* **2022**, *55*, 3362-3375; 'Biocatalytic Enantioselective Synthesis of Atropisomers'.

[88] J. Wencel-Delord, A. Panossian, F. Leroux, F. Colobert, *Chem. Soc. Rev.* **2015**, *44*, 3418-3430; 'Recent advances and new concepts for the synthesis of axially stereoenriched biaryls'.

[89] X. Li, J. Yang, M. C. Kozlowski, *Org. Lett.* **2001**, *3*, 1137-1140; 'Enantioselective oxidative biaryl coupling reactions catalyzed by 1,5-diazadecalin metal complexes'.

[90] X. Li, J. B. Hewgley, C. A. Mulrooney, J. Yang, M. C. Kozlowski, *J. Org. Chem.* **2003**, *68*, 5500-5511; 'Enantioselective oxidative biaryl coupling reactions catalyzed by 1, 5-diazadecalin metal complexes: Efficient formation of chiral functionalized BINOL derivatives'.

[91] M. C. Kozlowski, B. J. Morgan, E. C. Linton, *Chem. Soc. Rev.* **2009**, *38*, 3193-3207; 'Total synthesis of chiral biaryl natural products by asymmetric biaryl coupling'.

[92] M. C. Kozlowski, E. C. Dugan, E. S. DiVirgilio, K. Maksimenka, G. Bringmann, *Adv. Synth. Catal.* **2007**, *349*, 583-594; 'Asymmetric Total Synthesis of Nigerone and *ent*-Nigerone: Enantioselective Oxidative Biaryl Coupling of Highly Hindered Naphthols'.

[93] B. J. Morgan, S. Dey, S. W. Johnson, M. C. Kozlowski, *J. Am. Chem. Soc.* **2009**, *131*, 9413-9425; 'Design, synthesis, and investigation of protein kinase C inhibitors: total syntheses of (+)-calphostin D, (+)-phleichrome, cercosporin, and new photoactive perylenequinones'.

[94] E. M. O'Brien, B. J. Morgan, C. A. Mulrooney, P. J. Carroll, M. C. Kozlowski, *J. Org. Chem.* **2010**, *75*, 57-68; 'Perylenequinone natural products: total synthesis of hypocrellin A'.

[95] H. Wang, *Chirality* **2010**, *22*, 827-837; 'Recent advances in asymmetric oxidative coupling of 2-naphthol and its derivatives'.

[96] C. Zheng, S.-L. You, *Asymmetric oxidative biaryl coupling reactions*, The Royal Society of Chemistry, **2015**.

[97] H. Kang, Y. E. Lee, P. V. G. Reddy, S. Dey, S. E. Allen, K. A. Niederer, P. Sung, K. Hewitt, C. Torruellas, M. R. Herling, *Org. Lett.* **2017**, *19*, 5505-5508; 'Asymmetric oxidative coupling of phenols and hydroxycarbazoles'.

[98] H. Kang, C. Torruellas, J. Liu, M. C. Kozlowski, *Org. Lett.* **2018**, *20*, 5554-5558; 'Total synthesis of chaetoglobin A via catalytic, atroposelective oxidative phenol coupling'.

[99] L. Ackermann, H. K. Potukuchi, A. Althammer, R. Born, P. Mayer, *Org. Lett.* **2010**, *12*, 1004-1007; 'Tetra-*ortho*-substituted biaryls through palladium-catalyzed Suzuki−Miyaura couplings with a diaminochlorophosphine ligand'.

[100] T. Hoshi, T. Nakazawa, I. Saitoh, A. Mori, T. Suzuki, J.-i. Sakai, H. Hagiwara, *Org. Lett.* **2008**, *10*, 2063-2066; 'Biphenylene-substituted ruthenocenylphosphine for Suzuki–Miyaura coupling of aryl chlorides'.

[101] J. Yin, M. P. Rainka, X.-X. Zhang, S. L. Buchwald, *J. Am. Chem. Soc.* **2002**, *124*, 1162-1163; 'A highly active Suzuki catalyst for the synthesis of sterically hindered biaryls: novel ligand coordination'.

[102] O. M. Demchuk, B. Yoruk, T. Blackburn, V. Snieckus, *Synlett* **2006**, *18*, 2908-2913; 'A mixed naphthyl-phenyl phosphine ligand motif for suzuki, heck, and hydrodehalogenation reactions'.

[103] Q. Zhao, C. Li, C. H. Senanayake, W. Tang, *Chem. Eur. J.* **2013**, *19*, 2261-2265; 'An efficient method for sterically demanding Suzuki–Miyaura coupling reactions'.

[104] C. Li, D. Chen, W. Tang, *Synlett* **2016**, *15*, 2183-2200; 'Addressing the challenges in Suzuki–Miyaura cross-couplings by ligand design'.

[105] G. Hedouin, S. Hazra, F. Gallou, S. Handa, *ACS Catal.* **2022**, *12*, 4918-4937; 'The catalytic formation of atropisomers and stereocenters via asymmetric Suzuki–Miyaura couplings'.

[106] N. D. Patel, J. D. Sieber, S. Tcyrulnikov, B. J. Simmons, D. Rivalti, K. Duvvuri, Y. Zhang, D. A. Gao, K. R. Fandrick, N. Haddad, *ACS Catal.* **2018**, *8*, 10190-10209; 'Computationally assisted mechanistic investigation and development of Pd-catalyzed asymmetric Suzuki–Miyaura and Negishi cross-coupling reactions for tetra-*ortho*-substituted biaryl synthesis'.

[107] R. Pearce-Higgins, L. N. Hogenhout, P. J. Docherty, D. M. Whalley, P. Chuentragool, N. Lee, N. Y. Lam, T. M. McGuire, D. Valette, R. J. Phipps, *J. Am. Chem. Soc.* **2022**, *144*, 15026-15032; 'An enantioselective Suzuki–Miyaura coupling to form axially chiral biphenols'.

[108] W. Tang, N. D. Patel, G. Xu, X. Xu, J. Savoie, S. Ma, M.-H. Hao, S. Keshipeddy, A. G. Capacci, X. Wei, *Org. Lett.* **2012**, *14*, 2258-2261; 'Efficient Chiral Monophosphorus Ligands for Asymmetric Suzuki–Miyaura Coupling Reactions'.

[109] G. Xu, W. Fu, G. Liu, C. H. Senanayake, W. Tang, *J. Am. Chem. Soc.* **2014**, *136*, 570-573; 'Efficient syntheses of korupensamines A, B and michellamine B by asymmetric Suzuki-Miyaura coupling reactions'.

[110] H. Yang, J. Sun, W. Gu, W. Tang, *J. Am. Chem. Soc.* **2020**, *142*, 8036-8043; 'Enantioselective cross-coupling for axially chiral tetra-*ortho*-substituted biaryls and asymmetric synthesis of gossypol'.

[111] B. H. Lipshutz, F. Kayser, Z. P. Liu, *Angew. Chem. Int. Ed.* **1994**, *33*, 1842-1844; 'Asymmetric synthesis of biaryls by intramolecular oxidative couplings of cyanocuprate intermediates'.

[112] B. H. Lipshutz, F. Kayser, Z. P. Liu, *Angew. Chem.* **1994**, *106*, 1962-1964; 'Asymmetrische Synthese von Biarylen durch intramolekulare oxidative Kupplung von Cyanocuprat-Zwischenstufen'.

[113] G.-Q. Lin, M. Zhong, *Tetrahedron Lett.* **1997**, *38*, 1087-1090; 'The first enantioselective synthesis of optically pure (*R*)- and (*S*)-5,5''-dihydroxy-4',4''',7,7''-tetramethoxy-8,8''-biflavone and the reconfirmation of their absolute configuration'.

[114] R. V. Kyasnoor, M. V. Sargent, *Chem. Commun.* **1998**, 2713-2714; 'A formal synthesis of both atropenantiomers of desertorin C'.

[115] G.-Q. Lin, M. Zhong, *Tetrahedron: Asymmetry* **1997**, *8*, 1369-1372; 'The first asymmetric synthesis of the naturally occurring (+)-Kotanin and the assignment of its absolute configuration'.
[116] T. D. Nelson, A. Meyers, *J. Org. Chem.* **1994**, *59*, 2655-2658; 'The asymmetric Ullmann reaction. 2. The synthesis of enantiomerically pure C2-symmetric binaphthyls'.
[117] A. Meyers, *J. Heterocycl. Chem.* **1998**, *35*, 991-1002; 'Chiral oxazolines-their legacy as key players in the renaissance of asymmetric synthesis'.
[118] A. Meyers, J. J. Willemsen, *Tetrahedron Lett.* **1996**, *37*, 791-792; 'An asymmetric synthesis of (+)-apogossypol hexamethyl ether'.
[119] A. Meyers, J. J. Willemsen, *Tetrahedron* **1998**, *54*, 10493-10511; 'An oxazoline based approach to (*S*)-gossypol'.
[120] J. M. Wilson, D. J. Cram, *J. Am. Chem. Soc.* **1982**, *104*, 881-884; 'Chiral leaving groups induce asymmetry in syntheses of binaphthyls in nucleophilic aromatic substitution reactions'.
[121] J. M. Wilson, D. J. Cram, *J. Org. Chem* **1984**, *49*, 4930-4943; 'Studies in stereochemistry. 47. Asymmetric induction by leaving group in nucleophilic aromatic substitution'.
[122] T. Suzuki, H. Hotta, T. Hattori, S. Miyano, *Chem. Lett.* **1990**, *19*, 807-810; 'An Efficient Asymmetric Synthesis of Atropisomeric 1,1'-Binaphthyls via Nucleophilic Aromatic Substitution Reaction'.
[123] T. Hattori, N. Koike, S. Miyano, *J. Chem. Soc., Perkin Trans.* **1994**, 2273-2282; 'Asymmetric synthesis of axially chiral 1,1'-biphenyl-2-carboxylates via nucleophilic aromatic substitution on 2-menthoxybenzoates by aryl Grignard reagents'.
[124] S. Lu, S. B. Poh, Y. Zhao, *Angew. Chem. Int. Ed.* **2014**, *53*, 11041-11045; 'Kinetic Resolution of 1,1'-Biaryl-2,2'-Diols and Amino Alcohols through NHC-Catalyzed Atroposelective Acylation'.
[125] S. Lu, S. B. Poh, Y. Zhao, *Angew. Chem.* **2014**, *126*, 11221-11225; 'Kinetic Resolution of 1,1'-Biaryl-2,2'-Diols and Amino Alcohols through NHC-Catalyzed Atroposelective Acylation'.
[126] T. Hayashi, S. Niizuma, T. Kamikawa, N. Suzuki, Y. Uozumi, *J. Am. Chem. Soc.* **1995**, *117*, 9101-9102; 'Catalytic asymmetric synthesis of axially chiral biaryls by palladium-catalyzed enantioposition-selective cross-coupling'.
[127] T. Kamikawa, Y. Uozumi, T. Hayashi, *Tetrahedron Lett.* **1996**, *37*, 3161-3164; 'Enantioposition-selective alkynylation of biaryl ditriflates by palladium-catalyzed asymmetric cross-coupling'.
[128] T. Kamikawa, T. Hayashi, *Tetrahedron* **1999**, *55*, 3455-3466; 'Enantioposition-selective arylation of biaryl ditriflates by palladium-catalyzed asymmetric Grignard cross-coupling'.
[129] E. S. Munday, M. A. Grove, T. Feoktistova, A. C. Brueckner, D. M. Walden, C. M. Young, A. M. Slawin, A. D. Campbell, P. H. Y. Cheong, A. D. Smith, *Angew. Chem. Int. Ed.* **2020**, *59*, 7897-7905; 'Isothiourea-Catalyzed Atropselective Acylation of Biaryl Phenols via Sequential Desymmetrization/Kinetic Resolution'.
[130] E. S. Munday, M. A. Grove, T. Feoktistova, A. C. Brueckner, D. M. Walden, C. M. Young, A. M. Slawin, A. D. Campbell, P. H. Y. Cheong, A. D. Smith, *Angew. Chem.* **2020**, *132*, 7971-7979; 'Isothiourea-Catalyzed Atropselective Acylation of Biaryl Phenols via Sequential Desymmetrization/Kinetic Resolution'.

[131] Y. Zhang, S.-M. Yeung, H. Wu, D. P. Heller, C. Wu, W. D. Wulff, *Org. Lett.* **2003**, *5*, 1813-1816; 'Highly enantioselective deracemization of linear and vaulted biaryl ligands'.
[132] G. Hu, D. Holmes, B. F. Gendhar, W. D. Wulff, *J. Am. Chem. Soc.* **2009**, *131*, 14355-14364; 'Optically active (*aR*)-and (*aS*)-linear and vaulted biaryl ligands: deracemization versus oxidative dimerization'.
[133] G. Bringmann, M. Breuning, R.-M. Pfeifer, W. A. Schenk, K. Kamikawa, M. Uemura, *J. Organomet. Chem.* **2002**, *661*, 31-47; 'The lactone concept—a novel approach to the metal-assisted atroposelective construction of axially chiral biaryl systems'.
[134] G. Bringmann, S. Tasler, R.-M. Pfeifer, M. Breuning, *J. Organomet. Chem.* **2002**, *661*, 49-65; 'The directed synthesis of axially chiral ligands, reagents, catalysts, and natural products through the 'lactone methodology''.
[135] R. Noyori, I. Tomino, Y. Tanimoto, *J. Am. Chem. Soc.* **1979**, *101*, 3129-3131; 'Virtually complete enantioface differentiation in carbonyl group reduction by a complex aluminum hydride reagent'.
[136] G. Bringmann, J. Hinrichs, T. Pabst, P. Henschel, K. Peters, E.-M. Peters, *Synthesis* **2001**, 0155-0167; 'From dynamic to non-dynamic kinetic resolution of lactone-bridged biaryls: Synthesis of mastigophorene B'.
[137] S. Tasler, G. Bringmann, *Chem. Rec.* **2002**, *2*, 113-126; 'Biarylic Biscarbazole Alkaloids: Occurrence, Stereochemistry, Synthesis, and Bioactivity: Biarylic Biscarbazole Alkaloids'.
[138] G. Bringmann, M. Ochse, R. Götz, *J. Org. Chem.* **2000**, *65*, 2069-2077; 'First atropo-divergent total synthesis of the antimalarial korupensamines A and B by the "lactone method"'.
[139] G. Bringmann, D. Menche, *Angew. Chem. Int. Ed.* **2001**, *40*, 1687-1690; 'First, Atropo-Enantioselective Total Synthesis of the Axially Chiral Phenylanthraquinone Natural Products Knipholone and 6'-*O*-Methylknipholone'.
[140] G. Bringmann, D. Menche, *Angew. Chem.* **2001**, *113*, 1733-1736; 'Erste, atropenantioselektive Totalsynthese der axial-chiralen Phenylanthrachinon-Naturstoffe Knipholon und 6'-O-Methylknipholon'.
[141] G. Carrea, S. Riva, *Angew. Chem. Int. Ed.* **2000**, *39*, 2226-2254; 'Properties and synthetic applications of enzymes in organic solvents'.
[142] G. Carrea, S. Riva, *Angew. Chem.* **2000**, *112*, 2312-2341; 'Enzyme in organischen Lösungsmitteln: Eigenschaften und Einsatz in der Synthese'.
[143] W. Hüttel, M. Müller, *Nat. Prod. Rep.* **2021**, *38*, 1011-1043; 'Regio- and stereoselective intermolecular phenol coupling enzymes in secondary metabolite biosynthesis'.
[144] J. Liu, A. Liu, Y. Hu, *Nat. Prod. Rep.* **2021**, *38*, 1469-1505; 'Enzymatic dimerization in the biosynthetic pathway of microbial natural products'.
[145] L. E. Zetzsche, J. A. Yazarians, S. Chakrabarty, M. E. Hinze, L. A. Murray, A. L. Lukowski, L. A. Joyce, A. R. Narayan, *Nature* **2022**, *603*, 79-85; 'Biocatalytic oxidative cross-coupling reactions for biaryl bond formation'.
[146] P. Gupta, A. Rouf, B. A. Shah, N. Mahajan, A. Chaubey, S. C. Taneja, *J. Mol. Catal.* **2014**, *101*, 35-39; 'Arthrobacter sp. lipase catalyzed kinetic resolution of BINOL: The effect of substrate immobilization'.
[147] N. Aoyagi, N. Ogawa, T. Izumi, *Tetrahedron Lett.* **2006**, *47*, 4797-4801; 'Effects of reaction temperature and acyl group for lipase-catalyzed chiral binaphthol synthesis'.

[148] Y. Fujimoto, H. Iwadate, N. Ikekawa, *J. Chem. Soc., Chem. Comm.* **1985**, 1333-1334; 'Preparation of optically active 2,2'-dihydroxy-1,1'-binaphthyl via microbial resolution of the corresponding racemic diester'.
[149] T. Takemura, G. Emoto, J. Satoh, Y. Kobayashi, C. Yaginuma, Y. Takahashi, T. Utsukihara, C. A. Horiuchi, *J. Mol. Catal. B: Enzym.* **2008**, *55*, 104-109; 'Optical resolution of hexamethylbiphenol by cholesterol esterase and porcine pancreas lipase'.
[150] M. Inagaki, J. Hiratake, T. Nishioka, O. Jun'ichi, *Agric. Biol. Chem.* **1989**, *53*, 1879-1884; 'Lipase-catalyzed Stereoselective Acylation of [1,1'-Binaphthyl]-2,2'-diol and Deacylation of Its Esters in an Organic Solvent'.
[151] M. Juárez-Hernandez, D. V. Johnson, H. L. Holland, J. McNulty, A. Capretta, *Tetrahedron: Asymmetry* **2003**, *14*, 289-291; 'Lipase-catalyzed stereoselective resolution and desymmetrization of binaphthols'.
[152] M. Jouffroy, K. Neufeld, *ACS Catalysis* **2022**, *12*, 8380-8385; 'Synthesis of Atropisomeric Biaryls via Chiral Suzuki–Miyaura/Enzymatic Kinetic Resolution'.
[153] C. Sanfilippo, N. D'Antona, G. Nicolosi, *Tetrahedron: Asymmetry* **2006**, *17*, 12-14; 'Lipase-catalysed resolution by an esterification reaction in organic solvent of axially chiral (±)-3,3'-bis (hydroxymethyl)-2,2'-bipyridine *N*,*N*-dioxide'.
[154] T. Takemura, G. Emoto, J. Satoh, Y. Kobayashi, C. Yaginuma, Y. Takahashi, T. Utsukihara, C. A. Horiuchi, *J. Mol. Catal.* **2008**, *55*, 104-109; 'Optical resolution of hexamethylbiphenol by cholesterol esterase and porcine pancreas lipase'.
[155] G. A. Moustafa, K. Kasama, K. Higashio, S. Akai, *RSC Adv.* **2019**, *9*, 1165-1175; 'Base-promoted lipase-catalyzed kinetic resolution of atropisomeric 1,1'-biaryl-2,2'-diols'.
[156] B. Skrobo, J. Deska, *Tetrahedron: Asymmetry* **2013**, *24*, 1052-1056; 'On the lipase-catalyzed resolution of functionalized biaryls'.
[157] Z. S. Seddigi, M. S. Malik, S. A. Ahmed, A. O. Babalghith, A. Kamal, *Coord. Chem. Rev.* **2017**, *348*, 54-70; 'Lipases in asymmetric transformations: Recent advances in classical kinetic resolution and lipase–metal combinations for dynamic processes'.
[158] G. A. Moustafa, Y. Oki, S. Akai, *Angew. Chem. Int. Ed.* **2018**, *57*, 10278-10282; 'Lipase-Catalyzed Dynamic Kinetic Resolution of C1-and C2-Symmetric Racemic Axially Chiral 2,2'-Dihydroxy-1,1'-biaryls'.
[159] G. A. Moustafa, Y. Oki, S. Akai, *Angew. Chem.* **2018**, *130*, 10435-10439; 'Lipase-Catalyzed Dynamic Kinetic Resolution of C1-and C2-Symmetric Racemic Axially Chiral 2,2'-Dihydroxy-1,1'-biaryls'.
[160] T. Matsumoto, T. Konegawa, T. Nakamura, K. Suzuki, *Synlett* **2002**, *1*, 122-124; 'Facile and highly enantioselective synthesis of axially chiral biaryls by enzymatic desymmetrization'.
[161] N. Takahashi, T. Kanayama, K. Okuyama, H. Kataoka, H. Fukaya, K. Suzuki, T. Matsumoto, *Chem. Asian J.* **2011**, *6*, 1752-1756; 'Enantioselective Total Synthesis of (−)-Euxanmodin B: An Axially Chiral Natural Product with an Anthraquinone–Xanthone Composite Structure'.
[162] M. Ochiai, Y. Akisawa, D. Kajiyama, T. Matsumoto, *Synlett* **2019**, *5*, 557-562; 'Desymmetrization of *σ*-Symmetric Biphenyl-2,6-diyl Diacetate Derivatives by Lipase-Catalyzed Hydrolysis: Unexpected Effect of C(3')-Substituent on the Enantiotopic Group Selectivity'.
[163] S. Yamaguchi, N. Takahashi, D. Yuyama, K. Sakamoto, K. Suzuki, T. Matsumoto, *Synlett* **2016**, *8*, 1262-1268; 'First Total Synthesis of Dermocanarin 2'.
[164] K. Kasama, H. Aoyama, S. Akai, *Eur. J. Org. Chem.* **2020**, *2020*, 654-661; 'Enantiodivergent Synthesis of Axially Chiral Biphenyls from *σ*-Symmetric 1,1'-

Biphenyl-2,6-diol Derivatives by Single Lipase-Catalyzed Acylative and Hydrolytic Desymmetrization'.

[165] S. Lu, J. Tian, W. Sun, J. Meng, X. Wang, X. Fu, A. Wang, D. Lai, Y. Liu, L. Zhou, *Molecules* **2014**, *19*, 7169-7188; 'Bis-naphtho-*γ*-pyrones from fungi and their bioactivities'.

[166] W. Sun, A. Wang, D. Xu, W. Wang, J. Meng, J. Dai, Y. Liu, D. Lai, L. Zhou, *J. Agric. Food Chem.* **2017**, *65*, 5151-5160; 'New ustilaginoidins from rice false smut balls caused by *Villosiclava virens* and their phytotoxic and cytotoxic activities'.

[167] R. Barrow, M. McCulloch, *Mini Rev. Med. Chem.* **2009**, *9*, 273-292; 'Linear naphtho-*γ*-pyrones: a naturally occurring scaffold of biological importance'.

[168] Y. Takahashi, *Bot. Mag.* **1896**, *10*, 16-20; 'On Ustilago virens Cooke and a new species of Tilletia parasitic on rice-plant'.

[169] S. Lu, W. Sun, J. Meng, A. Wang, X. Wang, J. Tian, X. Fu, J. Dai, Y. Liu, D. Lai, *J. Agric. Food Chem.* **2015**, *63*, 3501-3508; 'Bioactive bis-naphtho-*γ*-pyrones from rice false smut pathogen *Ustilaginoidea virens*'.

[170] J. N. Ashley, B. C. Hobbs, H. Raistrick, *Biochem. J.* **1937**, *31*, 385; 'Studies in the biochemistry of micro-organisms: the crystalline colouring matters of *Fusarium culmorum* (WG Smith) Sacc. and related forms'.

[171] G. H. Stout, L. Jensen, *Acta Crystallogr.* **1962**, *15*, 451-457; 'Rubrofusarin: a structure determination using direct phase calculation'.

[172] P. Rugbjerg, M. Naesby, U. H. Mortensen, R. J. Frandsen, *Microb. Cell Fact.* **2013**, *12*, 1-9; 'Reconstruction of the biosynthetic pathway for the core fungal polyketide scaffold rubrofusarin in *Saccharomyces cerevisiae*'.

[173] S. Obermaier, W. Thiele, L. Fürtges, M. Müller, *Angew. Chem. Int. Ed.* **2019**, *58*, 9125-9128; 'Enantioselective phenol coupling by laccases in the biosynthesis of fungal dimeric naphthopyrones'.

[174] S. Obermaier, W. Thiele, L. Fürtges, M. Müller, *Angew. Chem.* **2019**, *131*, 9223-9226; 'Enantioselective phenol coupling by laccases in the biosynthesis of fungal dimeric naphthopyrones'.

[175] D. Xu, R. Yin, Z. Zhou, G. Gu, S. Zhao, J.-R. Xu, J. Liu, Y.-L. Peng, D. Lai, L. Zhou, *Chem. Sci.* **2021**, *12*, 14883-14892; 'Elucidation of ustilaginoidin biosynthesis reveals a previously unrecognised class of ene-reductases'.

[176] S. Shibata, E. Morishita, Y. Arima, *Chem. Pharm. Bull.* **1963**, *11*, 821-823; 'Synthesis of rubrofusarin dimethyl ether'.

[177] E. Morishita, S. Shibata, *Chem. Pharm. Bull.* **1967**, *15*, 1772-1775; 'Metabolic products of fungi. XXVII. Synthesis of racemic ustilaginoidin A and its related compounds. (2). Synthesis of racemic ustilaginoidin A'.

[178] F. J. Leeper, J. Staunton, *J. Chem. Soc., Chem. Comm.* **1978**, 406-407; 'Biomimetic syntheses of heptaketide metabolites: alternariol and a derivative of rubrofusarin'.

[179] W. Hüttel, M. Müller, *ChemBioChem* **2007**, *8*, 521-529; 'Regio- and stereoselective intermolecular oxidative phenol coupling in kotanin biosynthesis by *Aspergillus niger*'.

[180] J. A. Laakso, E. D. Narske, J. B. Gloer, D. T. Wicklow, P. F. Dowd, *J. Nat. Prod.* **1994**, *57*, 128-133; 'Isokotanins A-C: New bicoumarins from the sclerotia of *Aspergillus alliceus*'.

[181] K. Nozawa, S. Nakajima, K.-I. Kawai, S.-I. Udagawa, M. Miyaji, *Phytochem.* **1994**, *35*, 1049-1051; 'Bicoumarins from ascostromata of *Petromyces alliaceus*'.

[182] H. Musso, W. Steckelberg, *Chem. Ber.* **1968**, *101*, 1510-1518; 'Über Orceinfarbstoffe, XXVI; letzte Mitteilung. Synthese, Konfiguration und ORD-CD-Spektren optisch aktiver Orceinfarbstoffe'.

[183] H. Kikuchi, M. Isobe, M. Sekiya, Y. Abe, T. Hoshikawa, K. Ueda, S. Kurata, Y. Katou, Y. Oshima, *Org. Lett.* **2011**, *13*, 4624-4627; 'Structures of the dimeric and monomeric chromanones, gonytolides A–C, isolated from the fungus *Gonytrichum sp.* and their promoting activities of innate immune responses'.

[184] J. Wang, A. Galgoci, S. Kodali, K. B. Herath, H. Jayasuriya, K. Dorso, F. Vicente, A. González, D. Cully, D. Bramhill, *J. Biol. Chem.* **2003**, *278*, 44424-44428; 'Discovery of a small molecule that inhibits cell division by blocking FtsZ, a novel therapeutic target of antibiotics'.

[185] T. Drennhaus, Bachelor thesis, Fachhochschule Aachen **2019**; 'Studien zur Synthese axial-chiraler Hydroxyacetophenon-Dimere als Schlüsselbausteine in der Naturstoffsynthese. '

[186] H. Musso, W. Steckelberg, *Justus Liebigs Ann. Chem.* **1966**, *693*, 187-196; '(−)-(*S*)-2,2'-Diamino-4,4'-dimethoxy-6,6'-dimethyl-biphenyl. Zur Konfigurationsbestimmung optisch aktiver 2,2'-Diamino-biphenyle mittels Rotationsdispersion und Circulardichroismus'.

[187] G. Solladié, P. Hugelé, R. Bartsch, A. Skoulios, *Angew. Chem. Int. Ed.* **1996**, *35*, 1533-1535; 'New family of enantiomerically pure liquid crystals containing a chiral biphenyl core'.

[188] G. Solladié, P. Hugelé, R. Bartsch, A. Skoulios, *Angew. Chem.* **1996**, *108*, 1640-1642; 'Bildung von enantiomerenreinen Flüssigkristallen aus axial-chiralen Biphenylen'.

[189] R. Holzwarth, R. Bartsch, Z. Cherkaoui, G. Solladié, *Chem. Eur. J.* **2004**, *10*, 3931-3935; 'New 2,2'-Substituted 4,4'-Dimethoxy-6,6'-dimethyl[1,1'-biphenyls], Inducing a Strong Helical Twisting Power in Liquid Crystals'.

[190] G. Feutrill, R. Mirrington, *Aust. J. Chem.* **1972**, *25*, 1719-1729; 'Reactions with thioethoxide ion in dimethylformamide. I. Selective demethylation of aryl methyl ethers'.

[191] R. N. Mirrington, G. I. Feutrill, *Org. Synth.* **1973**, *53*, 90; 'Orcinol Monomethyl Ether: Phenol, 3-methoxy-5-methyl-'.

[192] V. Snieckus, *Chem. Rev.* **1990**, *90*, 879-933; 'Directed *ortho* metalation. Tertiary amide and *O*-carbamate directors in synthetic strategies for polysubstituted aromatics'.

[193] U.S. Department of Health and Human Services, Public Health Service, National Toxicology Program, *Report on Carcinogens: Carcinogen Profiles*, **2011**, p. 71.

[194] Bundesministerium der Justiz, *Verordnung zum Schutz vor Gefahrstoffen (Gefahrstoffverordnung - GefStoffV) Besondere Herstellungs- und Verwendungsbeschränkungen für bestimmte Stoffe, Gemische und Erzeugnisse*, **2010**, pp. 1674-1676.

[195] N. C. Bruno, S. L. Buchwald, *Org. Lett.* **2013**, *15*, 2876-2879; 'Synthesis and application of palladium precatalysts that accommodate extremely bulky di-*tert*-butylphosphino biaryl ligands'.

[196] N. C. Bruno, M. T. Tudge, S. L. Buchwald, *Chem. Sci.* **2013**, *4*, 916-920; 'Design and preparation of new palladium precatalysts for C–C and C–N cross-coupling reactions'.

[197] N. C. Bruno, N. Niljianskul, S. L. Buchwald, *J. Org. Chem.* **2014**, *79*, 4161-4166; '*N*-Substituted 2-aminobiphenylpalladium methanesulfonate precatalysts and their use in C–C and C–N cross-couplings'.

[198] N. Li, J. Shen, X. Liu, *Eur. J. Inorg. Chem.* **2021**, *2021*, 2797-2800; 'Hydrolysis of B_2pin_2 over Pd/C catalyst: high efficiency, mechanism, and *in situ* tandem reaction'.

[199] A. Fulton, M. R. Hayes, U. Schwaneberg, J. Pietruszka, K.-E. Jaeger, in *Protein Engineering: Methods and Protocols*, **2018**, pp. 209-231.
[200] P. D. De Maria, J. M. Sánchez-Montero, J. V. Sinisterra, A. R. Alcántara, *Biotechnol. Adv.* **2006**, *24*, 180-196; 'Understanding *Candida rugosa* lipases: an overview'.
[201] P. Khunnamwong, N. Lertwattanasakul, S. Jindamorakot, S. Limtong, M.-A. Lachance, *Int. J. Syst. Evol. Micr.* **2015**, *65*, 4701-4709; 'Description of *Diutina* gen. nov., *Diutina siamensis*, fa sp. nov., and reassignment of *Candida catenulata*, *Candida mesorugosa*, *Candida neorugosa*, *Candida pseudorugosa*, *Candida ranongensis*, *Candida rugosa* and *Candida scorzettiae* to the genus *Diutina*'.
[202] C. C. Akoh, G.-C. Lee, J.-F. Shaw, *Lipids* **2004**, *39*, 513-526; 'Protein engineering and applications of *Candida rugosa* lipase isoforms'.
[203] E. Vanleeuw, S. Winderickx, K. Thevissen, B. Lagrain, M. Dusselier, B. P. Cammue, B. F. Sels, *ACS Sustainable Chem. Eng.* **2019**, *7*, 15828-15844; 'Substrate-specificity of *Candida rugosa* lipase and its industrial application'.
[204] *Candida rugosa* lipase (CRL) from Sigma Aldrich, CAS-Number: 9001-62-1, Article Number: 62316
[205] M. Cygler, J. D. Schrag, *Biochim. Biophys. Acta, Mol. Cell Biol. Lipids* **1999**, *1441*, 205-214; 'Structure and conformational flexibility of *Candida rugosa* lipase'.
[206] C. S. Chen, C. J. Sih, *Angew. Chem. Int. Ed.* **1989**, *28*, 695-707; 'General aspects and optimization of enantioselective biocatalysis in organic solvents: The use of lipases '.
[207] C. S. Chen, C. J. Sih, *Angew. Chem.* **1989**, *101*, 711-724; 'Enantioselektive Biokatalyse in organischen Solventien am Beispiel Lipase-katalysierter Reaktionen'.
[208] C. Laane, S. Boeren, K. Vos, C. Veeger, *Biotechnol. Bioeng.* **1987**, *30*, 81-87; 'Rules for optimization of biocatalysis in organic solvents'.
[209] A. Kumar, K. Dhar, S. S. Kanwar, P. K. Arora, *Biol. Proced. Online* **2016**, *18*, 1-11; 'Lipase catalysis in organic solvents: advantages and applications'.
[210] A. Bollinger, R. Molitor, S. Thies, R. Koch, C. Coscolín, M. Ferrer, K.-E. Jaeger, *Appl. Environ. Microbiol.* **2020**, *86*, e00106-00120; 'Organic-solvent-tolerant carboxylic ester hydrolases for organic synthesis'.
[211] A. Bollinger, S. Thies, E. Knieps-Grünhagen, C. Gertzen, S. Kobus, A. Höppner, M. Ferrer, H. Gohlke, S. H. Smits, K.-E. Jaeger, *Front. Microbiol.* **2020**, *11*, 114; 'A Novel Polyester Hydrolase From The Marine Bacterium *Pseudomonas aestusnigri*–Structural and Functional Insights'.
[212] A. Höppner, A. Bollinger, S. Kobus, S. Thies, C. Coscolin, M. Ferrer, K. E. Jaeger, S. H. Smits, *FEBS J.* **2021**, *288*, 3570-3584; 'Crystal structures of a novel family IV esterase in free and substrate-bound form'.
[213] S. Narute, R. Parnes, F. D. Toste, D. Pappo, *J. Am. Chem. Soc.* **2016**, *138*, 16553-16560; 'Enantioselective oxidative homocoupling and cross-coupling of 2-naphthols catalyzed by chiral iron phosphate complexes'.
[214] A. Ghanem, H. Y. Aboul-Enein, *Tetrahedron: Asymmetry* **2004**, *15*, 3331-3351; 'Lipase-mediated chiral resolution of racemates in organic solvents'.
[215] K. Kasama, Y. Hinami, K. Mizuno, S. Horino, T. Nishio, C. Yuki, K. Kanomata, G. A. Moustafa, H. Gröger, S. Akai, *Chem. Pharm. Bull.* **2022**, *70*, 391-399; 'Lipase-Catalyzed Kinetic Resolution of C1-Symmetric Heterocyclic Biaryls'.
[216] M. Eckert, A. Brethon, Y.-X. Li, R. A. Sheldon, I. W. C. E. Arends, *Adv. Synth. Catal.* **2007**, *349*, 2603-2609; 'Study of the Efficiency of Amino-Functionalized Ruthenium and Ruthenacycle Complexes as Racemization Catalysts in the Dynamic Kinetic Resolution of 1-Phenylethanol'.

[217] O. Verho, J.-E. Bäckvall, *J. Am. Chem. Soc.* **2015**, *137*, 3996-4009; 'Chemoenzymatic dynamic kinetic resolution: a powerful tool for the preparation of enantiomerically pure alcohols and amines'.
[218] P. M. Dinh, J. A. Howarth, A. R. Hudnott, J. M. Williams, W. Harris, *Tetrahedron Lett.* **1996**, *37*, 7623-7626; 'Catalytic racemisation of alcohols: Applications to enzymatic resolution reactions'.
[219] B. Martín-Matute, M. Edin, K. Bogár, J.-E. Bäckvall, *Angew. Chem. Int. Ed.* **2004**, *43*, 6535-6539; 'Highly compatible metal and enzyme catalysts for efficient dynamic kinetic resolution of alcohols at ambient temperature'.
[220] B. Martín-Matute, M. Edin, K. Bogár, J.-E. Bäckvall, *Angew. Chem.* **2004**, *115*, 6697-6701; 'Highly compatible metal and enzyme catalysts for efficient dynamic kinetic resolution of alcohols at ambient temperature'.
[221] J. H. Choi, Y. H. Kim, S. H. Nam, S. T. Shin, M. J. Kim, J. Park, *Angew. Chem. Int. Ed.* **2002**, *41*, 2373-2376; 'Aminocyclopentadienyl ruthenium chloride: catalytic racemization and dynamic kinetic resolution of alcohols at ambient temperature'.
[222] J. H. Choi, Y. H. Kim, S. H. Nam, S. T. Shin, M. J. Kim, J. Park, *Angew. Chem.* **2002**, *114*, 2479-2482; 'Aminocyclopentadienyl ruthenium chloride: catalytic racemization and dynamic kinetic resolution of alcohols at ambient temperature'.
[223] Y.-B. Wang, B. Tan, *Acc. Chem. Res.* **2018**, *51*, 534-547; 'Construction of axially chiral compounds via asymmetric organocatalysis'.
[224] G. Buechi, D. H. Klaubert, R. Shank, S. M. Weinreb, G. Wogan, *J. Org. Chem.* **1971**, *36*, 1143-1147; 'Structure and Synthesis of Kotanin and Desmethylkotanin, Metabolites of *Aspergillus glaucus*'.
[225] S. Ahmad, S. Razaq, *Tetrahedron* **1976**, *32*, 503-506; 'New synthesis of biflavones of cupressuflavone series'.
[226] S. Duprat de Paule, S. Jeulin, V. Ratovelomanana-Vidal, J.-P. Genêt, N. Champion, G. Deschaux, P. Dellis, *Org. Process Res. Dev.* **2003**, *7*, 399-406; 'Synphos: A new atropisomeric diphosphine ligand. From laboratory-scale synthesis to scale-up development'.
[227] T. Saito, T. Yokozawa, T. Ishizaki, T. Moroi, N. Sayo, T. Miura, H. Kumobayashi, *Adv. Synth. Catal.* **2001**, *343*, 264-267; 'New chiral diphosphine ligands designed to have a narrow dihedral angle in the biaryl backbone'.
[228] H. Jiang, Y. Zhang, W. Xiong, J. Cen, L. Wang, R. Cheng, C. Qi, W. Wu, *Org. Lett.* **2018**, *21*, 345-349; 'A Three-Phase Four-Component Coupling Reaction: Selective Synthesis of *o*-Chloro Benzoates by KCl, Arynes, CO_2, and Chloroalkanes'.
[229] M. Runge, G. Haufe, *J. Org. Chem.* **2000**, *65*, 8737-8742; 'Enantioselective synthesis of a fluorinated analogue of the orsellinic acid-type twelve-membered lactone lasiodiplodin'.
[230] M. P. Bernstein, F. E. Romesberg, D. J. Fuller, A. T. Harrison, D. B. Collum, Q. Y. Liu, P. G. Williard, *J. Am. Chem. Soc.* **1992**, *114*, 5100-5110; 'Structure and reactivity of lithium diisopropylamide in the presence of *N*,*N*,*N*',*N*'-tetramethylethylenediamine'.
[231] D. B. Collum, *Acc. Chem. Res.* **1992**, *25*, 448-454; 'Is N,N,N',N'-tetramethylethylenediamine a good ligand for lithium?'.
[232] S. Usui, Y. Hashimoto, J. V. Morey, A. E. Wheatley, M. Uchiyama, *J. Am. Chem. Soc.* **2007**, *129*, 15102-15103; 'Direct *ortho* cupration: A new route to regioselectively functionalized aromatics'.
[233] N. Tezuka, K. Shimojo, K. Hirano, S. Komagawa, K. Yoshida, C. Wang, K. Miyamoto, T. Saito, R. Takita, M. Uchiyama, *J. Am. Chem. Soc.* **2016**, *138*, 9166-9171; 'Direct hydroxylation and amination of arenes via deprotonative cupration'.

[234] N. Tezuka, K. Hirano, M. Uchiyama, *Org. Lett.* **2019**, *21*, 9536-9540; 'A Direct, Chemo-, and Regioselective Cross-Coupling Reaction of Arenes via Sequential Directed ortho Cuprations and Oxidation'.
[235] T. Sawada, M. Aono, S. Asakawa, A. Ito, K. Awano, *J. Antibiot.* **2000**, *53*, 959-966; 'Structure determination and total synthesis of a novel antibacterial substance, AB0022A, produced by a cellular slime mold'.
[236] Y.-L. Zeng, Y. Ai, S.-Y. Tang, X.-J. Song, X.-G. Chen, Y.-Y. Tang, Z.-X. Zhang, Y.-M. You, R.-G. Xiong, H.-Y. Zhang, *J. Am. Chem. Soc.* **2022**, *144*, 19559-19566; 'Axial-Chiral BINOL Multiferroic Crystals with Coexistence of Ferroelectricity and Ferroelasticity'.
[237] T. Ishiyama, J. Takagi, J. Hartwig, N. Miyaura, *Angew. Chem. Int. Ed.* **2002**, *41*, 3056-3058; 'A stoichiometric aromatic CH borylation catalyzed by iridium (I)/2, 2â ²-bipyridine complexes at room temperature'.
[238] T. Ishiyama, J. Takagi, J. Hartwig, N. Miyaura, *Angew. Chem.* **2002**, *114*, 3182-3184; 'A stoichiometric aromatic CH borylation catalyzed by iridium (I)/2, 2â ²-bipyridine complexes at room temperature'.
[239] T. Ishiyama, J. Takagi, K. Ishida, N. Miyaura, N. R. Anastasi, J. F. Hartwig, *J. Am. Chem. Soc.* **2002**, *124*, 390-391; 'Mild iridium-catalyzed borylation of arenes. High turnover numbers, room temperature reactions, and isolation of a potential intermediate'.
[240] T. Ishiyama, Y. Nobuta, J. F. Hartwig, N. Miyaura, *Chem. Commun.* **2003**, 2924-2925; 'Room temperature borylation of arenes and heteroarenes using stoichiometric amounts of pinacolborane catalyzed by iridium complexes in an inert solvent'.
[241] M. K. T. Klischan, Dissertation, Heinrich-Heine-Universität Düsseldorf **2024**; 'Biaryl-based natural products as structural motif for pharmaceutically relevant compounds.'
[242] M. K. Klischan, C. David, D. Grudzinski, W. Frey, B. Stork, J. Pietruszka, *Org. Lett.* **2024**, *26*, 5258-5262; 'Application of Cyclic Diaryliodonium Salts in the Synthesis of Axially Chiral Natural Product Analogues'.
[243] A. L. Thompson, G. W. Kabalka, M. R. Akula, J. W. Huffman, *Synthesis* **2005**, 547-550; 'The conversion of phenols to the corresponding aryl halides under mild conditions'.
[244] Y. Li, M. Wang, Z. Liu, K. Zhang, F. Cui, W. Sun, *Environ. Microbiol.* **2019**, *21*, 2629-2643; 'Towards understanding the biosynthetic pathway for ustilaginoidin mycotoxins in *Ustilaginoidea virens*'.
[245] C. D. Donner, *Tetrahedron* **2013**, *69*, 3747-3773; 'Tandem Michael-Dieckmann/Claisen reaction of *ortho*-toluates-the Staunton-Weinreb annulation'.
[246] A. Fürstner, O. R. Thiel, N. Kindler, B. Bartkowska, *J. Org. Chem.* **2000**, *65*, 7990-7995; 'Total syntheses of (*S*)-(−)-zearalenone and lasiodiplodin reveal superior metathesis activity of ruthenium carbene complexes with imidazol-2-ylidene ligands'.
[247] M. Mondal, V. G. Puranik, N. P. Argade, *J. Org. Chem.* **2007**, *72*, 2068-2076; 'A facile phenol-driven intramolecular diastereoselective thermal/base-catalyzed dipolar [2+2] annulation reactions: An easy access to complex bioactive natural and unnatural benzopyran congeners'.
[248] S. Fang, L. Chen, M. Yu, B. Cheng, Y. Lin, S. L. Morris-Natschke, K.-H. Lee, Q. Gu, J. Xu, *Org. Biomol. Chem.* **2015**, *13*, 4714-4726; 'Synthesis, antitumor activity, and mechanism of action of 6-acrylic phenethyl ester-2-pyranone derivatives'.

[249] M. G. Charest, C. D. Lerner, J. D. Brubaker, D. R. Siegel, A. G. Myers, *Science* **2005**, *308*, 395-398; 'A convergent enantioselective route to structurally diverse 6-deoxytetracycline antibiotics'.

[250] K. R. Anderson, S. p. L. Atkinson, T. Fujiwara, M. E. Giles, T. Matsumoto, E. Merifield, J. T. Singleton, T. Saito, T. Sotoguchi, J. A. Tornos, *Org. Process Res. Dev.* **2010**, *14*, 58-71; 'Routes for the Synthesis of (2*S*)-2-Methyltetrahydropyran-4-one from Simple Optically Pure Building Blocks'.

[251] R. Nakamura, K. Tanino, M. Miyashita, *Org. Lett.* **2005**, *7*, 2929-2932; 'Stereoselective synthesis of premisakinolide A, the monomeric counterpart of the marine 40-membered dimeric macrolide misakinolide A'.

[252] A. G. Cook, P. M. Feltman, *J. Chem. Educ.* **2007**, *84*, 1827; 'Determination of Solvent Effects on Keto-Enol Equilibria of 1,3-Dicarbonyl Compounds Using NMR'.

[253] X. Sun, D. B. Collum, *J. Am. Chem. Soc.* **2000**, *122*, 2452-2458; 'Lithium diisopropylamide-mediated enolizations: solvent-independent rates, solvent-dependent mechanisms'.

[254] A. S. Galiano-Roth, D. B. Collum, *J. Am. Chem. Soc.* **1989**, *111*, 6772-6778; 'Structure and reactivity of lithium diisopropylamide (LDA). The consequences of aggregation and solvation during the metalation of an *N*,*N*-dimethylhydrazone'.

[255] M. Ronn, Z. Zhu, P. C. Hogan, W.-Y. Zhang, J. Niu, C. E. Katz, N. Dunwoody, O. Gilicky, Y. Deng, D. K. Hunt, *Org. Process Res. Dev.* **2013**, *17*, 838-845; 'Process R&D of eravacycline: the first fully synthetic fluorocycline in clinical development'.

[256] C. Sun, Q. Wang, J. D. Brubaker, P. M. Wright, C. D. Lerner, K. Noson, M. Charest, D. R. Siegel, Y.-M. Wang, A. G. Myers, *J. Am. Chem. Soc.* **2008**, *130*, 17913-17927; 'A robust platform for the synthesis of new tetracycline antibiotics'.

[257] L. Gupta, A. C. Hoepker, K. J. Singh, D. B. Collum, *J. Org. Chem.* **2009**, *74*, 2231-2233; 'Lithium diisopropylamide-mediated *ortho* lithiations: Lithium chloride catalysis'.

[258] Y. Ma, A. C. Hoepker, L. Gupta, M. F. Faggin, D. B. Collum, *J. Am. Chem. Soc.* **2010**, *132*, 15610-15623; '1,4-addition of lithium diisopropylamide to unsaturated esters: Role of rate-limiting deaggregation, autocatalysis, lithium chloride catalysis, and other mixed aggregation effects'.

[259] A. C. Hoepker, L. Gupta, Y. Ma, M. F. Faggin, D. B. Collum, *J. Am. Chem. Soc.* **2011**, *133*, 7135-7151; 'Regioselective lithium diisopropylamide-mediated *ortho*-lithiation of 1-chloro-3-(trifluoromethyl) benzene: Role of autocatalysis, lithium chloride catalysis, and reversibility'.

[260] J. D. White, F. Demnitz, Q. Xu, W. H. Martin, *Org. Lett.* **2008**, *10*, 2833-2836; 'Synthesis of an Advanced Intermediate for (+)-Pillaromycinone. Staunton-Weinreb Annulation Revisited'.

[261] F. Weber, A. Weber, L. Schmitt, I. Lechtenberg, J. Greb, B. Henßen, S. Wesselborg, J. Pietruszka, *Chem. Eur. J.* **2024**, *30*, e202400559; 'From the Total Synthesis of Semi–Viriditoxin, Semi–Viriditoxic Acid and Dimeric Naphthopyranones to their Biological Activities in Burkitt B Cell Lymphoma'.

[262] B. B. Liau, B. C. Milgram, M. D. Shair, *J. Am. Chem. Soc.* **2012**, *134*, 16765-16772; 'Total syntheses of HMP-Y1, hibarimicinone, and HMP-P1'.

[263] F. Grein, A. C. Chen, D. Edwards, C. M. Crudden, *J. Org. Chem.* **2006**, *71*, 861-872; 'Theoretical and Experimental Studies on the Baeyer-Villiger Oxidation of Ketones and the Effect of α-Halo Substituents'.

[264] P. Sarver, M. Acker, J. T. Bagdanoff, Z. Chen, Y.-N. Chen, H. Chan, B. Firestone, M. Fodor, J. Fortanet, H. Hao, *J. Med. Chem.* **2019**, *62*, 1793-1802; '6-Amino-3-methylpyrimidinones as potent, selective, and orally efficacious SHP2 inhibitors'.
[265] J. J. Ma, W. B. Yi, G. P. Lu, C. Cai, *Org. Biomol. Chem.* **2015**, *13*, 2890-2894; 'Transition-metal-free C–H oxidative activation: persulfate-promoted selective benzylic mono-and difluorination'.
[266] E. Marzi, F. Mongin, A. Spitaleri, M. Schlosser, *Eur. J. Org. Chem.* **2001**, *2001*, 2911-2915; 'Fluorophenols and (Trifluoromethyl)phenols as Substrates of Site-Selective Metalation Reactions: To Protect or not To Protect'.
[267] S. E. Bode, D. Drochner, M. Müller, *Angew. Chem. Int. Ed.* **2007**, *46*, 5916-5920; 'Synthesis, Biosynthesis, and Absolute Configuration of Vioxanthin'.
[268] S. E. Bode, D. Drochner, M. Müller, *Angew. Chem.* **2007**, *119*, 6020-6024; 'Synthesis, biosynthesis, and absolute configuration of vioxanthin'.
[269] K. Tatsuta, T. Fukuda, T. Ishimori, R. Yachi, S. Yoshida, H. Hashimoto, S. Hosokawa, *Tetrahedron Lett.* **2012**, *53*, 422-425; 'The first total synthesis of hibarimicinone, a potent v-Src tyrosine kinase inhibitor'.
[270] I. M. Romaine, J. E. Hempel, G. Shanmugam, H. Hori, Y. Igarashi, P. L. Polavarapu, G. A. Sulikowski, *Org. Lett.* **2011**, *13*, 4538-4541; 'Assignment and stereocontrol of hibarimicin atropoisomers'.
[271] Y. S. Park, C. I. Grove, M. González-López, S. Urgaonkar, J. C. Fettinger, J. T. Shaw, *Angew. Chem. Int. Ed.* **2011**, *50*, 3730-3733; 'Synthesis of (−)-Viriditoxin: A 6,6'-Binaphthopyran-2-one that Targets the Bacterial Cell Division Protein FtsZ'.
[272] Y. S. Park, C. I. Grove, M. González-López, S. Urgaonkar, J. C. Fettinger, J. T. Shaw, *Angew. Chem.* **2011**, *123*, 3814-3817; 'Synthesis of (−)-Viriditoxin: A 6,6'-Binaphthopyran-2-one that Targets the Bacterial Cell Division Protein FtsZ'.
[273] S. Huang, T. B. Petersen, B. H. Lipshutz, *J. Am. Chem. Soc.* **2010**, *132*, 14021-14023; 'Total synthesis of (+)-korupensamine B via an atropselective intermolecular biaryl coupling'.
[274] H. F. Lewis, S. Shaffer, W. Trieschmann, H. Cogan, *Ind. Eng. Chem.* **1930**, *22*, 34-36; 'Methylation of Phenol by Dimethyl Sulfate'.
[275] C. I. Grove, M. J. Di Maso, F. A. Jaipuri, M. B. Kim, J. T. Shaw, *Org. Lett.* **2012**, *14*, 4338-4341; 'Synthesis of 6,6'-Binaphthopyran-2-one Natural Products: Pigmentosin A, Talaroderxines A and B'.
[276] G. Lunn, E. B. Sansone, *Am. Ind. Hyg. Assoc. J.* **1985**, *46*, 111-114; 'Validation of techniques for the destruction of dimethyl sulfate'.
[277] M. K. T. Klischan, Bachelor thesis, Heinrich Heine Universität **2018**; 'Funktionalisierte Chromonmethylester–Schlüsselintermediate für die Synthese von Tetrahydroxanthon-Dimeren.'
[278] W. Basiski, *Polish J. Chem.* **1995**, *69*, 376-384; 'Benzo-γ-pyrones. Part XV. Conversion of some 4-Oxo-4H-1-benzopyran-2-carboxylic Acids into 4H-1-Benzopyran-4-ones via Isoxazoles'.
[279] pKa value was computed by Chem3D.
[280] J. Clayden, N. Greeves, S. Warren, *Organic chemistry*, Oxford University Press, USA, **2012**.
[281] J.-F. Cui, H. Huang, H. N. Wong, *Synlett* **2011**, *7*, 1018-1022; 'A concise synthetic approach towards hydroxytetraphenylenes'.
[282] C. Chen, Y. Qiao, H. Geng, X. Zhang, *Org. Lett.* **2013**, *15*, 1048-1051; 'A novel triphosphoramidite ligand for highly regioselective linear hydroformylation of terminal and internal olefins'.

[283] W. Pan, C. Li, H. Zhu, F. Li, T. Li, W. Zhao, *Org. Biomol. Chem.* **2021**, *19*, 7633-7640; 'A mild and practical method for deprotection of aryl methyl/benzyl/allyl ethers with $HPPh_2$ and *t*-BuOK'.

[284] G. Delogu, D. Fabbri, M. A. Dettori, A. Forni, G. Casalone, *Tetrahedron: Asymmetry* **2000**, *11*, 4417-4427; 'Chiral nonracemic C2-symmetry biphenyls by desymmetrization of 6,6',2,2'-tetramethoxy-1,1'-biphenyl'.

[285] L. Jierry, S. Harthong, C. Aronica, J.-C. Mulatier, L. Guy, S. Guy, *Org. Lett.* **2012**, *14*, 288-291; 'Efficient Dibenzo[*c*]acridine Helicene-like Synthesis and Resolution: Scaleup, Structural Control, and High Chiroptical Properties'.

[286] S.-J. Tang, K.-H. Sun, G.-H. Sun, T.-Y. Chang, G.-C. Lee, *Protein Expr. Purif.* **2000**, *20*, 308-313; 'Recombinant Expression of the *Candida rugosa* lip4 Lipase in *Escherichia coli*'.

[287] S. Vorlová, U. T. Bornscheuer, I. Gatfield, J. M. Hilmer, H. J. Bertram, R. D. Schmid, *Adv. Synth. Catal.* **2002**, *344*, 1152-1155; 'Enantioselective Hydrolysis of D,L-Menthyl Benzoate to L-(–)-Menthol by Recombinant *Candida rugosa* Lipase LIP1'.

[288] P. Ferrer, M. Alarcón, R. Ramón, M. D. Benaiges, F. Valero, *Biochem. Eng. J.* **2009**, *46*, 271-277; 'Recombinant *Candida rugosa* LIP2 expression in Pichia pastoris under the control of the AOX1 promoter'.

[289] M. Stewart, R. J. Capon, J. M. White, E. Lacey, S. Tennant, J. H. Gill, M. P. Shaddock, *J. Nat. Prod.* **2004**, *67*, 728-730; 'Rugulotrosins A and B: Two new antibacterial metabolites from an Australian isolate of a Penicillium sp.'.

[290] M. Gill, P. M. Morgan, *Arkivoc* **2004**, *10*, 152-165; 'Absolute stereochemistry of fungal metabolites: icterinoidins A1 and B1, and atrovirins B1 and B2'.

[291] M. A. Rizzacasa, M. V. Sargent, *J. Chem. Soc., Perkin Trans.* **1988**, 2425-2428; 'The synthesis of desertorin C, a bicoumarin from the fungus *Emericella desertorum*'.

[292] S. Lorraine, K. Abdur-Rashid, W. Jia, K. Abdur-Rashid, P. Maragh, T. Dasgupta, *Inorg. Chim. Acta* **2020**, *511*, 119850; 'Biaryl diphosphine ligands and their ruthenium complexes: Preparation and use for catalytic hydrogenation of ketones'.

[293] L. F. Tietze, D. A. Spiegl, F. Stecker, J. Major, C. Raith, C. Große, *Chem. Eur. J.* **2008**, *14*, 8956-8963; 'Stereoselective Synthesis of 4-Dehydroxydiversonol Employing Enantioselective Palladium-Catalysed Domino Reactions'.

[294] J. Fang, D. Wang, G.-J. Deng, H. Gong, *Tetrahedron Lett.* **2017**, *58*, 4503-4506; 'Transition metal-free protodecarboxylation of electron rich aromatic acids under mild conditions'.

[295] J. MacMillan, *J. Chem. Soc.* **1954**, 2585-2587; 'Griseofulvin. Part IX. Isolation of the bromo-analogue from *Penicillium griseofulvum* and *Penicillium nigricans*'.

[296] P. M. Tadross, C. D. Gilmore, P. Bugga, S. C. Virgil, B. M. Stoltz, *Org. Lett.* **2010**, *12*, 1224-1227; 'Regioselective reactions of highly substituted arynes'.

[297] H. Lv, X. Wang, Y. Hao, C. Ma, S. Li, G. Li, J. Zhang, *Green Chem.* **2023**, *25*, 554-559; 'Rhodium(ii)-catalyzed C–H carboxylation of ferrocenes with CO_2'.

[298] R. Shintani, H. Otomo, K. Ota, T. Hayashi, *J. Am. Chem. Soc.* **2012**, *134*, 7305-7308; 'Palladium-catalyzed asymmetric synthesis of silicon-stereogenic dibenzosiloles via enantioselective C–H bond functionalization'.

[299] T. Hattori, Y. Shimazumi, H. Goto, O. Yamabe, N. Morohashi, W. Kawai, S. Miyano, *J. Org. Chem.* **2003**, *68*, 2099-2108; 'Synthesis, resolution, and absolute stereochemistry of (−)-Blestriarene C'.

[300] G. Pavé, J.-M. Léger, C. Jarry, M.-C. Viaud-Massuard, G. Guillaumet, *J. Org. Chem.* **2003**, *68*, 1401-1408; 'Enantioselective synthesis of spirocyclic aminochroman derivatives according to the CN (*R*, *S*) strategy'.

[301] M. Weimar, G. Dürner, J. W. Bats, M. W. Göbel, *J. Org. Chem.* **2010**, *75*, 2718-2721; 'Enantioselective synthesis of (+)-estrone exploiting a hydrogen bond-promoted Diels-Alder reaction'.

[302] C. Fricke, K. Deckers, F. Schoenebeck, *Angew. Chem. Int. Ed.* **2020**, *59*, 18717-18722; 'Orthogonal Stability and Reactivity of Aryl Germanes Enables Rapid and Selective (Multi)Halogenations'.

[303] C. Fricke, K. Deckers, F. Schoenebeck, *Angew. Chem.* **2020**, *128*, 674-678; 'Orthogonal Stability and Reactivity of Aryl Germanes Enables Rapid and Selective (Multi)Halogenations'.

[304] U. Lüning, F. Fahrenkrug, *Eur. J. Org. Chem.* **2004**, *2004*, 3119-3127; 'Synthesis of Concave 1, 10-Phenanthrolines by a Combination of Suzuki Coupling, Ring Closing Metathesis and Hydrogenation'.

[305] W. Kashikura, K. Mori, T. Akiyama, *Org. Lett.* **2011**, *13*, 1860-1863; 'Chiral phosphoric acid catalyzed enantioselective synthesis of *β*-amino-*α*,*α*-difluoro carbonyl compounds'.

[306] J.-M. Yoon, C.-Y. Lee, Y.-I. Jo, C.-H. Cheon, *J. Org. Chem.* **2016**, *81*, 8464-8469; 'Synthesis of Optically Pure 3,3'-Disubstituted-1,1'-Bi-6-Methoxy-2-Phenol (BIPhOL) Derivatives via Diastereomeric Resolution'.

[307] J. Magano, M. H. Chen, J. D. Clark, T. Nussbaumer, *J. Org. Chem.* **2006**, *71*, 7103-7105; '2-(Diethylamino) ethanethiol, a new reagent for the odorless deprotection of aromatic methyl ethers'.

[308] A. Adeyemi, J. Bergman, J. Branalt, J. Sävmarker, M. Larhed, *Org. Process Res. Dev.* **2017**, *21*, 947-955; 'Continuous flow synthesis under high-temperature/high-pressure conditions using a resistively heated flow reactor'.

[309] Q. Liu, D. G. Batt, G. V. DeLucca, Q. Shi, A. J. Tebben, *United States Patent* **2011**, *US8362065B2*; 'Carbazole carboxamide compounds useful as kinase inhibitors'.

[310] D. Zamora-Olivares, T. S. Kaoud, K. N. Dalby, E. V. Anslyn, *J. Am. Chem. Soc.* **2013**, *135*, 14814-14820; 'In-situ generation of differential sensors that fingerprint kinases and the cellular response to their expression'.

[311] W. Lin, O. Baron, P. Knochel, *Org. Lett.* **2006**, *8*, 5673-5676; 'Highly Functionalized Benzene Syntheses by Directed Mono or Multiple Magnesiations with TMPMgCl·LiCl'.

[312] D. He, B. Wang, K. Duan, Y. Zhou, M. Li, H. Jiang, W. Wu, *Org. Lett.* **2022**, *24*, 1292-1297; 'Synthesis of Densely Substituted Pyridine Derivatives from 1-Methyl-1,3-(ar)enynes and Nitriles by a Formal [4+2] Cycloaddition Reaction'.

[313] S. Jo, B. Kang, J.-W. Jung, *Molecules* **2022**, *28*, 62; 'Microwave-Assisted Cu-Catalyzed Diaryletherification for Facile Synthesis of Bioactive Prenylated Diresorcinols'.

[314] H. Miyakoshi, S. Miyahara, T. Yokogawa, K. Endoh, T. Muto, W. Yano, T. Wakasa, H. Ueno, K. T. Chong, J. Taguchi, *J. Med. Chem.* **2012**, *55*, 6427-6437; '1,2,3-Triazole-containing uracil derivatives with excellent pharmacokinetics as a novel class of potent human deoxyuridine triphosphatase inhibitors'.

[315] T. Fukuda, T. Umeki, K. Tokushima, G. Xiang, Y. Yoshida, F. Ishibashi, Y. Oku, N. Nishiya, Y. Uehara, M. Iwao, *Bioorg. Med. Chem.* **2017**, *25*, 6563-6580; 'Design, synthesis, and evaluation of A-ring-modified lamellarin N analogues as noncovalent inhibitors of the EGFR T790M/L858R mutant'.

[316] S. Kimura, S. Kobayashi, T. Kumamoto, A. Akagi, N. Sato, T. Ishikawa, *Helv. Chim. Acta* **2011**, *94*, 578-591; 'Syntheses of Prekinamycin and a Tetracyclic Quinone from Common Synthetic Intermediates'.
[317] R. K. Haynes, H. Heß, H. Musso, *Chem. Ber.* **1974**, *107*, 3733-3748; 'Die Oxidation von Orcin mit $K_3[Fe(CN)_6]$ im Strömungsrohr'.
[318] K. Kodama, F. Takase, T. Hirose, *RSC Adv.* **2021**, *11*, 18162-18170; 'Direct enantioseparation of axially chiral 1,1'-biaryl-2,2'-diols using amidine-based resolving agents'.
[319] D. R. Armstrong, C. Cameron, D. C. Nonhebel, P. G. Perkins, *J. Chem, Soc., Perkin Trans.* **1983**, 563-568; 'Oxidative coupling of phenols. Part 6. A study of the role of spin density factors on the product composition in the oxidations of 3, 5-dimethylphenol and phenol'.
[320] R. S. Coleman, J. M. Guernon, J. T. Roland, *Org. Lett.* **2000**, *2*, 277-280; 'Synthesis of the spirocyclic cyclohexadienone ring system of the schiarisanrins'.
[321] W. Logan, G. Newbold, *J. Chem. Soc.* **1957**, 1946-1951; '374. Lactones. Part V. Experiments relating to mycophenolic acid'.
[322] G. A. Kraus, I. Jeon, J. Mengwasser, A. C. West, T. L. Windus, *Synlett* **2010**, *13*, 1955-1958; 'Selective Metalation of 4, 6-Dibromoresorcinol Dimethyl Ether with LiTMP'.
[323] R. V. Cochrane, R. Sanichar, G. R. Lambkin, B. Reiz, W. Xu, Y. Tang, J. C. Vederas, *Angew. Chem.* **2016**, *128*, 674-678; 'Production of new cladosporin analogues by reconstitution of the polyketide synthases responsible for the biosynthesis of this antimalarial agent'.
[324] R. V. Cochrane, R. Sanichar, G. R. Lambkin, B. Reiz, W. Xu, Y. Tang, J. C. Vederas, *Angew. Chem. Int. Ed.* **2016**, *55*, 664-668; 'Production of new cladosporin analogues by reconstitution of the polyketide synthases responsible for the biosynthesis of this antimalarial agent'.
[325] K. Kumari, T. Syed, A. Krishna, S. Muvvala, A. Nowduri, C. Sridhar, A. Saxena, *Tetrahedron* **2022**, *112*, 132723; 'Steroselective total synthesis of Neocosmosin B'.
[326] R. Samala, M. K. Basu, K. Mukkanti, *Tetrahedron Lett.* **2022**, *88*, 153574; 'Regioselective functionalization of pyrones: Facile synthesis of 6-styrylpyrones *via* KHMDS-mediated aldol condensation'.
[327] L. Koser, V. M. Lechner, T. Bach, *Angew. Chem. Int. Ed.* **2021**, *60*, 20269-20273; 'Biomimetic Total Synthesis of Enterocin'.
[328] L. Koser, V. M. Lechner, T. Bach, *Angew. Chem.* **2021**, *133*, 20431-20435; 'Biomimetic Total Synthesis of Enterocin'.
[329] M. Wolberg, W. Hummel, M. Müller, *Chem. Eur. J.* **2001**, *7*, 4562-4571; 'Biocatalytic Reduction of *β*, *δ*-Diketo Esters: A Highly Stereoselective Approach to All Four Stereoisomers of a Chlorinated *β*, *δ*-Dihydroxy Hexanoate'.
[330] H. Zhao, A. Yang, N. Zhang, S. Li, T. Yuan, N. Ding, S. Zhang, S. Bao, C. Wang, Y. Zhang, *J. Agric. Food Chem.* **2020**, *68*, 1588-1595; 'Insecticidal Endostemonines A–J Produced by Endophytic *Streptomyces* from *Stemona sessilifolia*'.
[331] G. Späth, A. Fürstner, *Angew. Chem.* **2021**, *133*, 7979-7984; 'Scalable de novo synthesis of aldgarose and total synthesis of aldgamycin N'.
[332] G. Späth, A. Fürstner, *Angew. Chem. Int. Ed.* **2021**, *60*, 7900-7905; 'Scalable de novo synthesis of aldgarose and total synthesis of aldgamycin N'.
[333] M. Macías, M. Ulloa, A. Gamboa, R. Mata, *J. Nat. Prod.* **2000**, *63*, 757-761; 'Phytotoxic compounds from the new coprophilous fungus *Guanomyces polythrix*'.
[334] A. Ilangovan, P. Sakthivel, *RSC Adv.* **2014**, *4*, 55150-55161; 'Simple access to 5-carboalkoxy-2,3-dihydro-4*H*-pyran-4-ones via domino acylative electrocyclization:

the first three step total synthesis of the dihydronaphthopyran-4-one class of natural products'.

[335] J. Buter, D. Heijnen, C. Vila, V. Hornillos, E. Otten, M. Giannerini, A. J. Minnaard, B. L. Feringa, *Angew. Chem. Int. Ed.* **2016**, *55*, 3620-3624; 'Palladium-Catalyzed, *tert*-Butyllithium-Mediated Dimerization of Aryl Halides and Its Application in the Atropselective Total Synthesis of Mastigophorene A'.

[336] J. Buter, D. Heijnen, C. Vila, V. Hornillos, E. Otten, M. Giannerini, A. J. Minnaard, B. L. Feringa, *Angew. Chem.* **2016**, *128*, 3684-3688; 'Palladium-Catalyzed, *tert*-Butyllithium-Mediated Dimerization of Aryl Halides and Its Application in the Atropselective Total Synthesis of Mastigophorene A'.

[337] D. Drochner, W. Hüttel, S. E. Bode, M. Müller, U. Karl, M. Nieger, W. Steglich, *Eur. J. Org. Chem.* **2007**, *2007*, 1749-1758; 'Dimeric Orsellinic Acid Derivatives: Valuable Intermediates for Natural Product Synthesis'.

[338] D. Drochner, W. Hüttel, M. Nieger, M. Müller, *Angew. Chem.* **2003**, *115*, 961-963; 'Unselective Phenolic Coupling of Methyl 2-Hydroxy-4-methoxy-6-methylbenzoate—A Valuable Tool for the Total Synthesis of Natural Product Families'.

10 Acknowledgements

First, I would like to thank *Prof. Dr. Jörg Pietruszka* for giving me the opportunity to pursue my doctoral studies at his institute. I am grateful for the chance to work on this very interesting project. Your availability and support have greatly encouraged and helped me throughout this journey. I appreciate your trust and your belief in my potential as a lab leader, which I did not see in myself at the beginning. The experience has shaped me and has given me the opportunity to grow.

I would also like to thank *Prof. Dr. Thomas J. J. Müller* for his willingness to evaluate my doctoral thesis as a second evaluator.

Next, I would like to extend a big thank you to *Birgit Henßen*. Thank you for dedicating so much time to develop all the HPLC separation methods and for assisting with so many HPLC measurements. It was a great help. I appreciate your willingness to help with various organizational matters, despite all your many other responsibilities.

Furthermore, I thank *Thomas Classen* for his input and feedback during our seminars. I am grateful for your efforts in investigating the lipase docking studies and for taking the time to explain these complex topics to me.

I would also like to thank the analytics department at the Heinrich Heine University of Düsseldorf and the central analytics department (ZEA 3) at the Forschungszentrum Jülich for measuring the HRMS samples.

Thank you as well to *Stephan Thies* and *Alexander Bollinger*, who have provided their hydrolases and have offered support on topics regarding to lipases.

A huge thank you to the amazing Biaryl Team: *Julian Greb*, *Moritz Klischan* and *Sebastian Myllek*. I am very grateful to have the opportunity to work within this team. It was a great support to exchange ideas, discuss problems, and learn from each other. I would like to extend a special thanks to *Julian Greb* for creating the new projects and forming this team. Your hard work, alongside *Till Drennhaus,* provided a good foundation for my thesis. I greatly appreciate our conversations and your support with tips and ideas. Thank you also for the cooperation of our publication. Your input and corrections have helped me a lot to find the right concept for the paper. Next, I would like to thank *Moritz Klischan* as well. Without you, lab life would have been only half as enjoyable. It was fun to work with you.

Even on days when nothing seemed to work out, you could brighten the lab's mood with new jokes, imitations, videos or songs. Thank you for all your advices, ideas and for always being open to my questions.

Many thanks to the wonderful people who have supported me in reading and correcting my doctoral thesis: *Alexander Fejzagic*, *David Skinner*, *Marvin Mantel* and *Moritz Klischan*. Thank you for taking your time to help me in the final phases of this journey.

Furthermore, a big big thank you to *Cindy Zimmermann*. I am so glad that we could share all the experiences together since our master's thesis. I knew I could always come to you and share everything with you, knowing that you would understand me. It was always good to have a coffee break with you, where we could laugh together or have deep conversations. I think we handled the Asian invasion perfectly.

I also want to thank everyone in lab 2004: *Benedikt Baumer*, *Dorothea Kossmann*, *Julian Greb*, *Marvin Mantel*, *Max Schlamkow*, *Moritz Klischan*, *Teresa Friedrichs*. I am so grateful that I could work in such a cool and easy-going team. It was never boring, and I will never forget all the crazy game ideas.

I would also like to thank my students who have supported me with their commitment: *Alesia Hysenaj, Anas Salhani, Cornelius Pawlowsky*, *Jacqueline Kühnel* and *Jan Böcker*.

Furthermore, I want to thank *Jasmin Wloka*. It was very motivating for me to see how diligent you always were. I enjoyed sharing the same office with you and the time we spent together.

Finally, I would like to thank my entire family and my friends, who have been there for me in this whole journey and have supported me through the highs and lows. Their prayers and open ears have been a great help to me and have always lifted me up. A special thank you to *Sena Permadi* for being always supportive and for encouraging me. Thank you for all your love and patient. I am so grateful to have you by my side.

Last but not least, I would like to thank my God for bringing me here. It is only by His grace that I could be here. I am grateful for the paths He has made possible for me. Without Him, I wouldn't have made it this far.

11 Declaration

I hereby certify that the present doctoral thesis, supervised by Prof. Dr. Jörg Pietruszka at the Institute of Bioorganic Chemistry at the Heinrich Heine University Düsseldorf and Forschungszentrum Jülich, was written by me independently and without the use of unauthorized aids. The work and writing of this doctoral thesis were conducted in accordance with the 'Principles of ensuring good scientific practice' at the Heinrich Heine University Düsseldorf.

The present doctoral thesis has only been presented to the Faculty of Mathematics and Natural Sciences of the Heinrich Heine University Düsseldorf. There has been no other attempt of reaching a doctoral degree before.

_____

Ruth Christine Ganardi

12 List of Abbreviations

AIBN	Azobisisobutyronitrile
BINAM	1,1′-Bi-(2-naphthylamin)
BINAP	[2,2′-Bis(diphenylphosphino)-1,1′-binaphthyl
BINOL	1,1′-Bi-2-naphthol
BOP	Bis(2-oxo-3-oxazolidinyl)phosphinate
brs	Broad singlet
BTM	Benzotetramisole
CoA	Coenzyme A
CBS	Corey-Bakshi-Shibata
d	Doublet
DCC	Dicyclohexylcarbodiimide
DEKR	Dynamic enzymatic kinetic resolution
DiBAL-H	Diisobutylaluminiumhydrid
DKR	Dynamic kinetic resolution
DMAP	4-Dimethylaminopyridine
DMF	Dimethylformamide
DMG	Direct metalation group
DMPU	*N*,*N*′-Dimethylpropyleneurea
DMS	Dimethyl sulfate
DMSO	Dimethyl sulfoxide
DOC	Directed *ortho*-cupration
DPQ	Tetra-*tert*-butyldiphenoquinone
dtbpy	4,4′-Di-*tert*-butyl-2,2′-bipyridyl
EAA	Ethyl acetoacetate
ee	Enantiomeric excess
EKR	Enzymatic kinetic resolution
EOM	Ethoxymethylether
ESI	Electrospray ionization
IR	Infrared
KR	Kinetic resolution
LDA	Lithium diisopropylamide

LiHMDS	Lithium bis(trimethylsilyl)amide
LiTMP	Lithium tetramethylpiperidide
HMG	3-Hydroxy-3-methylglutaryl
HMBC	Heteronuclear multiple bond correlation
HMPA	Hexamethylphosphoramide
HPLC	High-performance liquid chromatography
m	Multiplet
MBSC	*Miyaura* borylation *Suzuki* coupling
MOM	Methoxymethylether
Mp	Melting point
MS	Mass spectrometry
MTBE	Methyl *tert*-butyl ether
NBS	*N*-Bromosuccinimide
NHC	*N*-heterocyclic carbene
NMR	Nuclear magnetic resonance spectroscopy
NOBIN	2-Amino-2′-hydroxy-1,1′-binaphthyl
PE	Petroleum ether
PKS	Polyketide synthase
r.t.	Room temperature
s	Singlet
SAH	*S*-Adenosyl-L- homocysteine
SAM	*S*-Adenosyl methionine
t	Triplet
TBAI	Tetra-*N*-butylammonium iodide
TBAT	Tetra-butylammonium difluorotriphenylsilicate
THF	Tetrahydrofuran
TLC	Thin layer chromatography
TMEDA	Tetramethylethylenediamine
TMP	2,2,6,6-Tetramethylpiperidine
TMS	Tetramethylsilane
VANOL	3,3′-Diphenyl-2,2′-bi-1-naphthol
VAPOL	2,2′-Diphenyl-(4-biphenanthrol)
WHO	World Health Organization

13 List of synthesized molecules

All the compounds synthesized in this work are listed with their corresponding reference to the structure number and the abbreviation in the laboratory journal.

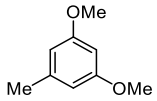	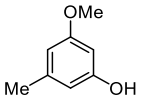	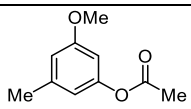
167	**168**	**169**
RGA001V125	RGA001V009	RGA001V015A
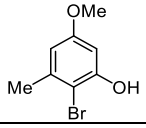	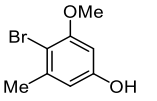	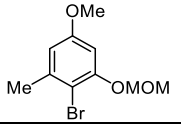
172	**173**	**174**
RGA001V035	JKU-RGA-001V006C	RGA001V024
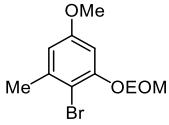	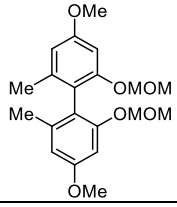	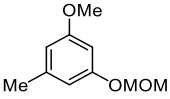
175	*rac*-**176a**	**177a**
RGA001V143	RGA001V048C	RGA001V065
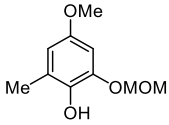	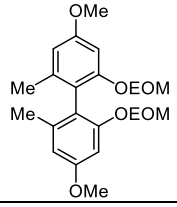	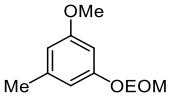
178a	*rac*-**176b**	**177b**
RGA001V098OxNP	RGA001V144D	RGA001V145A
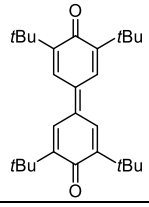	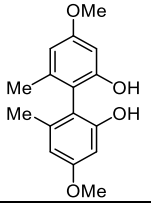	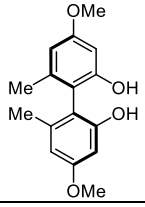
179	*rac*-**1**	(*P*)-**1**
RGA001V126	RGA001V056	RGA004V009C

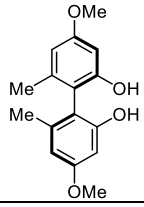	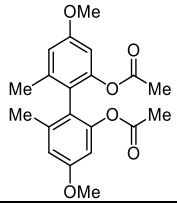	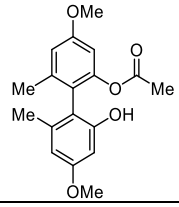
(*M*)-**1**	*rac*-**181a**	*rac*-**182a**
RGA004V100	RGA002V031	RGA002V034A
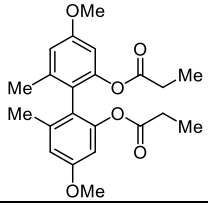	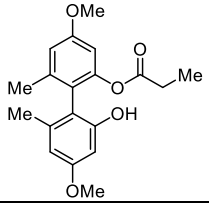	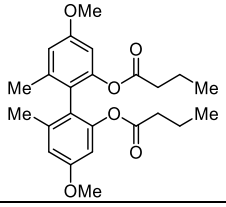
rac-**181b**	*rac*-**182b**	*rac*-**181c**
RGA002V002A	RGA002V004B	RGA002V003A
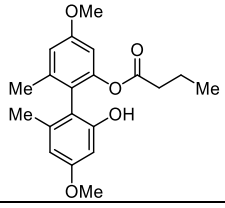	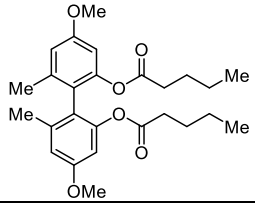	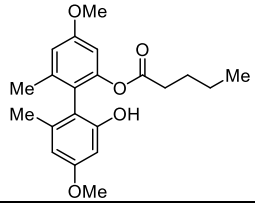
rac-**182c**	*rac*-**181d**	*rac*-**182d**
*R*GA002V005A	RGA002V016A	RGA002V016B
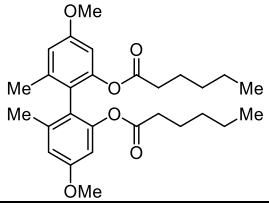	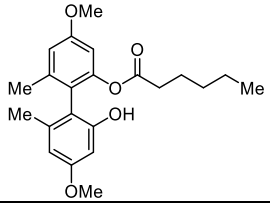	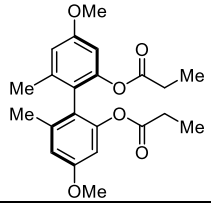
rac-**181e**	*rac*-**182e**	(*M*)-**181b**
RGA002V009A	RGA002V009C	RGA004V099A
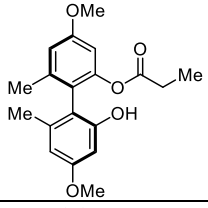	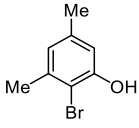	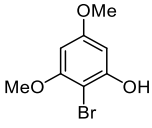
(*P*)-**182b**	**184**	**189**
RGA004V099B	RGA001V170B	RGA001V017

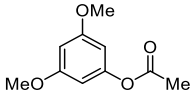	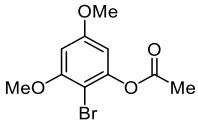	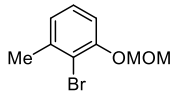
191	**192**	**193a**
RGA001V013	RGA001V014B	RGA001V010
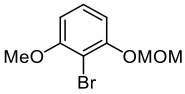	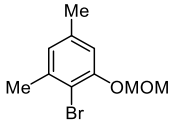	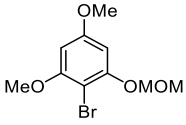
193b	**193c**	**193d**
AHY-RGA009	JKU-RGA001V027	RGA001V020
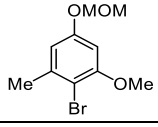	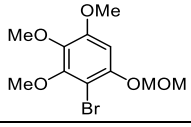	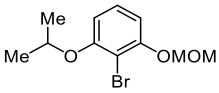
193e	**193f**	**193g**
JKU-RGA001V008	JKU-RGA001V015	JKU-RGA001V029A
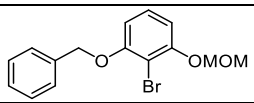	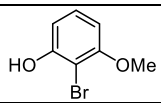	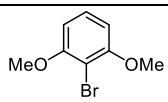
193h	**196**	**197**
RGA003V049	AHY-RGA008	AHY-RGA008NP
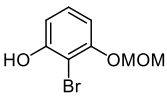	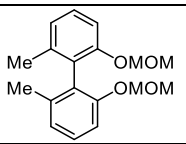	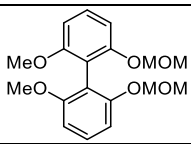
198	*rac*-**199a**	*rac*-**199b**
JKU-RGA001V028	RGA001V049B	JKU-RGA002V013
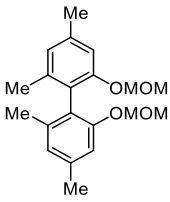	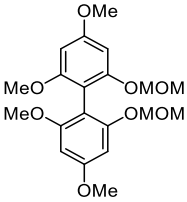	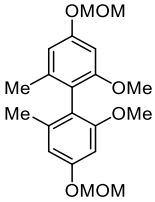
rac-**199c**	*rac*-**199d**	*rac*-**199e**
JKU-RGA002V019	RGA001V050C	JKU-RGA002V011
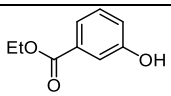	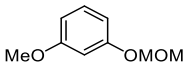	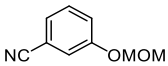
200	**201a**	**201b**
RGA001V077	RGA001V011	RGA001V120

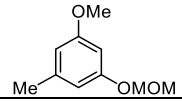	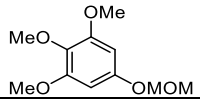	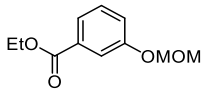
201c	**201d**	**201e**
RGA001V065	JKU-RGA001V014	RGA001V084
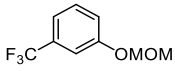	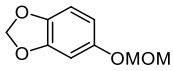	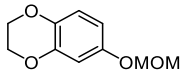
201f	**201g**	**201h**
RGA001V171	AHY-RGA001	AHY-RGA003
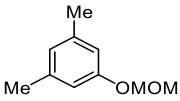	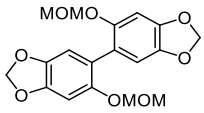	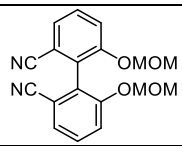
201i	**203**	*rac*-**207**
RGA001V051A	RGA003V026C	RGA003V039C
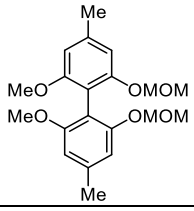	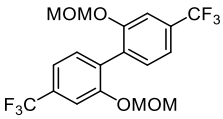	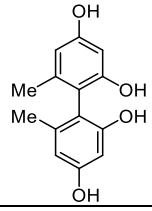
rac-**208**	**210**	*rac*-**153**
RGA003V029C	RGA003V032A	RGA001V169
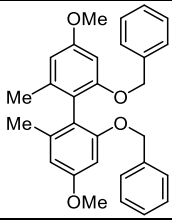	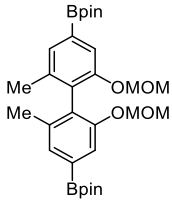	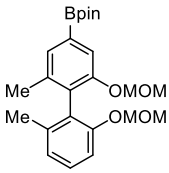
rac-**218**	*rac*-**220**	*rac*-**221**
RGA003V048A	MKL0185D	MKL0185C
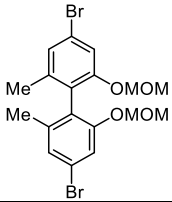	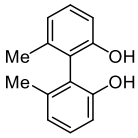	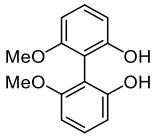
rac-**222**	*rac*-**223a**	*rac*-**223b**
RGA003V065A	RGA003V022	RGA003V024B

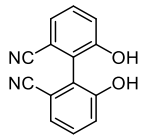	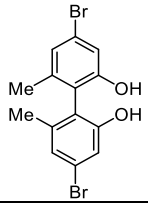	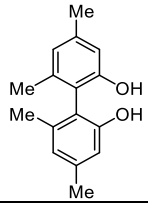
rac-**223c**	*rac*-**223d**	*rac*-**223e**
RGA003V042B	RGA003V068	JKU-RGA002V020
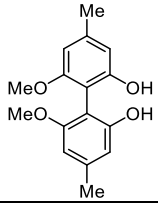	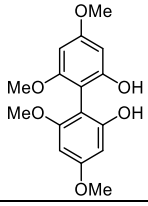	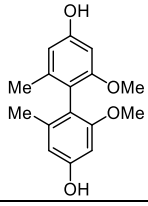
rac-**223f**	*rac*-**223g**	*rac*-**223h**
RGA003V047	RGA003V021	JKU-RGA002V014B
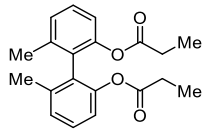	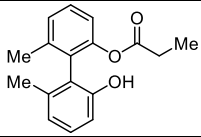	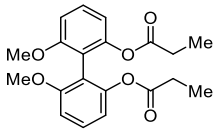
rac-**224a**	*rac*-**225a**	*rac*-**224b**
RGA002V039A	RGA002V039B	RGA002V043A
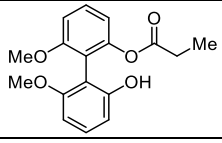	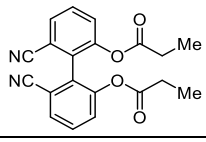	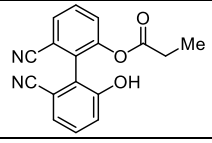
rac-**225b**	*rac*-**224c**	*rac*-**225c**
RGA002V043B	RGA002V047A	RGA002V047B
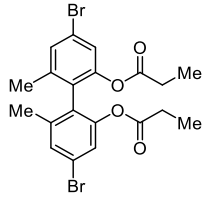	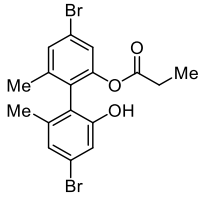	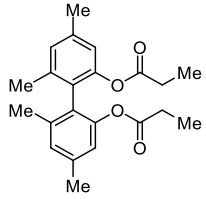
rac-**224d**	*rac*-**225d**	*rac*-**224e**
RGA002V049A	RGA002V049B	RGA002V046
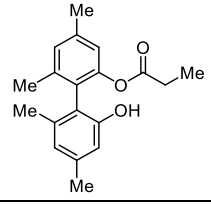	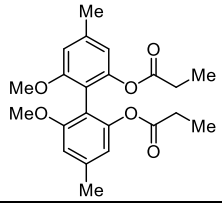	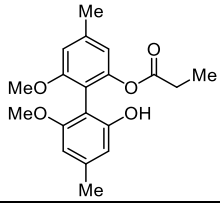
rac-**225e**	*rac*-**224f**	*rac*-**225f**
JKU-RGA002V021	RGA002V048A	RGA002V048B

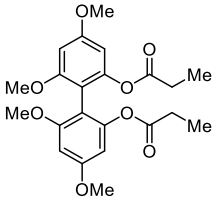	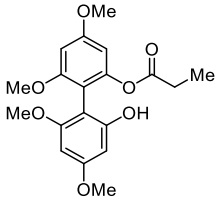	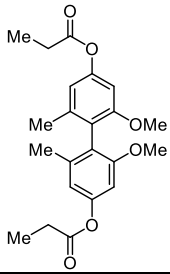
rac-**224g**	*rac*-**225g**	*rac*-**224h**
RGA002V037	RGA002V040B	RGA002V042A
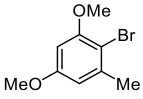	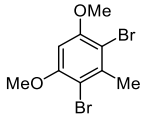	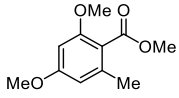
226	**227**	**228**
RGA006V002A	RGA006V002B	RGA006V005
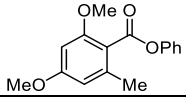	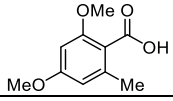	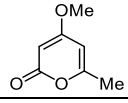
229	**230**	**232**
RGA006V020D	RGA006V006	RGA006V016
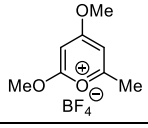	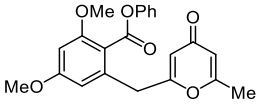	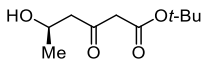
233	**235**	**238**
RGA006V021	RGA006V023A	RGA006V094
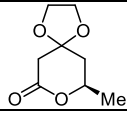		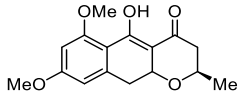
239	**241**	**242**
RGA006V095	RGA006V098	RGA006V113C
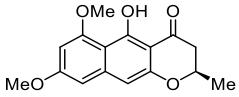	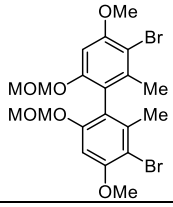	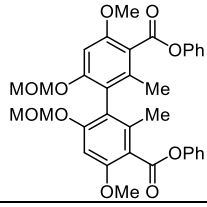
243	*rac*-**244**	*rac*-**245**
RGA006V055A	RGA006V126	RGA006V060B

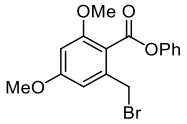	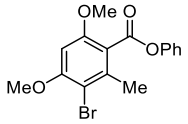	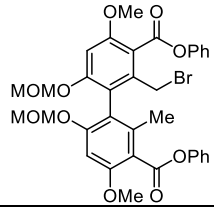
256	**260**	*rac*-**261**
RGA006V114C	RGA006V119	RGA006V116B
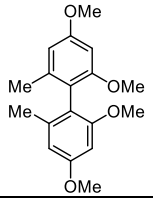	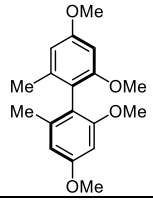	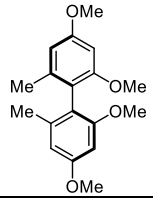
rac-**152**	(*M*)-**152**	(*P*)-**152**
RGA006V168	RGA006V179A	RGA004V099C
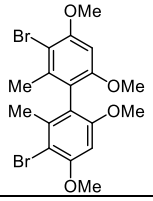	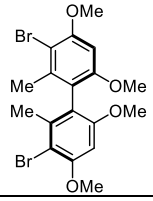	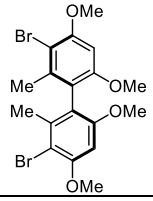
rac-**264**	(*M*)-**264**	(*P*)-**264**
RGA001V169	RGA006V183	RGA006V180
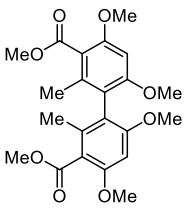	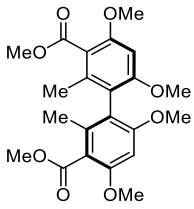	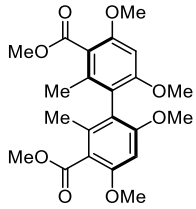
rac-**266**	(*M*)-**266**	(*P*)-**266**
RGA006V140C	RGA006V187C	RGA006V192B
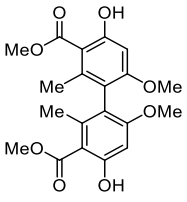	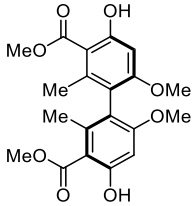	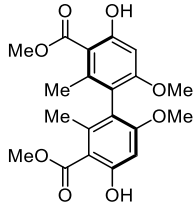
rac-**268**	(*M*)-**268**	(*P*)-**268**
RGA006V147A	RGA006V191A	RGA006V196

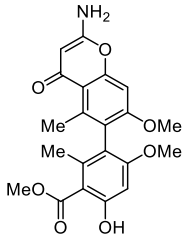	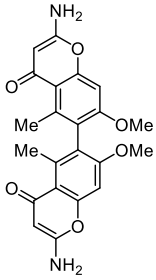	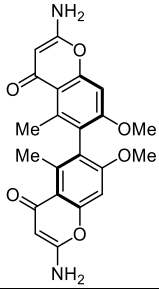
rac-**269**	*rac*-**270**	(*M*)-**270**
RGA006V204B	RGA006V182C	RGA006V198
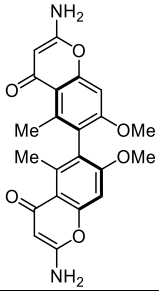	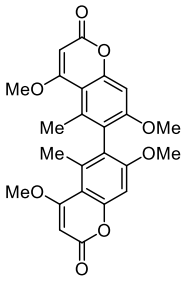	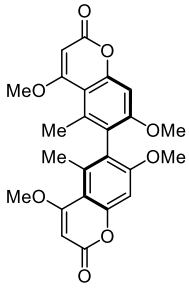
(*P*)-**270**	*rac*-**4**	(*M*)-**4**
RGA006V200	RGA006V188B	RGA006V214A

14 Appendix

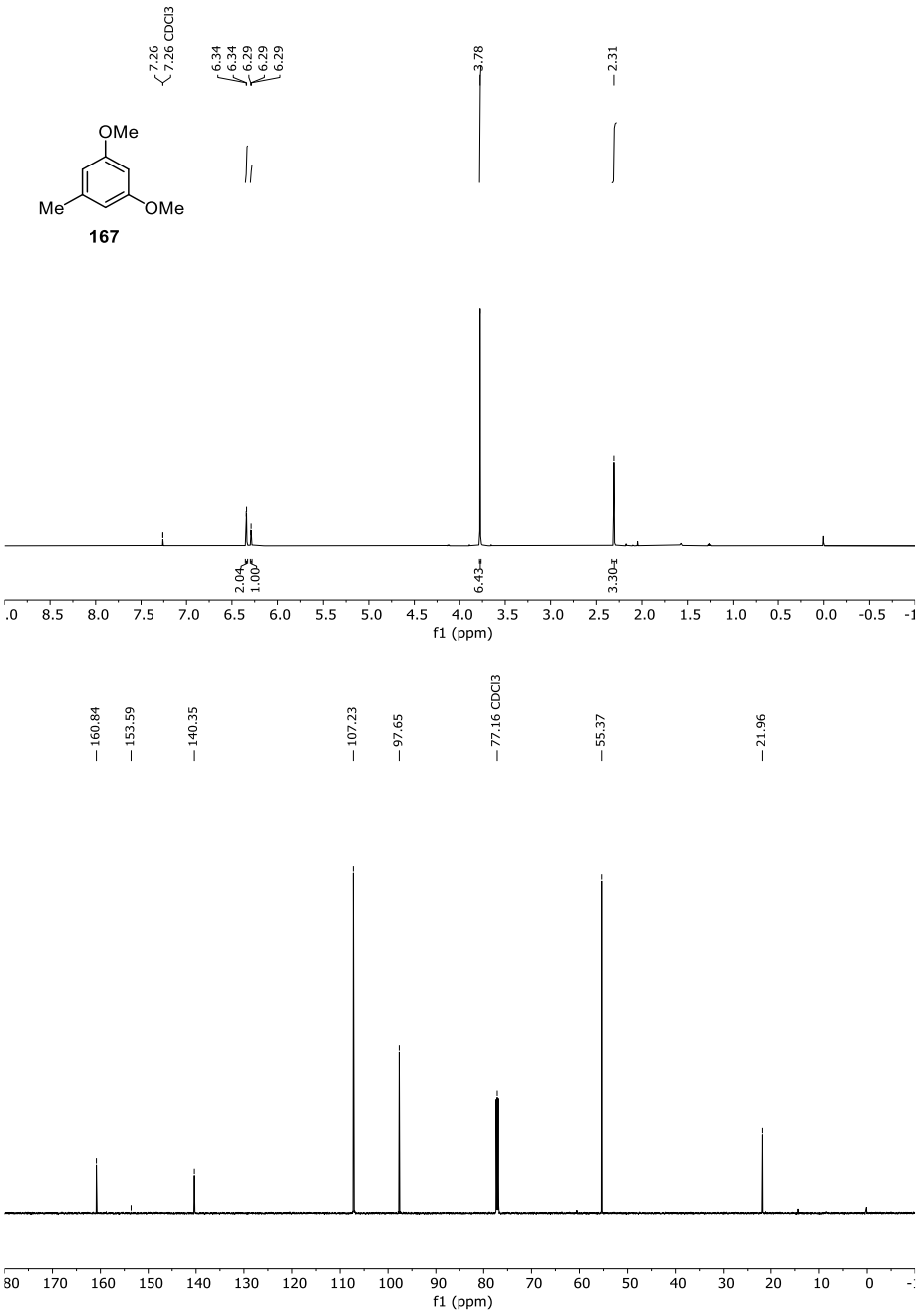

Figure 34 ^{1}H- and ^{13}C-NMR-Spectrum of **167** in $CDCl_3$ (600 MHz/151 MHz).

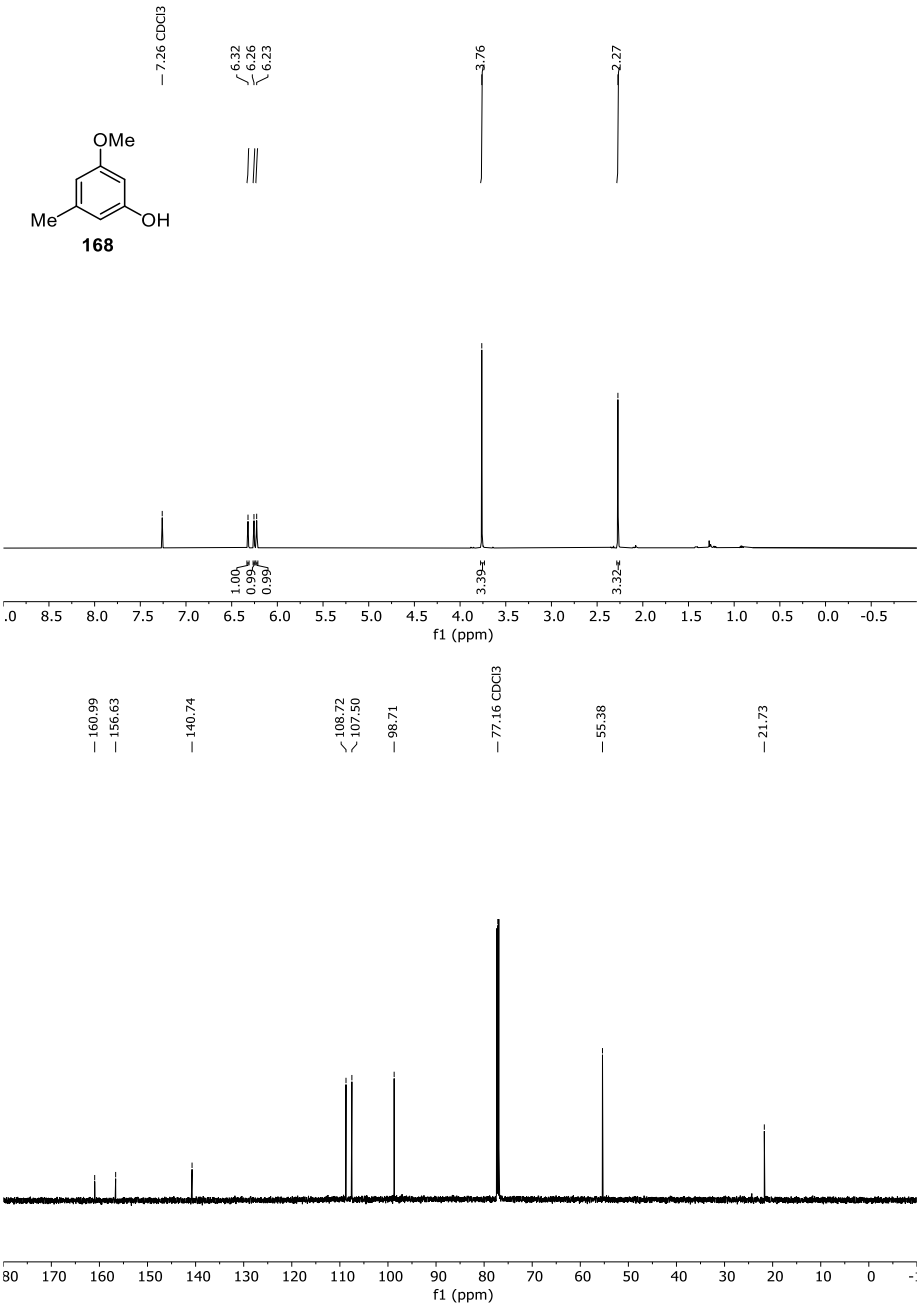

Figure 35 ^{1}H- and ^{13}C-NMR-Spectrum of **168** in $CDCl_3$ (600 MHz/151 MHz).

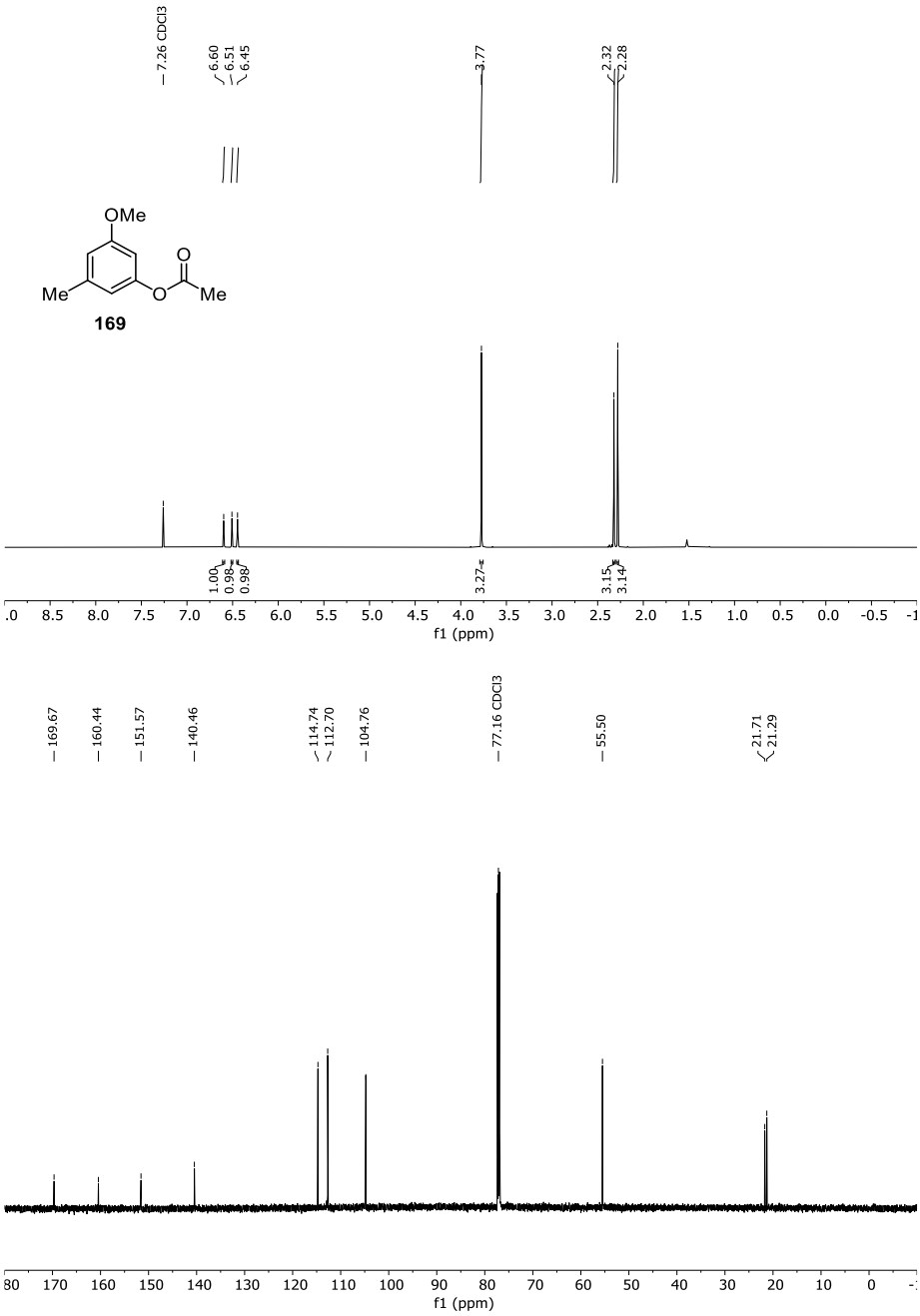

Figure 36 ^{1}H- and ^{13}C-NMR-Spectrum of **169** in $CDCl_3$ (600 MHz/151 MHz).

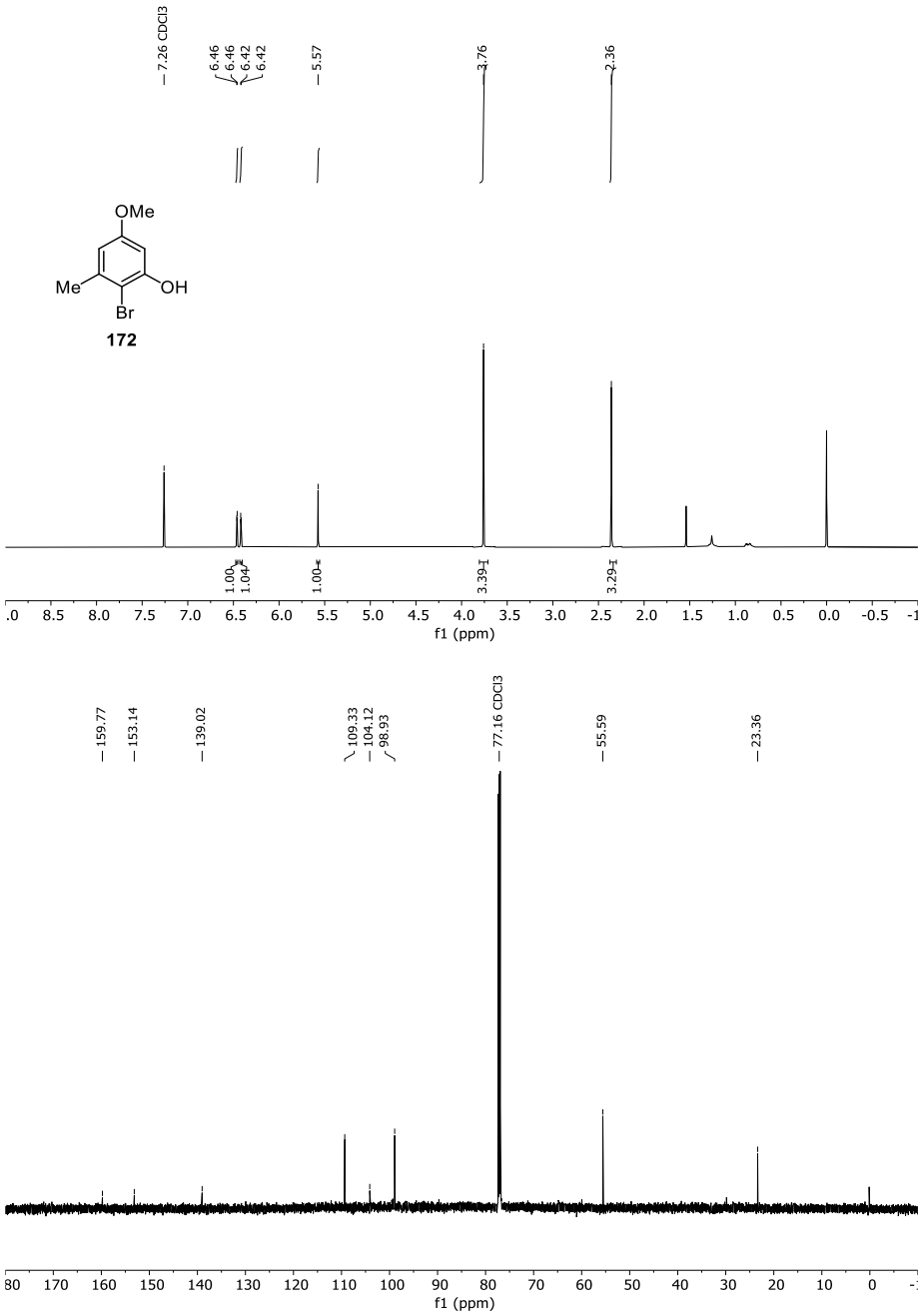

Figure 37 ^{1}H- and ^{13}C-NMR-Spectrum of **172** in $CDCl_3$ (600 MHz/151 MHz).

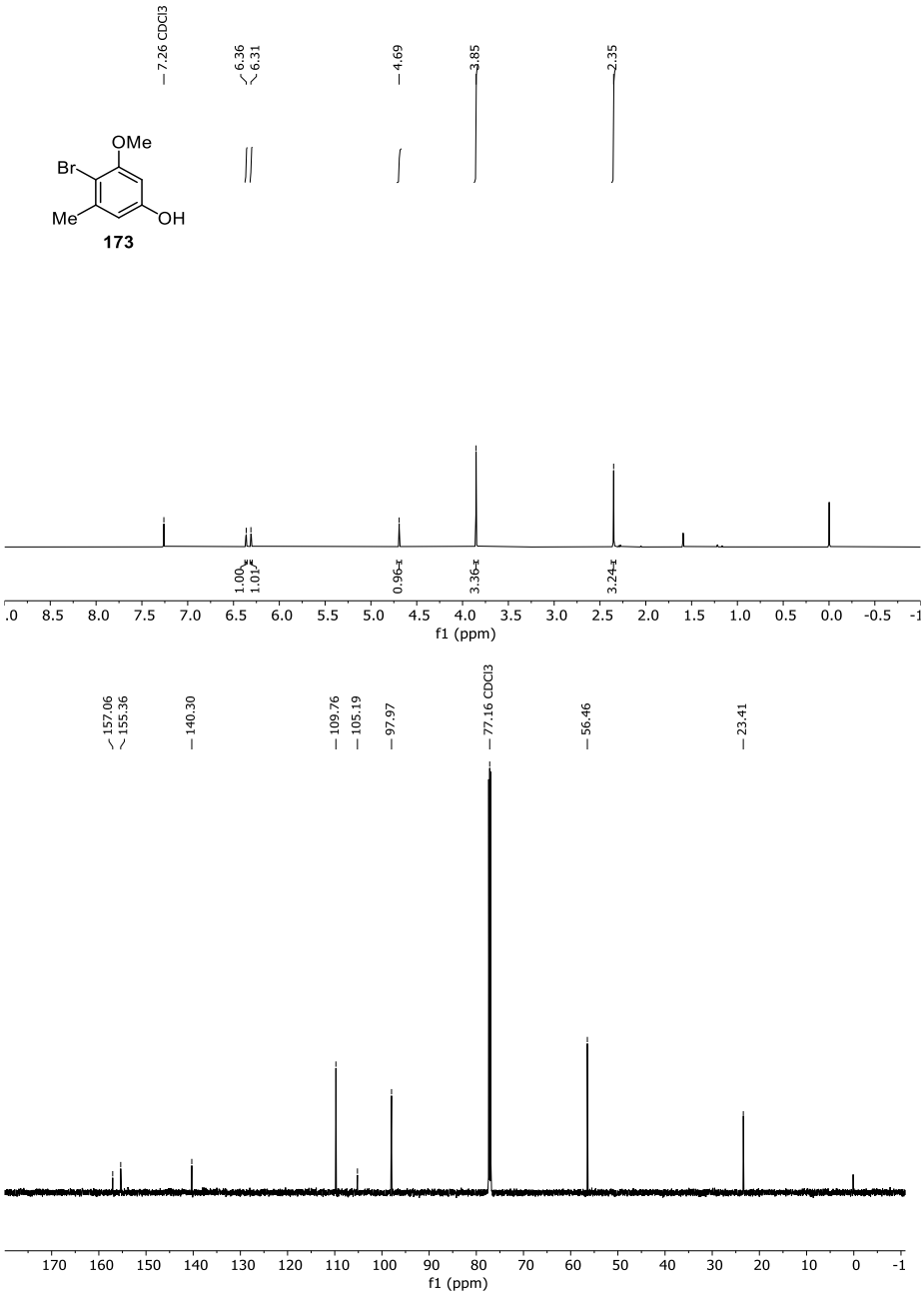

Figure 38 ^{1}H- and ^{13}C-NMR-Spectrum of **173** in $CDCl_3$ (600 MHz/151 MHz).

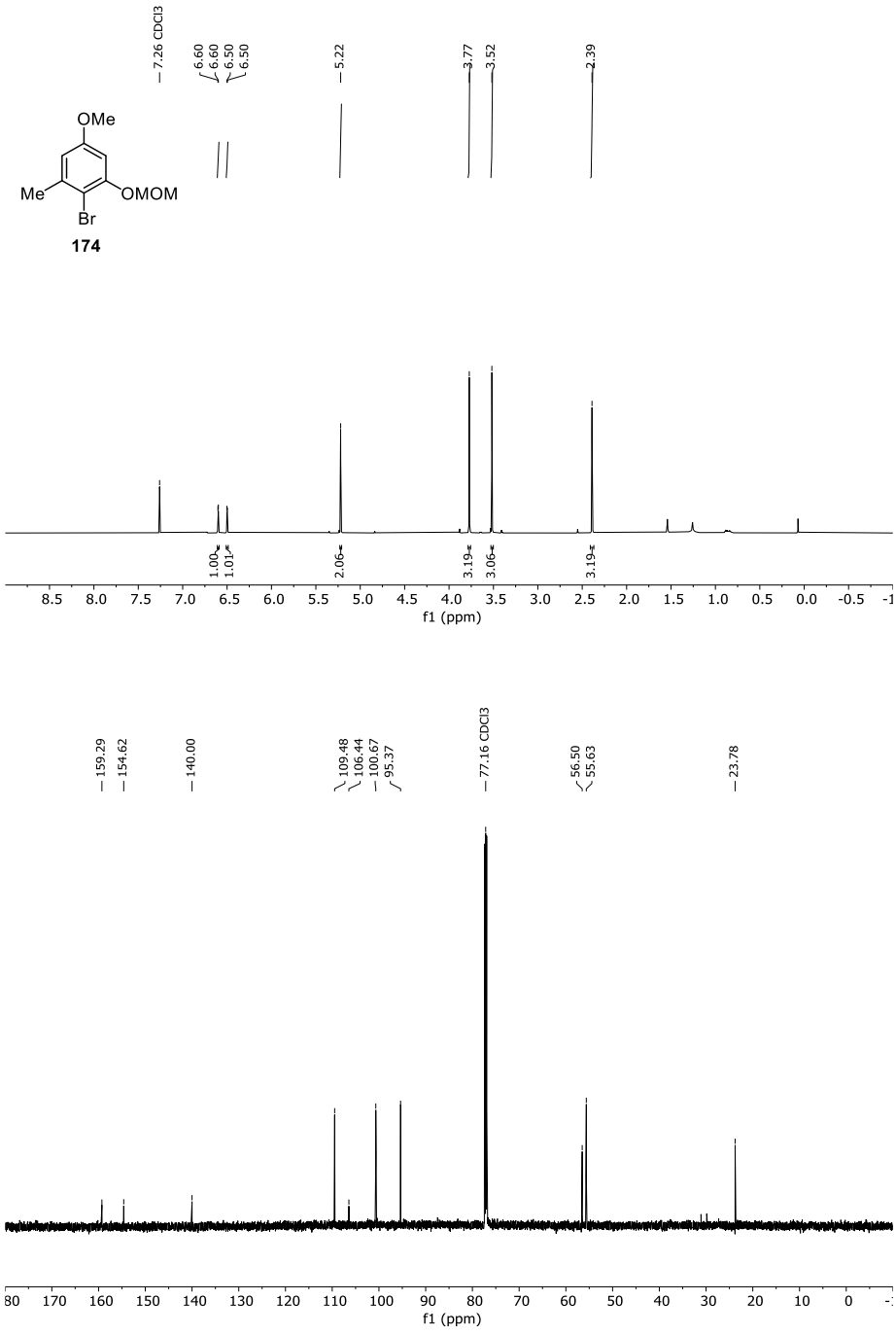

Figure 39 ^{1}H- and ^{13}C-NMR-Spectrum of **174** in $CDCl_3$ (600 MHz/151 MHz).

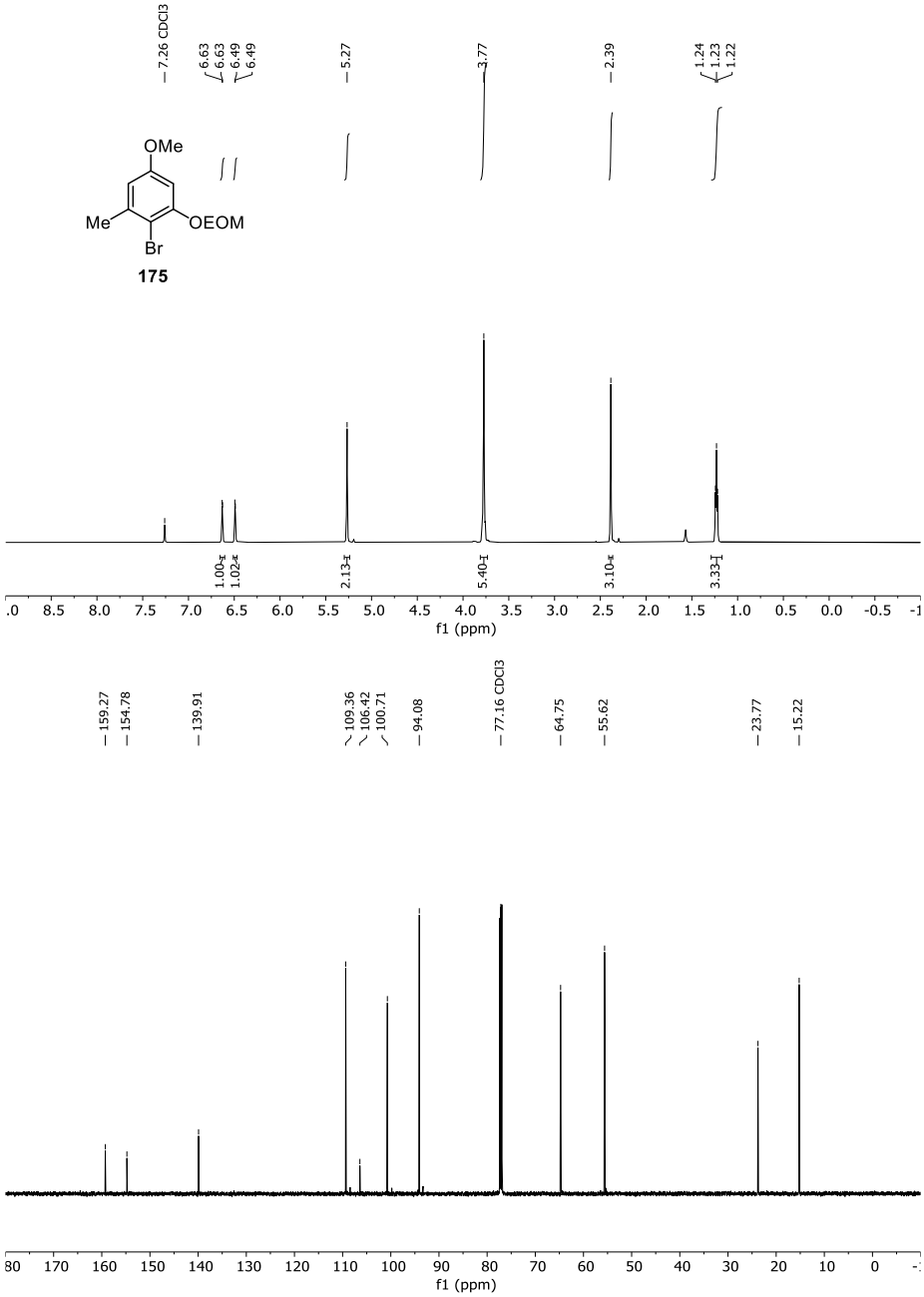

Figure 40 ^{1}H- and ^{13}C-NMR-Spectrum of **175** in $CDCl_3$ (600 MHz/151 MHz).

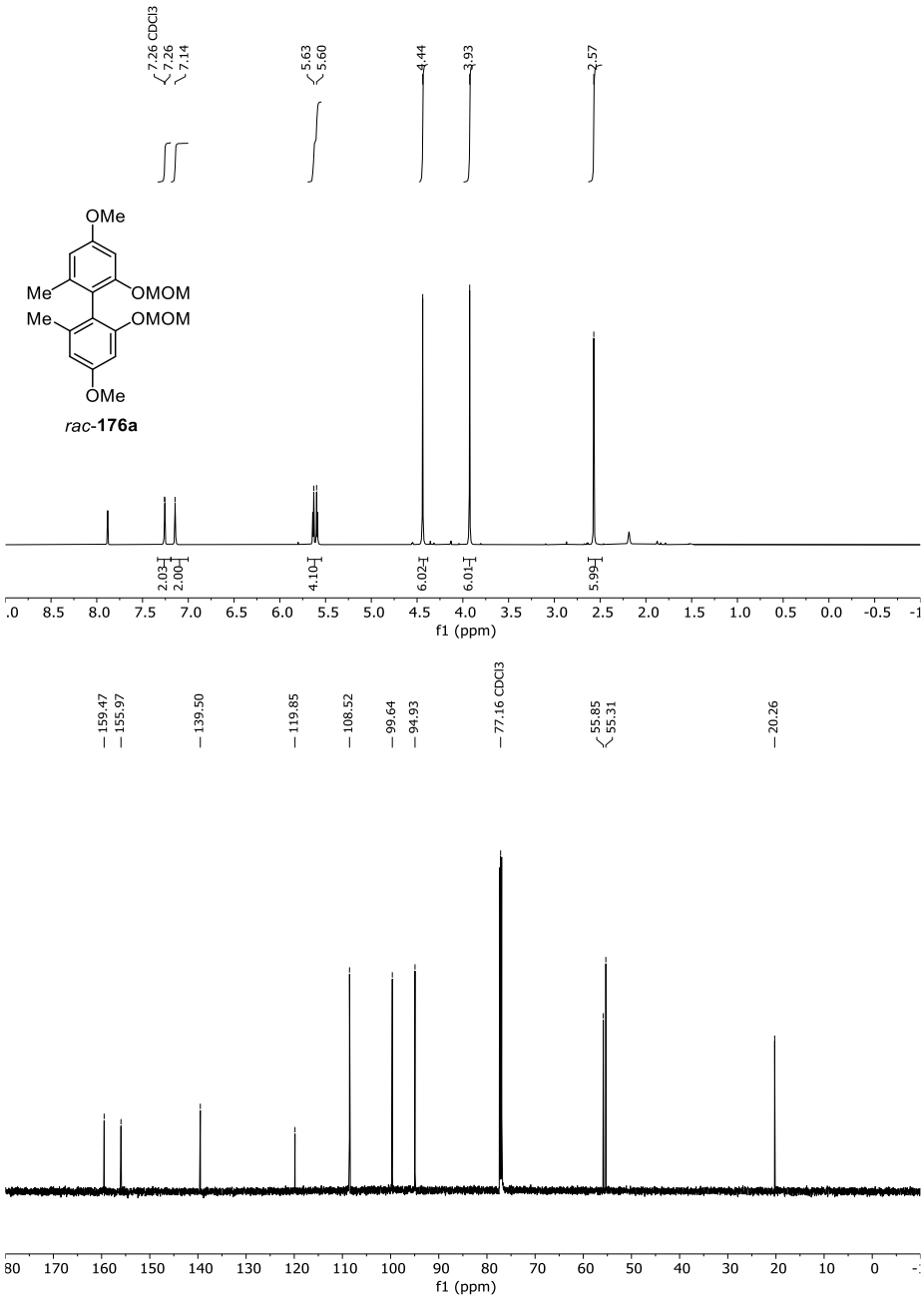

Figure 41 ^{1}H- and ^{13}C-NMR-Spectrum of *rac*-**176a** in $CDCl_3$ (600 MHz/151 MHz).

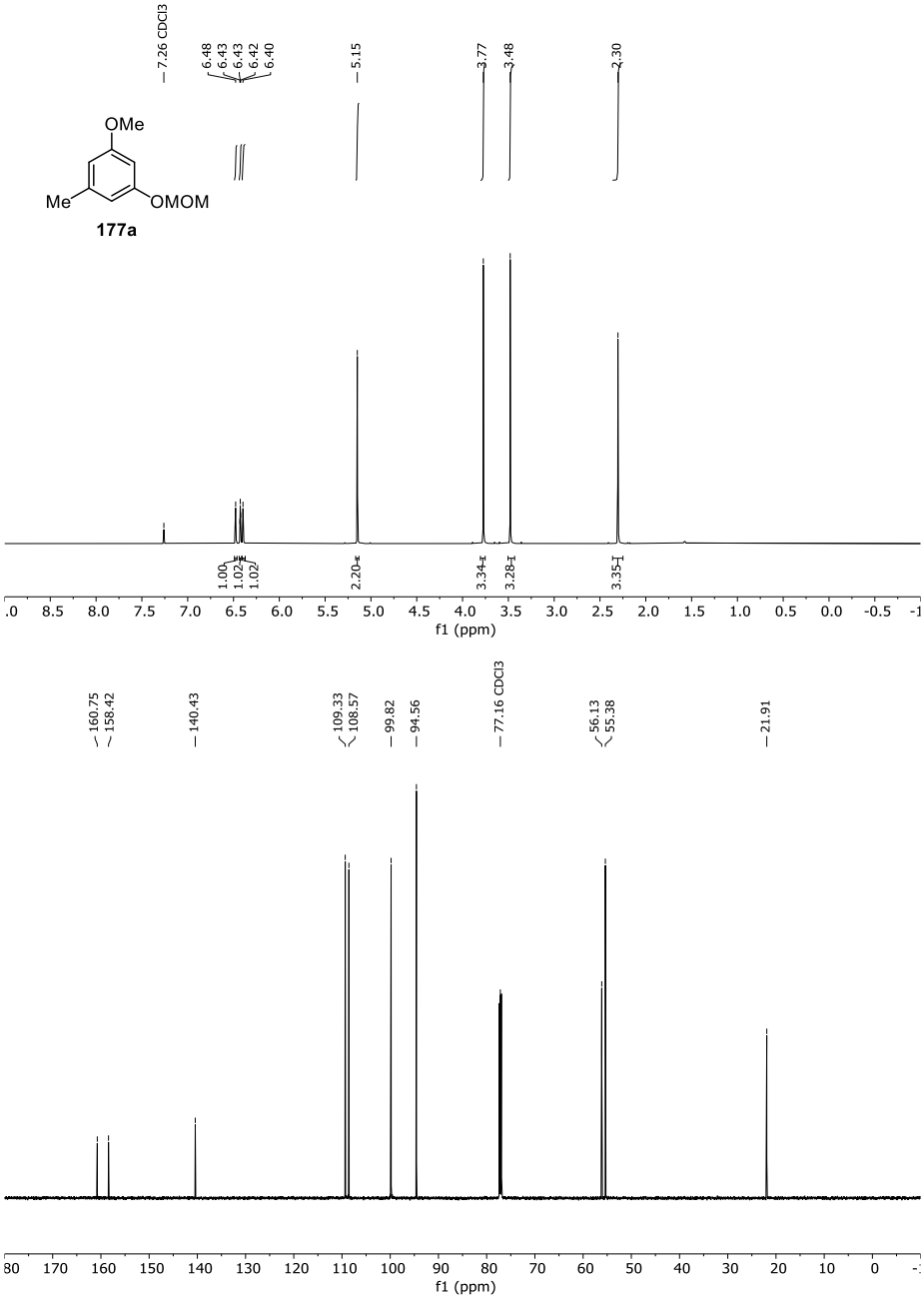

Figure 42 ^{1}H- and ^{13}C-NMR-Spectrum of **177a** in $CDCl_3$ (600 MHz/151 MHz).

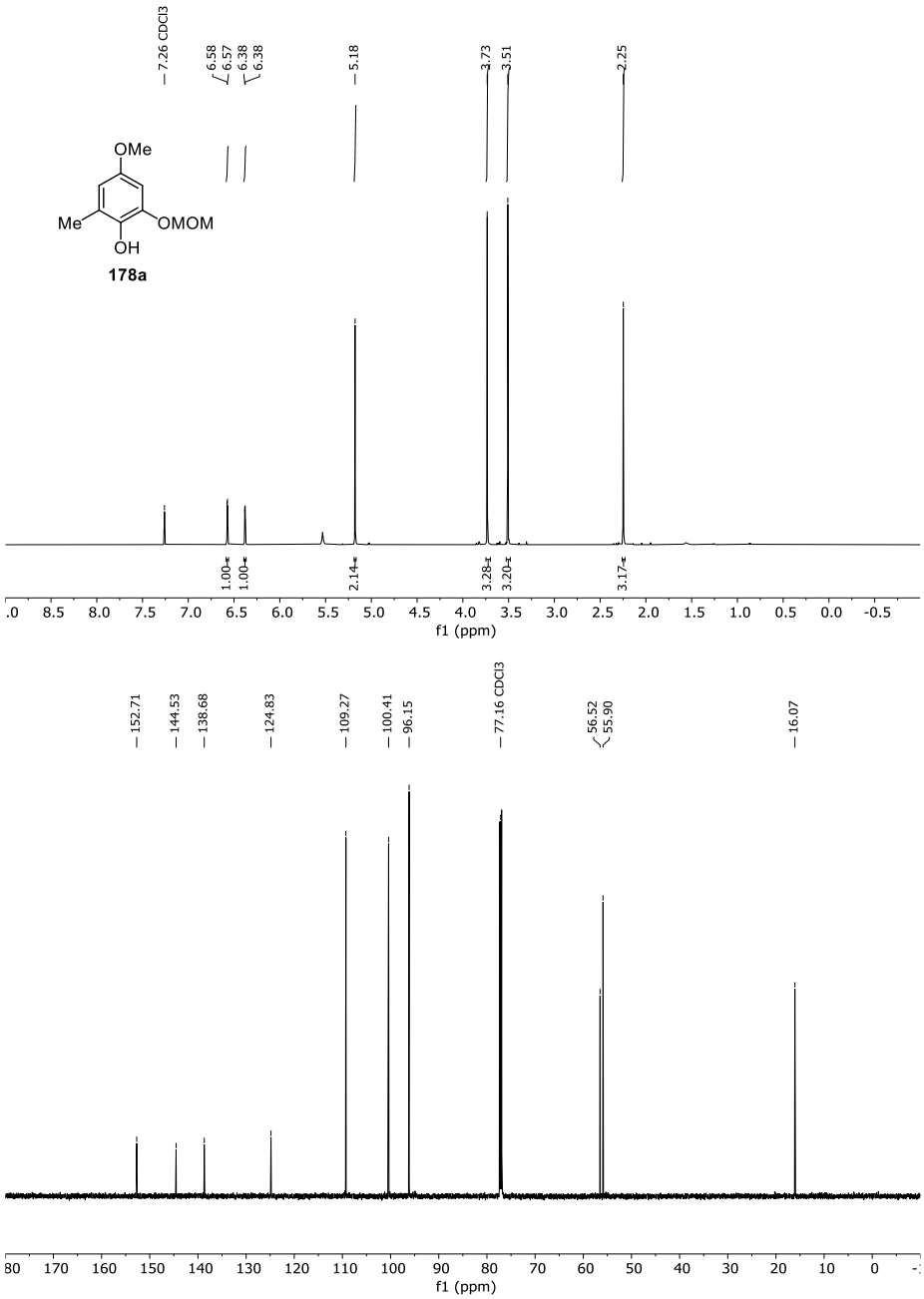

Figure 43 ^{1}H- and ^{13}C-NMR-Spectrum of **178a** in $CDCl_3$ (600 MHz/151 MHz).

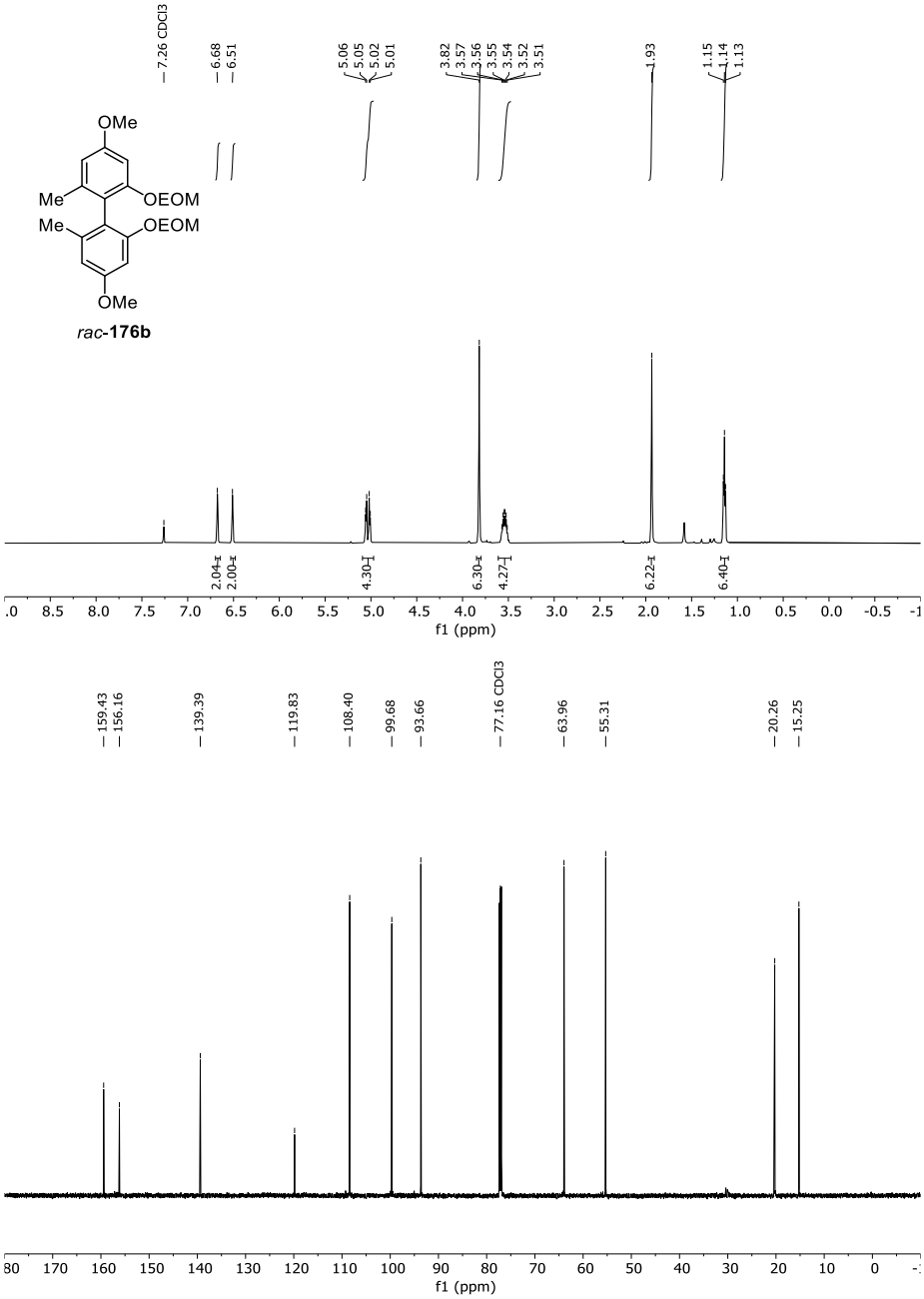

Figure 44 ^{1}H- and ^{13}C-NMR-Spectrum of *rac*-**176b** in $CDCl_3$ (600 MHz/151 MHz).

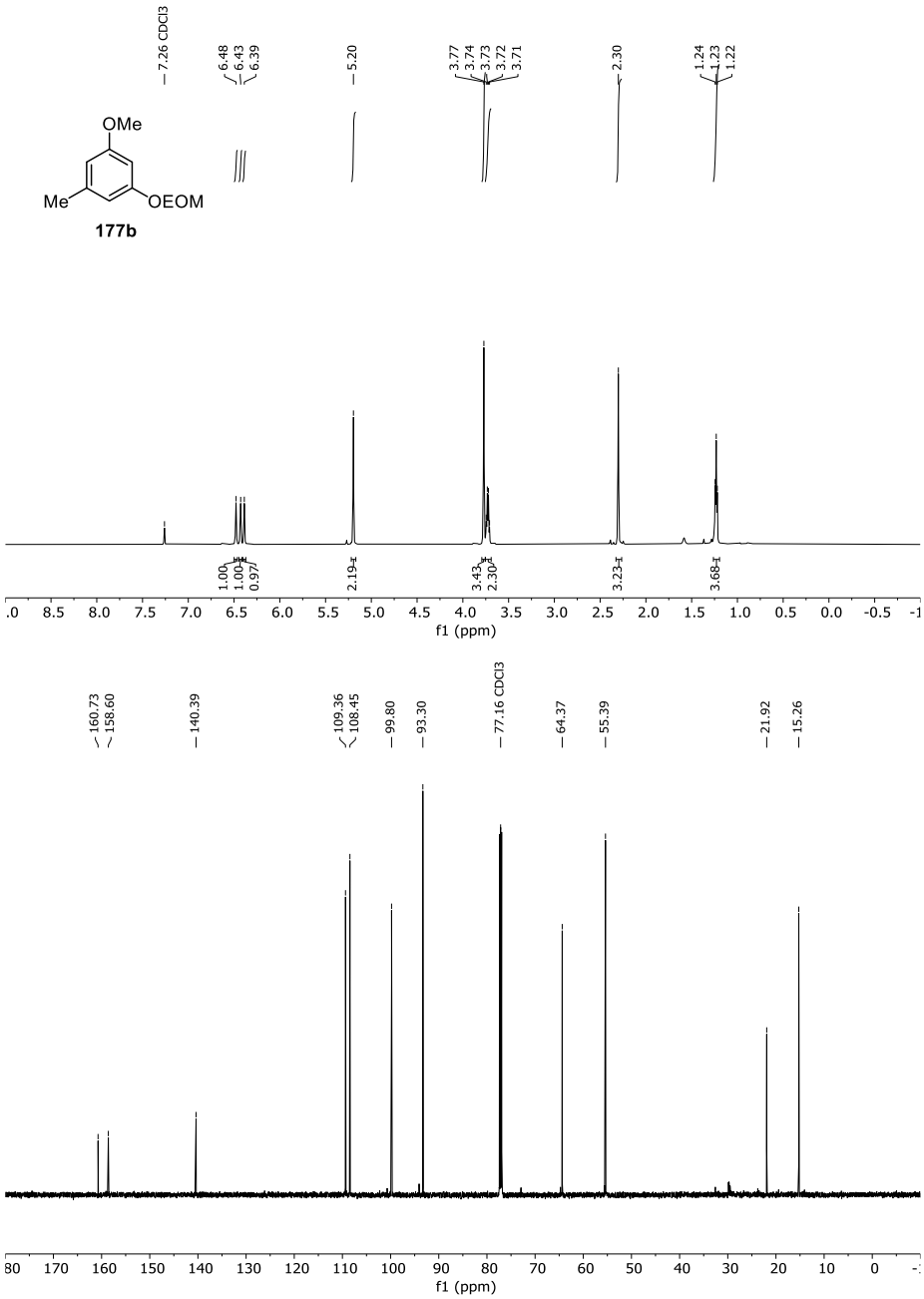

Figure 45 ^{1}H- and ^{13}C-NMR-Spectrum of **177b** in $CDCl_3$ (600 MHz/151 MHz).

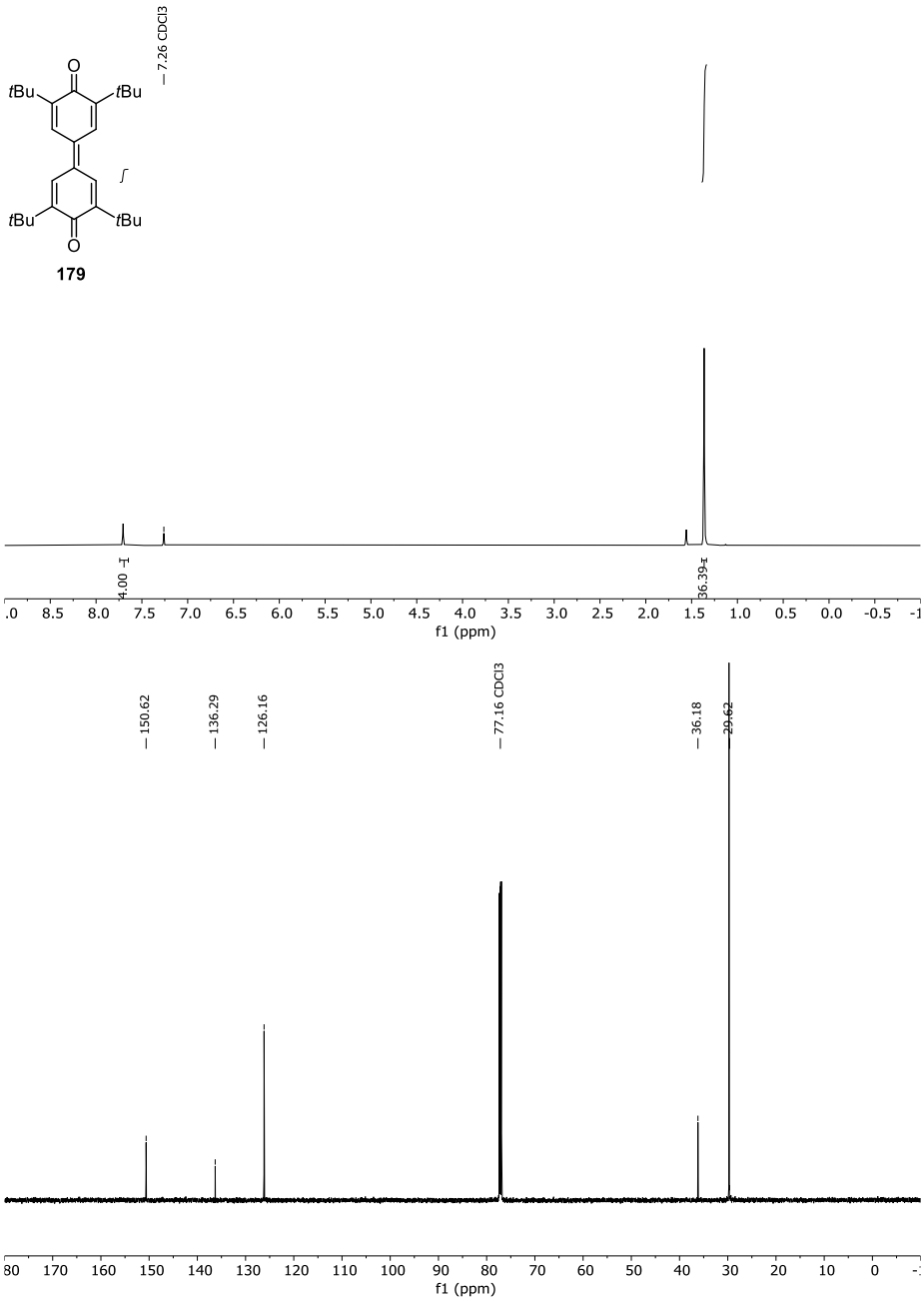

Figure 46 ^{1}H- and ^{13}C-NMR-Spectrum of **179** in $CDCl_3$ (600 MHz/151 MHz).

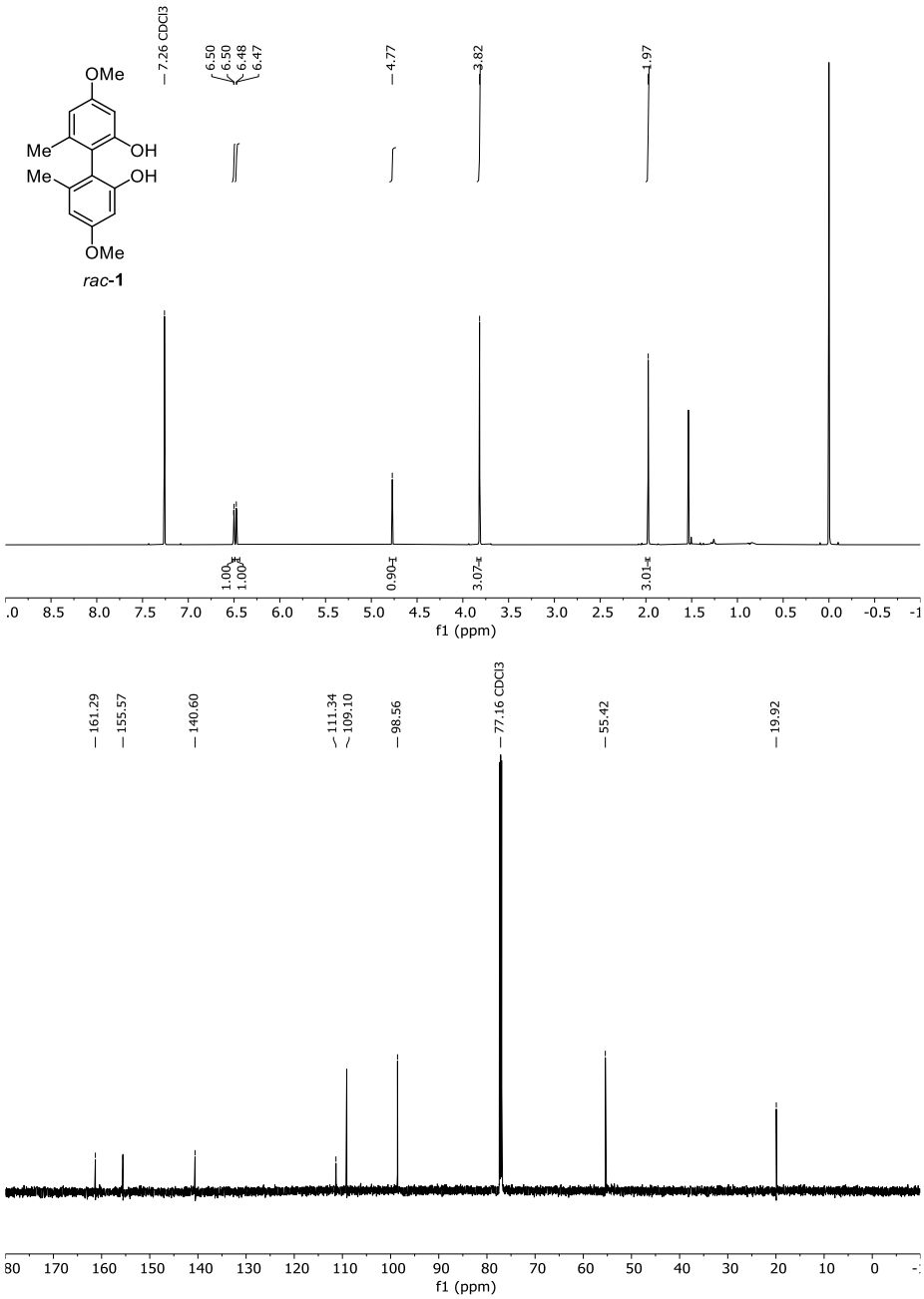

Figure 47 ^{1}H- and ^{13}C-NMR-Spectrum of *rac*-**1** in $CDCl_3$ (600 MHz/151 MHz).

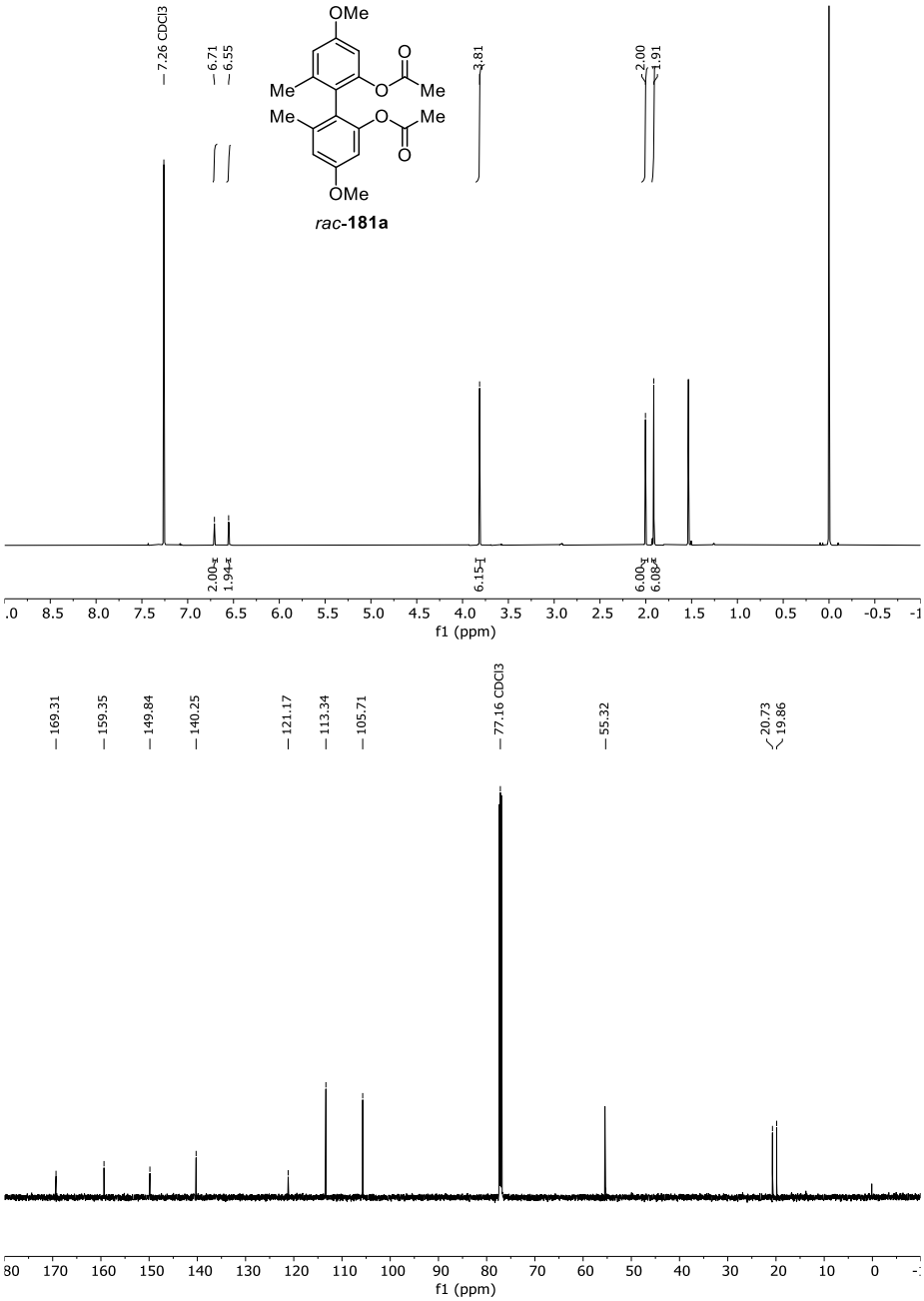

Figure 48 ^{1}H- and ^{13}C-NMR-Spectrum of *rac*-**181a** in $CDCl_3$ (600 MHz/151 MHz).

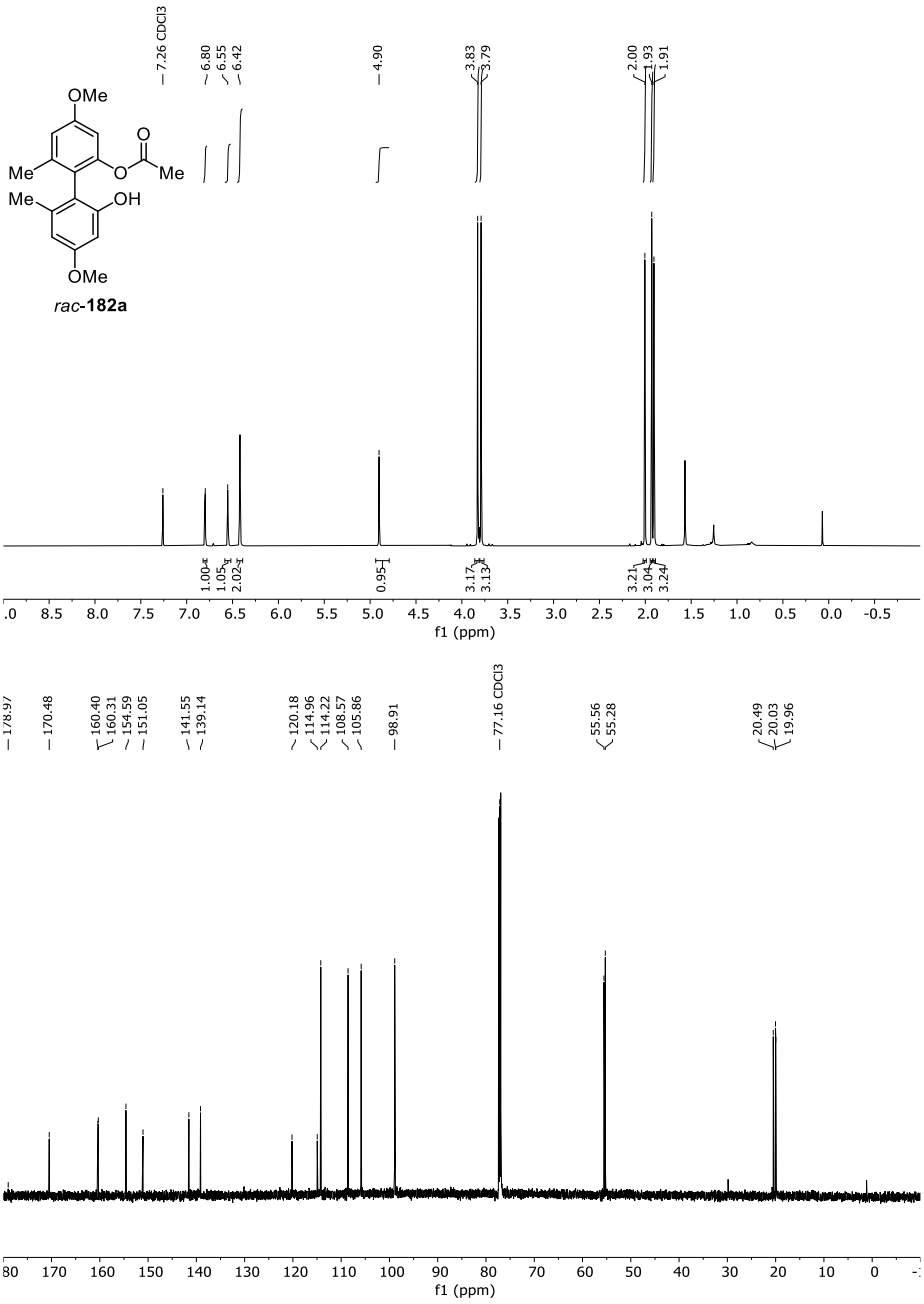

Figure 49 ^{1}H- and ^{13}C-NMR-Spectrum of *rac*-**182a** in $CDCl_3$ (600 MHz/151 MHz).

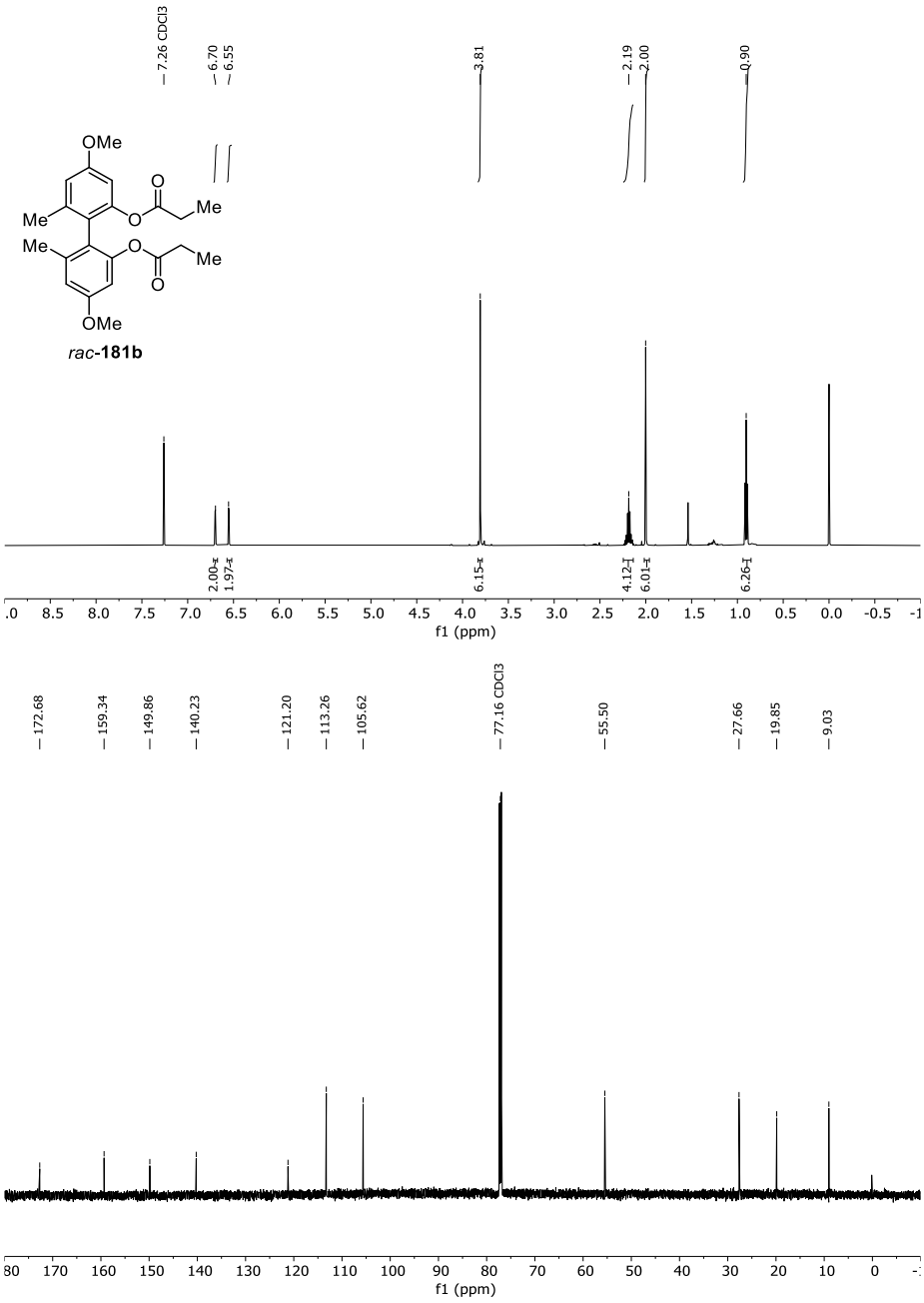

Figure 50 ^{1}H- and ^{13}C-NMR-Spectrum of *rac*-**181b** in $CDCl_3$ (600 MHz/151 MHz).

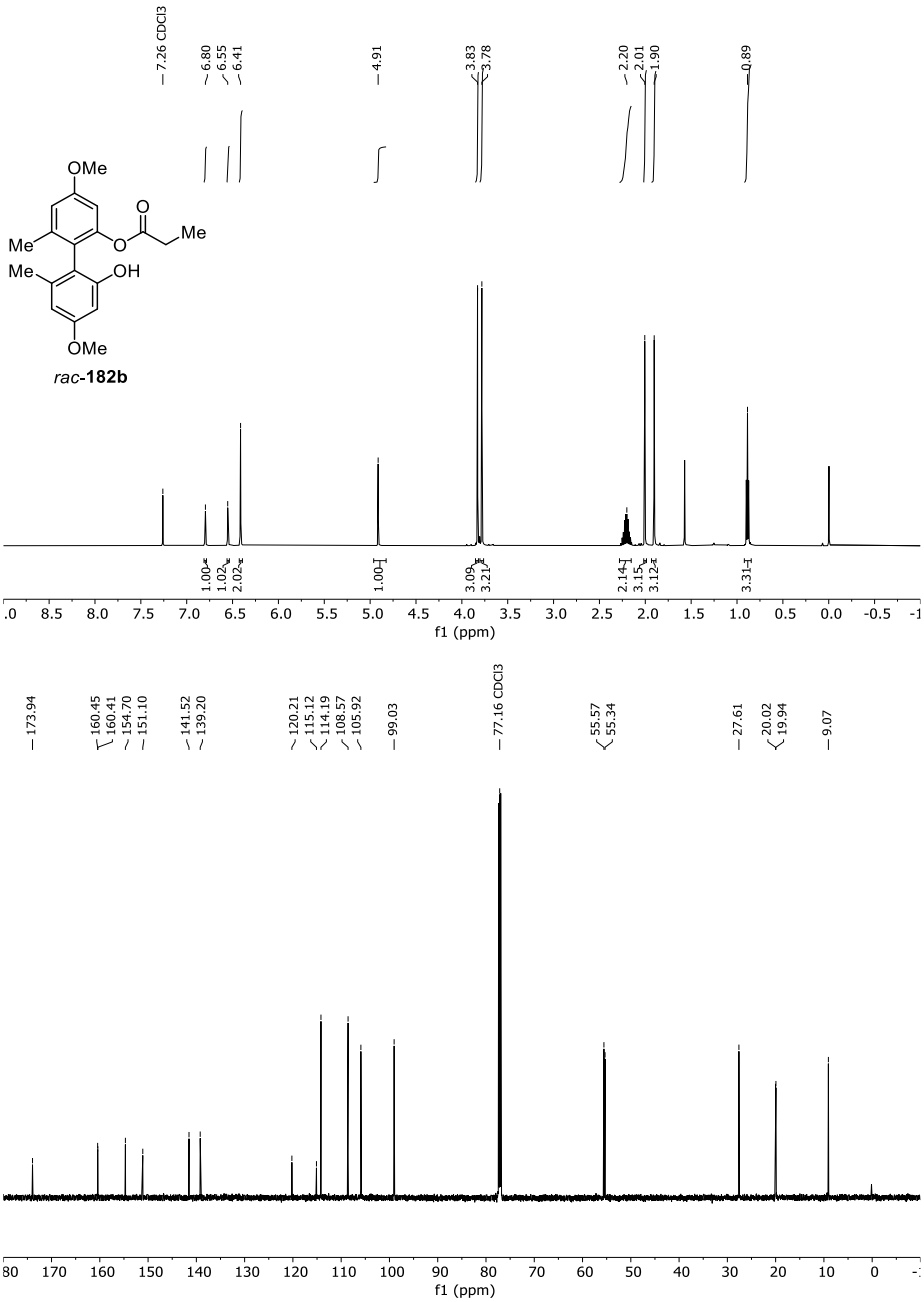

Figure 51 ^{1}H- and ^{13}C-NMR-Spectrum of *rac*-**182b** in $CDCl_3$ (600 MHz/151 MHz).

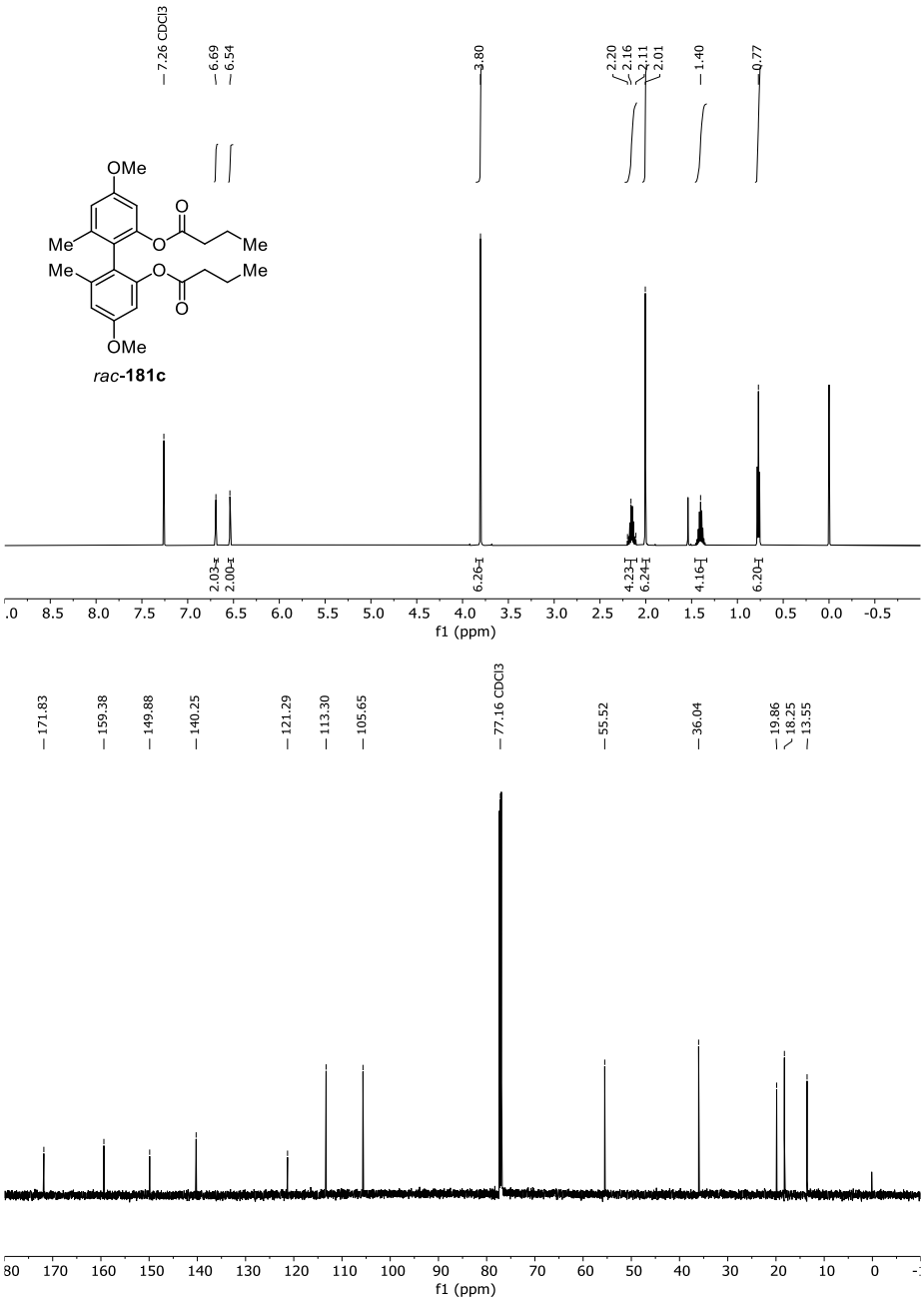

Figure 52 ^{1}H- and ^{13}C-NMR-Spectrum of *rac*-**181c** in $CDCl_3$ (600 MHz/151 MHz).

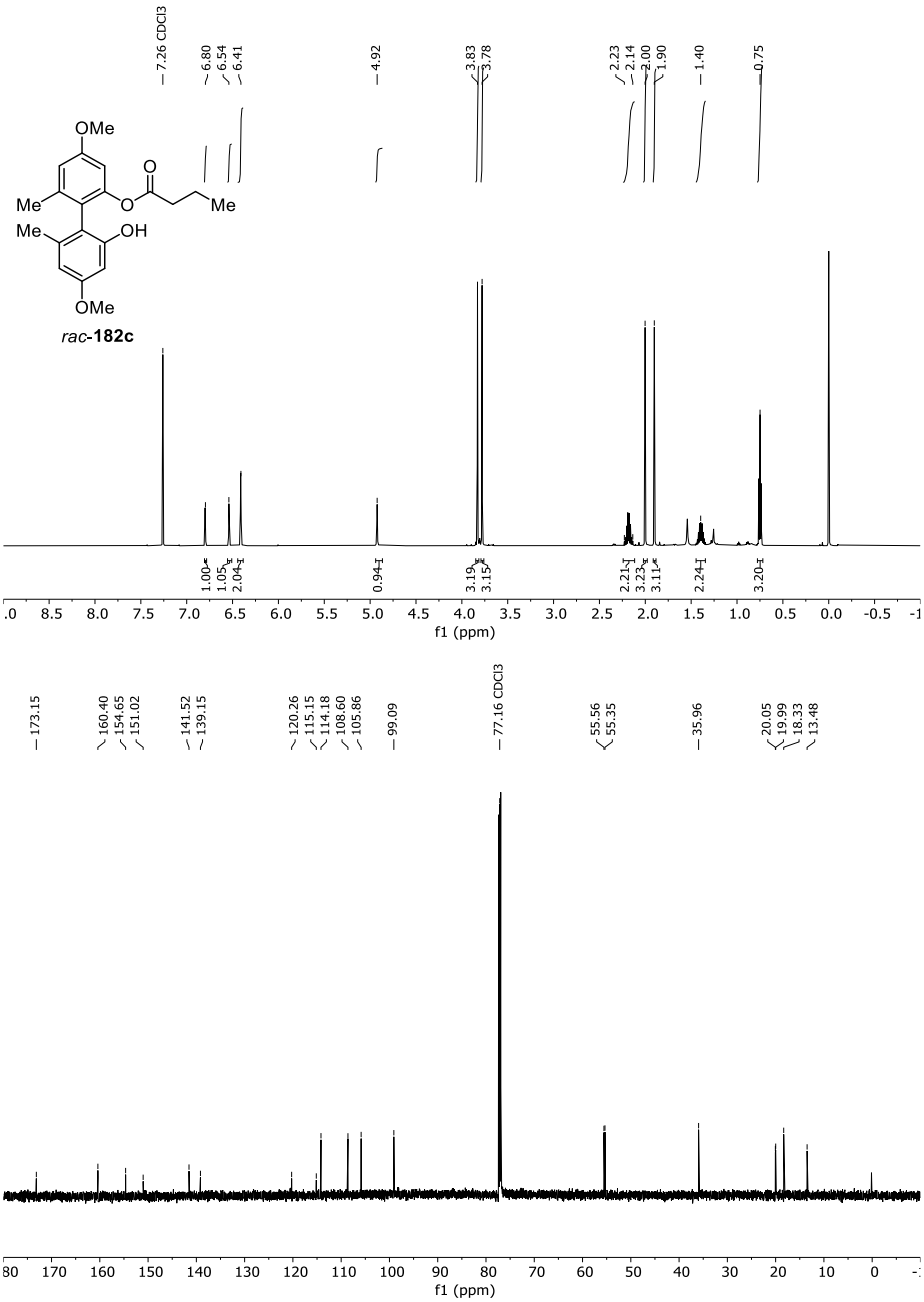

Figure 53 ^{1}H- and ^{13}C-NMR-Spectrum of *rac*-**182c** in $CDCl_3$ (600 MHz/151 MHz).

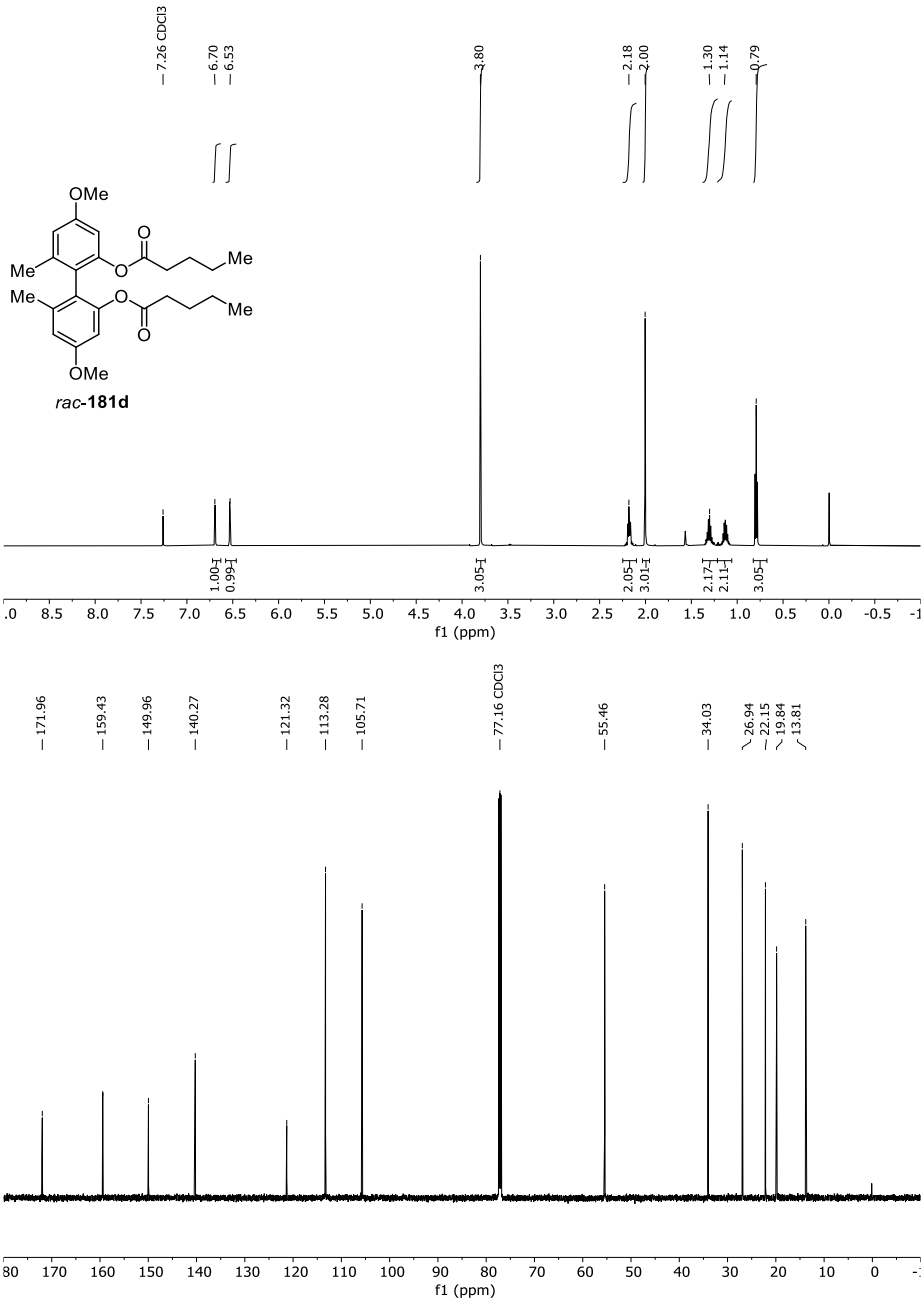

Figure 54 ^{1}H- and ^{13}C-NMR-Spectrum of *rac*-**181d** in $CDCl_3$ (600 MHz/151 MHz).

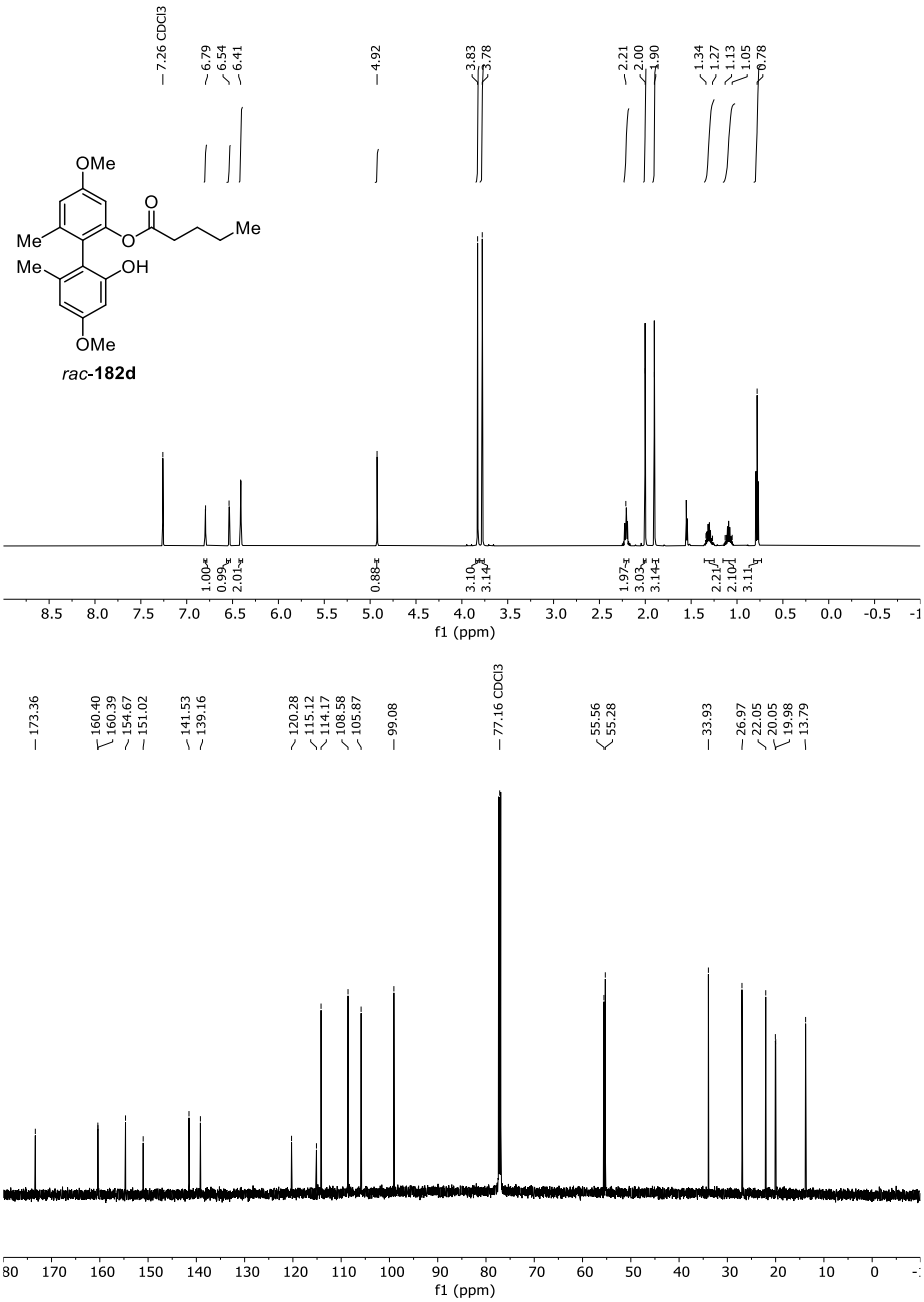

Figure 55 ^{1}H- and ^{13}C-NMR-Spectrum of *rac*-**182d** in $CDCl_3$ (600 MHz/151 MHz).

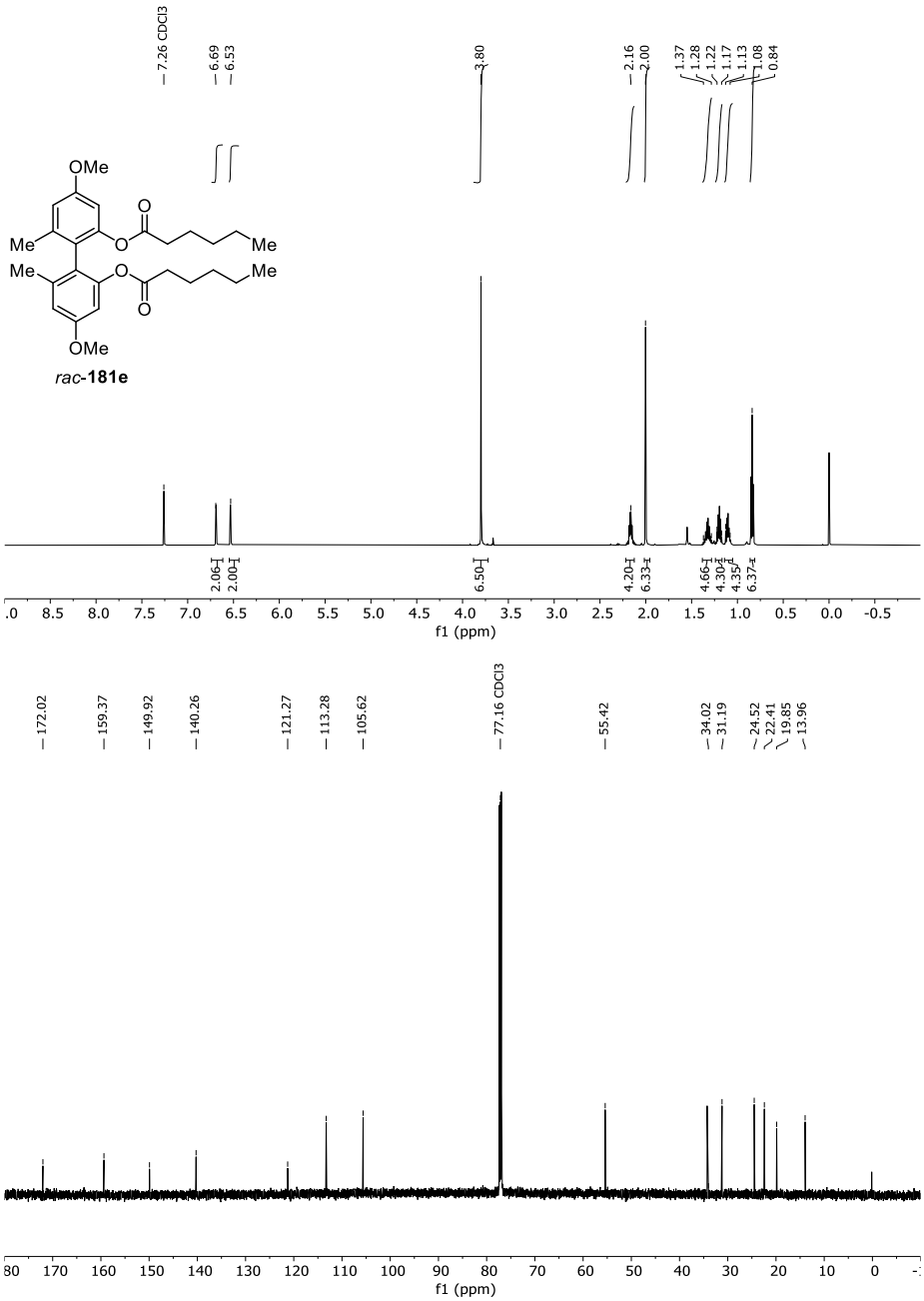

Figure 56 ^{1}H- and ^{13}C-NMR-Spectrum of *rac*-**181e** in $CDCl_3$ (600 MHz/151 MHz).

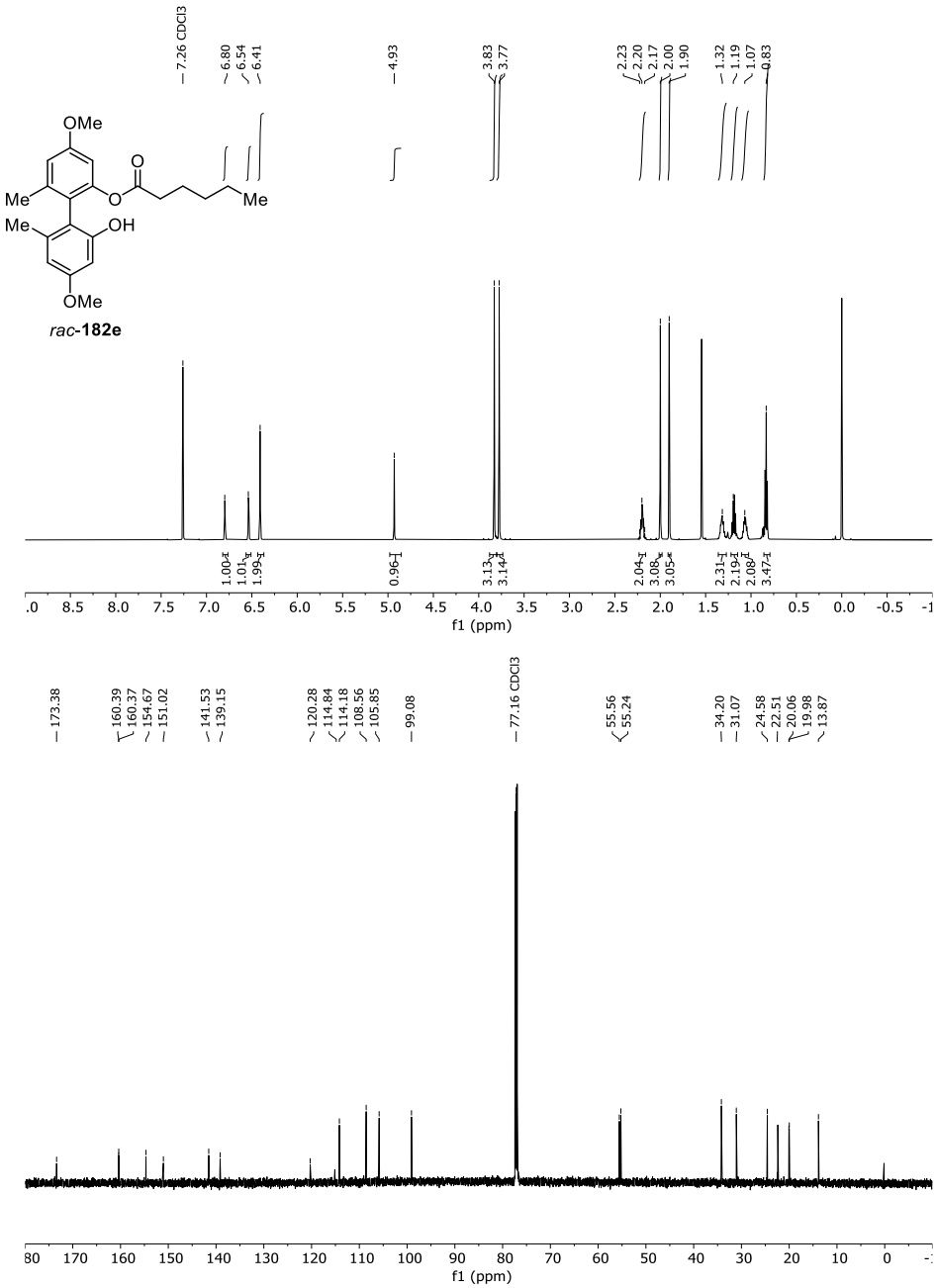

Figure 57 ^{1}H- and ^{13}C-NMR-Spectrum of *rac*-**182e** in $CDCl_3$ (600 MHz/151 MHz).

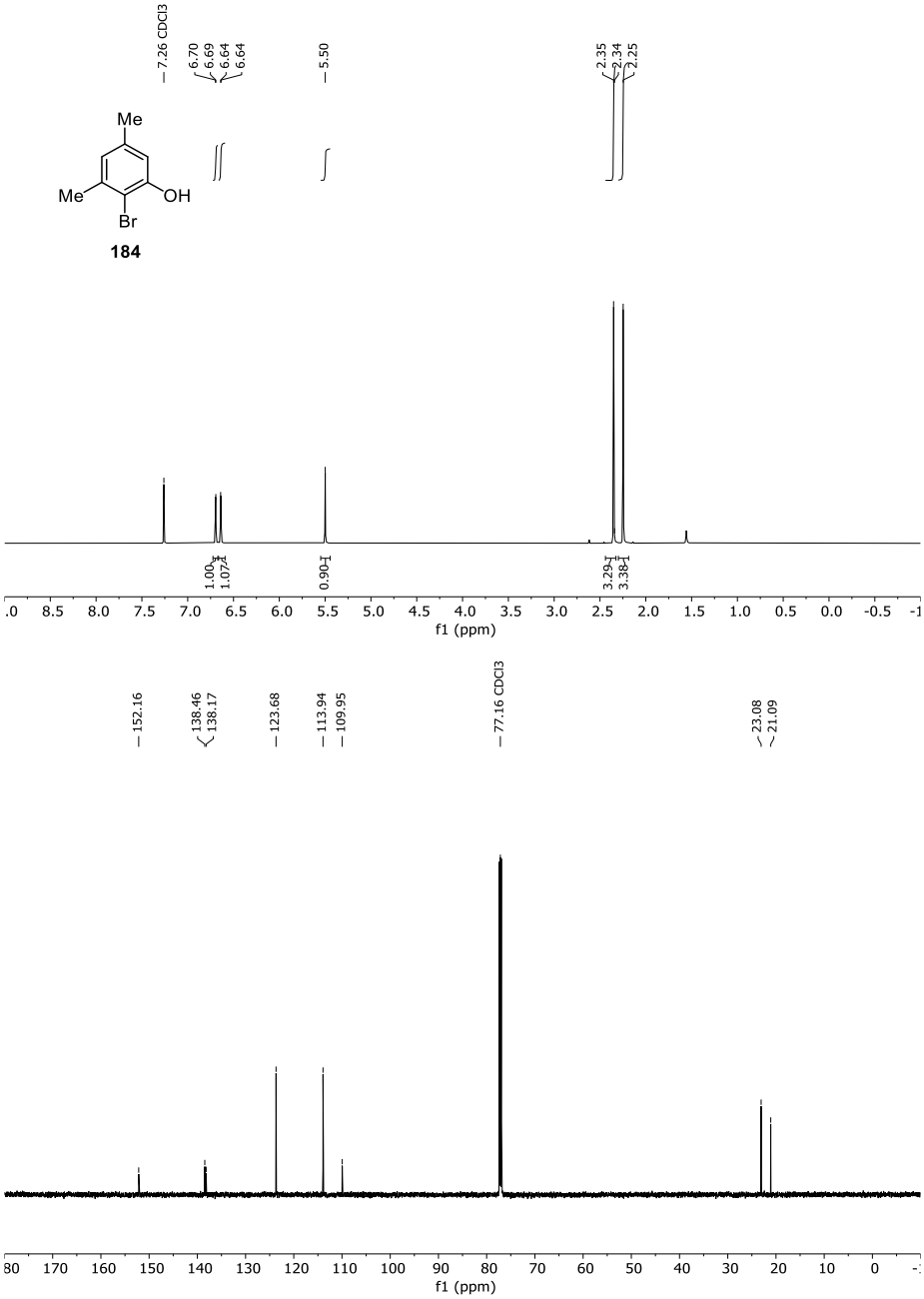

Figure 58 ^{1}H- and ^{13}C-NMR-Spectrum of **184** in $CDCl_3$ (600 MHz/151 MHz).

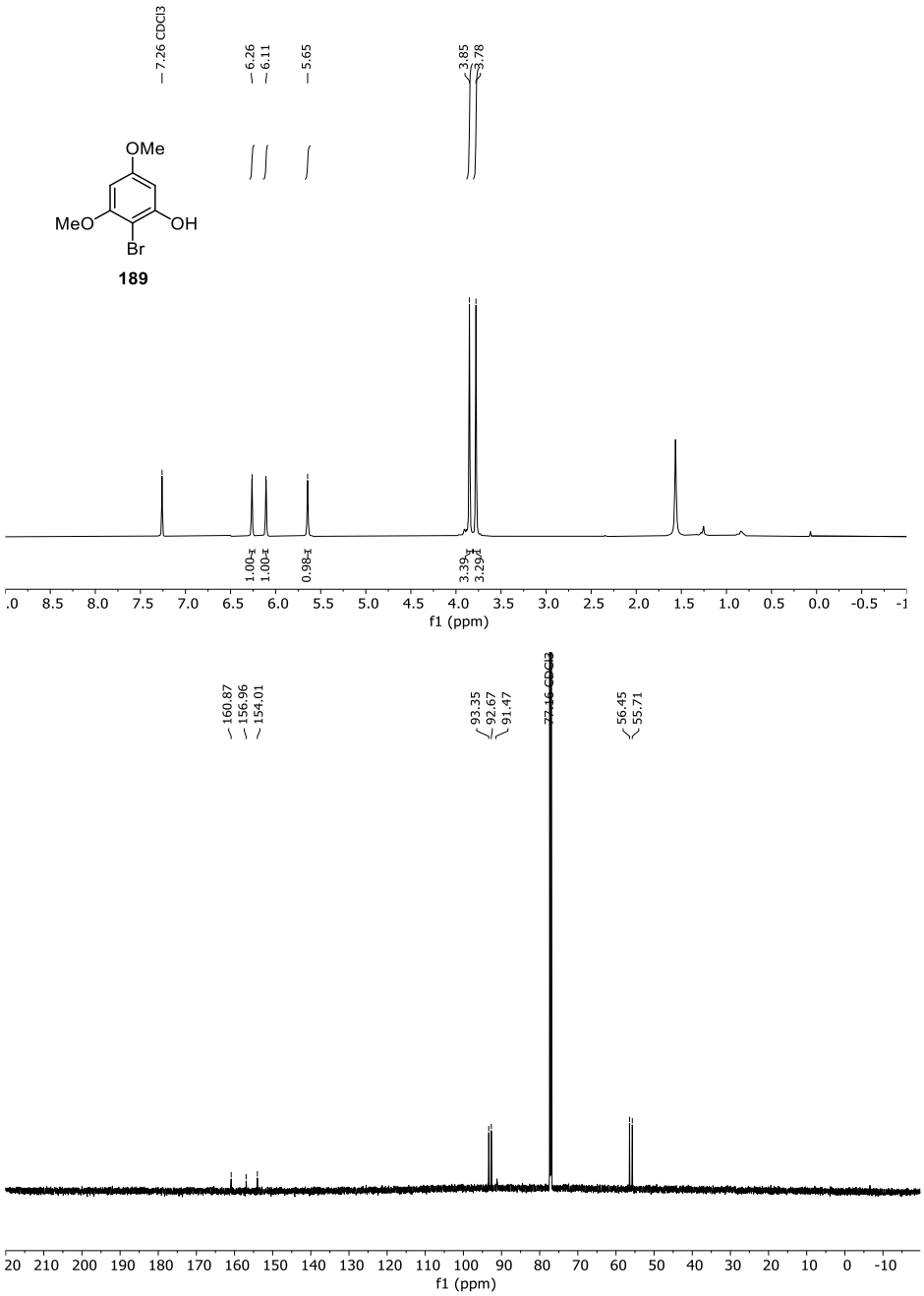

Figure 59 ^{1}H- and ^{13}C-NMR-Spectrum of **189** in $CDCl_3$ (600 MHz/151 MHz).

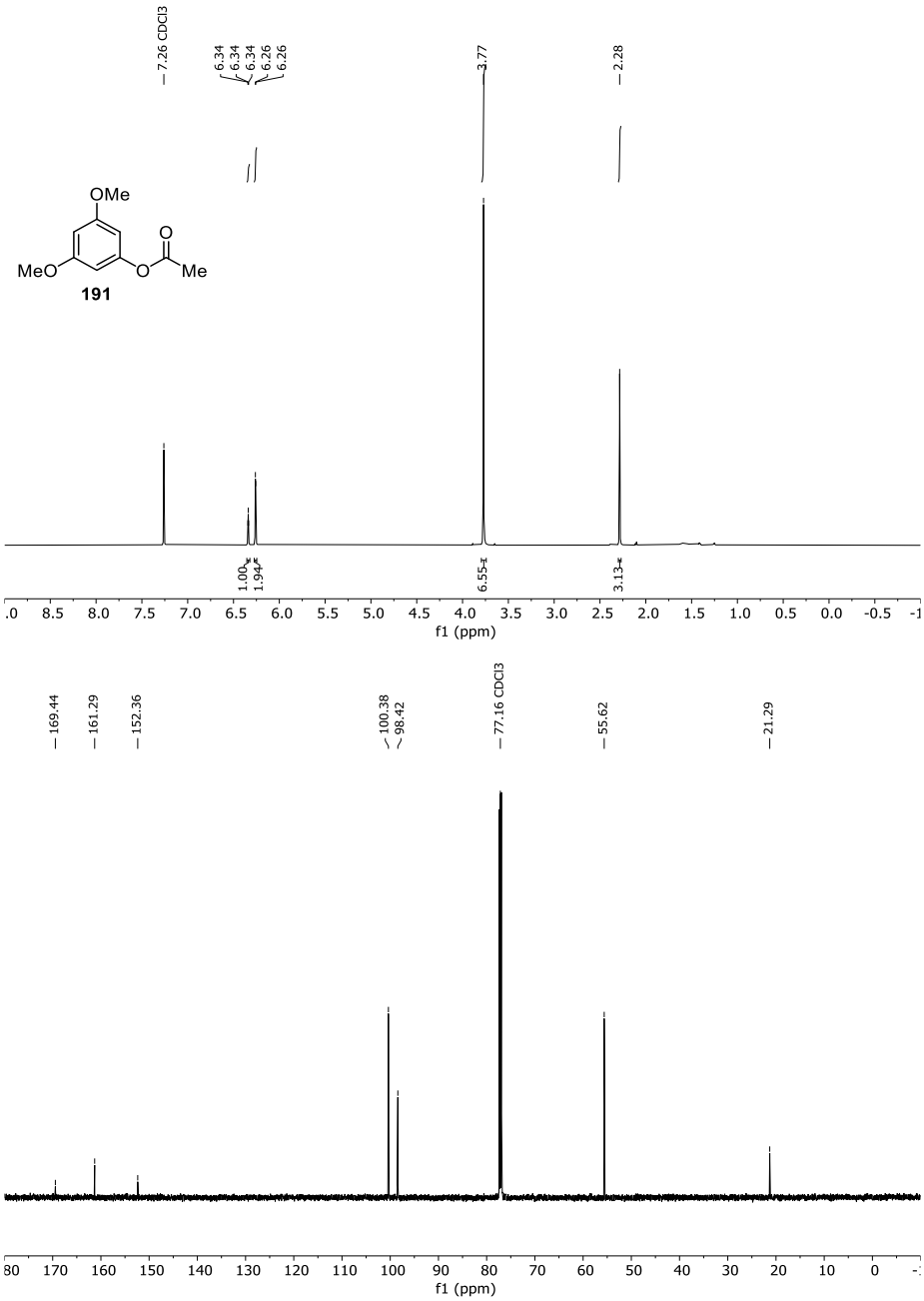

Figure 60 ^{1}H- and ^{13}C-NMR-Spectrum of **191** in $CDCl_3$ (600 MHz/151 MHz).

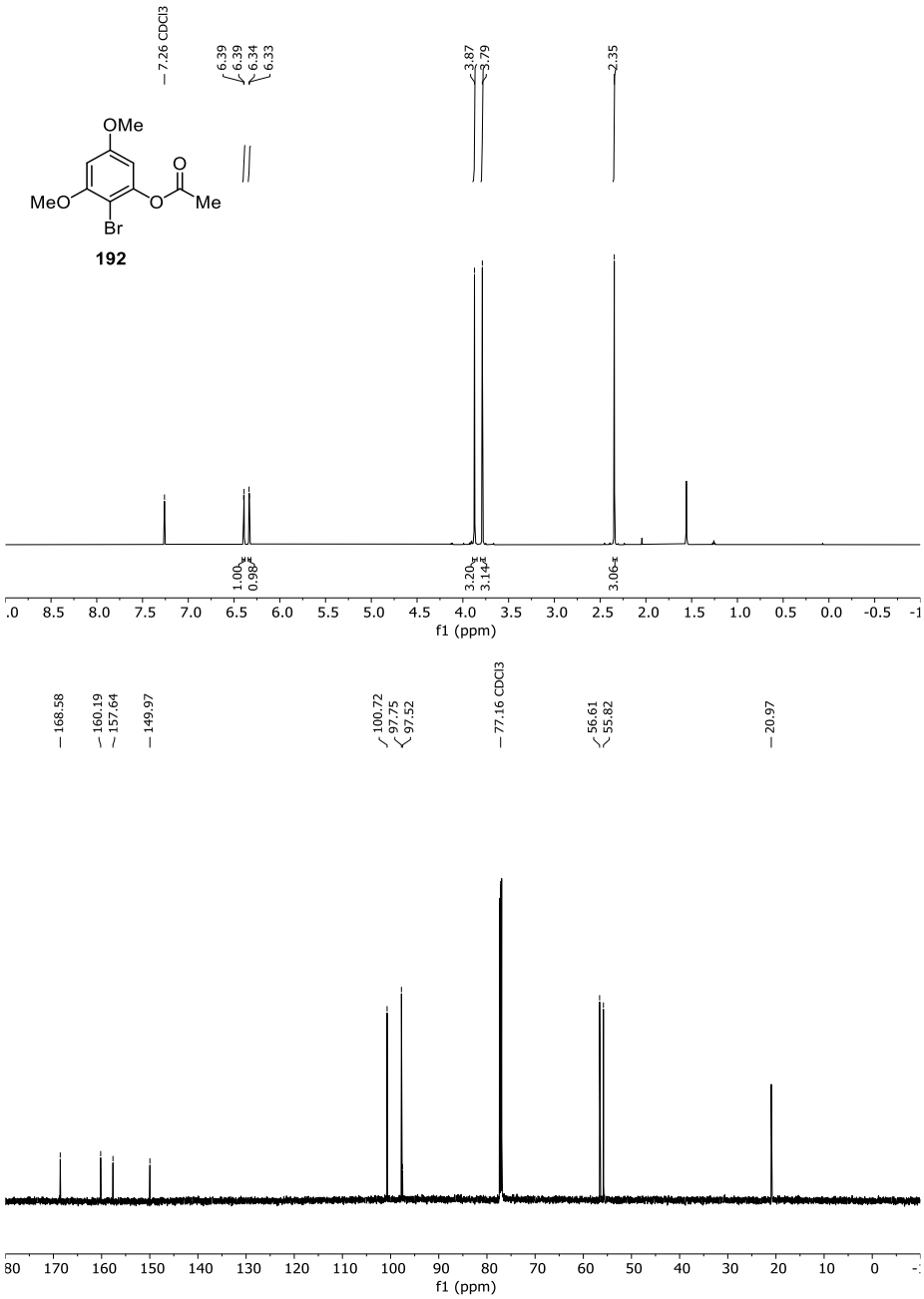

Figure 61 ^{1}H- and ^{13}C-NMR-Spectrum of **192** in $CDCl_3$ (600 MHz/151 MHz).

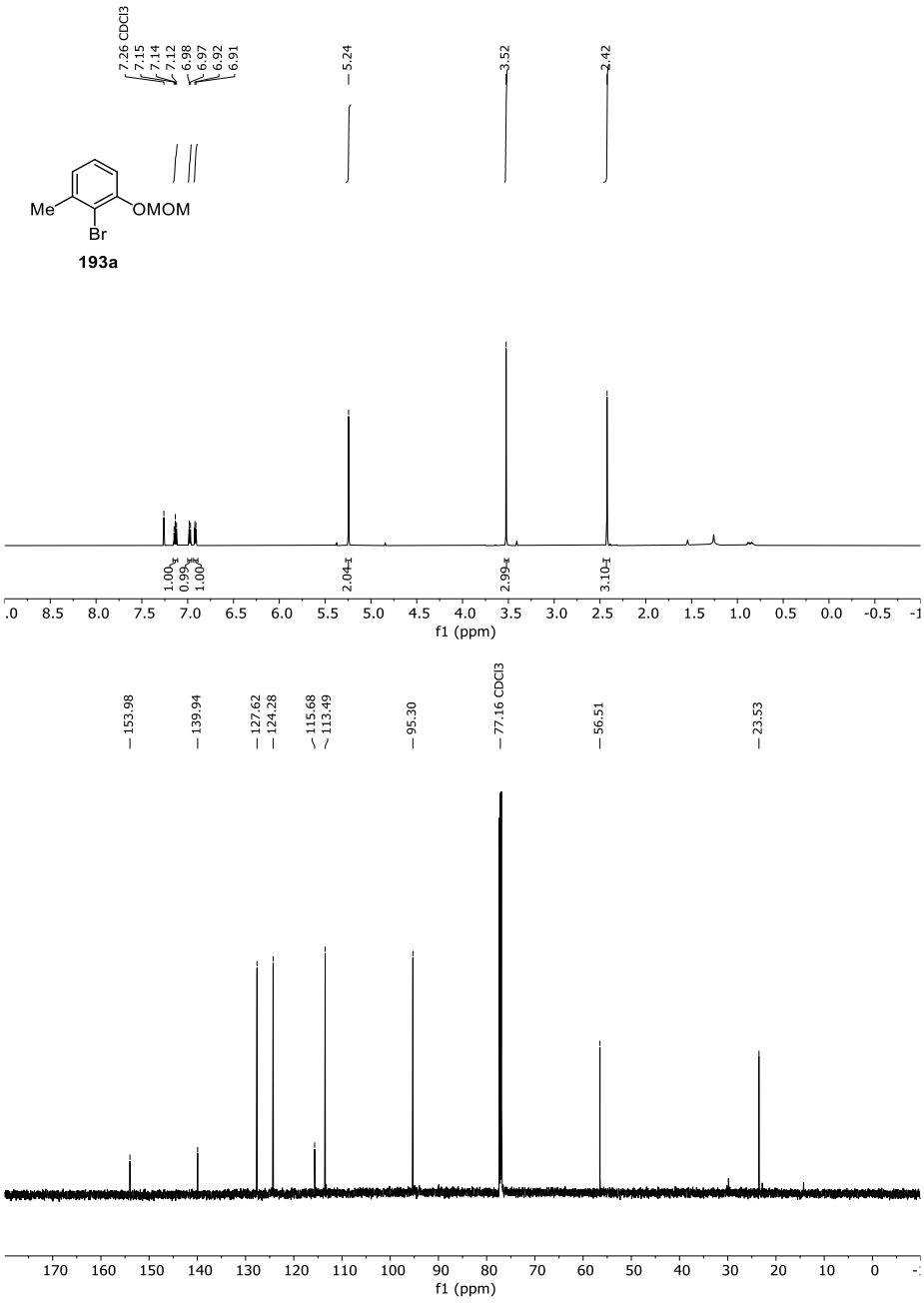

Figure 62 ^{1}H- and ^{13}C-NMR-Spectrum of **193a** in $CDCl_3$ (600 MHz/151 MHz).

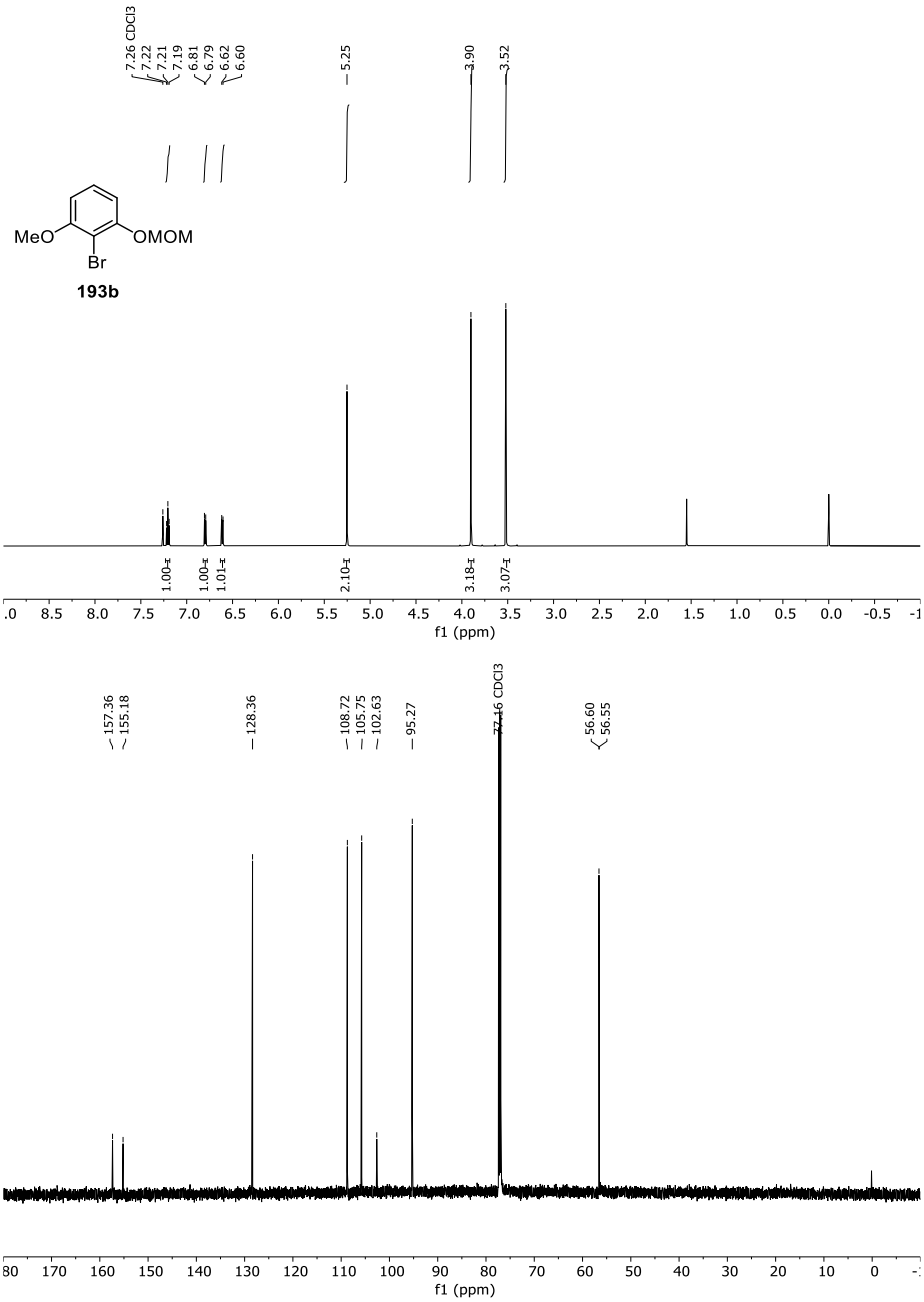

Figure 63 ^{1}H- and ^{13}C-NMR-Spectrum of **193b** in $CDCl_3$ (600 MHz/151 MHz).

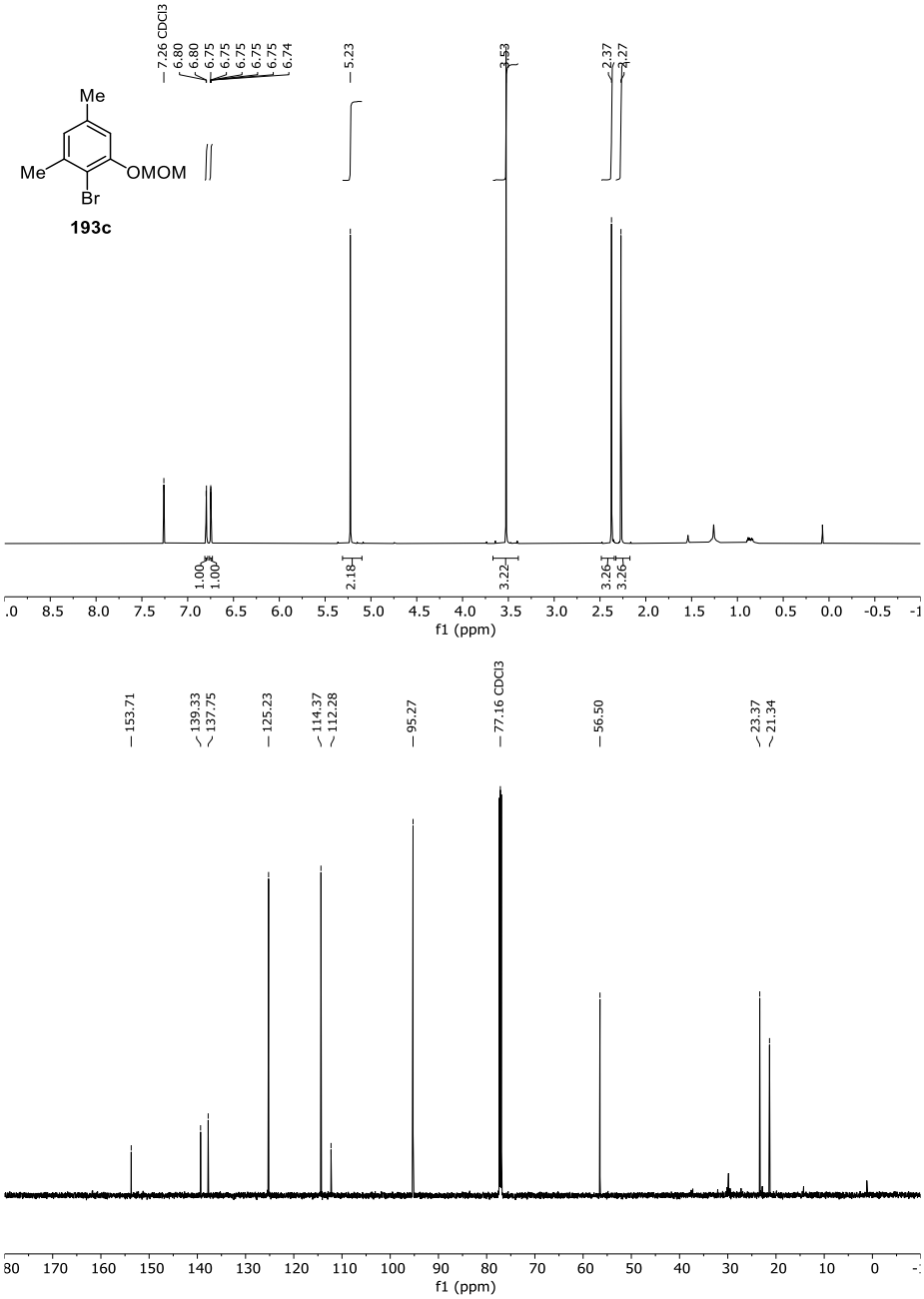

Figure 64 ^{1}H- and ^{13}C-NMR-Spectrum of **193c** in $CDCl_3$ (600 MHz/151 MHz).

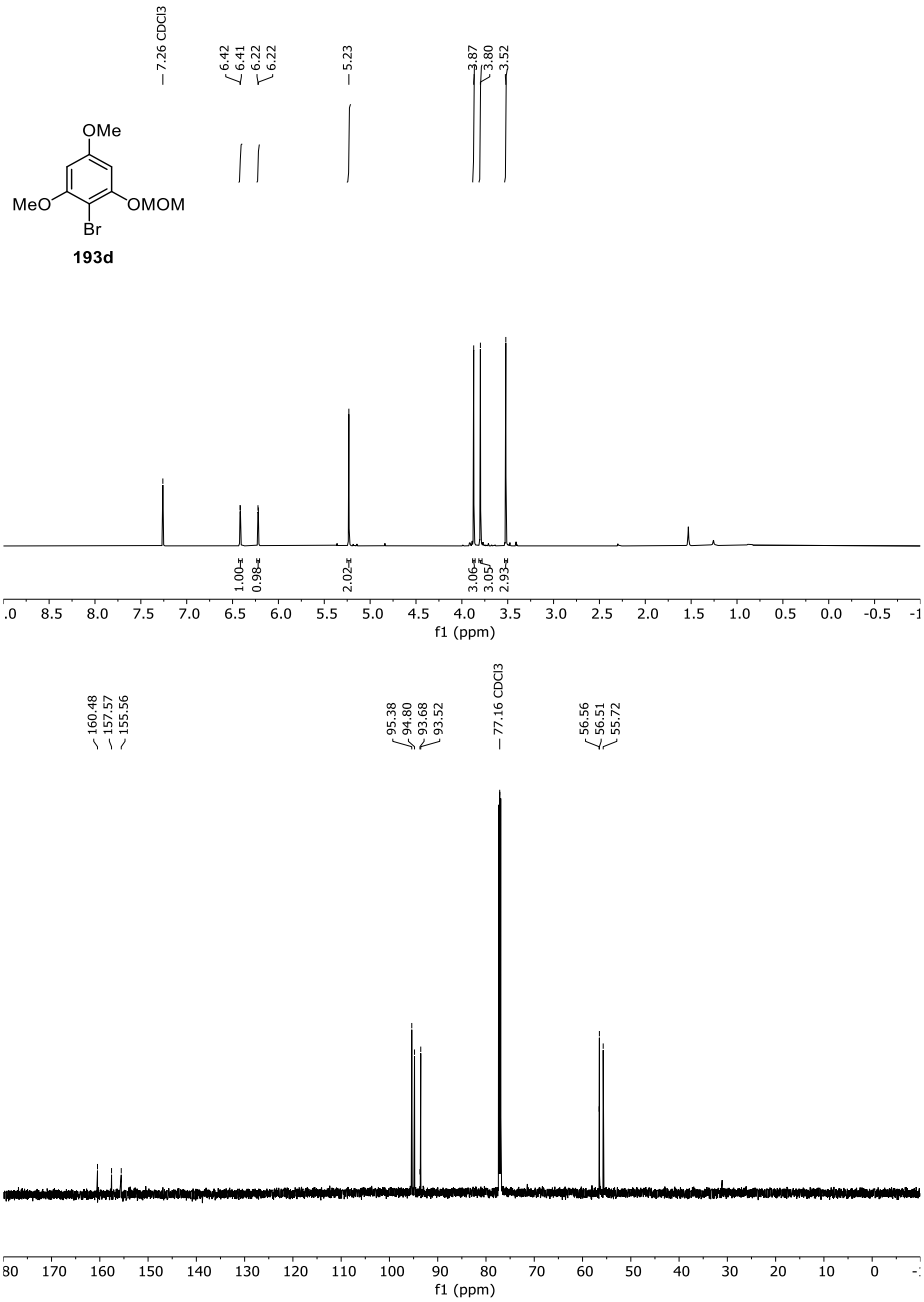

Figure 65 ^{1}H- and ^{13}C-NMR-Spectrum of **193d** in $CDCl_3$ (600 MHz/151 MHz).

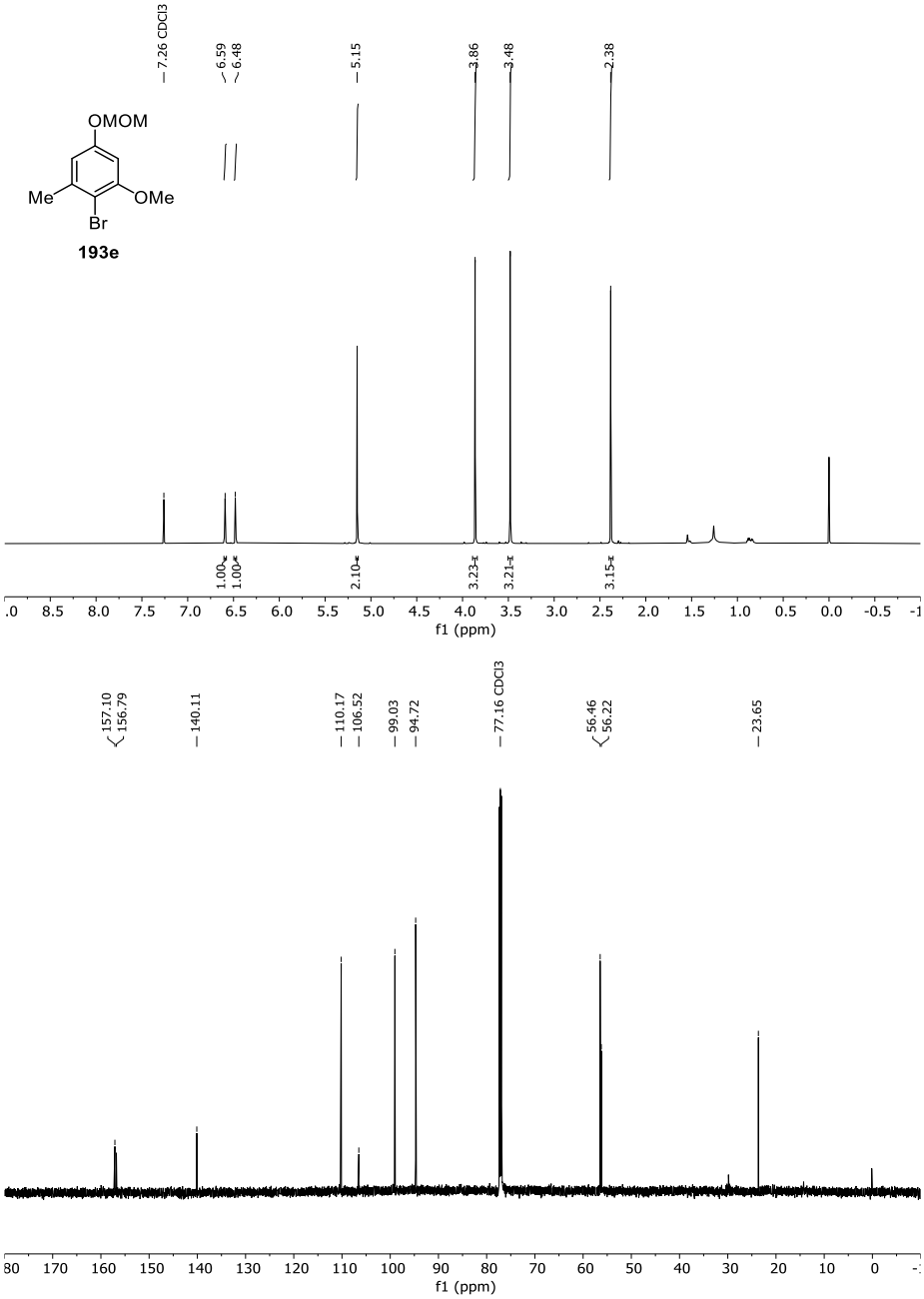

Figure 66 ^{1}H- and ^{13}C-NMR-Spectrum of **193e** in $CDCl_3$ (600 MHz/151 MHz).

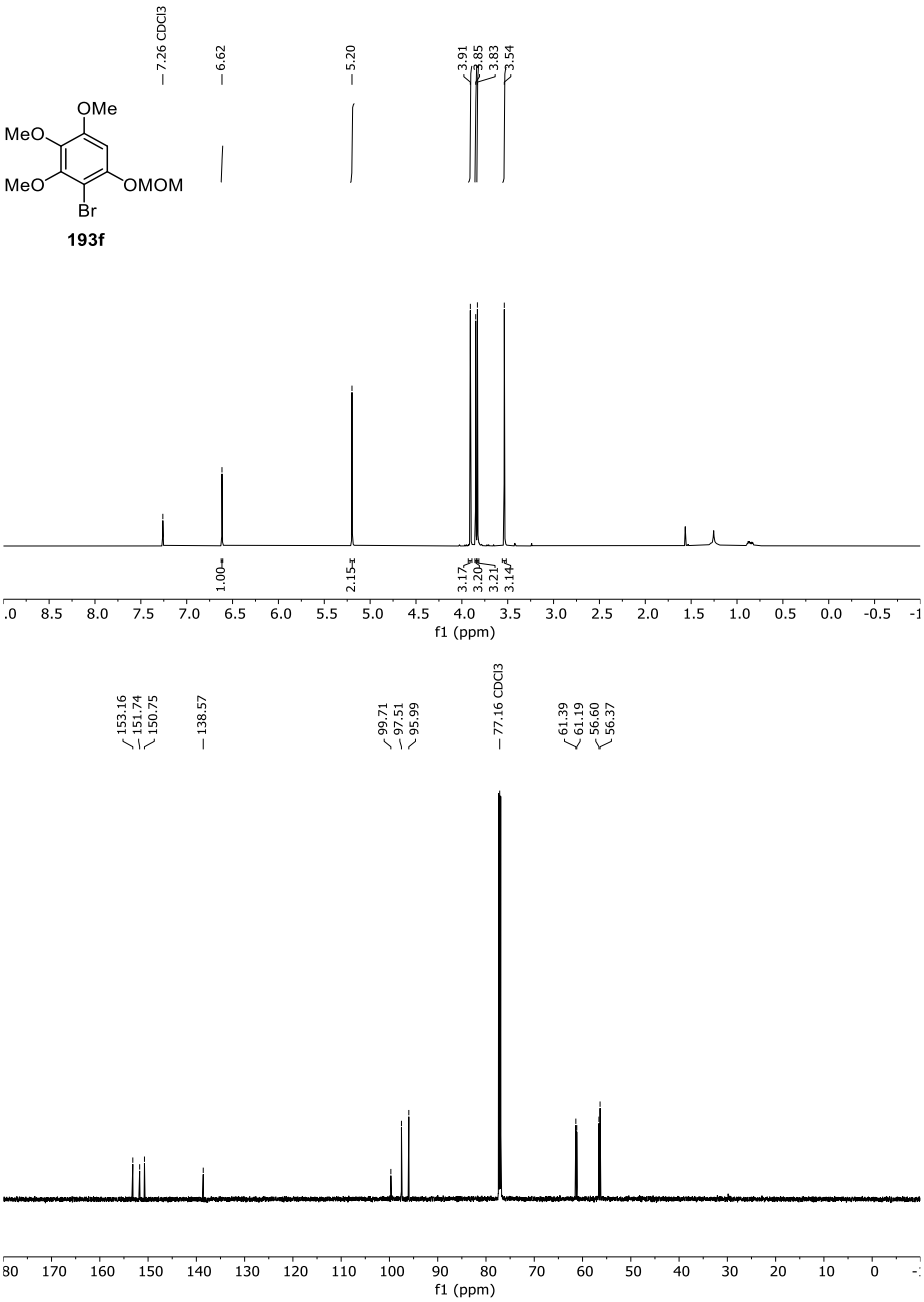

Figure 67 ^{1}H- and ^{13}C-NMR-Spectrum of **193f** in $CDCl_3$ (600 MHz/151 MHz).

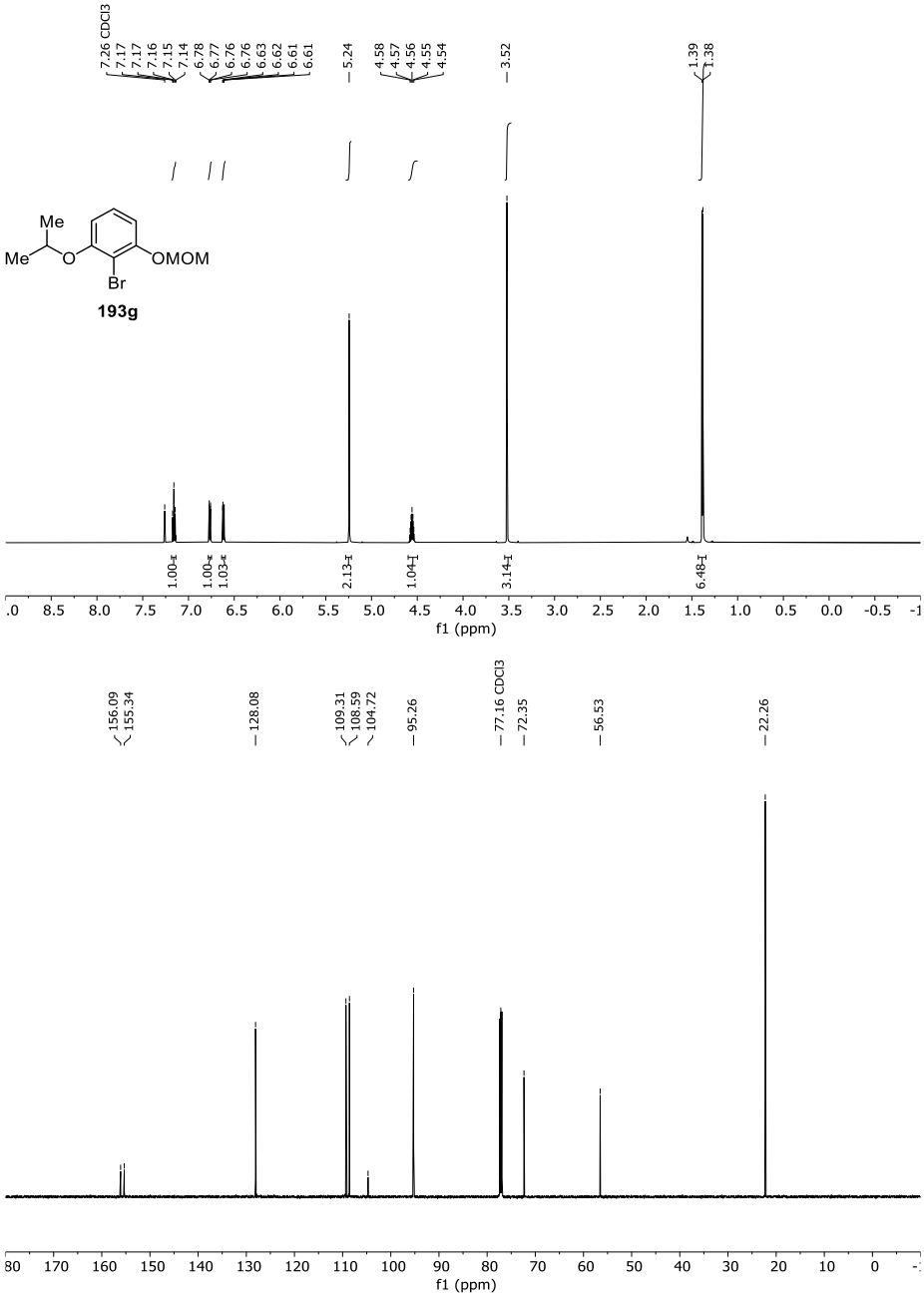

Figure 68 ^{1}H- and ^{13}C-NMR-Spectrum of **193g** in $CDCl_3$ (600 MHz/151 MHz).

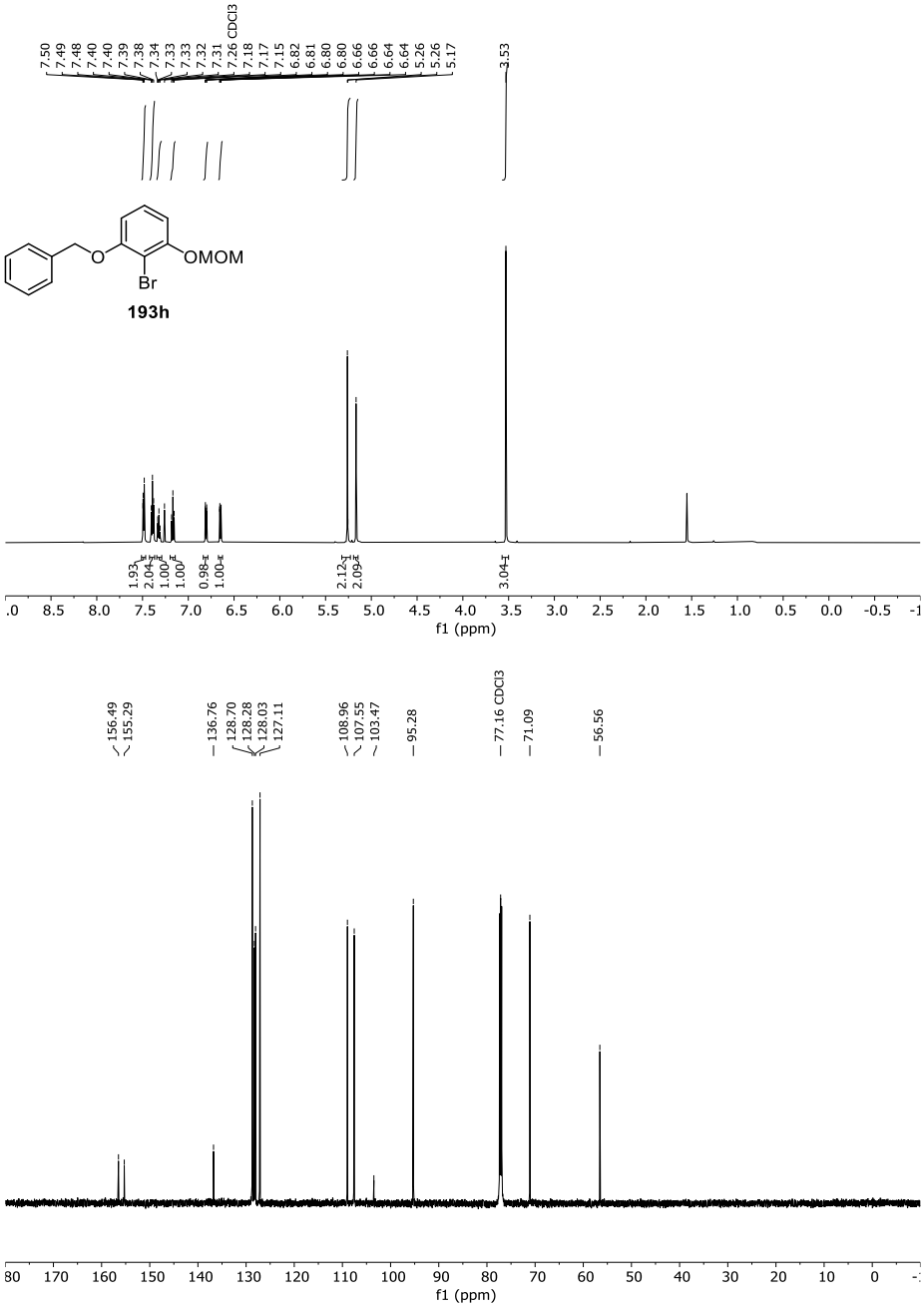

Figure 69 ^{1}H- and ^{13}C-NMR-Spectrum of **193h** in $CDCl_3$ (600 MHz/151 MHz).

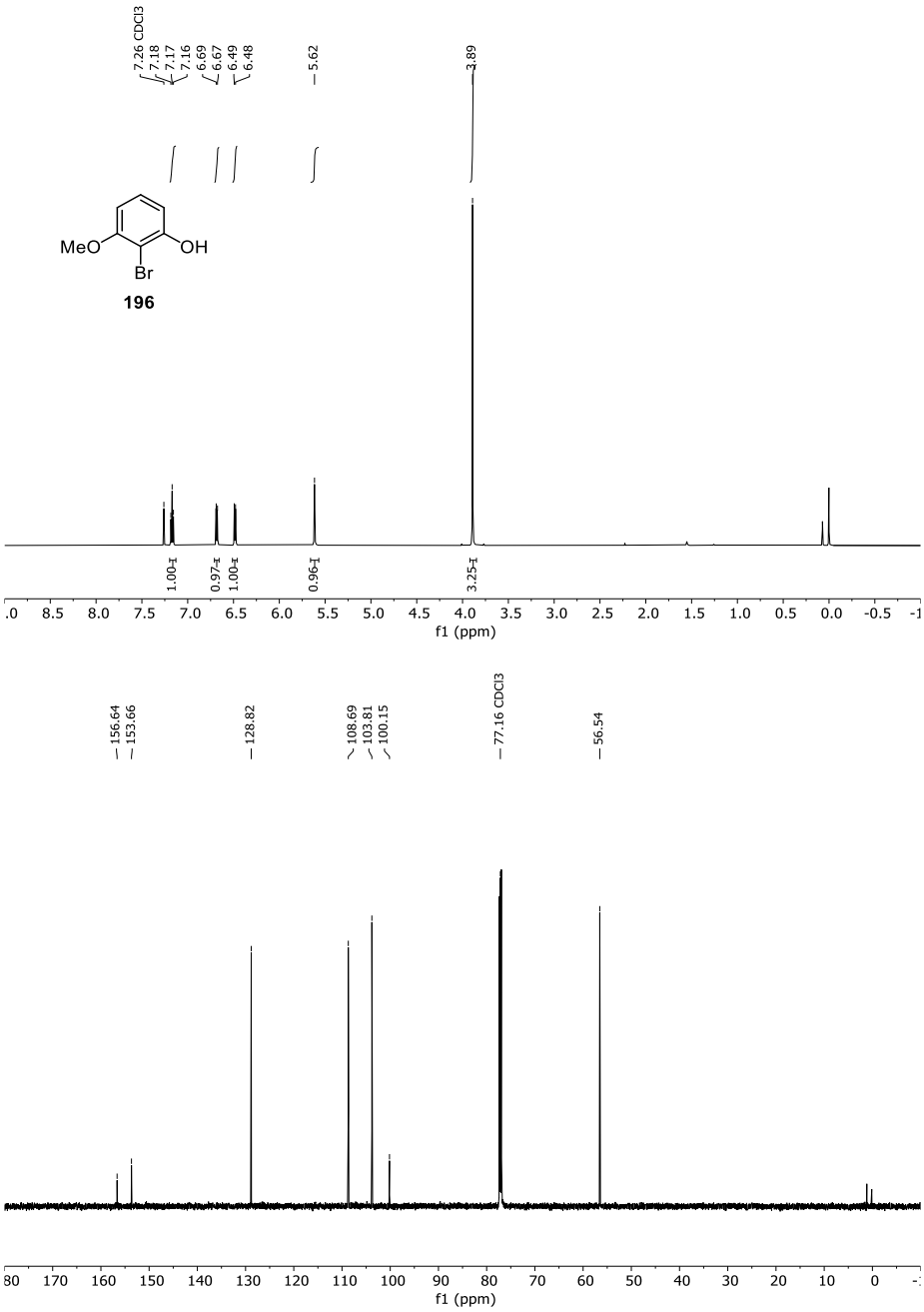

Figure 70 ^{1}H- and ^{13}C-NMR-Spectrum of **196** in $CDCl_3$ (600 MHz/151 MHz).

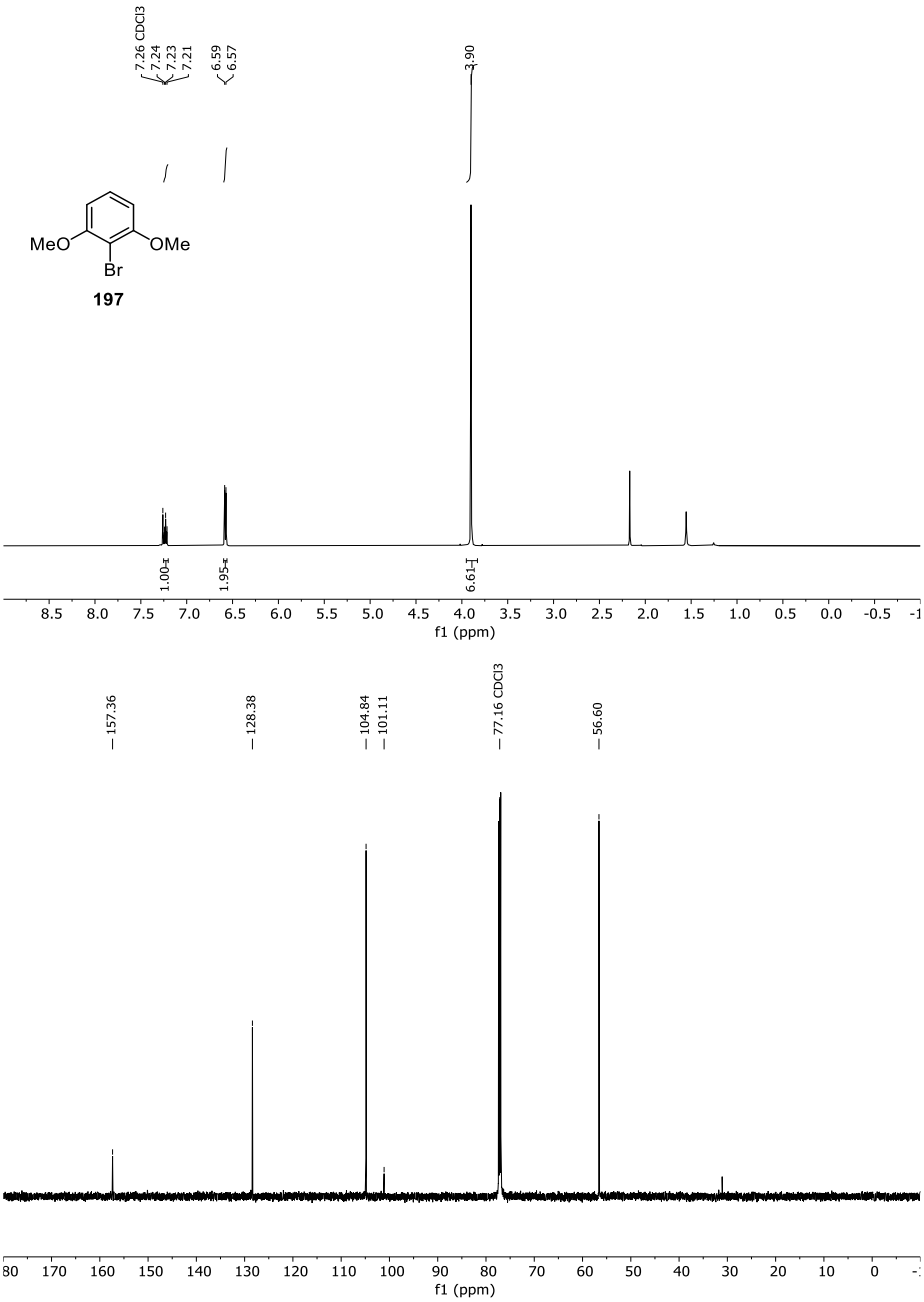

Figure 71 ^{1}H- and ^{13}C-NMR-Spectrum of **197** in $CDCl_3$ (600 MHz/151 MHz).

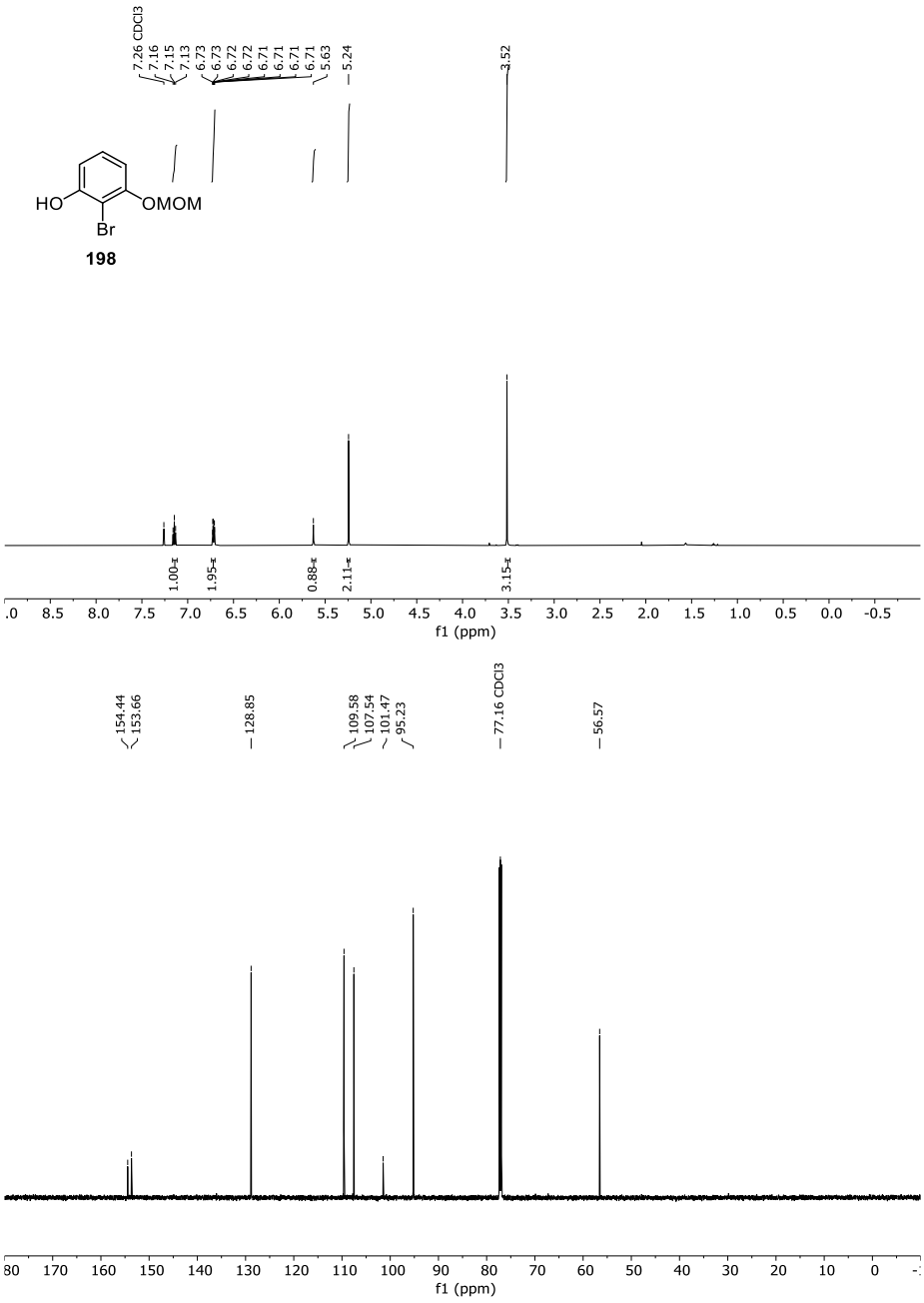

Figure 72 ^{1}H- and ^{13}C-NMR-Spectrum of **198** in $CDCl_3$ (600 MHz/151 MHz).

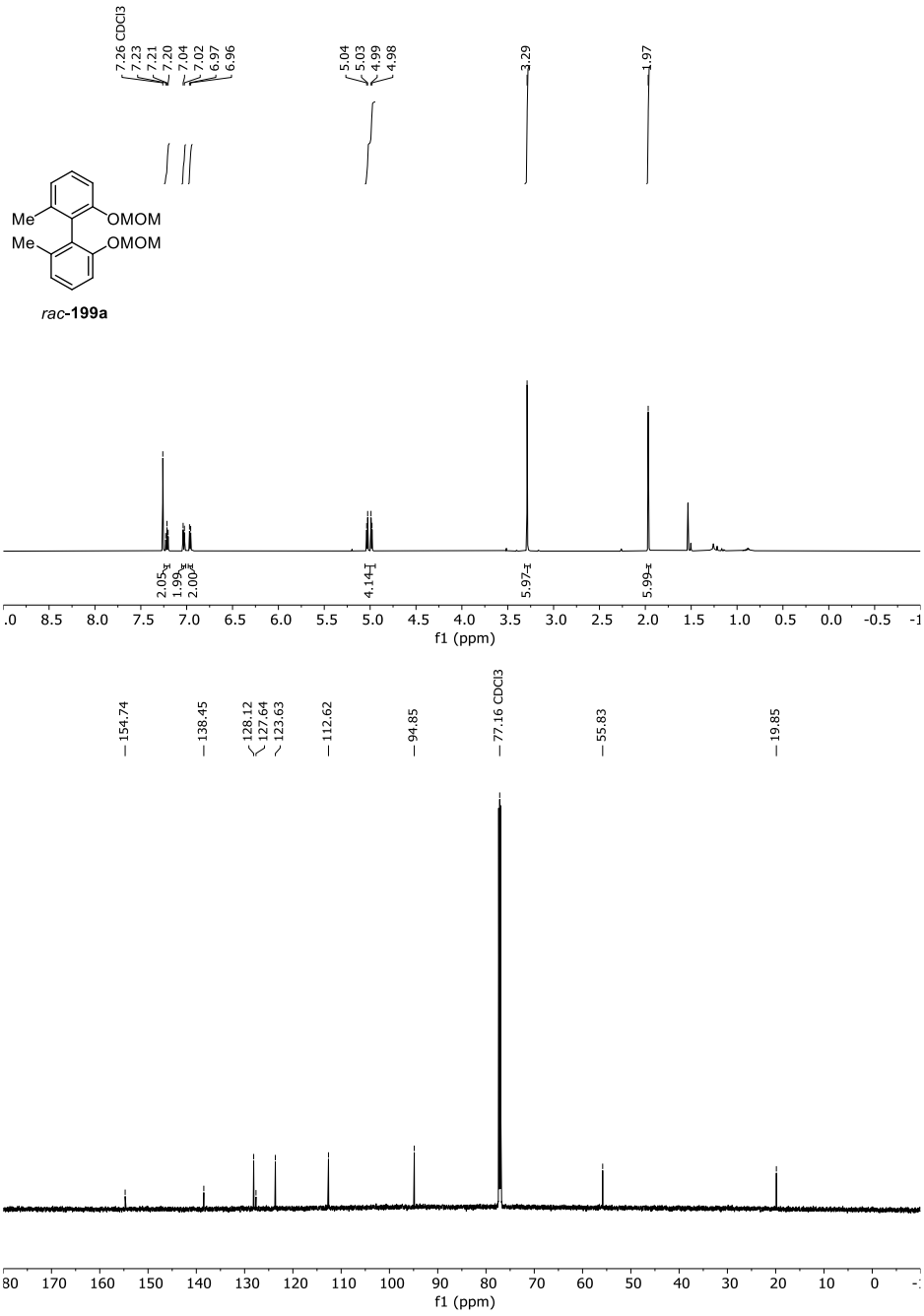

Figure 73 ^{1}H- and ^{13}C-NMR-Spectrum of *rac*-**199a** in $CDCl_3$ (600 MHz/151 MHz).

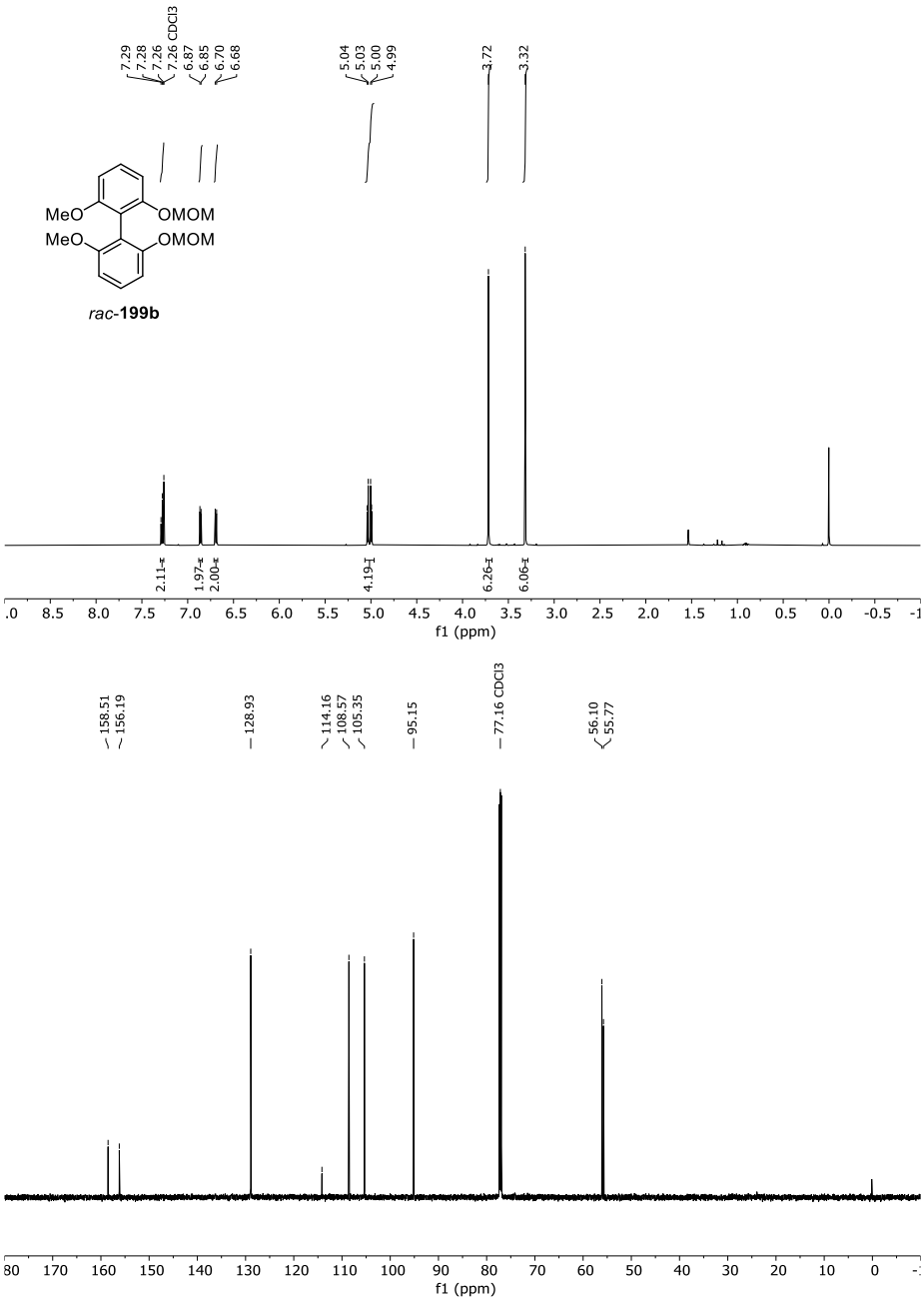

Figure 74 ^{1}H- and ^{13}C-NMR-Spectrum of *rac*-**199b** in $CDCl_3$ (600 MHz/151 MHz).

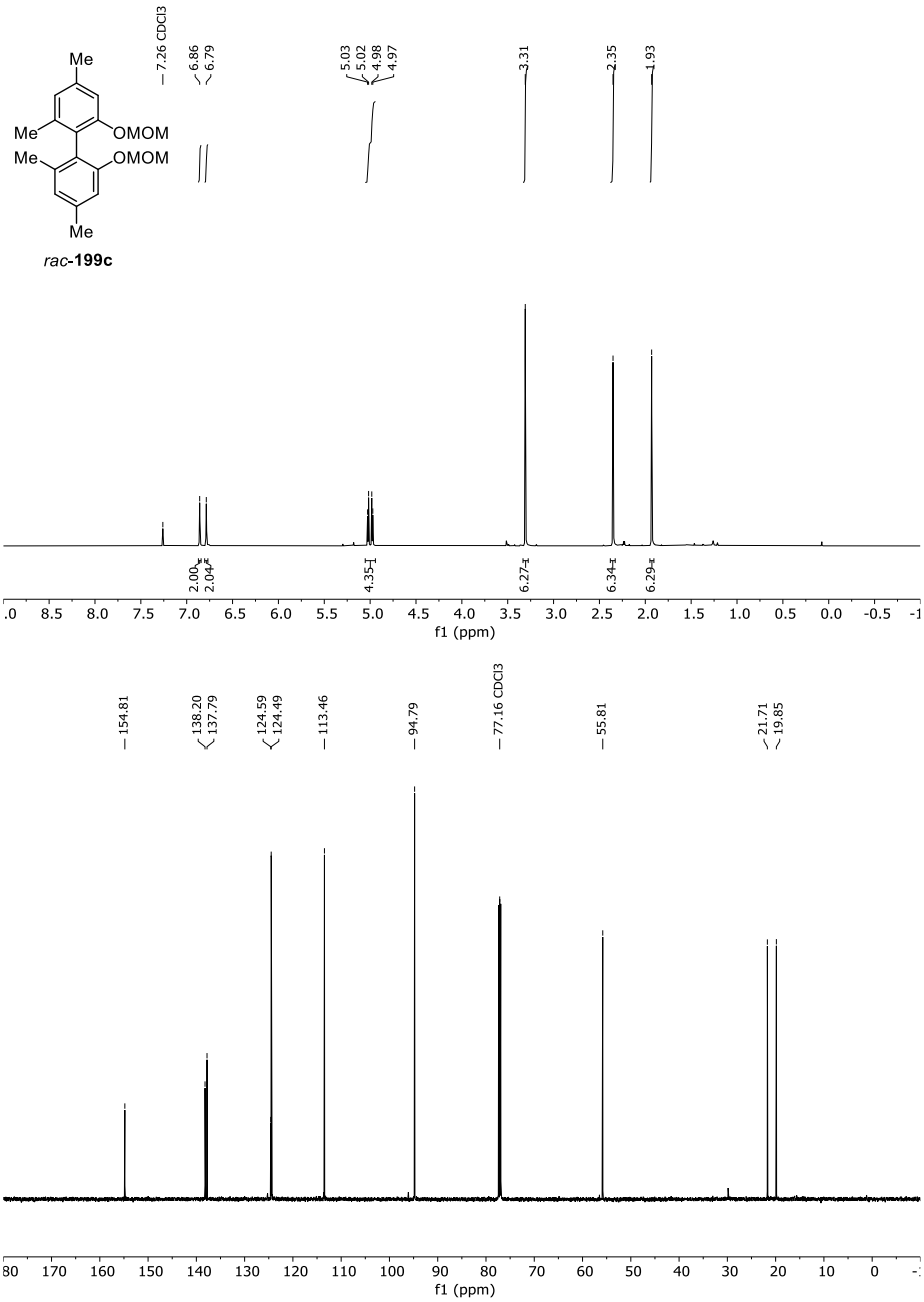

Figure 75 ^{1}H- and ^{13}C-NMR-Spectrum of *rac*-**199c** in $CDCl_3$ (600 MHz/151 MHz).

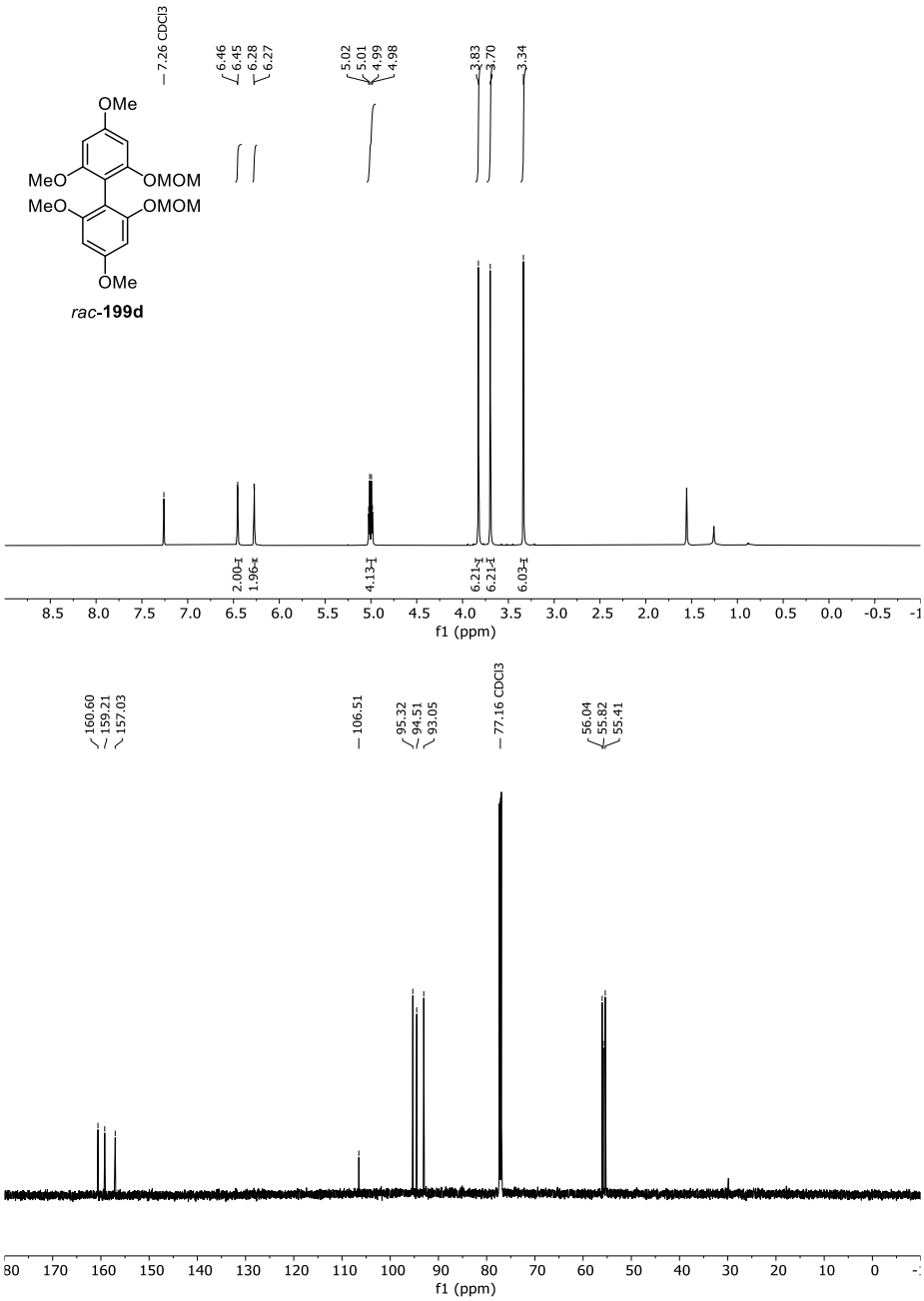

Figure 76 ^{1}H- and ^{13}C-NMR-Spectrum of *rac*-**199d** in $CDCl_3$ (600 MHz/151 MHz).

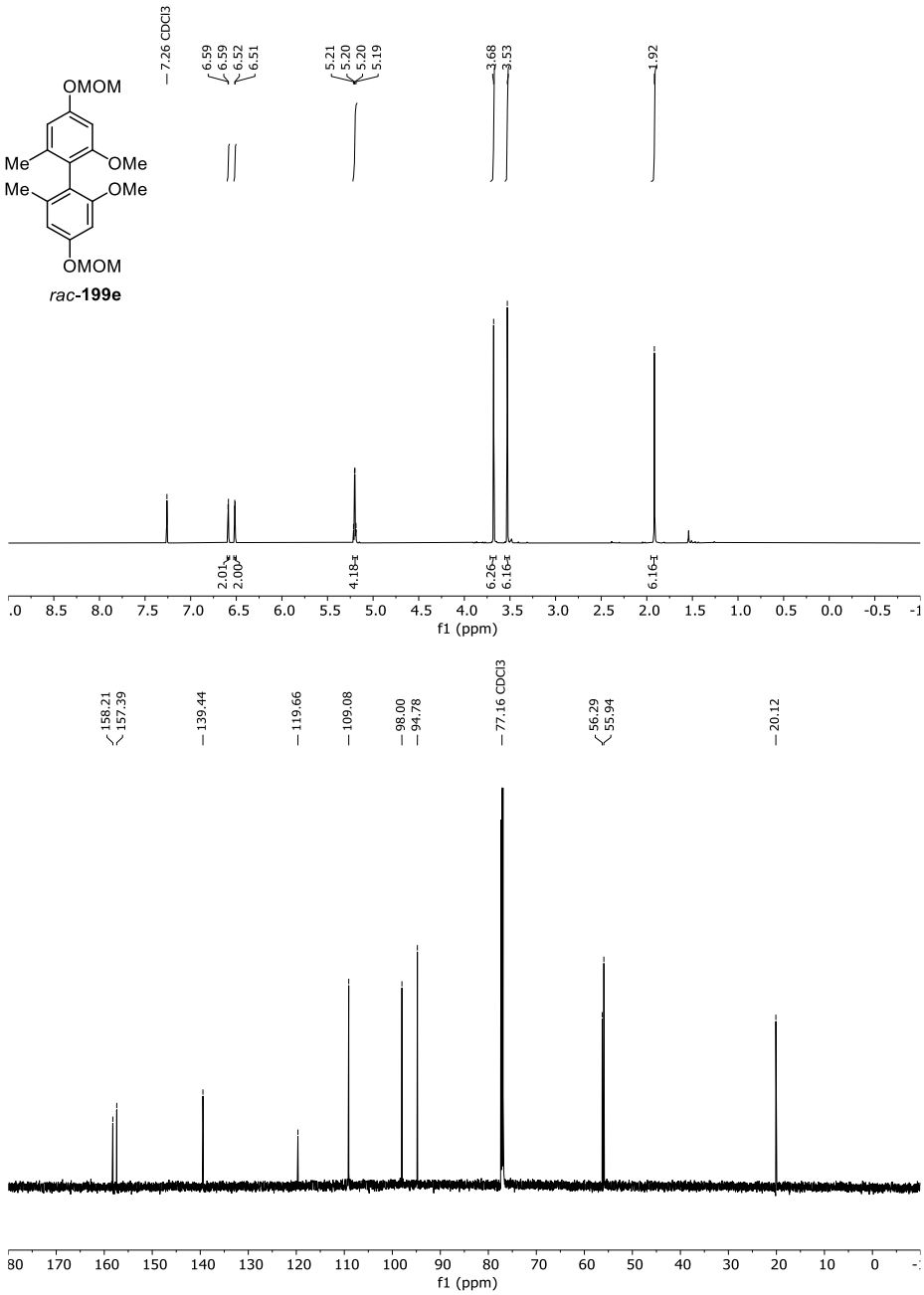

Figure 77 ^{1}H- and ^{13}C-NMR-Spectrum of *rac*-**199e** in $CDCl_3$ (600 MHz/151 MHz).

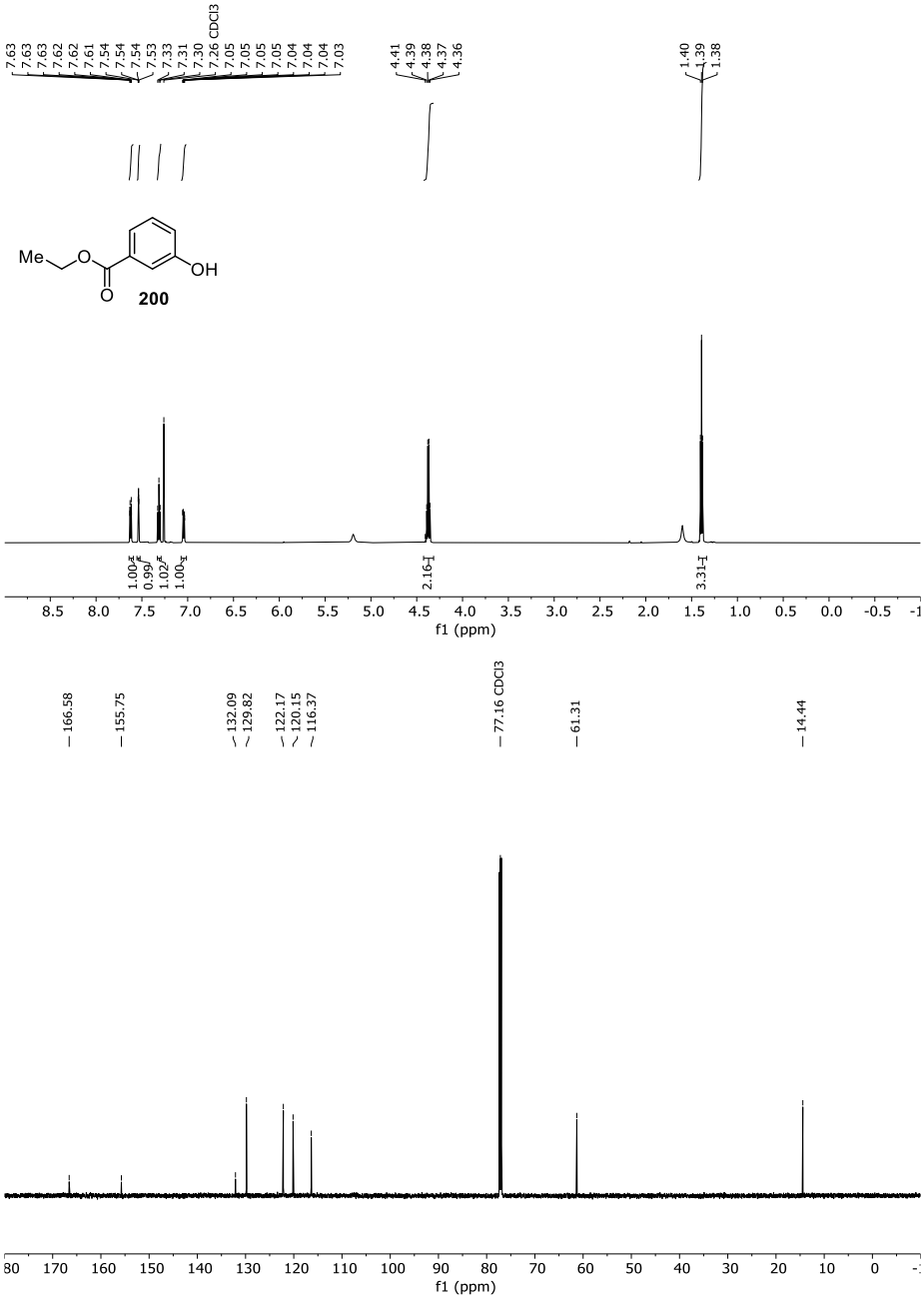

Figure 78 ^{1}H- and ^{13}C-NMR-Spectrum of **200** in $CDCl_3$ (600 MHz/151 MHz).

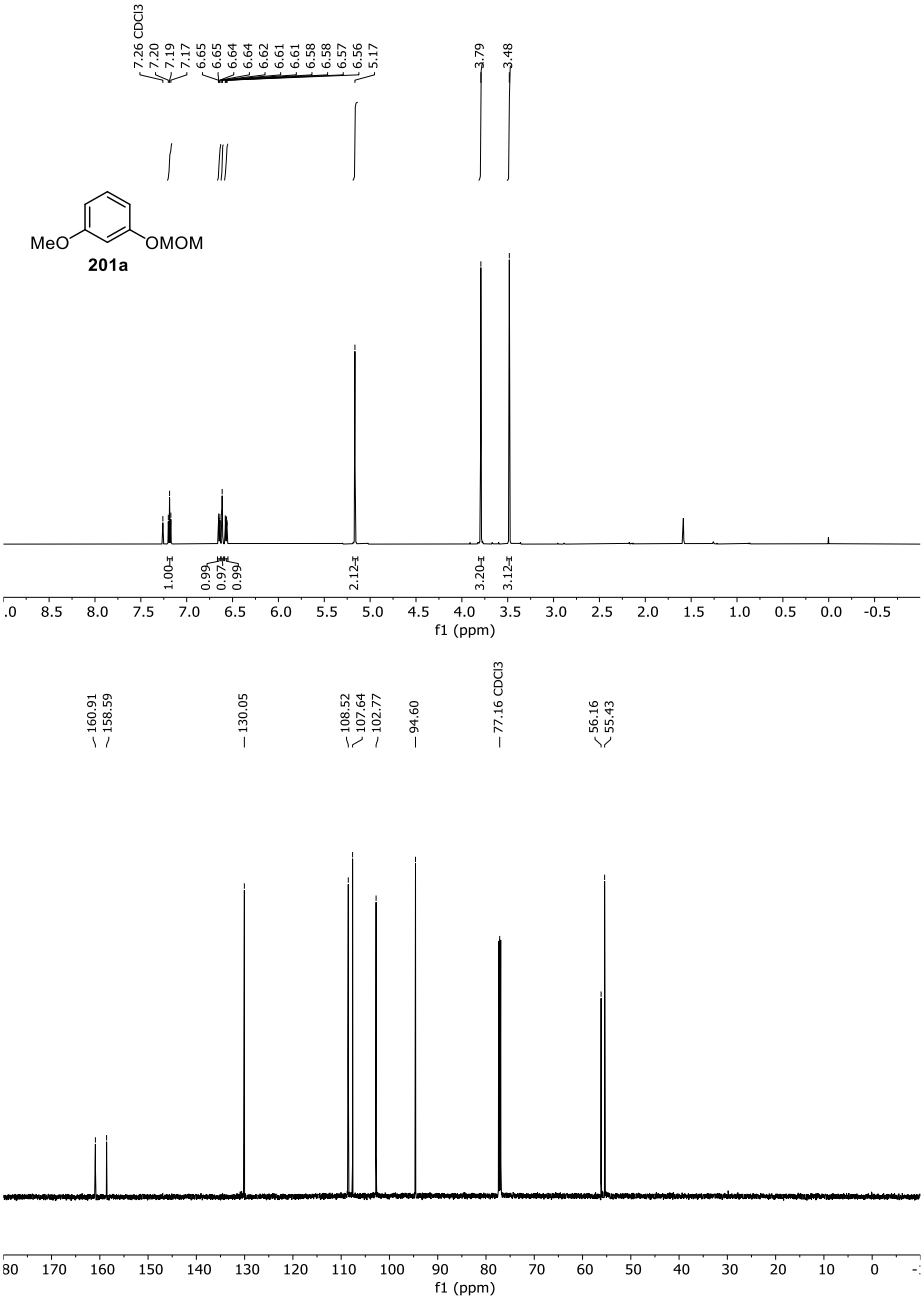

Figure 79 ^{1}H- and ^{13}C-NMR-Spectrum of **201a** in $CDCl_3$ (600 MHz/151 MHz).

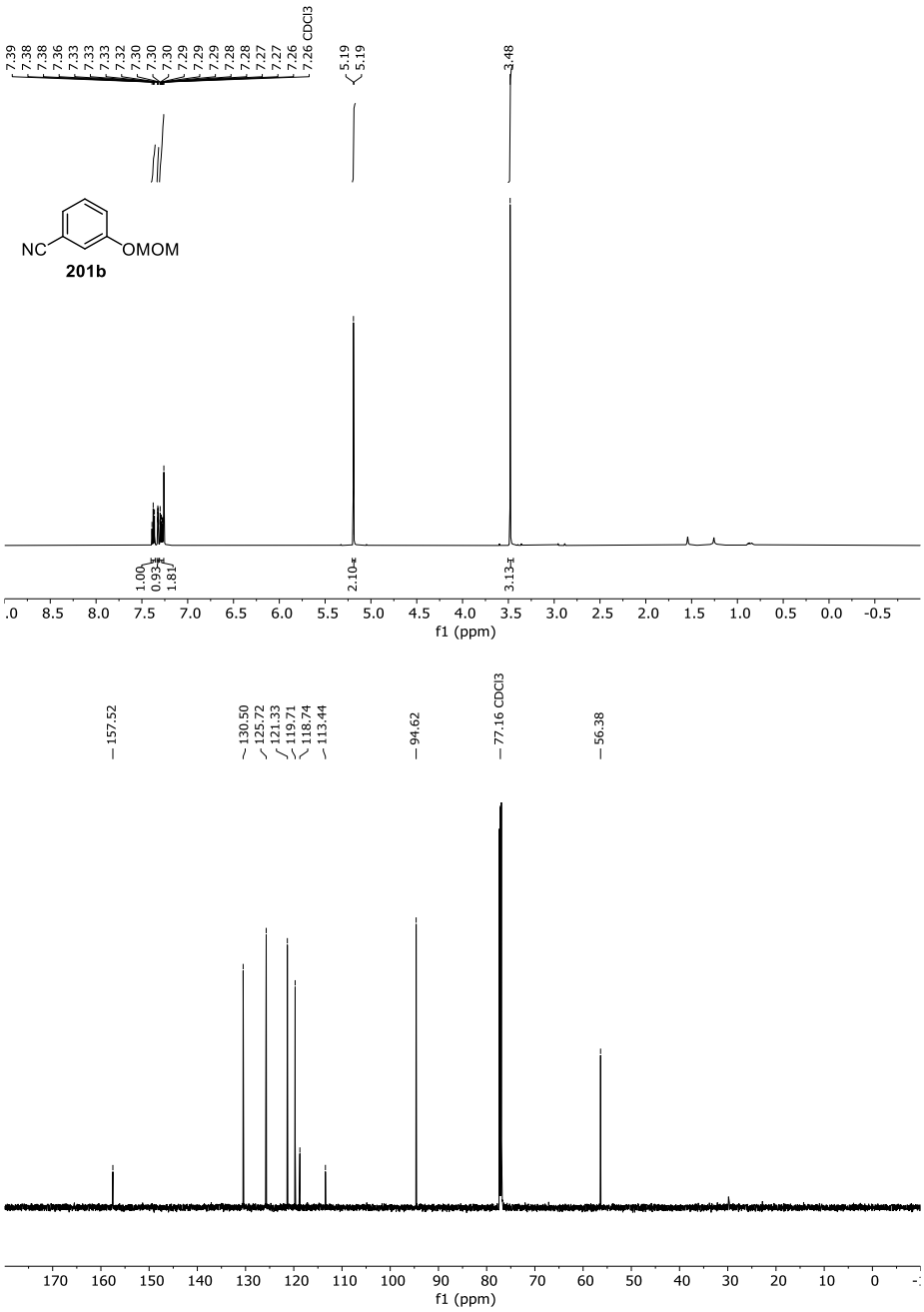

Figure 80 ^{1}H- and ^{13}C-NMR-Spectrum of **201b** in $CDCl_3$ (600 MHz/151 MHz).

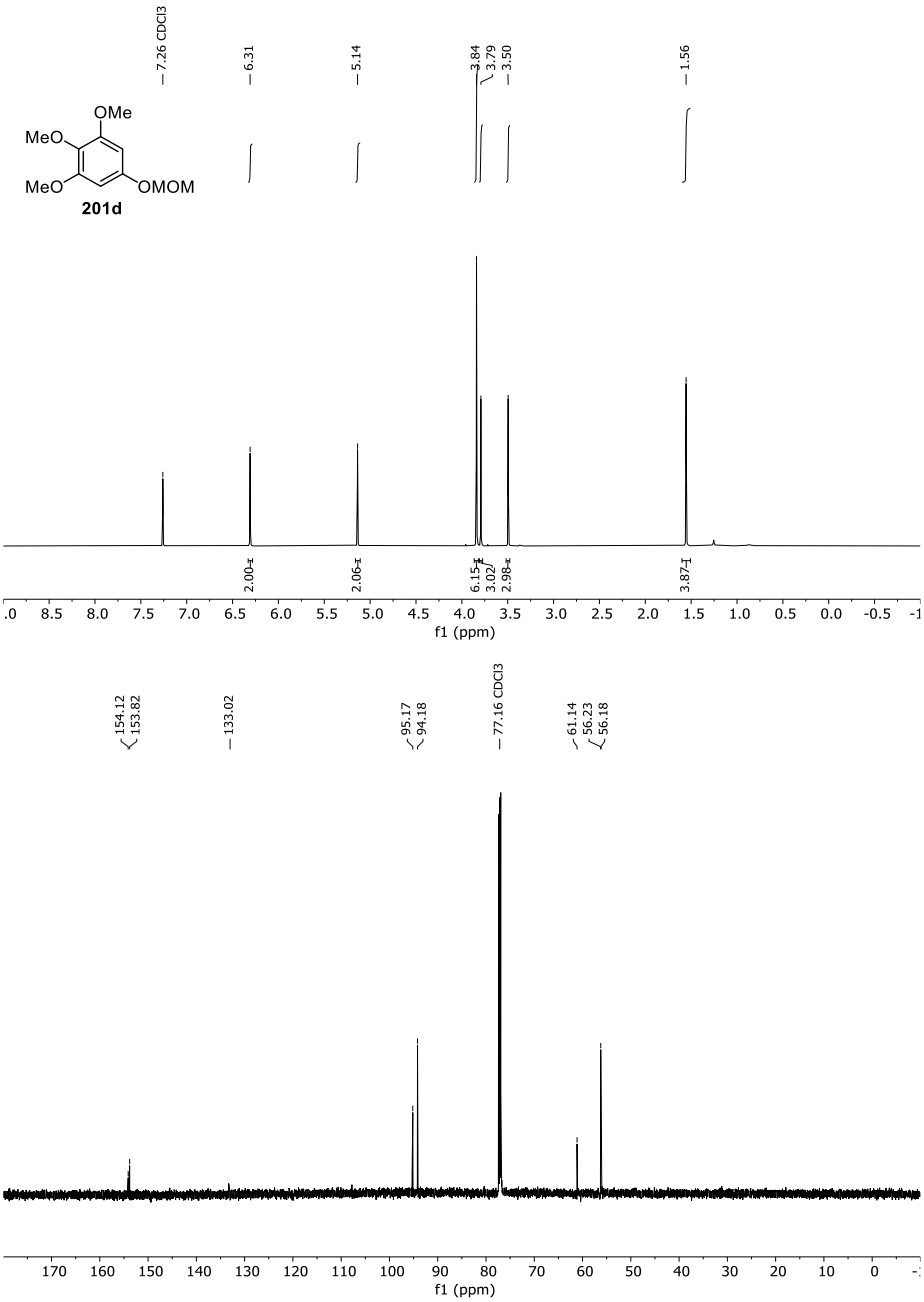

Figure 81 ^{1}H- and ^{13}C-NMR-Spectrum of **201d** in $CDCl_3$ (600 MHz/151 MHz).

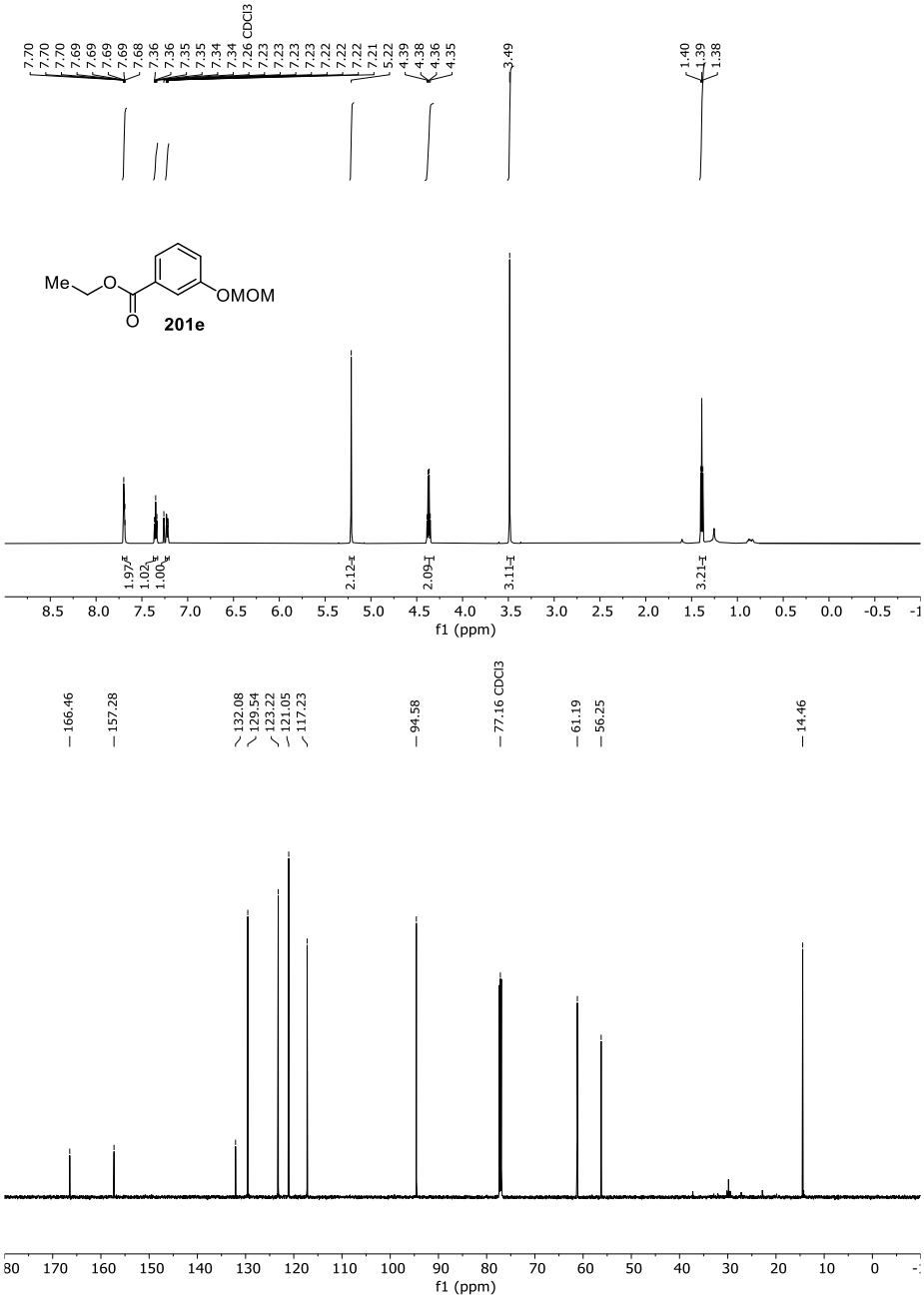

Figure 82 ^{1}H- and ^{13}C-NMR-Spectrum of **201e** in $CDCl_3$ (600 MHz/151 MHz).

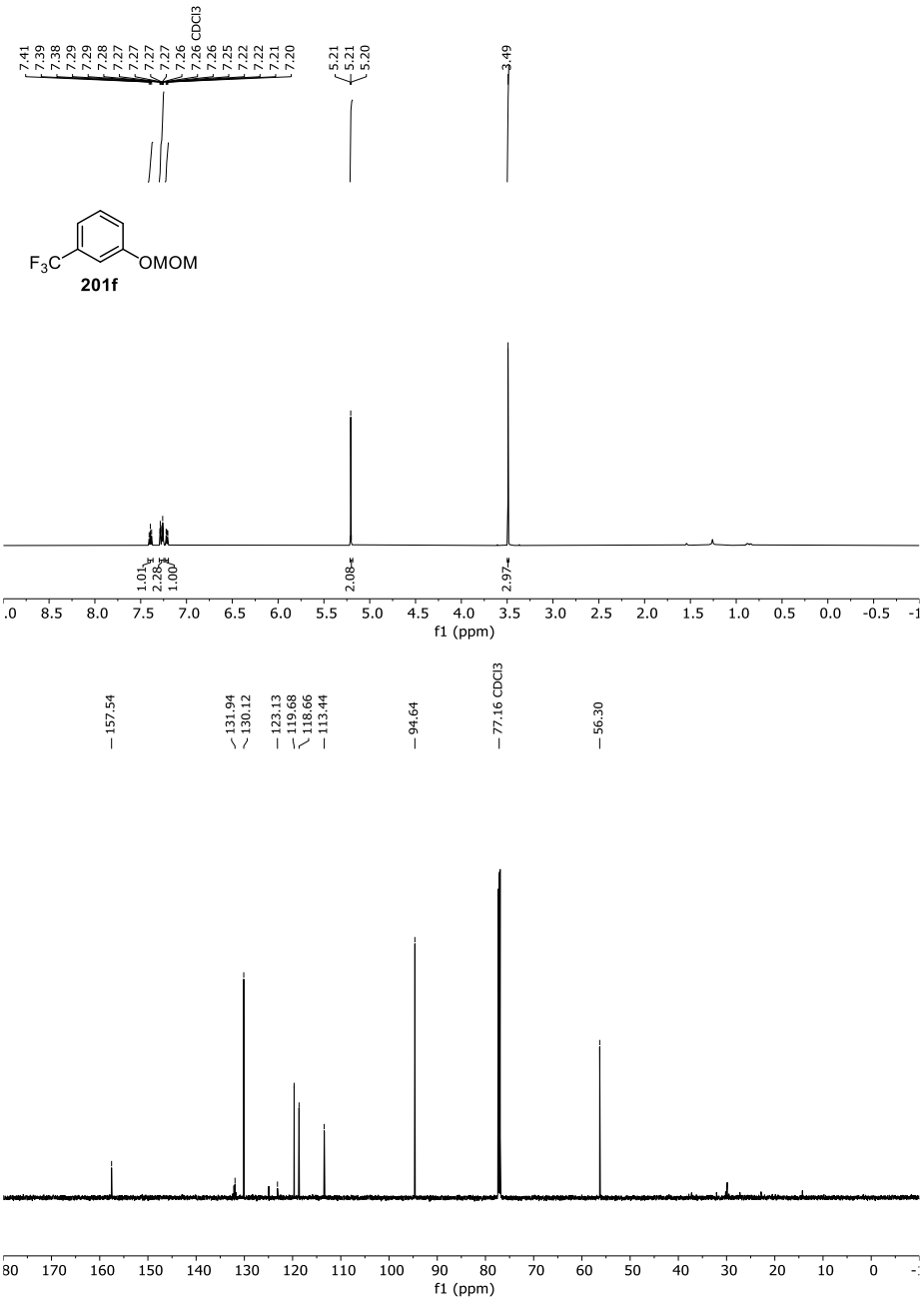
7.41
7.39
7.38
7.29
7.29
7.28
7.27
7.27
7.27
7.27
7.26 CDCl3
7.26
7.25
7.22
7.21
7.20
5.21
5.21
5.20
3.49
F3C
OMOM
201f
1.01
2.28
1.00
2.08
2.97
f1 (ppm)
157.54
131.94
130.12
123.13
119.68
118.66
113.44
94.64
77.16 CDCl3
56.30
f1 (ppm)

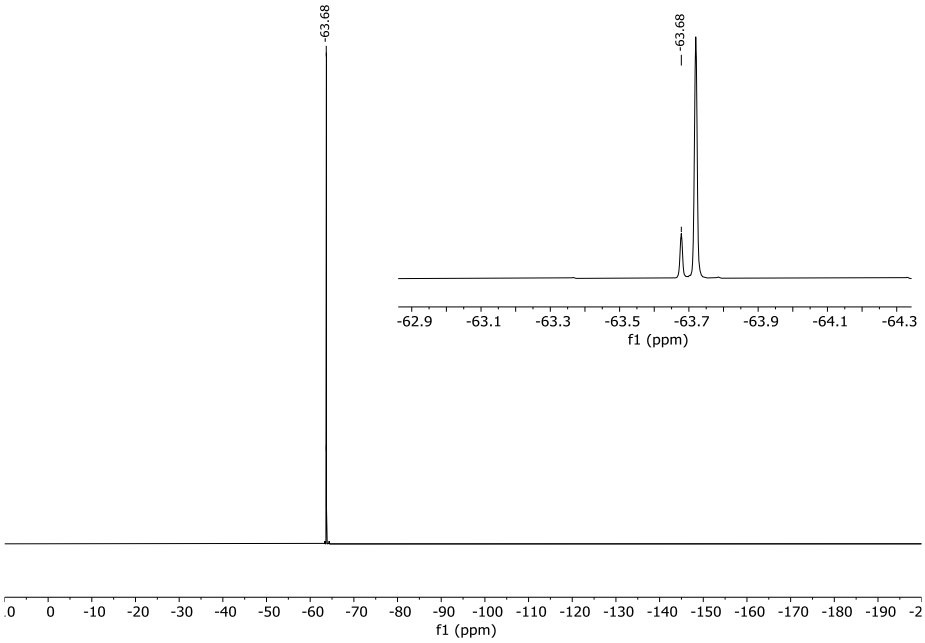

Figure 83 ^{1}H-, ^{13}C- and ^{19}F-NMR-Spectrum of **201f** in $CDCl_3$ (600 MHz/151 MHz).

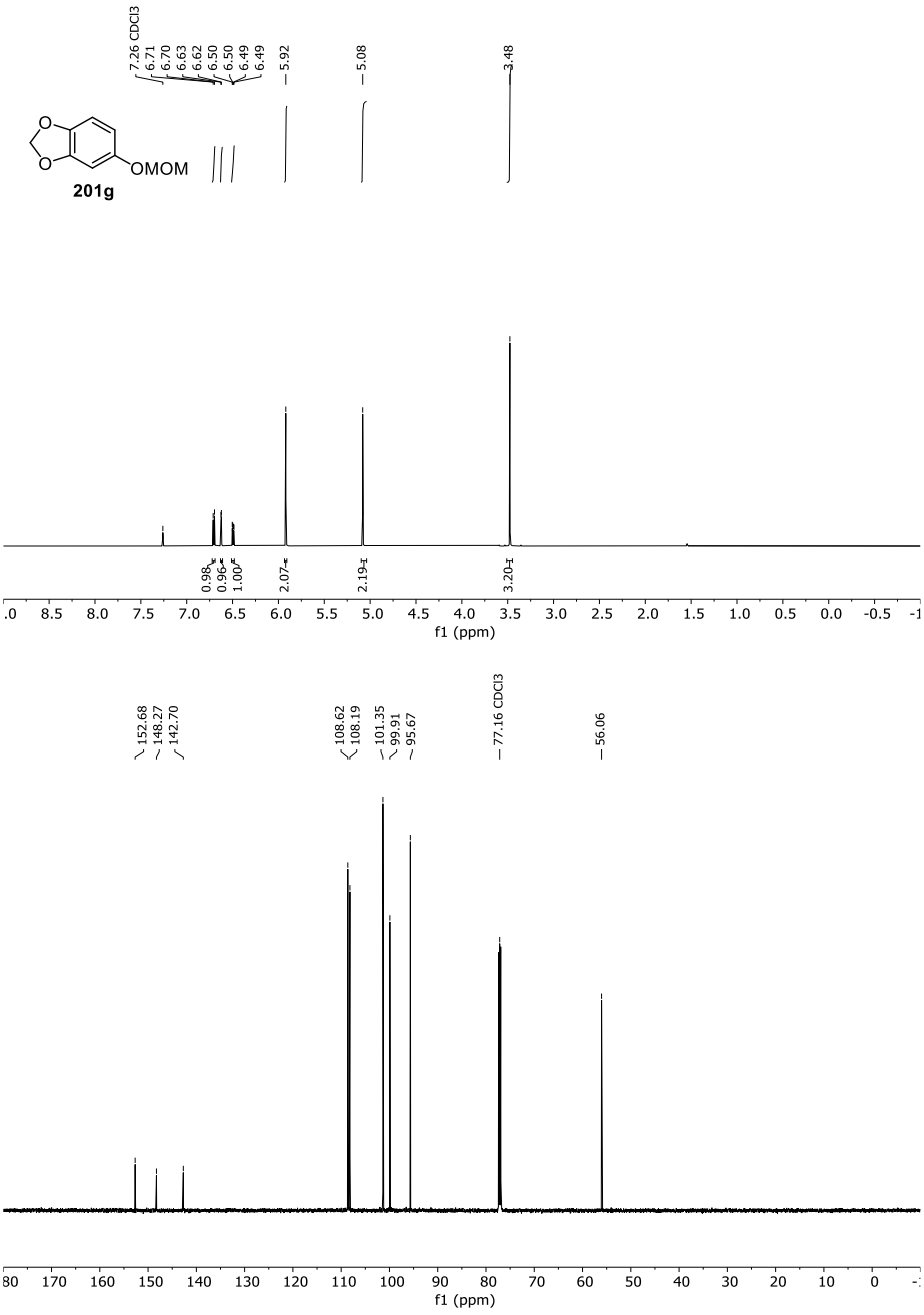

Figure 84 ^{1}H- and ^{13}C-NMR-Spectrum of **201g** in $CDCl_3$ (600 MHz/151 MHz).

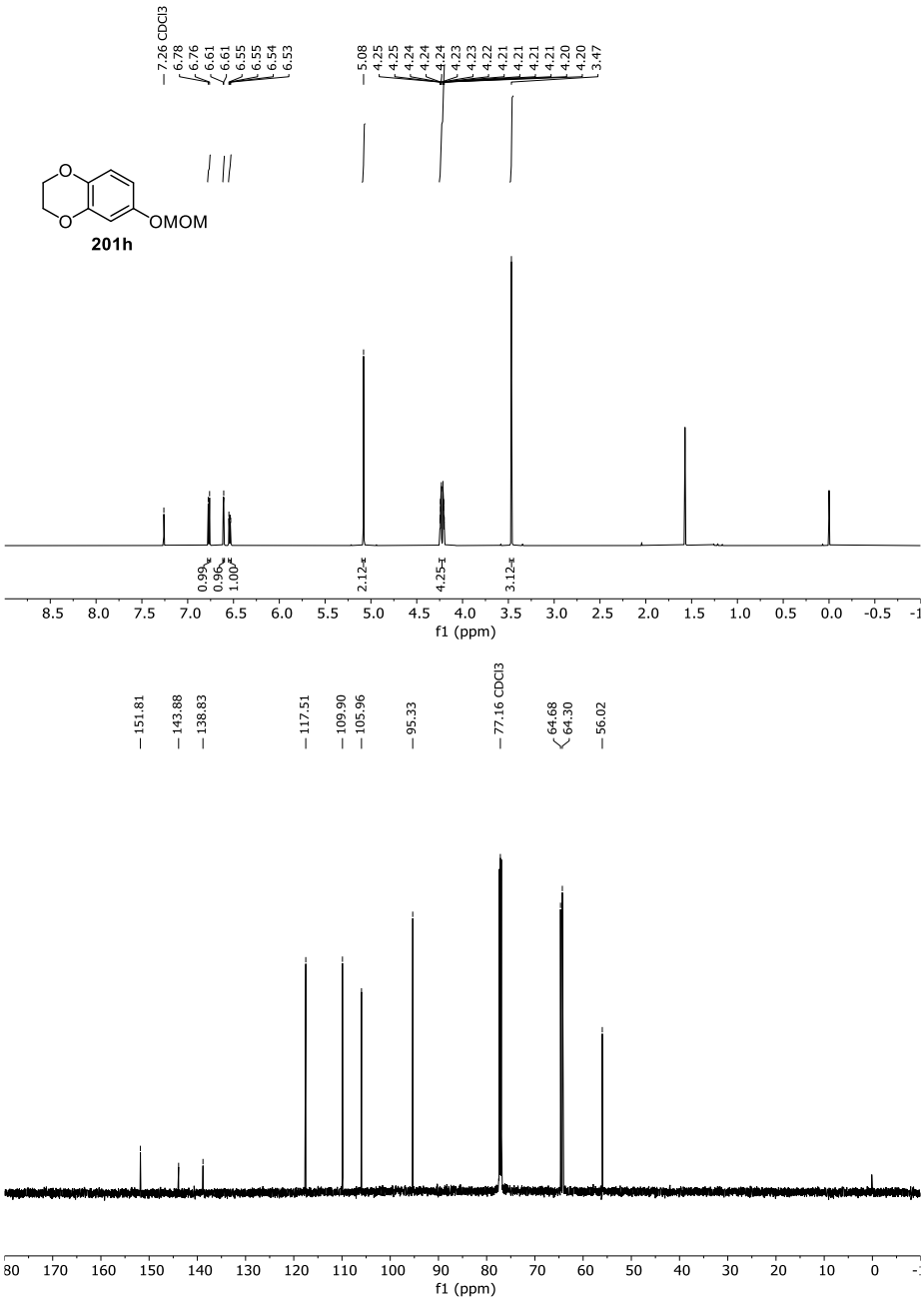

Figure 85 ^{1}H- and ^{13}C-NMR-Spectrum of **201h** in $CDCl_3$ (600 MHz/151 MHz).

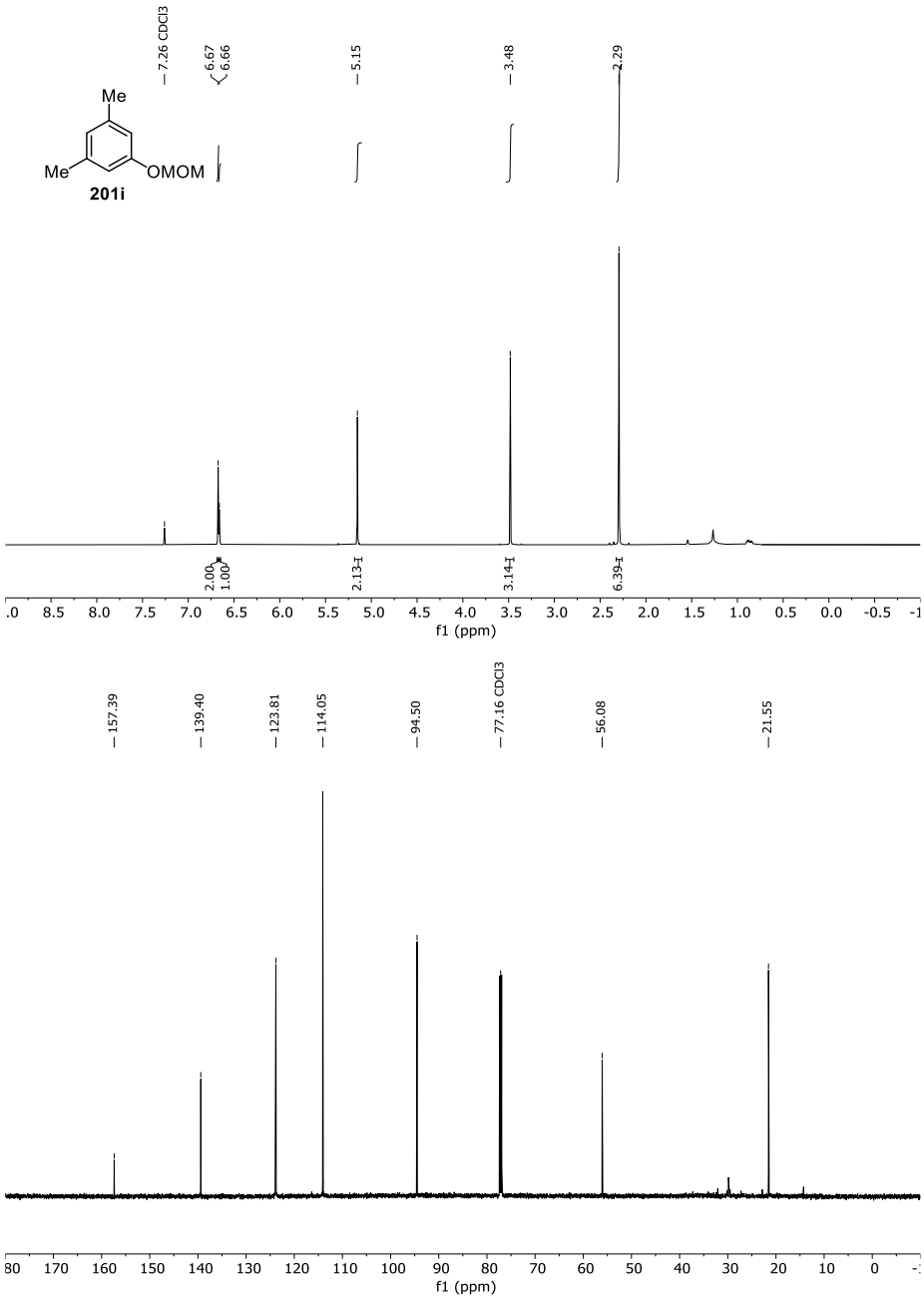

Figure 86 ^{1}H- and ^{13}C-NMR-Spectrum of **201i** in $CDCl_3$ (600 MHz/151 MHz).

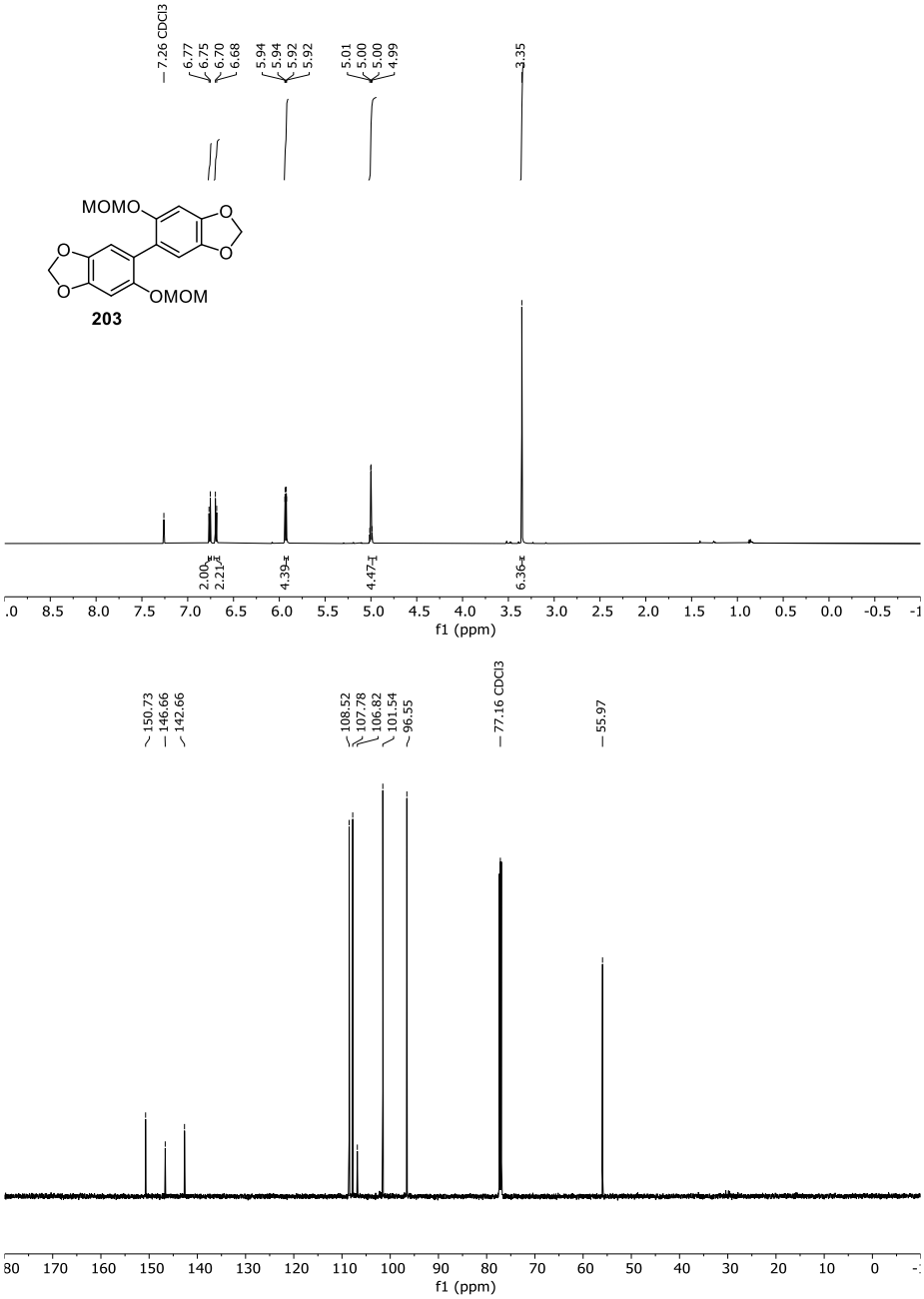

Figure 87 ^{1}H- and ^{13}C-NMR-Spectrum of **203** in $CDCl_3$ (600 MHz/151 MHz).

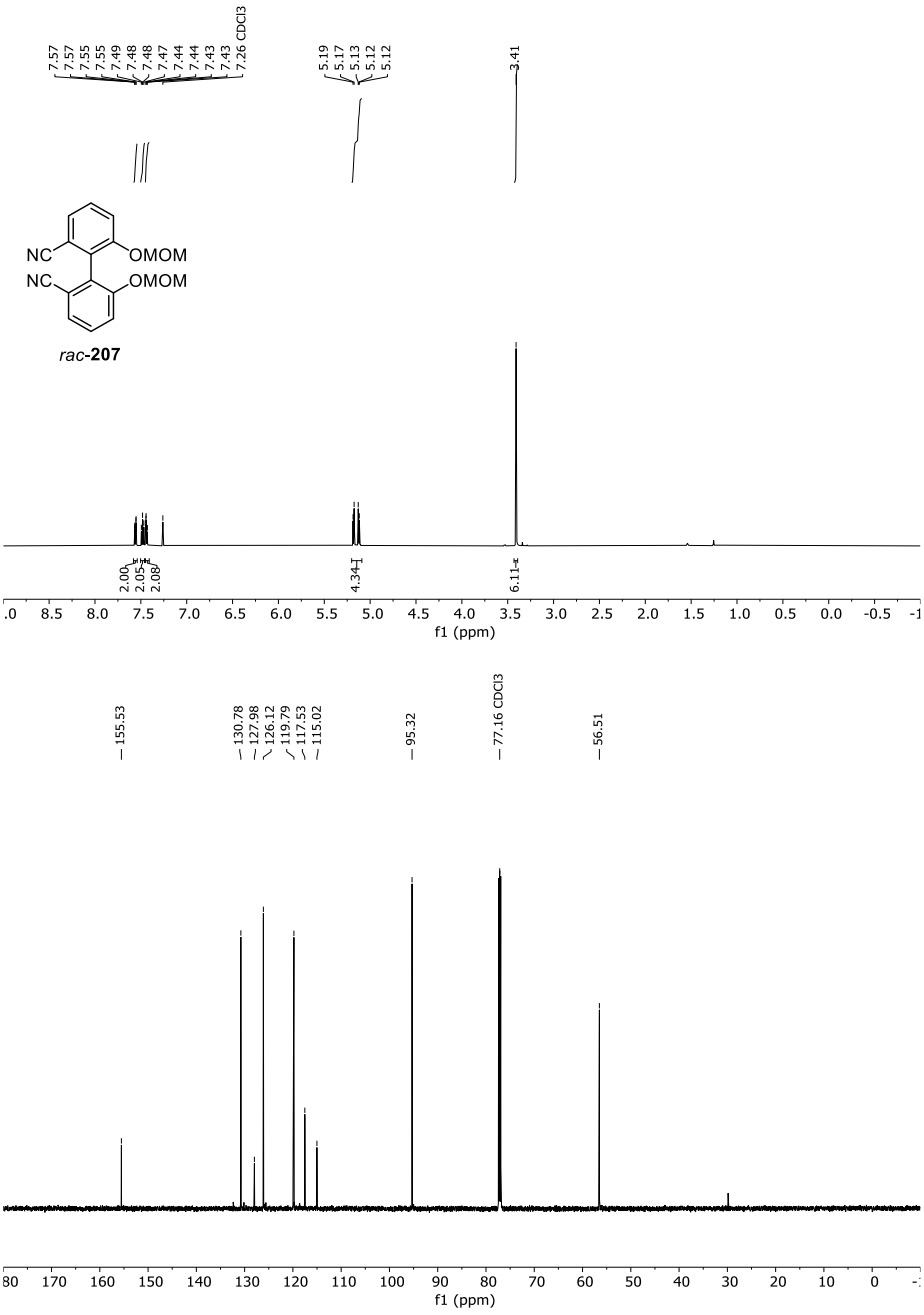

Figure 88 ^{1}H- and ^{13}C-NMR-Spectrum of *rac*-**207** in $CDCl_3$ (600 MHz/151 MHz).

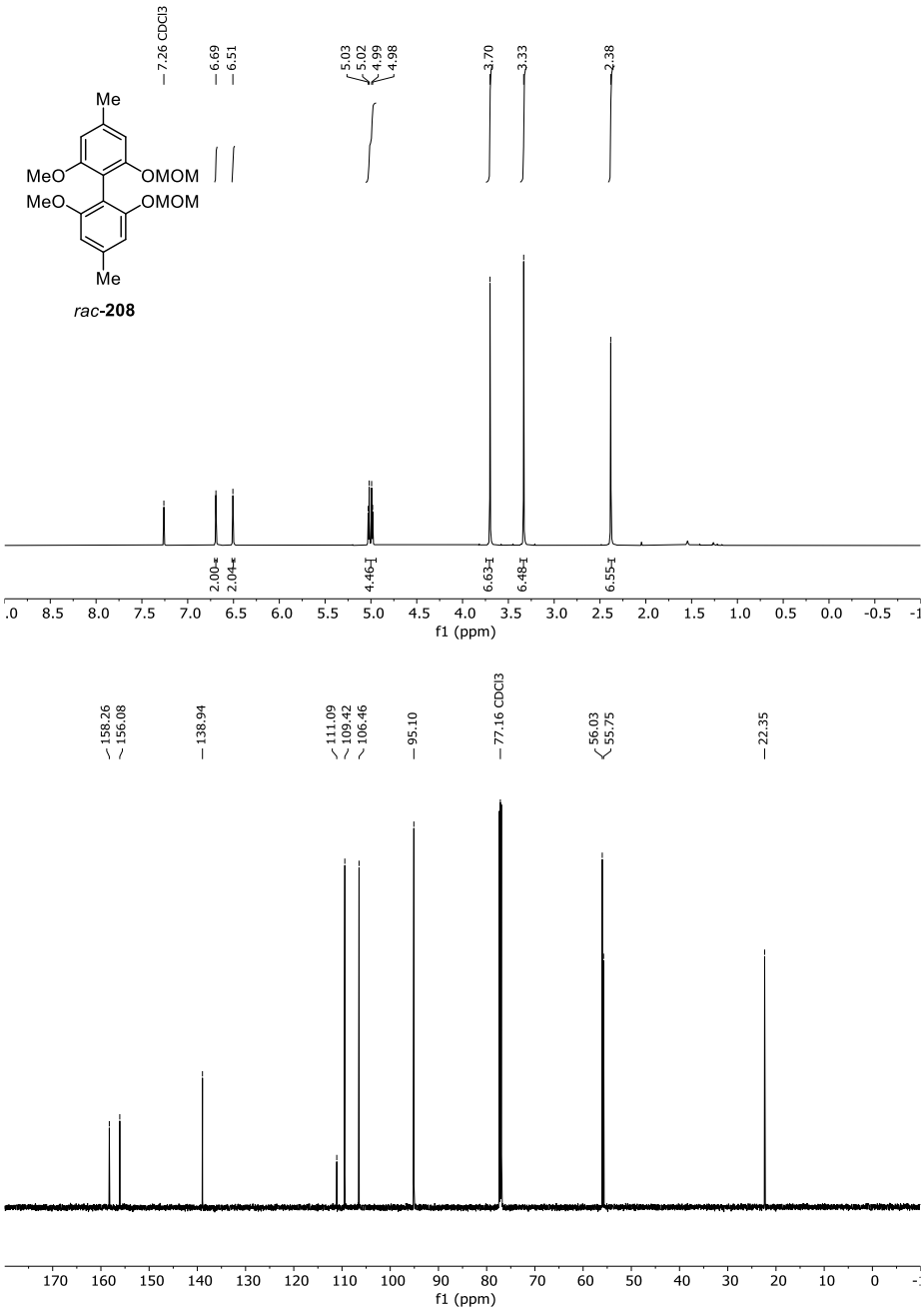

Figure 89 ^{1}H- and ^{13}C-NMR-Spectrum of *rac*-**208** in $CDCl_3$ (600 MHz/151 MHz).

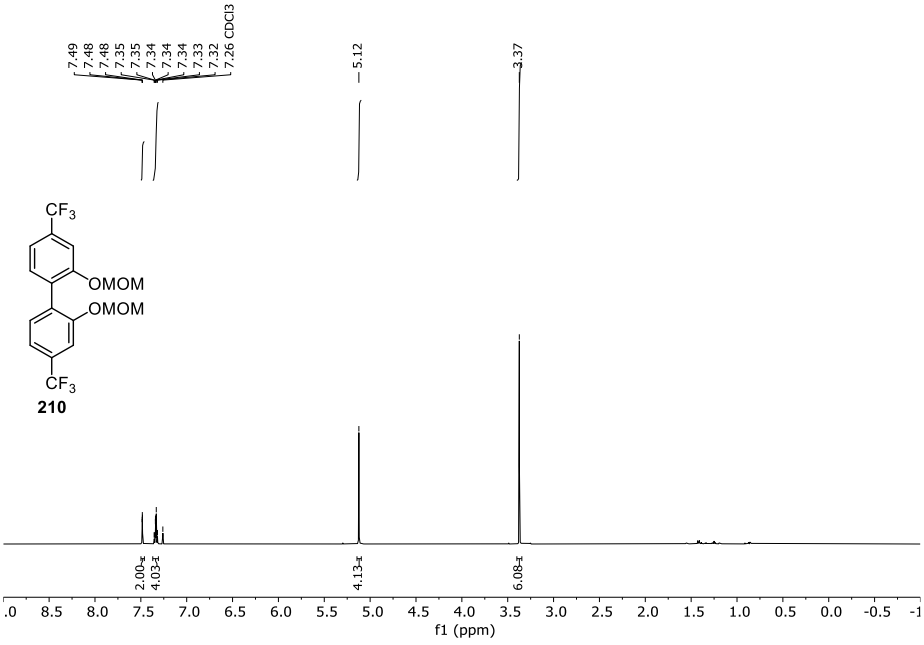
7.49
7.48
7.48
7.35
7.35
7.34
7.34
7.34
7.33
7.32
7.26 CDCl3
5.12
3.37
CF3
OMOM
OMOM
CF3
210
2.00
4.03
4.13
6.08
f1 (ppm)

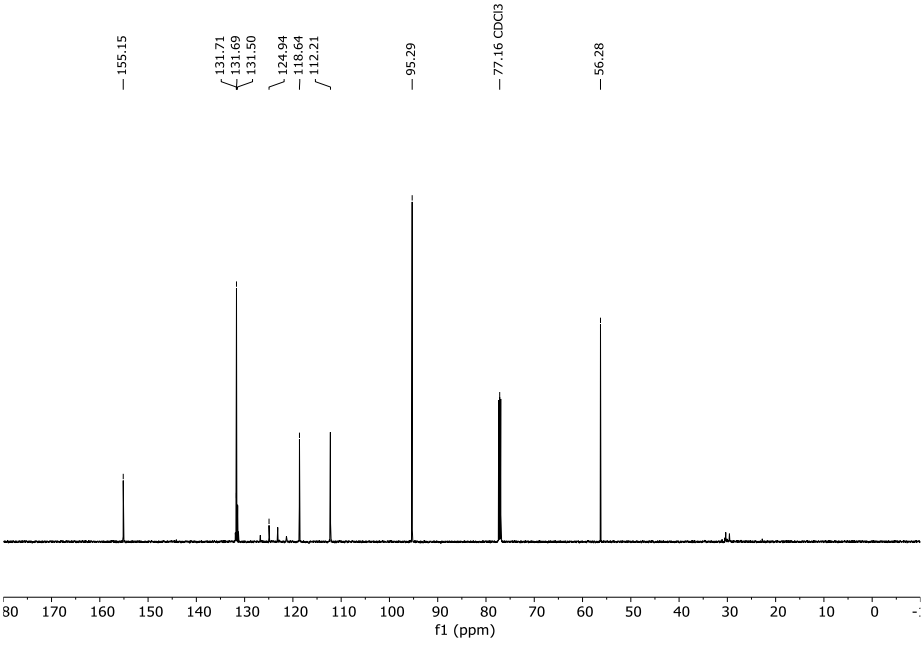
155.15
131.71
131.69
131.50
124.94
118.64
112.21
95.29
77.16 CDCl3
56.28
f1 (ppm)

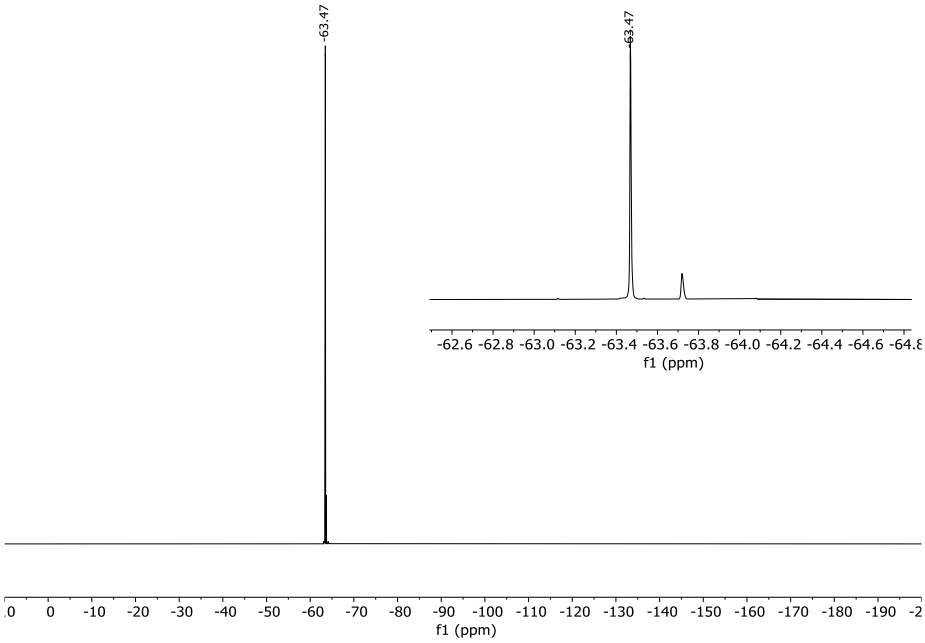

Figure 90 ^{1}H-, ^{13}C- and ^{19}F-NMR-Spectrum of **210** in $CDCl_3$ (600 MHz/151 MHz).

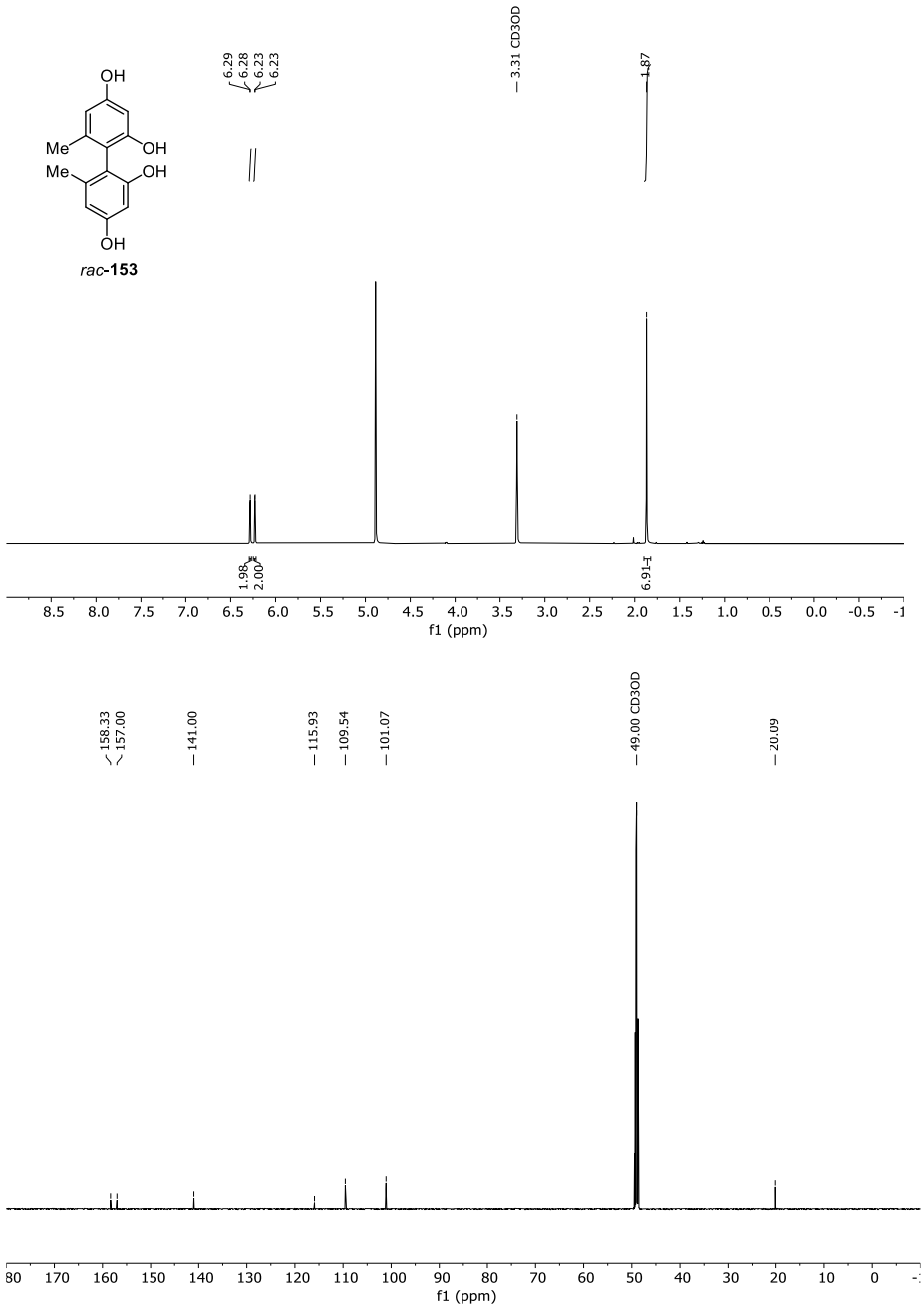

Figure 91 ^{1}H- and ^{13}C-NMR-Spectrum of *rac*-**153** in CD_3OD (600 MHz/151 MHz).

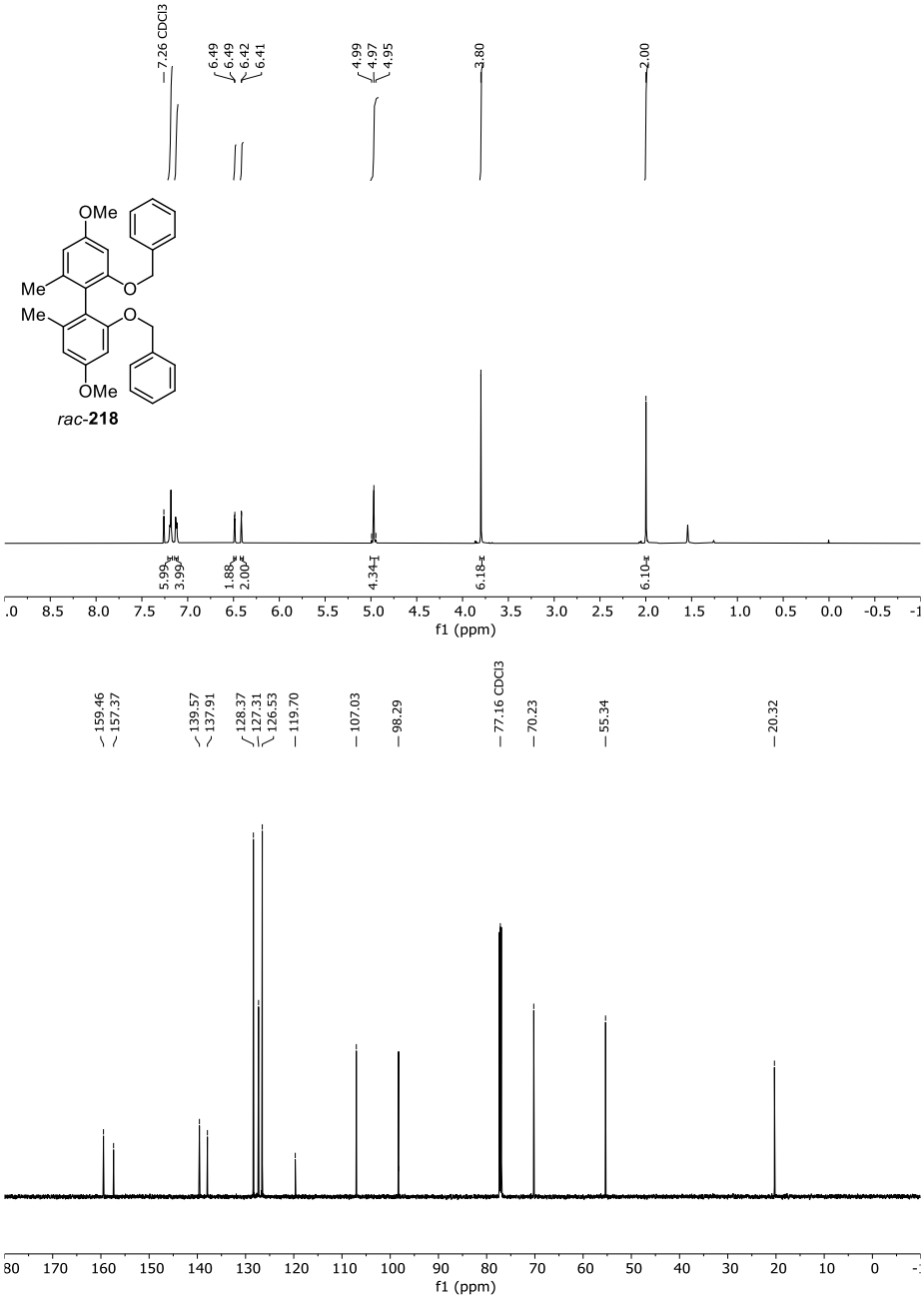

Figure 92 ^{1}H- and ^{13}C-NMR-Spectrum of *rac*-**218** in $CDCl_3$ (600 MHz/151 MHz).

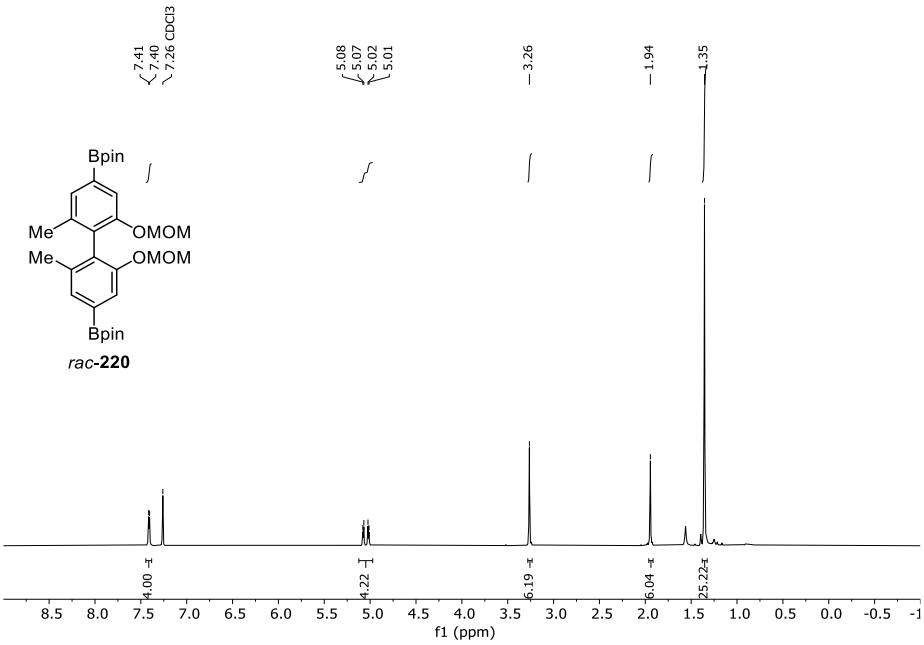
7.41
7.40
7.26 CDCl3
5.08
5.07
5.02
5.01
3.26
1.94
1.35
Bpin
Me
OMOM
Me
OMOM
Bpin
4.00
4.22
6.19
6.04
25.22
f1 (ppm)

rac-**220**

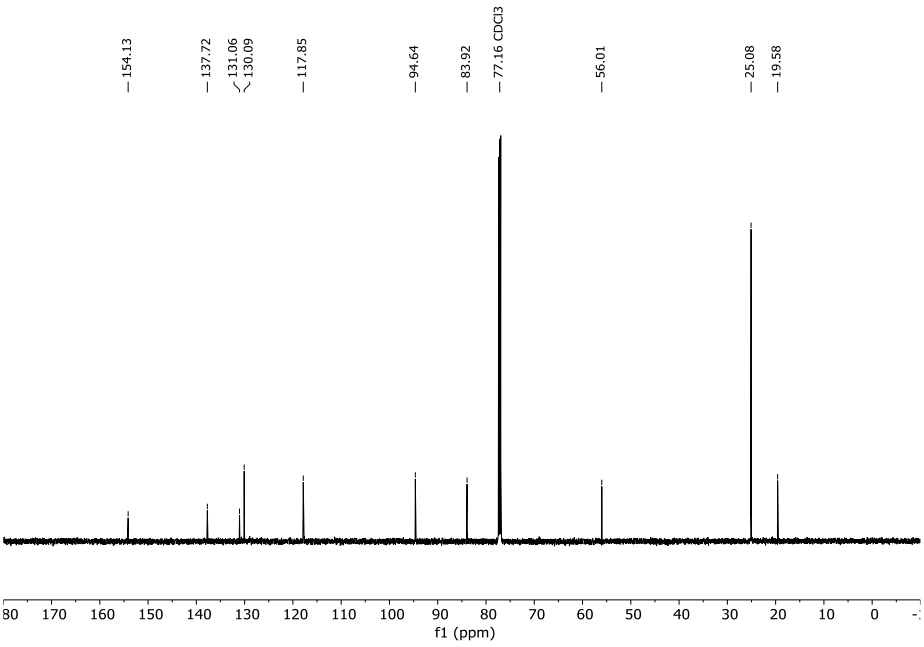
154.13
137.72
131.06
130.09
117.85
94.64
83.92
77.16 CDCl3
56.01
25.08
19.58
f1 (ppm)

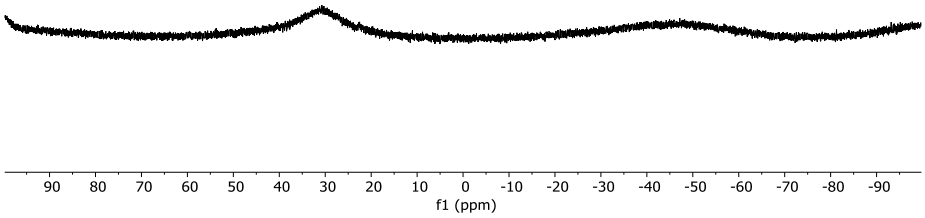

Figure 93 ^{1}H-, ^{13}C and ^{11}B-NMR-Spectrum of *rac*-**220** in $CDCl_3$ (600 MHz/151 MHz).

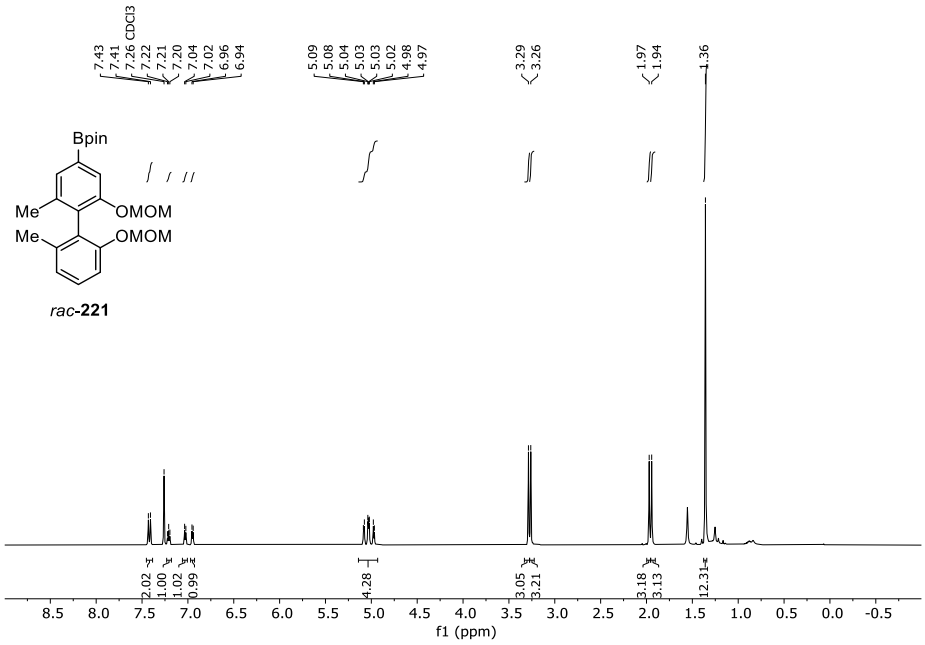

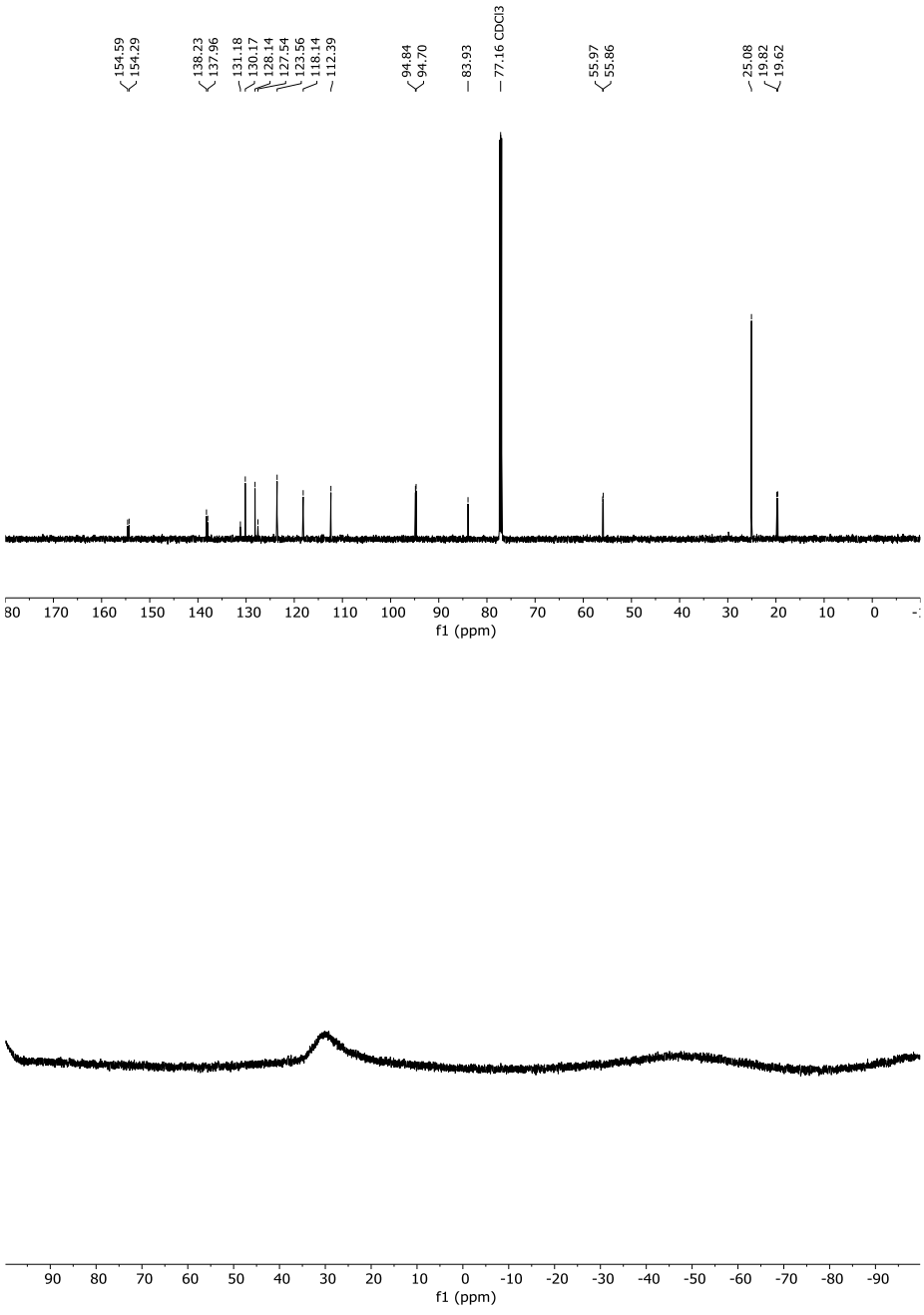

Figure 94 ^{1}H-, ^{13}C and ^{11}B-NMR-Spectrum of *rac*-**221** in $CDCl_3$ (600 MHz/151 MHz).

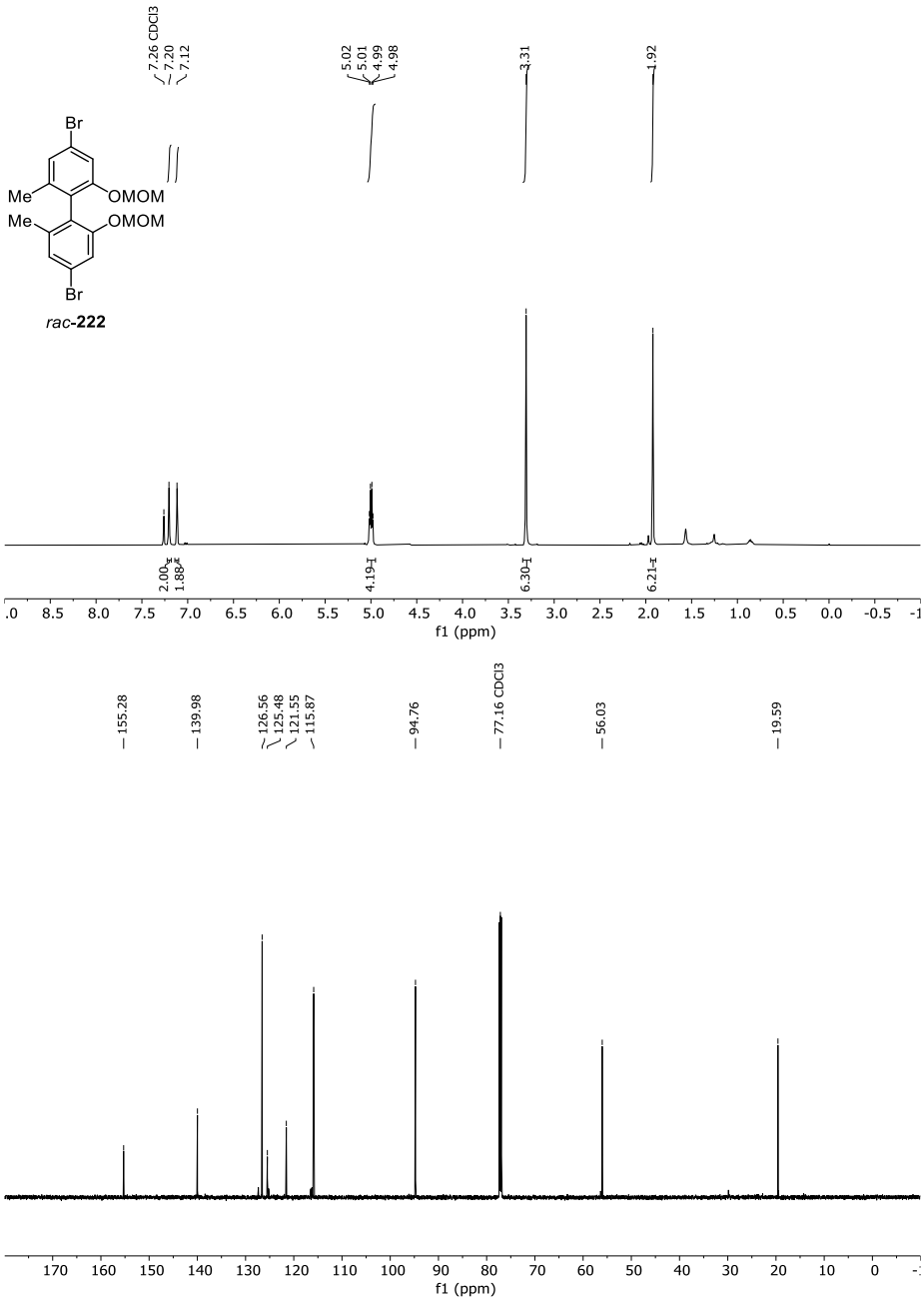

Figure 95 ^{1}H- and ^{13}C-NMR-Spectrum of *rac*-**222** in $CDCl_3$ (600 MHz/151 MHz).

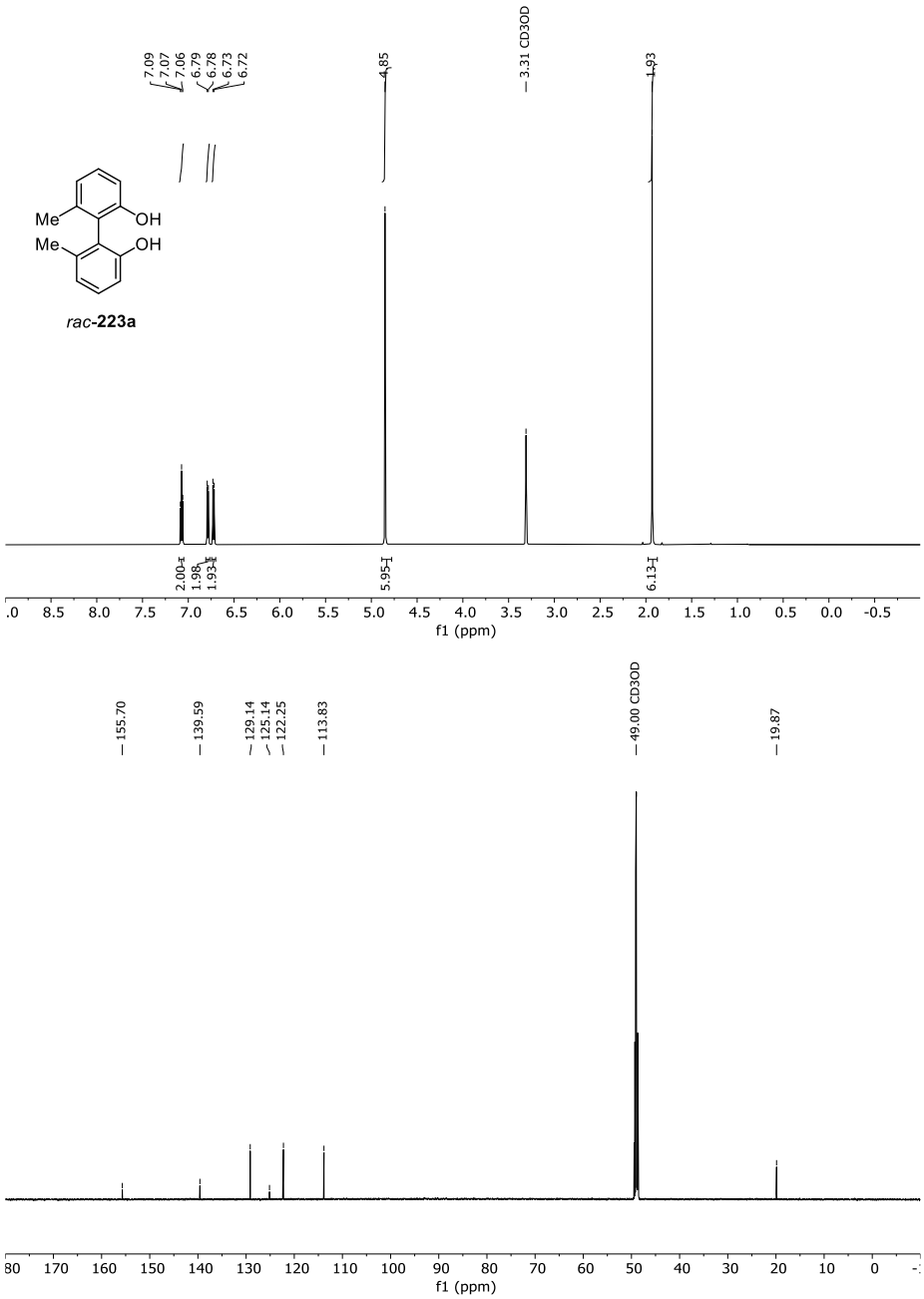

Figure 96 ^{1}H- and ^{13}C-NMR-Spectrum of *rac*-**223a** in CD_3OD (600 MHz/151 MHz).

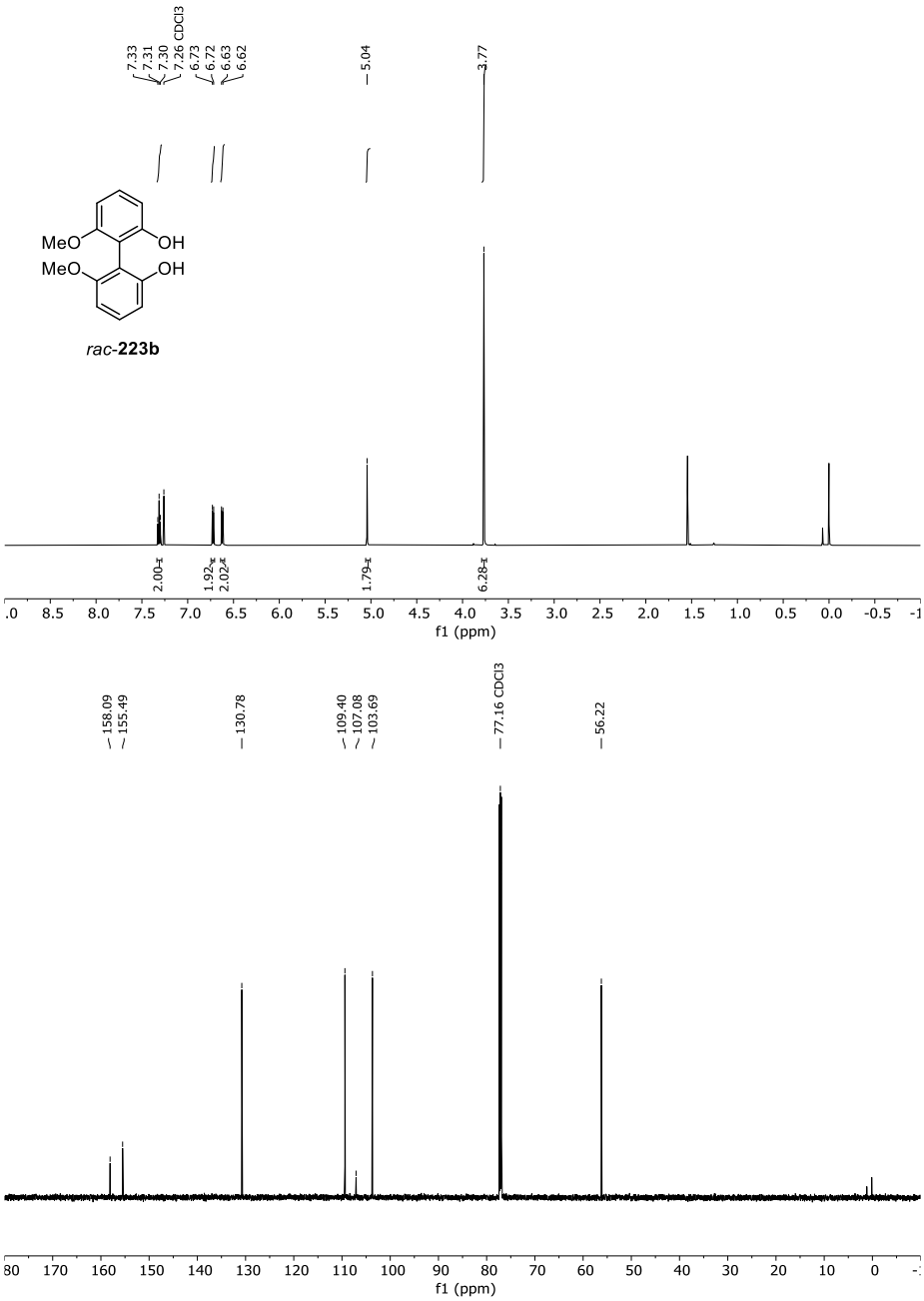

Figure 97 ^{1}H- and ^{13}C-NMR-Spectrum of *rac*-**223b** in $CDCl_3$ (600 MHz/151 MHz).

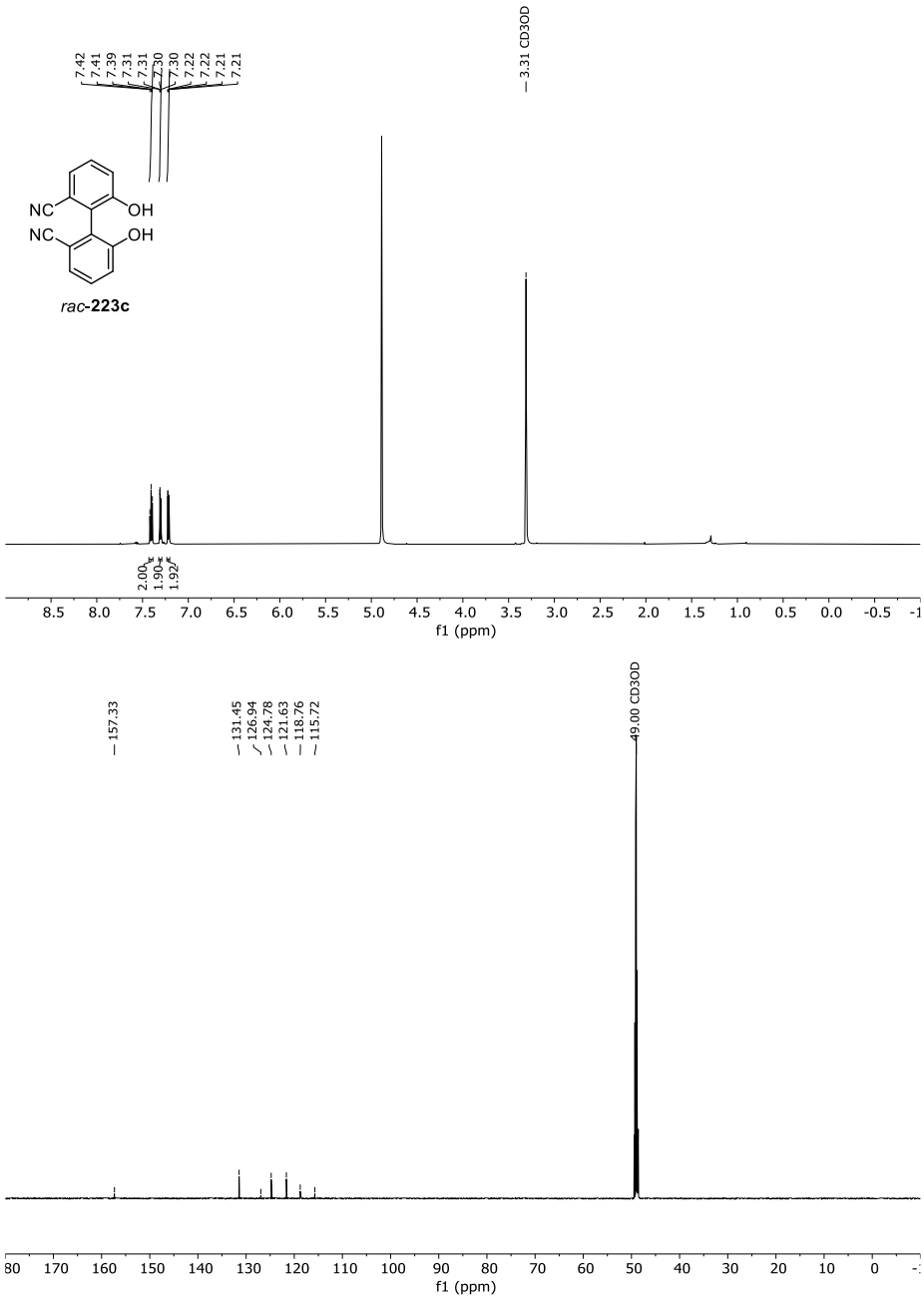

Figure 98 ^{1}H- and ^{13}C-NMR-Spectrum of *rac*-**223c** in CD_3OD (600 MHz/151 MHz).

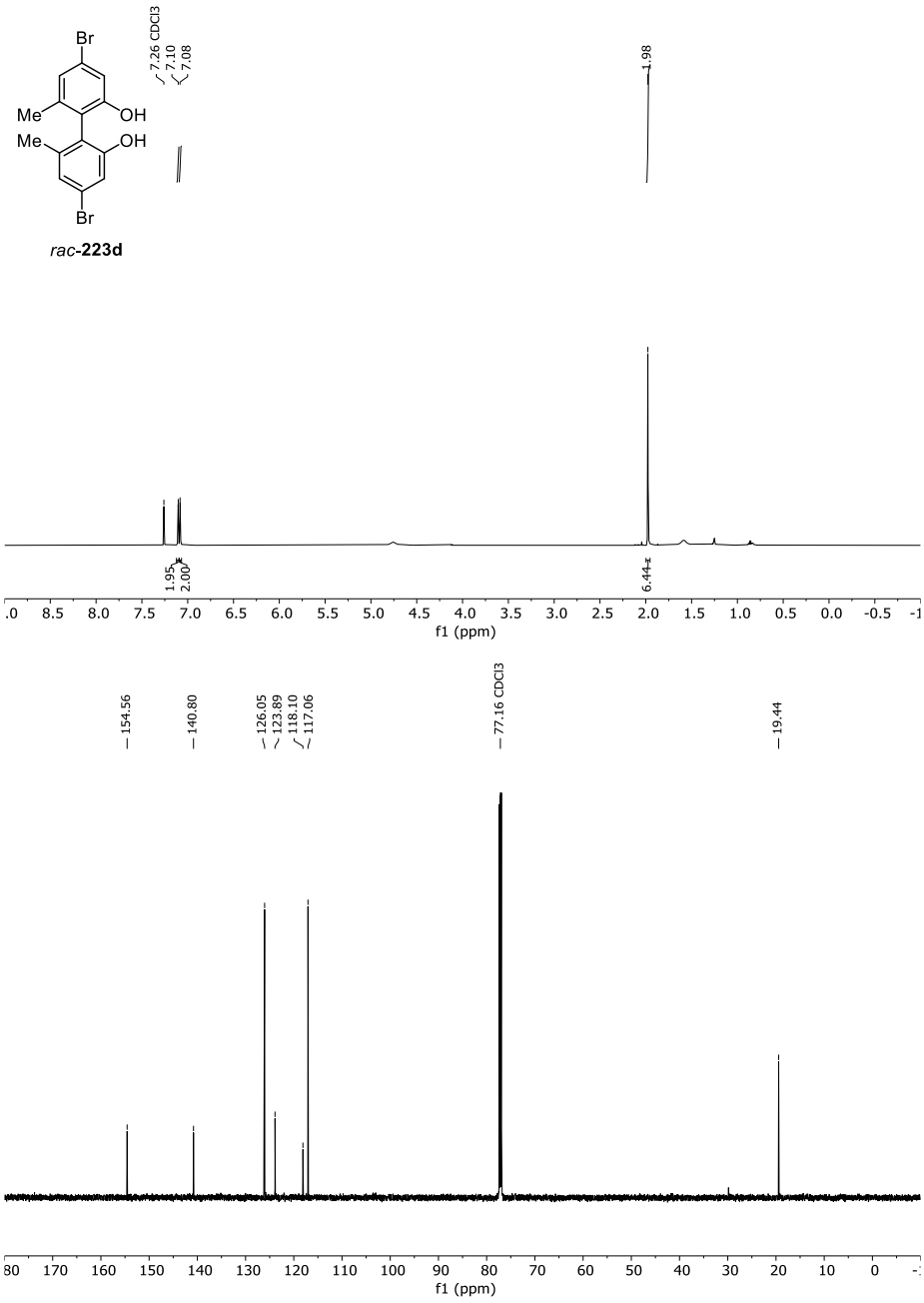

Figure 99 ^{1}H- and ^{13}C-NMR-Spectrum of *rac*-**223d** in $CDCl_3$ (600 MHz/151 MHz).

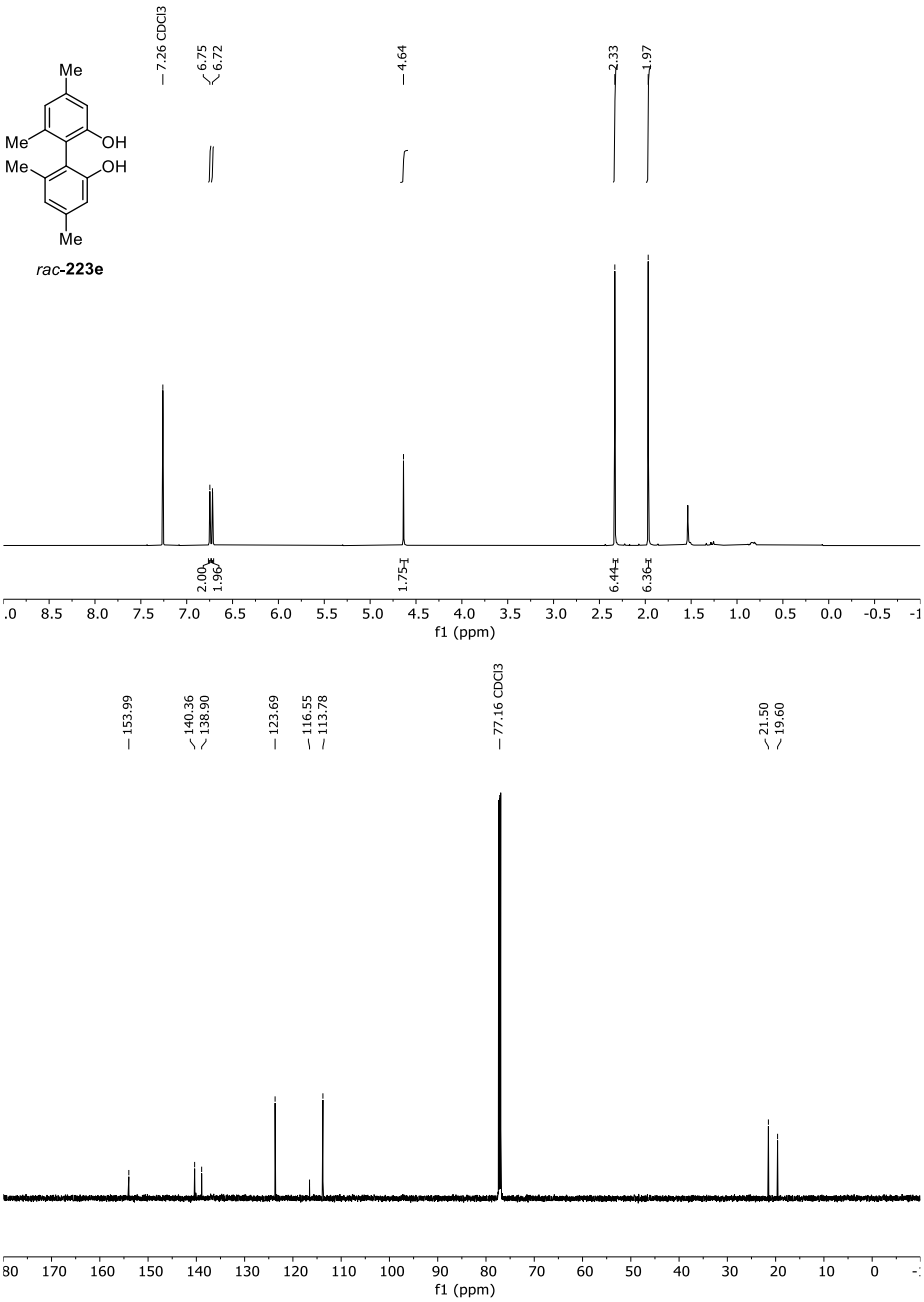

Figure 100 ^{1}H- and ^{13}C-NMR-Spectrum of *rac*-**223e** in $CDCl_3$ (600 MHz/151 MHz).

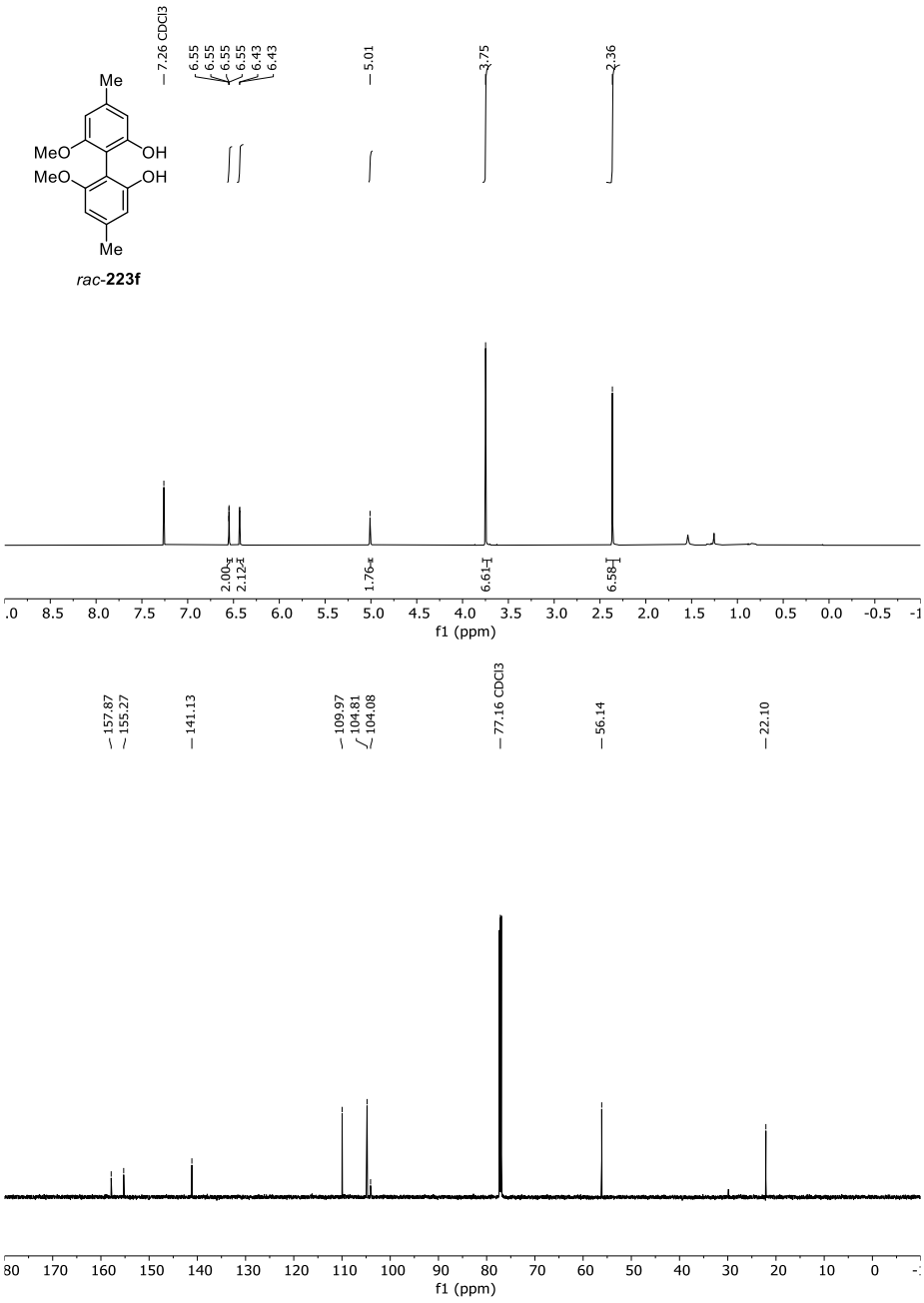

Figure 101 ^{1}H- and ^{13}C-NMR-Spectrum of *rac*-**223f** in $CDCl_3$ (600 MHz/151 MHz).

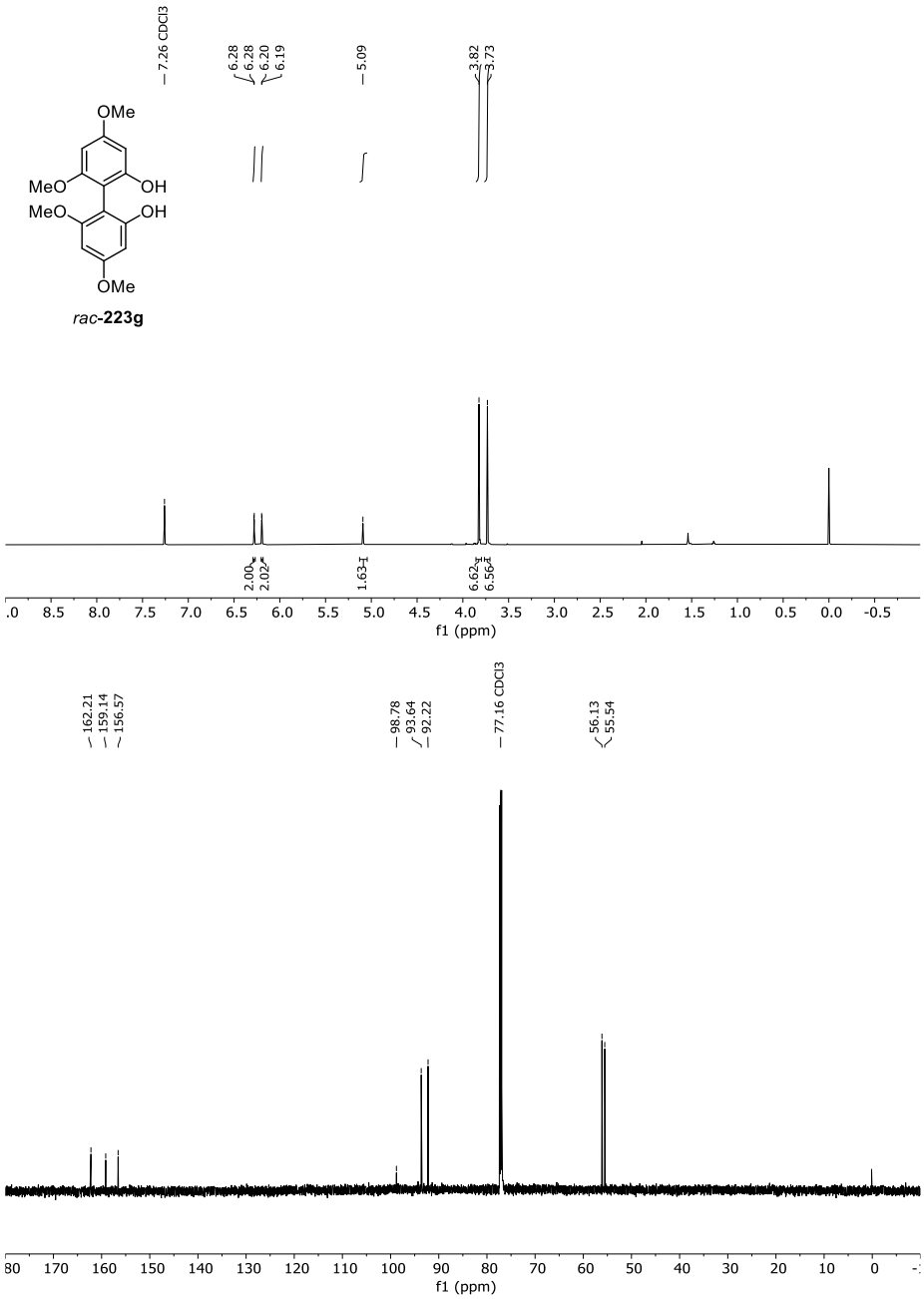

Figure 102 ^{1}H- and ^{13}C-NMR-Spectrum of *rac*-**223g** in $CDCl_3$ (600 MHz/151 MHz).

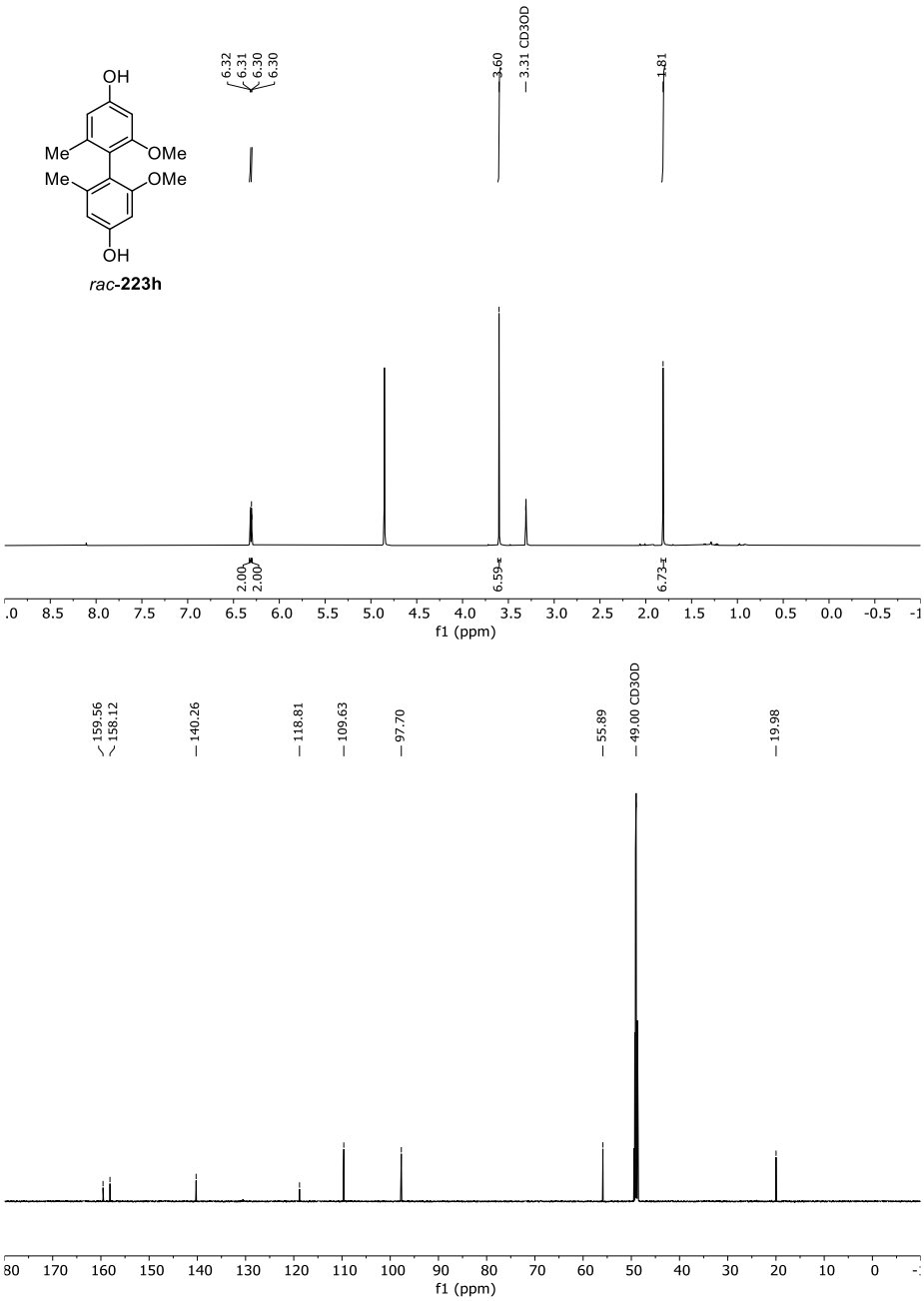

Figure 103 ^{1}H- and ^{13}C-NMR-Spectrum of *rac*-**223h** in CD_3OD (600 MHz/151 MHz).

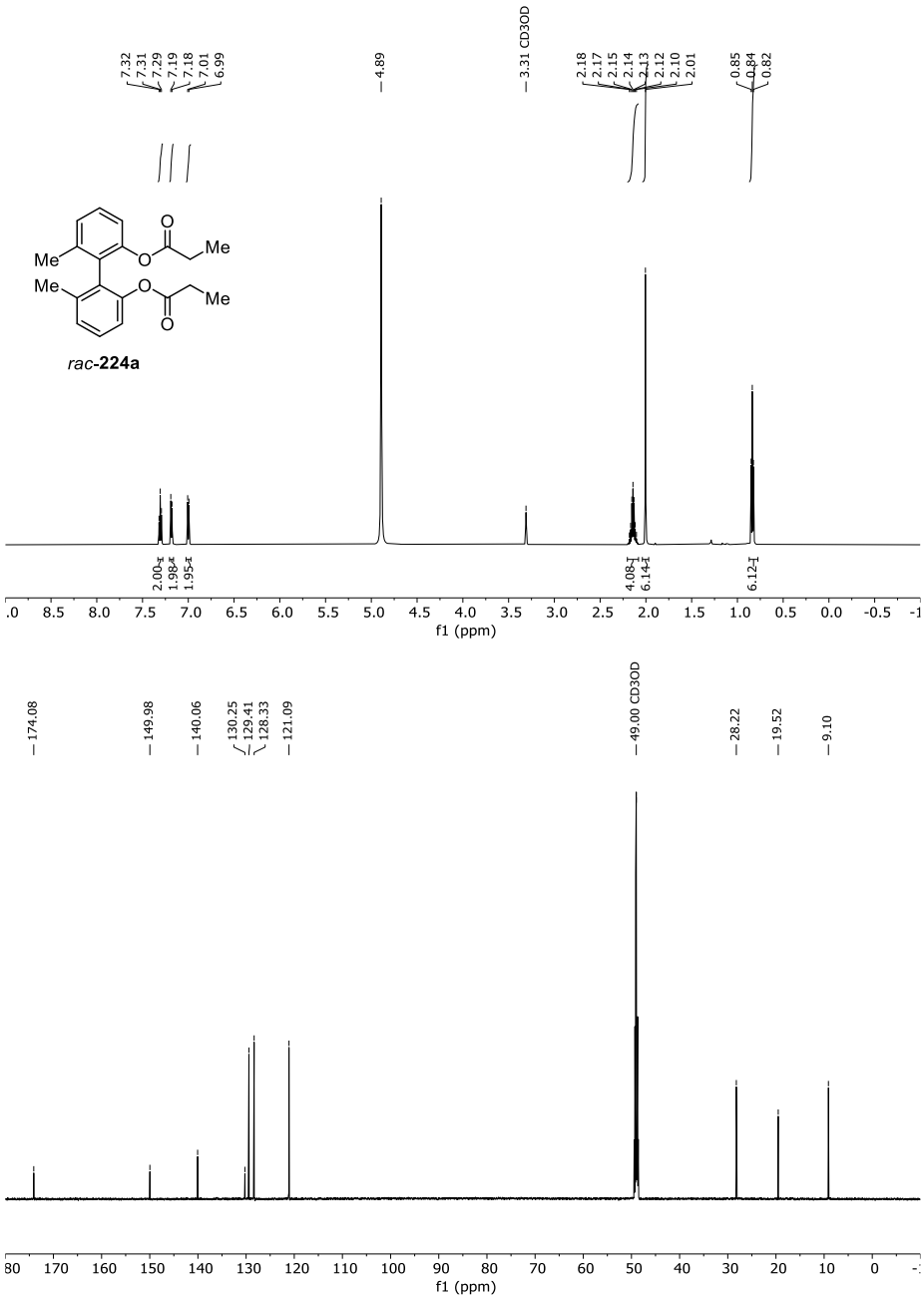

Figure 104 ^{1}H- and ^{13}C-NMR-Spectrum of *rac*-**224a** in CD_3OD (600 MHz/151 MHz).

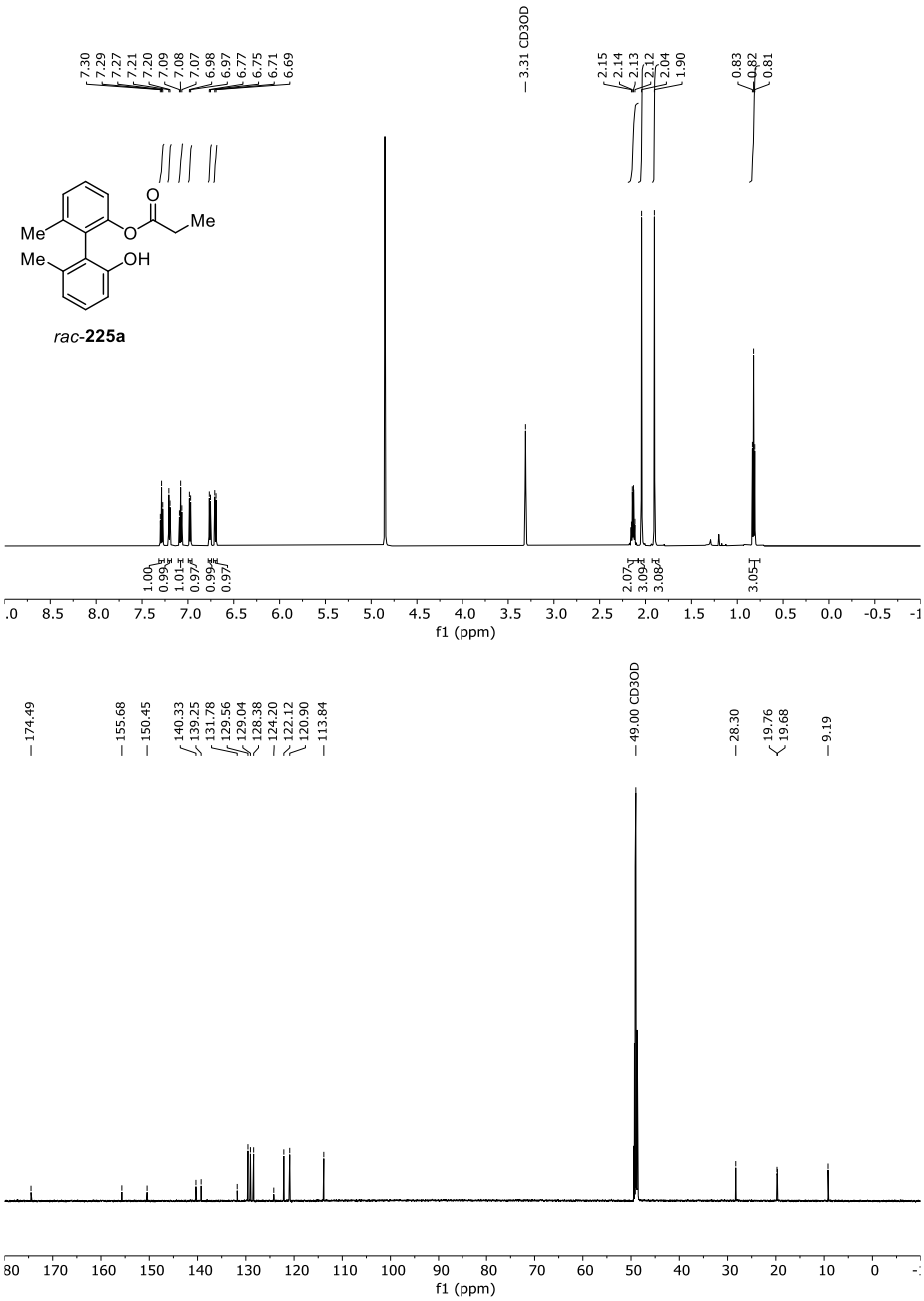

Figure 105 ^{1}H- and ^{13}C-NMR-Spectrum of *rac*-**225a** in $CDCl_3$ (600 MHz/151 MHz).

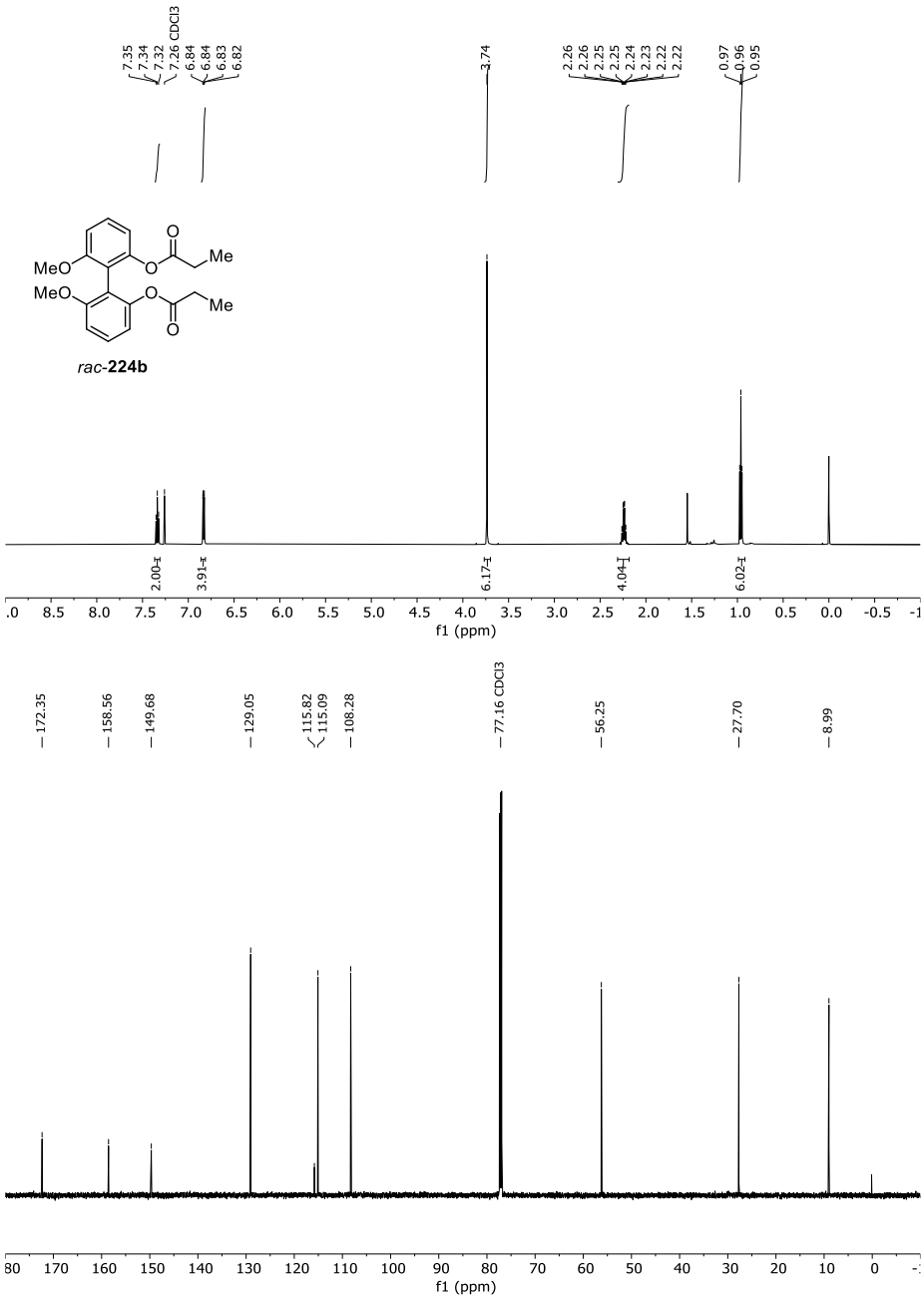

Figure 106 ^{1}H- and ^{13}C-NMR-Spectrum of *rac*-**224b** in $CDCl_3$ (600 MHz/151 MHz).

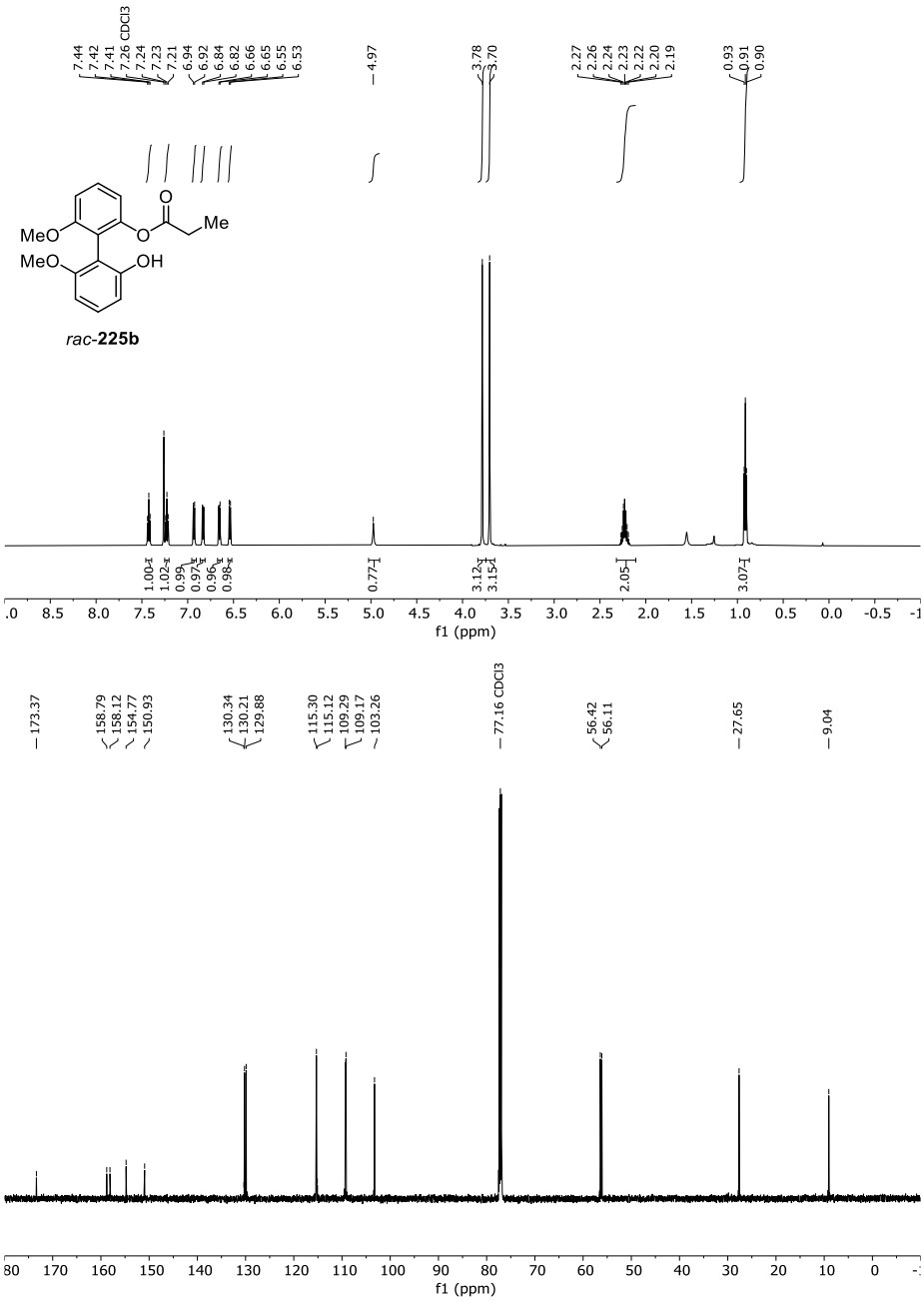

Figure 107 ^{1}H- and ^{13}C-NMR-Spectrum of *rac*-**225b** in $CDCl_3$ (600 MHz/151 MHz).

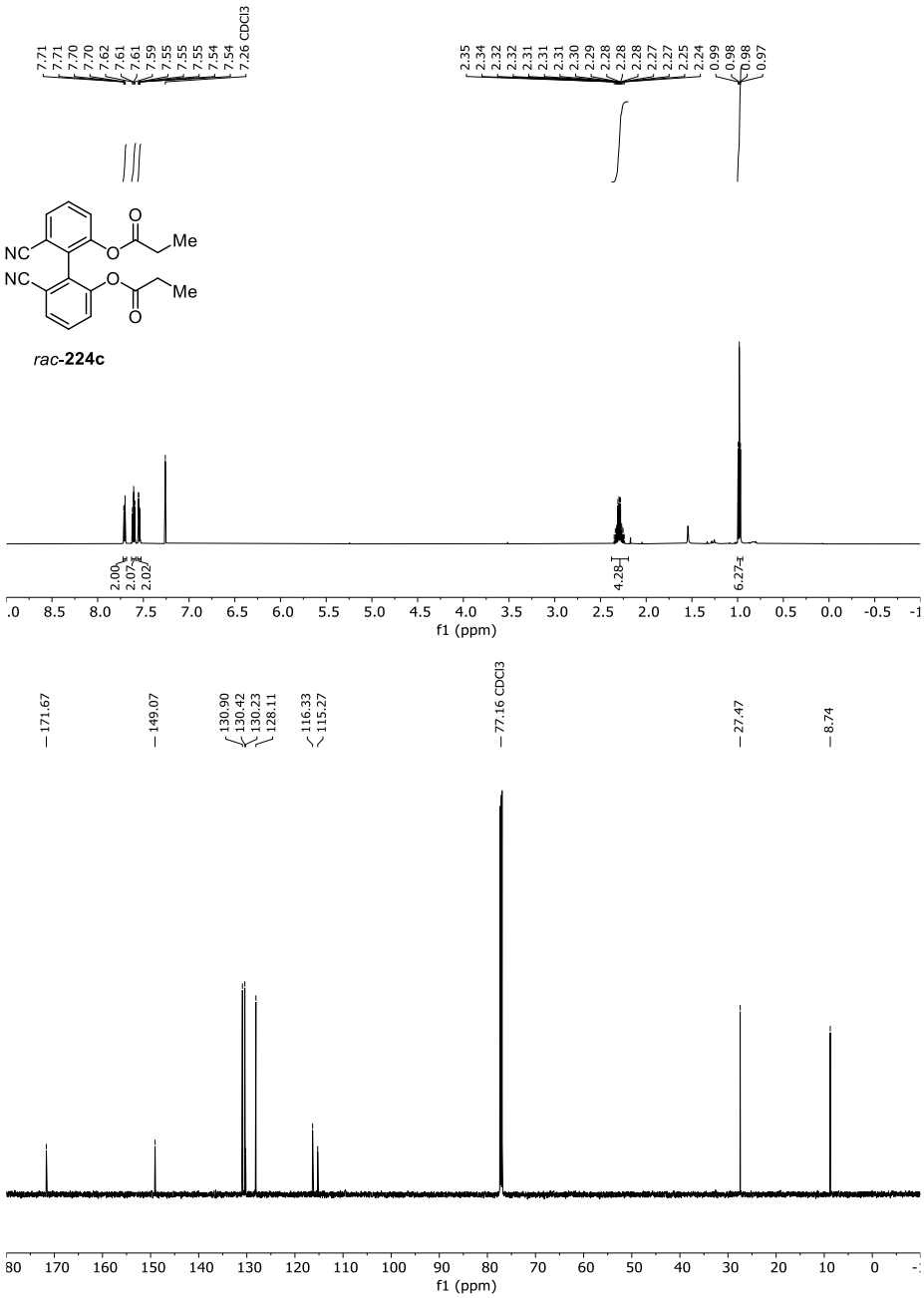

Figure 108 ^{1}H- and ^{13}C-NMR-Spectrum of *rac*-**224c** in $CDCl_3$ (600 MHz/151 MHz).

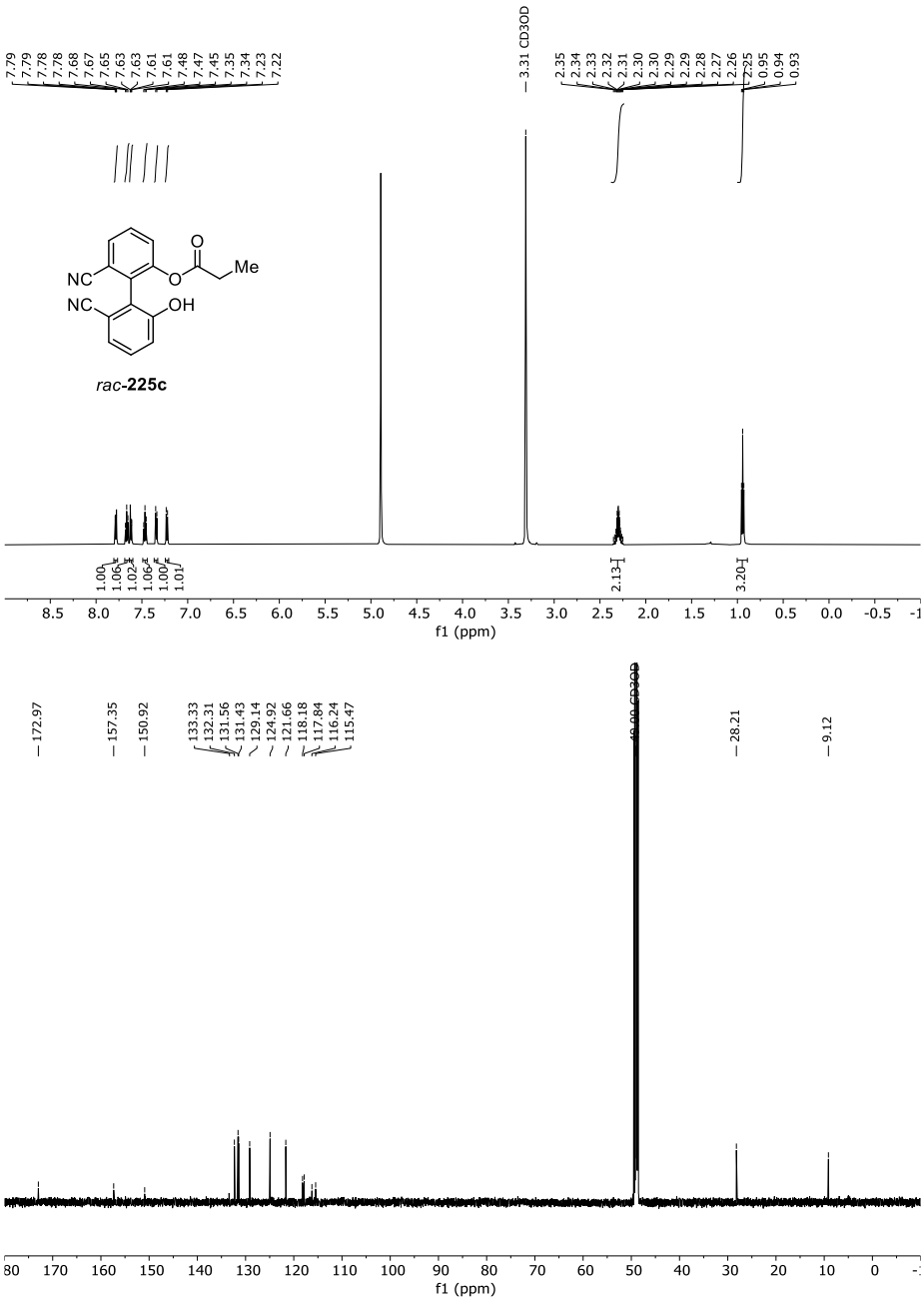

Figure 109 ^{1}H- and ^{13}C-NMR-Spectrum of *rac*-**225c** in CD_3OD (600 MHz/151 MHz).

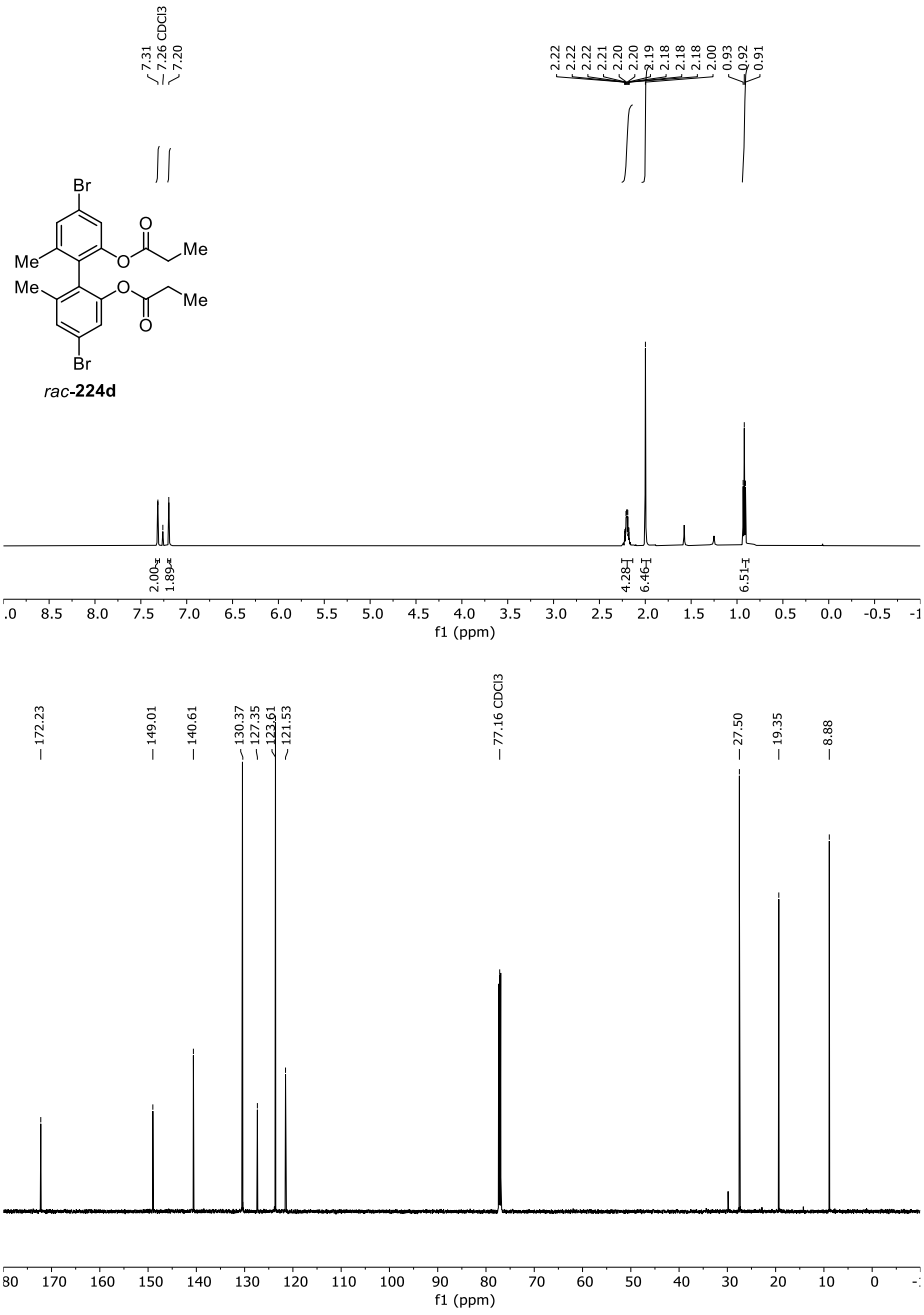

Figure 110 ^{1}H- and ^{13}C-NMR-Spectrum of *rac*-**224d** in $CDCl_3$ (600 MHz/151 MHz).

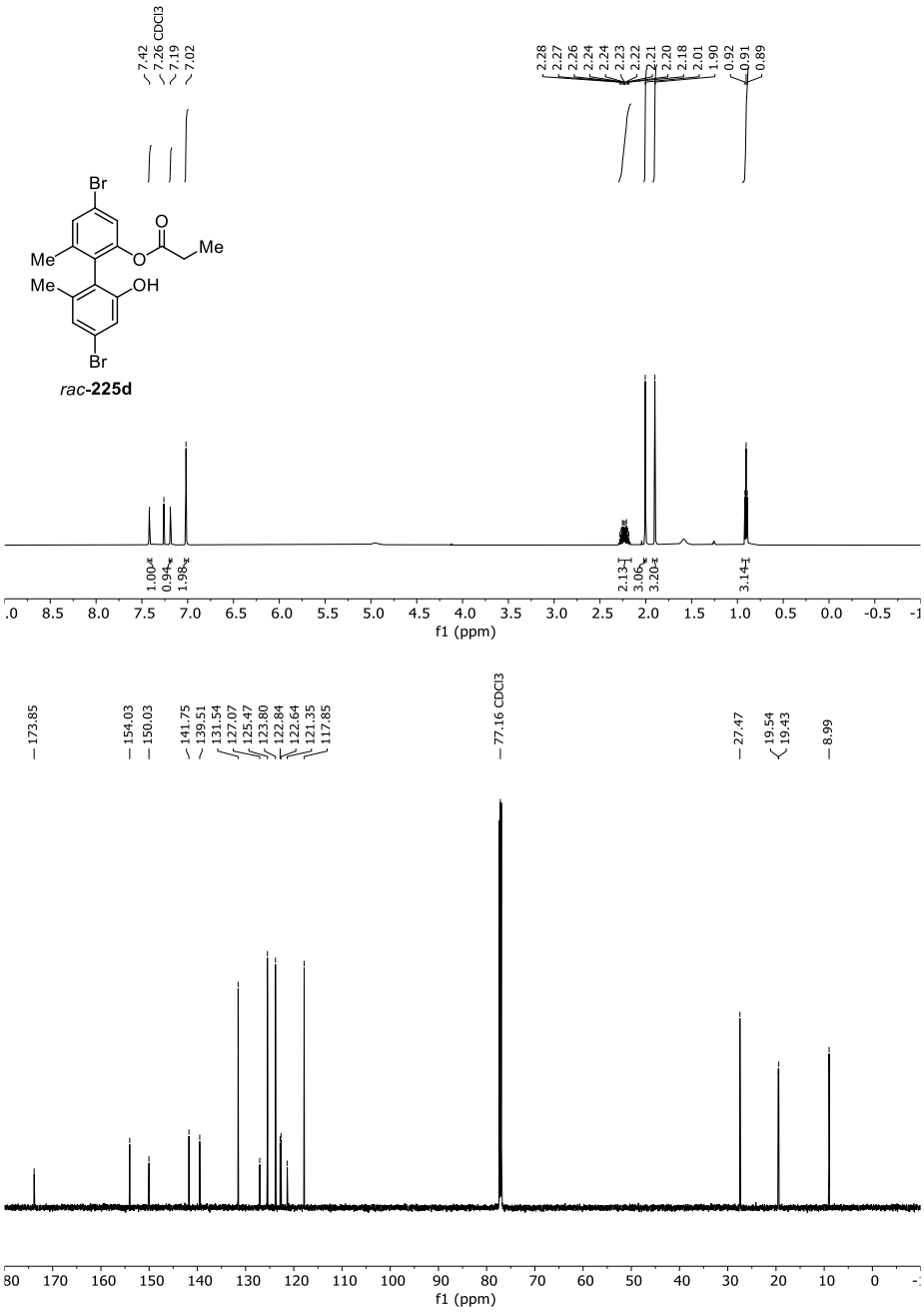

Figure 111 ^{1}H- and ^{13}C-NMR-Spectrum of *rac*-**225d** in $CDCl_3$ (600 MHz/151 MHz).

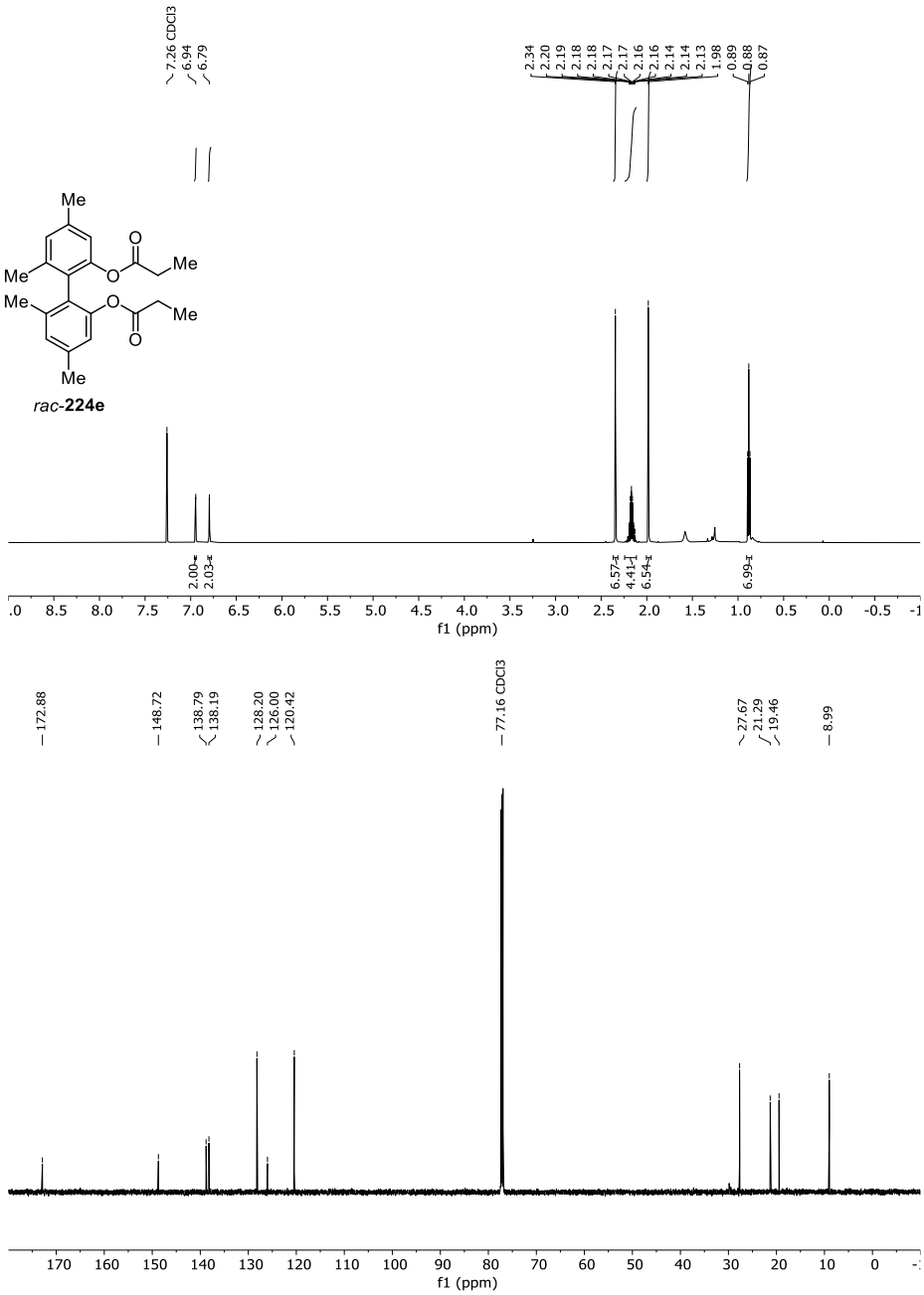

Figure 112 ^{1}H- and ^{13}C-NMR-Spectrum of *rac*-**224e** in $CDCl_3$ (600 MHz/151 MHz).

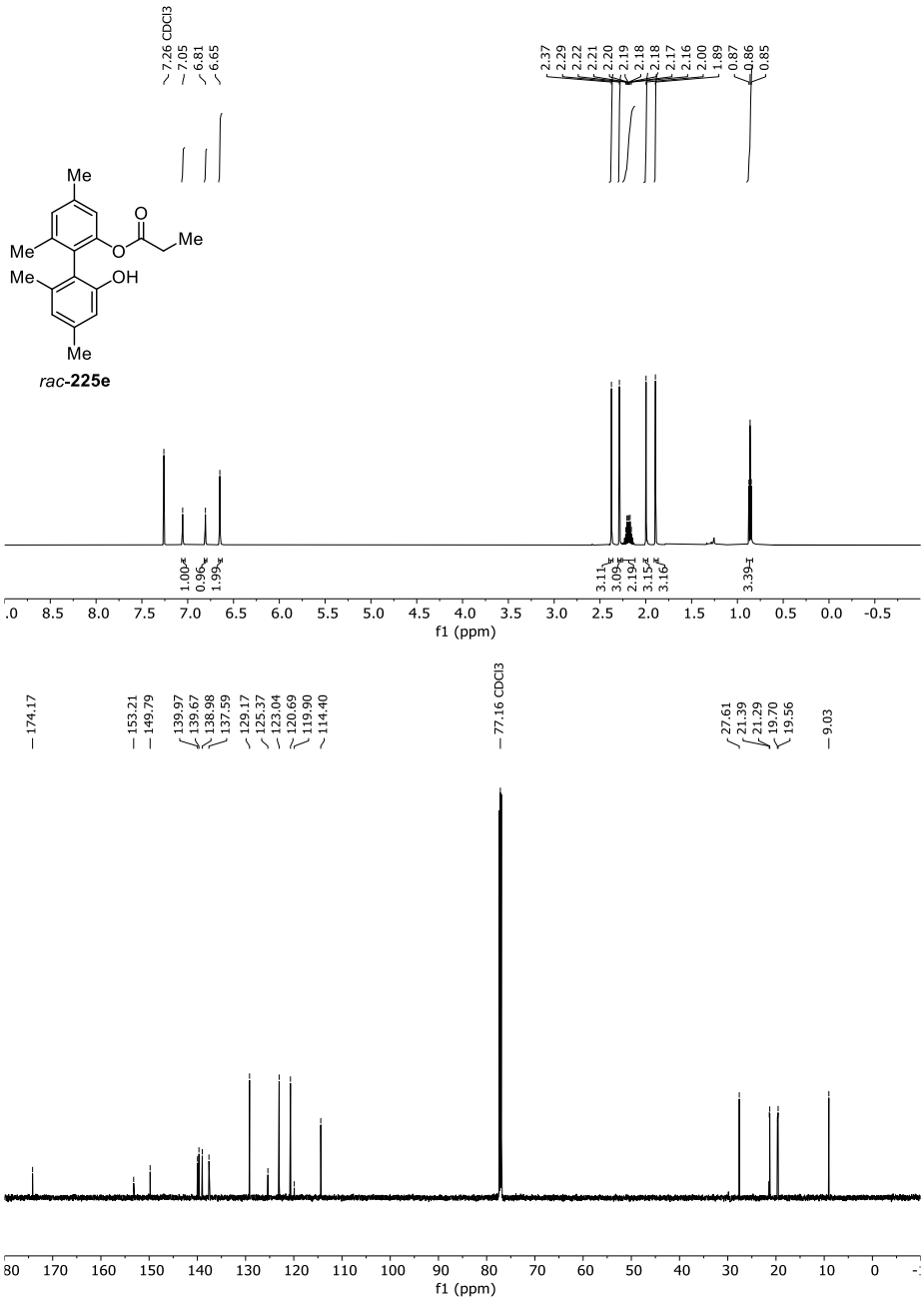

Figure 113 ^{1}H- and ^{13}C-NMR-Spectrum of *rac*-**225e** in $CDCl_3$ (600 MHz/151 MHz).

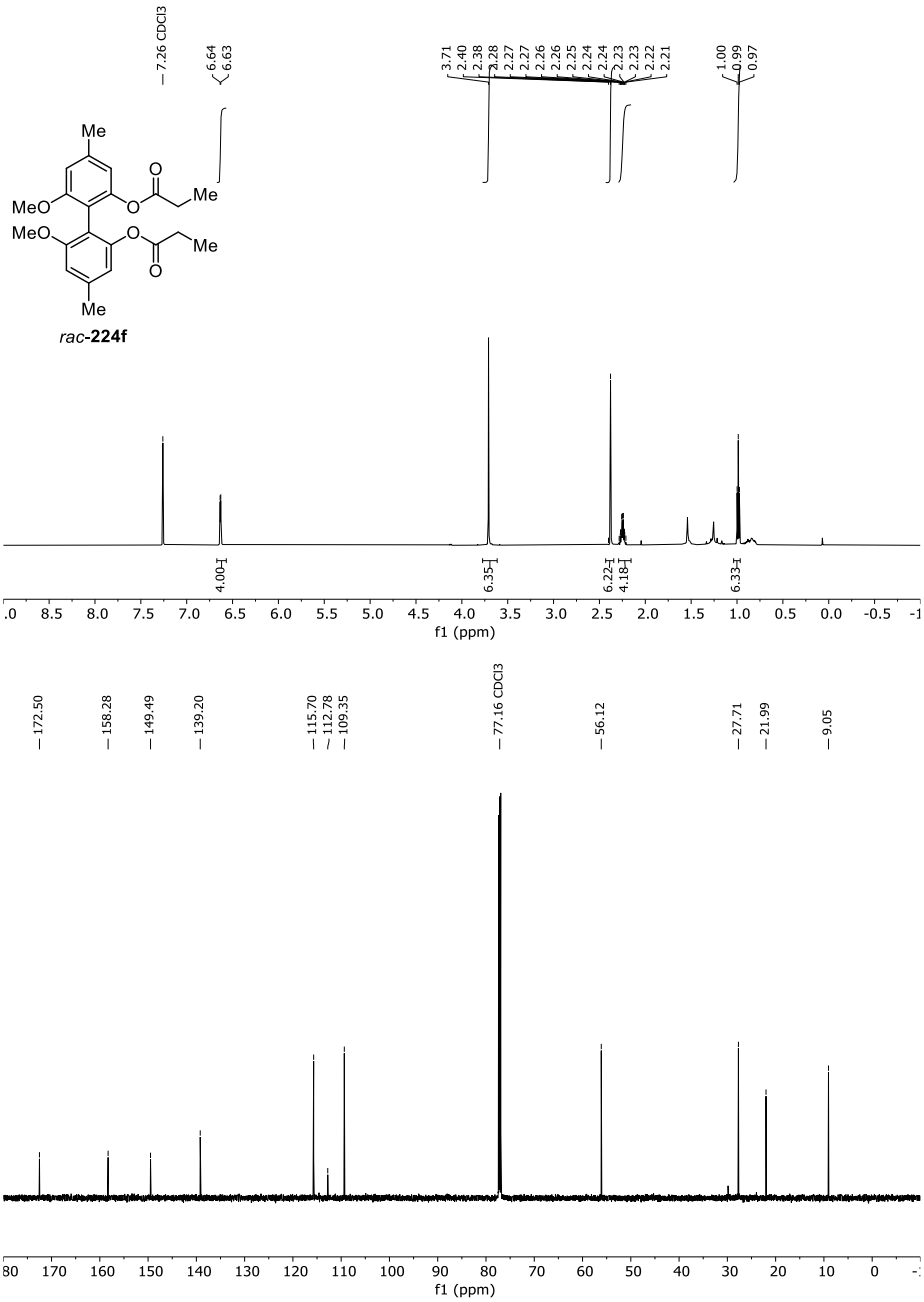

Figure 114 ^{1}H- and ^{13}C-NMR-Spectrum of *rac*-**224f** in $CDCl_3$ (600 MHz/151 MHz).

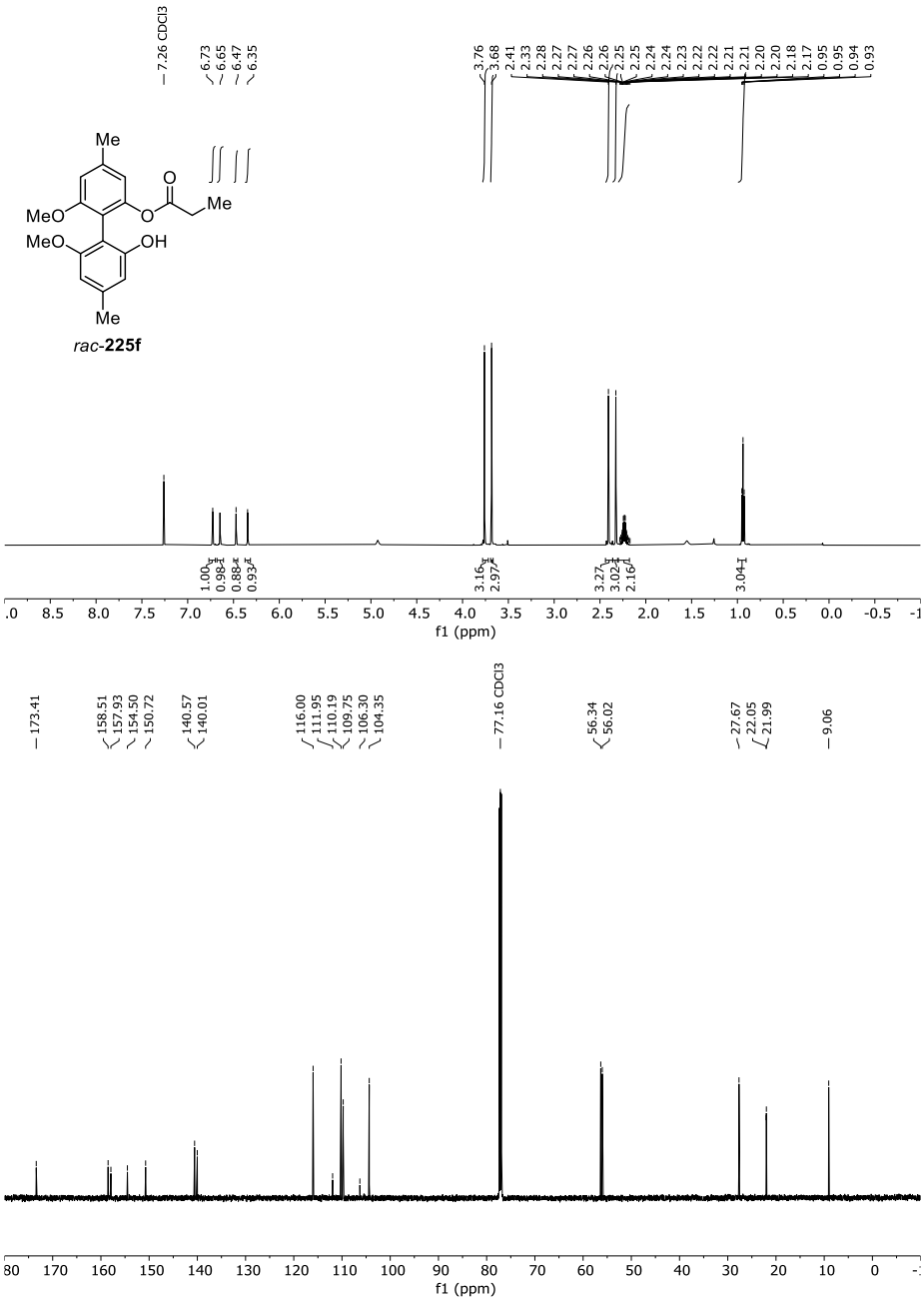

Figure 115 ^{1}H- and ^{13}C-NMR-Spectrum of *rac*-**225f** in $CDCl_3$ (600 MHz/151 MHz).

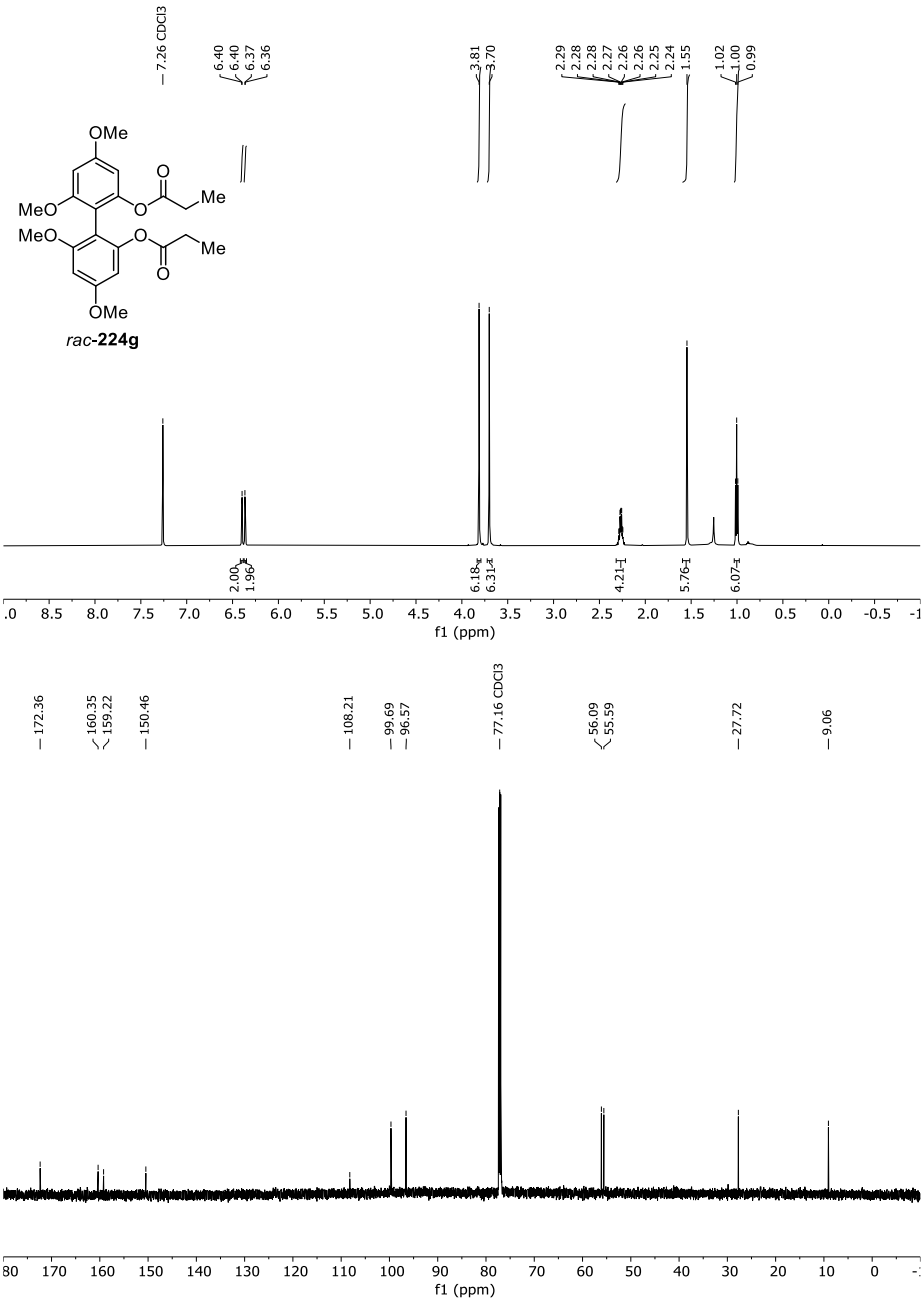

Figure 116 ^{1}H- and ^{13}C-NMR-Spectrum of *rac*-**224g** in $CDCl_3$ (600 MHz/151 MHz).

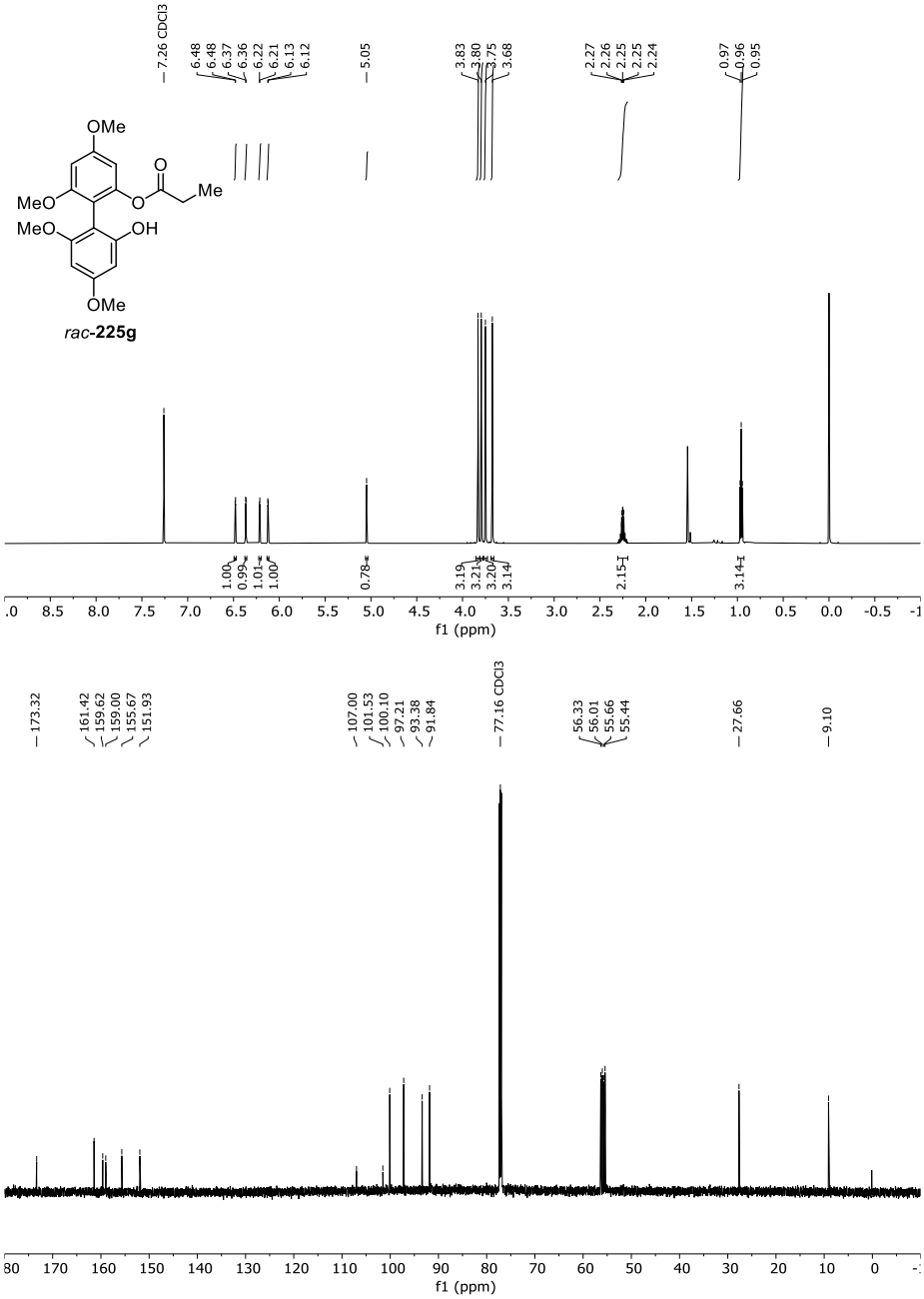

Figure 117 ^{1}H- and ^{13}C-NMR-Spectrum of *rac*-**225g** in $CDCl_3$ (600 MHz/151 MHz).

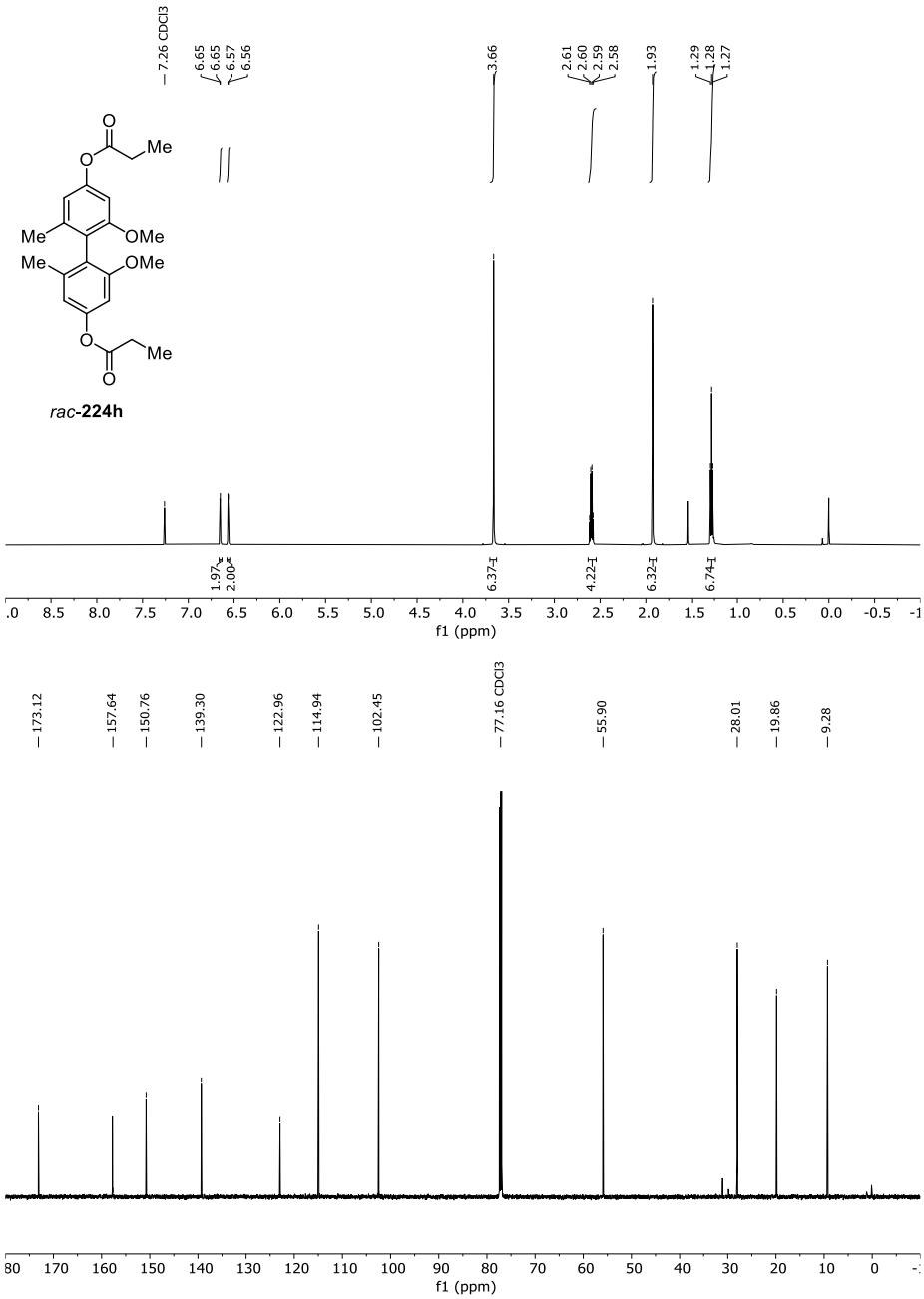

Figure 118 ^{1}H- and ^{13}C-NMR-Spectrum of *rac*-**224h** in $CDCl_3$ (600 MHz/151 MHz).

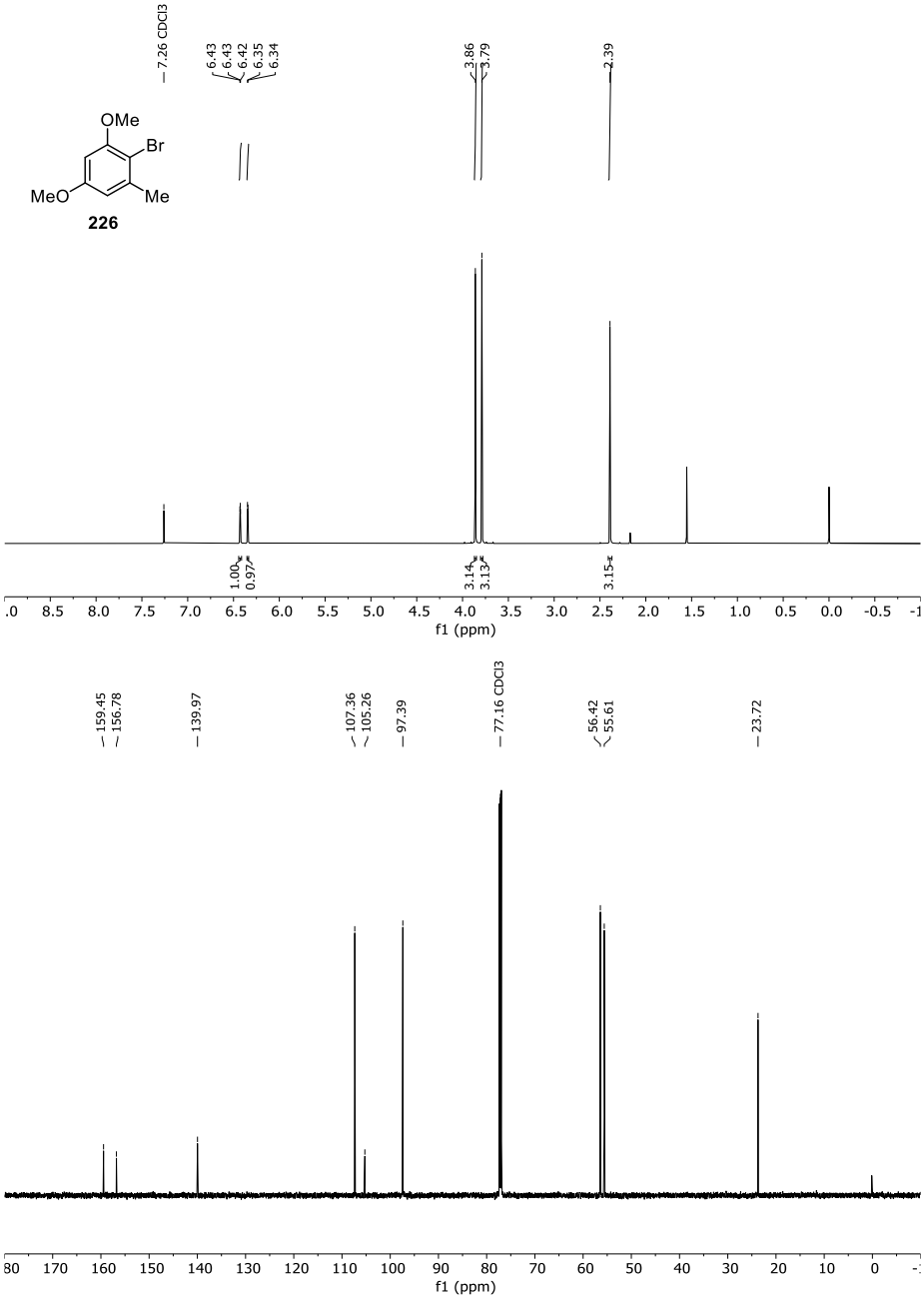

Figure 119 ^{1}H- and ^{13}C-NMR-Spectrum of **226** in $CDCl_3$ (600 MHz/151 MHz).

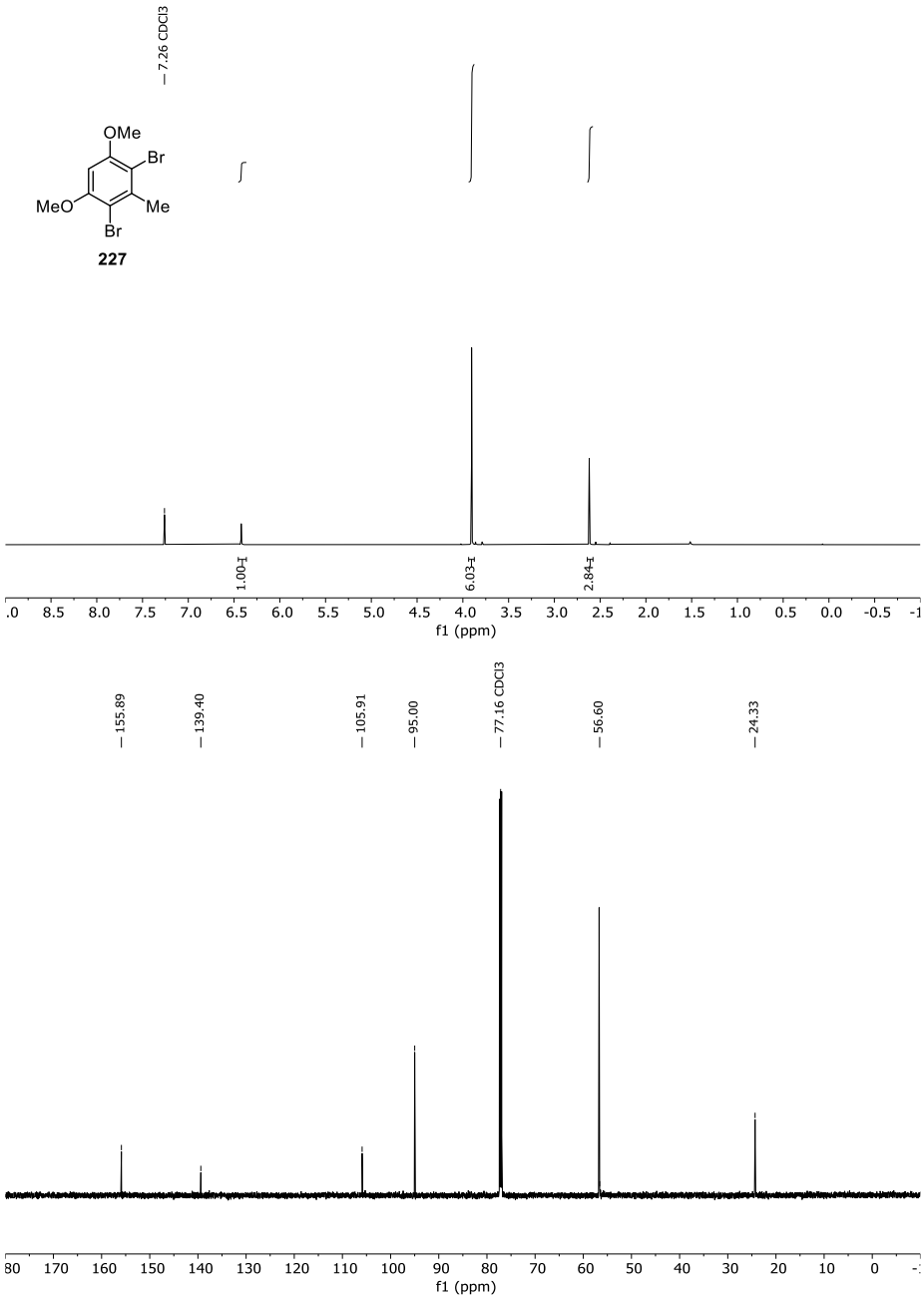

Figure 120 ^{1}H- and ^{13}C-NMR-Spectrum of **227** in $CDCl_3$ (600 MHz/151 MHz).

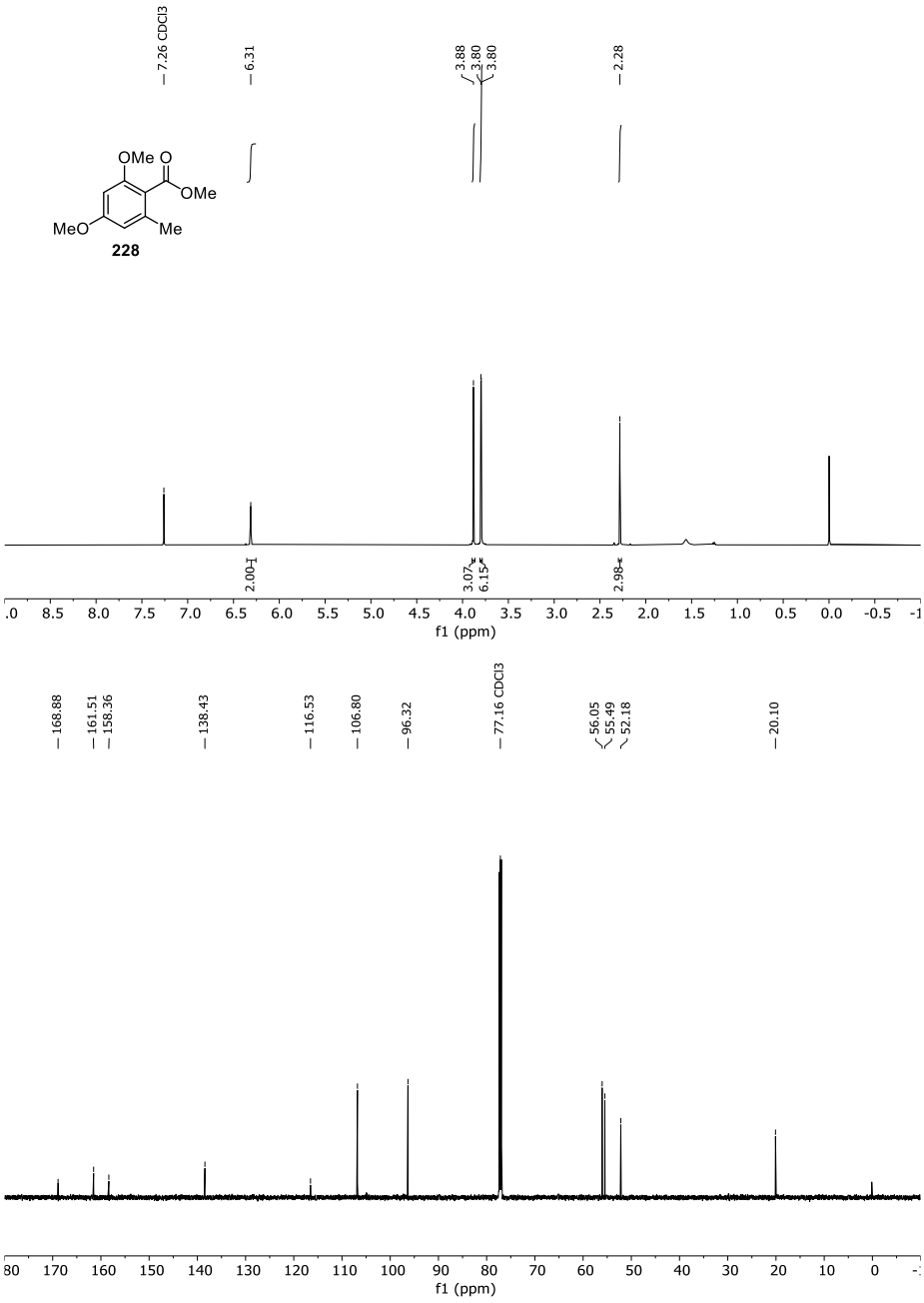

Figure 121 ^{1}H- and ^{13}C-NMR-Spectrum of **228** in $CDCl_3$ (600 MHz/151 MHz).

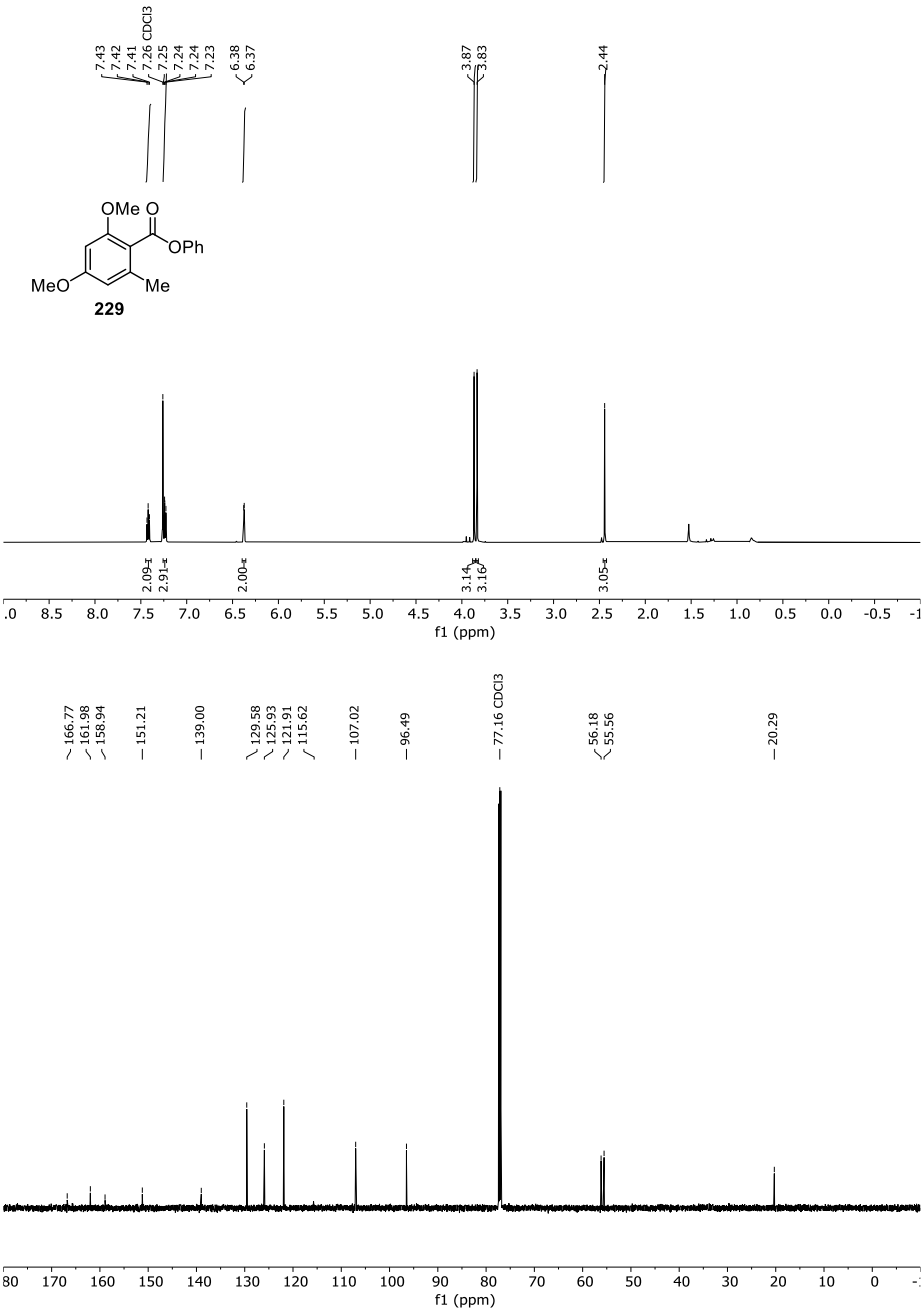

Figure 122 ^{1}H- and ^{13}C-NMR-Spectrum of **229** in $CDCl_3$ (600 MHz/151 MHz).

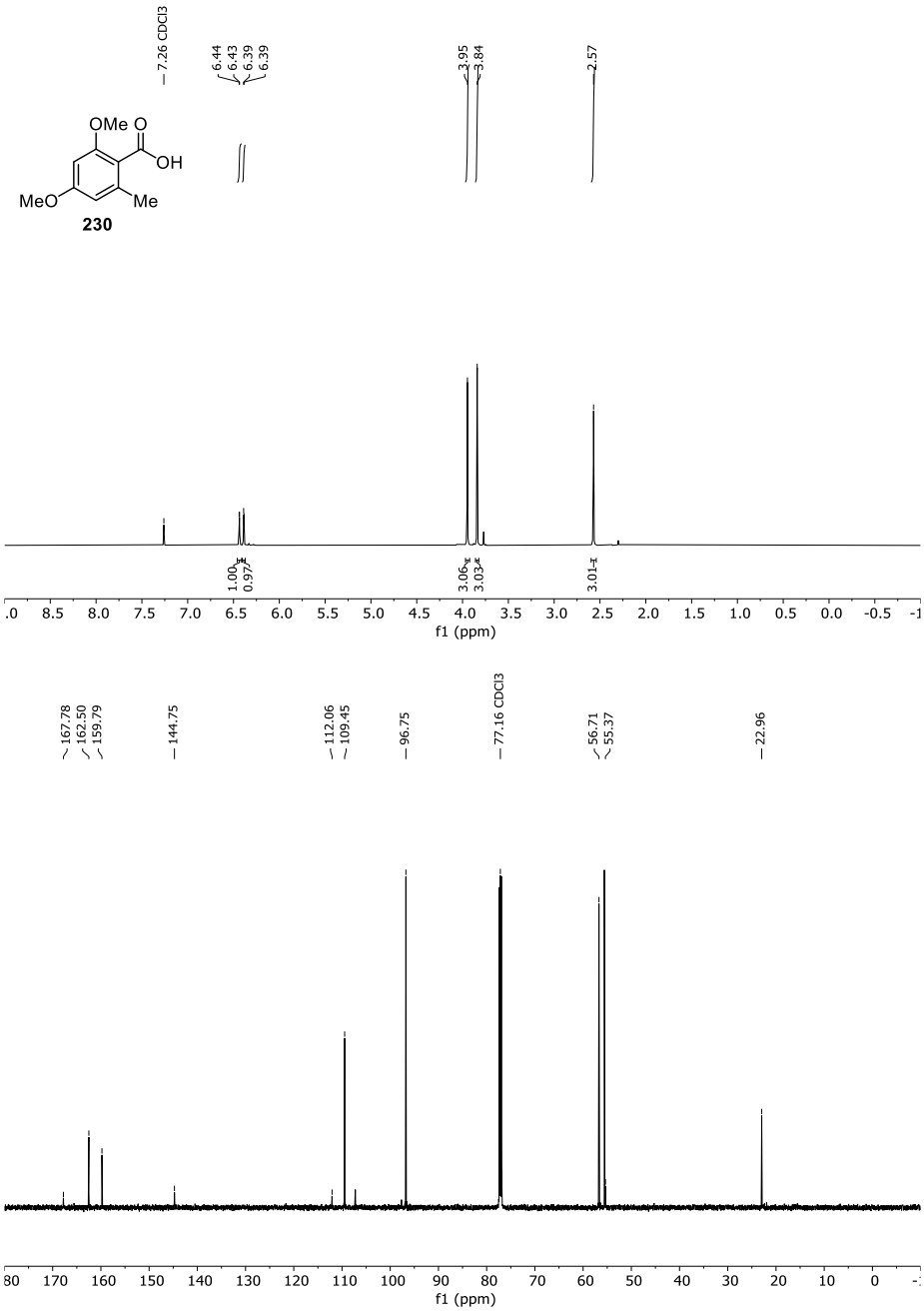

Figure 123 ^{1}H- and ^{13}C-NMR-Spectrum of **230** in $CDCl_3$ (600 MHz/151 MHz).

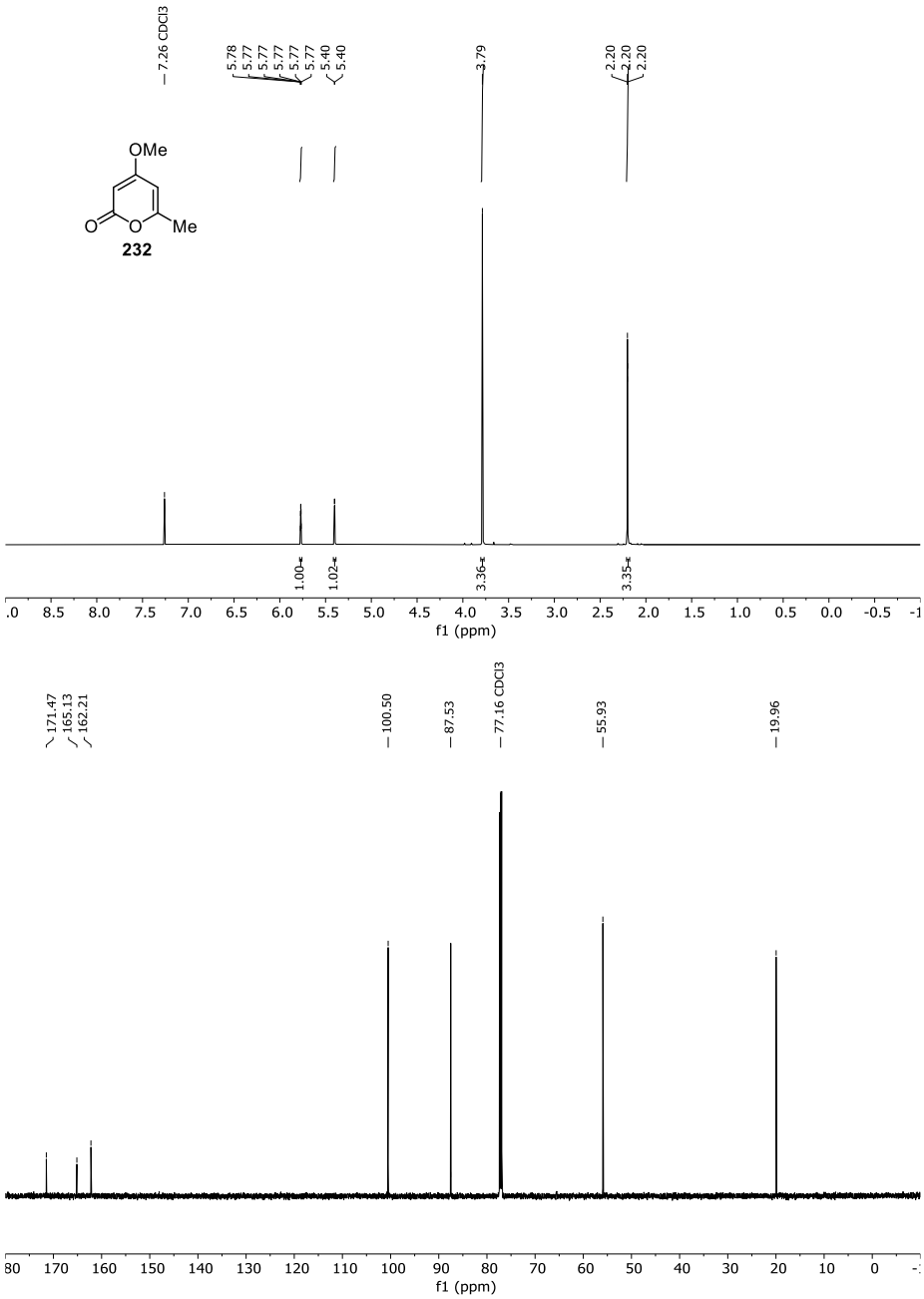

Figure 124 ^{1}H- and ^{13}C-NMR-Spectrum of **232** in $CDCl_3$ (600 MHz/151 MHz).

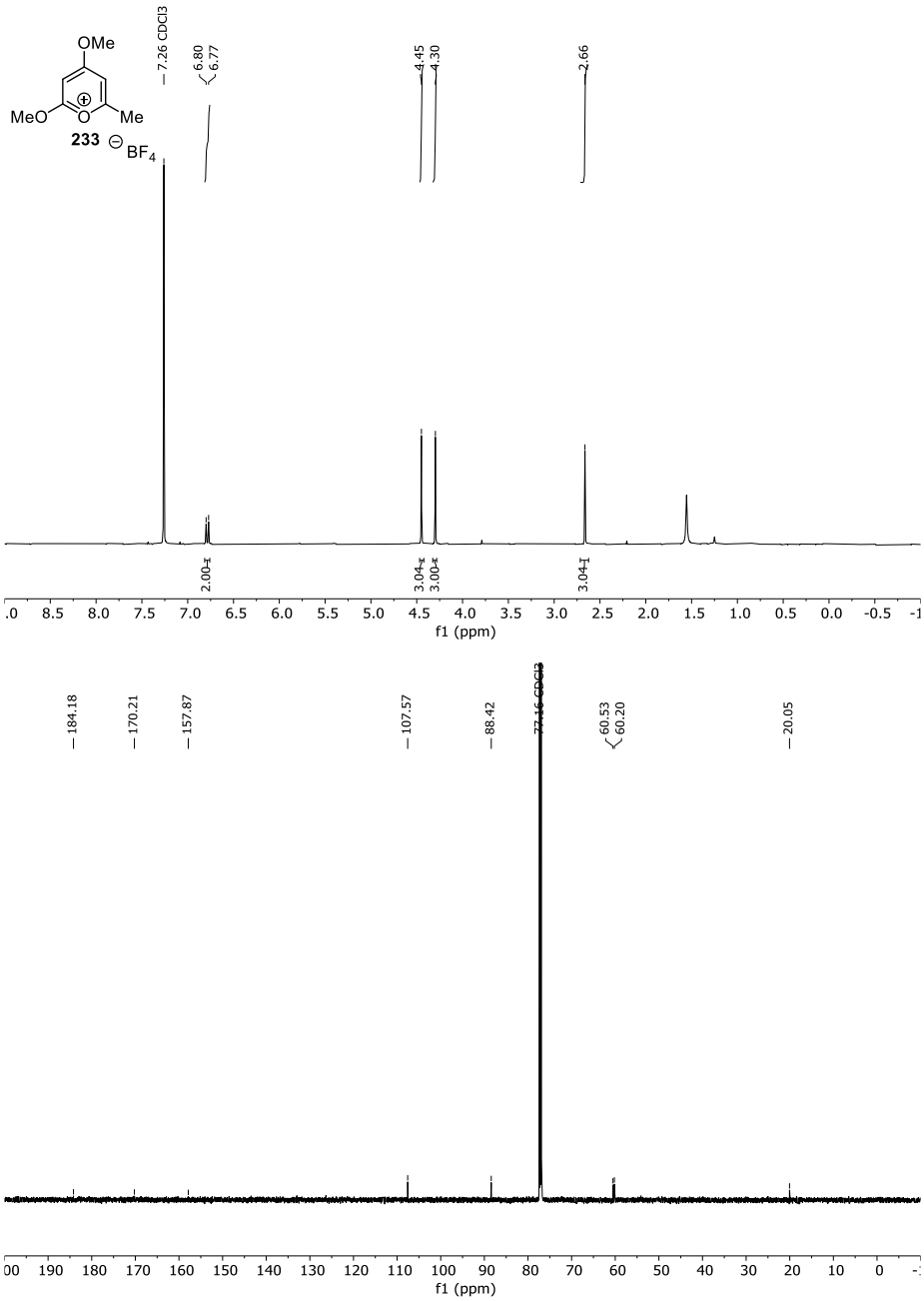

Figure 125 ^{1}H- and ^{13}C-NMR-Spectrum of **233** in $CDCl_3$ (600 MHz/151 MHz).

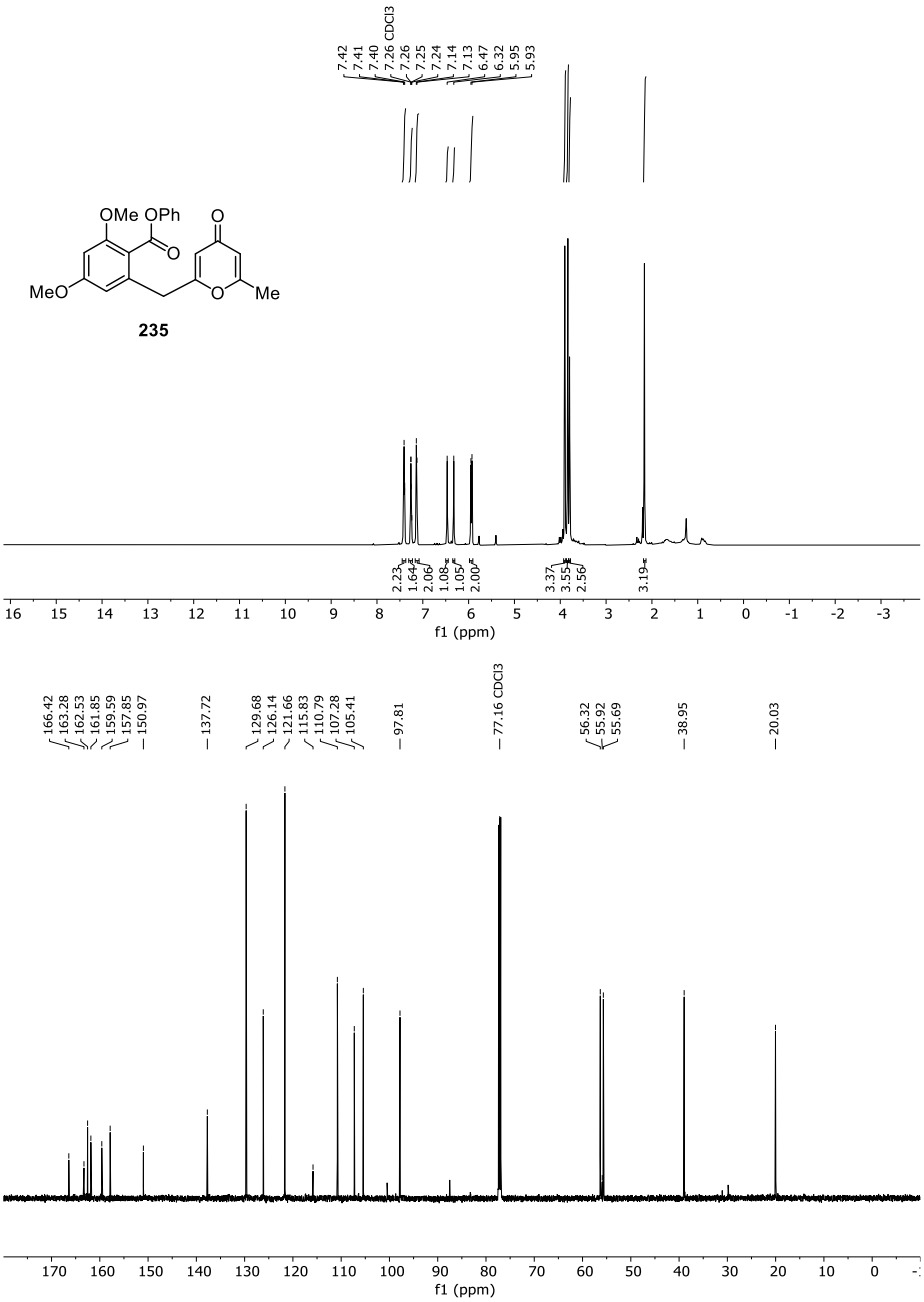

Figure 126 ^{1}H- and ^{13}C-NMR-Spectrum of **235** in $CDCl_3$ (600 MHz/151 MHz).

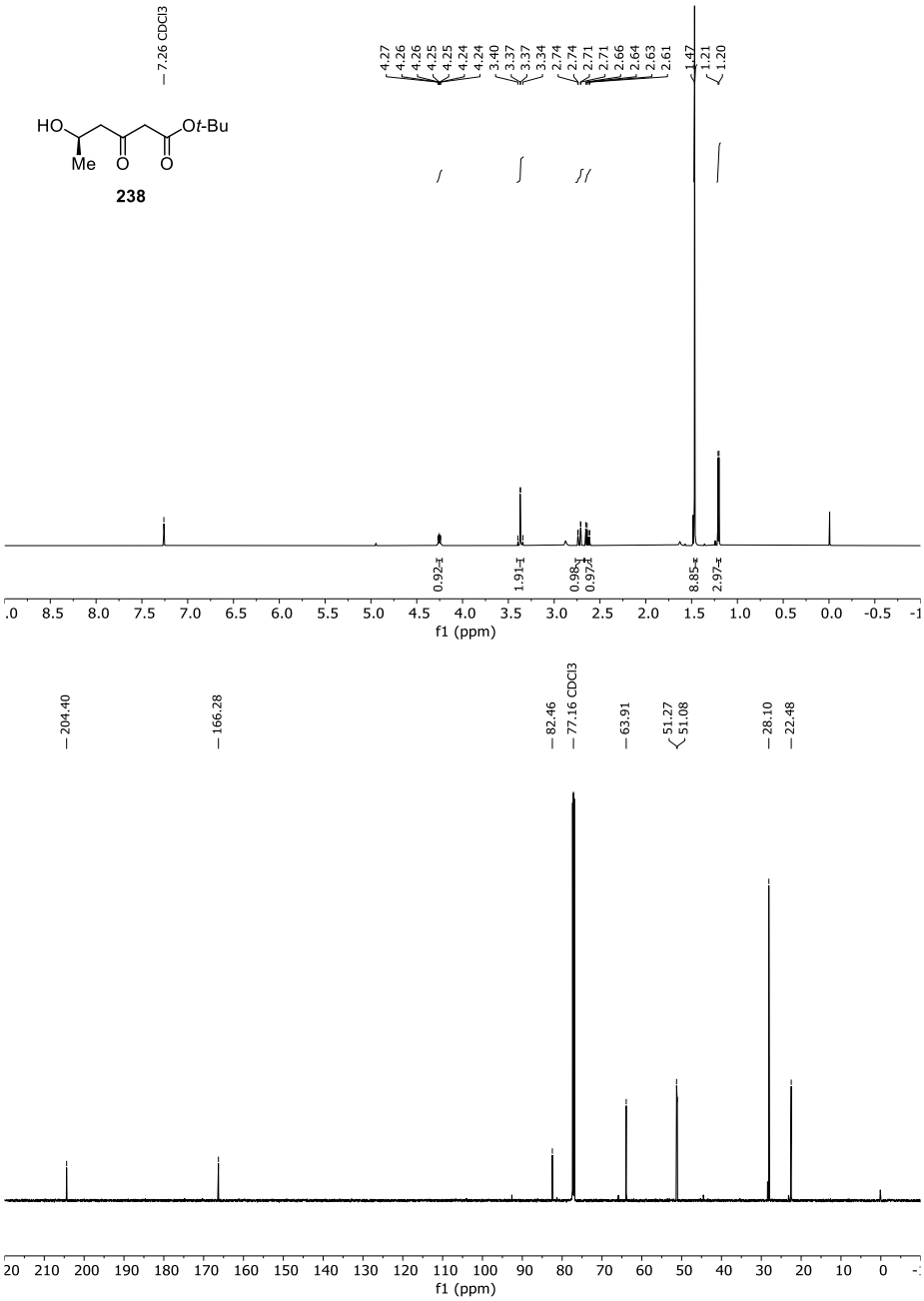

Figure 127 ^{1}H- and ^{13}C-NMR-Spectrum of **238** in $CDCl_3$ (600 MHz/151 MHz).

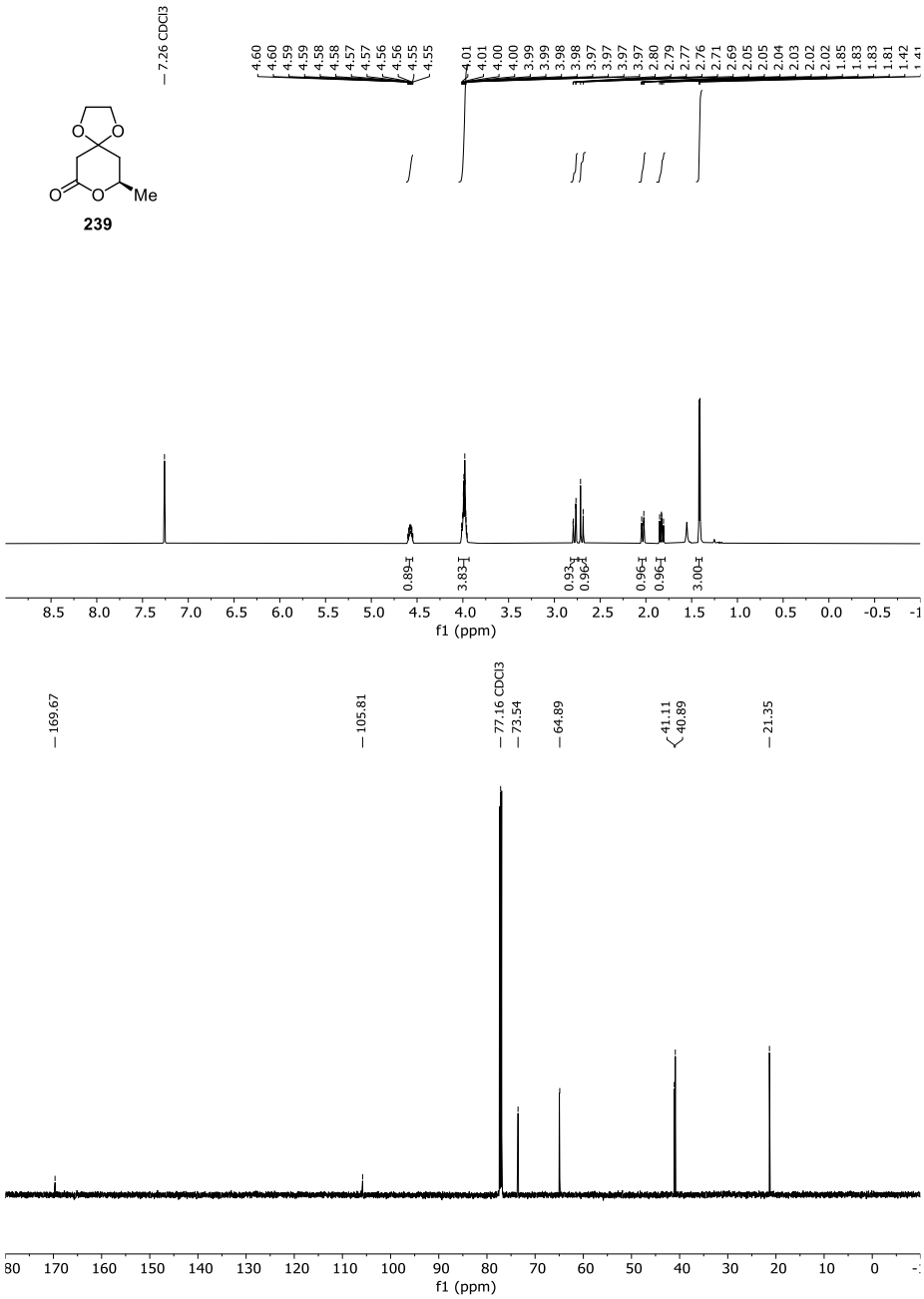

Figure 128 ^{1}H- and ^{13}C-NMR-Spectrum of **239** in $CDCl_3$ (600 MHz/151 MHz).

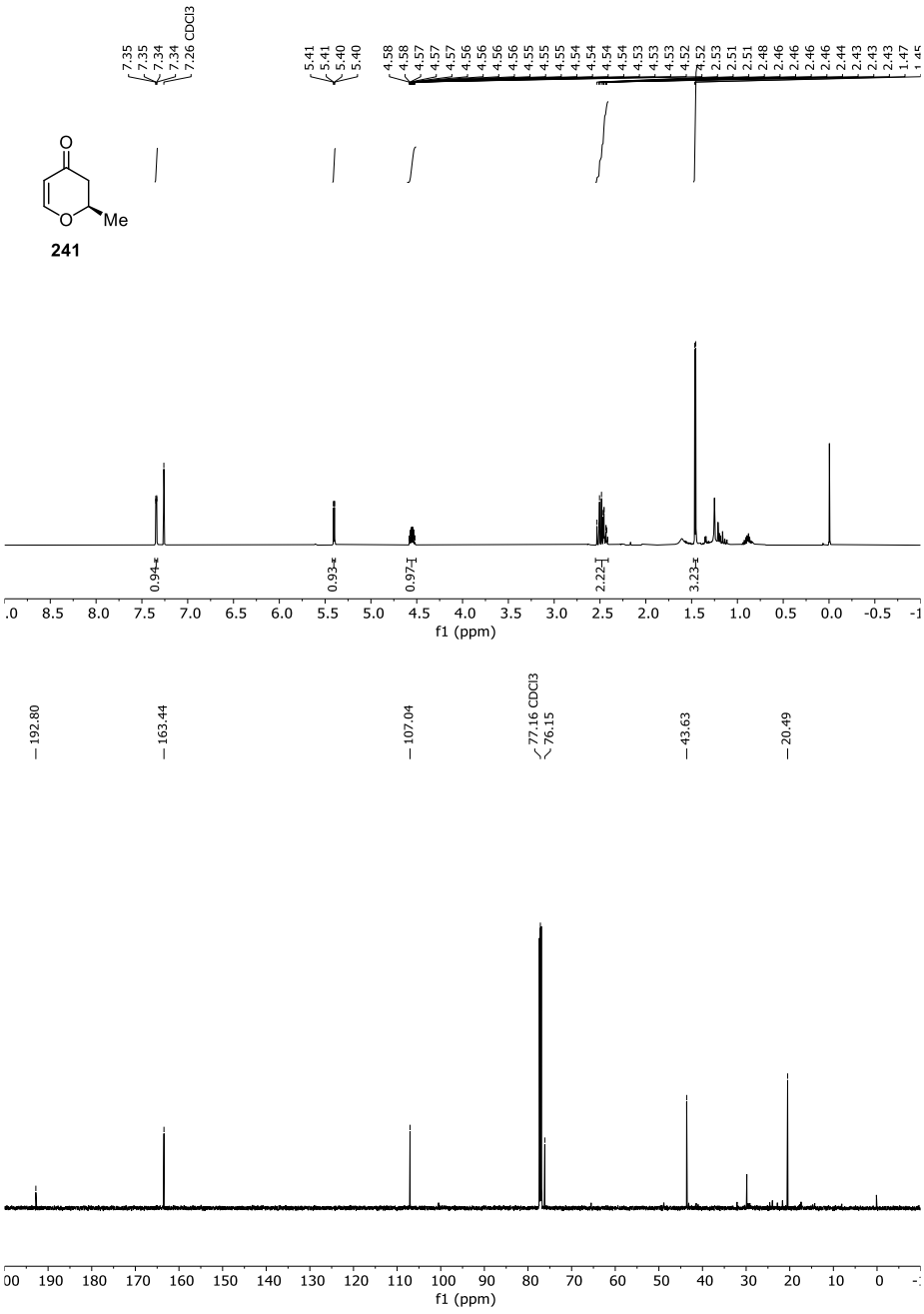

Figure 129 ^{1}H- and ^{13}C-NMR-Spectrum of **241** in $CDCl_3$ (600 MHz/151 MHz).

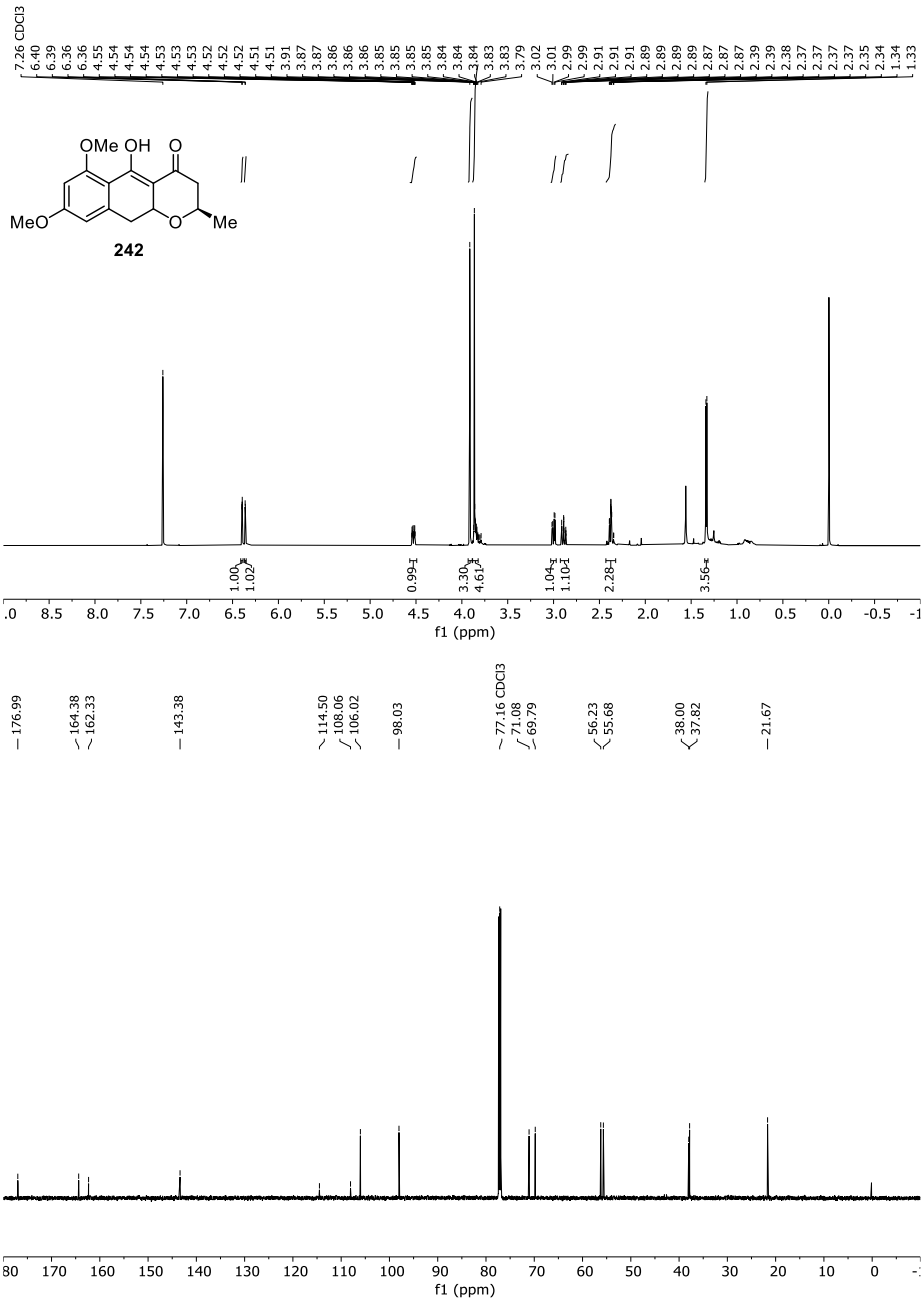

Figure 130 ^{1}H- and ^{13}C-NMR-Spectrum of **242** in $CDCl_3$ (600 MHz/151 MHz).

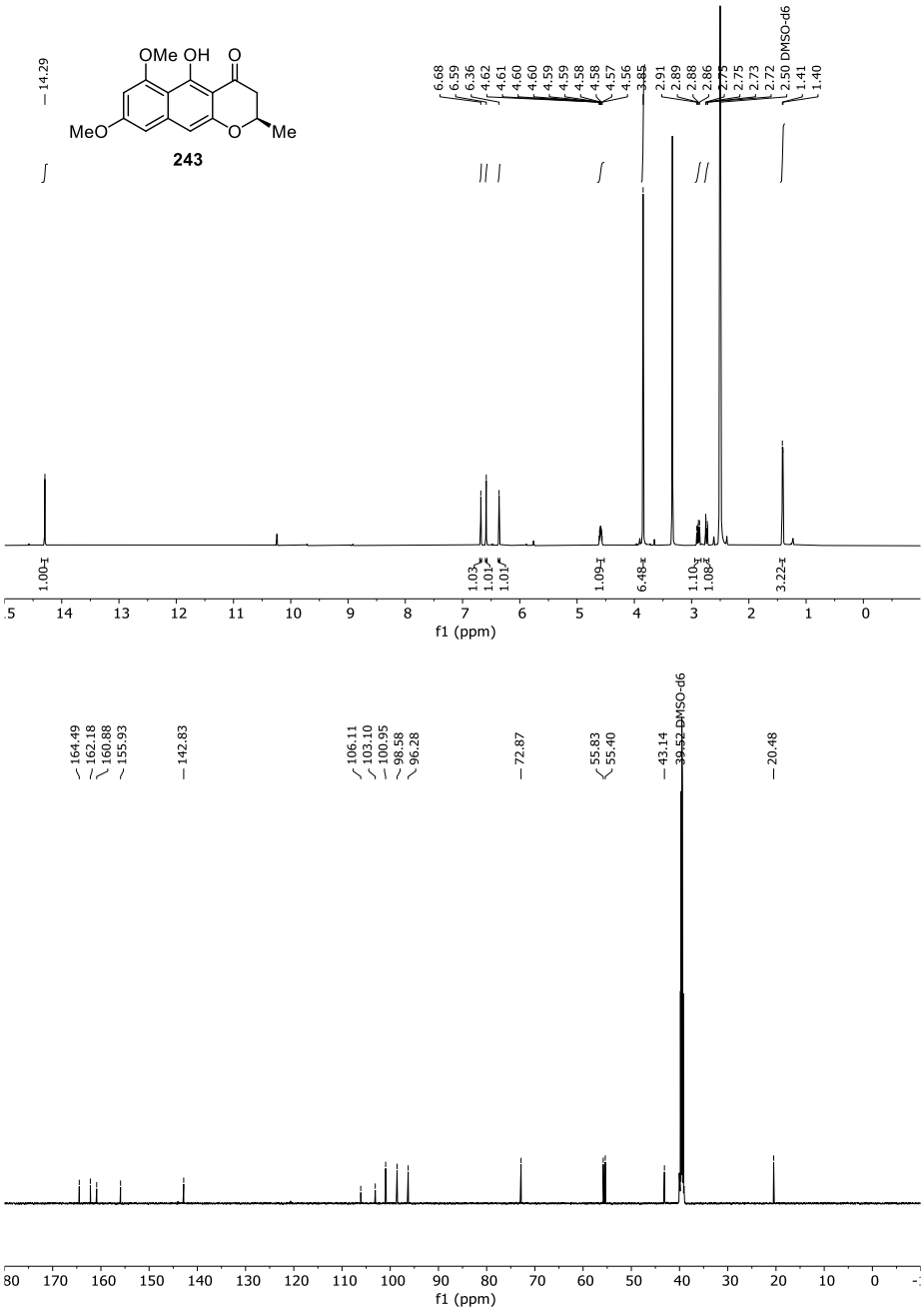

Figure 131 ^{1}H- and ^{13}C-NMR-Spectrum of **243** in DMSO-d_6 (600 MHz/151 MHz).

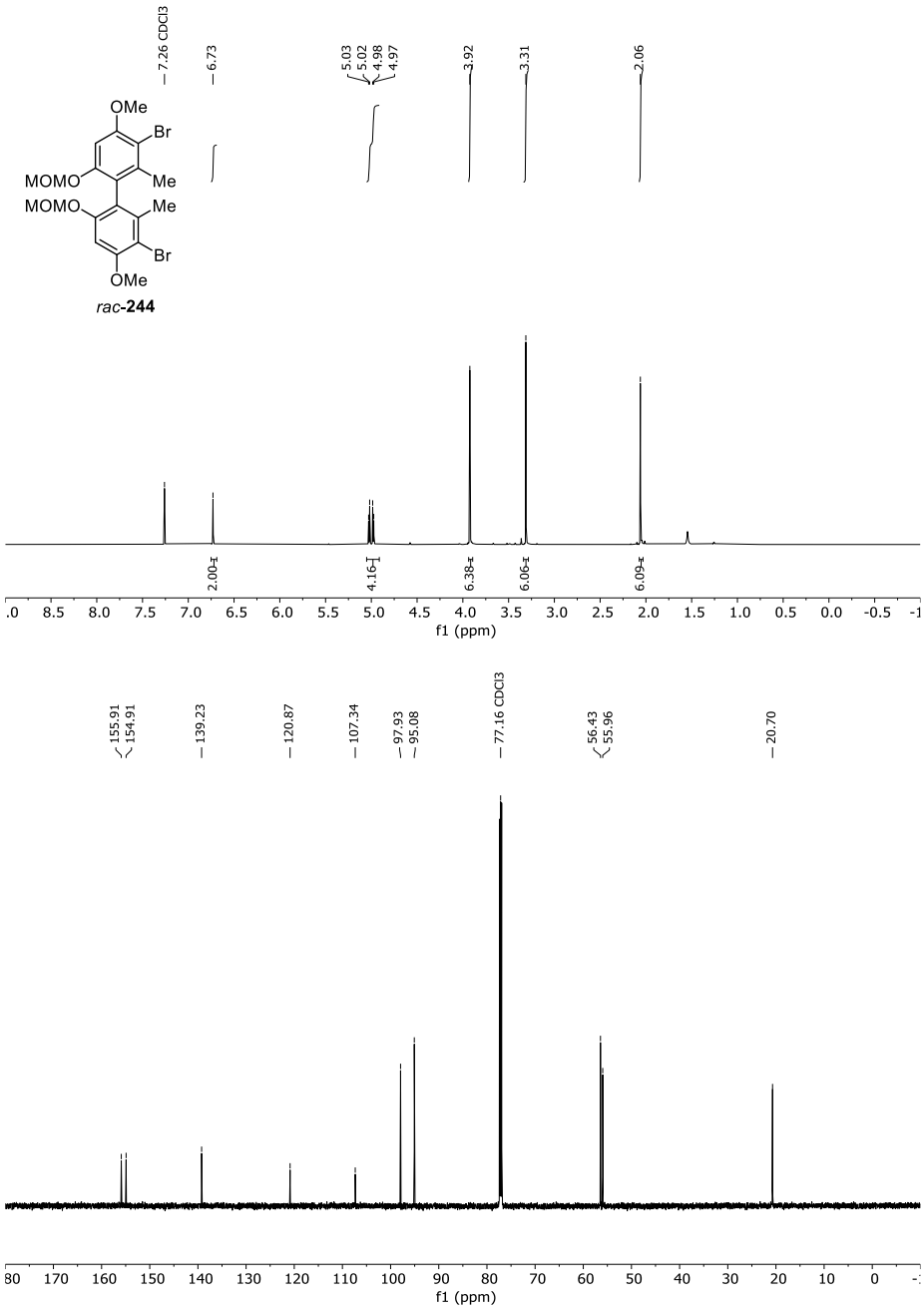

Figure 132 ^{1}H- and ^{13}C-NMR-Spectrum of *rac*-**244** in $CDCl_3$ (600 MHz/151 MHz).

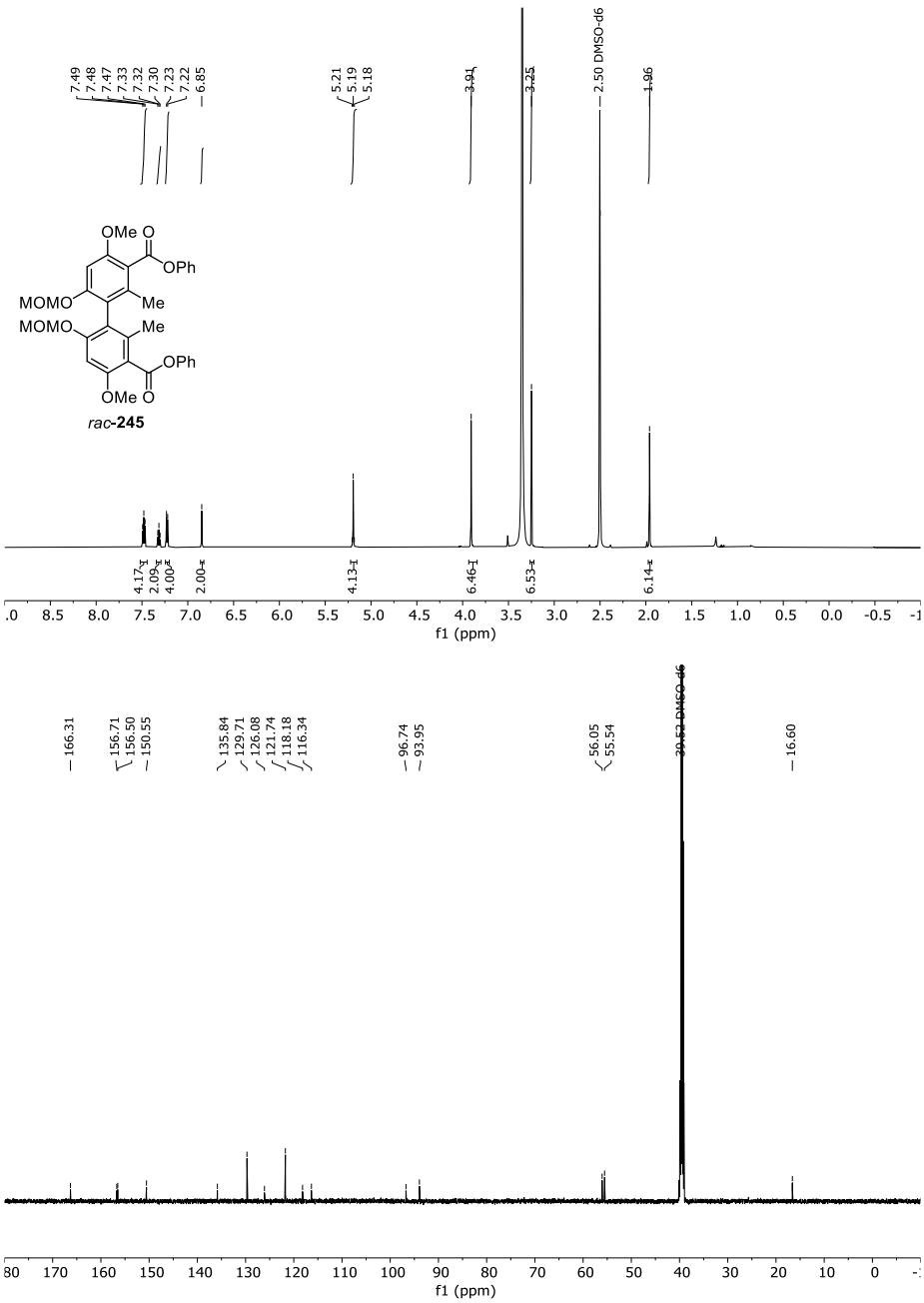

Figure 133 ^{1}H- and ^{13}C-NMR-Spectrum of *rac*-**245** in DMSO-d_6 (600 MHz/151 MHz).

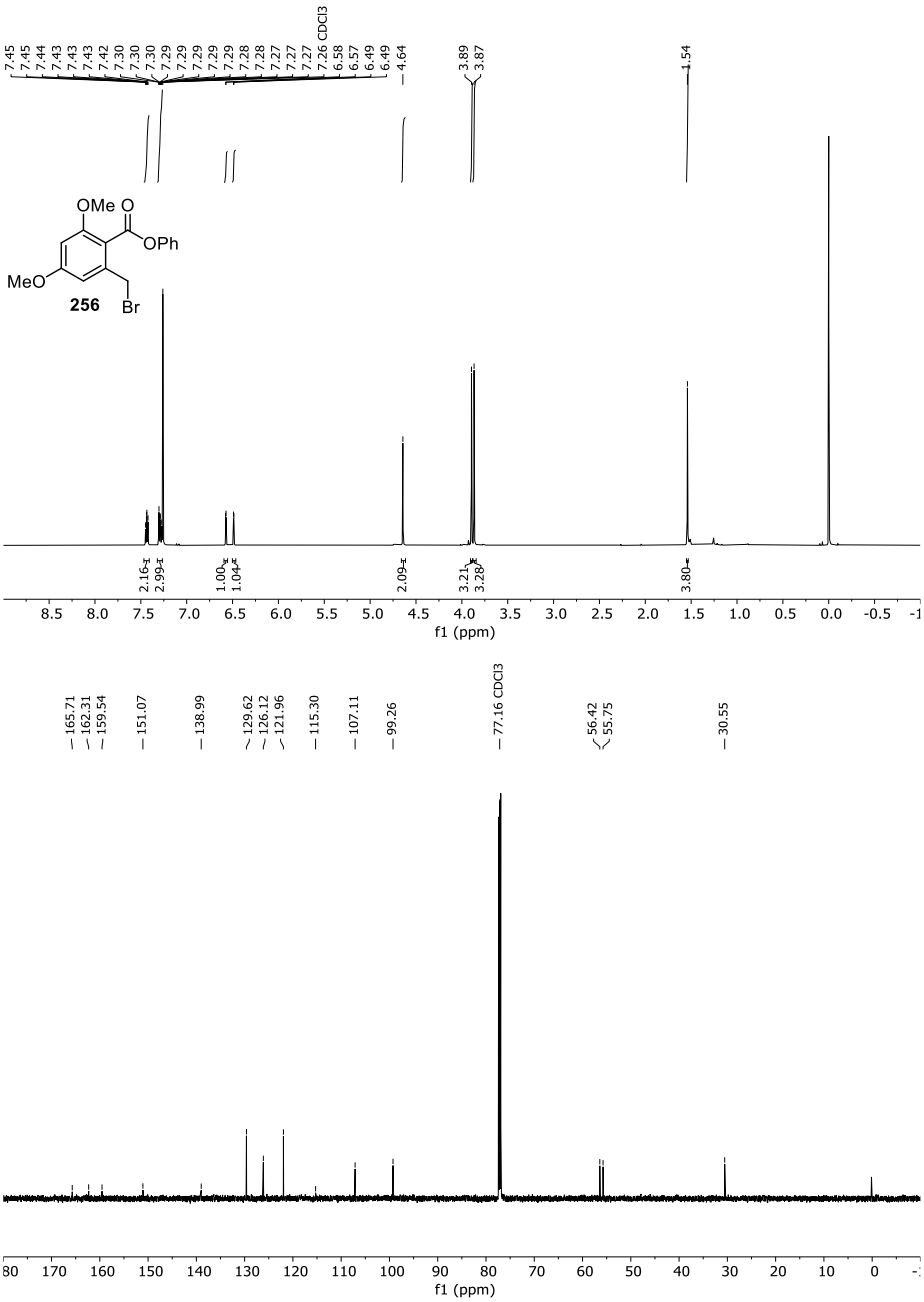

Figure 134 ^{1}H- and ^{13}C-NMR-Spectrum of **256** in $CDCl_3$ (600 MHz/151 MHz).

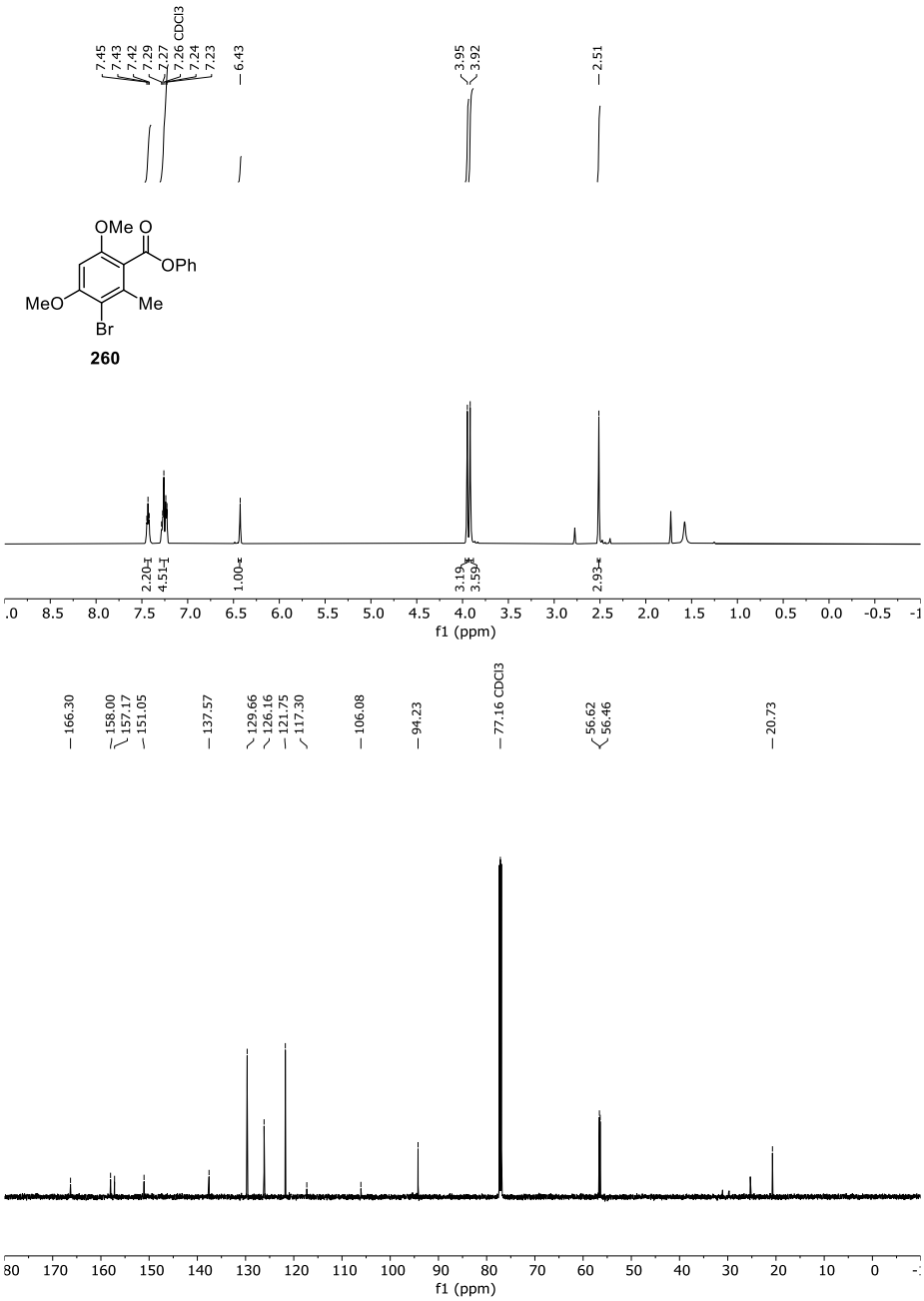

Figure 135 ^{1}H- and ^{13}C-NMR-Spectrum of **260** in $CDCl_3$ (600 MHz/151 MHz).

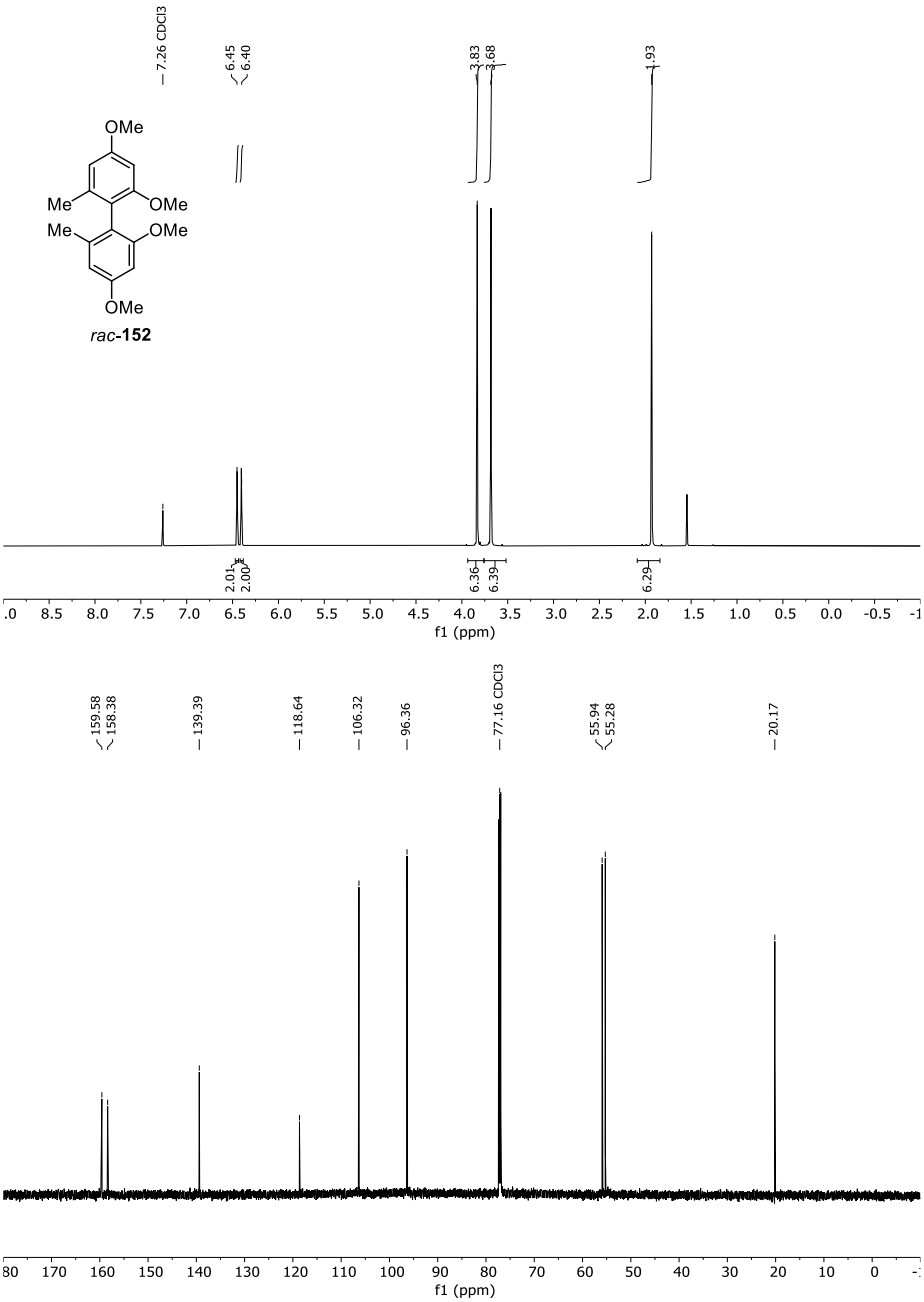

Figure 136 ^{1}H- and ^{13}C-NMR-Spectrum of *rac*-**152** in $CDCl_3$ (600 MHz/151 MHz).

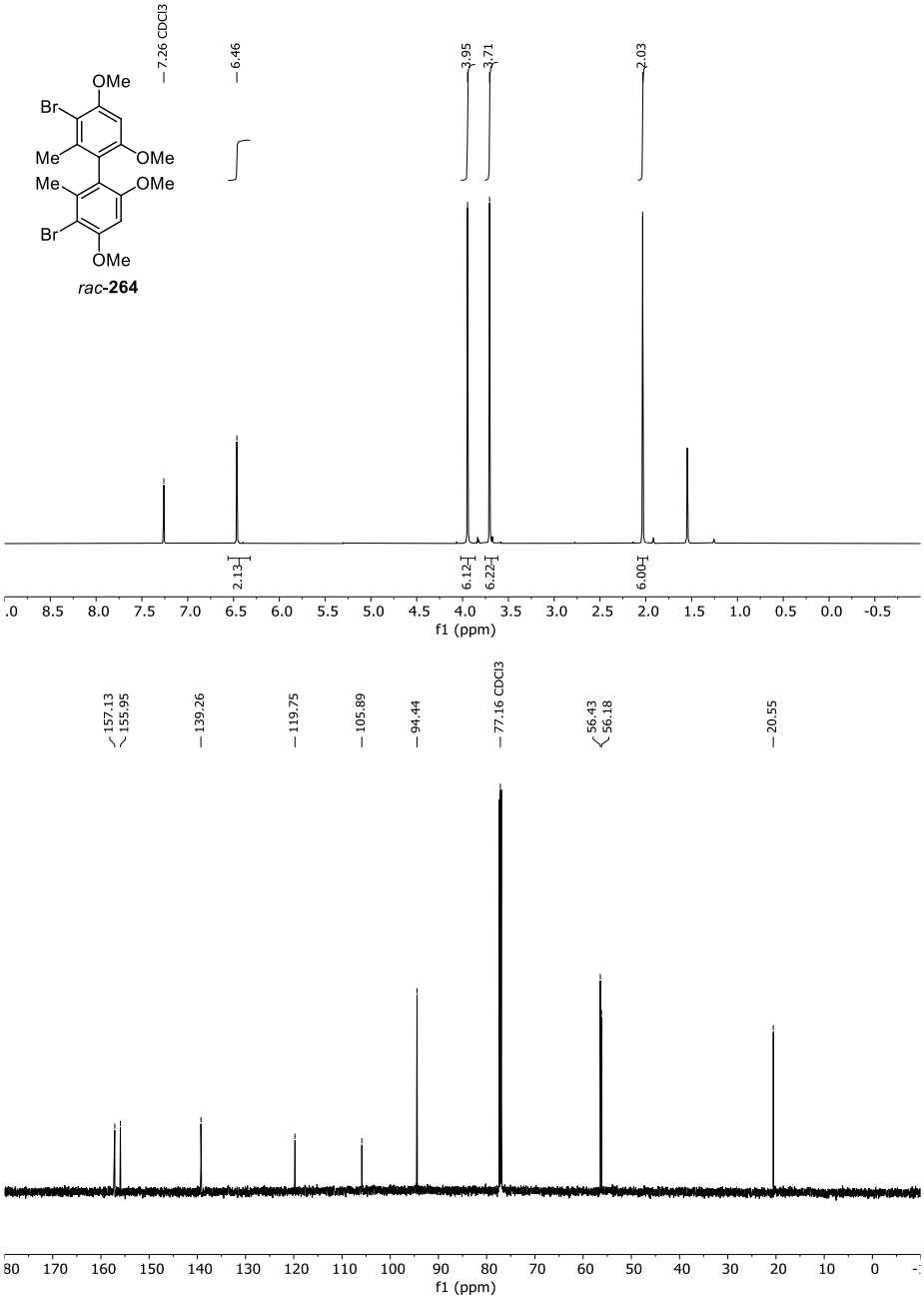

Figure 137 ^{1}H- and ^{13}C-NMR-Spectrum of *rac*-**264** in $CDCl_3$ (600 MHz/151 MHz).

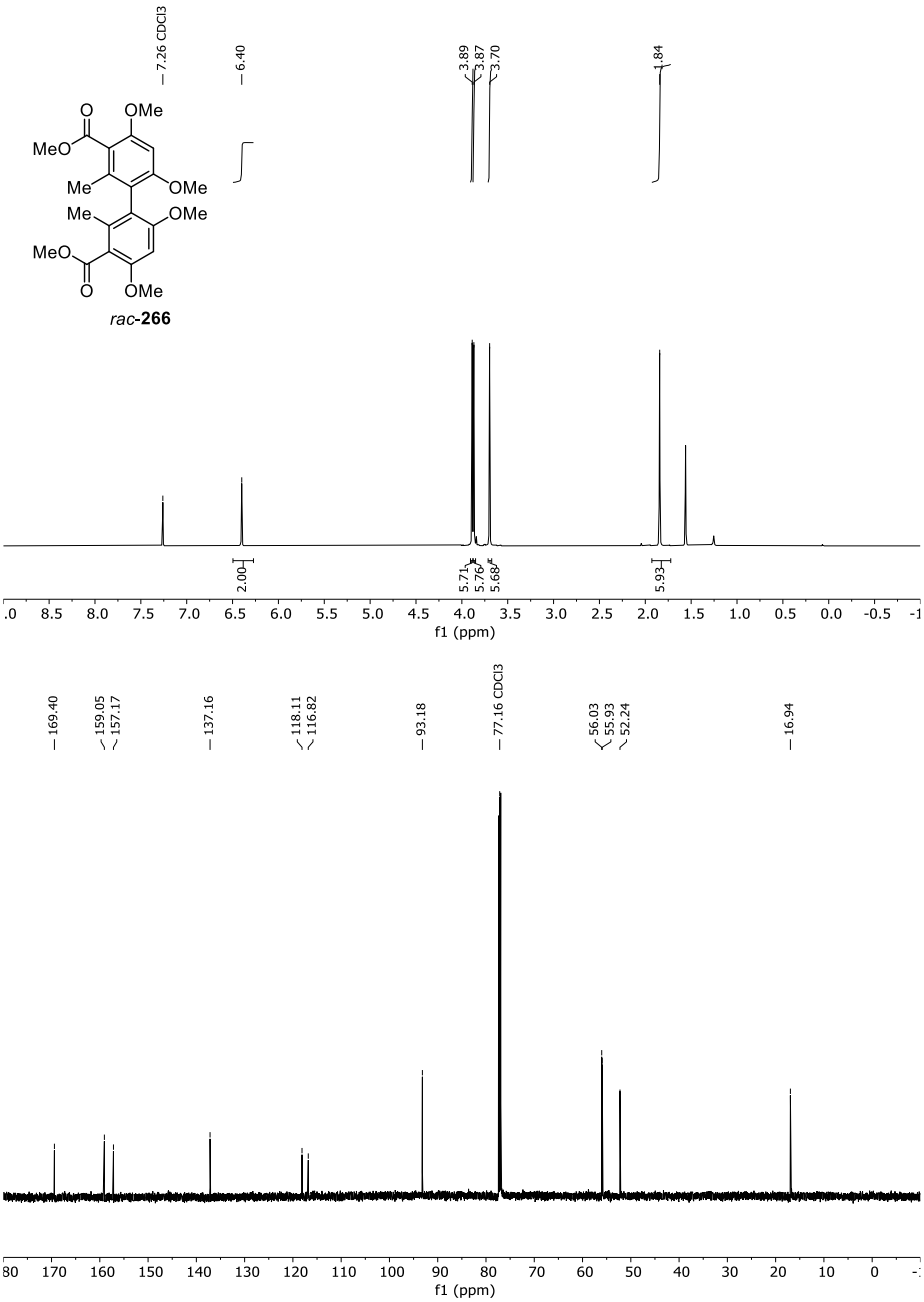

Figure 138 ^{1}H- and ^{13}C-NMR-Spectrum of *rac*-**266** in $CDCl_3$ (600 MHz/151 MHz).

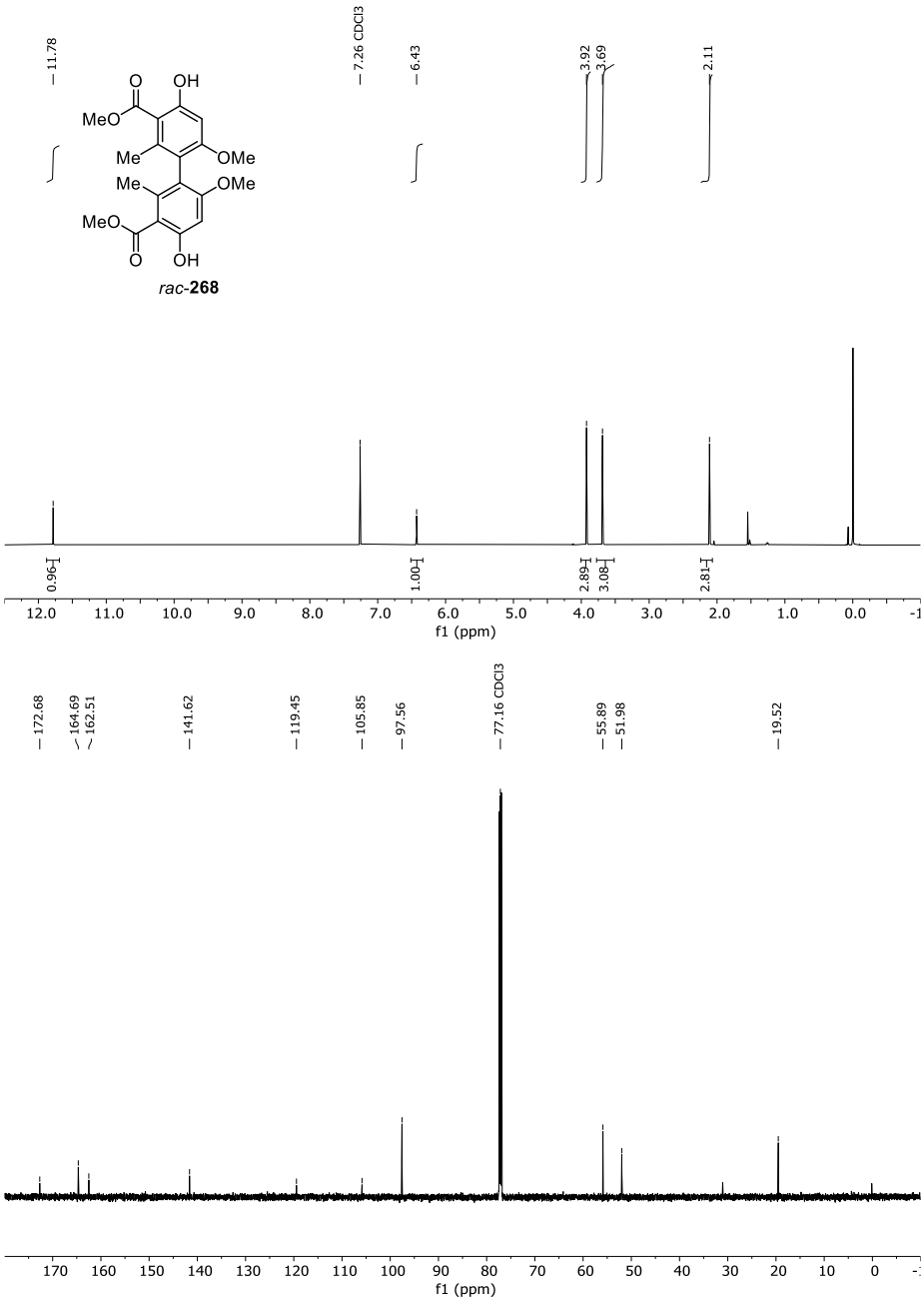

Figure 139 ^{1}H- and ^{13}C-NMR-Spectrum of *rac*-**268** in $CDCl_3$ (600 MHz/151 MHz).

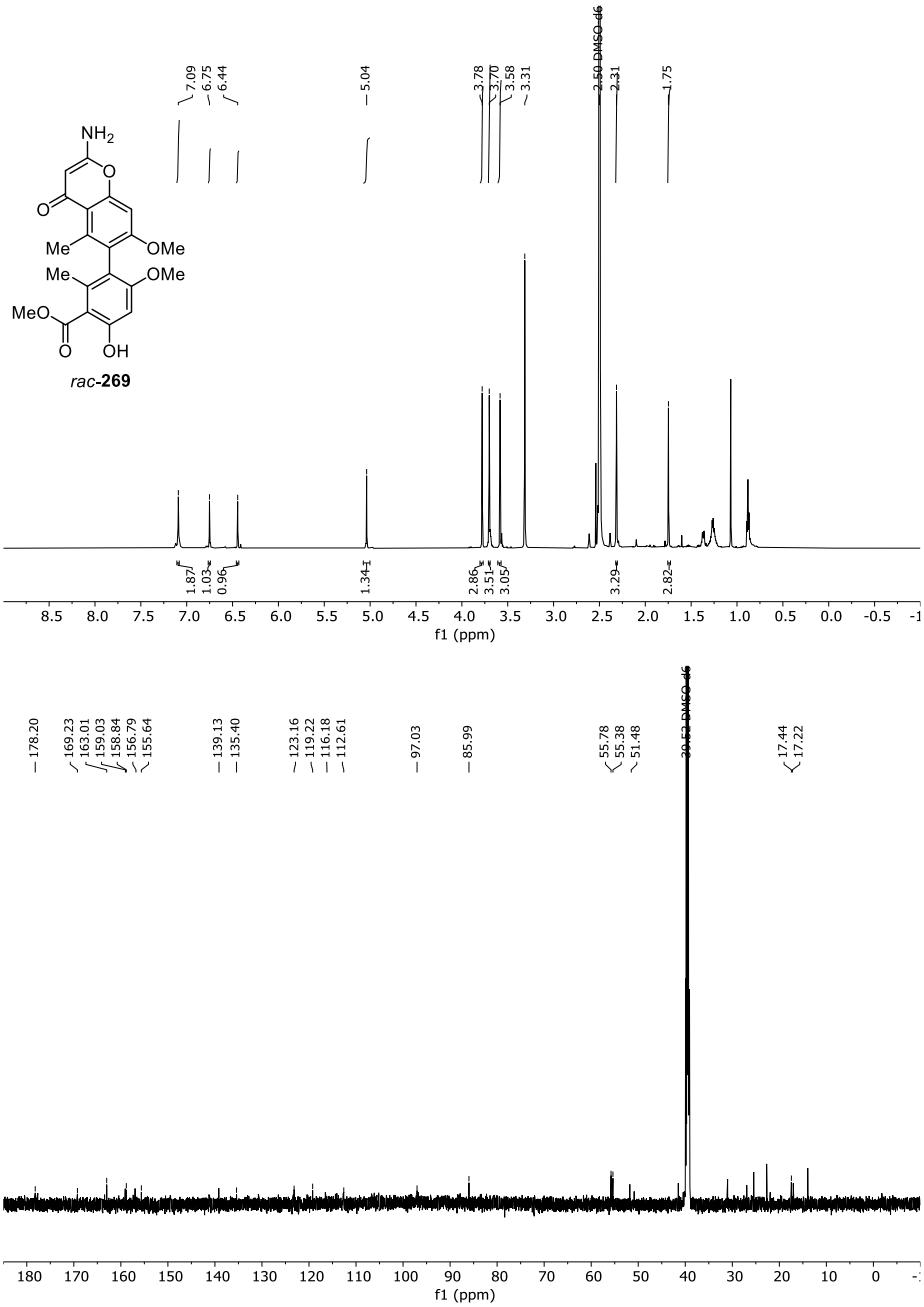

Figure 140 ^{1}H- and ^{13}C-NMR-Spectrum of *rac*-**269** in DMSO-d_6 (600 MHz/151 MHz).

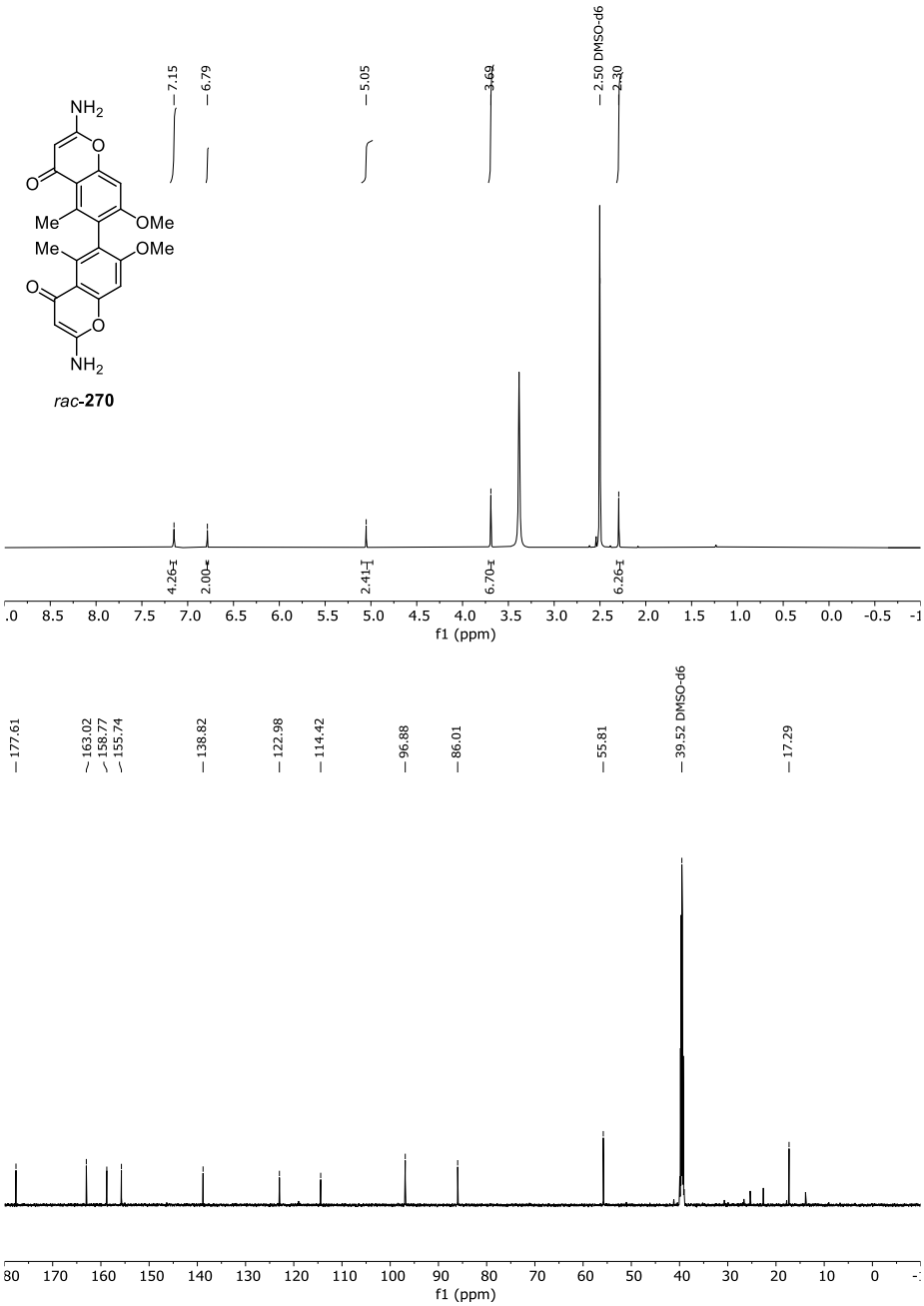

Figure 141 ^{1}H- and ^{13}C-NMR-Spectrum of *rac*-**270** in DMSO-d_6 (600 MHz/151 MHz).

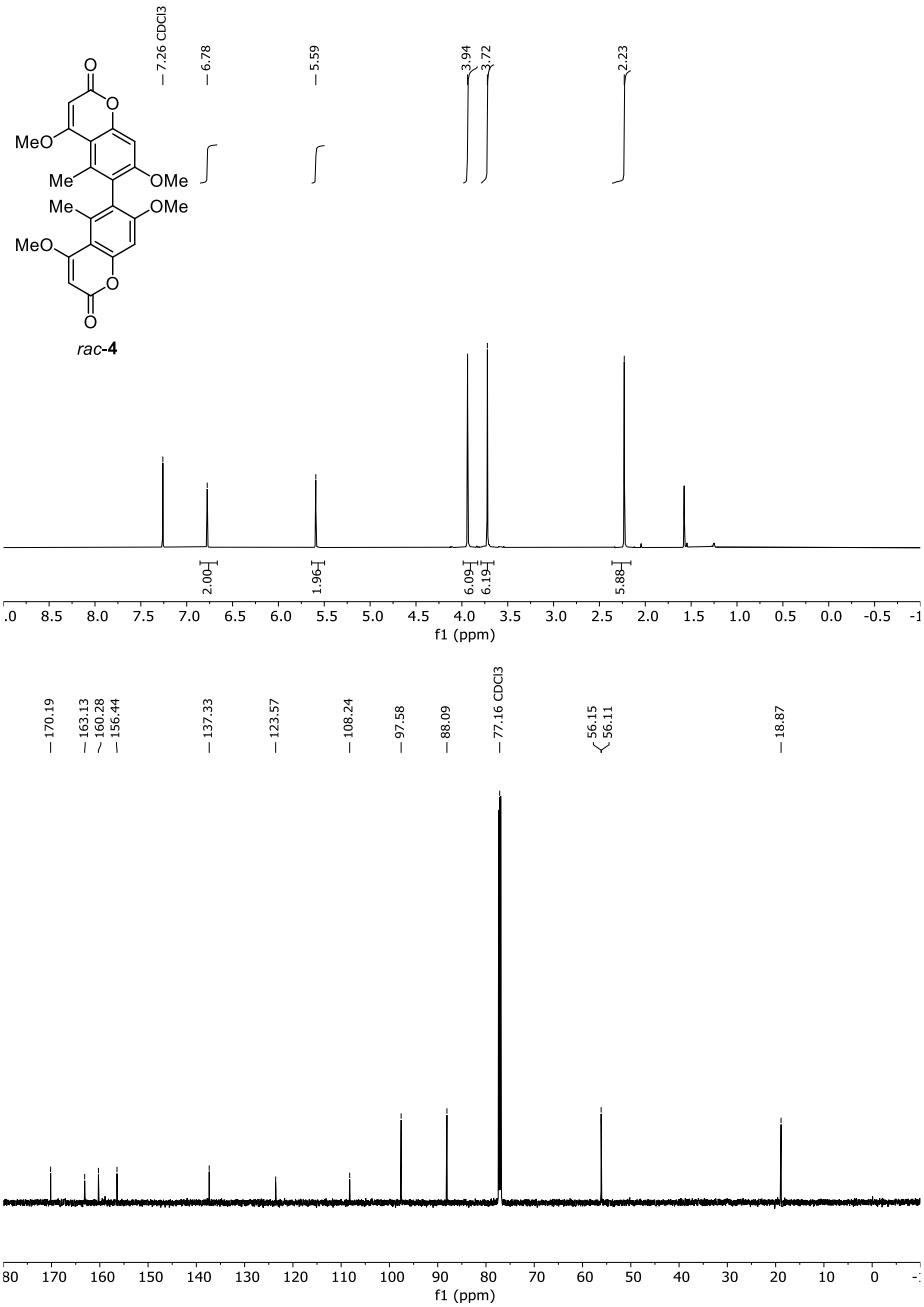

Figure 142 ^{1}H- and ^{13}C-NMR-Spectrum of *rac*-**4** in $CDCl_3$ (600 MHz/151 MHz).

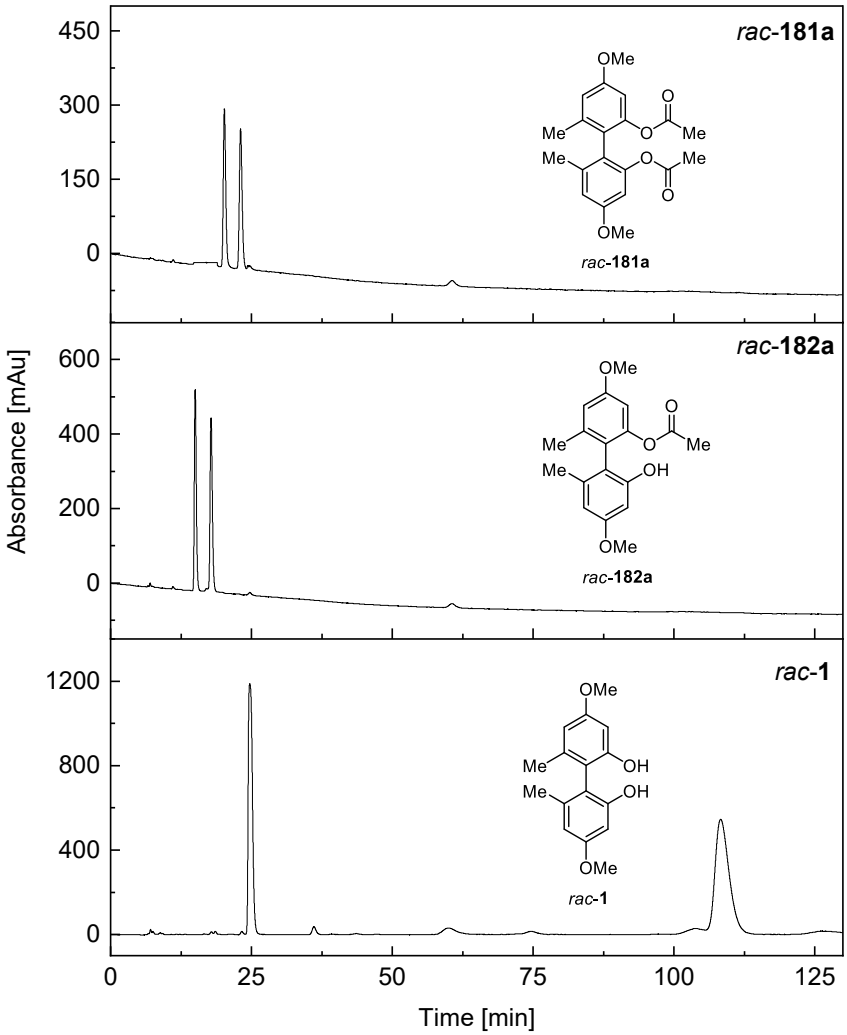

Column: Chiralpak IC, *Fa. Daicel* (250x4.6 mm); 5 µL, 25 °C, 0.5 mL/min, 205 nm; solvent: *n*-heptane:2-propanol (90:10).

	t_{R1} [min]	Area [mAu*min]	t_{R2} [min]	Area [mAu*min]
rac-**181a**	20.1	162.89	23.0	160.33
rac-**182a**	15.0	220.75	17.8	223.58
rac-**1**	24.7	1018.39	108.3	1495.77

Figure 143 HPLC Chromatogram of *rac*-**181a** and *rac*-**182a**.

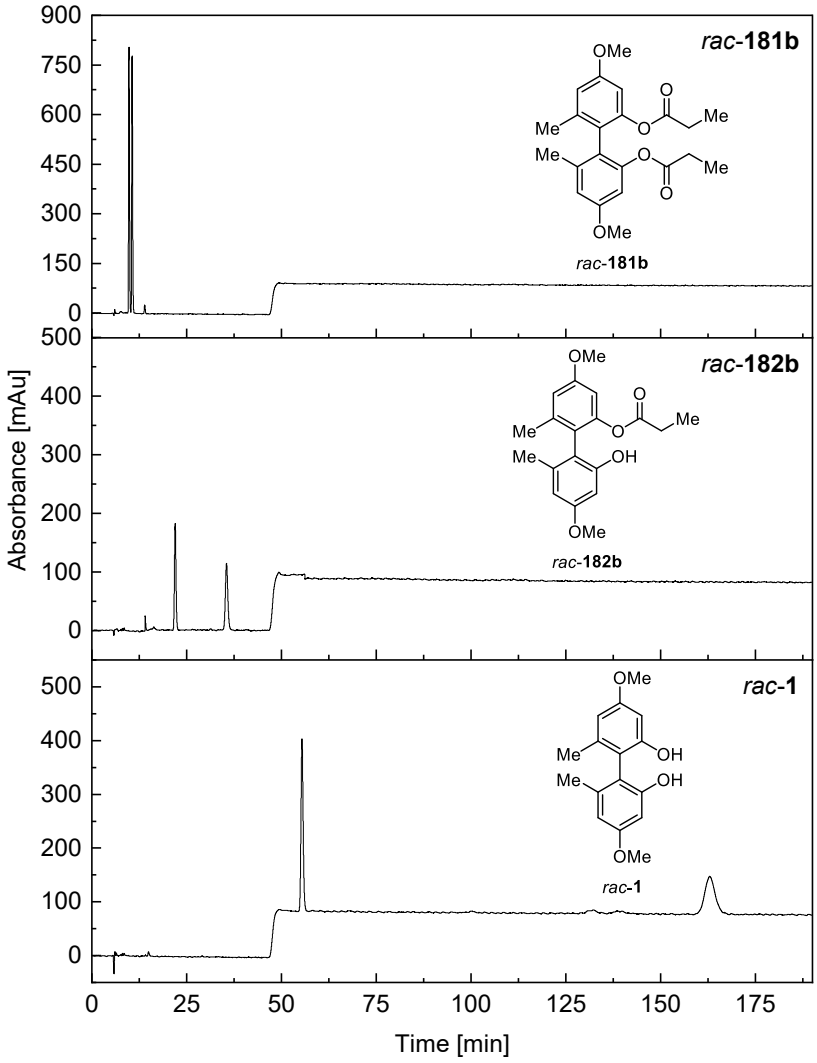

Column: Lux Amylose-1, *Fa. Phenomenex* (250x4.6 mm); 5 µL, 25 °C, 0.5 mL/min, 274 nm; solvent: *n*-heptane:2-propanol (90:10) for 40 min then (80:20) for 150 min.

	t_{R1} [min]	Area [mAu*min]	t_{R2} [min]	Area [mAu*min]
rac-**181b**	9.7	213.45	10.6	217.32
rac-**182b**	21.7	303.72	35.0	315.17
rac-**1**	55.4	210.82	162.9	228.4

Figure 144 HPLC Chromatogram of *rac*-**181b** and *rac*-**182b**.

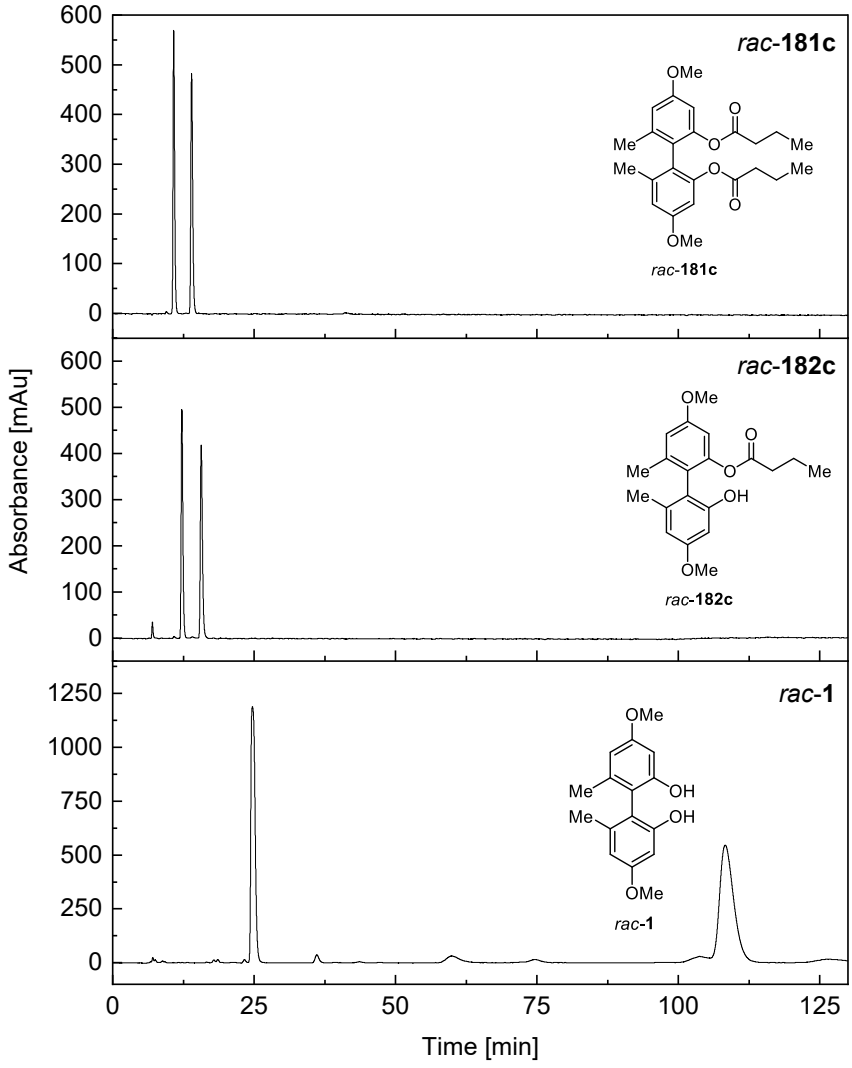

Column: Chiralpak IC, *Fa. Daicel* (250x4.6 mm); 5 µL, 25 °C, 0.5 mL/min, 205 nm; solvent: *n*-heptane:2-propanol (90:10).

	t_{R1} [min]	Area [mAu*min]	t_{R2} [min]	Area [mAu*min]
rac-**181c**	10.8	187.08	13.9	186.64
rac-**182c**	12.2	175.42	15.6	179.95
rac-**1**	24.7	1018.39	108.3	1495.77

Figure 145 HPLC Chromatogram of *rac*-**181c** and *rac*-**182c**.

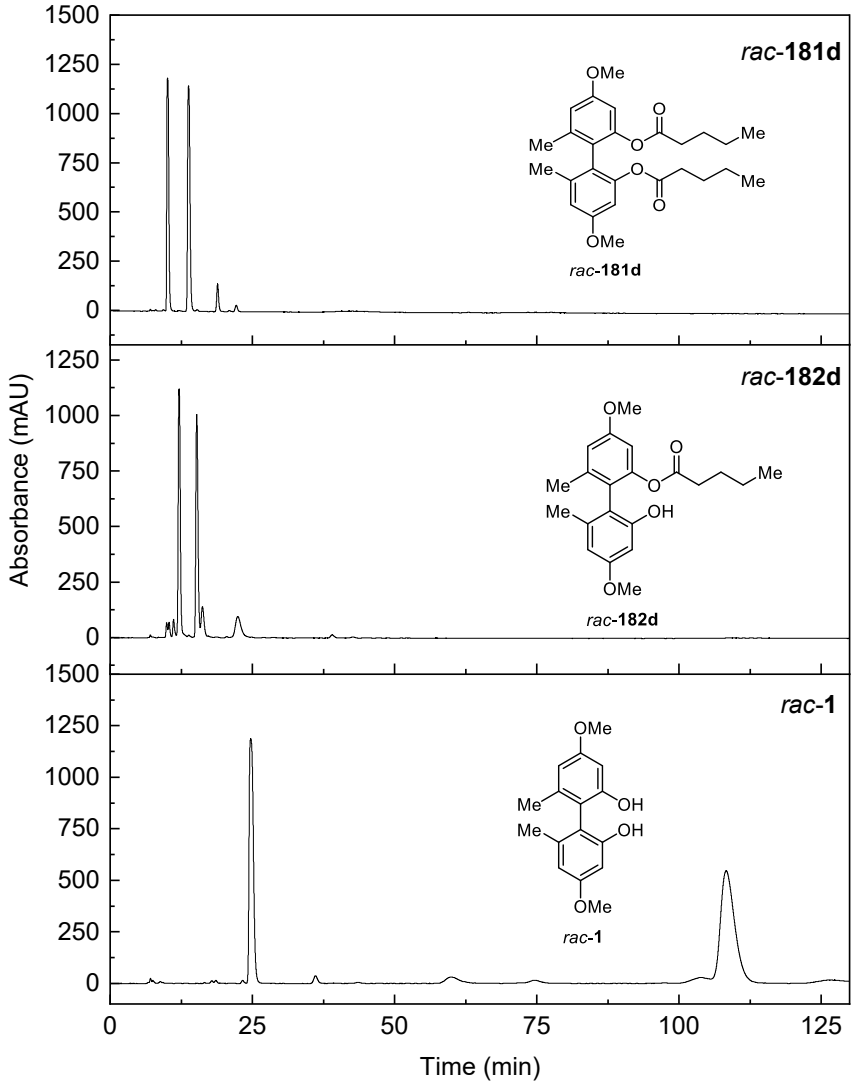

Column: Chiralpak IC, *Fa. Daicel* (250x4.6 mm); 5 µL, 25 °C, 0.5 mL/min, 205 nm; solvent: *n*-heptane:2-propanol (90:10).

	t_{R1} [min]	Area [mAu*min]	t_{R2} [min]	Area [mAu*min]
rac-**181d**	10.1	485.49	13.8	551.79
rac-**182d**	12.1	478.0	15.2	441.67
rac-**1**	24.7	1018.39	108.28	1495.77

Figure 146 HPLC Chromatogram of *rac*-**181d** and *rac*-**182d**.

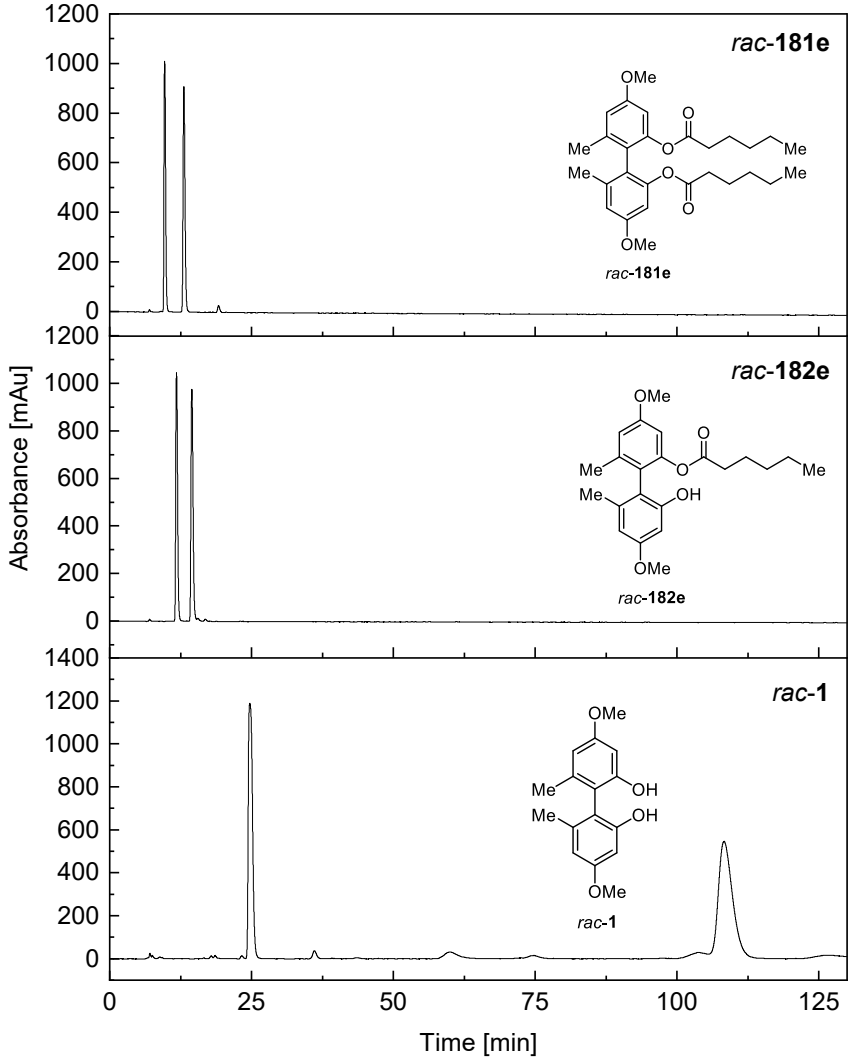

Column: Chiralpak IC, *Fa. Daicel* (250x4.6 mm); 5 µL, 25 °C, 0.5 mL/min, 205 nm; solvent: *n*-heptane:2-propanol (90:10).

	t_{R1} [min]	Area [mAu*min]	t_{R2} [min]	Area [mAu*min]
rac-**181e**	9.7	341.84	13.0	363.11
rac-**182e**	11.7	397.03	14.4	420.79
rac-**1**	24.7	1018.39	108.28	1495.77

Figure 147 HPLC Chromatogram of *rac*-**181e** and *rac*-**182e**.

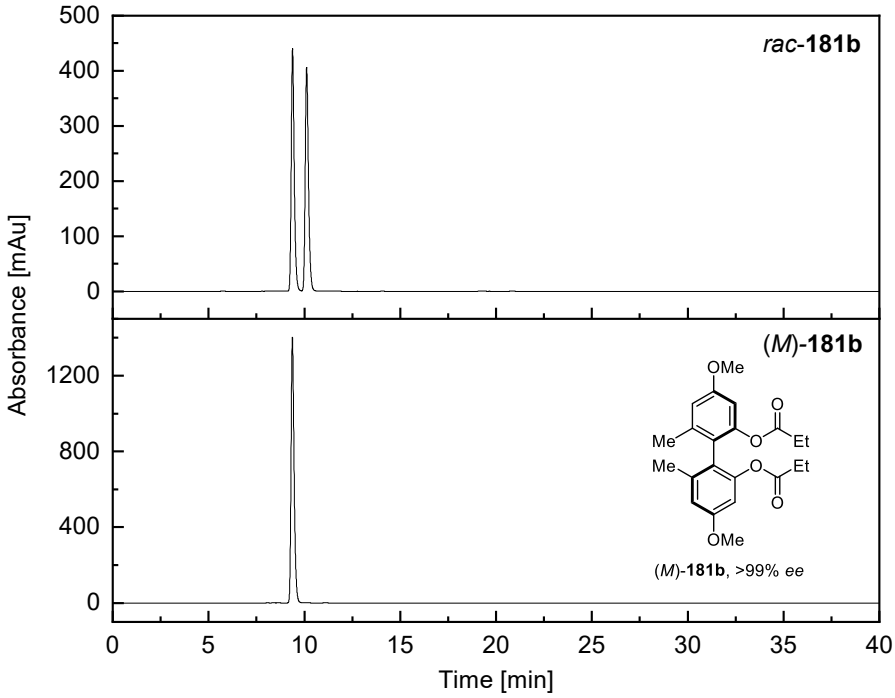

Column: Lux Amylose-1, *Fa. Phenomenex* (250x4.6 mm); 5 µL, 25 °C, 0.5 mL/min, 274 nm; solvent: *n*-heptane:2-propanol (90:10).

	t_{R1} [min]	Area [mAu*min]	t_{R2} [min]	Area [mAu*min]
rac-**181b**	9.4	79.50	10.1	79.49
(*M*)-**181b**	9.4	256.31	-	

Figure 148 HPLC Chromatogram of (*M*)-**181b**.

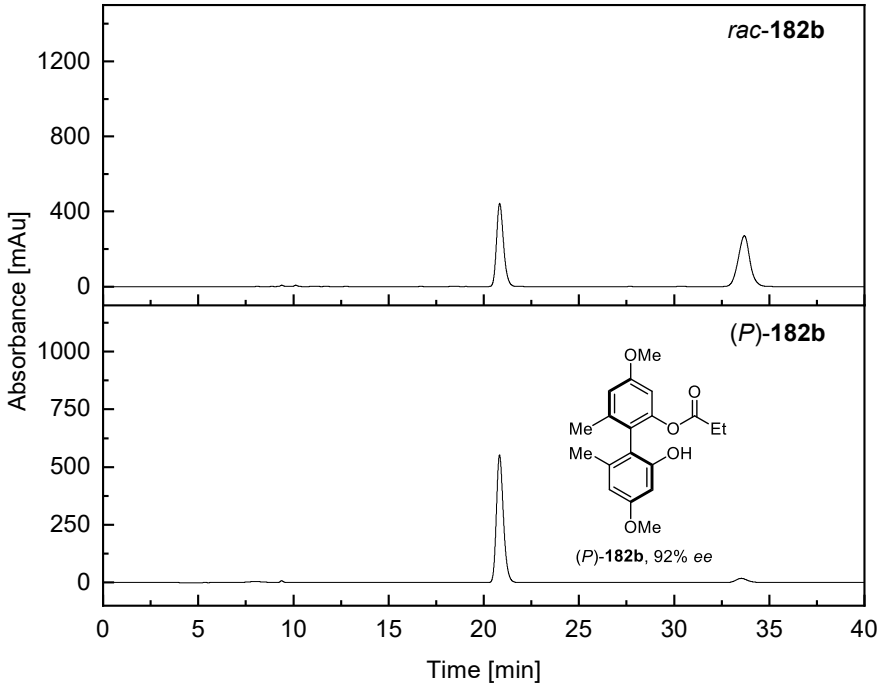

Column: Lux Amylose-1, *Fa. Phenomenex* (250x4.6 mm); 5 µL, 25 °C, 0.5 mL/min, 274 nm; solvent: *n*-heptane:2-propanol (90:10).

	t_{R1} [min]	Area [mAu*min]	t_{R2} [min]	Area [mAu*min]
rac-**182b**	20.8	188.50	33.7	193.36
(*M*)-**182b**	20.8	235.40	33.5	12.45

Figure 149 HPLC Chromatogram of (*M*)-**182b**.

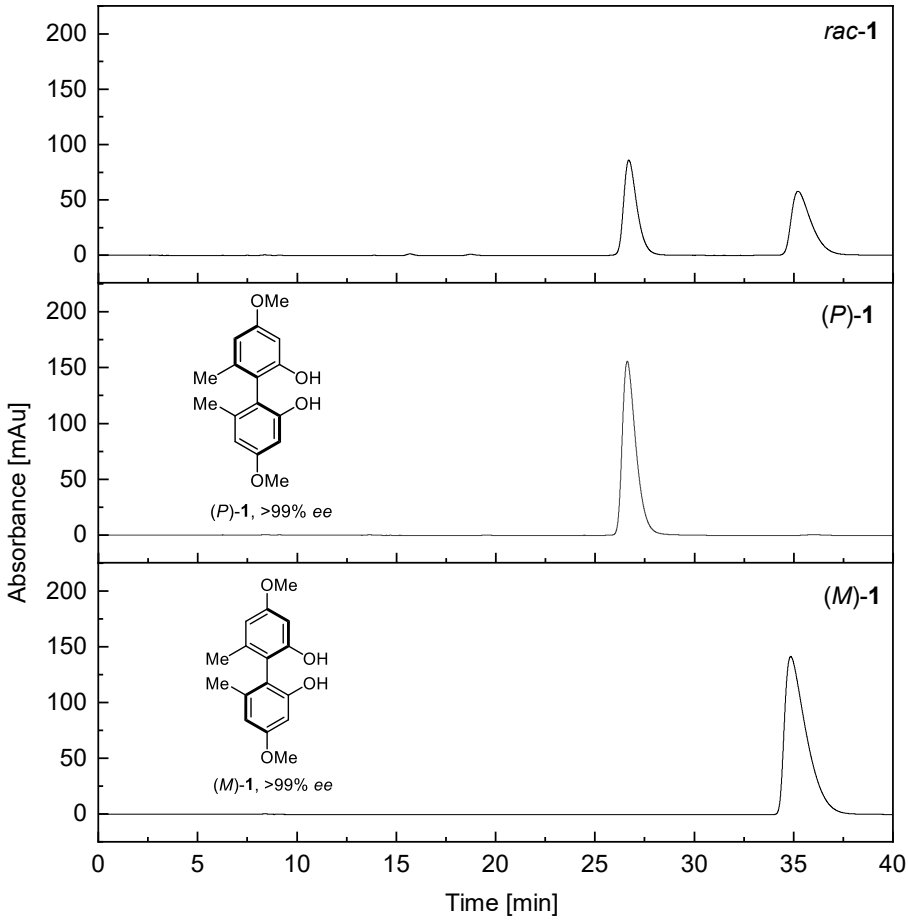

Column: Chiracel OD-H (250x4.6 mm); 5 µL, 25 °C, 0.5 mL/min, 274 nm; solvent: *n*-heptane:2-propanol (90:10).

	t_{R1} [min]	Area [mAu*min]	t_{R2} [min]	Area [mAu*min]
rac-**1**	26.7	66.98	35.2	66.99
(*M*)-**1**	-	-	34.9	179.58
(P)-**1**	26.6	124.64	-	-

Figure 150 HPLC Chromatogram of (*M*)-**1** and (*P*)-**1**.

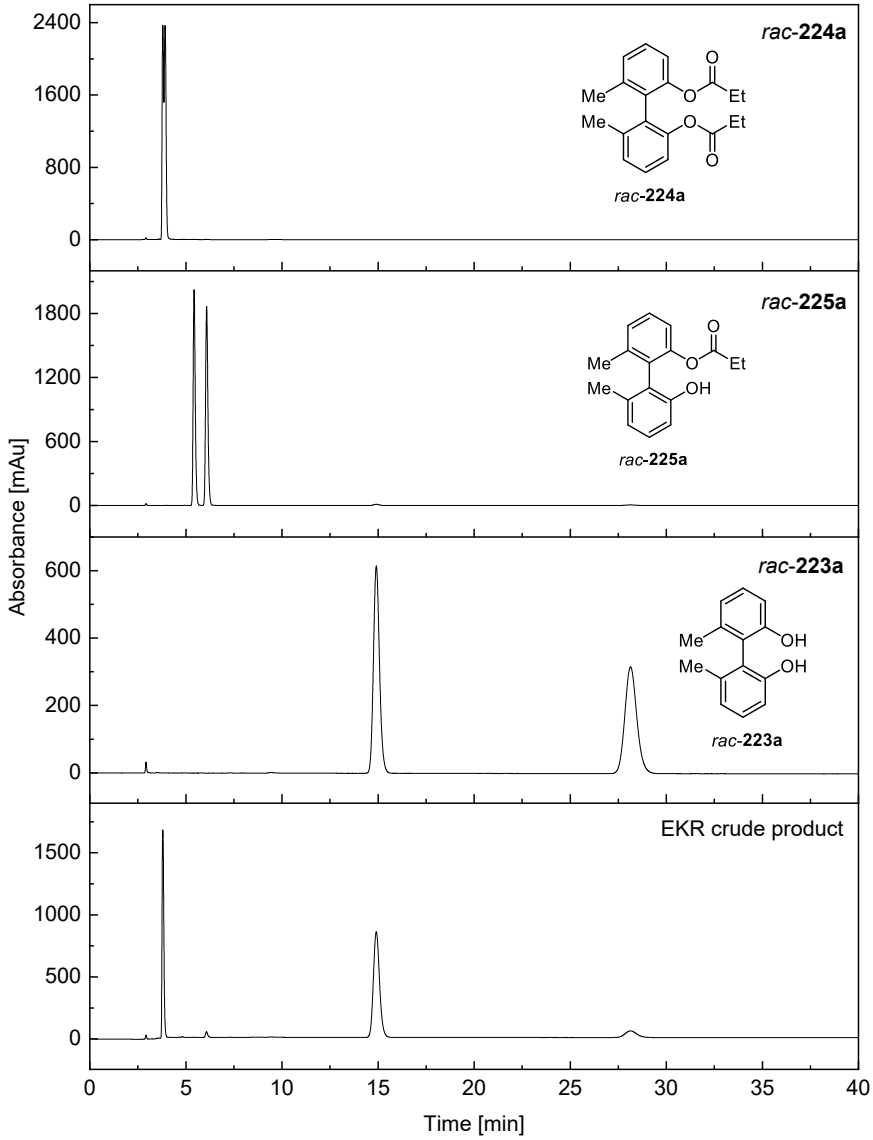

Column: Lux Amylose-1, *Fa. Phenomenex* (250x4.6 mm); 5 µL, 25 °C, 1 mL/min, 210 nm; solvent: *n*-heptane:2-propanol (90:10).

	t_{R1} [min]	Area [mAu*min]	t_{R2} [min]	Area [mAu*min]	
224a	3.8	197.19	3.9	1.47	98% *ee*
225a	-	-	-	-	-
223a	14.9	285.59	28.1	30.42	79% *ee*

Figure 151 HPLC Chromatogram of the crude product and reference substrates for the EKR of *rac*-**224a**.

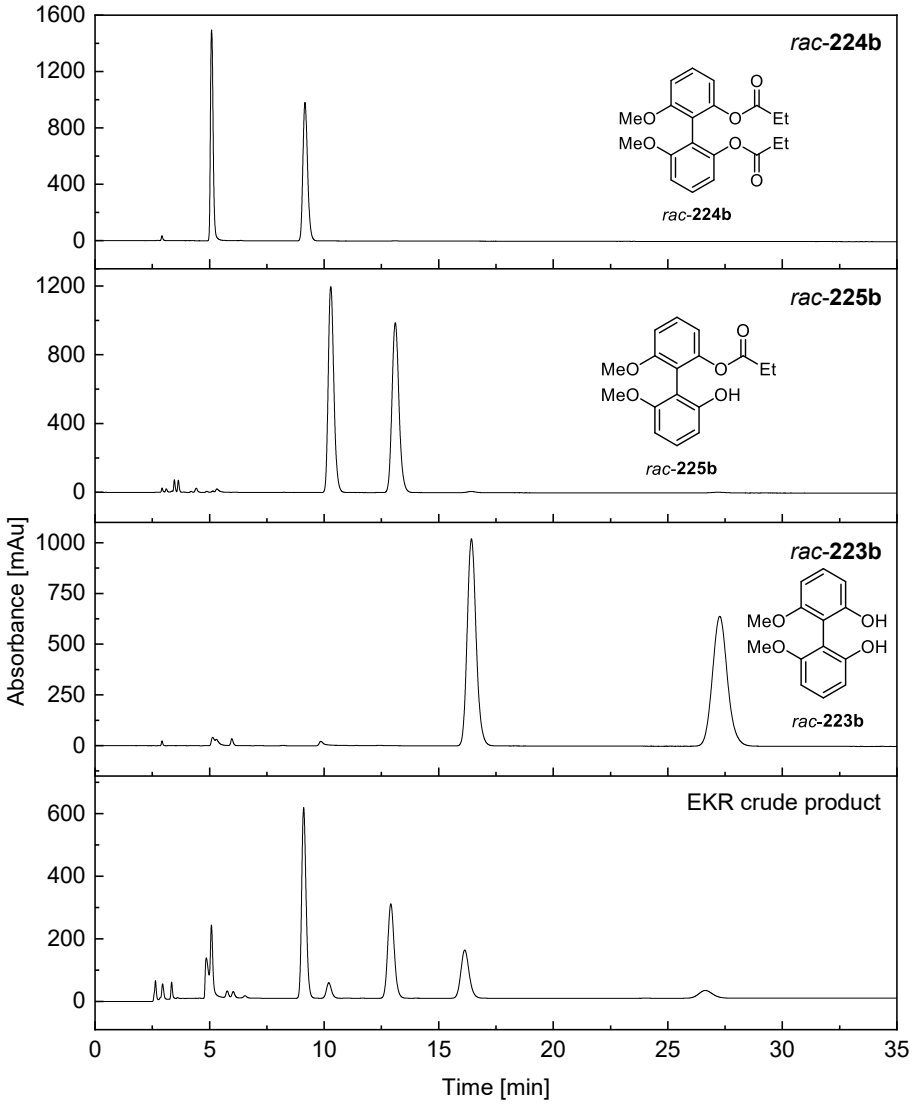

Column: Lux Amylose-1, *Fa. Phenomenex* (250x4.6 mm); 5 µL, 25 °C, 1 mL/min, 205 nm; solvent: *n*-heptane:2-propanol (80:20).

	t_{R1} [min]	Area [mAu*min]	t_{R2} [min]	Area [mAu*min]	
224b	5.1	33.24	9.1	202.48	72% *ee*
225b	10.2	15.71	12.9	99.37	73% *ee*
223b	16.1	64.66	26.6	18.90	54% *ee*

Figure 152 HPLC Chromatogram of the crude product and reference substrates for the EKR of *rac*-**224b**.

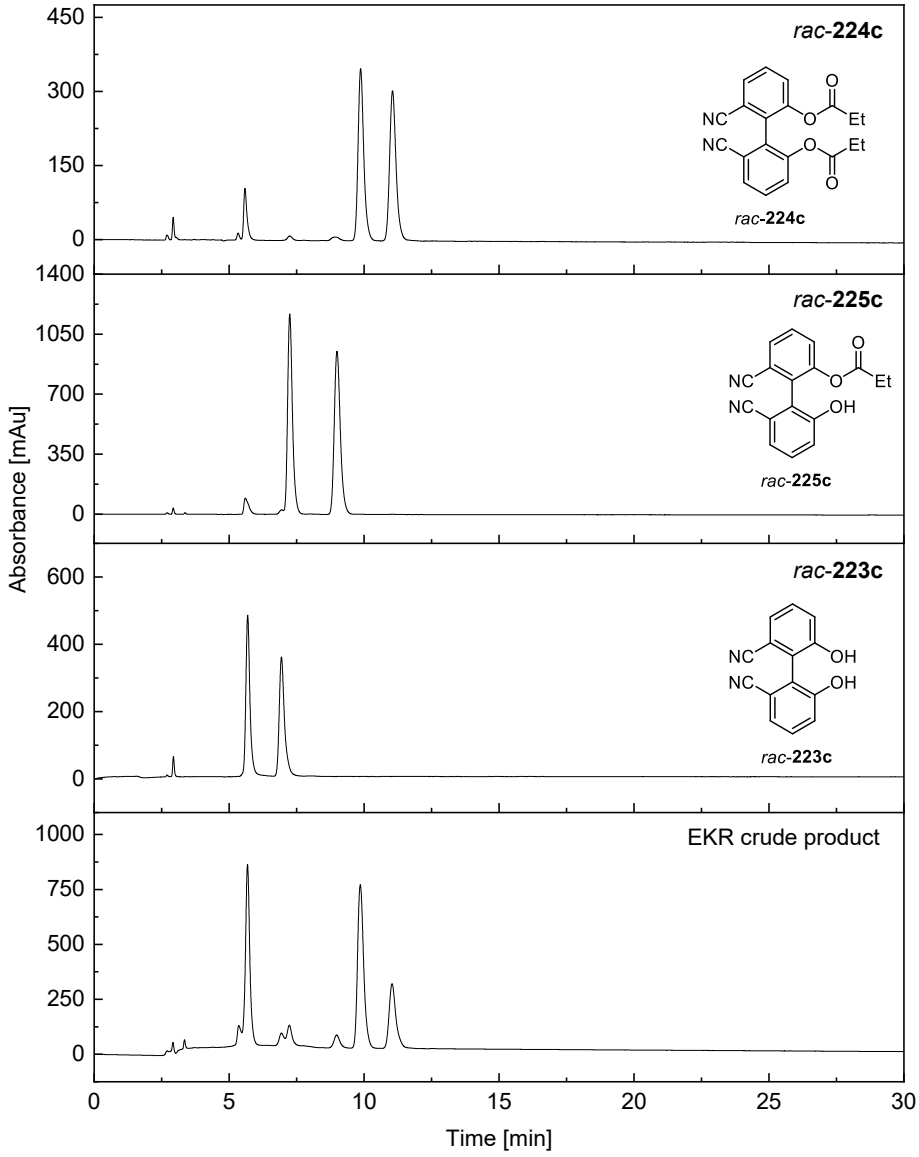

Column: Lux Amylose-1, *Fa. Phenomenex* (250x4.6 mm); 5 µL, 25 °C, 1 mL/min, 205 nm; solvent: *n*-heptane:2-propanol (80:20).

	t_{R1} [min]	Area [mAu*min]	t_{R2} [min]	Area [mAu*min]	
224c	9.8	145.21	11.0	117.18	11% *ee*
225c	7.2	20.46	8.9	19.13	rac.
223c	5.6	120.75	6.9	21.26	70% *ee*

Figure 153 HPLC Chromatogram of the crude product and reference substrates for the EKR of *rac*-**224c**.

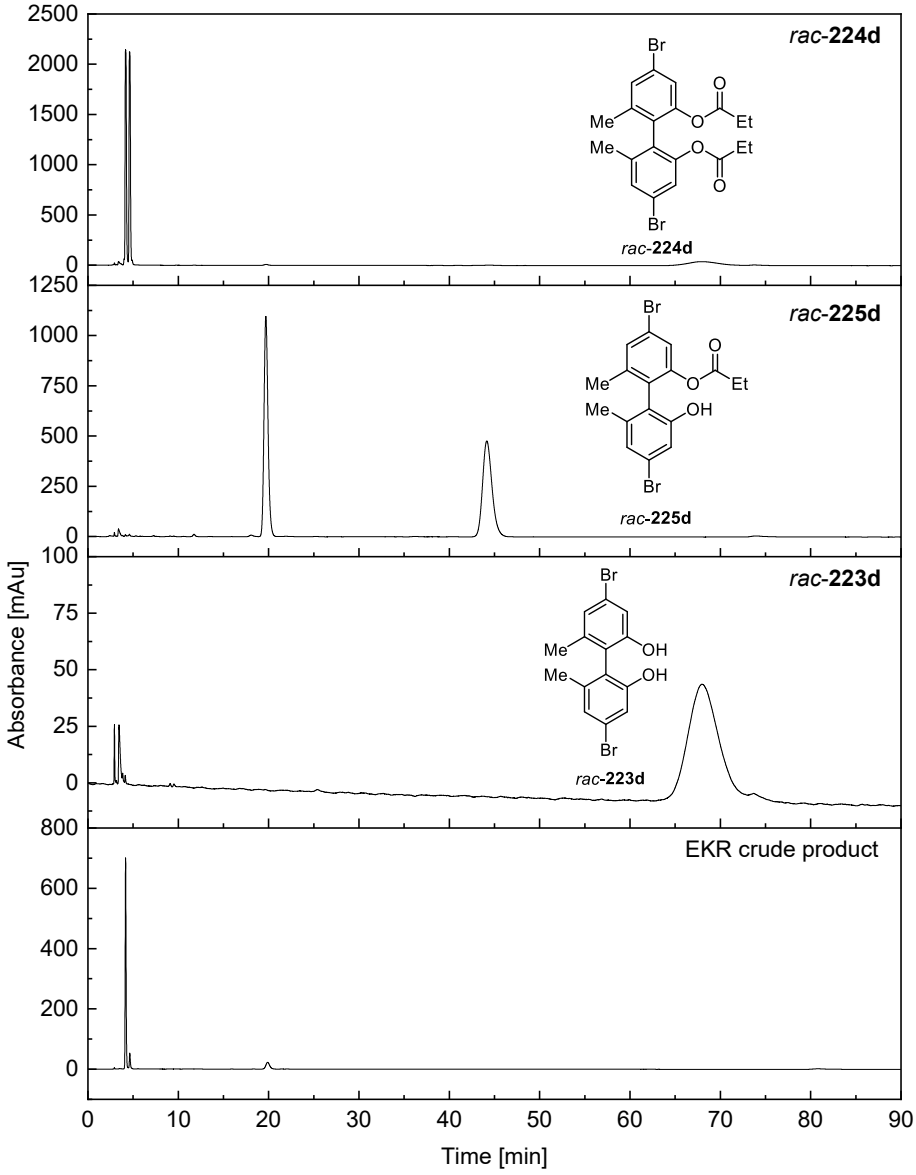

Column: Lux Amylose-1, *Fa. Phenomenex* (250x4.6 mm); 5 µL, 25 °C, 1 mL/min, 205 nm; solvent: *n*-heptane:2-propanol (98:2).

	t_{R1} [min]	Area [mAu*min]	t_{R2} [min]	Area [mAu*min]	
224d	4.1	189.68	4.6	15.27	85% *ee*
225d	19.6	28.13	-	-	>99% *ee*
223d	No baseline separation				

Figure 154 HPLC Chromatogram of the crude product and reference substrates for the EKR of *rac*-**224d**.

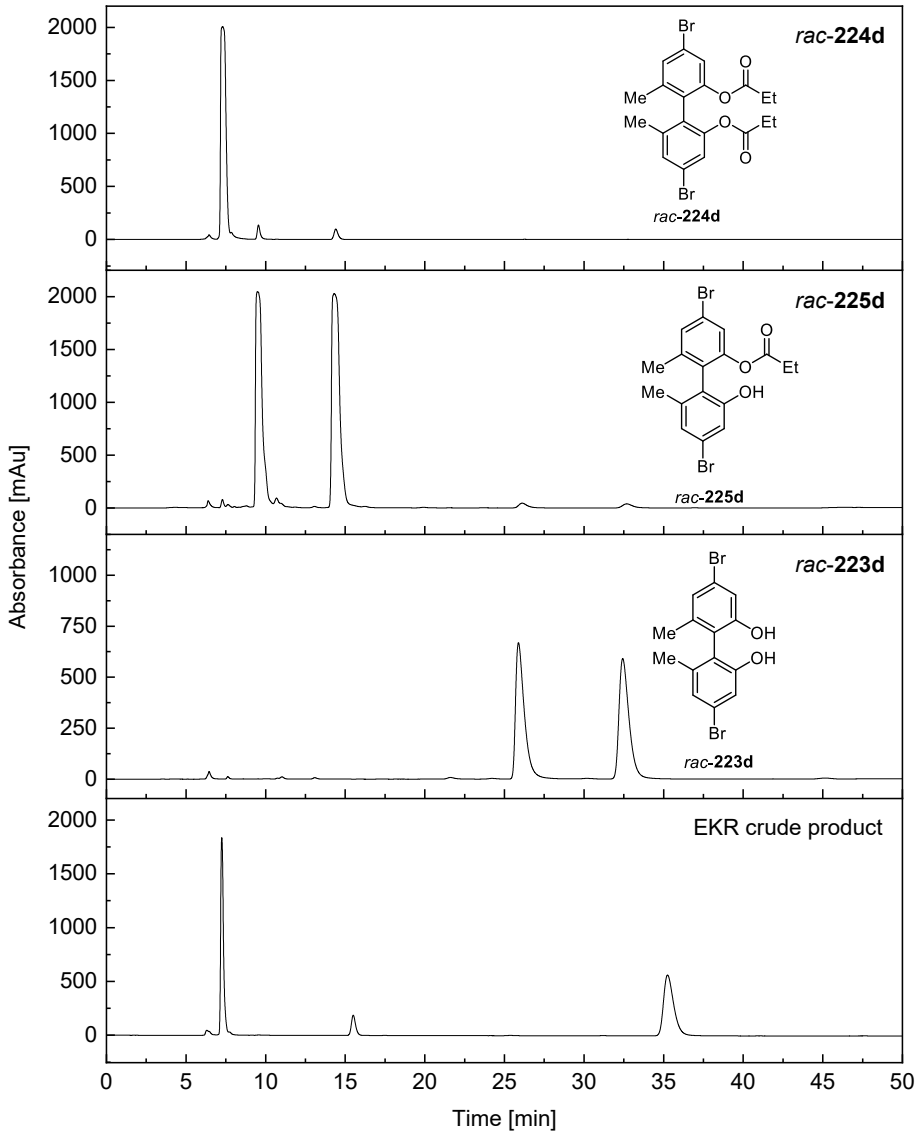

Column: Chiralpak IB, *Fa. Daicel* (250x4.6 mm); 5 µL, 25 °C, 0.5 mL/min, 205 nm; solvent: *n*-heptane:2-propanol (95:5).

	t_{R1} [min]	Area [mAu*min]	t_{R2} [min]	Area [mAu*min]	
224d		No baseline separation			
225d	-	-	15.5	58.60	99% *ee*
223d	25.4	1.48	35.3	417.46	99% *ee*

Figure 155 HPLC Chromatogram of the crude product and reference substrates for the EKR of *rac*-**224d**.

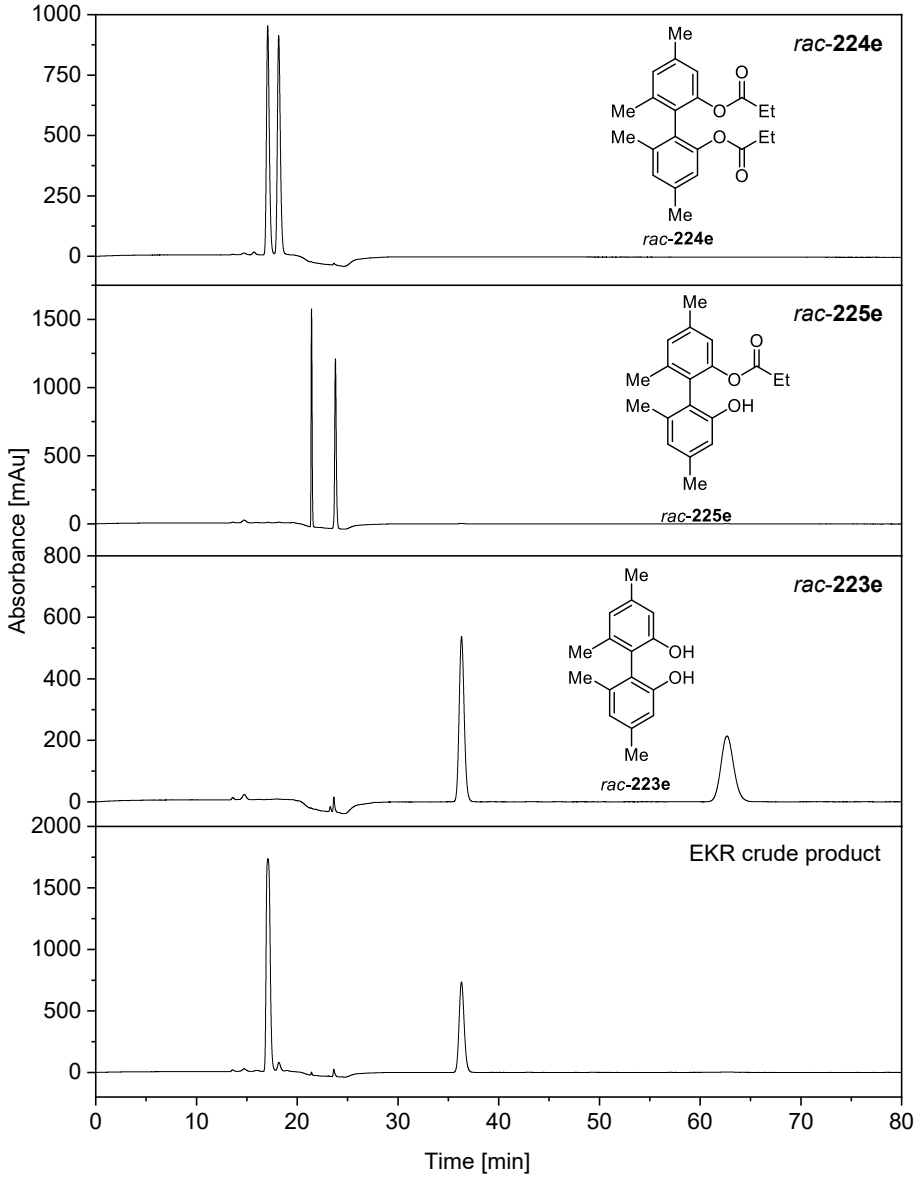

Column: Lux Amylose-1, *Fa. Phenomenex* (250x4.6 mm); 5 µL, 25 °C, 0.2 mL/min for 20 min then 1 mL/min, 205 nm; solvent: *n*-heptane:2-propanol (85:15).

	t_{R1} [min]	Area [mAu*min]	t_{R2} [min]	Area [mAu*min]	
224e	17.0	788.90	18.1	28.30	94% *ee*
225e	-	-	-	-	-
223e	36.3	433.44	62.7	3.63	98% *ee*

Figure 156 HPLC Chromatogram of the crude product and reference substrates for the EKR of *rac*-**224e**.

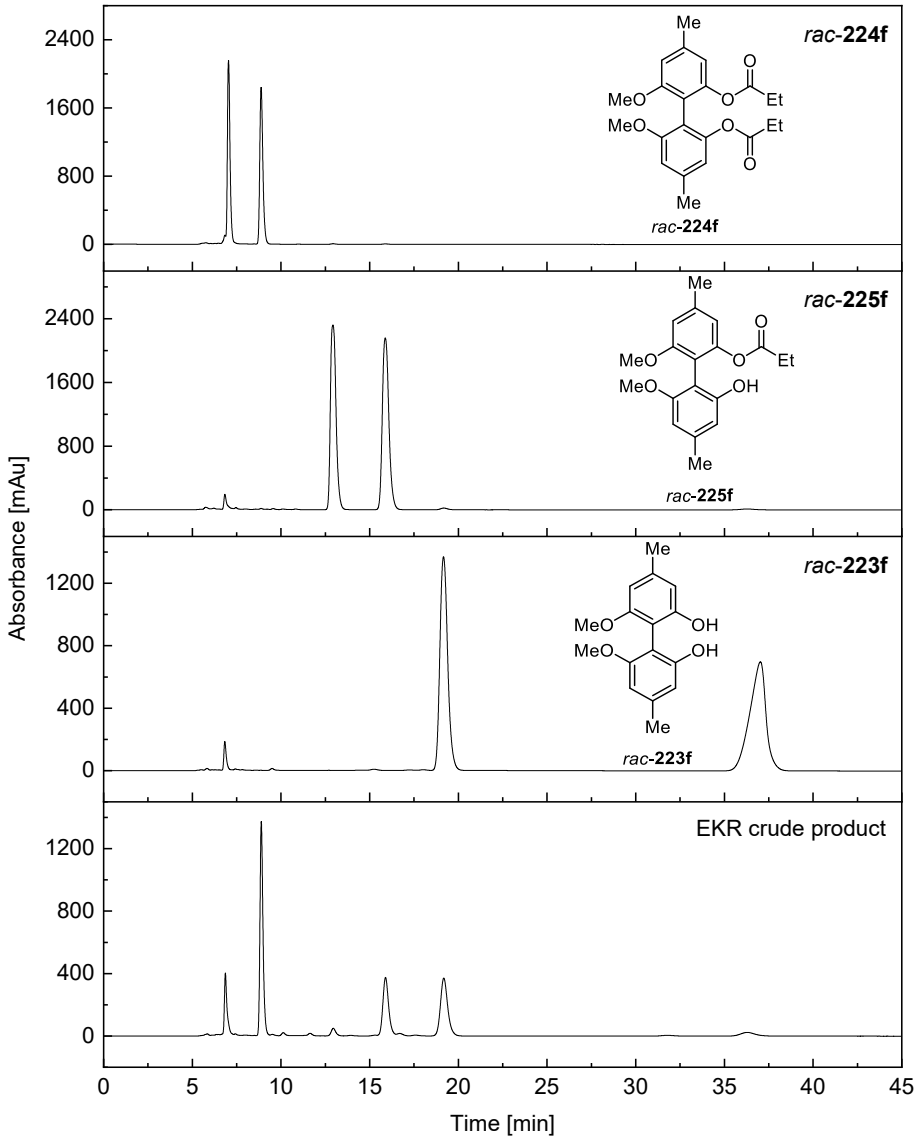

Column: Lux Amylose-1, *Fa. Phenomenex* (250x4.6 mm); 2 µL, 25 °C, 0.5 mL/min, 210 nm; solvent: *n*-heptane:2-propanol (55:45).

	t_{R1} [min]	Area [mAu*min]	t_{R2} [min]	Area [mAu*min]	
224f	7.43	9.45	8.8	169.20	89% *ee*
225f	12.9	14.76	15.8	142.73	81% *ee*
223f	19.1	175.31	36.3	22.16	78% *ee*

Figure 157 HPLC Chromatogram of the crude product and reference substrates for the EKR of *rac*-**224f**.

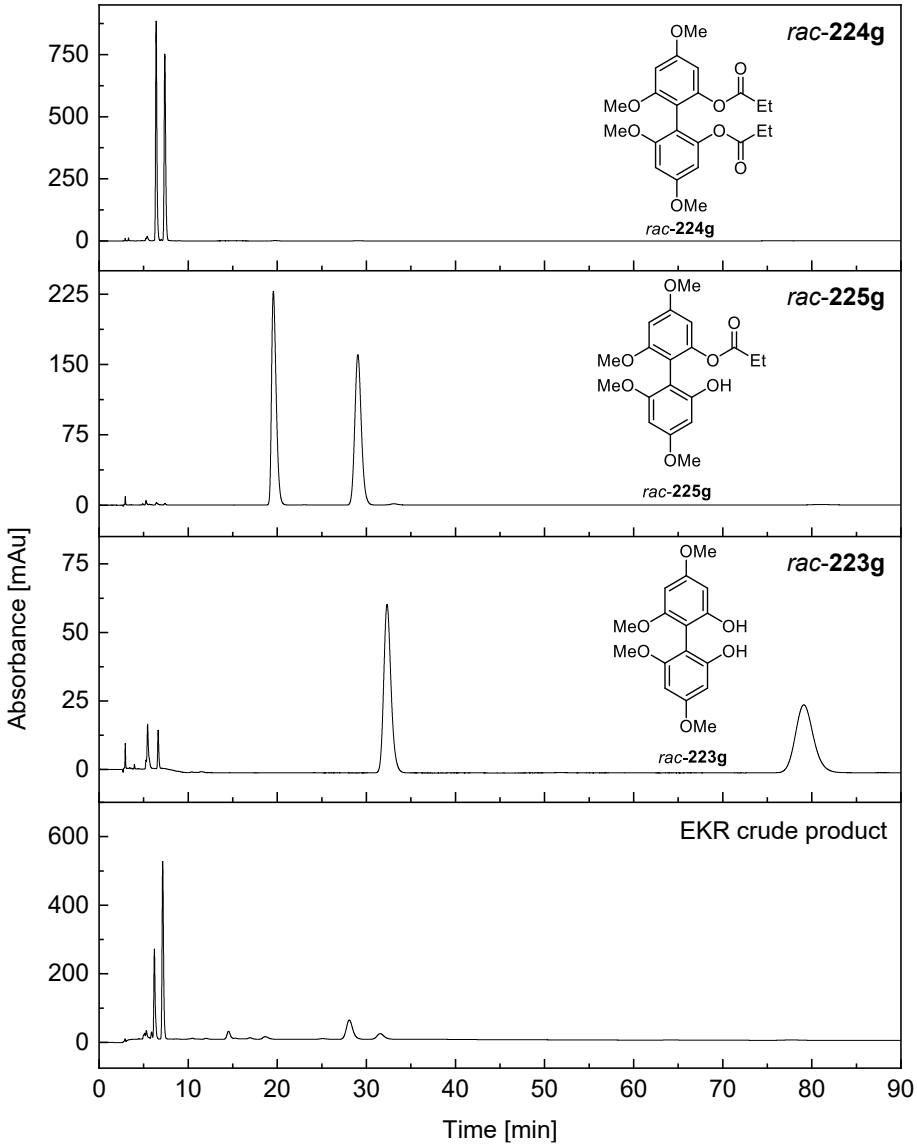

Column: Lux Amylose-1, *Fa. Phenomenex* (250x4.6 mm); 5 µL, 25 °C, 1 mL/min, 205 nm; solvent: *n*-heptane:2-propanol (80:20).

	t_{R1} [min]	Area [mAu*min]	t_{R2} [min]	Area [mAu*min]	
224g	6.2	46.09	7.1	99.73	37% *ee*
225g	18.6	5.21	28.1	47.66	80% *ee*
223g	31.6	15.77	77.8	2.65	71% *ee*

Figure 158 HPLC Chromatogram of the crude product and reference substrates for the EKR of *rac*-**224g**.

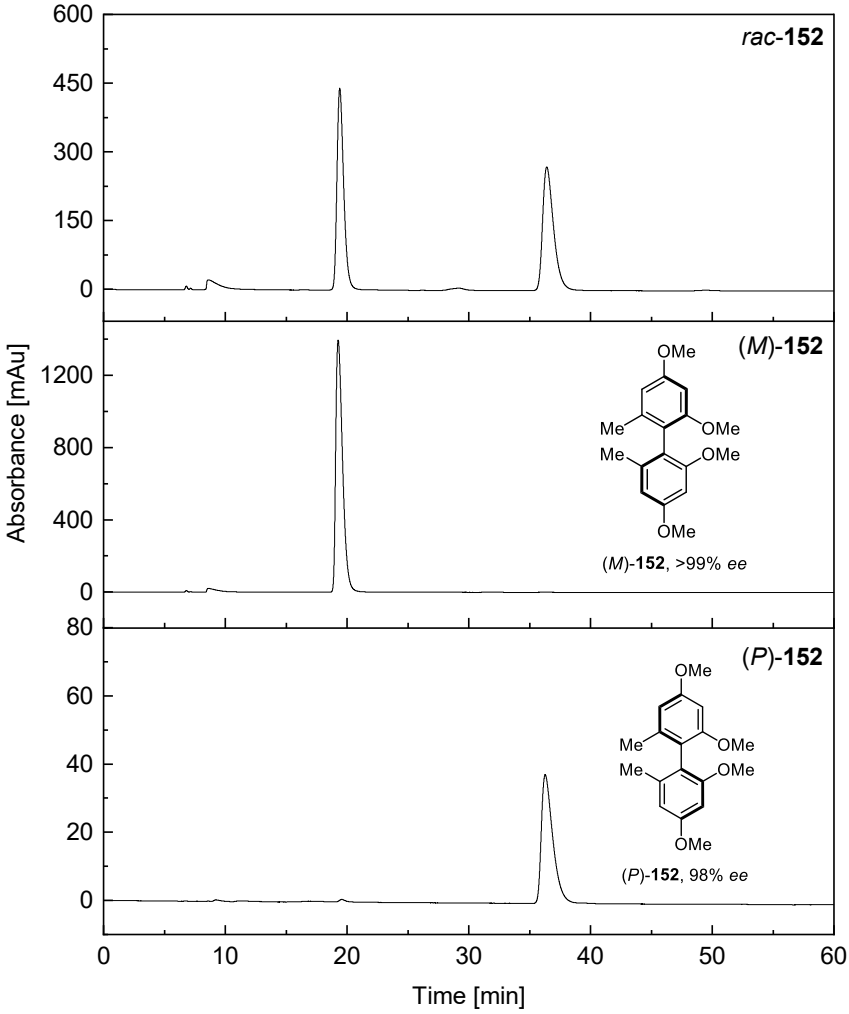

Column: Chiralpak IC, *Fa. Daicel* (250x4.6 mm); 5 µL, 25 °C, 0.5 mL/min, 210 nm; solvent: *n*-heptane:2-propanol (99:1).

	t_{R1} [min]	Area [mAu*min]	t_{R2} [min]	Area [mAu*min]
rac-**152**	19.4	281.15	36.4	279.97
(*M*)-**152**	19.02	174.54	-	-
(*P*)-**152**	19.6	6.26	36.3	613.54

Figure 159 HPLC Chromatogram of (*M*)-**152** and (*P*)-**152**.

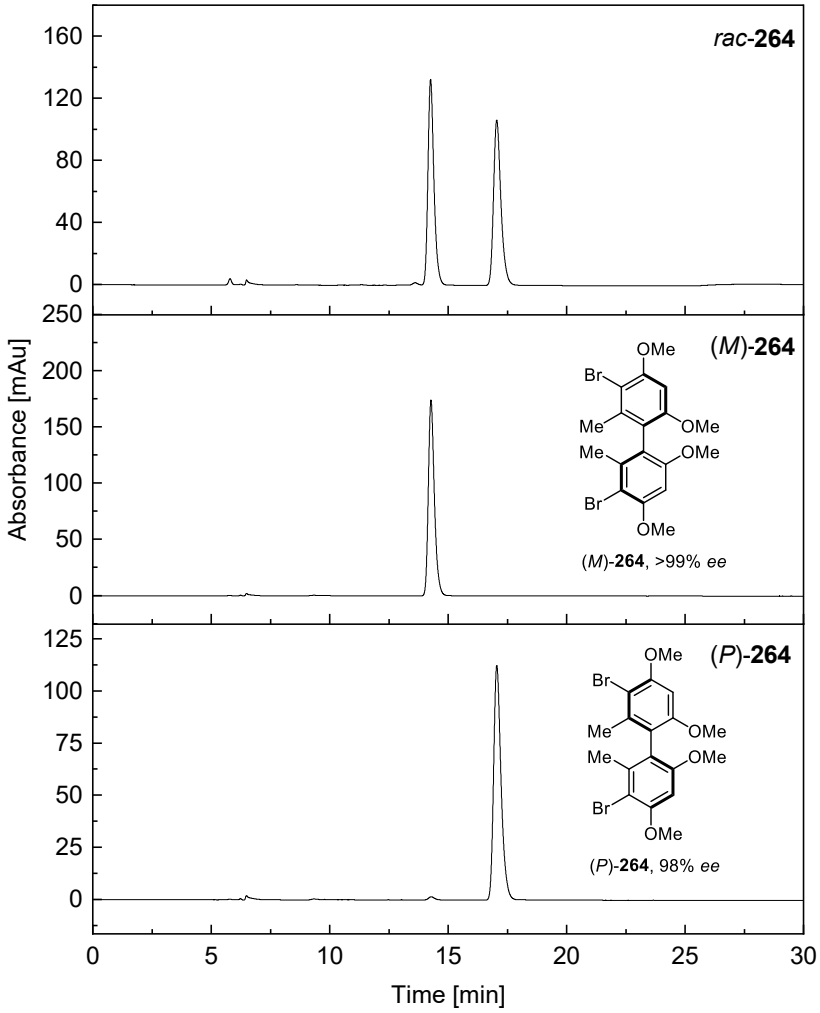

Column: Lux Amylose-1, *Fa. Phenomenex* (250x4.6 mm); 5 µL, 25 °C, 0.5 mL/min, 274 nm; solvent: *n*-heptane:2-propanol (98:2).

	t_{R1} [min]	Area [mAu*min]	t_{R2} [min]	Area [mAu*min]
rac-**264**	14.2	105.30	17.0	104.37
(*M*)-**264**	14.3	251.15	-	-
(*P*)-**264**	14.3	2.28	17.0	199.20

Figure 160 HPLC Chromatogram of (*M*)-**264** and (*P*)-**264**.

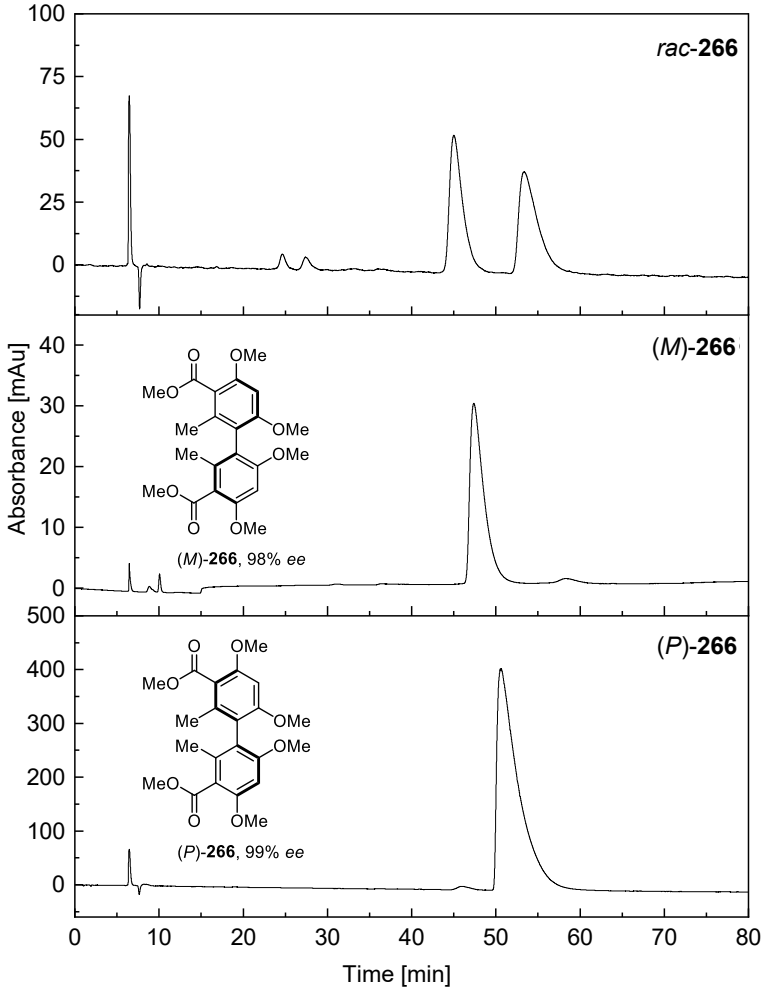

Column: Chiracel OD-H (250x4.6 mm); 5 µL, 25 °C, 0.5 mL/min, 331 nm; solvent: *n*-heptane:2-propanol (95:5).

	t_{R1} [min]	Area [mAu*min]	t_{R2} [min]	Area [mAu*min]
rac-**266**	44.9	102.80	53.4	108.19
(*M*)-**266**	47.4	56.44	58.4	0.56
(*P*)-**266**	45.9	0.74	50.5	114.60

Figure 161 HPLC Chromatogram of (*M*)-**266** and (*P*)-**266**.

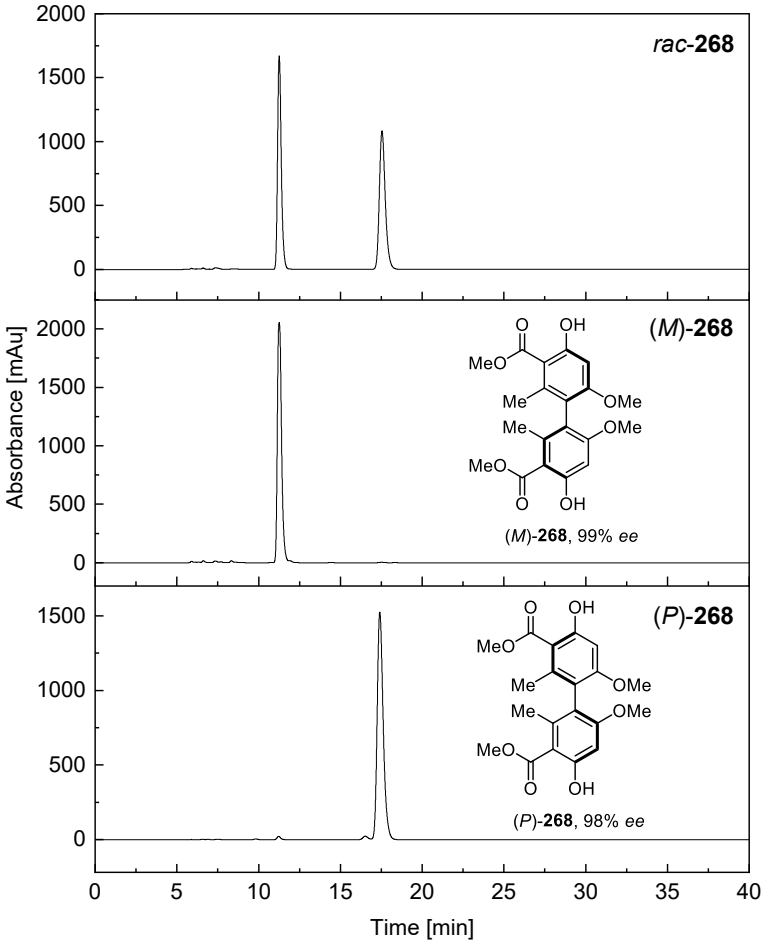

Column: Lux Amylose-1, *Fa. Phenomenex* (250x4.6 mm); 5 µL, 25 °C, 0.5 mL/min, 232 nm; solvent: *n*-heptane:2-propanol (50:50).

	t_{R1} [min]	Area [mAu*min]	t_{R2} [min]	Area [mAu*min]
rac-**268**	11.3	440.93	17.5	454.41
(*M*)-**268**	11.2	614.88	17.5	1.66
(*P*)-**268**	11.2	9.23	17.4	989.50

Figure 162 HPLC Chromatogram of (*M*)-**268** and (*P*)-**268**.

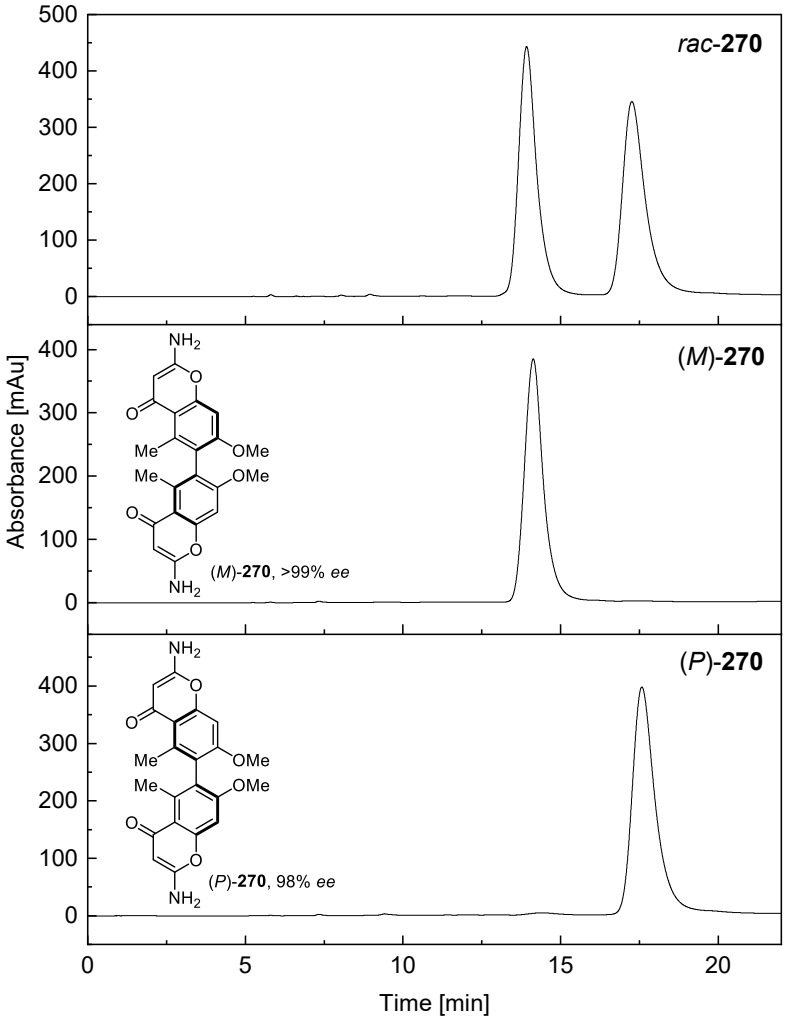

Column: Lux Amylose-1, *Fa. Phenomenex* (250x4.6 mm); 5 µL, 25 °C, 0.5 mL/min, 238 nm; solvent: *n*-heptane:2-propanol (75:25).

	t_{R1} [min]	Area [mAu*min]	t_{R2} [min]	Area [mAu*min]
rac-**270**	13.9	300.88	17.3	297.87
(*M*)-**270**	14.1	409.77	-	-
(*P*)-**270**	14.4	5.72	17.6	534.44

Figure 163 HPLC Chromatogram of (*M*)-**270** and (*P*)-**270**.

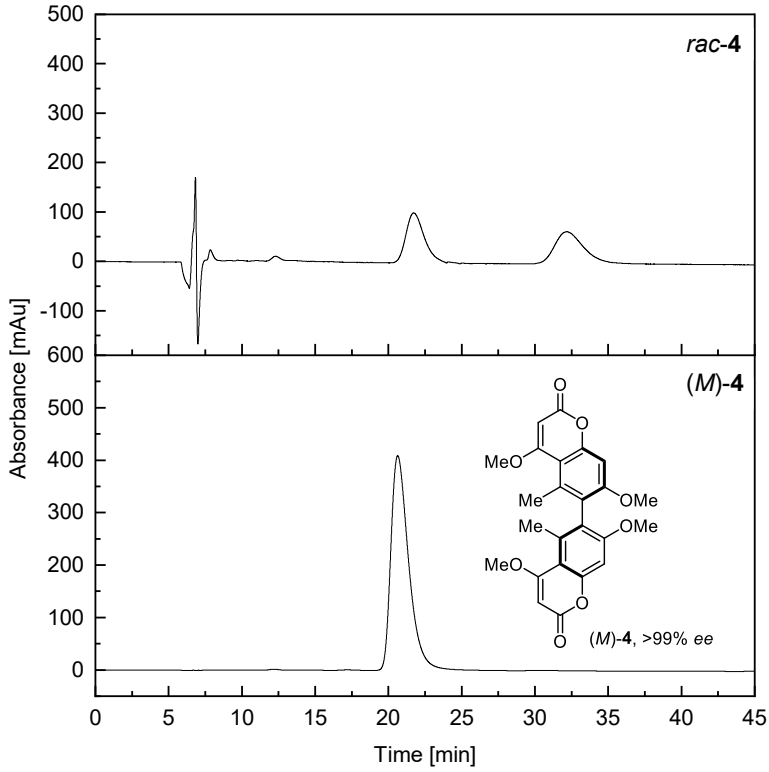

Column: Chiracel OD-H (250x4.6 mm); 5 µL, 25 °C, 0.5 mL/min, 331 nm; solvent: *n*-heptane:2-propanol (30:70).

	t_{R1} [min]	Area [mAu*min]	t_{R2} [min]	Area [mAu*min]
rac-**4**	21.7	146.51	32.2	146.71
(*M*)-**4**	20.6	574.70	-	-

Figure 164 HPLC Chromatogram of (*M*)-**4**.

Band 36
Enantioselektive Totalsynthese von Altersolanolen
B. Mechsner (2019), I, V, 311 pp
ISBN: 978-3-95806-412-6

Band 37
Glycosynthases – tuning glycosidase activity towards glycoside diversification and synthesis
M. R. Hayes (2019), VI, 225 pp
ISBN: 978-3-95806-441-6

Band 38
**Chemoenzymatische Synthesemethoden –
Zugang zur duftenden Welt der Chemie und darüber hinaus**
C. Kumru (2019), V, 338 pp
ISBN: 978-3-95806-446-1

Band 39
Oxidoreduktasen für die Bereitstellung von Schlüsselbausteinen der Natur- und Wirkstoffsynthese
R. Krug (2020), 216 pp
ISBN: 978-3-95806-454-6

Band 40
Die farbenfrohe Welt der Prodiginine – Neue Enzyme für die Synthese bioaktiver Naturstoffderivate
H. U. C. Braß (2021), IX, 349 pp
ISBN: 978-3-95806-523-9

Band 41
Oxidoreduktasen: Von neuen Biokatalysatoren bis zum fertigen Naturstoff
D. Dickmann (2021), 274 pp
ISBN: 978-3-95806-573-4

Band 42
**Chemie ohne Grenzen –
Biokatalysatoren und Bororganyle als wertvolle Hilfsmittel
für die zielmolekülorientierte, enantioselektive Synthese**
M. R. Mantel (2021), 487 pp
ISBN: 978-3-95806-585-7

Band 43
Über tetraolbasierte Allylboronsäureester und deren Potential in der stereoselektiven Synthese
P. Ullrich (2022), xii, 324 pp
ISBN: 978-3-95806-618-2

Band 44
Design, Synthese und Charakterisierung neuartiger *photocaged compounds* – Optimierte Werkzeuge zur Etablierung wellenlängenselektiver Genexpression
F. Hogenkamp (2022), V, 456 pp
ISBN: 978-3-95806-637-3

Band 45
Charakterisierung von Methyltransferasen zur enantioselektiven Synthese von Hexahydropyrrolo[2,3-*b*]indol basierten Naturstoffen
P. Schneider (2023), x, 315 pp
ISBN: 978-3-95806-690-8

Band 46
Untersuchungen zu enzymatischen Halogenierungsreaktionen in der organischen Synthese
A. V. Fejzagić (2023), XI, 264 pp
ISBN: 978-3-95806-728-8

Band 47
Biochemische Charakterisierung von modularen dirigierenden Proteinen
N. Huwa (2024), X, 235 pp
ISBN: 978-3-95806-745-5

Band 48
Immobilisierte Enzyme und Kofaktor-Regenerierung in der kontinuierlichen Durchflusssynthese
B. Baumer (2024), XVIII, 231 pp
ISBN: 978-3-95806-783-7

Band 49
Biaryl-based natural products as structural motif for pharmaceutically relevant compounds
M. K. T. Klischan (2025), V, 657 pp
ISBN: 978-3-95806-801-8

Band 50
Flavin-abhängige Halogenasen zur Derivatisierung von Naturstoffen
J. Gebauer (2025), XXIV, 321 pp
ISBN: 978-3-95806-850-6

Band 51
Lipase-catalyzed kinetic resolution: Synthesis and application of axially chiral biphenols
R. C. Ganardi (2025), 423 pp
ISBN: 978-3-95806-854-4

Bioorganische Chemie an der Heinrich-Heine-Universität Düsseldorf
im Forschungszentrum Jülich

Herausgegeben von Jörg Pietruszka

In this work, investigations on the atroposelective synthesis of axially chiral biphenols were carried out. The focus was on the construction and application of the important 2,2´-biphenol building block *rac*-4,4´-dimethoxy-6,6´-dimethyl-[1,1´-biphenyl]-2,2´-diol *rac*-(**1**), which represents a common motif of various aromatic polyketide dimers. The challenging construction of the sterically hindered *rac*-**1** was performed and discussed. The established methods were applied afterwards to the racemic synthesis of a dedicated library of tetra-*ortho*-substituted biphenols.

The atroposelective transformation of the racemic biphenol *rac*-**1** was investigated by an enzyme screening of hydrolases. A scalable enzymatic kinetic resolution using commercially available *Candida rugosa* lipase (CRL) was developed for the atroposelective hydrolysis towards both enantiomers (*M*)-**1** and (*P*)-**1** with excellent enantiomeric excesses. The applicability of CRL was tested on a scope of different biphenols to evaluate the influence of the substitution pattern on the enzyme's activity and selectivity. Finally, the combination of the metal-catalyzed homocoupling and the enzymatic kinetic resolution enabled a scalable and efficient method towards the total synthesis of the enantiopure (*M*)-isokotanin A.

Band 51
ISBN 978-3-95806-854-4